VISCOELASTIC BEHAVIOUR IN HYDROGENATED NITRILE RUBBER FOR INDUSTRIAL ROLL APPLICATIONS

PANJAPORN WONGWITTHAYAKOOL

A THESIS SUBMITTED IN PARTIAL FULFILLMENT
OF THE REQUIREMENTS FOR
THE DEGREE OF DOCTOR OF PHILOSOPHY
(POLYMER SCIENCE AND TECNOLOGY)
FACULTY OF GRADUATE STUDIES
MAHIDOL UNIVERSITY
2012

Thesis
entitled

VISCOELASTIC BEHAVIOUR IN HYDROGENATED NITRILE RUBBER FOR INDUSTRIAL ROLL APPLICATIONS

……
Miss Panjaporn Wongwitthayakool
Candidate

……
Assoc. Prof. Chakrit Sirisinha,
Ph.D.
Major advisor

……
Mr. Pongdhorn Sae-Oui,
Ph.D.
Co-advisor

……
Mr. Ekkawit Pianhanuruk,
Ph.D.
Co-advisor

……
Prof. Banchong Mahaisavariya,
M.D., Dip Thai Board of Orthopedics
Dean
Faculty of Graduate Studies
Mahidol University

……
Asst. Prof. Panya Sunintaboon,
Ph.D.
Program Director
Doctor of Philosophy Program in
Polymer Science and Technology
Faculty of Science, Mahidol University

Thesis
entitled

VISCOELASTIC BEHAVIOUR IN HYDROGENATED NITRILE RUBBER FOR INDUSTRIAL ROLL APPLICATIONS

was submitted to the Faculty of Graduate Studies, Mahidol University
for the degree of Doctor of Philosophy (Polymer Science and Technology)
on
December 27, 2012

……
Miss Panjaporn Wongwitthayakool
Candidate

……
Prof. Narongrit Sombatsompop,
Ph.D.
Chair

……
Assoc. Prof. Chakrit Sirisinha,
Ph.D.
Member

……
Mr. Ekkawit Pianhanuruk,
Ph.D.
Member

……
Mr. Pongdhorn Sae-Oui,
Ph.D.
Member

……
Prof. Banchong Mahaisavariya,
M.D., Dip Thai Board of Orthopedics
Dean
Faculty of Graduate Studies
Mahidol University

……
Prof. Skorn Mongkolsuk,
Ph.D.
Dean
Faculty of Science
Mahidol University

ACKNOWLEDGEMENTS

I would like to express my sincere gratitude to my advisor, Assoc. Prof. Dr. Chakrit Sirisinha, for his excellent supervision, inspiring guidance and encouragement throughout this research. Sincere appreciation is also extended to Dr. Pongdhorn Sae-Oui, and Dr. Narongrit Sombatsompop for their valuable advices and comments for completion of this thesis.

I gratefully acknowledge Prof. Dr. Jean L. Leblanc for helpful discussion in my research in his Polymer Rheology and Processing Laboratory at Paris, France. Sincere appreciation is extended to Prof. Dr. Ekkawit Pianhanuruk for suggestion about living and survival in France.

I wish to thank teachers, staffs of Polymer Science and Technology Program in the Department of Chemistry, Faculty of Science, Mahidol University, and my nice friends whose names are not mentioned here, for their help, kindness, suggestion, and encouragement.

I would like to thank The Royal Golden Jubilee Ph.D. Program, The Thailand Research Fund, French embassy in Thailand and Thai Industrial Rollers Co., Ltd, for the financial support on this research.

Finally, I am deeply grateful to my parents and my family for their love, support, understanding, and inspiration throughout the course of my graduate study.

Panjaporn Wongwitthayakool

VISCOELASTIC BEHAVIOUR IN HYDROGENATED NITRILE RUBBER FOR INDUSTRIAL ROLL APPLICATIONS

PANJAPORN WONGWITTHAYAKOOL 5038025 SCPO/D

Ph.D. (POLYMER SCIENCE AND TECHNOLOGY)

THESIS ADVISORY COMMITTEE: CHAKRIT SIRISINHA, Ph.D., PONGDHORN SAE-OUI, Ph.D., EKKAWIT PIANHANURAK, Ph.D.

ABSTRACT

Hydrogenated nitrile rubber (HNBR) was mixed with reinforcing fillers, namely, carbon black (CB), silica and organoclay. Cure, viscoelastic and mechanical properties of HNBR filled with various types and loadings of reinforcing fillers were investigated. Fourier transform (FT) rheometry was used to study the non-linear viscoelastic behaviour of filled rubber compounds. Filler loading appears to play a strong role on cure characteristics and non-linear viscoelastic response.

The HNBR vulcanisate hardness of 80 Shore A was of interest in this work as a typical hardness used in industrial rollers, especially steel and paper mill rollers. Such hardness could be achieved by various reinforcing fillers. Among CB, silica and organoclay, the CB was found to be the most effective reinforcing filler, giving good mechanical properties. This was attributed to the superiority in magnitudes of filler dispersion and rubber-filler interaction as evidenced by the broadest linear viscoelastic (LVE) region.

The reinforcement magnitude of N326/N990, N326/N774 and N550/N990 carbon black (CB) hybrid systems in HNBR vulcanisates was compared. The increase in loading portion of CB having larger surface area and/or greater structure in hybrid systems gives rise to the greater magnitudes of CB transient network formation and filler-rubber interaction. The relatively high structure of N550 leads to the high extents of bound rubber and crosslink density, yielding the comparable crosslink density, mechanical and viscoelastic properties of HNBR vulcanisates with N550/N990 and N326/N990 hybrid systems.

Heat build-up (HBU) of HNBR filled with various CB loadings (i.e., 0 to 60 phr) and CB characteristics (i.e., N326, N550, N774 and N990) was determined using Gabometer 4000 flexometer equipped with high load cell of 4000 N. The HBU measured was then correlated with loss modulus measured from RPA 2000, giving the logarithmic relationship of: $HBU_G = 18.019\ln(G'') - 54.138$ with R^2 of 0.9214. However, the relationship between HBU measured from RPA 2000 and Gabometer 4000 of HNBR vulcanisates filled various CB loadings and characteristics was relatively poor. In other words, the HBU measurement with RPA 2000 could not satisfactorily replace the standard HBU technique in the systems studied.

KEY WORDS: HYDROGENATED NITRILE RUBBER/
VISCOELASTIC PROPERTIES/ FILLER REINFORCEMENT/
FOURIER TRANSFORM REOMETRY/ HEAT BUILD-UP

360 pages

พฤติกรรมหยุ่นหนืดในยางไฮโดรเจนเนตเทดไนไตรล์เพื่อการประยุกต์ใช้ในงานลูกกลิ้งอุตสาหกรรม
VISCOELASTIC BEHAVIOUR IN HYDROGENATED NITRILE RUBBER FOR INDUSTRIAL ROLL APPLICATIONS

ปัญจพร วงศ์วิทยากูล 5038025 SCPO/D

ปร.ด. (วิทยาศาสตร์และเทคโนโลยีพอลิเมอร์)

คณะกรรมการที่ปรึกษาวิทยานิพนธ์: ชาคริต สิริสิงห, Ph.D., พงษ์ธร แซ่อุย, Ph.D., เอกวิทย์ เพียรอนุรักษ์, Ph.D.

บทคัดย่อ

ยางไฮโดรเจนเนตเทดไนไตรล์ (HNBR) ได้นำมาผสมกับตัวเติมเสริมแรง ได้แก่ เขม่าดำ (carbon black; CB) ซิลิกา (silica) และออรกาโนเคลย์ (organoclay) และนำไปตรวจสอบพฤติกรรมการวัลคาไนซ์ (cure properties) สมบัติหยุ่นหนืด (viscoelastic properties) และสมบัติเชิงกล (mechanical properties) พบว่าปฏิกิริยาการวัลคาไนซ์ เกิดได้ดีขึ้นเมื่อเพิ่มปริมาณตัวเติมมากขึ้น และจากการศึกษาพฤติกรรมหยุ่นหนืดที่ไม่ใช่เชิงเส้น (non-linear viscoelastic) ของยางคอมพาวด์โดยใช้เทคนิคฟูเรียร์ทรานสฟอร์ม (Fourier transform) พบว่าปริมาณของตัวเติมเป็นตัวแปรหลักที่มีอิทธิพลต่อการตอบสนองของการหยุ่นหนืดที่ไม่ใช่เชิงเส้น

ในงานวิจัยนี้สนใจยางที่มีความแข็ง 80 Shore A เนื่องจากเป็นความแข็งที่เป็นความแข็งทั่วไปที่ใช้ในอุตสาหกรรมการผลิตลูกกลิ้งโดยเฉพาะลูกกลิ้งในโรงงานเหล็กและโรงงานกระดาษ ตัวเติมเสริมแรง ได้แก่ เขม่าดำ ซิลิกา และดินขาวนำมาใช้ในการเตรียมยางวัลคาไนซ์ที่มีระดับความแข็งนี้ได้ พบว่าเขม่าดำเป็นตัวเติมเสริมแรงที่มีประสิทธิภาพที่ดีที่สุด เนื่องจากแสดงสมบัติเชิงกลที่ดี ซึ่งสามารถอธิบายได้ด้วยอันตรกิริยาที่ดีกว่าระหว่างเขม่าดำและยางไฮโดรเจนเนตเทดไนไตรล์ (CB-HNBR interaction) ดังเห็นได้จากช่วงกว้างของการหยุ่นหนืดเชิงเส้น (linear viscoelastic region) ของยางวัลคาไนซ์

เมื่อเปรียบเทียบการเสริมแรงของยางวัลคาไนซ์ที่ผสมกับเขม่าดำลูกผสมในระบบที่แตกต่างสามระบบ ได้แก่ ระบบ N326/N990, N326/N774 และ N550/N990 พบว่าการเพิ่มปริมาณเขม่าดำที่มีพื้นที่ผิวและ/หรือโครงสร้างสูงมากขึ้นในระบบลูกผสมส่งผลต่อการเพิ่มปริมาณโครงสร้างตาข่ายชั่วคราวของเขม่าดำ (CB transient network) และทำให้แรงอันตรกิริยาระหว่างเขม่าดำและยางมีมากขึ้น โครงสร้างที่ค่อนข้างสูงของ N550 จะทำให้มีปริมาณยางบาวด์ (bound rubber) และความหนาแน่นเชื่อมขวางมาก ยางวัลคาไนซ์ที่ผสมกับเขม่าดำลูกผสมระบบ N550/N990 จึงมีสมบัติเชิงกลและสมบัติหยุ่นหนืดใกล้เคียงกับยางวัลคาไนซ์ที่ผสมกับเขม่าดำลูกผสมระบบ N326/N990

การทดสอบการสะสมความร้อน (heat build-up; HBU) ของยางไฮโดรเจนเนตเทดไนไตรล์ที่เติมเขม่าดำต่างชนิดกัน (ได้แก่ N326, N550, N774 และ N990) ในปริมาณต่างๆ (ได้แก่ 0 ถึง 60 phr) ทดสอบด้วยเครื่อง Gabometer 4000 flexometer ภายใต้น้ำหนักกดสูงสุด 4000 นิวตัน พบว่าเมื่อนำการสะสมความร้อนที่วัดได้มาสร้างความสัมพันธ์กับค่าโมดูลัสสูญเสียที่วัดจาก RPA 2000 ได้ความสัมพันธ์เชิงลอการิทึมตามสมการ $HBU_G = 18.019\ln(G'') - 54.138$ โดยมีค่าของความผิดพลาด (R^2) เท่ากับ 0.9214 อย่างไรก็ตาม การสะสมความร้อนของยางไฮโดรเจนเนตเทดไนไตรล์ที่เติมเขม่าดำต่างชนิดกัน (ได้แก่ N326, N550, N774 และ N990) ในปริมาณต่างๆที่วัดจาก RPA 2000 กับ Gabometer 4000 มีความสัมพันธ์ในแง่ที่ไม่ดี หรืออาจกล่าวได้ว่าการวัดการสะสมความร้อนด้วยเครื่อง RPA 2000 ไม่สามารถใช้แทนวิธีมาตรฐานได้ในยางระบบที่ทำการศึกษา

360 หน้า

CONTENTS

CONTENTS (cont.)

CONTENTS (cont.)

CONTENTS (cont.)

LIST OF TABLES

LIST OF TABLES (cont.)

LIST OF TABLES (cont.)

LIST OF TABLES (cont.)

LIST OF TABLES (cont.)

LIST OF TABLES (cont.)

LIST OF FIGURES

LIST OF FIGURES (cont.)

LIST OF FIGURES (cont.)

LIST OF FIGURES (cont.)

LIST OF FIGURES (cont.)

LIST OF FIGURES (cont.)

LIST OF FIGURES (cont.)

LIST OF FIGURES (cont.)

LIST OF FIGURES (cont.)

LIST OF FIGURES (cont.)

LIST OF FIGURES (cont.)

LIST OF FIGURES (cont.)

LIST OF FIGURES (cont.)

LIST OF FIGURES (cont.)

LIST OF FIGURES (cont.)

LIST OF FIGURES (cont.)

LIST OF FIGURES (cont.)

LIST OF ABBREVIATIONS

ACN	Acrylonitrile
ASTM	American society for testing and materials
BRC	Bound rubber content
CB	Carbon black
DBP	Dibutyl phthalate
DSS	Dynamic strain softening
EB	Elongation at break
FT	Fourier transform
HBU	Heat build-up
HNBR	Hydrogenated nitrile rubber
LAOS	Large amplitude oscillatory
LVE	Linear viscoelastic
M100	Modulus at 100% strain
NBR	Nitrile rubber
PSi	Precipitated silica
SEM	Scanning electron microscopy
SBR	Styrene butadiene rubber
VTA	Variable temperature analysis

CHAPTER I
INTRODUCTION

Rubber industrial rolls are generally utilised in various types of industries including steel, textile, paper, printing and packaging industries. Practically, each type of industries requires different physical properties to match the service conditions. Typically, good mechanical properties especially abrasion and tear resistances and elasticity associated with good processability are desirable. In order to achieve such properties, the appropriate rubber formulation is known to be one of key factors. In the case of rubber covering rolls to be used in paper mill industry, the rubber covers must be subjected to extreme service conditions (i.e., high compression load at high temperature (ca. 120-150°C) in conjunction with chemicals used in paper production). Therefore, high hardness, tensile strength, tear and abrasion resistance as well as low heat build-up (HBU) are necessary.

In the present study, hydrogenated nitrile rubber (HNBR) is selected due to its excellent thermal stability, high chemical resistance, very good mechanical strength with high elasticity. Typically, HNBR has widely been employed in automotive and industrial applications (1). HNBR is known to be curable with either peroxide or sulfur/sulfurdonor cure systems, depending on its degree of unsaturation on the backbone as well as on product properties required. Laboratory comparisons of sulfur/sulfur-donor and peroxide cured HNBR compounds reveal that the peroxide vulcanisation provides considerably superior compression set and heat resistance (2).

Although HNBR offers relatively good mechanical properties due to its highly saturated structure facilitating the molecular packing, an incorporation of filler into HNBR is still necessary for further enhancing mechanical properties as well as performance per cost of the final products (3, 4). The reinforcement performance of filler has been reported to depend typically on filler characteristics including specific surface area, surface chemistry and structure (or degree of aggregation). In general, the greater loading of reinforcing filler will result in the higher hardness and modulus.

Simultaneously, property improvement and processability are found to reach its maxima at certain filler loading relying on the mixing efficiency for filler dispersion and distribution (i.e., state-of-mix). There are numerous works on enhancement in mechanical properties of HNBR vulcanisates by reinforcing fillers including carbon black (CB), silica, carbon nanotubes and organoclay (5-12).

Nonetheless, the published work on viscoelastic properties of CB filled HNBR is still limited. It is reported that storage modulus (G′) increases and damping factor peak ($\tan\delta_{max}$) decreases with CB loading which is attributed to the changes in occluded rubber, bound rubber and shell rubber (13, 14). By increasing CB specific surface area, the tanδ appears to decrease in the transition zone and then increase in the plateau zone (rubber plateau). The magnitude of G′ enhancement is more obvious with increasing specific surface area of CB. Numerous works (15-18) reveal that CB surface area and loading play strong roles in viscoelastic behaviour of filled rubber.

Basically, the reinforcement mechanism of CB filled rubber is believed to be caused by hydrodynamic effect and CB-CB together with rubber-CB interactions (19). Although the presence of rubber-CB interaction leads to a high extent of reinforcement, such interaction gives rise to the high magnitude of HBU found in rubber products. This is because of the fact that the rubber-CB interaction is dominated by the physical over chemical interactions (20), allowing molecular flow at rubber-CB interfaces, and thus the occurrence of energy dissipation via hysteretic process (21). The HBU is reported to increase with increasing hysteresis loss, implying a correlation of HBU to viscoelastic behaviour to some extent (22).

In this work, the viscoelastic behaviour and mechanical properties as well as HBU of HNBR compounds and vulcanisates filled with various types of CB are studied. A correlation between viscoelastic behaviour and HBU of rubber vulcanisates is established. Moreover, the effects of filler types on properties of HNBR compounds and vulcanisates are investigated.

CHAPTER II
OBJECTIVES

The present research aims to investigate cure characteristics, viscoelastic behaviour and mechanical properties of HNBR compounds and vulcanisates filled with various types and loadings of fillers. Then, a correlation between viscoelastic behaviour and HBU of rubber vulcanisates is established. The scope of this work consists of two main parts, as follows:

2.1 Effects of filler type and loading

The main purpose of this part is to study the influences of filler type and loading on cure and viscoelastic behaviour as well as mechanical properties of HNBR. The following studies are carried out.

- Investigation of CB type (i.e. N326, N550, N774 and N990) and loading effects on properties of HNBR compounds and vulcanisates.
- Investigation of precipitated silica (i.e. Hi-Sil 233-S) loading effect on properties of HNBR compounds and vulcanisates.
- Investigation of organoclay (i.e. Bentone® 38) loading effect on properties of HNBR compounds and vulcanisates.
- Investigation of CB hybrid system effects on properties of HBNR compounds and vulcanisates. Three systems of CB hybrid, i.e. N326/N990, N550/N990 and N326/N774, having different surface area and structure will be focused.

2.2 Correlation between viscoelastic behaviour and heat build-up of HNBR vulcanisates

The final part focuses on a correlation between viscoelastic properties, such as, loss modulus and damping factor with HBU of HNBR vulcanisates. The correlation of viscoelastic behaviour to HBU results as measured from Gabometer 4000 and RPA 2000 will be established.

CHAPTER III
LITERATURE REVIEW

3.1 Hydrogenated nitrile rubber (HNBR)

Hydrogenated nitrile rubber, or HNBR as designated by ASTM 1418, was first commercialised in 1984 by Zeon Corporation (Nippon Zeon Co., Ltd.) under the trade name Zetpol. Later in the same year, HNBR was introduced by Bayer under the trade name Therban as a new material for applications in temperatures between -25°C and 150°C. The HNBR is a synthetic rubber produced through a hydrogenation of nitrile rubber (NBR). The process is the addition of hydrogen atoms into carbon-to-carbon double bonds (C=C) on butadiene segment resulting in a decrease in amount of unsaturation in the polymer backbone. The chemical structure of HNBR is presented in Figure 3.1. The subscripted "x-z" after the initial ethylene unit shows the variation in the ethylene unit concentration as a function of the degree of hydrogenation of butadiene units.

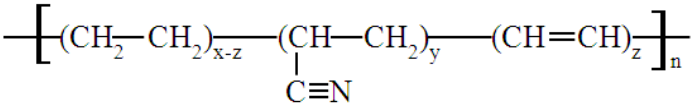

Figure 3.1 Chemical structure of hydrogenated nitrile rubber (HNBR)

Typically, grades of HNBR are classified by hydrogenation level, i.e., a saturation degree ranges from 85% to 99.9%. The HNBR grades containing 4-8% (partially hydrogenated) or virtually no double bonds (fully hydrogenated) are used in most cases. Partially hydrogenated materials can be crosslinked using both sulphur and peroxide cure systems, and the fully hydrogenated grades can be crosslinked with peroxides. This further expands the range of grades, and opens up more applications for these HNBR materials.

Mechanical properties of HNBR vulcanisates are extremely good generally with high tensile strength at room temperature and elevated service temperatures up to

100-140°C. In addition, the HNBR provides outstanding abrasion resistance and significantly improved heat resistance, compared to NBR, while retaining its excellent oil and fuel resistances. The addition of hydrogen atoms causes many of the carbon-to-carbon double bonds (C=C) in the polymer backbone to become single bonds (C-C), which is desirable because of its high thermal stability. The higher the percent of saturation, the greater the number of C-C bonds, and thus the greater the chemical and heat resistances. However, the acrylonitrile (ACN) content is unaffected by the hydrogenation process, and provides swelling resistance to oils and fuels in a similar manner to the parent polymer. With increasing ACN content, oil and fuel resistances of HNBR are improved with the expense of low temperature properties.

Unsaturated HNBR elastomers are typically cured with either peroxide or sulfur/sulfur-donor cure systems (2). Sulphur curing systems are used to provide certain advantage, such as, elongation, tear strength and flex fatigue (1). On the contrary, the peroxide/coagent systems can be used for improving resistances to heat and compression set. To enhance low-temperature flexibility as well as to optimise physical properties and processing characteristics, the appropriate plasticisers are incorporated to the compounds. The addition of reinforcing filler (such as, carbon black, silica, clay and etc.) into compound formulations is known to enhance the physical properties of HNBR compounds effectively.

The applications for HNBR elastomers are in a variety of areas, including oilfield, automotive, industrial, and assorted performance-demanding applications. The HNBR is used for a wide range of products, including o-rings, packings, wellhead seals, drill bit seals, blowout preventers, and drill pipe protectors. Belts, seals and hoses are among the most important applications of HNBR. Automotive belts, especially synchronous timing belts, are the largest application in automotive market due to the good strength and dynamic properties of HNBR. As for sealing application, the HNBR is selected because of its excellent resistances to heat, hot oils and swelling in a variety of fluids and chemicals. The HNBR is also employed in industrial rolls for steel processing, pulp and paper milling, textile manufacturing and many other materials handling applications due to its unique properties, particularly fluid, abrasion and high-pressure decompression resistances as well as broad service temperature and pressure.

3.2 Filler reinforcement in rubber industry

The vulcanisation process of rubber used in rubber industry yields resilient products having elastic properties sometimes with low strength. Such low strength could be overcome by the addition of certain fillers to the rubber. Carbon black (CB) and precipitated silica (PSi) have mainly been used as reinforcing fillers in the rubber industry for decades. Such fillers offer improvement in mechanical properties of rubber compounds and vulcanisates. The degree of property improvement is strongly dependent on a dispersion degree of filler particles and their principal relevant properties (e.g., particle size, surface area, aggregate structure and surface activity) in conjunction with the rubber-filler interaction (23-25).

3.2.1 Filler dispersion in rubber reinforcement

The uniform dispersion of reinforcing filler throughout the rubber matrix is essential for rubber compounding to achieve optimum vulcanisate properties, and the degree of dispersion is a crucial factor which ultimately controls the mechanical properties of the filled rubbers (26, 27). The poor dispersion gives the detrimental effect in vulcanisates which can be summarised as follows (28): (i) reduced product life, (ii) poor performance in service, (iii) poor product appearance, (iv) poor processing characteristics, (v) poor product uniformity, (vi) raw material waste and high finished-product rejection rates and (vii) excessive energy usage. The dispersion of filler agglomerates in rubber matrix considerably influences mechanical properties of rubber products. Typically, large filler agglomerates cause poor mechanical properties, and therefore must be broken down into aggregates (see Figure 3.2).

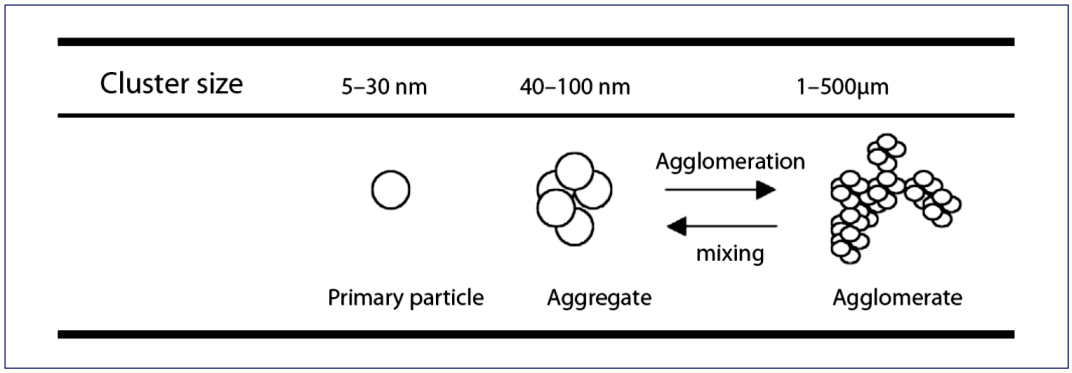

Figure 3.2 Filler aggregation and dispersion (29)

The dispersion of filler takes place in three major steps within the mixing stage, i.e., incorporation, distribution and dispersion steps (30). In the incorporation step, when filler is added in conventional mixing equipment, the filler must be wetted by rubber matrix. The completion of wetting can be indicated by the absence of loose filler (1). Distribution is the step that the incorporated or wetted fillers are distributed uniformly throughout the matrix. Dispersion, the final step, occurs simultaneously with the transformation of agglomerates into aggregates, accompanied by the formation of bound rubber and three dimensional networks. An optimal particle size distribution has to be achieved to gain the best performance in a specific application. Therefore, the break-up of filler agglomerates in the mixing process has extensively been studied by various researchers (31-33).

Factors controlling the filler dispersion and distribution in rubber matrix could be summarised as shown below (34):

- Filler type, size distribution and surface activity
- Type of a rubber matrix and its molecular and physico-chemical characteristics
- Overall mix composition
- Efficiency of mixing (deciding a degree of filler dispersion and uniformity of its distribution)
- Parameters of vulcanisation

It is very important to choose the suitable filler to match the mixing and processing as well as final performance properties. An incorrect choice of filler could lead to excessive mixing time or the compounds with poor dispersion level. For example, CBs having lower structure can be wetted more quickly, because of fewer spaces to be filled with rubber in its aggregate. On the other hand, during the dispersion stage, the low structure CBs develop relatively low viscosity in the compound, causing relatively small magnitude of shear in the mixer. Therefore, the lower structure CBs are harder to be dispersed. Alternatively, the dispersion step of rubber compound filled with low structure CBs must be extended to achieve the desired dispersion level. Conversely, CBs possessing higher structure take longer time to wet out. Nevertheless, in the dispersion step, such CBs are easier to be disrupted due to its relatively high bulk viscosity. Its dispersion rate, therefore, is faster. Higher

surface area CBs have substantial cohesive force, and need relatively high magnitude of shear to break up the agglomerates into their constituent aggregates, making them more difficult to be dispersed. Consequently, high surface area CBs and low structure CBs are the most difficult, while low surface area CBs and high structure CBs are the easiest to be dispersed in the rubber matrix. CB spectrum shown in Figure 3.3 is generally utilised to choose proper CBs for mixing. It is worth noting that as CB surface area increases, only the CBs with high structure are practical. Conversely, at high surface area, there is no practical demand for CBs possessing lower structure, since it is too difficult to disperse (1).

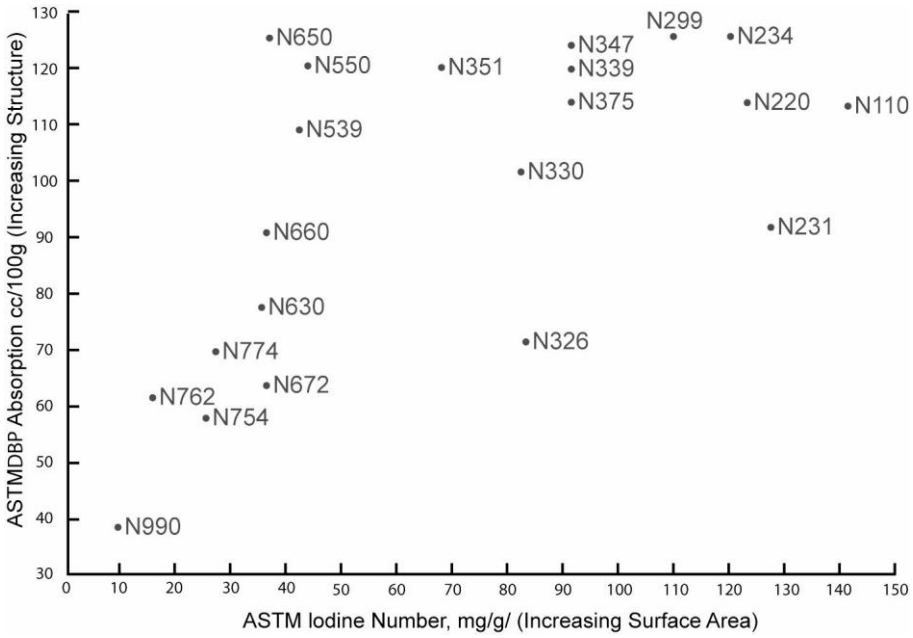

Figure 3.3 Carbon black spectrum (1)

The stiffness and plasticity of rubber matrix play major roles in determining the level of filler dispersion. The rubber matrix has to be stiff enough to break-up the filler agglomerates into aggregates. On the other hand, the rubber matrix has to be sufficiently flowable to facilitate the filler incorporation, and to give a uniform distribution of the filler throughout the compound. Generally, the stiffness of rubber matrix can be reduced by the addition of plasticiser (softener) into rubber compound during the mixing process. As defined by ASTM D883, the plasticiser is a substance incorporated into a plastic or elastomer to increase its flexibility, workability

or distensibility. Plasticisers are grouped into the following categories: phthalates, aliphatics (mainly adipates), epoxy, trimellitates, polymerics, phosphates and others. Ester plasticisers divided as phthalates and specialties (e.g., trimellitates, adipates, sebacates, etc.), play significant roles in rubber manufacturing, and are selected based upon cost-performance evaluation (35, 36). A plasticiser compatibility is the major factor determining a compound processability.

The sequence of a plasticiser incorporation to gain the best mixing procedure has been reported that the filler should be added into masticated rubber sooner than the plasticiser. However, this method does not work well in view of the economy of production, due to the high power consumption. The elimination of the shortcomings of separate incorporation and the reduction of mixing time were proposed by Rostler and Du Pont (37). The premixed preparations of fillers and plasticisers in compounding rubber are used in their study. The advantages of this method are the decreases in milling time and power consumption during the mixing process as well as the elimination of dust in handling dry fillers and the inconveniences in handling the highly viscous plasticisers. Nevertheless, the use of premixed preparation is limited to the plasticiser content. It is found that the concentration of plasticiser in the premixed preparation must not be too high. Otherwise, the poor filler dispersion is resulted.

The good filler dispersion and distribution can also be improved significantly by the uses of dispersants and coupling agents. A silane is widely used as a coupling agent and an adhesion promoter, and also as a dispersant for non-black filler in rubber matrix especially silica (38, 39). Generally, the silane can improve compatibility between silica and rubber matrix through its dual functionality. A typical structure of silane coupling agent is shown below:

$$(RO)_3SiCH_2CH_2CH_2\text{-}X$$

where RO is a hydrolysable functional group, such as, methoxy, ethoxy or acetoxy, etc. that reacts with inorganic materials, such as, filler, and X is an organofunctional group, such as amino, methacryloxy, epoxy, etc., that reacts with organicmaterials, such as, rubber matrix. The silane is typically used as a primer for treating filler

surfaces to make the filler more suitable for usage in rubber. A strong filler–filler interaction is significantly reduced, and the dispersion of filler in the rubber matrix is, therefore, improved. Figure 3.4 shows a simplified picture of the coupling linkage between rubber and filler by silane (29).

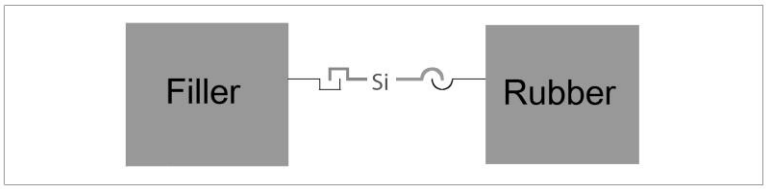

Figure 3.4 The coupling linkage between rubber and filler by silane (29)

Initially, the filler surface treatment is executed, i.e., a reactive silanol group reacts with silane through a hydrolysis reaction, which can then condense with other silanol groups on filler surfaces. Then, the bonding between silane treated filler and rubber is achieved, i.e., a reactive hydrocarbon chain in organic part of the silane will interact or react with the rubber matrix. The assumed mechanism for the silica-silane reaction and the formation of filler-rubber bond is shown in Figure 3.5.

The characterisation of filler dispersion degree in the rubber matrix seems to be important. Several experimental techniques have been proposed (40-44). The degree of filler dispersion practically requires powerful analytical techniques, being able to examine inside structure of filler agglomerates. Such techniques include a scanning electron microscopy (SEM). The SEM is a type of electron microscope which images a sample surface by scanning the surfaces with a high-energy beam of electrons in a raster scan pattern. The electrons interact with the atoms that make up the sample, producing the signals corresponding to the sample's surface topography, composition, and other properties, such as, electrical conductivity. The SEM image analysis is typically based on the use of atomic number contrast from backscattered electron images to determine the dispersion of filler. The fillers with higher atomic number elements, such as, calcium (Ca), magnesium (Mg) and zinc (Zn) will be visually lighter in colour in the image, and the fillers with lower atomic number elements, such as, carbon (C) and sulphur (S) will be darker, while rubber matrix is

dark. The SEM micrographs have a large depth of field yielding a characteristic three-dimensional appearance useful for understanding the surface structure of a sample.

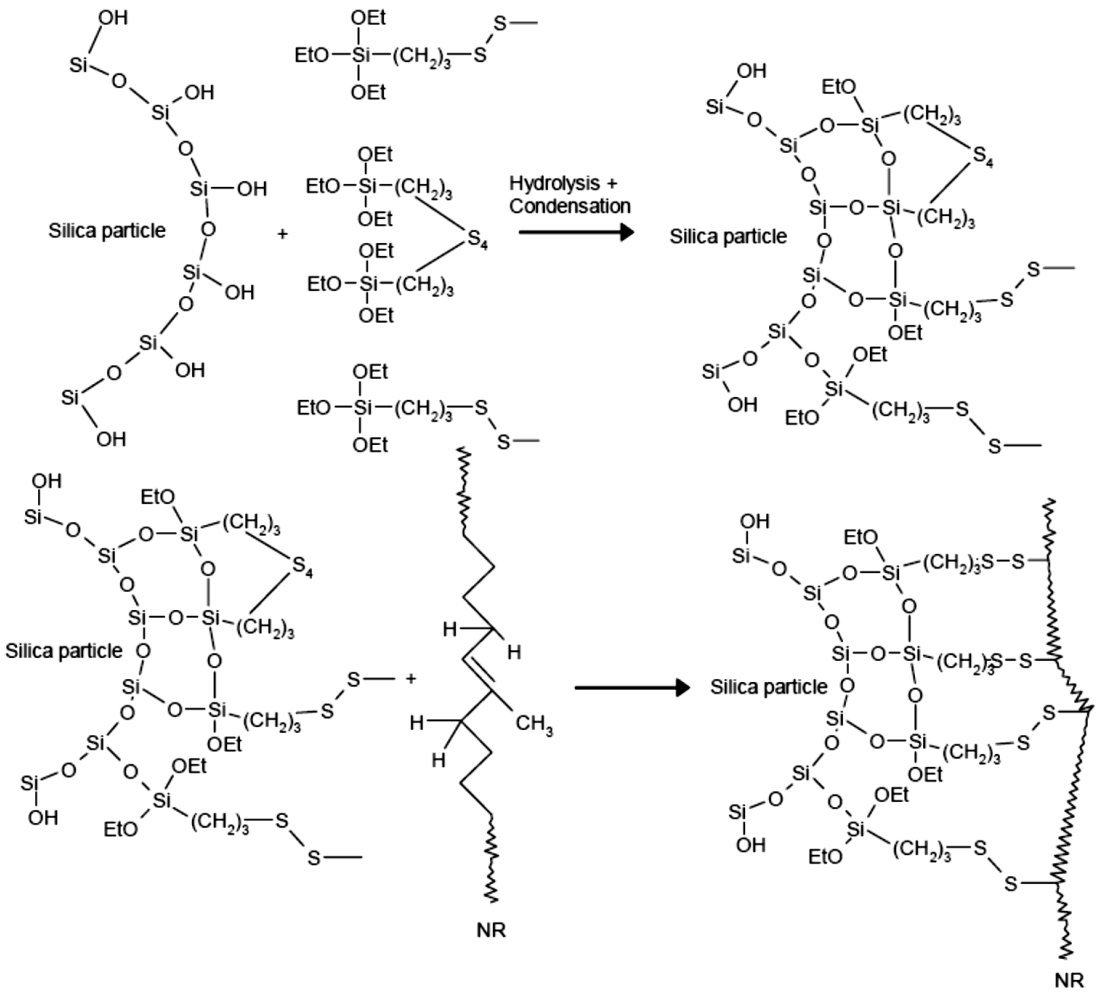

Figure 3.5 Reaction steps for silica treatment and formation of rubber-to-filler bonds (45)

The state of filler dispersion in rubber matrix can be characterised by the statistical processing of SEM micrographs. The quadrate method and index value (I_δ) proposed by Morishita, is utilised as a tool for characterisation (46-48). Karásek and Sumita (49) reviewed that the I_δ index is one of the most useful quadrate methods, in which the total area of the SEM pattern is divided into small elementary parts with equal area, and the number of the points in each element is calculated. The I_δ index

which plays an important role in the characterisation of dispersion of points is given as shown in Equation (3.1) (49).

$$I_\delta = q\delta \tag{3.1}$$

with

$$\delta = \frac{\sum_{i=1}^{q} n_i(n_i - 1)}{N(N-1)} \tag{3.2}$$

where q = dividing number (total number of sample sections)

n_i = number of particles in the i-th section (i = 1,2,3,...,q)

N = total number of particles

Figure 3.6 shows schematically the dependence of I_δ on q for various distribution modes of particles. For Poisson's distribution, all the δ are equal to q^{-1}, independently of the value of q, i.e., I_δ is always unity (Figure 3.6a). For the regular mode of distribution, I_δ gradually decreases with increasing q value (Fig. 3.6b). For the aggregate mode, the I_δ increases as the q value increases (Figure 3.6c-f). The smaller the size of the aggregate, the larger the value of q at which the I_δ becomes larger than unity (smaller size of aggregate: Figure 3.6d and 3.6f; larger size of aggregate: Figure 3.6c and 3.6e). Furthermore, when the particles are distributed in the regular mode in each aggregate, the I_δ has a maximum peak at a certain value of q (Figures 3.6e and 3.6f). For CB-SBR compounds, it is observed that the distribution mode changes from aggregate mode to Poisson's with increasing CB loading (Figure 3.7).

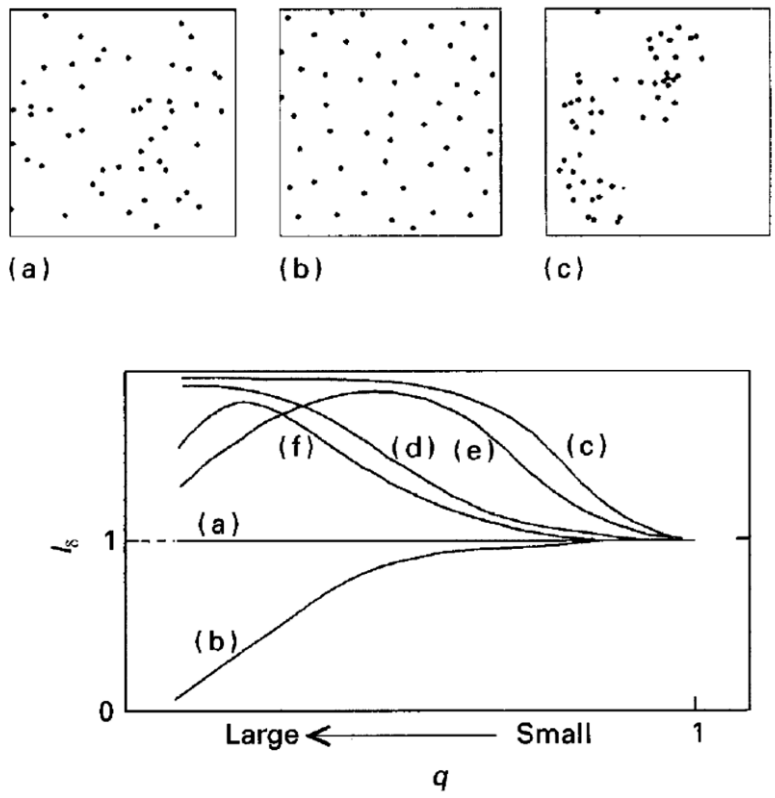

Figure 3.6 Schematic representation of the relationship between I_δ index and dividing number (q) for various distribution modes of particles: (a) Poisson's distribution; (b) regular distribution; (c) aggregate distribution in which the size of each aggregate is large and the particles are distributed in Poisson's mode in each aggregate; (d) aggregate distribution in which the size of each aggregate is small and the particles are distributed in Poisson's mode in each aggregate; (e) aggregate distribution in which the size of each aggregate is large and the particles are distributed in regular mode in each aggregate; (f) aggregate distribution in which the size of each aggregate is small and the particles are distributed in regular mode in each aggregate (49)

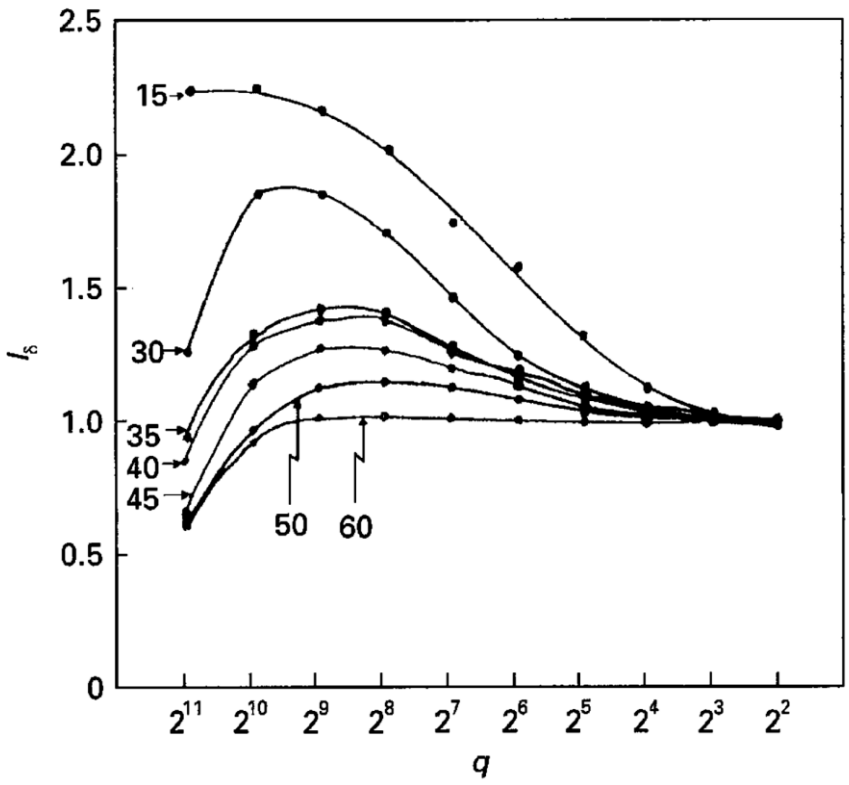

Figure 3.7 The I_δ index for carbon black filled SBR composite materials with various carbon black contents (phr.) as a function of dividing number (q) (49)

3.2.2 Polymer-filler interactions in filler reinforcement

It is generally accepted that the reinforcement of rubbers and the improvement of other properties, to a large extent, are associated with the chemical and physical interactions between the rubber matrix and fillers. Thus, researchers have attempted to explain the improved performance of rubber products from the microscopic view by relating the observed cure kinetics and mechanical properties with the interactions between rubbers and fillers. (38, 50, 51) The development of rubber-filler interactions is dependent on the characteristics of filler, particularly specific surface area and structure. The specific surface area or primary particle size determines the effective contact area between the filler and rubber matrix. The structure or the degree of irregularity of the filler plays an essential role in the restrictive motion of rubber chains under strain. The surface activity refers to the strength of the filler surface interaction with the polymer, via either physical or

chemical adsorption. The strong interaction between rubber and filler plays an important role on the improved filler dispersion, which contributes to the adjustment of important physical characteristics, such as, modulus, extensibility and resilience in rubber vulcanisates (52). The most possible way to enhance the strength of the bonding is the modification of the filler surfaces, which should be considered in conjunction with the improvement in filler dispersion by either changing the polarity of the filler particles or sterically avoiding their aggregration (53, 54).

Generally, the incorporation of reinforcing filler, including CB into rubber results in a certain fraction of rubber strongly adsorbed on the filler surfaces. When an uncured compound of filled rubber is dissolved in its good solvent, only a free rubber portion can be extracted into solvent, therefore, highly swollen filler rubber gel is found in the rubber solution. By definition, a bound rubber is the rubber content in such gel (55). At higher filler concentration or higher bound-rubber content in compound, the bound rubber forms an enormous gel of filler particles held together in a three-dimensional lattice by longer interparticle rubber molecules, which is an indication of higher filler-rubber interaction. Therefore, the bound rubber is considered as a factor in filler reinforcement of rubber, a measure of filler surface activity and filler-polymer interaction (56-59). The bound rubber content is almost proportional to filler content, i.e. bound rubber content increases with increasing filler loading. At a certain filler loading, the bound rubber depends on characteristics of filler, such as surface area, structure or morphology, and surface activity. Regarding the rubber nature, the chemical structure (saturated or unsaturated and polar or non-polar) and the microstructure (configuration, molecular weight, and molecular weight distribution) influence strongly the level of bound rubber content. Effect of bound rubber on properties of filled rubber compounds and vulcanisates has been studied (60-63).

Choi investigated the influence of CB structure on the bound rubber formation of styrene butadiene rubber (SBR) by employing three types of CB with similar primary particles but different structures (64). The results were studied within the concept that the bound rubber is composed of loosely and tightly bound ones (65, 66). The loosely bound rubber exists in an outer shell around the filler while the tightly bound rubber is in the immediate vicinity of the filler particle. The tightly bound rubber is much less mobile than the loosely bound rubber (67, 68). At high extracting

temperature, some loosely bound rubber can be extracted, i.e. bound rubber content is decreased as the extraction temperature becomes higher (69). From the experiment, the result implies that the total and tightly bound rubber contents increase with increasing CB content and the magnitude of increment increases with the development of filler structure, as shown in Figure 3.8.

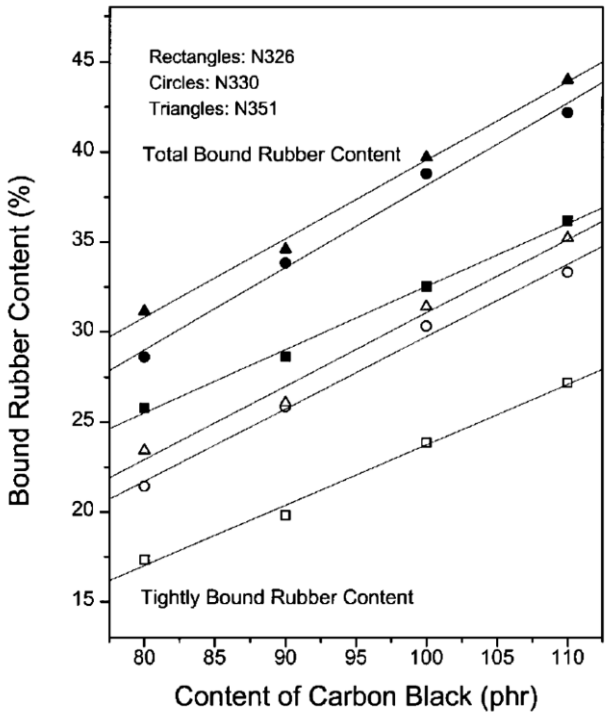

Figure 3.8 Variation of the bound rubber contents with the carbon black content: rectangles, circles, and triangles represent the N326, N330 and N351, respectively; the solid and open symbols stand for the total and tightly bound rubber contents, respectively (64)

The bound rubber effect is correlated to viscosity and cure behaviour of CB filled SBR compound. Mooney viscosity and Mooney peak (which is the initial viscosity after the preheating) increase with increasing of the CB content, as shown in Figure 3.9. Choi explained these results with the increased bound rubber content.

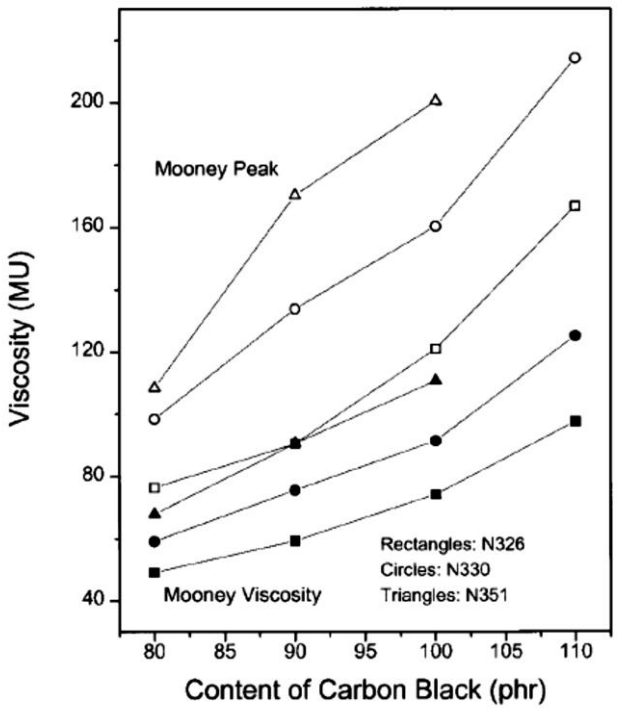

Figure 3.9 Variation of the Mooney viscosity and Mooney peak with the carbon black content: rectangles, circles, and triangles represent the N326, N330 and N351, respectively; the solid and open symbols stand for the Mooney viscosity and Mooney peak, respectively (64)

Figure 3.10 shows the variation of the cure characteristics as a function of the CB content, which the t_3 and t_{18} means the times taken for the viscosity to reach from the minimum point to increases of t_3 and t_{18} MU, respectively, and the Δt (= t_{18}-t_3) is used as the cure rate index. Evidently, the t_3, t_{18}, and Δt decrease with increase of the CB content. At a given CB content, compound filled with CB having high structure is found to be more effective to increase the bulk viscosity, and to make the cure times faster than the one filled with lower structure CB. The faster cure time found in the compounds with higher bound rubber content is explained by the difficulty for the curatives to move through the bound rubber phase particularly in the tightly bound region, leading to more free curatives available in rubber matrix, and then the crosslinking reaction in rubber bulk is promoted (64).

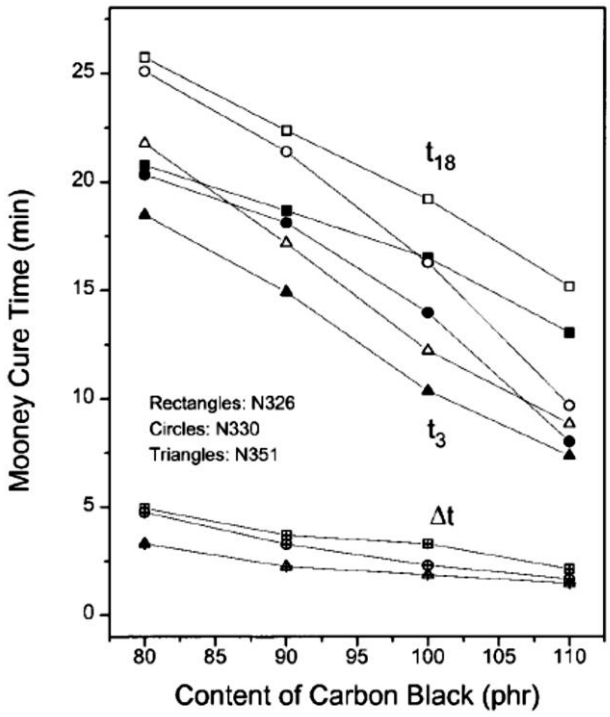

Figure 3.10 Variation of the Mooney cure times (cure characteristics) at 135°C with the carbon black content: rectangles, circles, and triangles represent the N326, N330 and N351, respectively; the solid and open symbols stand for the t_3, t_{18}, and Δt, respectively (64)

Choi and his coworkers also studied the influence of bound rubber content on the cure characteristics of filled rubber (70). Two types of CB possessing different both surface area and structure, namely, N220 and N550 filled NR were used. The result shows that the cure rate of the compound filled with N550 is more sensitive to the filler content than the compound filled with N220 (see Figure 3.11). The more tightly bound rubber in higher developed CB structure is used to explain the result. It is known that the N550 possesses smaller surface area but more developed structure than N220. Thus, the N550 having more tightly bound rubber than N220 with less developed structure, reveals lower curative adsorption. The greater amount of curative in matrix, therefore, causes the cure promotion phenomenon in the compound with N550.

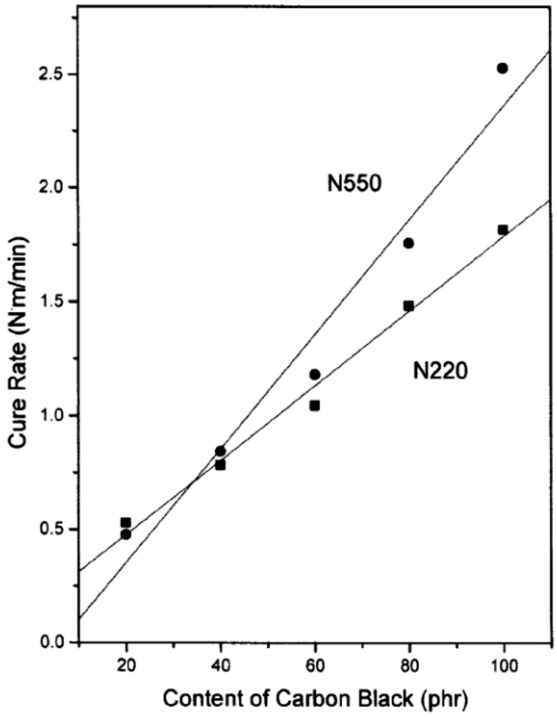

Figure 3.11 Variation of the cure rate as a function of carbon black loading at a cure rate of $(T_{90}-T_2)/(t_{90}-t_2)$ for compounds filled with (■) N220 and (●) N550 (70)

In principle, a measurement of bound rubber is a simple, in which small pieces of uncured compound of filler rubber are immersed in a large excess of good solvent, such as, toluene, for several days at room temperature in order to presumably achieve full extraction of soluble rubber. Factors affecting the bound rubber content during the measurement are solvent nature and extraction temperature. Weights of the samples before and after the extraction were measured and the bound rubber contents could be calculated from Equation (3.3).

$$R_b(\%) = \frac{100\times\left[W_{fg} - W_t\left(\frac{m_f}{m_f + m_r}\right)\right]}{W_t\left(\frac{m_r}{m_f + m_r}\right)} \qquad (3.3)$$

where R_b = bound rubber content

W_{fg} = weight of filler and gel

W_t = weight of sample

m_f = fraction of filler in compound

m_r = fraction of rubber in compound

On the basis of developed method by Le and his co-worker (71-73), the characterisation of a wetting behaviour of filler by rubber chains is realised. When filler is mixed with a rubber, a part of the rubber chains will be bonded to the existing reactive groups or active centre available on the filler surface. The bound rubber cannot be separated from the filler when the filled compound is extracted in a good solvent during a certain period of time, the bound part of the rubber forming a layer around the filler particles remains in the rubber-filler gel. The larger the amount of rubber that stays on the filler surface, the better the polymer-filler interaction, which has also been related to improved final properties. In contrast to the bound rubber often reported in literature, the determination of the amount of rubber bound to the surface of the filler is proposed according to Equation (3.4).

$$L = \frac{m_2 - m_1 C_R}{m_2} \qquad (3.4)$$

where L = rubber-layer bonded on filler surface

m_1 = mass of composite before extracting

m_2 = mass of rubber-filler gel

C_R = mass concentration of filler in composite

3.3 Viscoelastic properties of filled rubber compounds and vulcanisates

Viscoelastic properties of filled rubber can be investigated by a dynamic mechanical analysis. When a strain is imposed periodically with a sinusoidal alternation at a frequency (ω) on a test specimen, the stress will respond sinusoidally with phase lag (δ), as shown in Figure 3.11. Thus, the relationship between strain (γ) and stress (σ) could be expressed as shown in Equations 3.5 and 3.6, respectively.

$$\gamma = \gamma_0 \sin \omega t \qquad (3.5)$$

$$\sigma = \sigma_0 \sin (\omega t + \delta) \qquad (3.6)$$

where t = time

δ = phase angle between stress and strain

γ_0 = maximum amplitude of strain

σ_0 = maximum amplitude of stress

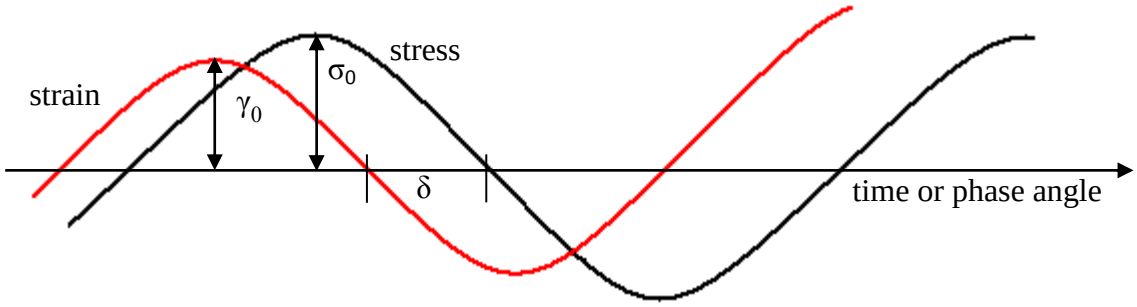

Figure 3.12 Sinusoidal stress and strain correspondence

In an alternative form, the σ can be sub-divided further into two components, i.e., in-phase and out-of-phase with strain, as shown in Equation (3.7).

$$\sigma = \sigma_0 \sin \omega t \cos\delta + \sigma_0 \cos \omega t \sin\delta \qquad (3.7)$$

Accordingly, the dynamic stress-strain behaviour of rubber material can be expressed in terms of storage modulus or elastic modulus (G′), which is in-phase with the applied strain, and loss modulus or viscous modulus (G″), which is 90° out-of-phase with the applied strain.

$$\sigma = \gamma_0 G' \sin \omega t + \gamma_0 G'' \cos \omega t \qquad (3.8)$$

$$G' = (\sigma_0/\gamma_0) \cos\delta \qquad (3.9)$$

$$G'' = (\sigma_0/\gamma_0) \sin\delta \qquad (3.10)$$

Additional frequency-dependent material functions, including complex modulus (G^*), complex viscosity (η^*), dynamic viscosity (η') and the elastic viscosity (η''), are defined by Equations (3.11) to (3.14), respectively.

$$G^* = (\sigma_0/\gamma_0) = G' + iG'' \quad (3.11)$$

$$\eta^* = G^*/\omega \quad (3.12)$$

$$\eta' = G''/\omega \quad (3.13)$$

$$\eta'' = G'/\omega \quad (3.14)$$

where i = imaginary number ($\sqrt{-1}$)

ω = frequency (rad/s)

Another widely used material function for describing the viscoelastic behaviour is the tangent of the phase angle (or the so-called damping or loss factor) as illustrated in Equation (3.15).

$$\tan\delta = G''/G' \quad (3.15)$$

The addition of filler into rubber systems is known to cause a considerable change in viscoelastic behaviour of rubber materials. The effect of strain amplitude on the dynamic modulus has been studied very intensively. Fletcher and Gent reported a detailed study of the low frequency dynamic properties of filled NR (74), which was later extended by Payne (75). The dynamic modulus of a filled rubber material displays very strong deformation amplitude dependence (non-linear properties), which is known as the Payne effect (75, 76). This effect is described by the breakdown and reformation of the filler network structure during dynamic mechanical testing. At low strain amplitudes, high storage modulus is observed, due to the presence of the filler network. The filler network is deformed by the increase in strain amplitude. It is observed as a drastic decrease of the storage modulus when the strain amplitude is increased. At sufficiently high strain amplitude, the network is permanently broken and can no longer reform. An example of this phenomenon is given in Figure 3.13.

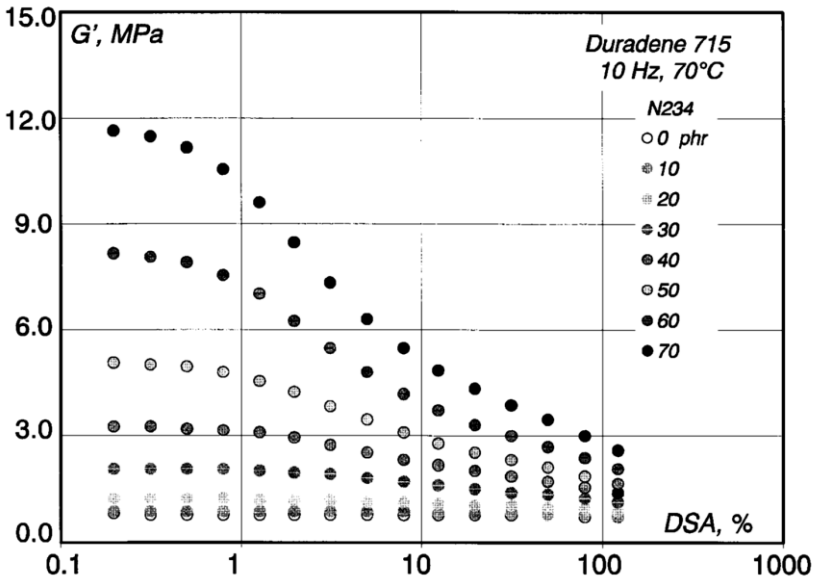

Figure 3.13 Strain dependence of G′ at 70°C and 10 Hz for SBR compounds with different loadings of carbon black N234 (21)

A qualitative description of this phenomenon is given in Figure 3.13. Fröhlich et al. (77) described the behaviour of the complex shear modulus of filled rubber samples versus dynamic shear deformation similar to the model of Payne, i.e., the strain-independent part of (i) the modulus as a combination of the polymer network, (ii) the contribution from the hydrodynamic effect and (iii) the modulus resulting from the in-rubber structure, as shown in Figure 3.14. The explanation of idealised form of a typical elastic modulus curve is summarised as follows:

(a) The polymer network contribution depends on the crosslink density of the matrix and the nature of the polymer.

(b) The hydrodynamic effect, in this model, is caused by the effect of strain amplification, in which the filler is the undeformable phase. As a consequence, the intrinsic strain of the polymer matrix is higher than the external strain yielding a strain-independent contribution to the modulus.

(c) The effect of the structure is attributed to the "in-rubber structure", which can be understood as a combination of the structure of the filler in the in-rubber state ("in-rubber DBP") and the extent of filler-polymer interaction. The in-rubber structure is a measure of the occluded rubber, which is shielded from deformation, and

therefore increases the effective filler content leading also to a strain-independent contribution to the modulus. The filler-polymer interaction can be attributed to either physical (Van der Waals), chemical linkages or both. In the case of the silica-silane system, this interaction is formed by chemical linkages, for example.

(d) The stress softening at large amplitudes is attributed to the breakdown of the inter-aggregate association respectively to the breakdown of the filler network. This stress softening at small deformations called the Payne-effect, plays an important role in the understanding of reinforcement mechanism of filled rubber samples.

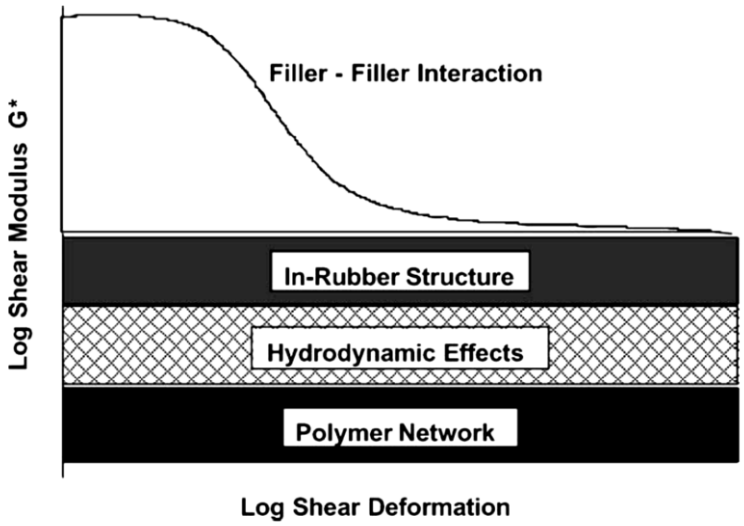

Figure 3.14 A qualitative interpretation of the Payne effect (77)

Wang (21) used the Payne effect to explain what happens to the trapped rubber between aggregates. As the filler network breaks down and reforms, it is proposed that the trapped rubber is allowed to rejoin the rubber matrix, and decrease the effective filler volume. The decreased effective filler volume causes the modulus to drop off, even further at higher temperature or higher strain amplitudes. While this model of change in occluded rubber with temperature and strain amplitude seems to explain the changes occurring in filled rubber under dynamic testing, the model is still an oversimplification for the effect of filler loading on reinforcement. Wang also investigated how filler surface area and structure influence the dynamic mechanical behaviour. It has been found that increases in surface area and filler structure promote

the storage modulus. A rational explanation for these reinforcement mechanisms based on filler structure and filler loading is still lacking.

3.4 Viscoelastic characterisation through large amplitude harmonic experiment

Fourier transform (FT) rheometry is a development of the so-called dynamic (or harmonic) testing to investigate both the linear and the non-linear viscoelastic properties of polymers, through performing large amplitude oscillatory strain (LAOS) experiments. Full strain and torque signals are captured under harmonic deformations at fixed frequency and temperature. Any commercial torsional dynamic rheometer can be conveniently modified for FT testing.

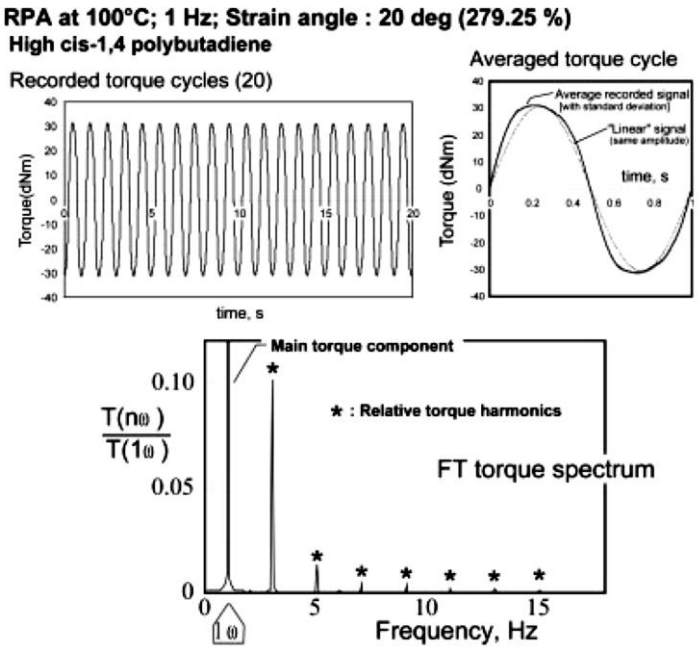

Figure 3.15 Typical recorded torque signal when submitting a high cis-1,4 polybutadiene sample to a harmonic strain of 20° at 1 Hz frequency; average torque cycle and Fourier Transform spectrum (78)

It is well known that the conventional open gap rheometers, such as, parallel plates and cone-and-plate instruments are not suitable for testing on very stiff and/or highly elastic polymers. The Rubber Process Analyser (RPA 2000, Alpha Technologies) offering the capability of testing very stiff materials, such as, filled polymer compounds, is suitably modified for FT experiments (78-82).

The modified RPA 2000 yields both strain and torque signals as recorded data files of actual harmonic strain and stress readings versus time at given temperature and frequency. The FT calculation technique converts a material property observed in the time domain, i.e., the torque signal, into the similar property expressed in the frequency domain, i.e., the torque spectrum, as shown in Figure 3.15.

Strain sweep test is performed at fixed frequency and temperature. The effect of strain amplitude on FT rheometry results is modeled with mathematical relationships, such as, Equation (3.16) (78-82).

$$G^*(\gamma_0) = G_f^* + \left[\frac{G_0^* - G_f^*}{1+(A\gamma_0)^B}\right] \tag{3.16}$$

where G_0^* = modulus in the linear region

G_f^* = modulus for an infinite strain

A = reverse of a critical strain which corresponds to $(G_0^* - G_f^*/2)$

B = parameter describing strain sensitivity of material

γ_0 = strain amplitude (that usually expressed in % strain)

As shown in Figure 3.16, a G^* versus γ_0 curve can be drawn with the equation and the inset parameters largely outside the experimental window. The G_f^* is a mere fitting parameter with obviously no physical meaning but G_0^* can be considered as a true material parameter because one would indeed expect any virgin polymer to exhibit this behaviour and also because a number of experimental results on gum rubbers really document the linear plateau (where the modulus is not dependent on strain amplitude). The critical strain (1/A) corresponds to the mid modulus values

between zero and infinite strain. Parameter B is called the strain sensitivity parameter because such parameter affects the steepness of the curve in the non-linear region.

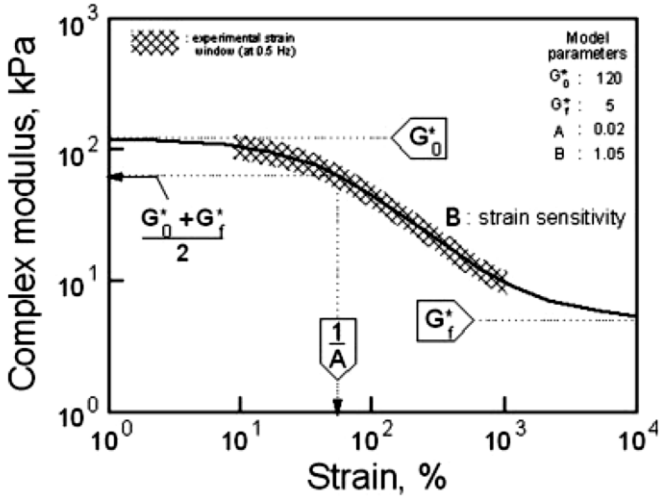

Figure 3.16 Modeling G^* variation with strain amplitude; physical meaning of model parameters (78)

A non-linear viscoelasticity of tested compounds is described by odd torque harmonics up to the 15th harmonic at high strain amplitude, reported as the total torque harmonic content (TTHC), 3rd relative torque harmonic (T(3/1)) and 5th relative torque harmonic (T(5/1)). Fitting parameter of Equation (3.17) is successfully used to fit the non-linear viscoelastic behaviour of filled rubber compounds.

$$TH(\gamma) = (TH_0+\alpha\gamma)\left[1-\exp\left(-C\gamma\right)\right]^D \qquad (3.17)$$

where γ is the strain magnitude. The TH_0, α, C and D are parameters of the model. The member $(TH_0+\alpha\gamma)$ expresses a linear variation of harmonics in the high strain region, while the member $\left[1-\exp\left(-C\gamma\right)\right]^D$ describes the transition from the linear to the non-linear viscoelastic response. Parameter D is related to the onset of significant harmonics while Parameter C indicates the strain sensitivity of the non-linear character. Model of the variation of relative torque harmonics against strain amplitude is shown in Figure 3.17.

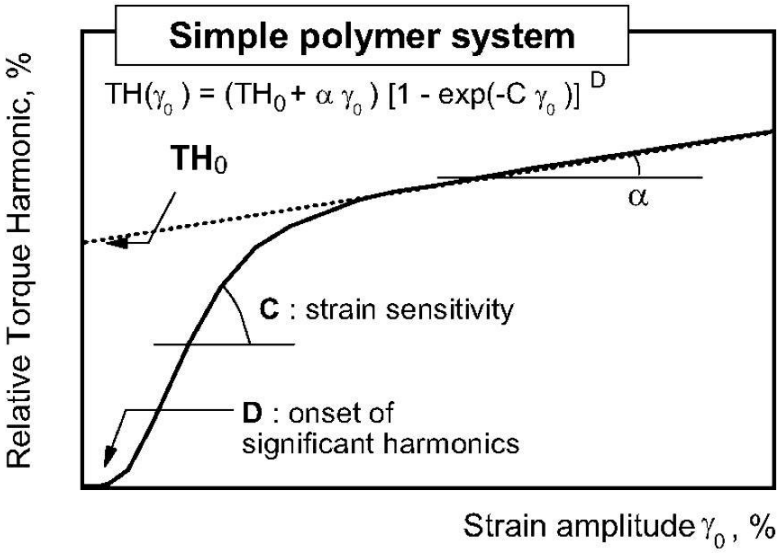

Figure 3.17 Modeling relative torque harmonics variation with strain amplitude; physical meaning of model parameters (82)

Under the application of a sufficiently large strain, there is a significant different between the non-linear viscoelastic behaviour of a neat (unfilled) rubber and of a filled rubber. The non-linearity of neat rubbers occurs through external causes, i.e., the applied strain. It is, therefore, called extrinsic non-linear viscoelasticity. While the non-linearity behaviour of filled rubbers is called intrinsic non-linear viscoelasticity, due to the strain response depends on internal morphology of filled rubbers.

The observation in quarter cycle integration of averaged torque signal is added to the FT analysis in order to distinguish the extrinsic and intrinsic non-linear viscoelasticity. The non-linear behaviour of filled rubber compounds is considered with respect to the ratio of the first to the second quarter torque signal integration, i.e., Q1/Q2 ratio.

From Figure 3.18, it is obvious that the Q1/Q2 ratio of unfilled homogeneous polymers is generally higher than 1, and increases with strain amplitude. In this case, the torque signal is always distorted “on the left” (i.e., Q1 > Q2), indicating extrinsic non-linear viscoelasticity.

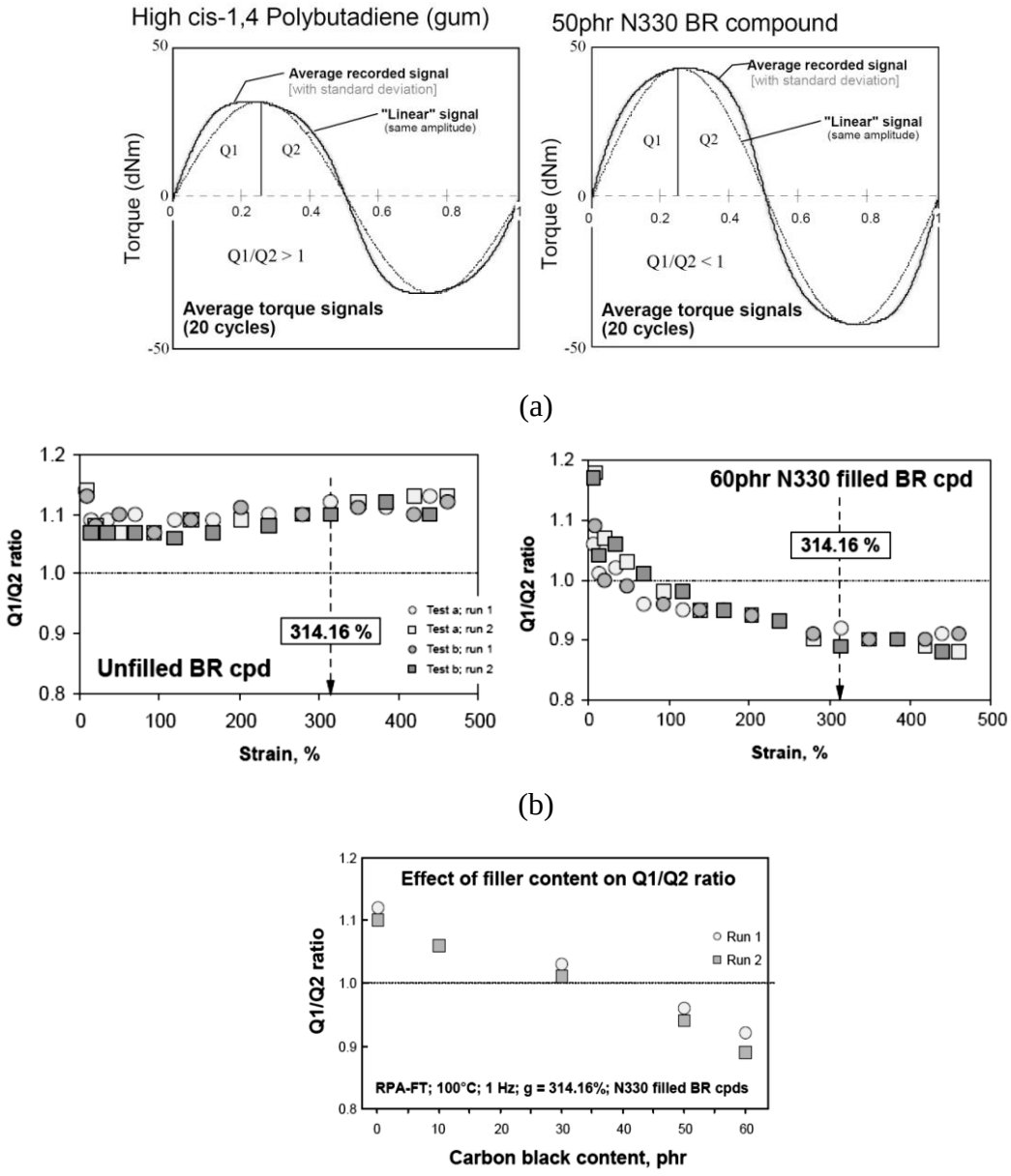

Figure 3.18 Documenting extrinsic and intrinsic non-linear viscoelastic characters through quarter cycle integration of averaged torque signal: (a) recorded torque signals during RPA tests at high strain on gum and 50 phr N330 filled polybutadiene compound; (b) effect of strain amplitude on Q1/Q2 ratio of gum and 60 phr N330 filled polybutadiene compound; (c) effect of filler content on Q1/Q2 ratio (81)

As for high load filled compound, the ratio of Q1/Q2 is generally higher than 1 at very low strain, and then quickly passes below 1 as strain increases, which correspond to a distortion “on the right” of the torque signal. It is considered that the Q1/Q2 lower than 1 reflects some structural character of material, which enhances their non-linearity as intrinsic non-linear viscoelasticity.

With the effect of filler level on Q1/Q2 ratio at high strain (see Figure 3.18(c)), the Q1/Q2 ratio decreases, as filler content increases. The transition from extrinsic into intrinsic non-linear viscoelasticity takes place at filler content corresponding to the so-called percolation level (78, 80, 81, 83).

3.5 Viscoelastic properties and heat build-up of filled rubbers

Rubber components undergo cyclic deformations of sufficient magnitude and frequency to cause some part of the energy. The energy of deformation is transformed into heat as a result of various dissipative processes. The heat generated internally is not conducted away rapidly enough, and the internal temperature becomes high enough, and therefore, the energy dissipation gives rise to a temperature rise. Viscoelastic behaviour, such as G′, G″ and tanδ has been used to evaluate heat generation in rubber materials. The G″ can be used as representative of the energy dissipated as heat. The ratio of G″ to G′ or generally known as a damping factor or loss factor (tanδ) is a measure of the energy dissipated by various processes, such as, molecular mobility (84, 85) breakdown and reformation of the filler transient network (84) or slippage of rubber molecules under high strain amplitudes (86). The energy loss during one cycle of strain (ΔE) is given by Equation (3.18).

$$\Delta E = \int \sigma d\gamma = \int_0^{2\pi\omega} \frac{\sigma d\gamma}{dt} dt \qquad (3.18)$$

From Equations (3.5) and (3.8), the amount of energy dissipated in a full cycle of oscillatory straining can be written as Equation (3.19):

$$\Delta E = \omega\gamma_0^2 \int_0^{2\pi\omega} \left(G' \sin\omega t \cos\omega t + G'' \cos^2 \omega t\right) dt = \pi\gamma_0^2 G'' \qquad (3.19)$$

By the definitions of G″ and G^*, ΔE can be also written as Equations (3.20) and (3.21).

$$\Delta E = \pi\sigma_0\gamma_0 \sin\delta \approx \pi\sigma_0\gamma_0 \tan\delta \qquad (3.20)$$

$$\Delta E = \omega\sigma_0^2 G''/G^{*2} = \omega\sigma_0^2 J'' \qquad (3.21)$$

where J″ = loss compliance which is defined as G''/G^{*2} or $G''/(G''^2 + G'^2)$

It can be seen that, depending on whether γ_0, σ_0 or $\gamma_0\sigma_0$, is kept constant during the dynamic deformation (corresponding to the constant strain, constant stress or constant energy input), the dissipated energy (or also called hysteresis loss) is proportional to G″, J″ or tanδ, respectively.

The incorporation of reinforcing filler, such as, CB and silica, into rubber greatly influences the viscous component. The effect of filler on hysteresis of rubber vulcanisates is dominated by the filler specific area, structure and loading (87, 88). At constant filler loading, the increase in surface area of filler results in the increase in tendency of secondary network formation. Under sufficient deformation, the breakdown of these secondary structures increases, i.e., the hysteresis loss increases, leading to a higher heat generation in rubber vulcanisates. Such heat generation without adequate heat dissipation then leads to a heat buildup (HBU), i.e., temperature rise. In theory, the HBU in a rubber vulcanisate is proportional to the hysteresis loss. Relationships between HBU of CB filled NR and hysteresis loss were examined by Park and co-workers (22). The results reveal that the HBU is a complicated function of the hysteresis loss. Figure 3.19 shows the variation of HBU with G″ for filled vulcanisates at a constant stroke. The HBU of filled NR increases either with increasing hysteresis or loading of CB, even though the proportionality is not linear.

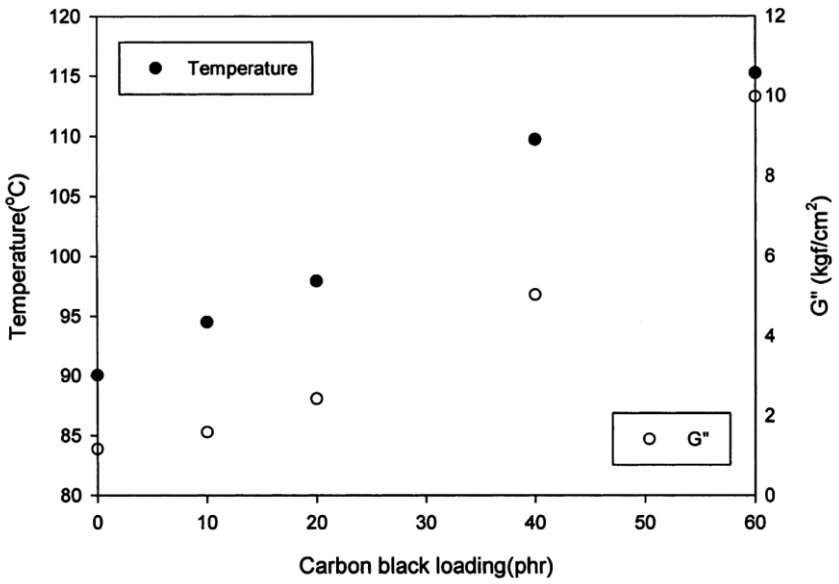

Figure 3.19 Relationship among heat buildup (HBU), loss modulus (G″) and carbon black loading of NR vulcanisates with heat buildup test at stroke amplitude of 4.45 mm and pre-load of 25 kgf (22)

Generally, the HBU measurement is carried out using a conventional Goodrich flexometer (ASTM D623 or DIN 53 533). A cyclic deformation is applied to a standard cylindrically shaped cured rubber specimen under standard conditions of frequency and temperature. The temperature rise in the specimen is recorded as a function of time. Although the Goodrich Flexometer has the practical advantage of being relatively simple to operate and cost-effective, the rubber compounds must be moulded and cured as cylinder shape specimens under high pressure in accordance with ASTM D623-93. Such standard practices do not favour routine testing however.

The Rubber Process Analyser (RPA 2000) is a dynamic rheometer especially designed for the measurement of viscoelastic properties of rubber before, during and after the vulcanisation process. The rubber sample is enclosed and moulded in a sealed and pressurised cavity of bi-conical design, so that the thin test specimen with the full contact with the die surface could be ensured. The instrument has the capability to measure rubber viscoelastic properties in a relatively large range of variable test parameters, i.e., temperature, oscillation frequency and strain/angle of oscillation, and time.

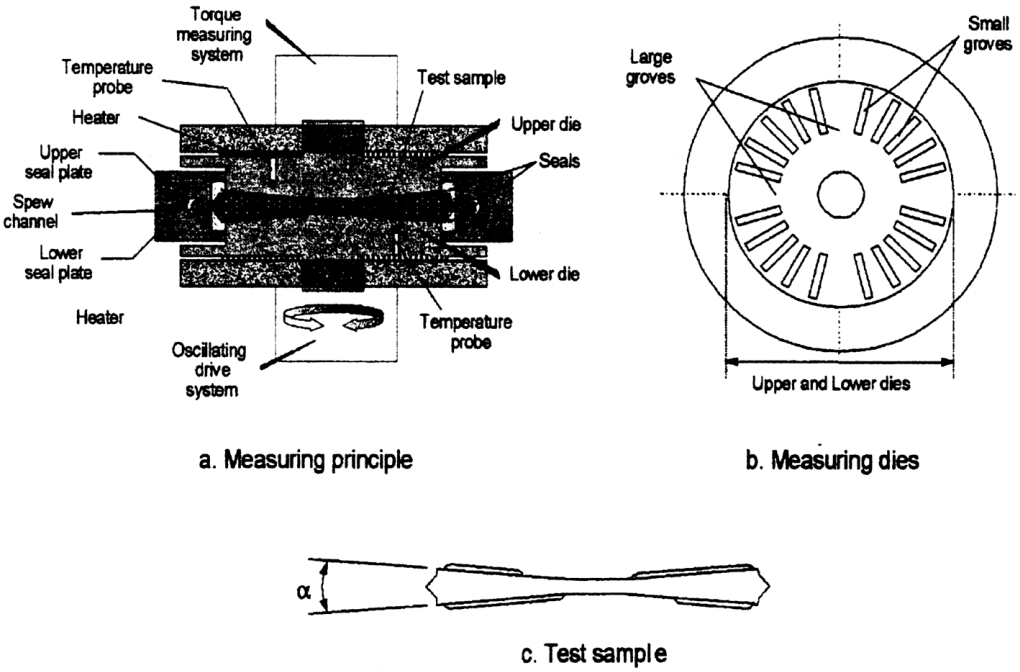

Figure 3.20 Rubber Process Analyser; measuring principle and sealed test cavity (89)

At first, the RPA 2000 could be considered as an ideal tester for measuring viscous heating associated with sustained oscillatory strain because the sample has a favourable surface area to sample volume ratio, and the instrument can apply large strains within the limits of the load cell capabilities. However in normal operating conditions, the set temperature is automatically controlled and maintained, so that any heating of the test material during a test is compensated for with respect to desired isothermal conditions. As reported by Dick and Pawlowski (90), it is however possible to short-cut the thermal control, so that a direct measure of viscous heating can be performed on cured rubbers with an excellent repeatability. The authors published results showing successful measurements of HBU on rubber vulcanisates (Figure 3.21).

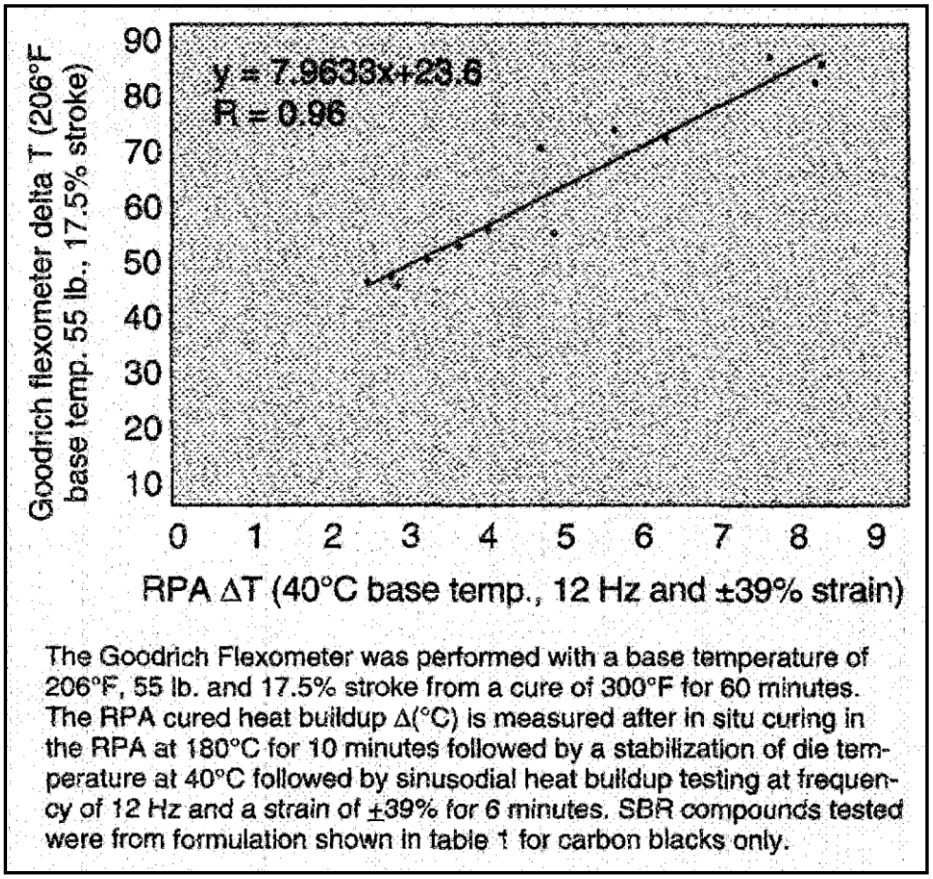

Figure 3.21 Relationship between heat build-up (HBU) measured from RPA 2000 and Goodrich flexometer of cured SBR vulcanisates filled with carbon black (90)

CHAPTER IV
MATERIALS AND METHODS

4.1 Compound preparation

4.1.1 Materials

The materials used in the present study are summarised in Table 4.1.

Table 4.1 Materials used in the present study

Chemical name	Grade/Supplier
Hydrogenated nitrile rubber (HNBR)	Therban® VP KA 8837 (34% acrylonitrile content, Mooney viscosity (ML1+4 at 100°C) = 55)/Lanxess Co., Ltd., Thailand
Zinc oxide (ZnO)	Commercial grade/Petch Thai Chemical Co., Ltd., Thailand
Stearic acid	Commercial grade/Petch Thai Chemical Co., Ltd., Thailand
2, 2, 4-trimethyl-1, 2-dihydroquinoline (TMQ)	Vulkanox® HS/Bayer International S. A., Bayer Thai Co., Ltd., Thailand
Tri-2-ethylhexyl trimellitate (TOTM)	TOTM (STAB)/Behn Meyer Chemical (Thailand) Co., Ltd., Thailand
Trimethylolpropane trimethacrylate (TRIM)	SR350/Sartomer, Chemical Innovation Co., Ltd., Thailand
Zinc diacrylate (ZDA)	Saret SR416/Sartomer, Chemical Innovation Co., Ltd., Thailand

Table 4.1 Materials used in the present study (cont.)

Chemical name	Grade/Supplier
Dicumyl peroxide (DCP)	Percumyl® D/Petch Thai Chemical Co., Ltd., Thailand
Carbon black (CB)	N326, N550, N774 and N990/Loxley Public Co., Ltd., Thailand and Siam Luck Trading Co., Ltd., Thailand
Precipitated silica (PSi)	Tokusil® 233/ Tokuyama Siam Silica Co., Ltd., Thailand
Quaternium-18 Hectorite	Bentone® 38/Elementis, Belgium
Vinyltriethoxysilane (VTEO)	Commercial grade/Evonik-Degussa, GmbH
Methyl ethyl ketone	Commercial grade/V.S. Chem House, Thailand

4.1.2 Apparatus

The apparatus used in the present study are summarised in Table 4.2.

Table 4.2 List of apparatus used in the present study

Apparatus	Model/Manufacturer
Laboratory two-roll mill	LRM 150/Labtech Engineering Co., Ltd., Thailand
Hydraulic hot press	G30H /Wabash Genesis Series Hydraulic Press, USA
Instron tester	4301/Instron Universal, USA
Rubber Process Analyser	RPA® 2000/Alpha Technology, USA

Table 4.2 List of apparatus used in the present study (cont.)

Apparatus	Model/Manufacturer
Shore A Hardness tester	H17A/Wallace, UK
DIN abrasion tester	6102/Zwick, , USA
Dynamic mechanical thermal analyser	Explexor 25 N/Gabo, Germany
Flexometer	Gabometer 4000/Gabo, Germany
Scanning electron microscope	SEM S-2500/Hitachi, Japan
Videomeasuring machine	VMZ-1510/Itokin Technology Co., Ltd., Thailand

4.1.3 Compound formulation

Raw rubber was compounded according to the formulation as given in Table 4.3. Remarkably, for the study of silica loading effect, silane coupling agent was charged to PSi at 6% by weight of PSi.

Table 4.3 Compound formulation used in the study of filler type and loading effects

Ingredients	Amount (phr)	Function
HNBR	100	Raw rubber
Filler[a]	Variable[b]	Reinforcing filler
TMQ	1	Antioxidant
ZnO	5	Activator/Filler
Stearic acid	1	Activator/Softener
TOTM	5	Plasticiser
TRIM	10	Coagent
Saret SR416	6	Metallic coagent
DCP	2	Curing agent

[a] Filler was used with various categories: Carbon black (N326, N550, N774 and N990), Clay (Bentone38), Silica (Hisil233/6%vinyl silane)

[b] Carbon black loading was varied: 0, 10, 20, 40 and 60 phr
Clay loading was varied: 0, 5, 10, 20 and 30 phr
Silica loading was varied: 0, 10, 20, 30 and 40 phr

For the study of CB hybrid system effect (having different CB surface area and structure) on properties of HBNR compounds and vulcanisates, three CB hybrid systems were prepared by blending two grades of CB having different surface area and/or structure. The total CB lading was kept constant at 60 phr. The CB hybrid ratios were as follows: 0/100, 20/80, 40/60, 60/40, 80/20 and 100/0. Detail of compound formulation used is illustrated in Table 4.4.

Table 4.4 Compound formulation used in the study of carbon black hybrid system effect

Ingredients	Amount (phr)	Function
HNBR	100	Raw rubber
Carbon black hybrid[a]	60	Reinforcing filler
TMQ	1	Antioxidant
TOTM	5	Plasticiser
TRIM	10	Coagent
Saret SR416	10	Coagent
DCP	2	Curing agent

[a] CB hybrid was used with various systems: N326/N990, N326/N774 and N550/N990

4.1.4 Mixing procedure

Initially, HNBR was masticated at 40°C using a two-roll mill with mastication time of 3 minutes. Afterward, the compounding ingredients and filler were sequentially added and mixed. Total mixing time of 20 minutes was used throughout the whole work. Detail of mixing procedure in the study of filler type and loading effects is shown in Table 4.5.

Table 4.5 Mixing procedure used in the study of filler type and loading effects

Action	Time (min)
Add HNBR	0
Add compounding ingredients[a]	3
Add filler	7
Add remaining compounding ingredients[b]	12
Dump and sheet	20

[a] Compounding ingredients were: ZnO, stearic acid and TMQ

[b] Remaining chemicals were: TOTM, TRIM, DCP and ZDA

For the study of CB hybrid system effect, the mixing procedure is illustrated in Table 4.6. In the first step, HNBR was charged to the mixer, and allowed 3 minute for mastication at the set temperature of 40°C. Then, antioxidant (TMQ) was added, and mixed further for 1 minute. Filler and remaining compounding ingredients were subsequently incorporated, and mixed for 16 minutes. The mix was finally discharged and sheeted.

Table 4.6 Mixing procedure used in the study of carbon black hybrid system

Action	Time (min)
Add HNBR	0
Add TMQ	3
Add filler	4
Add remaining compounding ingredients[a]	6
Dump and sheet	20

[a] Remaining chemicals were: TOTM, TRIM, DCP and ZDA

4.2 Determination of cure characteristics

Cure characteristics of prepared HNBR compounds were measured at 145°C using the Rubber Process Analyser (RPA 2000) with test frequency and strain of 6.28 rad/s and 15%, respectively. Scorch time (t_{s2}) and cure time (t_{c90}) were determined from the time to achieve torque rise of 2 units above the minimum torque, and the time to reach 90% complete cure state, respectively. The torque difference ($\Delta S'$) between the maximum (S'_{max}) and minimum (S'_{min}) storage torque was considered as an indication of crosslink density (91). Cure rate was calculated by dividing the difference between the storage torques at t_{c90} and t_{s2} by the difference at t_{c90} and t_{s2}, i.e., cure rate = $(\Delta S')/(t_{c90} - t_{s2})$ (92).

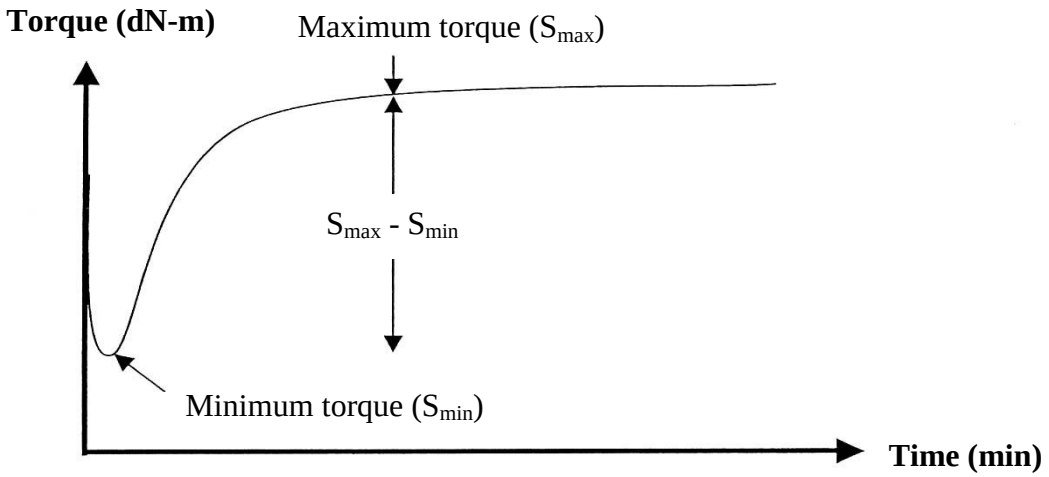

Figure 4.1 Typical cure characteristics

4.3 Determination of filler-rubber interaction

The filler-rubber interaction of filled HNBR compounds was investigated through the measurement of bound rubber content (BRC), as developed by Le and co-workers (71-73). The rubber-layer bonded on the CB surface was determined by extracting the unbound materials, such as, ingredients and free rubbers with methyl ethyl ketone for 7 days at room temperature and drying at 80°C in an oven for 2 hours until reaching a constant mass. Weights of the samples before and after the extraction were measured, and the rubber-layer bonded on the surface of CB was calculated using Equation 3.4 (as shown in section 3.2.2).

4.4 Determination of viscoelastic properties

The viscoelastic behaviour of HNBR compounds and vulcanisates were measured using the Rubber Process Analyser (RPA 2000).

A version of the instrument, suitably modified for Fourier Transform experiments (78, 79), was used for large amplitude oscillatrory strain (LAOS) experiments on uncured HNBR compounds. Strain sweep tests were performed at 100°C and test frequency of 3.14 rad/s (0.5 Hz). Two tests were performed on each sample, namely test "a" and "b", in order to check material's homogeneity. Strain history effects, if any, were considered by running two successive strain sweep runs on the same sample, with a dwell time of 2 minutes between both runs. The data were recorded as belonging to run 1 and run 2. Both linear and non-linear viscoelastic properties of filled HNBR compounds were investigated, and reported through complex modulus (G^*) and torque harmonics of filled HNBR compounds as a function of strain amplitude as well as quarter torque signal integration.

As for HNBR vulcanisates, the viscoelastic behaviour of HNBR vulcanisates was measured using the RPA 2000. Strain sweep test was conducted, and the resultant storage modulus or elastic modulus (G'), loss modulus or viscous modulus (G'') and damping factor or loss factor ($\tan\delta$) were recorded at 60°C. It must be noted that the time sweep test was initially performed to monitor thermal stability of test specimens, so that it could be ensured that any change in results of strain sweep tests is not caused mainly by a thermal degradation.

4.5 Determination of dynamic mechanical properties

Dynamic mechanical properties of HNBR vulcanisates were measured using a dynamic mechanical analyser (Gabo, Explexor^{TM} 25N) with tension mode under static and dynamic strain amplitudes of 2% and 0.1%, respectively. Temperature sweep tests were performed in a temperature range of -80 to 140°C with a heating rate of 2°C/min. The test frequency was kept constant at 62.8 rad/s (10 Hz).

4.6 Determination of heat build-up

The flexometer (Gabometer 4000) was used to assess the magnitude of heat build-up (HBU) in HNBR vulcanisates, according to ASTM D623 under high static stress of 1.97 MPa at test temperature, frequency and dynamic strain of 100°C, 15 Hz and 2.2 mm, respectively. The test specimen having cylindrical in shape with diameter of 17.8±0.1 mm and height of 25±0.15 mm was placed in the test chamber. Specimen temperature was monitored as a function of time. The test was terminated after 25 minutes, and temperature rise (ΔT) was determined as a HBU.

Apart from Gabometer 4000, the RPA 2000 could be used to predict HBU. HNBR compounds were first cured at 145°C for 120 minutes within the test cavity. Then, the temperature was reduced to 40°C using the so-called variable temperature analysis (VTA) feature of the built-in instrument monitoring system, and held at this level for 5 minutes before starting the heat build-up test. The delay feature was set at 5°C for 1 minute in order to switch-off temperature control system of the RPA 2000. By this means, the test specimen temperature is not controlled under temperature probe. Then cured specimen was tested under oscillation at 75.36 rad/s (12 Hz) frequency and 30% strain for 5 minutes. The rise in the temperature of the lower die was used as a measure of HBU of cured HNBR as calculated from Equation 4.1.

$$HBU = T_f - T_i \quad (4.1)$$

where HBU = heat build-up (°C)

T_f = final temperature of lower die (°C)

T_i = initial temperature of lower die (°C)

From the RPA die design, there is a rubber seal between the lower seal plate and lower die. This rubber seal could release a small amount of frictional heat build-up during oscillating, which must be accounted for and subtracted from the total lower die temperature rise when a rubber specimen is being tested. Therefore, the lower die temperature from the HBU test in RPA 2000 with empty cavity was recorded, and the HBU difference, or the so-called real HBU, was calculated using Equation 4.2.

$$HBU_r = HBU_a - HBU_e \quad (4.2)$$

where HBU_r = real heat build-up (°C)

HBU_a = heat build-up from filled cavity (°C)

HBU_e = heat build-up from empty cavity (°C)

4.7 Mechanical property measurement

To prepare vulcanised HNBR, the uncured compounds were compression moulded under clamping pressure of 15 MPa at 145°C for 120 minutes by hydraulic hot press.

4.7.1 Hardness

Hardness of 6-mm-thick specimens was measured at room temperature according to ASTM D2240-97 with a Shore A durometer. The hardness value is determined by the penetration of the durometer indenter foot into the sample. At least 6 readings at different areas were taken for an average as the hardness value of the tested sample.

4.7.2 Tensile properties

Tensile strength, modulus and elongation at break were performed as per ASTM D412-98, using the Instron universal tensile tester at a crosshead speed of 500 mm/min with the load cell of 1 kN. Dumbbell-shaped test pieces were punched out from the moulded 1-mm-thick sheets using ASTM die C.

4.7.3 Tear strength

The tear strength of HNBR vulacnisates was measured according to ASTM D624-98 using the Instron universal tensile tester at a crosshead speed of 500 mm/min with the load cell of 1 kN. Winkelmann-shaped tear test specimens were punched out from the moulded 1-mm-thick sheets using ASTM 624 die B. The test measures the strength required to initiate a tear in a material. The values of tear properties were the average of 4-5 specimens.

4.7.4 Abrasion resistance

Abrasion resistance of HNBR vulcanisates was measured using abrasion tester (Zwick model 6120) in accordance with DIN 53516. The rubber vulcanisates were moulded in cylindrical shapes with diameter and thickness of 16.0±0.2 mm and 12 mm, respectively. The abrasion resistance was measured by moving a test piece across the surface of an abrasive sheet mounted to a revolving drum, and is expressed as volume loss in cubic millimetres. The specimen surface was observed by videomeasuring machine to support the explanation of wear mechanism.

4.8 Determination of dispersion and/or distribution of filler

A scanning electron microscope (SEM) with 15 kV accelerating voltage was utilised for evaluating the quality of dispersion and distribution of filler in the rubber matrix. The cryogenic fractured surfaces of rubber specimens were prepared and sputtered with gold before viewing.

CHAPTER V
RESULTS AND DISCUSSION

The results and discussion of this research consist of 2 parts. The first part concerns the effects of filler type and loading on properties of HNBR. Viscoelastic behaviour of HNBR compounds is investigated to predict processability as well as reinforcement of a HNBR products. The reinforcement of HNBR vulcanisates is determined by measuring their cure characteristics, mechanical and dynamic properties, i.e., hardness, tensile properties, tear strength and abrasion resistance. The second part, a correlation of viscoelastic properties to HBU as measured from different instruments of filled HNBR vulcanisates will be focused and compared.

5.1 Effects of filler type and loading on reinforcement of hydrogenated nitrile rubber

5.1.1 Influences of carbon black loading and characteristics

In this study, a CB added to HNBR is expected to improve mechanical properties via rubber-filler interaction between HNBR matrix and CB. The reinforcement performance of filler has been reported to depend typically on CB loading and characteristics including specific surface area, surface chemistry and structure (or degree of aggregation) (14, 52, 57, 77). Simultaneously, property improvement and processability are found to reach its maxima at a certain CB loading relying on the mixing efficiency for CB dispersion and distribution (i.e., state-of-mix) (1). The cure characteristics and mechanical properties of HNBR filled with various CB loadings and types are compared in order to reach at a comprehensive understanding of the influences of the concentration and characteristics of the CB on the CB filled HNBR compounds and vulcanisates.

5.1.1.1 Cure characteristics

Results of scorch time (t_{s2}), cure time for 90% of cure completion (t_{c90}), and torque difference between the maximum and minimum torques ($\Delta S'$) as an indication of crosslink density (91) are presented in Figures 5.1 to 5.3, respectively. It can be seen that the scorch time (t_{s2}) and the cure time (t_{c90}) decrease while the torque difference (or crosslink density) increases with increasing CB loading. These results evidently imply a cure promotion phenomenon by the incorporation of CB. The explanations are postulated by (i) a thermal history, (ii) an alkalinity of CB, (iii) a relatively high thermal conductivity of CB and (iv) a restriction of curative migration to the tightly bound rubber (70).

It has been known that, as filler loading increases, bulk viscosity increases with the magnitude depending on filler specific surface area, filler structure and filler-rubber interaction. This would lead to a rise in bulk temperature via shear heating and thus the thermal history applied to the rubber bulk. By this means, the high magnitude of thermal history experienced in compound leads to an acceleration of curative dissociation in compounds.

In peroxide vulcanisation, the crosslinking is initiated by the thermal decomposition of the peroxide to produce alkoxy radicals. Next, the active radicals abstract hydrogen atom from elastomer chains to form macro-radicals. Finally, crosslinking is resulted either from the combination of two macro-radicals or from the addition of a macro-radical to an unsaturated moiety of another primary elastomer chain (93, 94). The alkalinity of the CB allows the peroxide decomposition to follow a free radical mechanism which results in the crosslinking of polymer (95, 96).

In terms of thermal conductivity effect, compared with raw rubber, the CB as solid particles possesses much higher thermal conductivity (0.1-0.6 W/mK for rubber (97) and ~2 W/mK for CB(98)) which helps transferring heat from mould surface to rubber.

Regarding the restriction of curative migration to the tightly bound rubber, Choi (64) reported that the effective prevention of curative adsorption of tightly bound rubber allows more free curatives to locate in rubber matrix, and therefore the crosslinking reactions become faster.

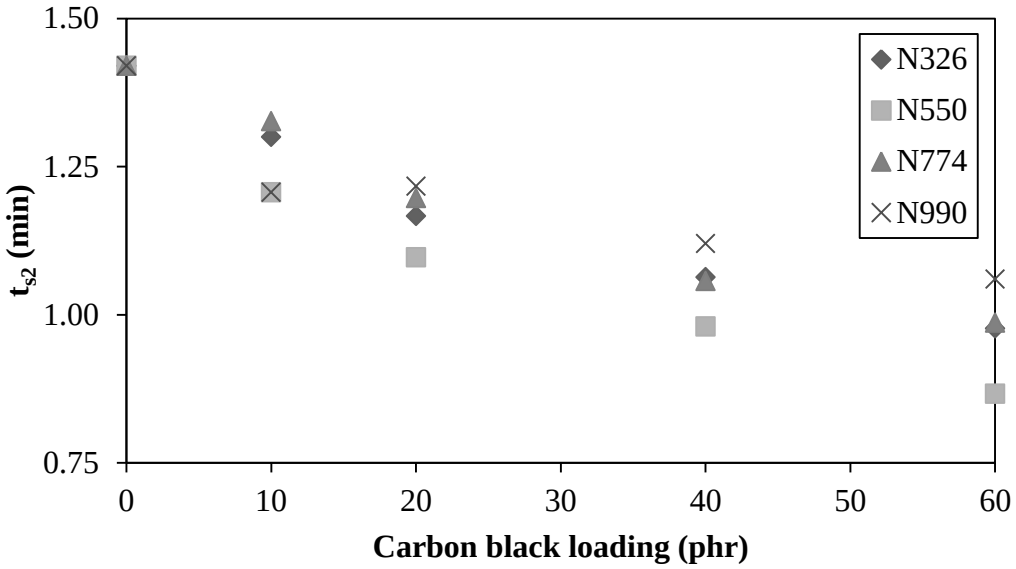

Figure 5.1 Relationship among scorch time (t_{s2}), carbon black loading and characteristics in HNBR compounds

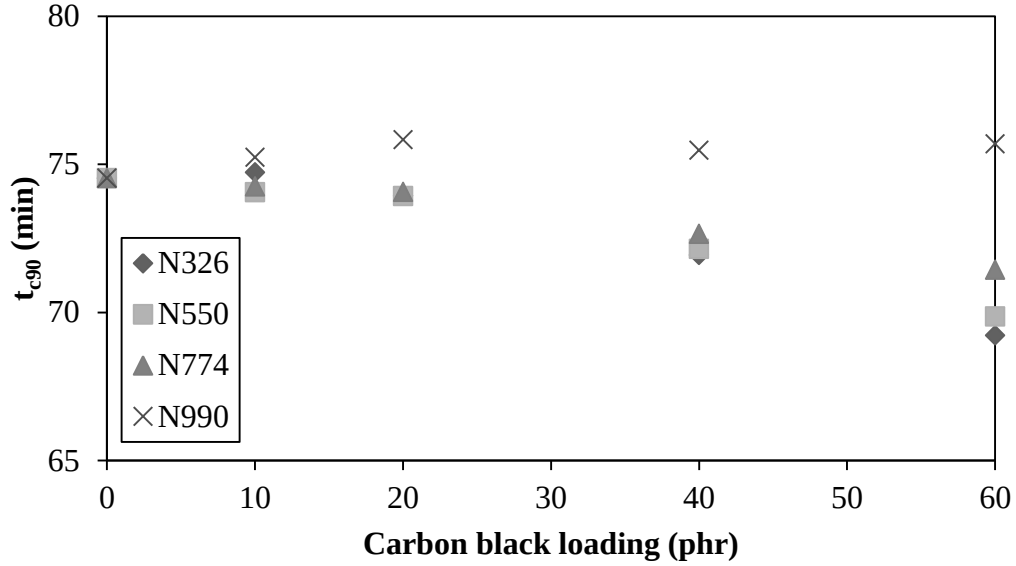

Figure 5.2 Relationship among cure time (t_{c90}), carbon black loading and characteristics in HNBR compounds

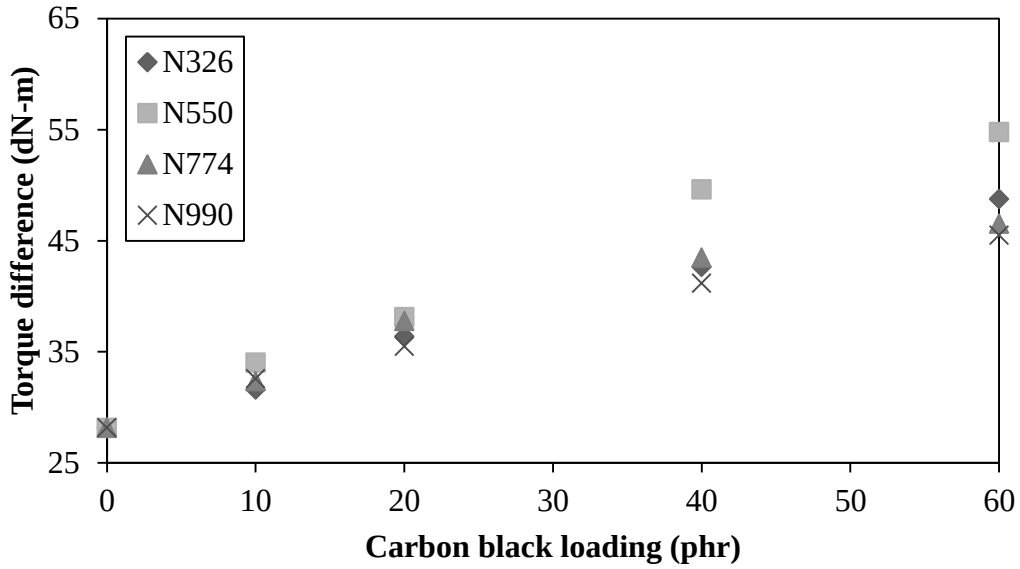

Figure 5.3 Relationship among torque difference (or crosslink density), carbon black loading and characteristics in HNBR compounds

However, it is evident that, at any given CB loading, the specific surface area of CB affects cure behaviour to some extent, but with the lower magnitude than the CB loading. As specific surface area of CB increases, the formation of rubber-filler interaction due to the rise in contacting area increases, and then crosslink density also increases (99, 100). Exceptionally, the crosslink density appears to be highest in HNBR filled with N550, which is due probably to bound rubber and/or crosslinking reaction effects.

The crosslinking reaction is proposed to correlate to the bound rubber as follows: there are some rubber molecules adsorbed on the surfaces of CB aggreates, leading to the increased rubber-filler interaction and thus the bound rubber. The curatives added into compound will prefer locating in the free rubber matrix rather than the bounded rubber. The higher the CB surface area and structure, the higher the bound rubber. As mentioned previously, with increasing bound rubber content, the rate of cure reaction could be promoted, leading to the higher crosslink density as observed in this work.

Table 5.1 shows the results of bound rubber content of HNBR compounds filled with CB having different surface areas and structures as measured through rubber-layer bonded on CB surface. It is evident that the bound rubber content

of HNBR compounds filled with CB having relatively high surface area is higher. Notably, the bound rubber content of HNBR compound filled with N550 having relatively low surface area is comparable to that filled with N326. Such high content of bound rubber found in the vulcanisates filled with N550 is believed to arise from the high structure of N550. Choi and coworker (70) have reported that the CB with highly developed structure provides the tightly bound rubber. Such tightly bound rubber then obstructs a curative absorption process on filler surfaces. This means a migration of free curatives to the free rubber matrix is promoted leading to the increased cure rate reaction and the state-of-cure.

Table 5.1 The rubber-layer bonded on the surface of carbon black of HNBR compound filled with different carbon black characteristics

Carbon black type	Rubber-layer (L)
N326	0.213 ± 0.01
N550	0.205 ± 0.00
N774	0.0468± 0.07
N990	N/A

5.1.1.2 Viscoelastic properties

Generally, the study of viscoelastic behaviour is capable of predicting a processability and mechanical properties of compounds and vulcanisates. In this work, the viscoelastic properties of CB filled HNBR compounds and vulcanisates (i.e., uncured and cured CB filled HNBR, respectively) were investigated using oscillatory shear rheometer, namely, RPA 2000. The viscoelastic behaviour of CB filled HNBR compounds and vulcanisates as a function of deformation strain was examined.

a) Uncured carbon black filled HNBR systems

In this section, the viscoelastic properties of uncured HNBR filled with CB having different characteristics (specific surface area and structure) and contents are investigated by RPA 2000, suitably modified for Fourier Transform (FT)

experiments. Both the linear and non-linear viscoelastic domains are investigated with respect to various characteristics and contents of CB filled HNBR compounds.

(RPA-FT) Complex modulus vs. Strain amplitude

Figures 5.4 to 5.7 show plots of complex modulus (G^*) versus strain amplitude (%) for HNBR filled with different loadings of N326, N550, N774 and N990, respectively. In all cases, it is evident that results from the two tests (a and b) are identical, indicating the homogenous compounds. It is also found that the difference between run 1 and run 2 is minimal, meaning either that there are no significant strain history effects or that the 2 minutes dwell time between runs is sufficient for strain recovery. An exception is the case of the 60 phr N550 filled HNBR compound, which exhibits a deviation of run 2 curve at high strain. This anomalous result could be explained by a premature scorching of the compound. The fast crosslinking reaction due to a large amount of tightly bound rubber is used to explain this phenomenon, as discussed previously.

It is clearly seen from Figures 5.4 to 5.8 that, at low strain, the G^* of unfilled compound is lowest, while the G^* of filled compound with CB loading of 60 phr is highest for all CB surface area. Expectedly, the G^* of CB filled HNBR increases with increasing CB content, which is due mainly to the reinforcing effects, i.e., the hydrodynamic effect, the filler-filler interaction as well as the CB-HNBR interaction (17, 21). Moreover, it is evident that the lightly filled compounds exhibit a relatively extended linear viscoelastic (LVE) region until the CB loading reaches 20 phr, then the compounds with CB loading of 40 phr show a narrow LVE region. Compounds with CB loading of 60 phr show no significant LVE region within the experimental strain windows of the RPA 2000.

The shortening of the LVE region is associated with an increase in G^*, likely indicating an increase in magnitude of filler network formation and hence a higher dynamic strain softening (DSS) effect. At high CB content, the filler network is expected to play a key role at low strain, but its magnitude of DSS appears to reduce at high strain due to the filler network disruption.

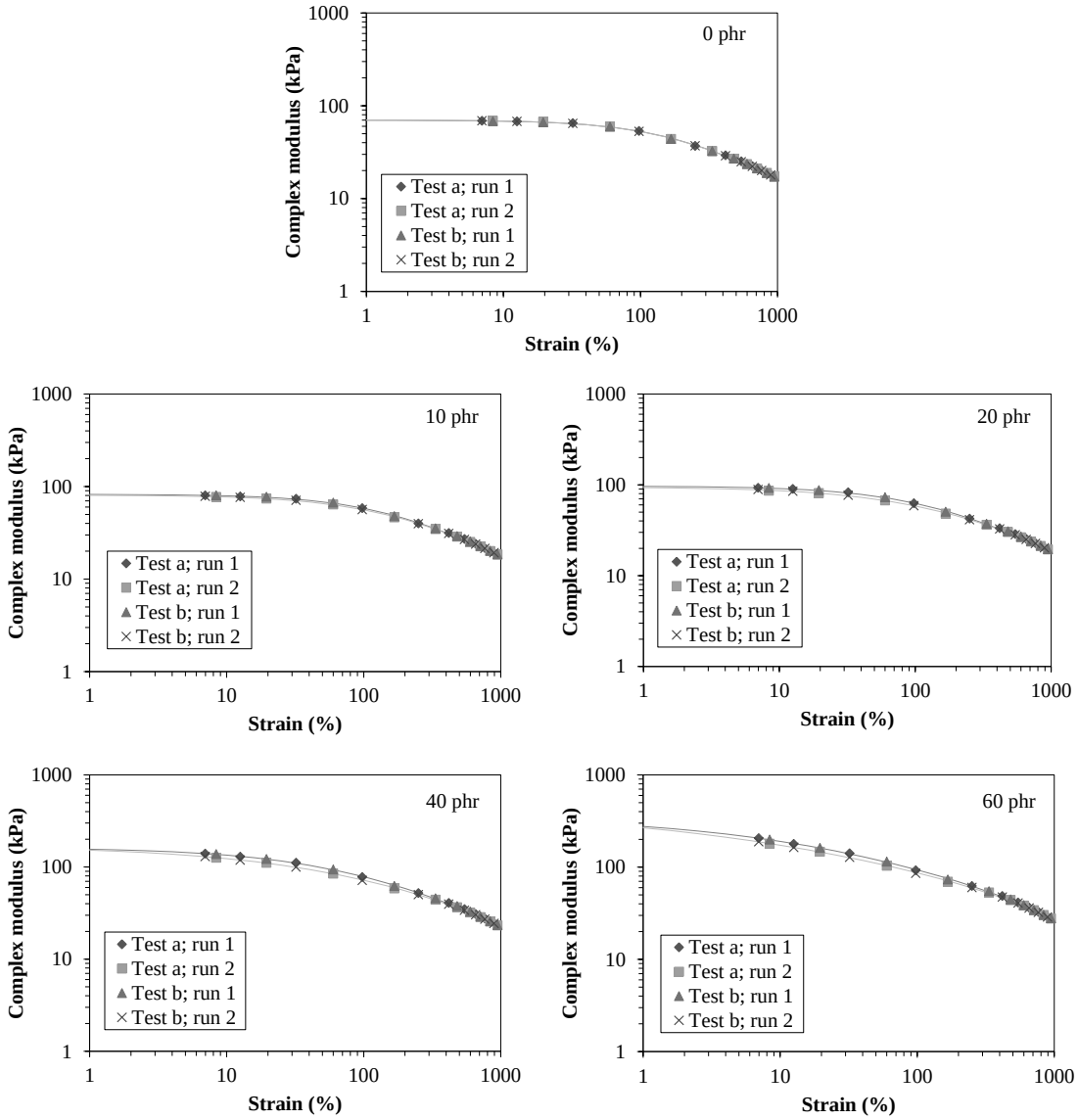

Figure 5.4 Complex modulus (G^*) as a function of strain amplitude at 3.14 rad/s and 100°C as measured by the RPA-FT of HNBR compounds filled with various N326 loadings

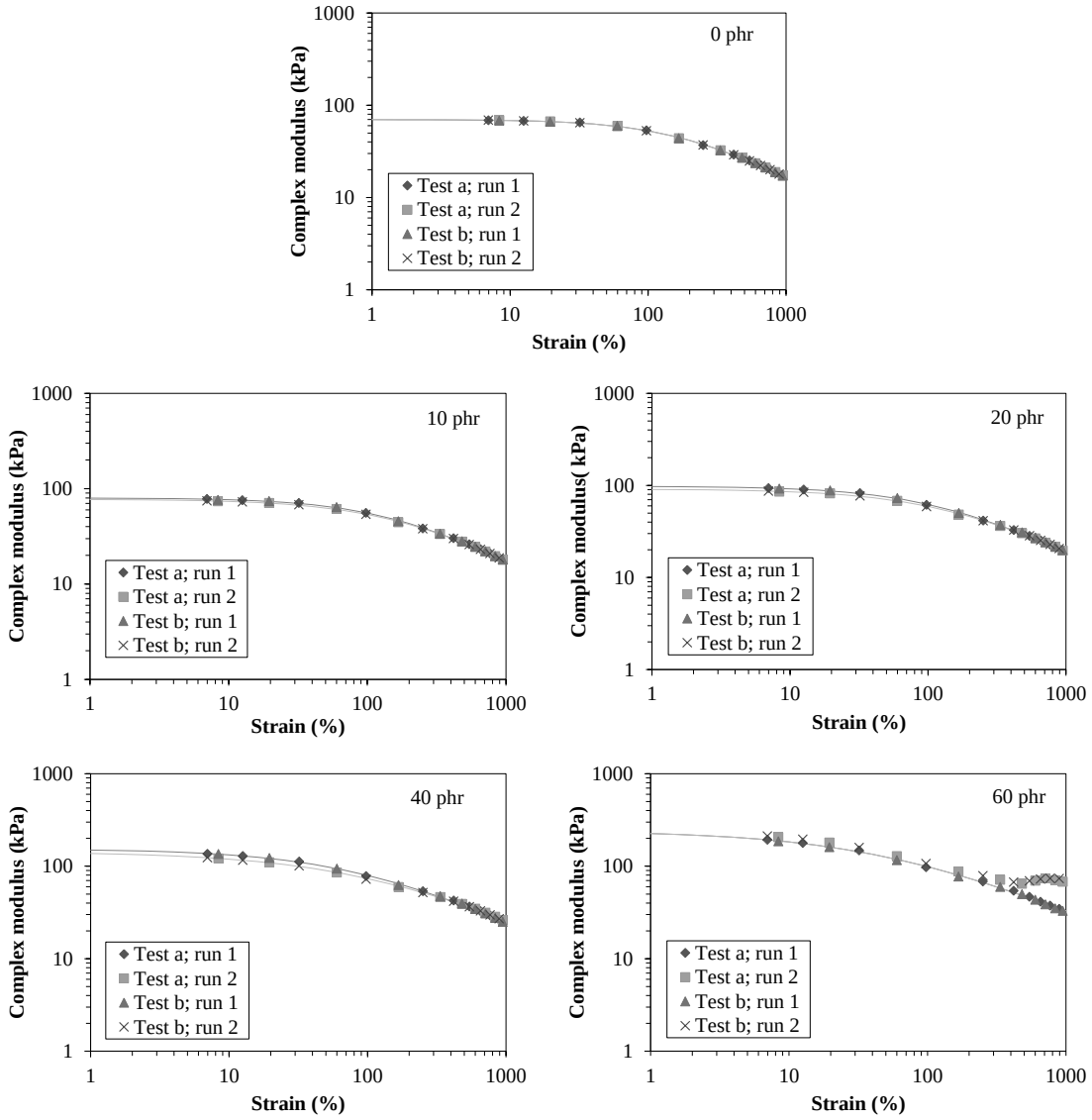

Figure 5.5 Complex modulus (G^*) as a function of strain amplitude at 3.14 rad/s and 100°C as measured by the RPA-FT of HNBR compounds filled with various N550 loadings

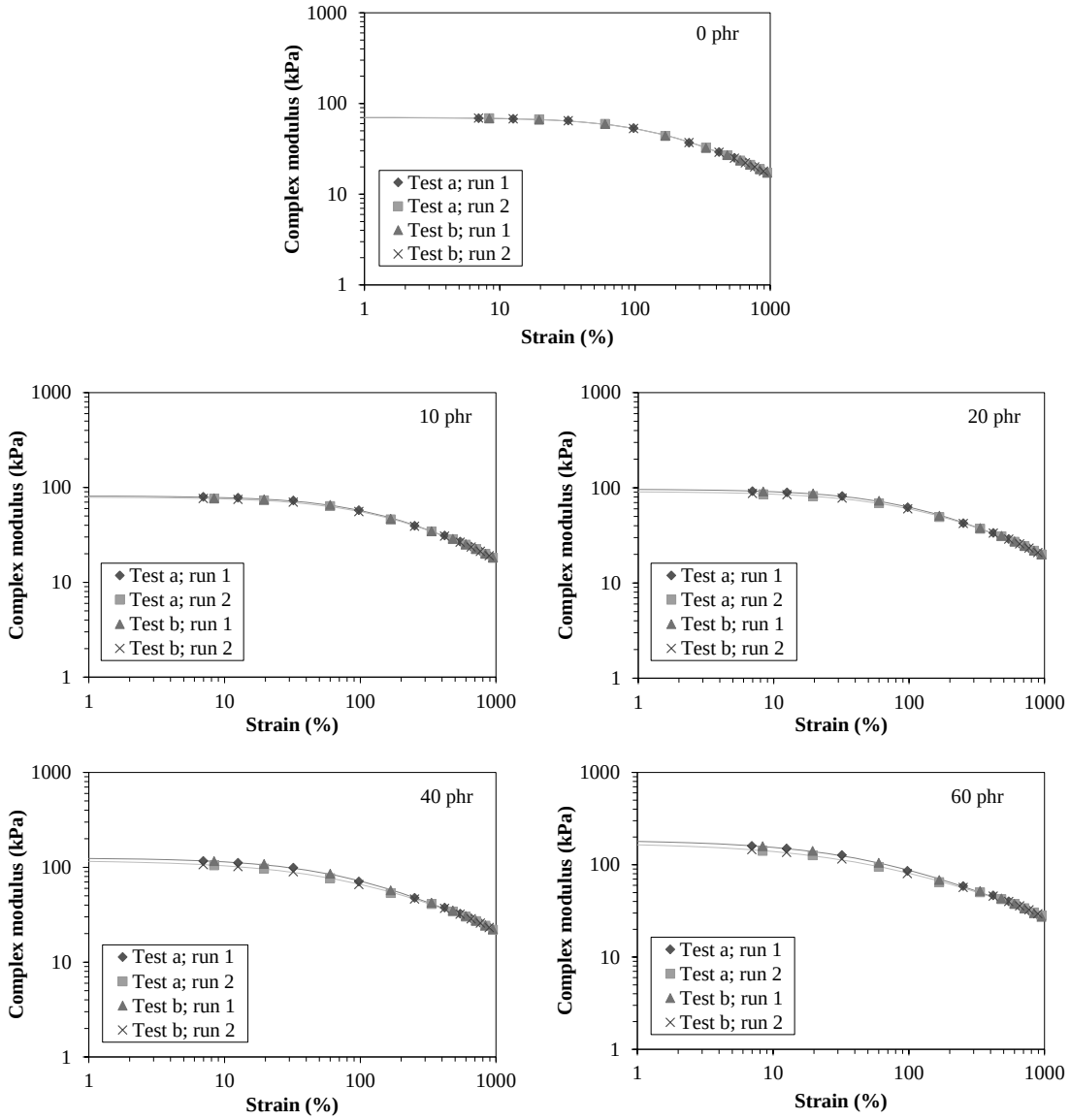

Figure 5.6 Complex modulus (G^*) as a function of strain amplitude at 3.14 rad/s and 100°C as measured by the RPA-FT of HNBR compounds filled with various N774 loadings

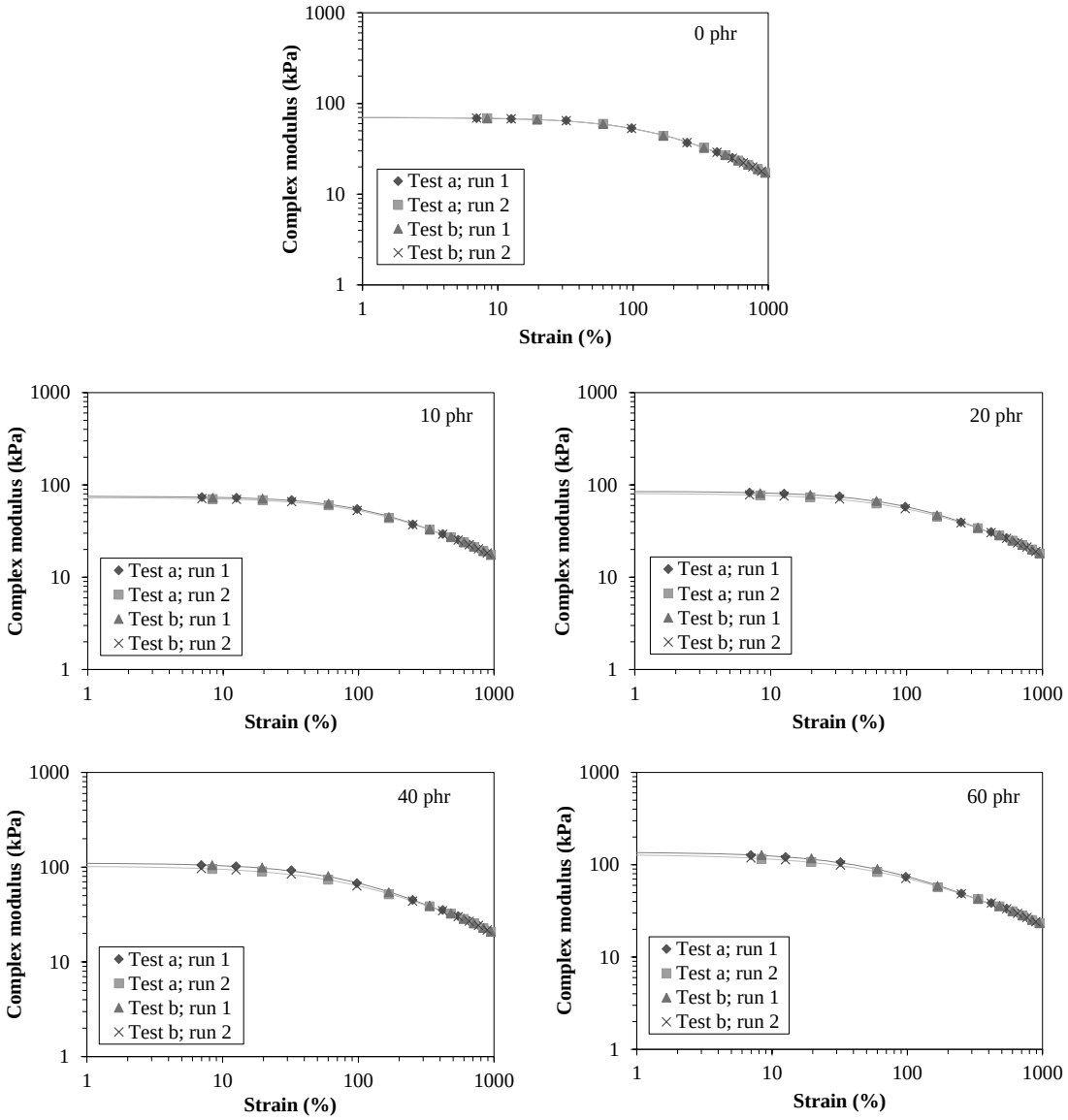

Figure 5.7 Complex modulus (G^*) as a function of strain amplitude at 3.14 rad/s and 100°C as measured by the RPA-FT of HNBR compounds filled with various N990 loadings

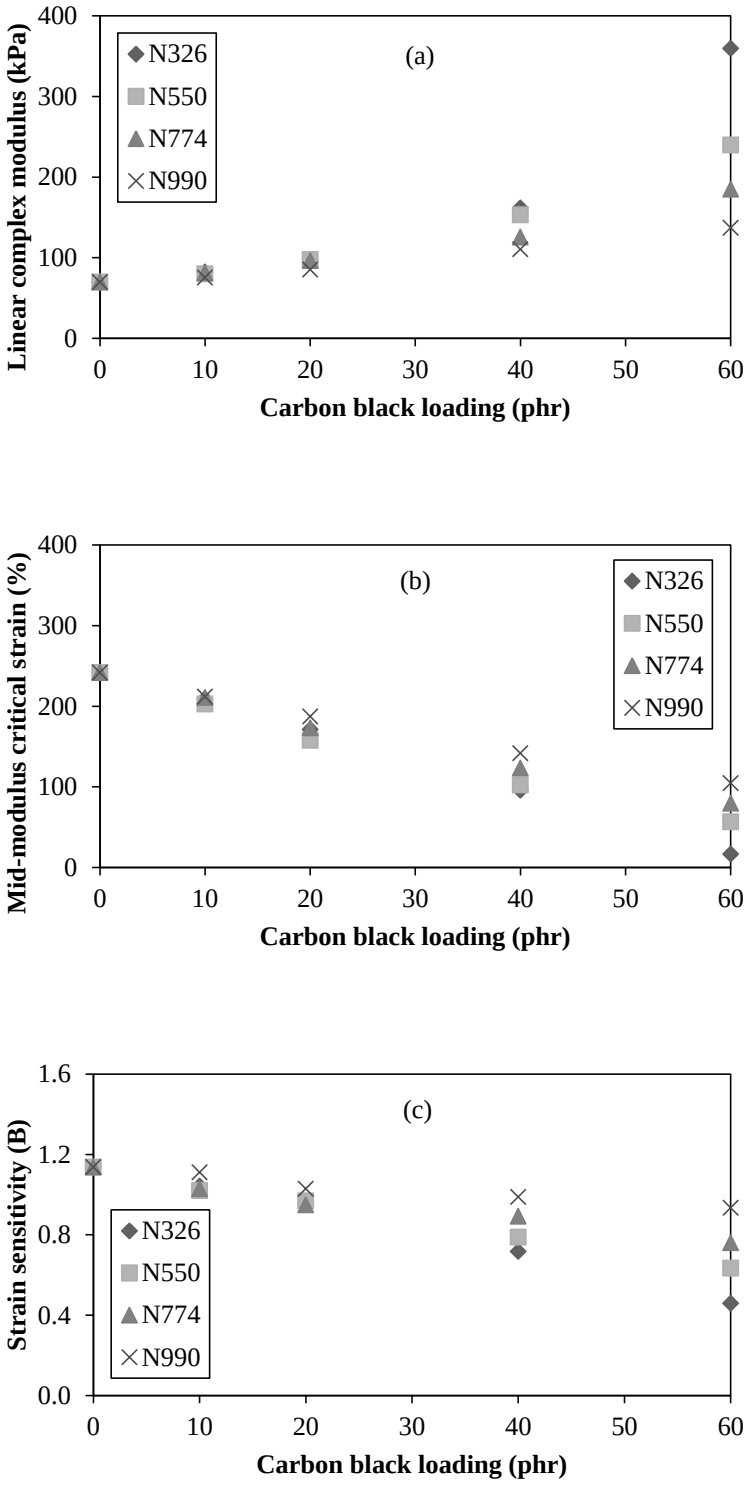

Figure 5.8 Relationship among fit parameters of Equation 3.16, carbon black loading and characteristics in HNBR compounds: (a) linear complex modulus $\left(G_0^*\right)$; (b) mid-modulus critical strain (1/A); (c) strain sensitivity (B)

At the 60 phr CB loading regardless of the CB specific surface area, the strain-dependent G^* is clearly observed in all uncured compounds with the greater magnitude in the compounds filled with CB having higher specific surface area. Also, at low strain amplitude, the magnitude of G^* rise is greater in HNBR filled with higher specific surface area (or smaller particle size) of CB. This is likely due to the greater possibility of formation of a CB tridimensional transient network through larger contacting area.

To support the proposed explanation of the CB characteristics (surface area and structure) and loading effects, the Equation 3.16 (as shown in literature review section) is used to perform the regression, and the fit parameters that govern the viscoelastic properties of filled HNBR compounds will be discussed in a very concise manner. As evidenced in Figure 5.8, the linear complex modulus $\left(G_0^*\right)$ increases with increasing CB loading and surface area. This supports the explanation of reinforcing effect as discussed earlier. To consider the extent of the LVE region, the mid-modulus critical strain (1/A) is used. Figure 5.8 (b) reveals that the 1/A values decrease with increasing CB loading and surface area, which is in good agreement with the DSS effect, as discussed previously. The B parameter appears to decrease with increasing CB content and surface area, indicating a strong dependency of the strain sensitivity of HNBR compounds.

(RPA-FT) Torque Harmonics vs. Strain amplitude

The non-linear viscoelasticity of tested compounds is described by odd torque harmonics at high strain amplitude, reported as the total torque harmonic content (TTHC), 3^{rd} relative torque harmonic (T(3/1)) and 5^{th} relative torque harmonic (T(5/1)).

Figures 5.9 to 5.12 show the variation of torque harmonics versus strain amplitude at the test frequency of 0.5 Hz in HNBR filled with different loadings of N326, N550, N774 and N990, respectively. It can be seen that there are no significant differences between test a and b, indicating that all the tested compounds are homogeneous.

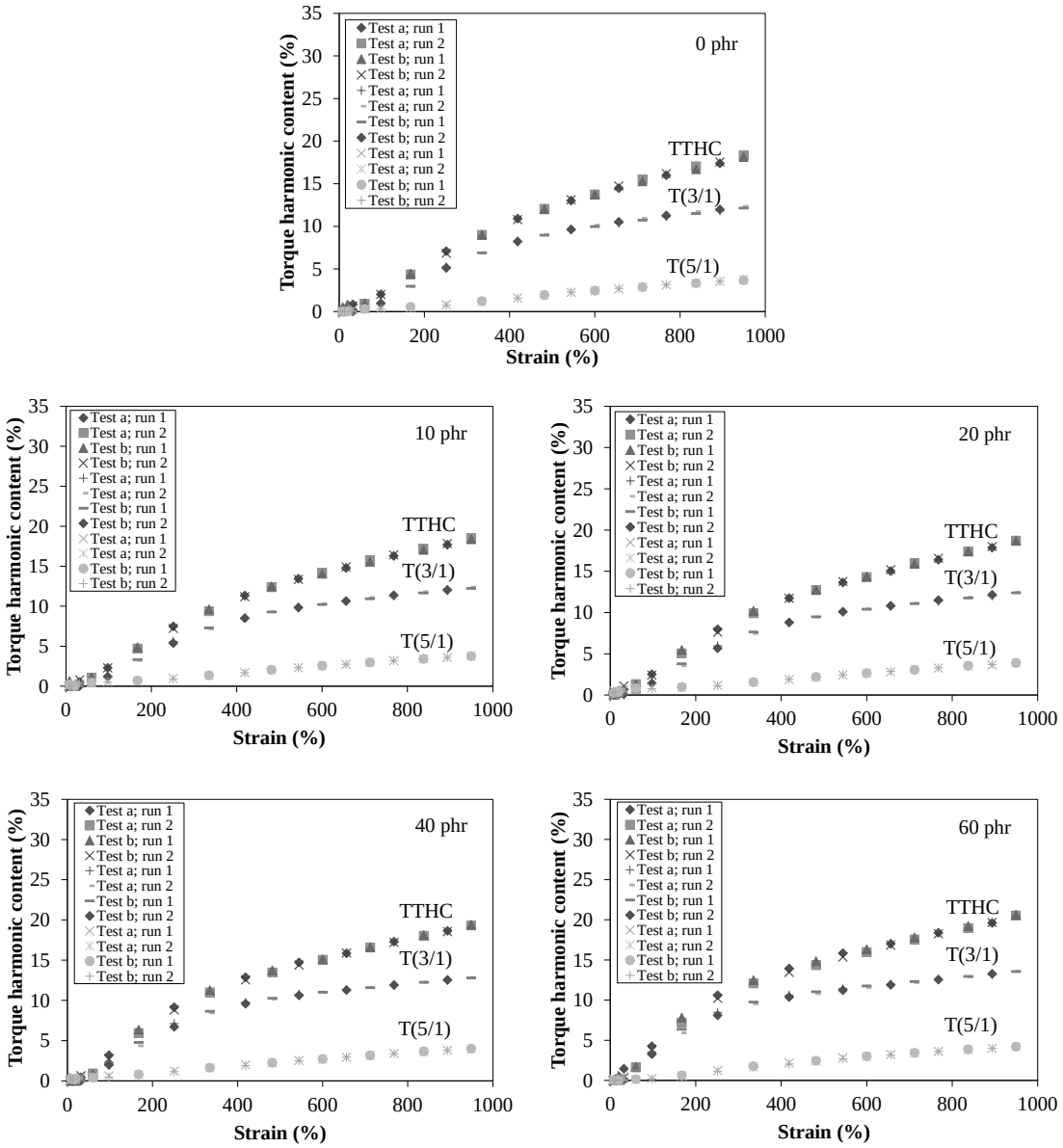

Figure 5.9 Torque harmonics as a function of strain amplitude at 3.14 rad/s and 100°C as measured by the RPA-FT of HNBR compounds filled with various N330 loadings

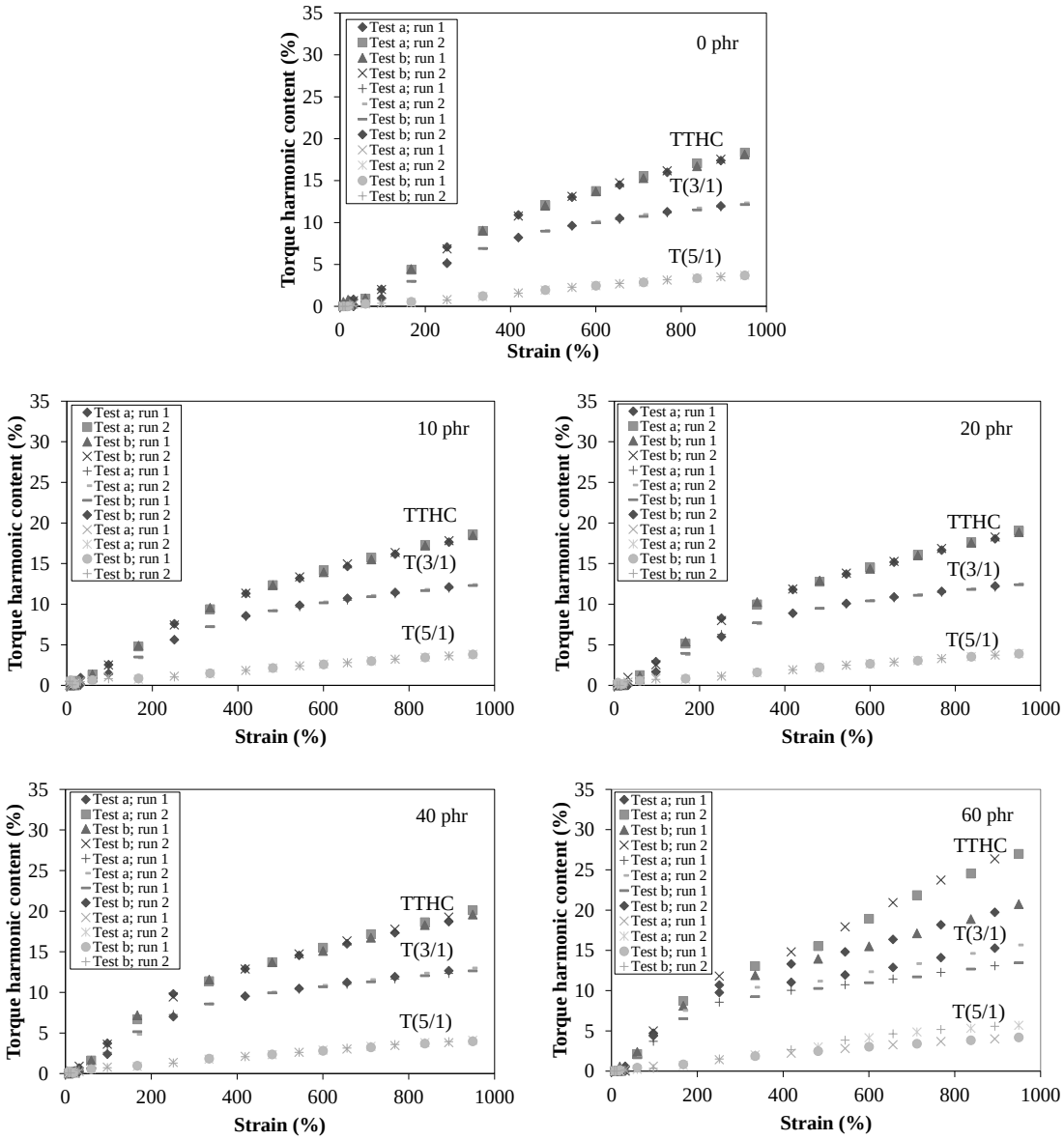

Figure 5.10 Torque harmonics as a function of strain amplitude at 3.14 rad/s and 100°C as measured by the RPA-FT of HNBR compounds filled with various N550 loadings

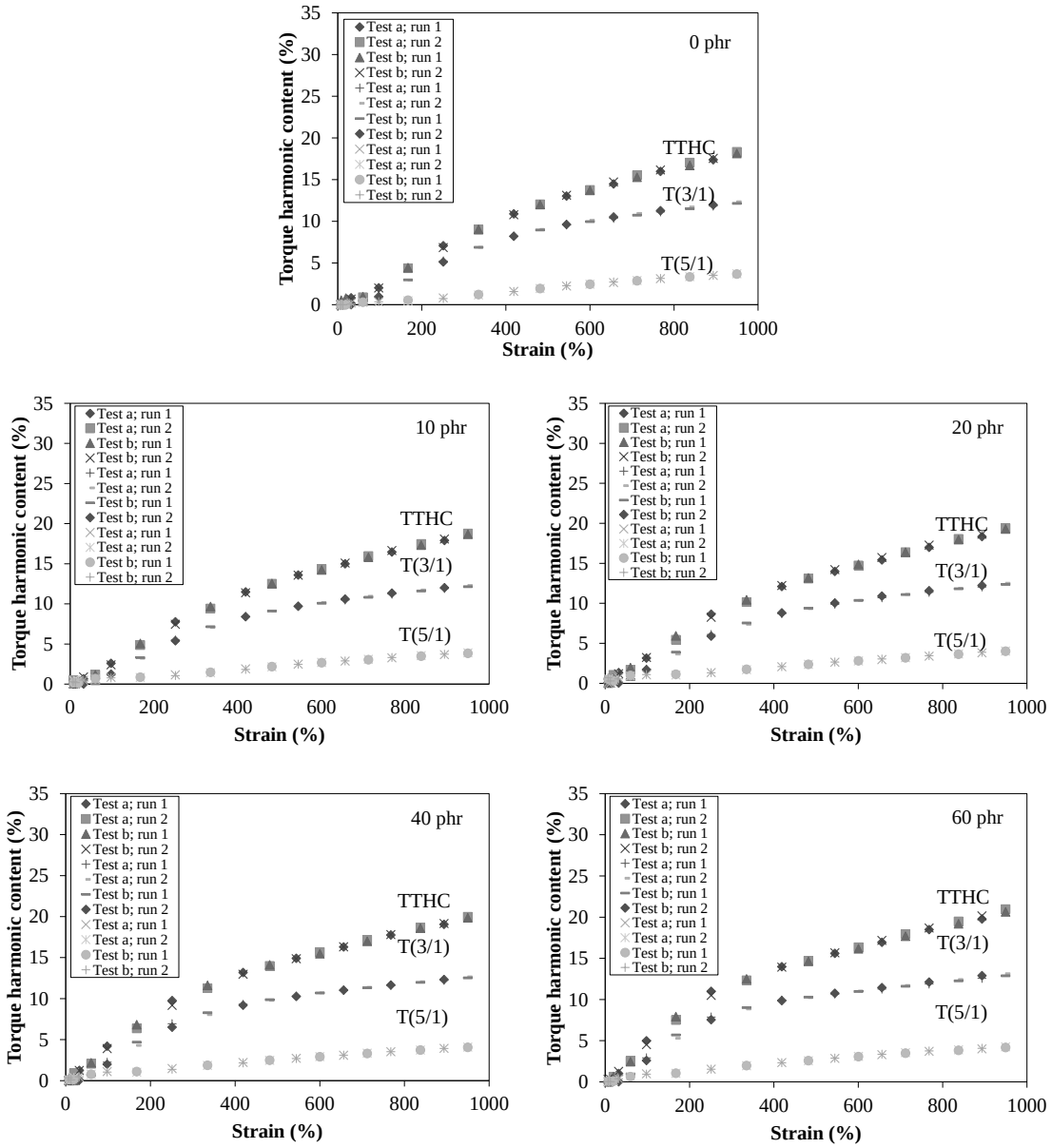

Figure 5.11 Torque harmonics as a function of strain amplitude at 3.14 rad/s and 100°C as measured by the RPA-FT of HNBR compounds filled with various N774 loadings

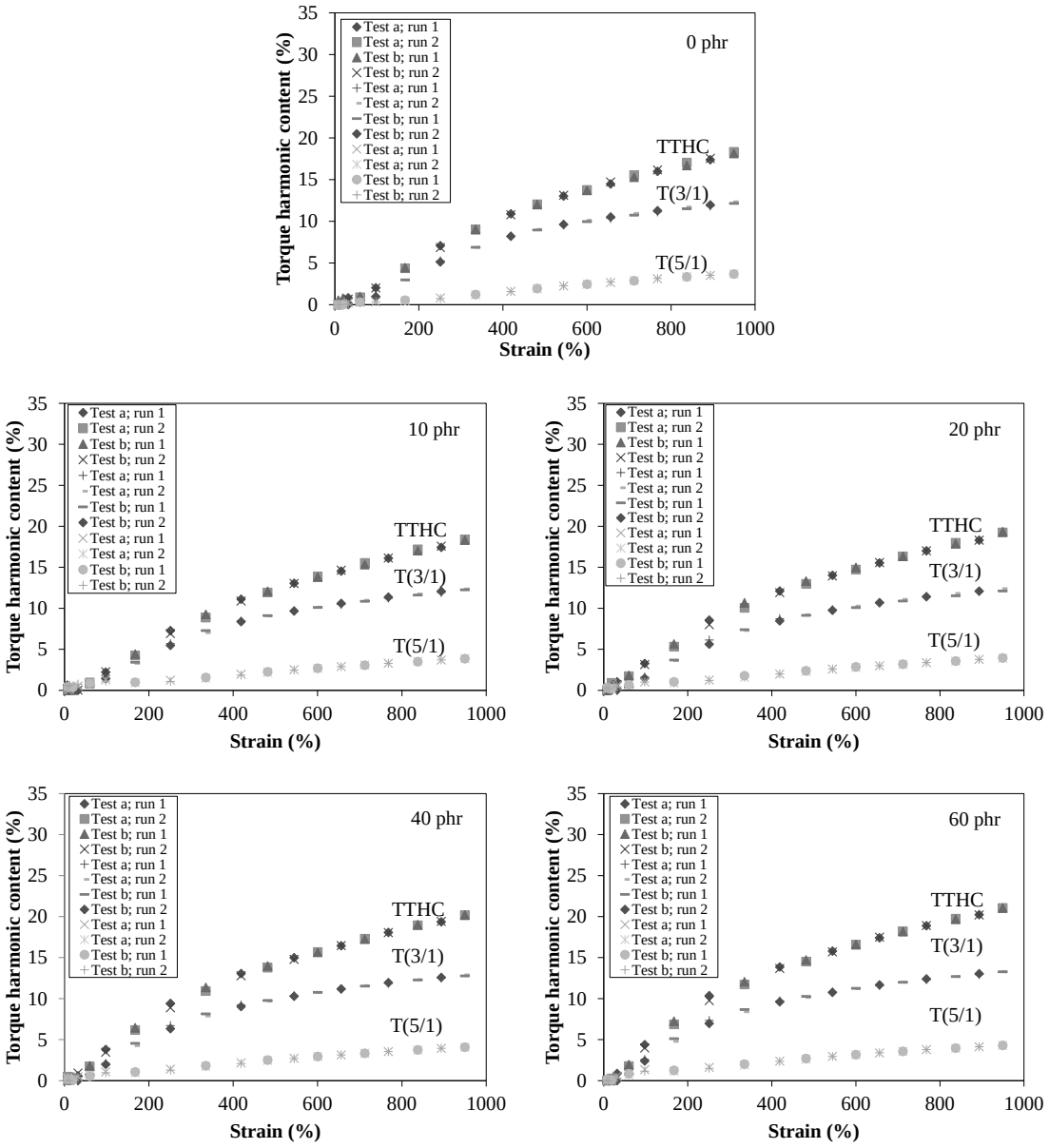

Figure 5.12 Torque harmonics as a function of strain amplitude at 3.14 rad/s and 100°C as measured by the RPA-FT of HNBR compounds filled with various N990 loadings

In addition, it is found that the difference between run 1 and 2 of all the tested compounds is insignificant, which allows to conclude that the torque signal harmonic is insensitive to strain. Except in the case of HNBR compound filled with N550 at loading of 60 phr, the difference between run 1 and 2 could be seen clearly. The scorch effect in the compound is believed to be responsible for the

obtained result, as mentioned previously in the complex modulus results (see Figure 5.5).

Obviously, the torque harmonics versus strain amplitude of all the tested compounds shows S-shape curves, meaning that, at high strain, there is a linear variation with strain. Therefore, the non-linear viscoelastic behaviour of all the tested compounds can easily be documented by the fit parameters of Equation 3.17. The T(3/1) is the largest and convenient to capture the essential of the non-linear behaviour, as a consequence, the fit parameters for T(3/1) of tested compounds are performed and the result are compared as shown in Figure 5.13. It is evident that the TH_0 and α (used to describe the high strain behaviour of all the tested compounds), slightly change with the increasing CB loading and surface area. It could be said that, at high strain, the CB characteristics and loading do not influence the viscoelastic properties of HNBR compounds. This is due to the disruption of rubber-filler interaction. Therefore, the viscoelastic character is maintained only by the stretched rubber phase. At low and middle strain behaviour, the most significant information of non-linear viscoelastic behaviour is provided by parameters C and D (81).

To quantify the effect of strain on CB filled HNBR compounds, the parameter C is evidently more stable than the parameter D. This is because the parameter C tends to increase with increasing CB content, which is noticeable in all CB characteristics. The decreases in parameter D values are insignificantly. The parameter C result is in good agreement with the concept of DSS effect, i.e., the extent of LVE region decreases with the increase in magnitude of filler network formation. At given CB loadings of 40 and 60 phr, it is evident that the parameter C of N550 is highest followed by N326 and N774 which are comparable. The lowest value is found in the compound with N990. It is clear that the change in parameter C is in line with the CB structure (N550 > N326 ≈ N774 > N990). The non-linear viscoelastic character of such filled HNBR compound is noticeable through the quarter cycle integration method to be discussed in the next section.

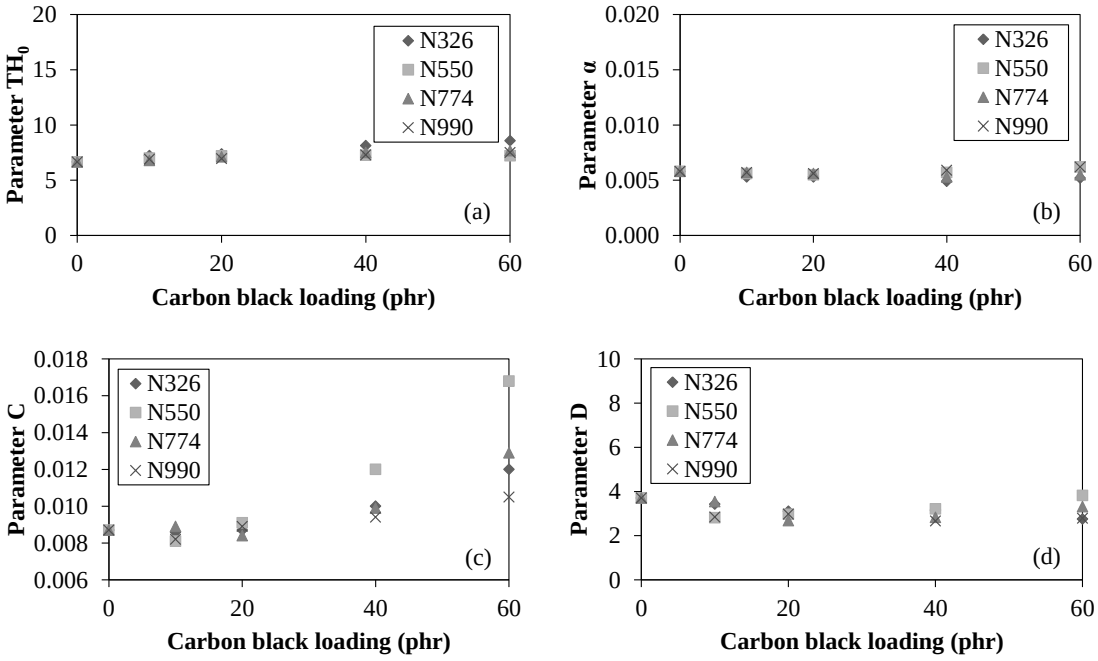

Figure 5.13 Relationship among fit parameters of Equation 3.17, carbon black loading and characteristics in HNBR compounds: (a) parameter TH_0; (b) parameter α; (c) parameter C; (d) parameter D

Quarter Torque Signal Integration

Further to the FT analysis, the non-linear viscoelastic behaviour of unfilled and filled rubber compounds can be considered with respect to the ratio of the first to the second quarter torque signal integration, i.e., Q1/Q2 ratio.

The Q1/Q2 ratio of unfilled rubber compounds is generally higher than 1, and increases with strain amplitude. The non-linear viscoelastic behaviour specified by external causes as applied strain is called extrinsic non-linear viscoelasticity. As for filled rubber compounds, the Q1/Q2 is higher than 1 at very low strain, and then quickly decreases until the minimum value is reached as strain increases. At last, the Q1/Q2 increases with increasing strain. The non-linear viscoelastic behaviour through the application of a sufficiently large strain of filled compounds refers to the intrinsic non-linear viscoelasticity. The internal morphology of the rubber compounds is determined. Remarkably, as filler level increases, the non-linear character changes from extrinsic to intrinsic.

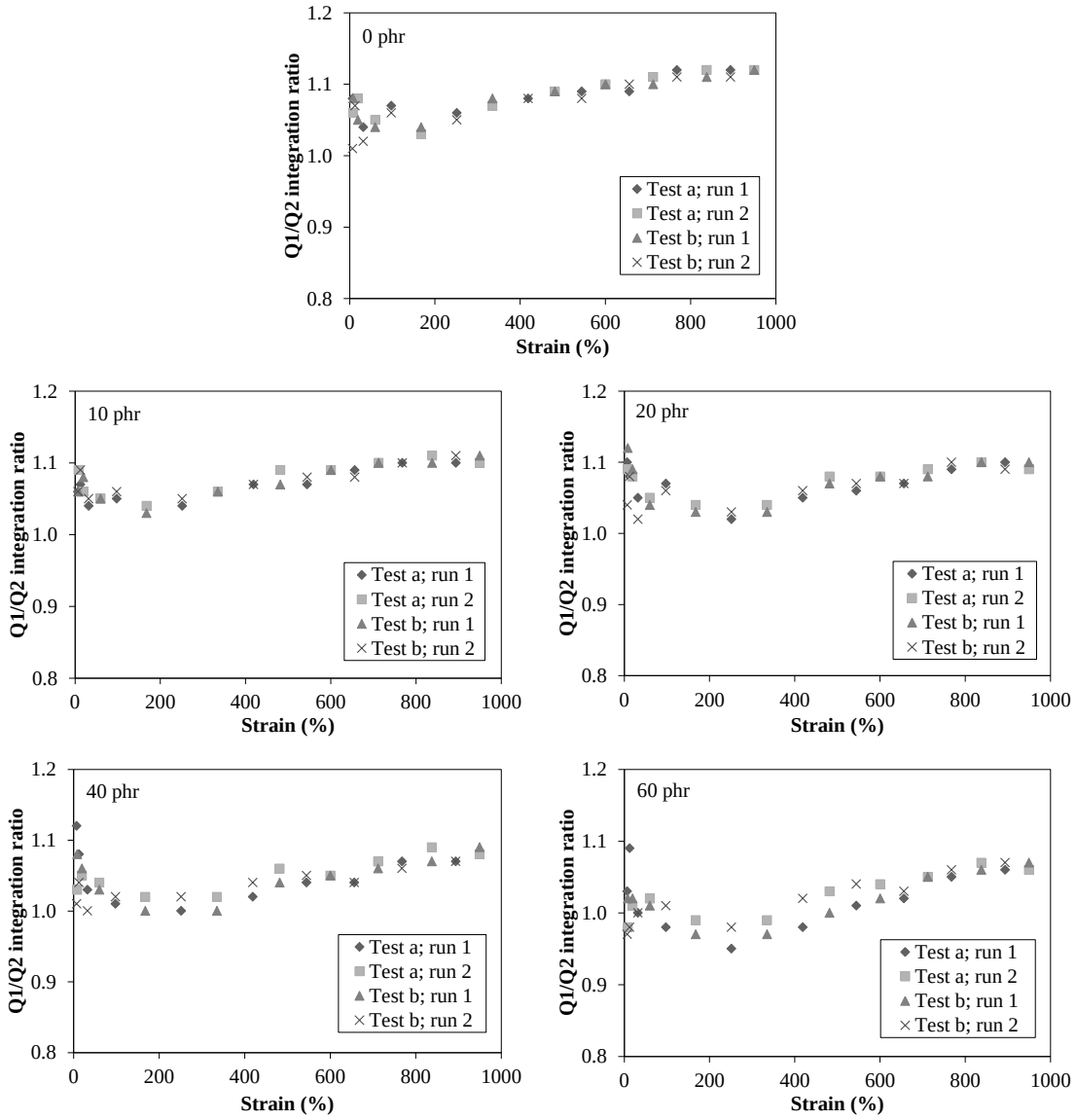

Figure 5.14 RPA-FT at 100°C on HNBR compounds filled with N326 assessing extrinsic or intrinsic non-linear viscoelastic character through the quarter cycle torque integration; strain sweep tests at 3.14 rad/s

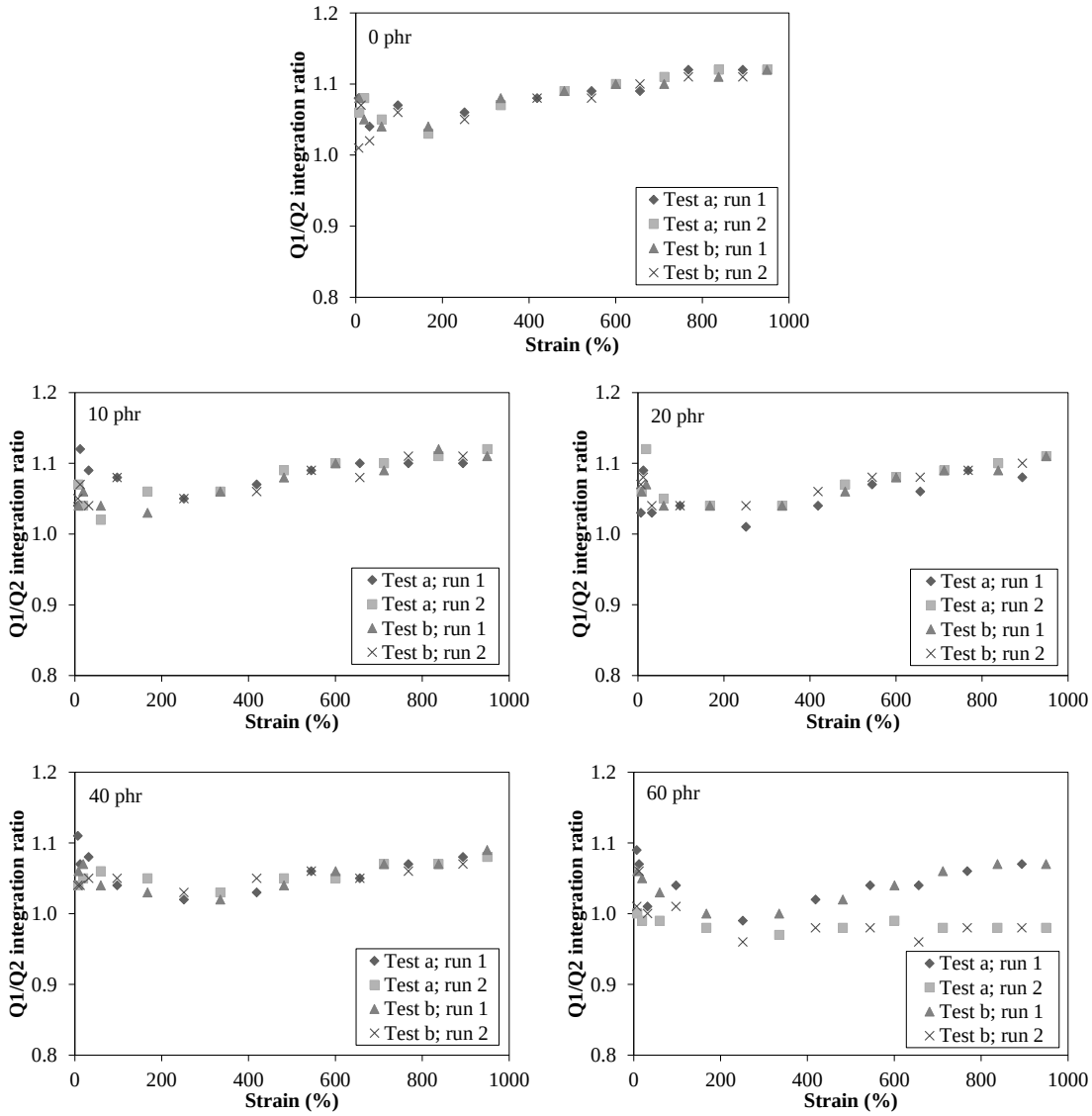

Figure 5.15 RPA-FT at 100°C on HNBR compounds filled with N550 assessing extrinsic or intrinsic non-linear viscoelastic character through the quarter cycle torque integration; strain sweep tests at 3.14 rad/s

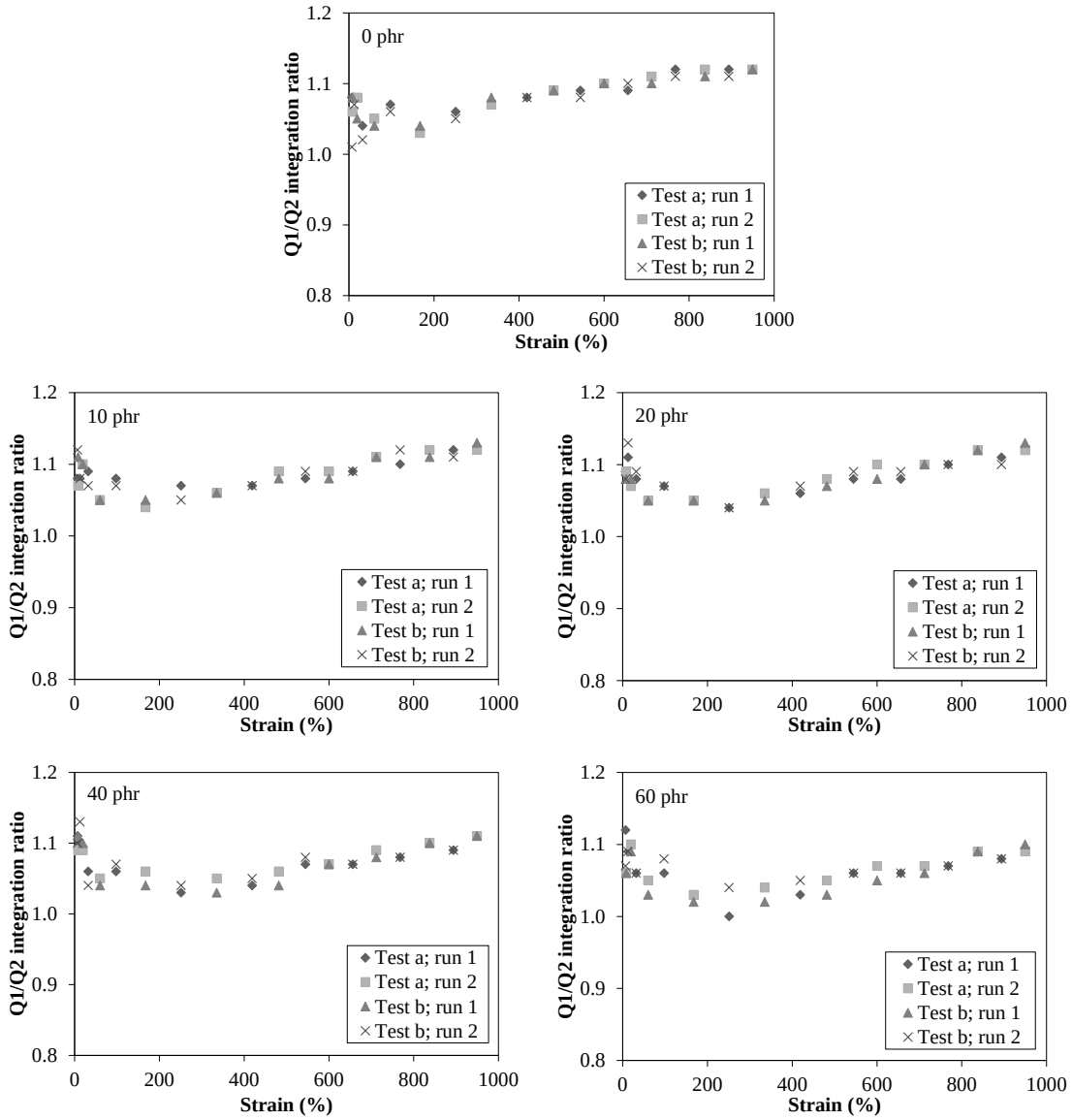

Figure 5.16 RPA-FT at 100°C on HNBR compounds filled with N774 assessing extrinsic or intrinsic non-linear viscoelastic character through the quarter cycle torque integration; strain sweep tests at 3.14 rad/s

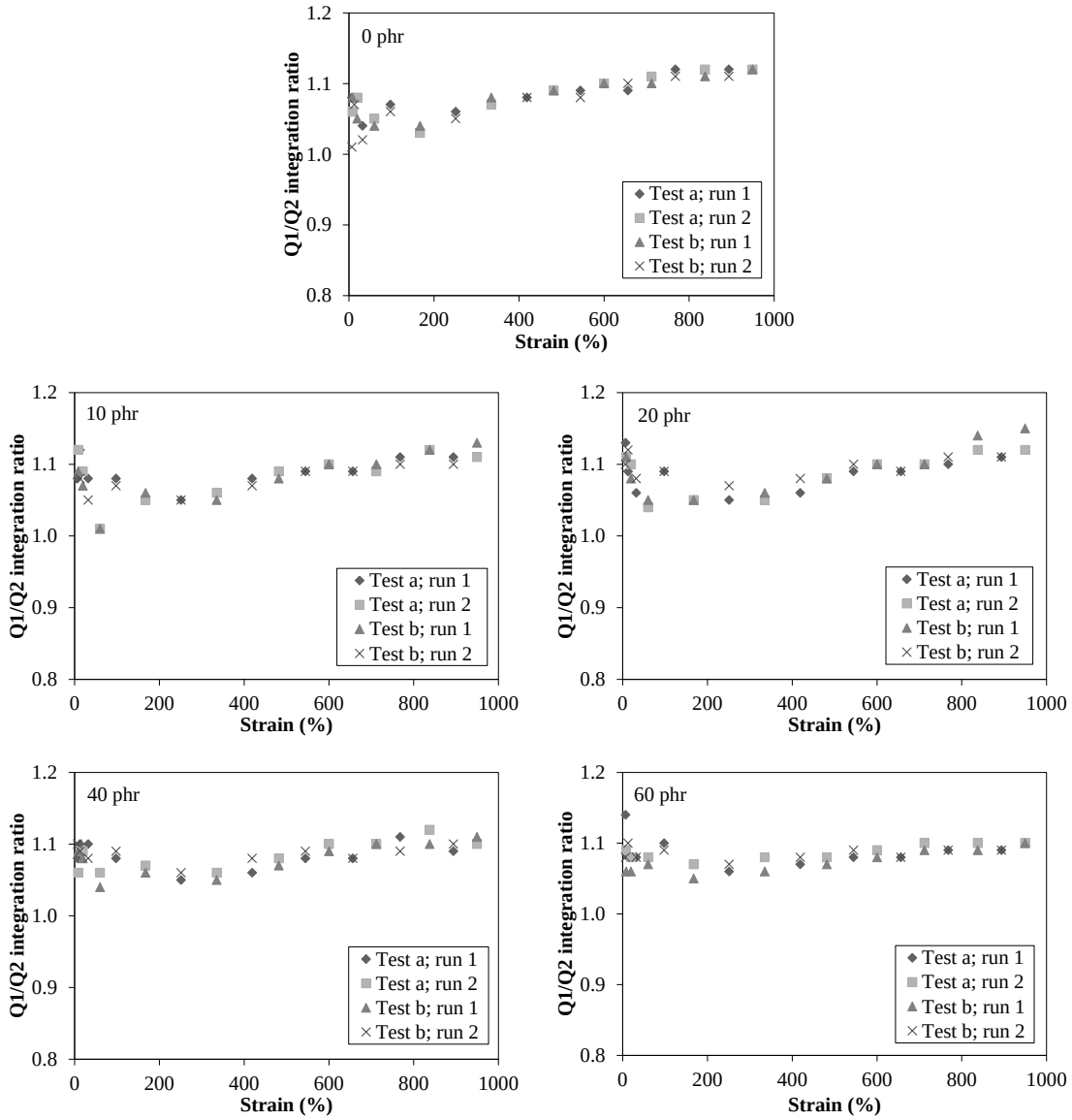

Figure 5.17 RPA-FT at 100°C on HNBR compounds filled with N990 assessing extrinsic or intrinsic non-linear viscoelastic character through the quarter cycle torque integration; strain sweep tests at 3.14 rad/s

The change in non-linear character of filled HNBR compounds with various CB loadings and characteristics is presented in Figures 5.14 to 5.17. It is obvious that the Q1/Q2 ratio at a given strain, i.e., 251.32%, decreases as filler content increases. The CB with large surface area and high structure, i.e., N326 and N550, gives the remarkable decrease, so that, generally speaking, it is clear that the intrinsic

non-linear behaviour of HNBR compounds increases with increasing CB content and characteristics, as shown in Figure 5.18.

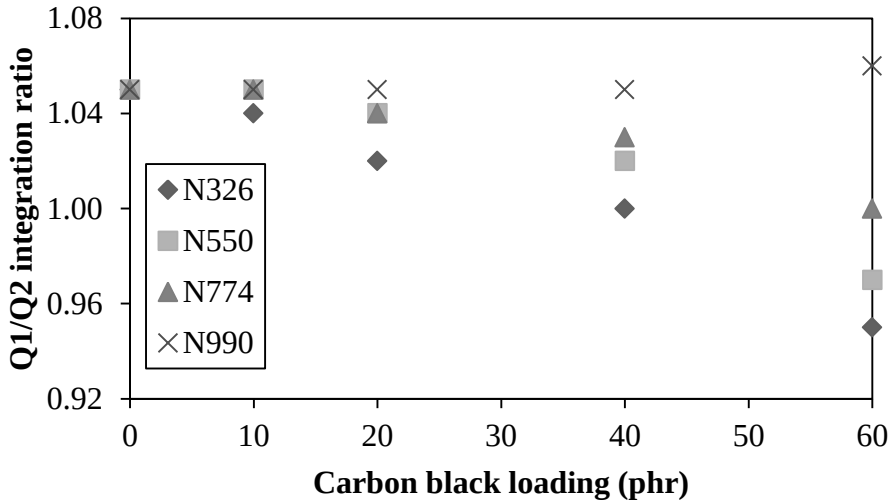

Figure 5.18 Relationship among quarter torque signal integration ratio, carbon black loading and characteristics in HNBR compounds at strain amplitude of 251.32%

b) Cured carbon black filled HNBR systems

In order to use HNBR in different engineering applications, particularly in the areas where the product is subjected to high vibration and pulsating loads, the viscoelastic behaviour, including storage modulus (G′), loss modulus (G″) and damping factor (tanδ), as functions of % strain and temperature must be considered.

Strain sweep test

Figure 5.19 shows the plot of G′ as a function of strain of vulcanised HNBR filled with various loadings and characteristics of CB at the test temperature of 60°C measured by the use of RPA 2000. The G′ of the cured HNBR apparently increases with increasing CB loading for all CB systems, which is a combined result of reinforcement (including, hydrodynamic effect, filler-rubber and filler-filler interactions) and crosslink density. Additionally, the cured HNBR filled with CB loading of 60 phr show a remarkable magnitude of Payne effect, which is

more obvious in the HNBR filled with larger surface area (i.e., the filler three-dimension transient network is a major role).

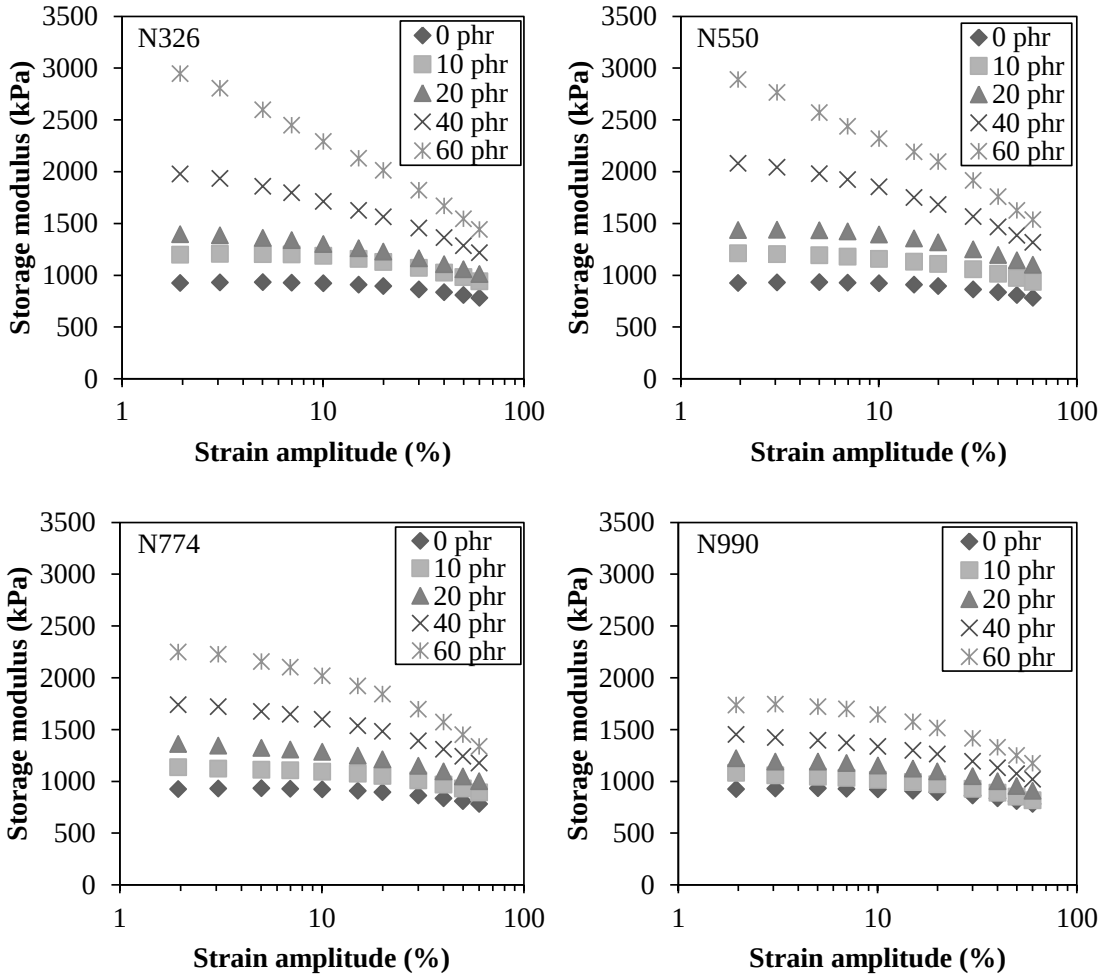

Figure 5.19 Storage modulus (G′) as a function of strain amplitude of filled HNBR vulcanisates with various carbon black loadings and characteristics at test temperature and frequency of 60°C and 1 rad/s, respectively

The effects of CB characteristics on G′ of vulcanised HNBR are exhibited in Figure 5.20, where the G′ at strain amplitude of 10% is plotted as a function of CB loading. It is obvious that the G′ rises with increasing CB surface area, which could be explained by the increase in contacting area available for the interaction between rubber and CB as well as between filler aggregates (or three-dimensional transient filler network). It must be noted that, although the N550 possesses smaller CB specific surface area than the N326, the vulcanisate with N550

shows comparable G′ to that with N326, which is in agreement with the relatively high structure and crosslink density in the vulcanisate filled with N550 (as shown in Figure 5.3).

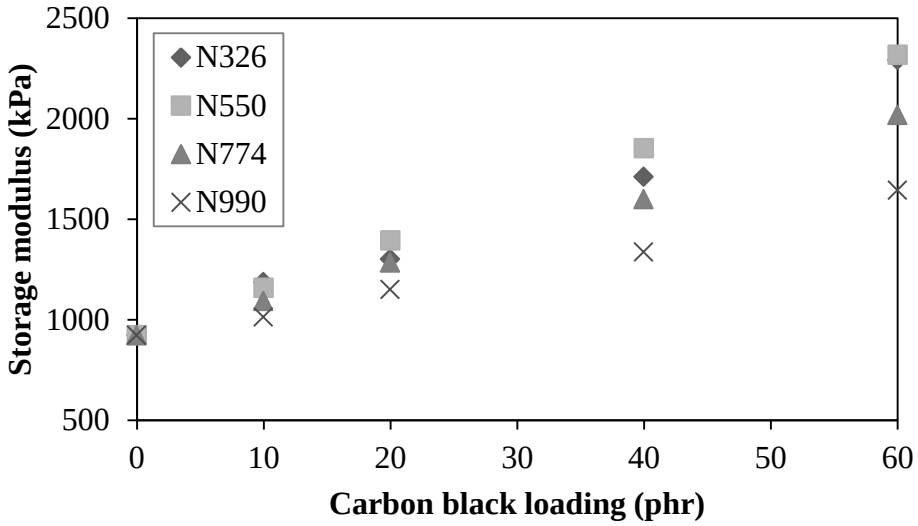

Figure 5.20 Relationship among storage modulus (G′), carbon black loading and characteristics in HNBR vulcanisates at test strain, temperature and frequency of 10%, 60°C and 1 rad/s, respectively

Figure 5.21 reveals the results of G″ versus strain amplitude of HNBR vulcanisates filled with various CB loadings and characteristics. Evidently, the G″ of all vulcanisates increases with increasing CB loading regardless of the strain amplitude. This is because of the effect of CB reinforcement and crosslink density, as discussed in the G′ results. It is reported that the G″ is dependent on rates of transient network breakdown and reformation processes under dynamic strain, and the processes of filler network breakdown and reformation cause additional energy dissipation (21). The breakdown magnitude of filler network increases with increasing strain amplitude while the reformation of this structure takes place instantly, thus the strain independence of G″ is observed. On the other hand, if filler network is destroyed and the reconstruction takes place slower than its disruption, the strain independence of G″ will be invalid. Therefore, the decrease in G″ with strain amplitude is observed.

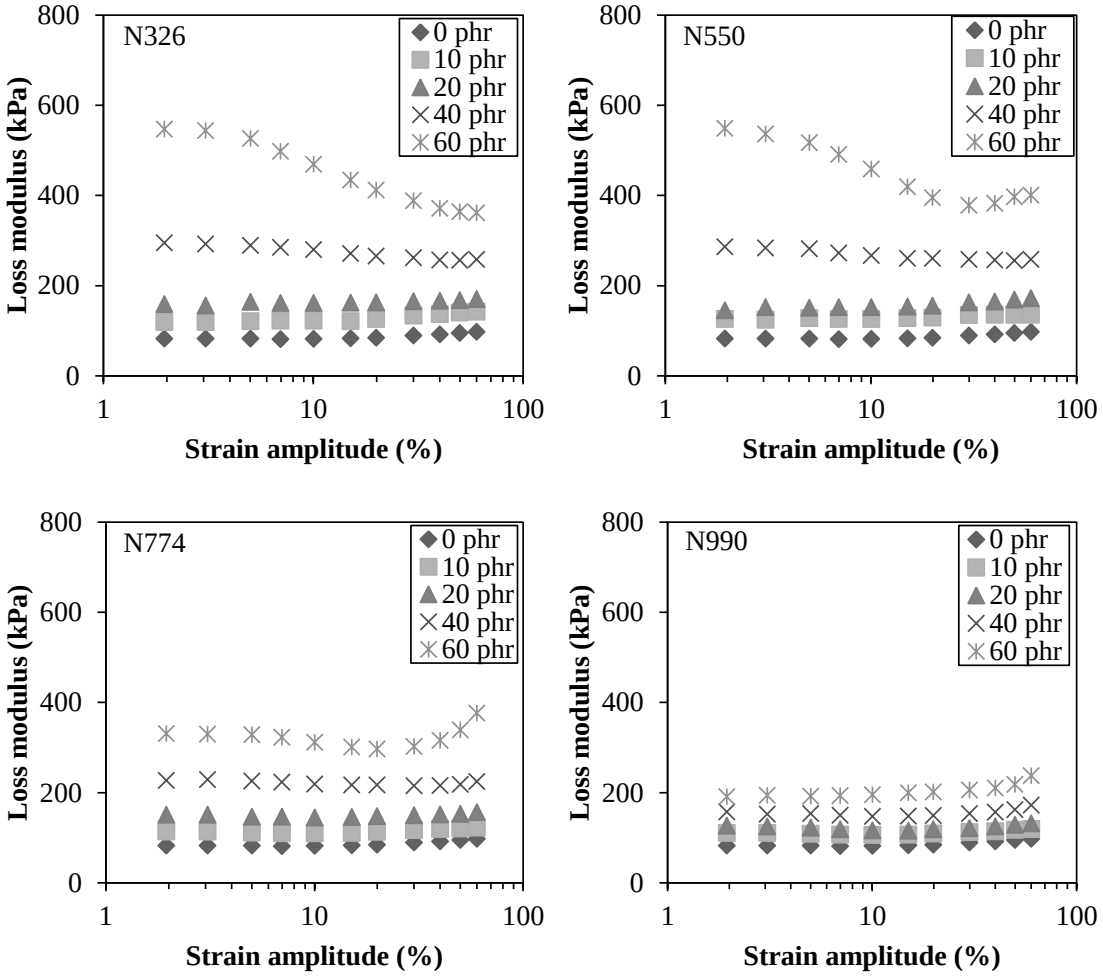

Figure 5.21 Loss modulus (G″) as a function of strain amplitude of filled HNBR vulcanisates with various carbon black loadings and characteristics at test temperature and frequency of 60°C and 1 rad/s, respectively

In HNBR vulcanisates filled with CB loading up to 40 phr, the G″ appears to be independent of strain up to around 30%, and then slightly increase with increasing shear strain. The increase in G″ at high strain could be caused by the viscous dissipation via molecular flow at CB surfaces. By contrast, with CB loading of 60 phr (except for N990 filled vucanisate), where the magnitude of filler transient network is relatively large (see Figure 5.19), the HNBR vulcanisates initially reveal the reduction in G″ with strain amplitude followed by the somewhat rise in G″ at high strain. The reduction in G″ is in good accordance with the fact that the transient filler network is destroyed and could not be fully reconstructed. At high strain of

deformation where the filler transient network is already disrupted, the viscous dissipation via molecular flow at CB surfaces is believed to be responsible for the slight increase in G″. The influence of CB characteristics on G″ of HNBR vulcanisates is illustrated in Figure 5.22. Evidently the specimens with high magnitude of filler network demonstrate high value of G″.

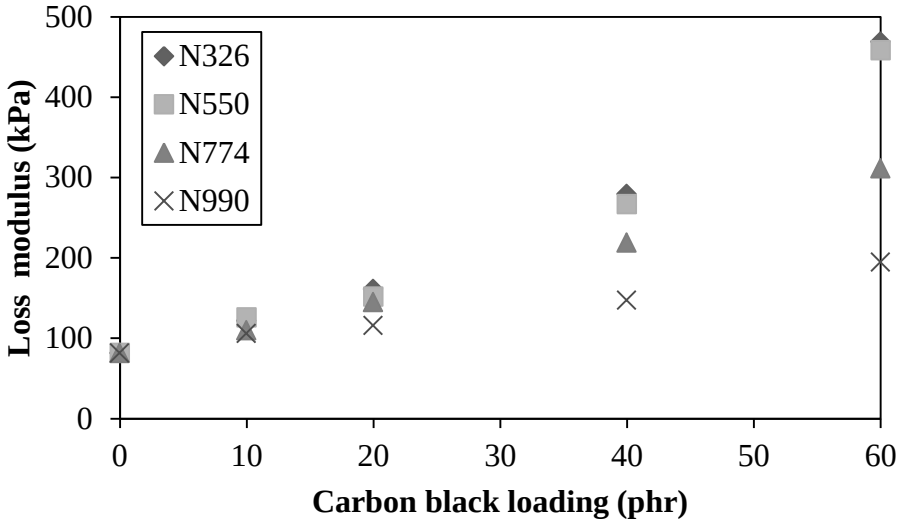

Figure 5.22 Relationship among loss modulus (G″), carbon black loading and characteristics in HNBR vulcanisates at test strain, temperature and frequency of 10%, 60°C and 1 rad/s, respectively

Figure 5.23 demonstrates the alteration in damping factor or tanδ, which is the ratio of loss to storage moduli, as a function of deformation strain. In general, the damping factor could be used to imply the magnitude of viscous response per unit of elastic response. It is evident that the damping factor of all vulcanisates increases with increasing strain amplitude, indicating the rise in magnitude of viscous contribution dominating over the elastic one. The increase in damping factor is reported to be the result of energy dissipation through a molecular slippage associated with the breakdown of the three dimensional filler transient network. This phenomenon is sometimes known as hysteretic process (17).

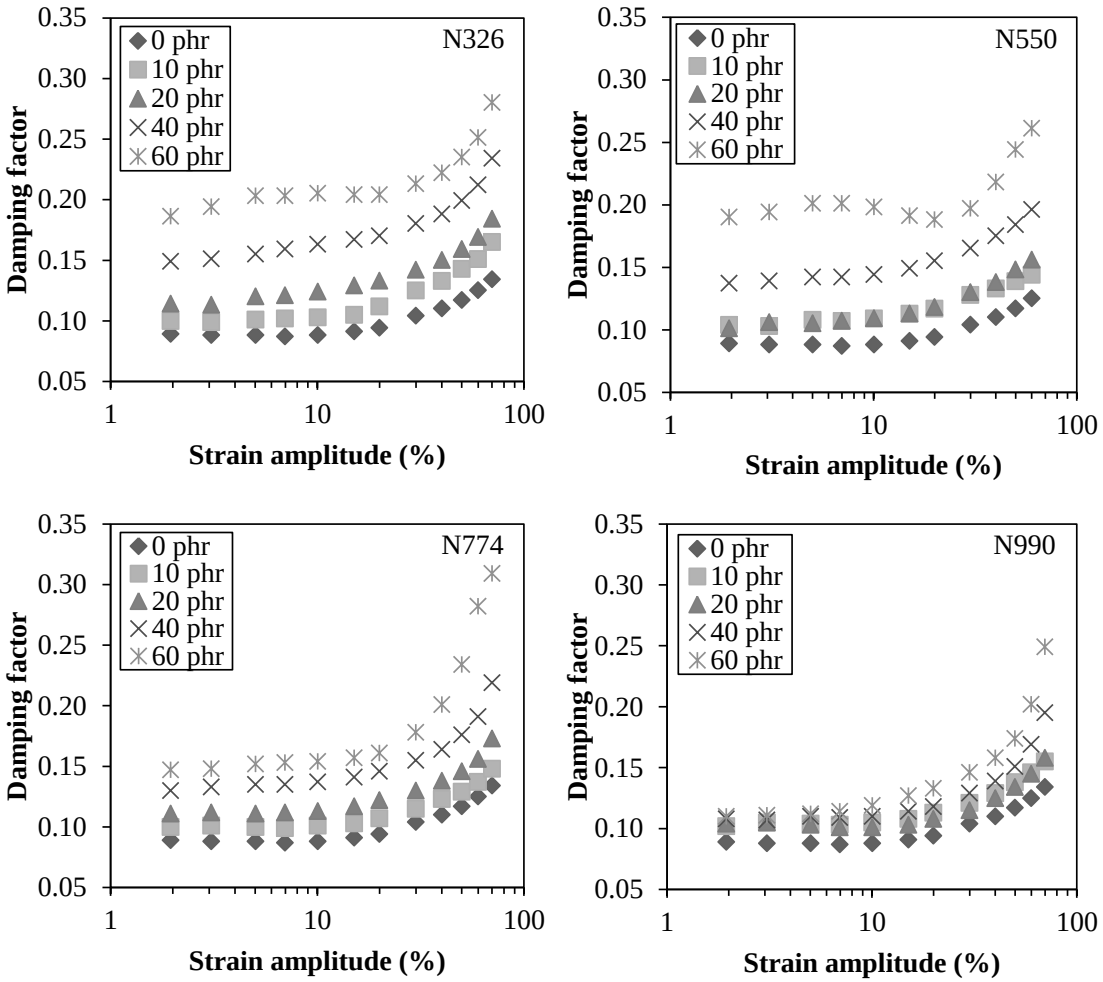

Figure 5.23 Damping factor (tanδ) as a function of strain amplitude of filled HNBR vulcanisates with various carbon black loadings and characteristics at test temperature and frequency of 60°C and 1 rad/s, respectively

In the case of CB characteristics effect on damping factor of filled vulcanisates, it is clearly seen from Figure 5.24 that the damping factor increases as the specific surface area of CB increases. As mentioned in CB loading effect, the increase in contacting area (by increasing surface area in this case) available for physical interaction between rubber and CB would lead to the rise in energy dissipation via molecular flow at the CB surfaces.

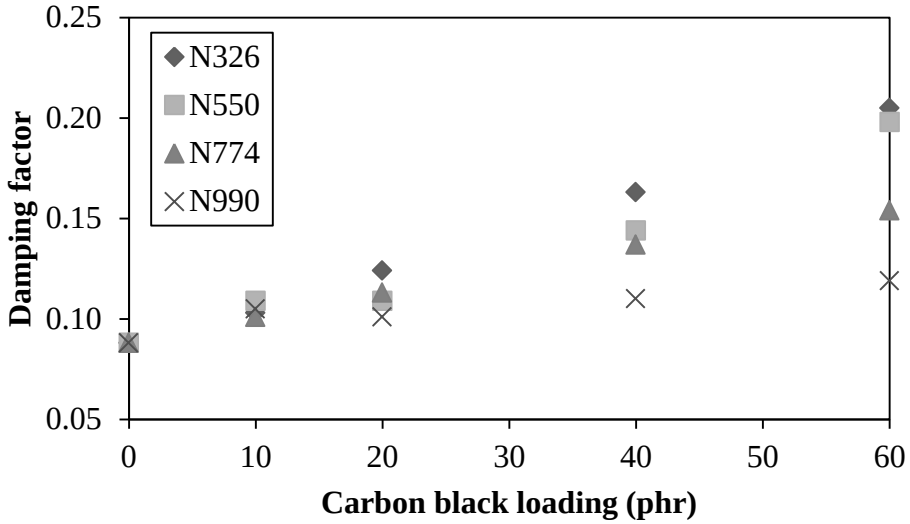

Figure 5.24 Relationship among damping factor (tanδ), carbon black loading and characteristics in HNBR vulcanisates at test strain, temperature and frequency of 10%, 60°C and 1 rad/s, respectively

Temperature sweep test

Figures 5.25 to 5.30 reveal that the filler loading can influence temperature dependence of G′, G″ and tanδ of filled vulcanisates as measured from DMA (Gabo, Explexor^{TM} 25N). Figure 5.25 exhibits that the G′ of the whole temperature range increases with CB loading, which is attributed to the filler reinforcement effect, i.e. hydrodynamic effect, filler-filler interaction as well as filler-rubber interaction, and the crosslink density effect, as discussed previously.

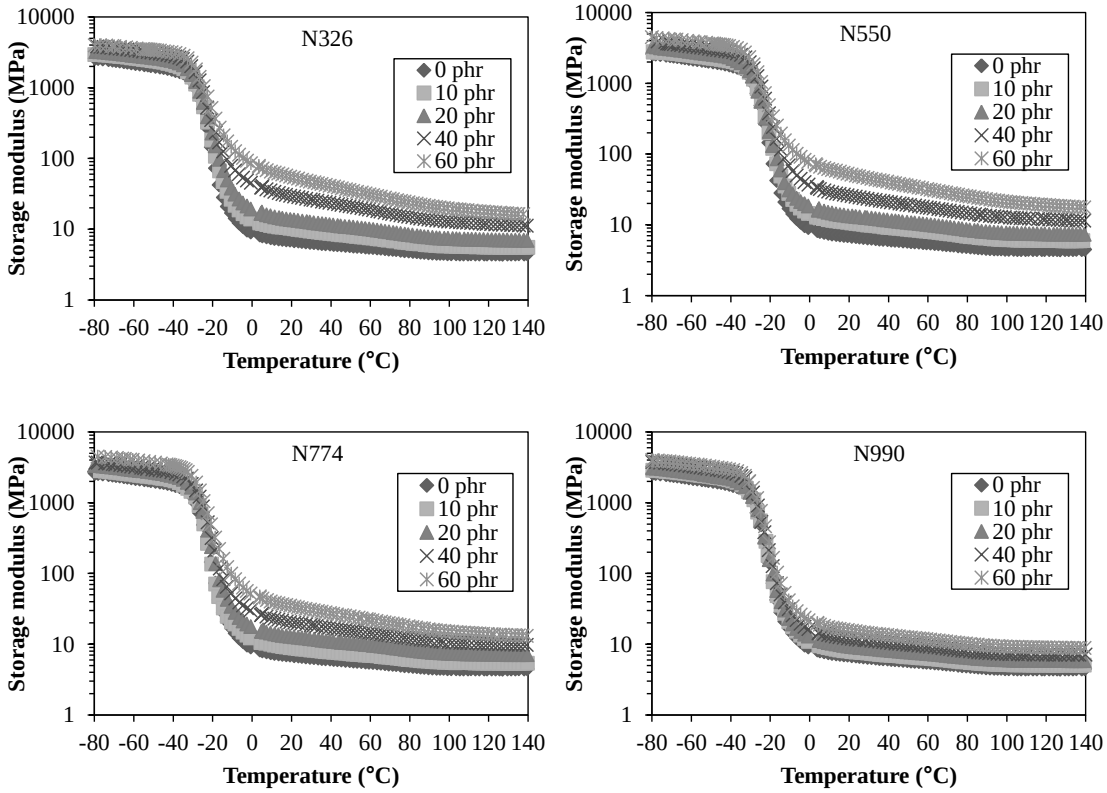

Figure 5.25 Storage modulus (G′) as a function of temperature of filled HNBR vulcanisates with various carbon black loadings and characteristics at test static strain, dynamic strain and frequency of 2%, 0.1% and 62.8 rad/s, respectively

Figure 5.26 illustrates the influences of CB characteristics on G′ of filled vulcanisates. As expected, the values of G′ agree well with those determined from the strain sweep test, as evidenced earlier in Figure 5.19. The vulcanisates filled with N550 exhibit the comparable G′ to those with N326, which is due to the balancing effects of crosslink density and surface area.

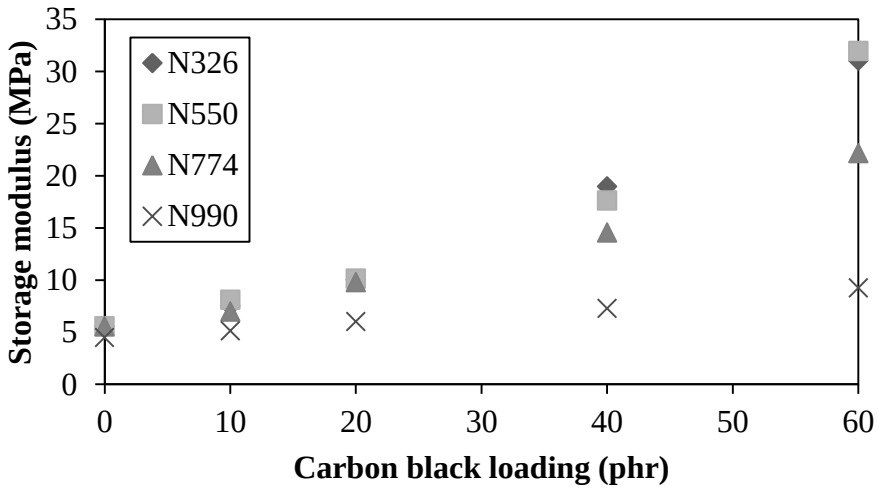

Figure 5.26 Relationship among storage modulus (G′), carbon black loading and characteristics in HNBR vulcanisates at test static strain, dynamic strain, frequency and temperature of 2%, 0.1%, 62.8 rad/s and 60°C, respectively

Figure 5.27 shows a temperature dependence of G″ in HNBR vulcanisates with different CB loadings. It can be seen that the G″ increases with increasing CB loading over the range of temperature investigated. It is well known that the G″ can be used as representative of the energy dissipated as heat, which is sometimes called as hysteresis loss. The incorporation of filler into rubber increases the energy dissipation resulting in increasing hysteresis. The different CB characteristics give different responses to the temperature dependence of the hysteresis loss.

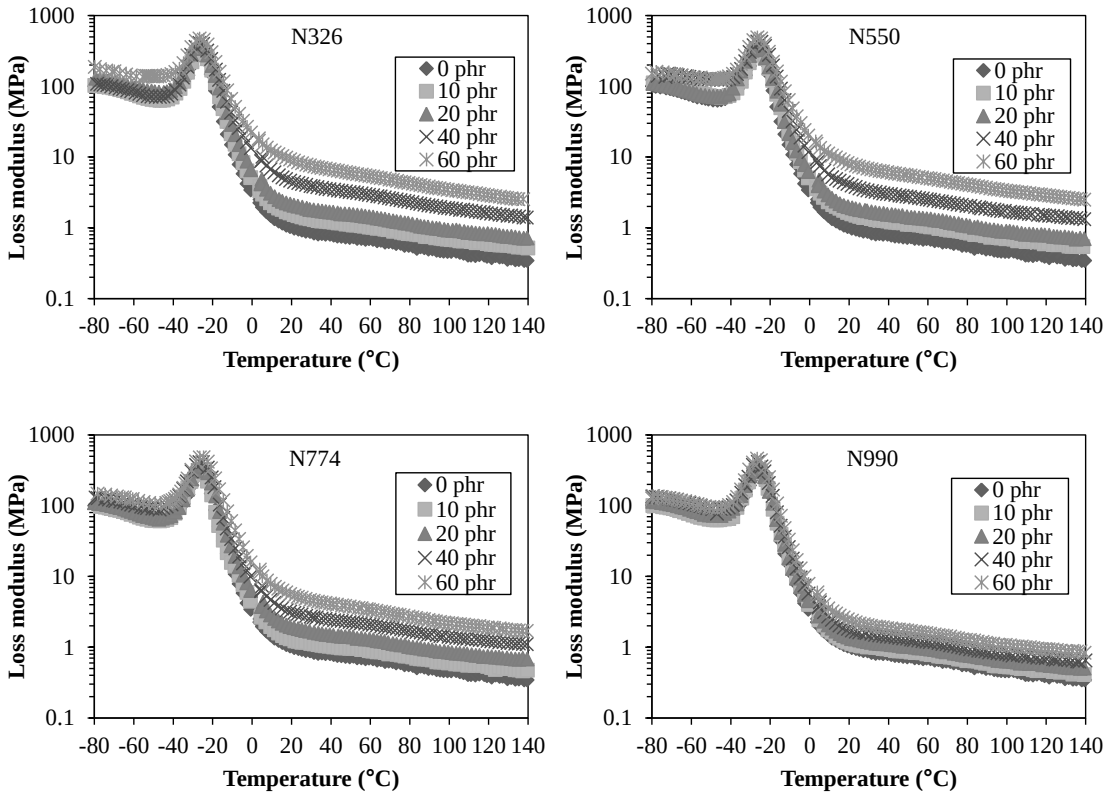

Figure 5.27 Loss modulus (G″) as a function of temperature of filled HNBR vulcanisates with various carbon black loadings and characteristics at test static strain, dynamic strain and frequency of 2%, 0.1% and 62.8 rad/s, respectively

The effects of CB characteristics on the hysteresis loss at 60°C (in the rubbery region) are revealed in Figure 5.28. Undoubtedly, the G″ increases with the incorporation of CB having relatively high surface area in HNBR vulcanisates. As mentioned previously, the rise in magnitude of three-dimension transient network results in the larger portion of energy dissipation of the vulcanisates, leading to the increase in hysteresis loss.

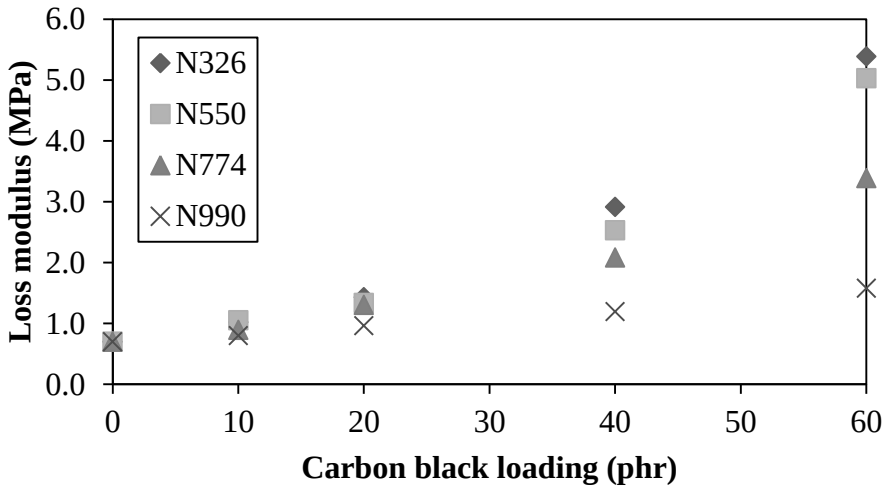

Figure 5.28 Relationship among loss modulus (G″), carbon black loading and characteristics in HNBR vulcanisates at test static strain, dynamic strain, frequency and temperature of 2%, 0.1%, 62.8 rad/s and 60°C, respectively

Figure 5.29 reveals tanδ results over a temperature range from -80 to 140°C. It can be seen that, the tanδ peaks of filled HNBR decreases with increasing CB loading due mainly to: (i) the reduction in rubber volume fraction by the CB incorporated (dilution effect) and (ii) the restricted molecular mobility (or HNBR segmental motions) via the increased filler-rubber interaction. The dilution effect and the interaction between filler and rubber result in increased G′ with lowered energy dissipation. Generally, the increase in filler-rubber interaction leads to a shift in T_g to the high temperature as a result of molecular restriction. From Figure 5.28, the T_g does not change with increasing CB loading, which is due to the temperature tolerance of ± 2°C of DMTA.

On the contrary, the tanδ in the rubbery region appears to increase with increasing CB loading, which is consistent with the results measured from the strain sweep test as shown previously in Figure 5.24. The hysteresis is responsible for the change in tanδ, which is increased by the incorporation of CB. The higher tanδ in rubbery region would cause the higher extent of heat build-up found in rubber product under vibration condition.

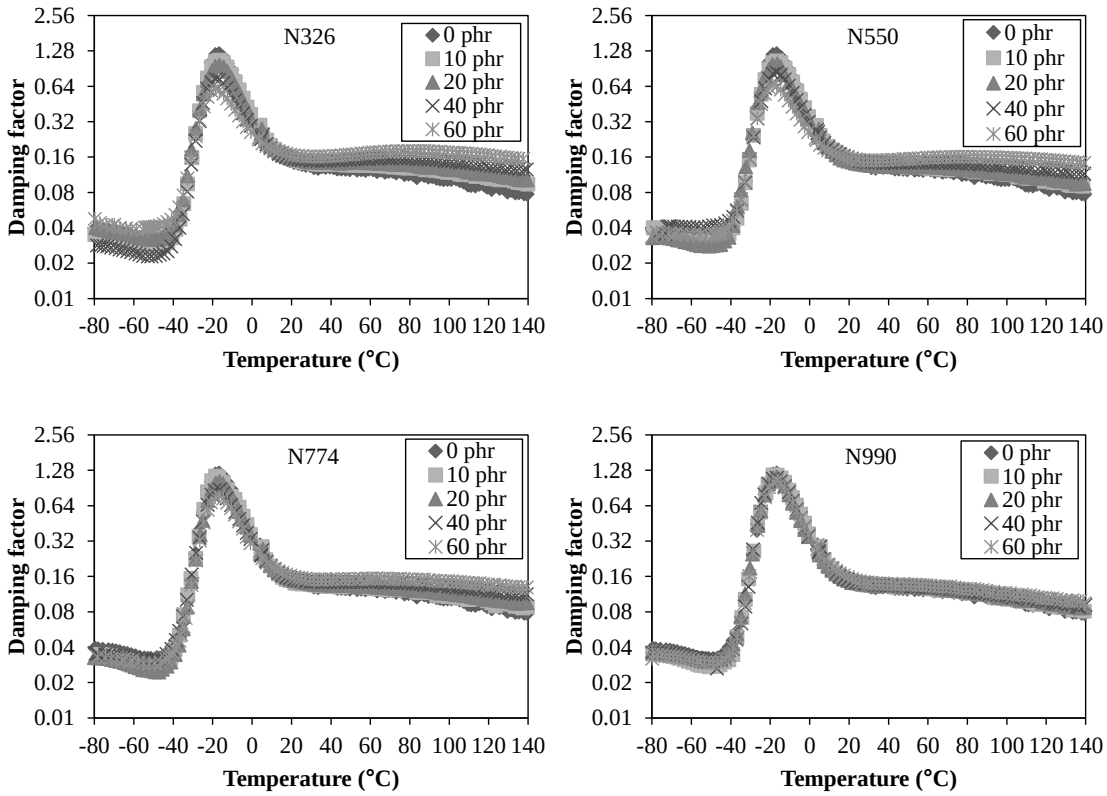

Figure 5.29 Damping factor (tanδ) as a function of temperature of filled HNBR vulcanisates with various carbon black loadings and characteristics at test static strain, dynamic strain and frequency of 2%, 0.1% and 62.8 rad/s, respectively

At any given CB loading, the characteristics of CB, i.e., surface area and structure give different responses to the temperature dependence of tanδ. The effects of CB characteristics on tanδ at the T_g and 60°C are illustrated in Figure 5.30. Apparently, the tanδ at T_g is diminished, and the tanδ at 60°C is increased by increasing surface area of CB. The interaction between filler and rubber is utillised as an explanation. It is well known that the CB having larger surface area shows the stronger rubber-filler interaction. Wang (21) explained that the stronger rubber-filler interaction would result in greater immobilised rubber shell, causing the effective volume of filler increases. Thus, the lower hysteresis at T_g and the higher increase in hysteresis at 60°C are resulted.

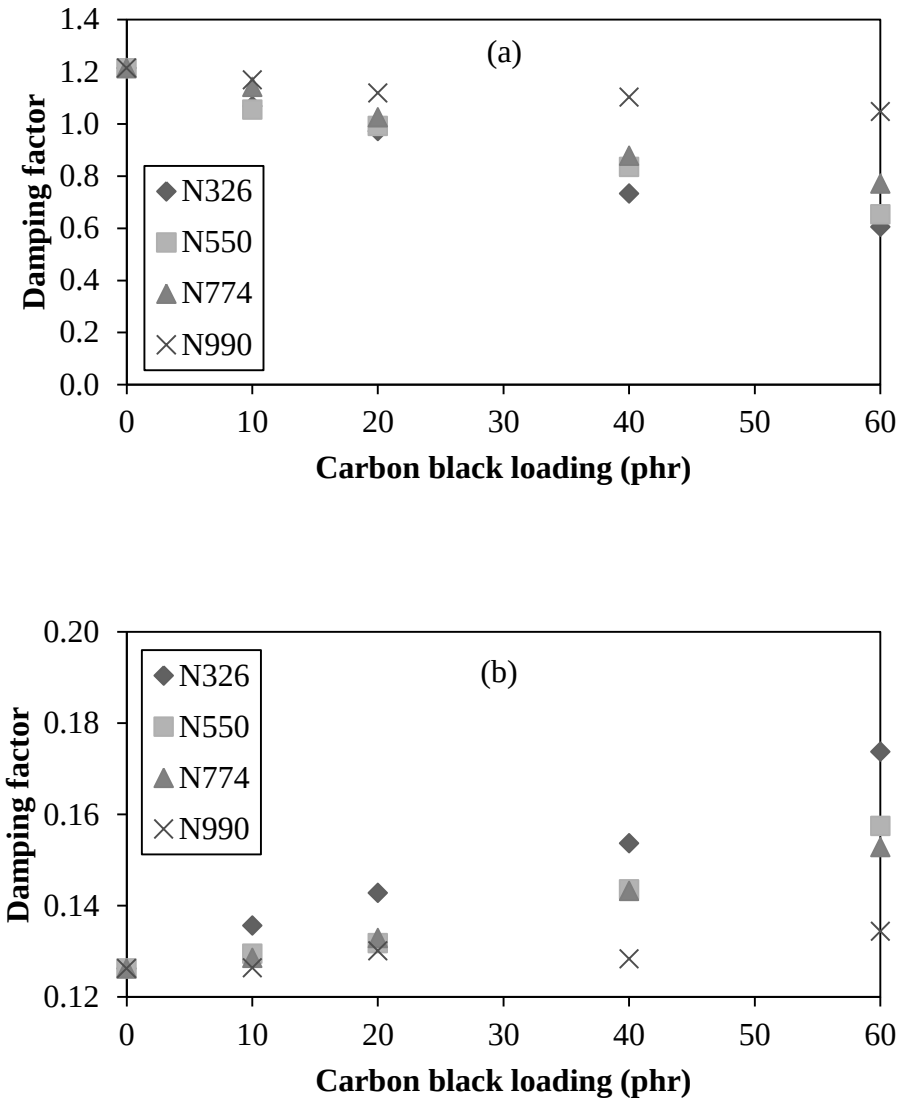

Figure 5.30 Relationship among damping factor (tanδ) carbon black loading and characteristics in HNBR vulcanisates at test static strain, dynamic strain, frequency of 2%, 0.1%, 62.8 rad/s, respectively: (a) at the glass transition temperature; (b) 60°C

5.1.1.3 Filler dispersion and distribution

Scanning electron microscopy (SEM) is used to study dispersion of CB in HNBR matrix. Figure 5.31 reveals SEM micrographs of the N550 filled HNBR vulcansates with various CB loadings. The CB phase in vulcanisates appears as bright spots in the micrographs. It can be seen that the CB disperses

thoroughly in the HNBR matrix. The degree of CB dispersion and distribution in HNBR matrix can be observed in detail by the the statistical processing of SEM micrographs using the quadrate method and Morishita's Index (I_δ) value (49) (see also section 3.2.1 for measurement).

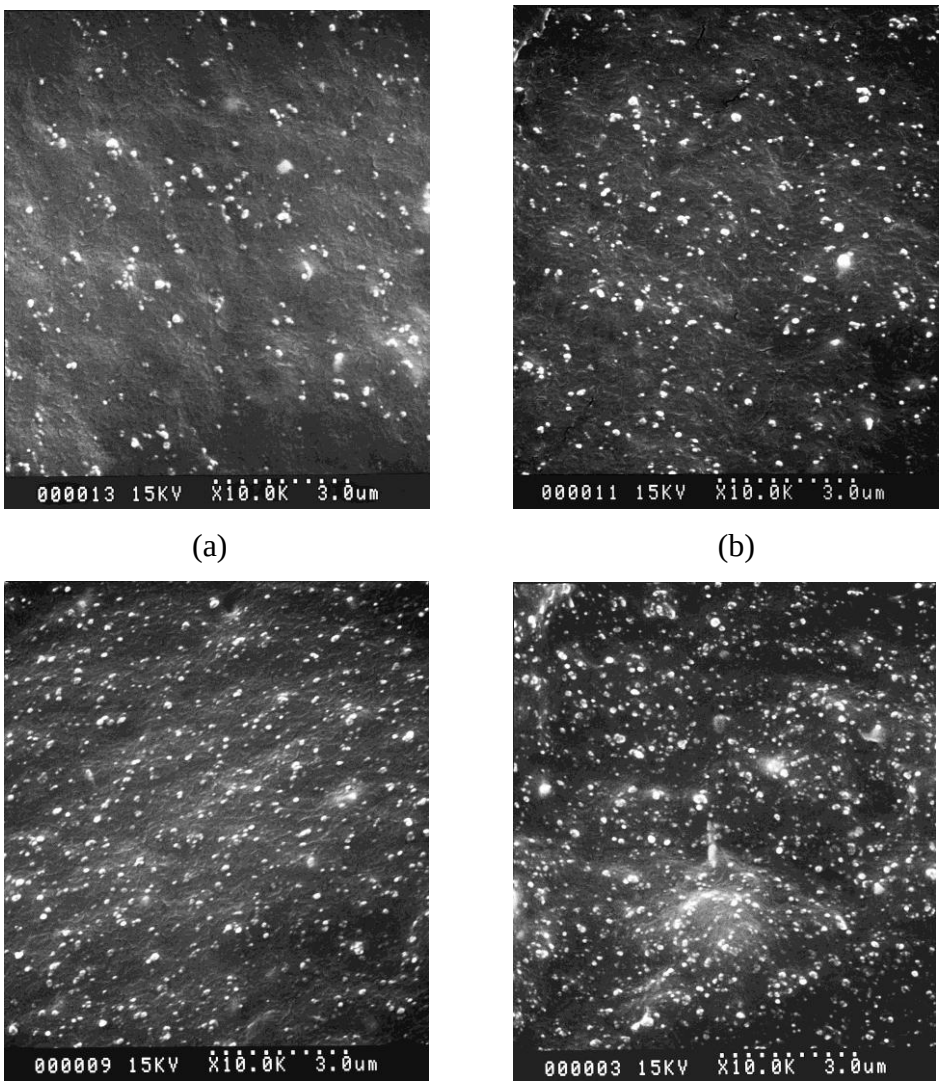

Figure 5.31 SEM micrographs of HNBR vulcanisates filled with various N550 loadings: (a) 10 phr; (b) 20 phr; (c) 40 phr; (d) 60 phr

The relationship between Morishita's index (I_δ) and quadrate number (q) for various distribution modes of particles is presented in Figure 5.32. Both values are utilised as a tool in a characterisation of filler dispersion and

distribution (49). The results are explained according to the schematic representation as shown previously in Figure 3.6 (section 3.2.1). Apparently, the cured HNBR systems filled with low CB loadings, i.e., 10 and 20 phr, show aggregate distribution in which the size of each aggregate is large, and the particles are distributed in regular mode in each aggregate (see Figure 3.6e). The filler agglomerates could be broken down more effectively by an increase in bulk viscosity (i.e., the increase in shear stress). The increase in bulk viscosity depends on filler loading, i.e., the higher the filler loading, the higher the bulk viscosity. Thus, the HNBR vulcanisate filled with CB loading of 40 phr reveals distribution mode as illustrated in Figure 3.6f, i.e., the size of each aggregate is small and the particles are distributed in regular mode in each aggregate. However, the incorporation of excessive CB leads to the filler agglomeration. Consequently, the CB particles are distributed in Poisson's mode (see Figure 3.6d) as evidenced in the vulcanisate filled with CB loading of 60 phr.

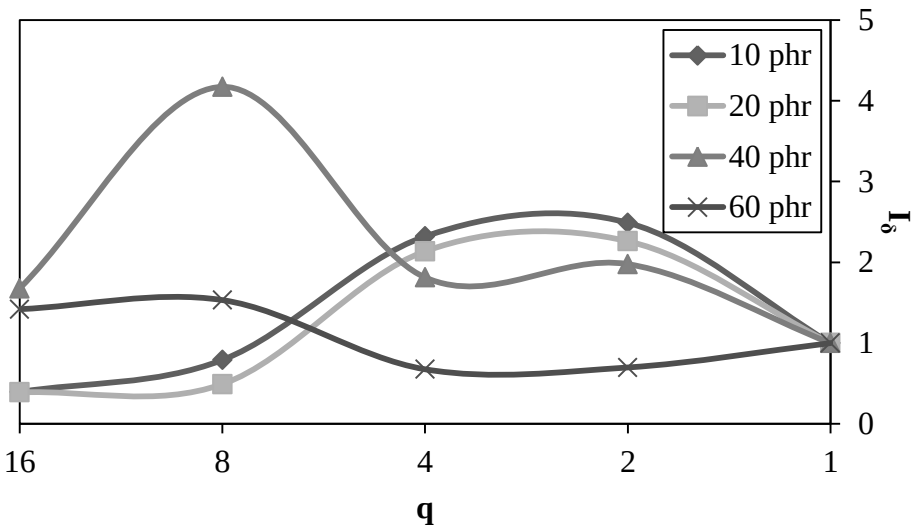

Figure 5.32 Morishita's index (I_δ) for HNBR vulcanisates filled with various N550 loadings as a function of quadrat number (q)

Regarding the effects of CB characteristics on the dispersion and distribution of filler, the SEM micrographs are revealed in Figure 5.33. At a given state-of-mix, the filler dispersion magnitude generally increases with increases in particle size (decreasing surface area) and structure of CB. The large particle size

enhances wetting and incorporation efficiencies while the high structure increases the viscosity of the compound, thereby leading to shear stresses available for a disruption of CB agglomerates (28).

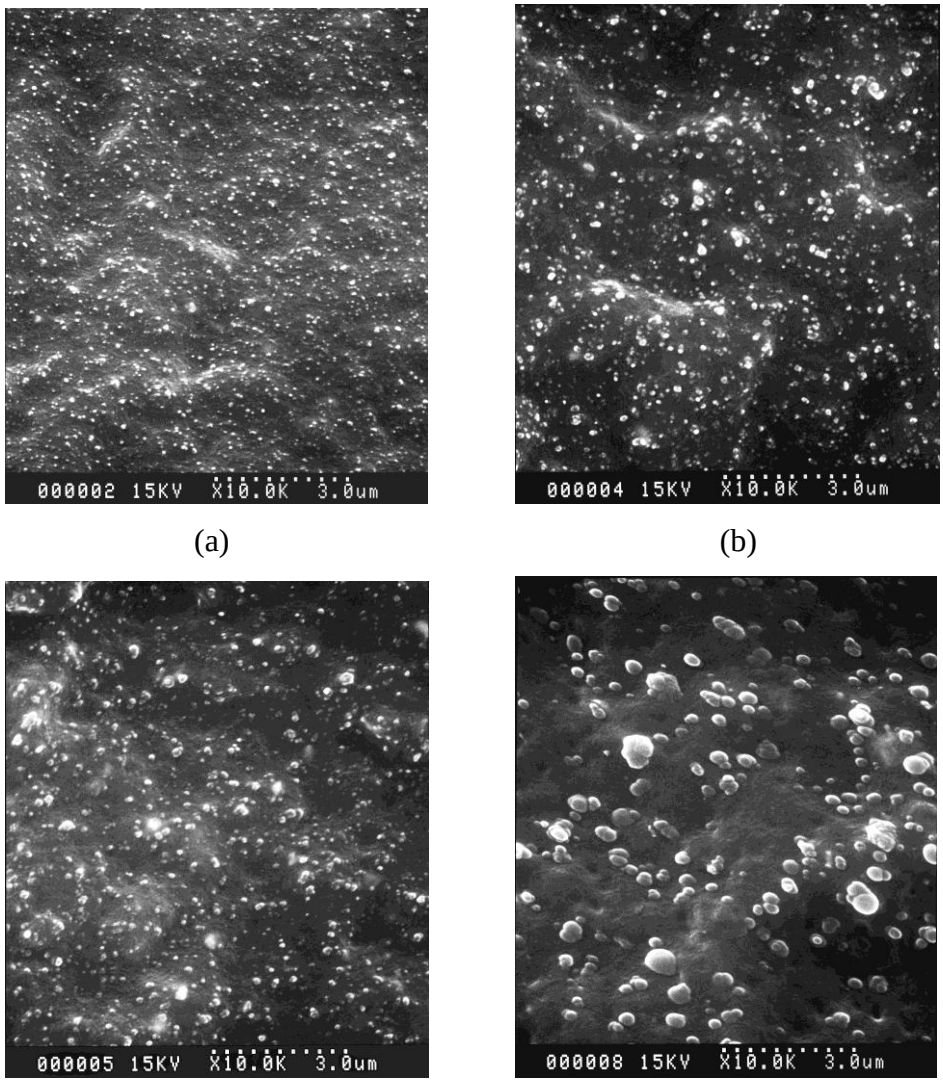

(a) (b)

(c) (d)

Figure 5.33 SEM micrographs of HNBR vulcanisates filled with various carbon black characteristics: (a) N326; (b) N550; (c) N774; (d) N990

Figure 5.34 illustrates the I_{δ} result of filled HNBR vulcanisates with various CB surface areas and structures as a function of q. The HNBR vulcanisates filled with N326, N550 and N774 show the distribution mode in the direction of Figure 3.6d, i.e., the distribution of each small aggregate is in Poisson's

mode. However, the distribution mode of the HNBR vulcanisates filled with N550 and N774 approach the Poisson's mode more obviously than those filled with N326, meaning the filler dispersion of N326 is poorer. Expectedly, the distribution mode of the HNBR vulcanisates filled with N990 follows the distribution in the same way as shown in Figure 3.6e, the particles in each large aggregate are distributed in the regular mode, which is due to the increased wetting and incorporation efficiencies as discussed previously.

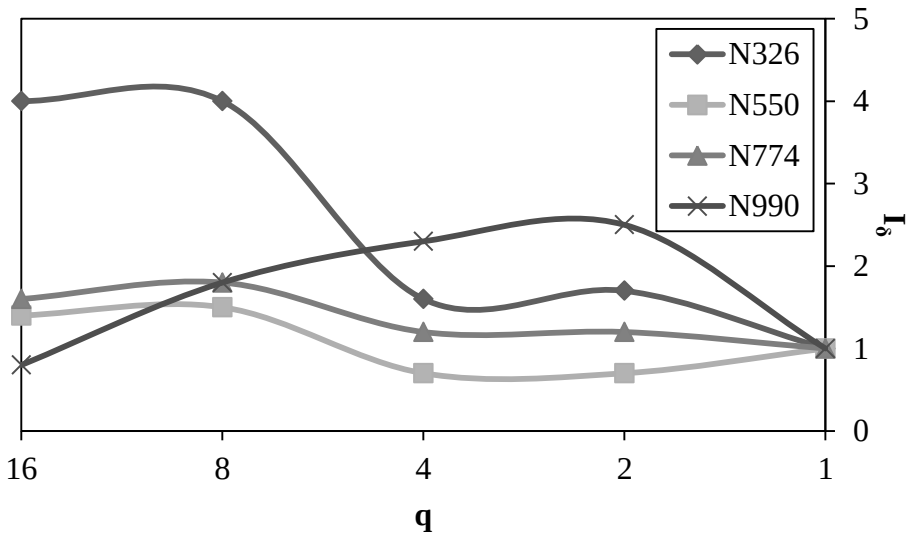

Figure 5.34 Morishita's index (I_δ) for HNBR vulcanisates filled with various carbon black characteristics as a function of quadrat number (q)

5.1.1.4 Mechanical properties

Mechanical properties of HNBR vulcanisates as functions of CB loading and specific surface area are shown in Figures 5.35 to 5.40. It is evident from Figure 5.35 that the modulus at 100% strain (M100) of cured HNBR increases with increasing CB loading and/or specific surface area. There are two main factors controlling the M100 of vulcanisates, namely, the crosslink density and the filler reinforcement. According to Figure 5.3, the crosslink density apparently increases with CB loading, and the increased crosslink density would thus yield the greater resistance to deformation via covalent bonds between rubber chains. Based on the results of the viscoelastic behaviour (Figures 5.20 and 5.24), the increase in damping

factor as functions of CB loading and specific surface area is in good agreement with the increase in the M100 of the corresponding vulcanisates. The increased CB loading and specific surface area mean a rise in contacting positions available for interaction between rubber molecules and CB surfaces. Also, the dilution of rubber molecules by undeformable filler particles (or the hydrodynamic reinforcement) could be another part of reasons for an enhancement in the M100. Notably, the M100 of vulcanisates with CB N550 appears to be close to that of CB N326 and becomes greater at high CB loading (60 phr) despite the relatively small specific surface area of CB N550. The results trend is similar to the one observed for G′ results discussed earlier. Thus, it is proposed that the reinforcement provided by N550 is governed mainly by the crosslink density enhancement rather than the rubber-filler interaction.

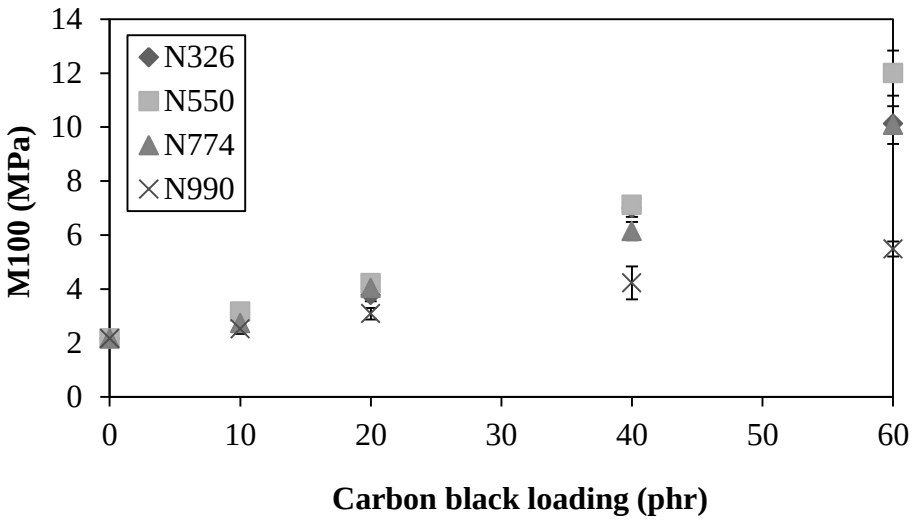

Figure 5.35 Relationship among modulus at 100% strain (M100), carbon black loading and characteristics in HNBR vulcanisates

The tensile strength results of filled HNBR vulcanisates are shown in Figure 5.36. It is evident that the tensile strength of HNBR vulcanisates increases with increasing CB loading, which could be explained by the filler reinforcement and/or crosslink density effects. Furthermore, it can be seen that the tensile strength of HNBR filled with high specific surface area CBs is apparently superior to the ones observed with low specific surface area CBs, which is typically

caused by filler reinforcement, as mentioned previously. However, an excessive crosslink density found particularly in vulcanisate filled with N550 might restrict molecular mobility, and thus a reduction in energy dissipation during being strained. This would end up with a decrease in mechanical strength (101). One might notice that the tensile strength of vulcanisate filled with N774 at high loading (60 phr) is highest among vulcanisates with N326, N550 and N990. The lowest tensile strength found in cured N990 filled HNBR systems is not surprising as the N990 possesses relatively small specific surface area and low structure (low DBPA value) and thus the low rubber-filler interaction. The apparently low tensile strength observed in N326 filled HNBR vulcanisates at high loading is probably attributed to its relatively poor dispersion in HNBR as discussed in Figure 5.34. It is known that the capability of CB incorporation, distribution and dispersion is reduced with increasing specific surface area of the filler. Thus, some of undispersed N326 agglomerates might act as flaws in specimens leading to a reduction in tensile strength. In the case of cured N550 filled HNBR vulcanisates, the excessive crosslink density might be responsible for a relatively low tensile strength.

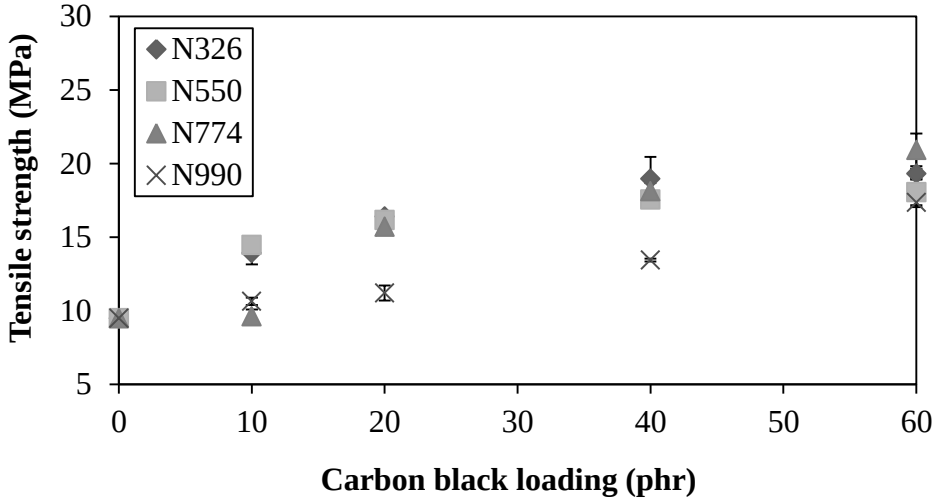

Figure 5.36 Relationship among tensile strength, carbon black loading and characteristics in HNBR vulcanisates

Results of elongation at break (%EB) as illustrated in Figure 5.37 agree well with the tensile strength results, i.e., the greater the reinforcement, the lower the %EB. High extents of crosslink density and rubber-filler interaction would restrict molecular deformation and thus leads to a decrease in %EB.

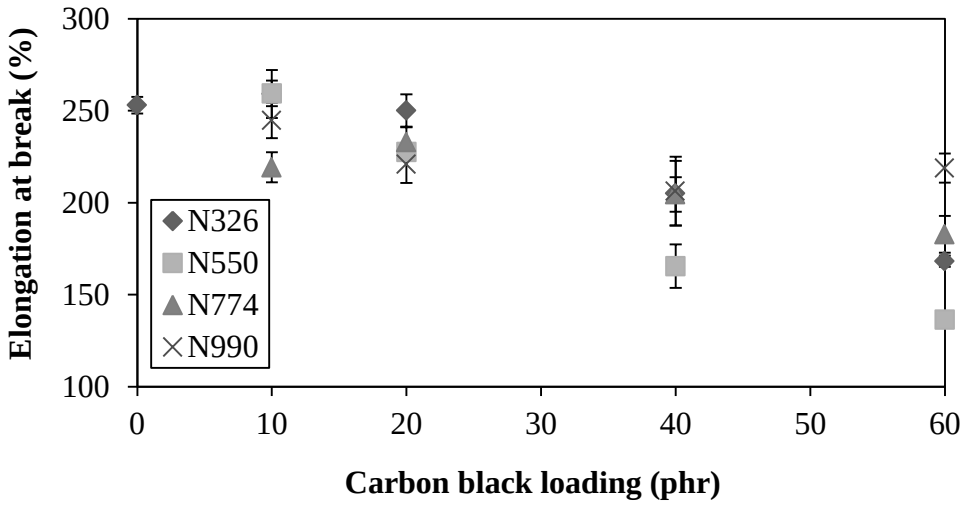

Figure 5.37 Relationship among elongation at break, carbon black loading and characteristics in HNBR vulcanisates

Tear strength is a measure of the resistance to failure of a material when it is subjected to tearing. Figure 5.38 shows that the tear strength of filled vulcanisates increases with increasing CB loading as a result of reinforcement and crosslink density. However, it should be noted that the tear strength of N326 system is highest while that of N990 system is lowest. The HNBR vulcanisates filled with N550 show similar tear strength to the ones filled with N774. In short, as surface area of CB increases, the tear strength is enhanced.

Figure 5.39 reveals that the hardness increases with increasing CB loading. It is acknowledged that the deformation magnitude taking place in the hardness test is relatively small and locates mainly at specimen surfaces. Consequently, the transient filler network in highly filled vulcanisates (i.e., HNBR vulcanisates with 60 phr of N326) might still influence the modulus at low strain (or

hardness), and its effect is comparable to the crosslink density effect found in vulcanisates with N550.

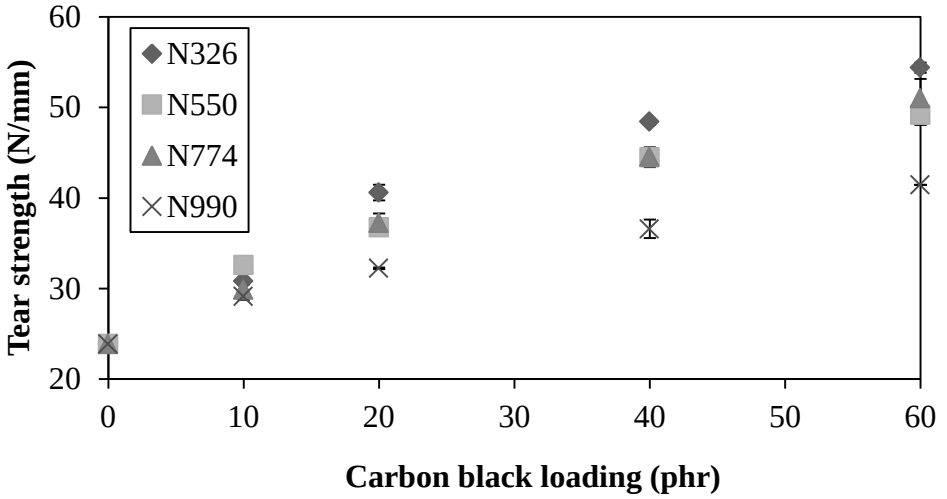

Figure 5.38 Relationship among tear strength, carbon black loading and characteristics in HNBR vulcanisates

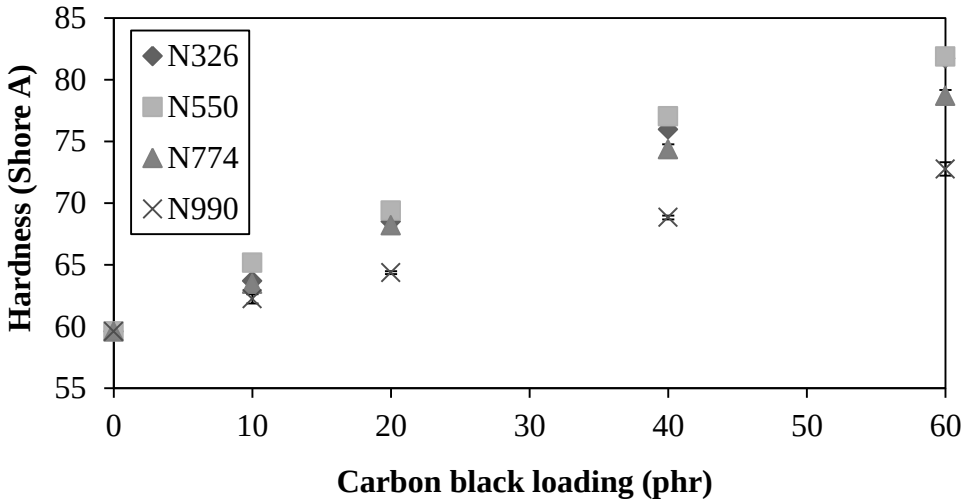

Figure 5.39 Relationship among hardness, carbon black loading and characteristics in HNBR vulcanisates

It has been reported that abrasion resistance is controlled mainly by the modulus and the friction coefficient of the vulcanisate (113). Higher modulus and lower friction coefficient give the vulcanisates with superior abrasion resistance. Figure 5.40 (a) demonstrates comparison of abrasion loss in vulcanisates reinforced with various CB surface area. Compared to unfilled vulcanisates, the CB filled ones exhibit higher volume loss which appears to increase with increasing CB loading. It is believed that the difference in abrasion loss is caused by the discrepancy in wear mechanisms. To support the proposed explanation, the abraded surfaces of test specimens were photographed, and the images are shown in Figure 5.40 (b). In the case of unfilled HNBR vulcanisate, the rubber layer is created on the specimen surfaces, and thereafter adheres tightly to the surfaces of the test specimen. This means this layer is practically not removable during the whole abrasion process, giving rise to the small volume loss, i.e., relatively high abrasion resistance. This proposed mechanism is evidenced by smooth surface of the test specimen. In the case of filled vulcanisates, the CB particles could escape from the specimen surfaces during the abrasion process as demonstrated by the scratches on specimen surfaces. With the increasing CB loading, the decrease in abrasion resistance is due to the increase in abrasive action of CB. Also, at a given specific surface area of CB, the abrasion resistance tends to decrease with increasing CB loading, particularly at high CB loading.

Regarding the CB surface area effect on abrasion loss, Figure 5.40 (a) shows high volume loss in the systems with N326 and N990. This phenomenon is probably due to the poor filler dispersion at high loading of N326 having large specific surface area, and due to low magnitude of rubber-filler interaction of N990 possessing relatively low structure and specific surface area.

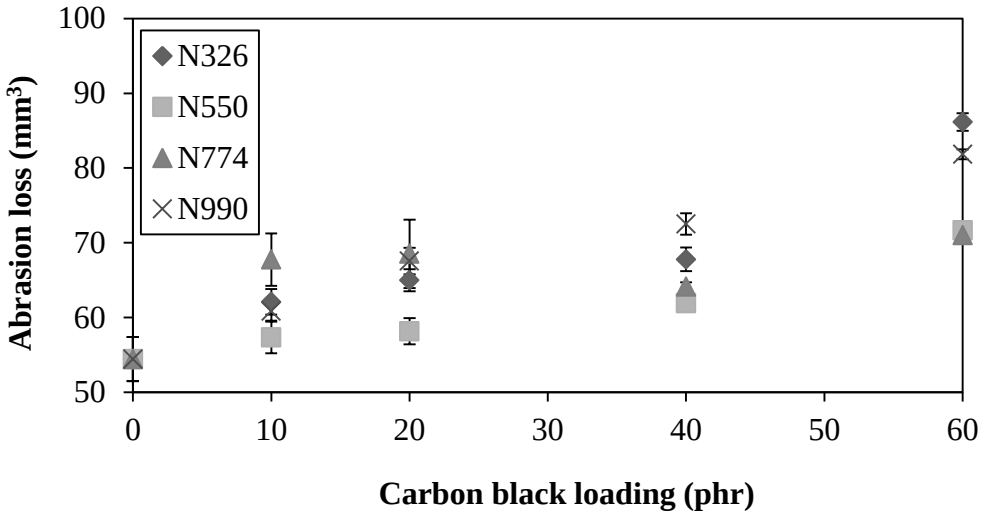

(a)

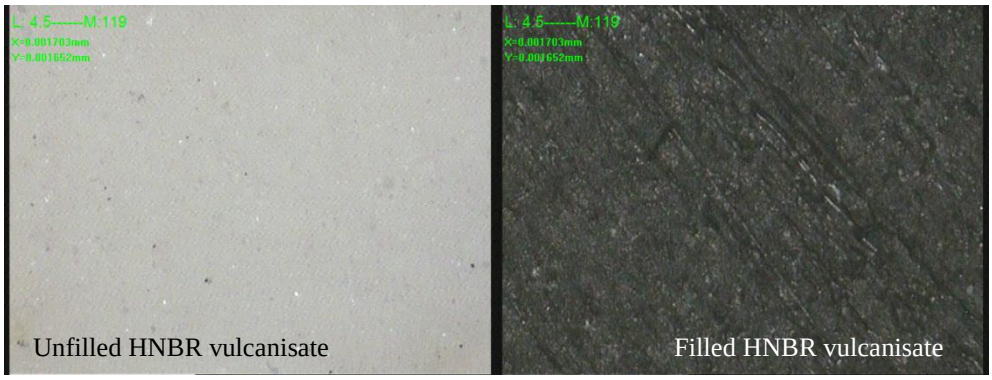

(b)

Figure 5.40 Abrasion resistance: (a) relationship among abrasion loss, carbon black loading and characteristics in HNBR vulcanisates; (b) abraded surfaces of HNBR vulcanisates after the abrasion process

5.1.2 Influences of precipitated silica loading

The silica has plenty of hydrophilic silanol groups (Si-OH) on its surface, resulting in strong filler-filler interaction and poor polymer-filler interaction (102). Since the intermolecular hydrogen bonds between silanol groups on silica surfaces are strong, the silica can form clusters tightly (103, 104) causing a poor dispersion of silica in a hydrophobic rubber matrix. Silane coupling agents have been known to

effectively reduce the filler-filler interaction and promote the polymer-filler interaction (105). In this study, a vinylsilane is used as coupling agent and dispersing aid in peroxide-cured HNBR compounds. The vinylsilane could also act as a cure activator which enhances the curing behaviour and crosslinking density (106). The effect of silica loading on polymer-filler interaction, cure characteristics, viscoelastic behaviour, dynamic mechanical properties and mechanical properties of silica-filled HNBR is investigated in this section.

5.1.2.1 Cure characteristics

The results of scorch time and cure time of silica filled HNBR compounds are presented in Figures 5.41 and 5.42, respectively. It is obvious that both scorch time and optimum cure time decrease with increasing silica loading, which can be explained by an increase in thermal history with increasing silica loading. Since the shear heating during the mixing process increases with increasing silica loading as a result of increased compound viscosity, the compounds with high loadings of silica would be subjected to a high thermal history, leading to the reduction in scorch and cure time (107).

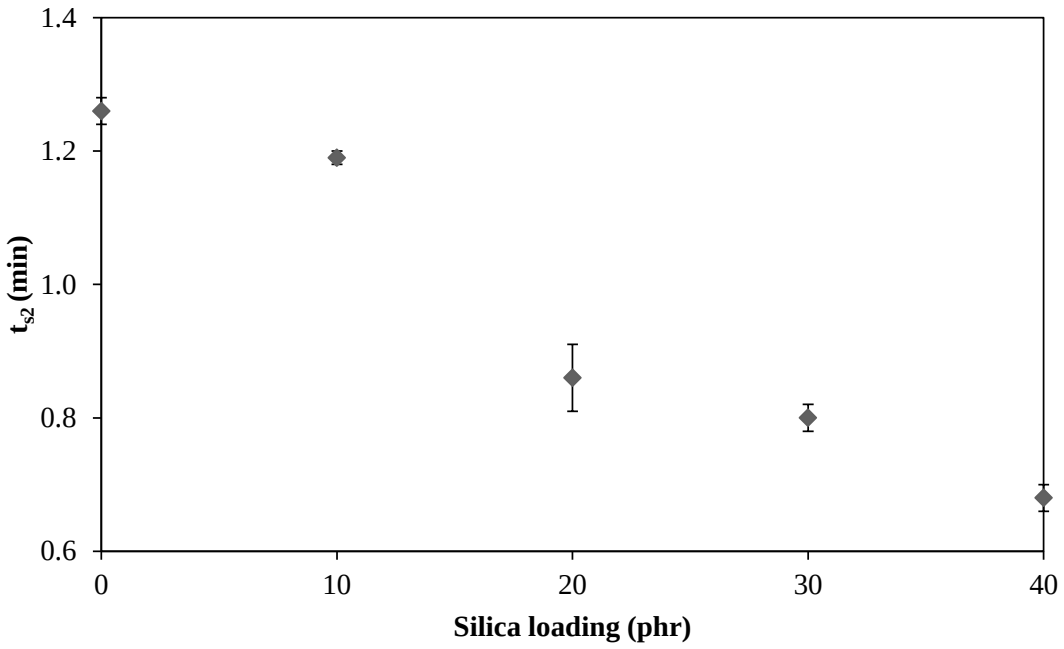

Figure 5.41 Relationship between scorch time (t_{s2}) and silica loading in HNBR compounds

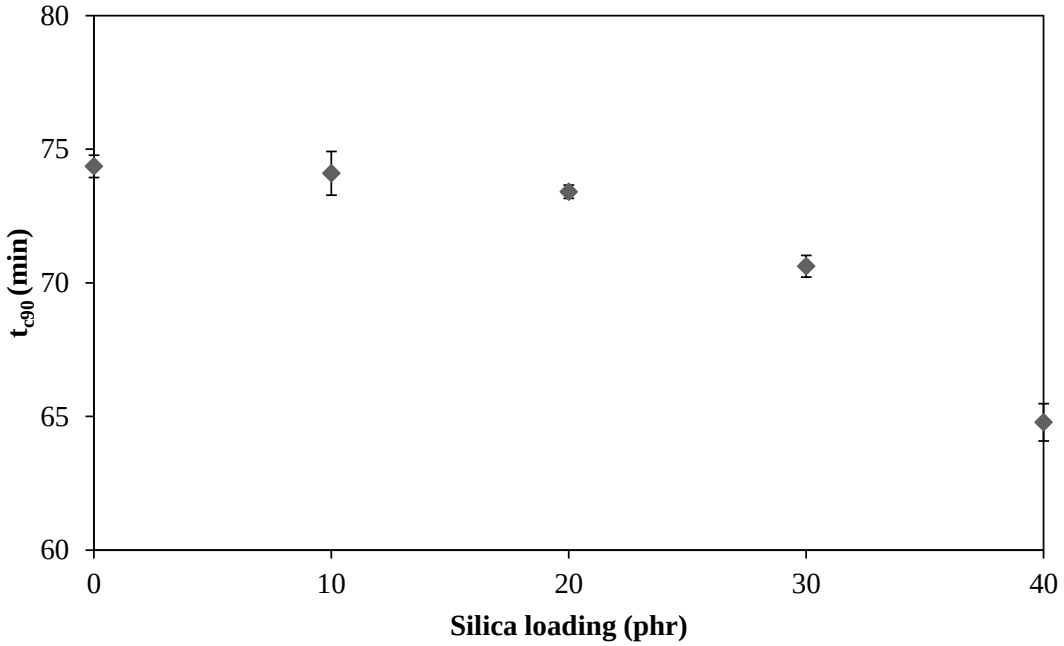

Figure 5.42 Relationship between optimum cure time (t_{c90}) and silica loading in HNBR compounds

Regarding the crosslink density, Figure 5.43 shows the rise in torque difference of cured silica filled HNBR system with increasing silica loadings. The results reveal an increase in crosslink density with increasing silica loading, which is in good agreement with the results of scorch time and cure time. In this study, the silica is utillised together with vinylsilane to enhance the interaction between rubber and filler. The rubber-filler interaction could be increased with increasing silica loading, leading to the increase in the adsorption of rubber molecular chain on the silica surfaces. The mobility of the rubber segment is therefore diminished, which restricts the migration of peroxide into the tightly bound rubber. This would result in a relatively high concentration of peroxide in the bulk and thus the crosslink density.

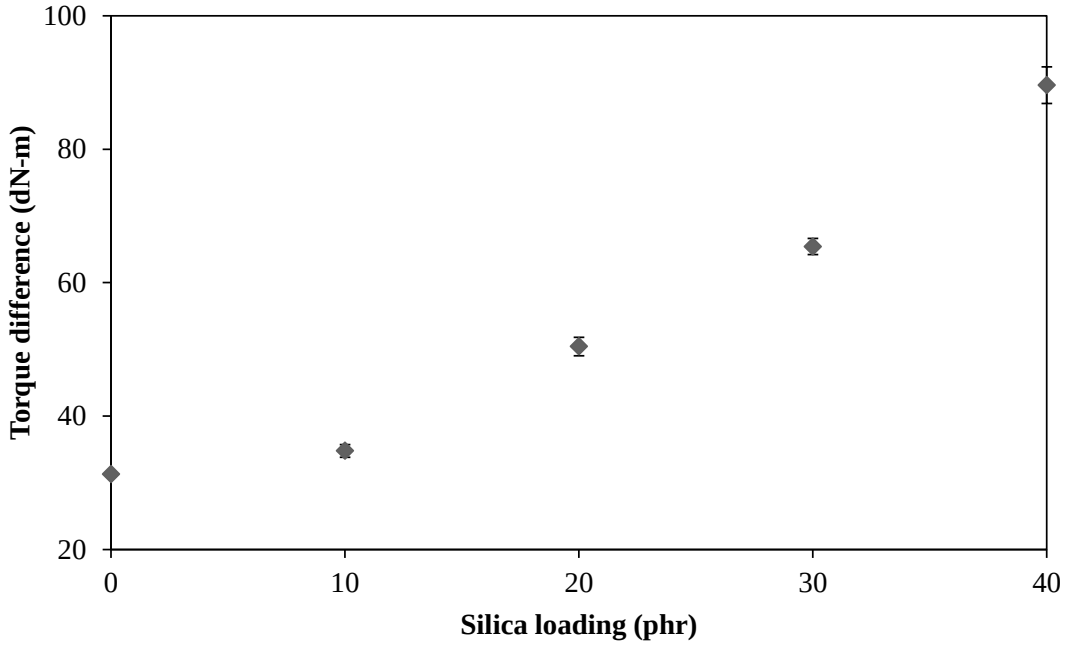

Figure 5.43 Relationship between torque difference (or crosslink density) and silica loading in HNBR compounds

5.1.2.2 Viscoelastic properties

a) Uncured silica filled HNBR systems

(RPA-FT) Complex modulus vs. Strain amplitude

The results of G^* versus strain curves are shown in Figure 5.44. Evidently, in all cases, the 2 test samples (a and b) give identical results, which exhibits the excellent homogeneity of tested materials and the reproducibility of the testing method. The difference between run 1 and run 2 is not noticeable, indicating none of significant strain history effects, and/or the strain effects are immediately recovered during the 2 minutes resting period between runs.

It is apparent that the unfilled HNBR compound reveals the lowest G^* and broadest plateau of LVE region. Also, the G^* increases with increasing silica loading, which is due mainly to the reinforcing effect, i.e., the hydrodynamic effect, the filler-filler interaction via hydrogen bonding as well as the strong rubber-filler interaction. Highly silica filled compounds, i.e. the compounds filled with 30 and 40 phr silica loading, show also a strain-dependent G^* as a result of strong filler-filler interaction (usually known as the Payne effect).

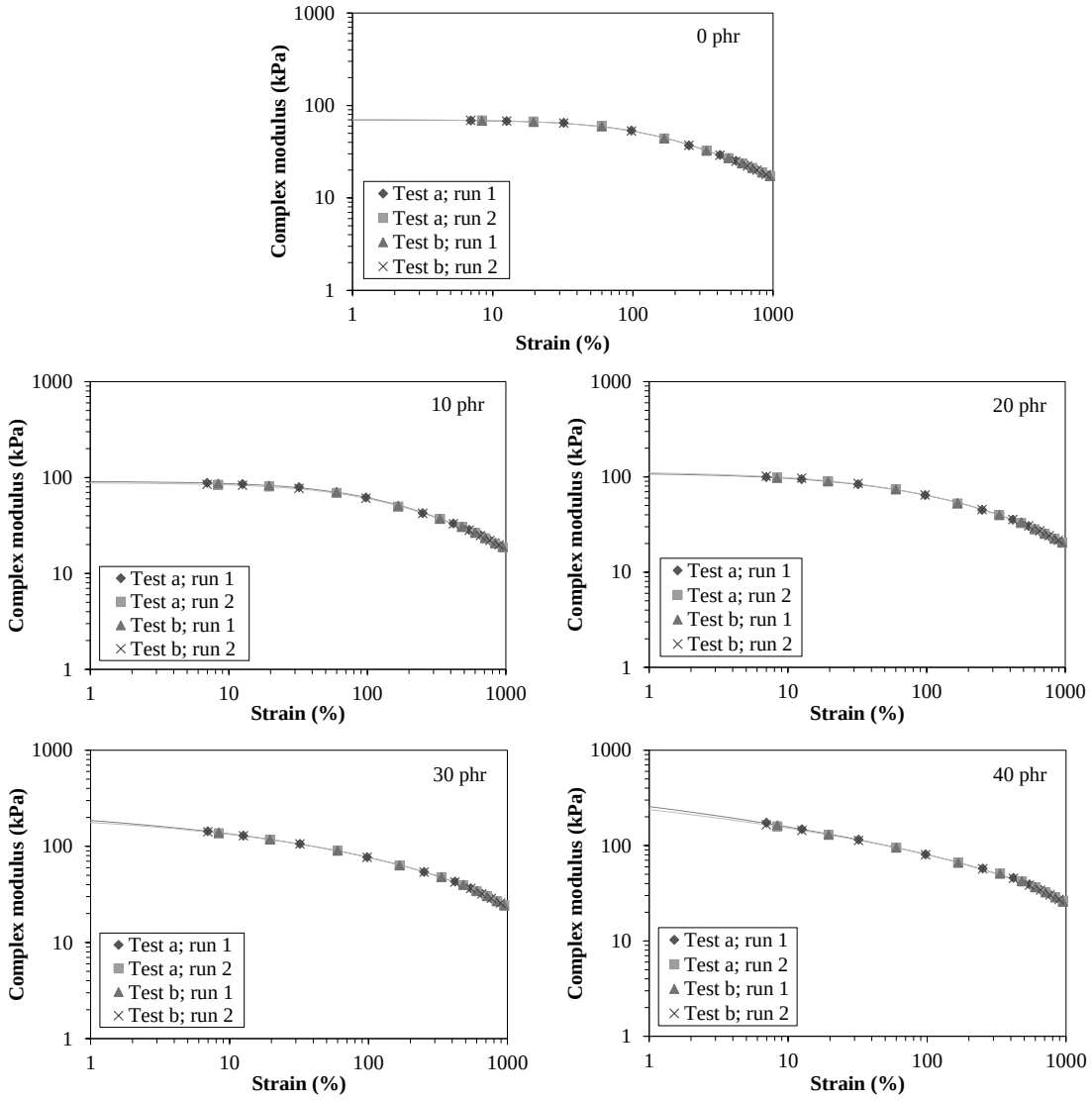

Figure 5.44 Complex modulus (G^*) as a function of strain amplitude at 3.14 rad/s and 100°C as measured by the RPA-FT of HNBR compounds filled with various silica loadings

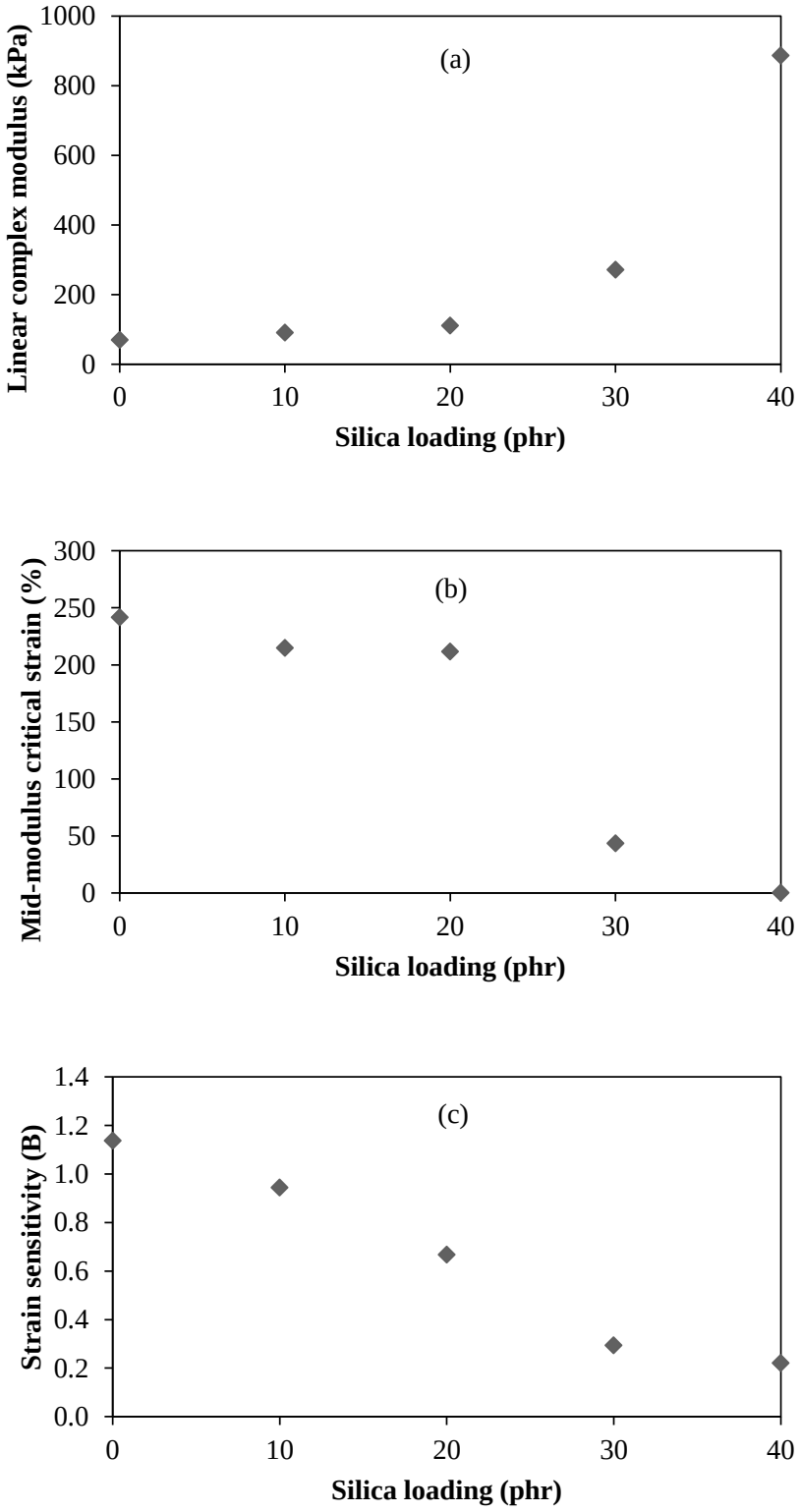

Figure 5.45 Relationship between fit parameters of Equation 3.16 and silica loading in HNBR compounds: (a) linear complex modulus $\left(G_0^*\right)$; (b) mid-modulus critical strain (1/A); (c) strain sensitivity (B)

Fit parameters of Equation 3.16 are given in Figure 5.45. The G_0^* increases with increasing silica loading, and increases extremely when the silica content is more than 20 phr. The hydrodynamic effect, filler network and rubber-filler interaction are taken into consideration. The parameter A in Equation 3.16 is the reverse of a critical strain, and thus the 1/A value is ploted with silica loading. It can be seen that the 1/A value decreases with increasing silica loading. Expectedly, the decrease in the value of 1/A is significant in the highly silica filled compound (i.e. the compounds filled with 30 and 40 phr). The higher the filler loading, the larger the dynamic strain softening (DSS) effect. Also, the strain sensitivity as expressed by parameter B decreases with the loading of silica.

(RPA-FT) Torque Harmonics vs. Strain amplitude

Figure 5.46 shows the torque harmonics varying with increasing strain amplitude for all the tested silica filled HNBR compounds. Data are well reproducible with no difference between tests a and b, and no difference between runs 1 and 2. Torque signal harmonics thus appear to be insensitive to strain history.

As expected, the total torque harmonic content (TTHC) curve envelops the 3rd relative torque harmonic (T(3/1)) and the 5th relative torque harmonic (T(5/1)). The T(3/1) behaves as the most significant part of the information, i.e., an S-shape curve is generally observed for all tested compounds.

Fit parameters followed Equation 3.17 for T(3/1) as a function of strain are given in Figure 5.47. As mentioned previously, the parameters TH_0 and α describe the principle of asymptotic non-linear behaviour at infinite strain where all rubber-filler interaction is completely destroyed, meaning that the viscoelastic character is maintained only by the stretched rubber phase, then the amount of silica does not affect the change in the values of TH_0 and α, as shown in Figures 5.47 (a) and 5.47 (b). However, the most significant information of non-linear viscoelastic behaviour can be expressed by the parameters C and D. The strain sensitivity of the non-linear response increases, and the extent of the LVE region decreases with increasing silica loading, as exhibited in Figures 5.47 (c) and 5.47 (d), respectively. The result is in complete agreement with the concept of DSS effect, i.e., the extent of LVE region decreases with the increase in magnitude of filler network formation.

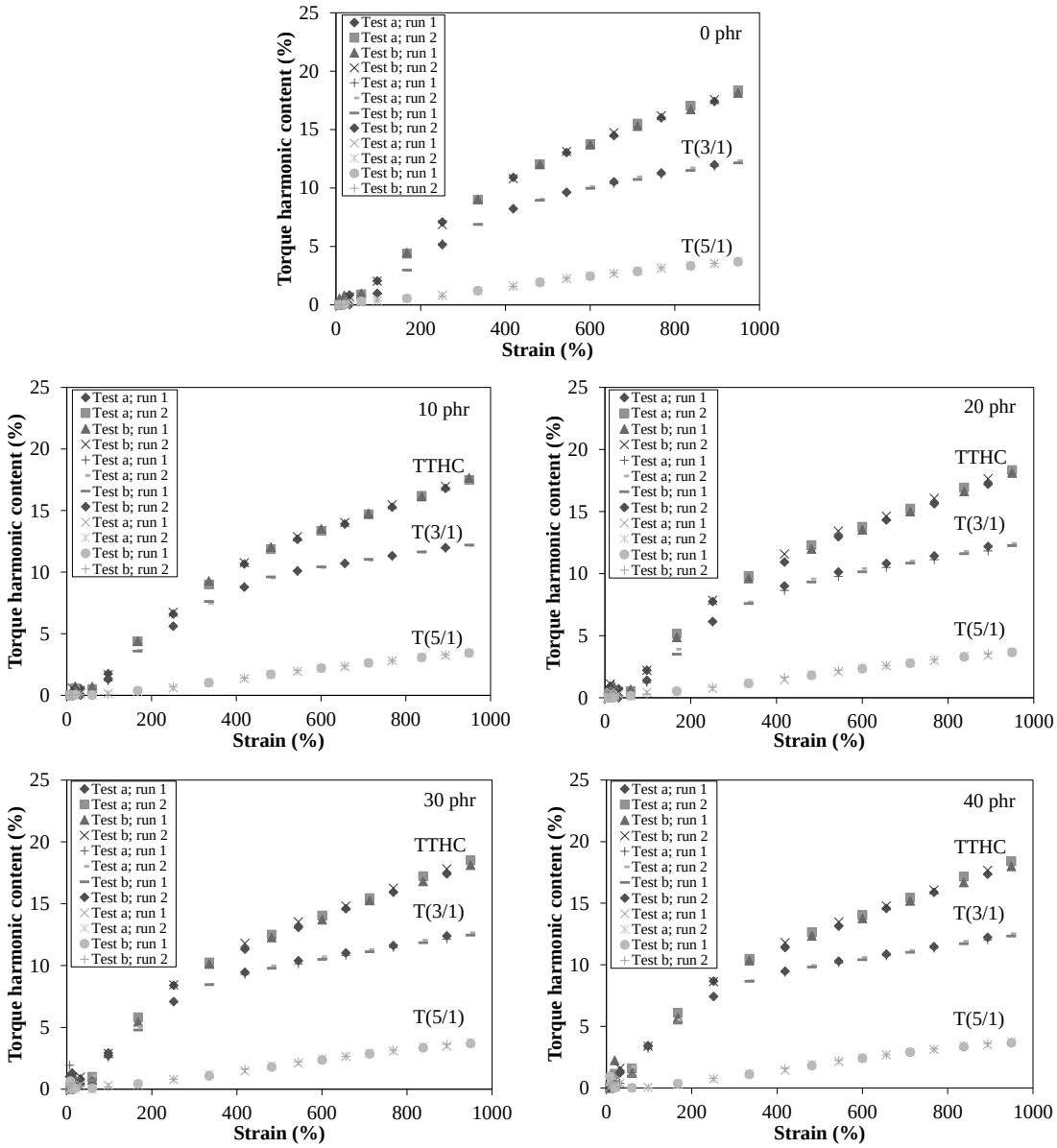

Figure 5.46 Torque harmonics as a function of strain amplitude at 3.14 rad/s and 100°C as measured by the RPA-FT of HNBR compounds filled with various silica loadings

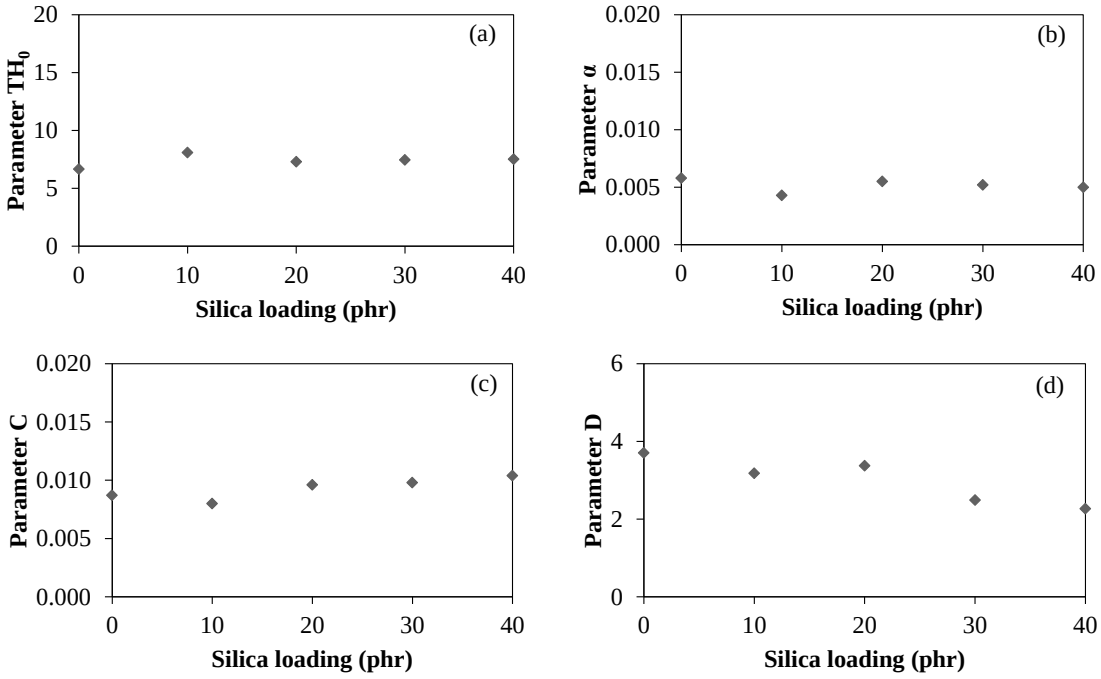

Figure 5.47 Relationship between fit parameters of Equation 3.17 and silica loading in HNBR compounds: (a) parameter TH_0; (b) parameter α; (c) parameter C; (d) parameter D

Quarter Torque Signal Integration

The change from extra (strain-induced) to intra (morphology-induced) non-linear viscoelastic character as silica loading increases is evidenced by the Q1/Q2 ratio, as shown in Figure 5.48. The minimum Q1/Q2 ratio occurs at strain of approximately 168%. It is known that the value of the minimum Q1/Q2 ratio can be considered as an indication of the nonlinear behaviour due to the filler content (78).

Figure 5.49 illustrates the minimum Q1/Q2 ratio of filled HNBR compounds with various silica loadings. It is clearly seen that the non-linear character changes as silica loading increases. The filled HNBR compounds change from extrinsic to intrinsic non-linear behaviour as filler loading increases, and the transition occurs expectedly at silica loading greater than 20 phr, i.e., at silica loading of 30 and 40 phr, the minimum Q1/Q2 ratio is below 1. Evidently, there are greater interactions between HNBR and silica for highly filled compounds.

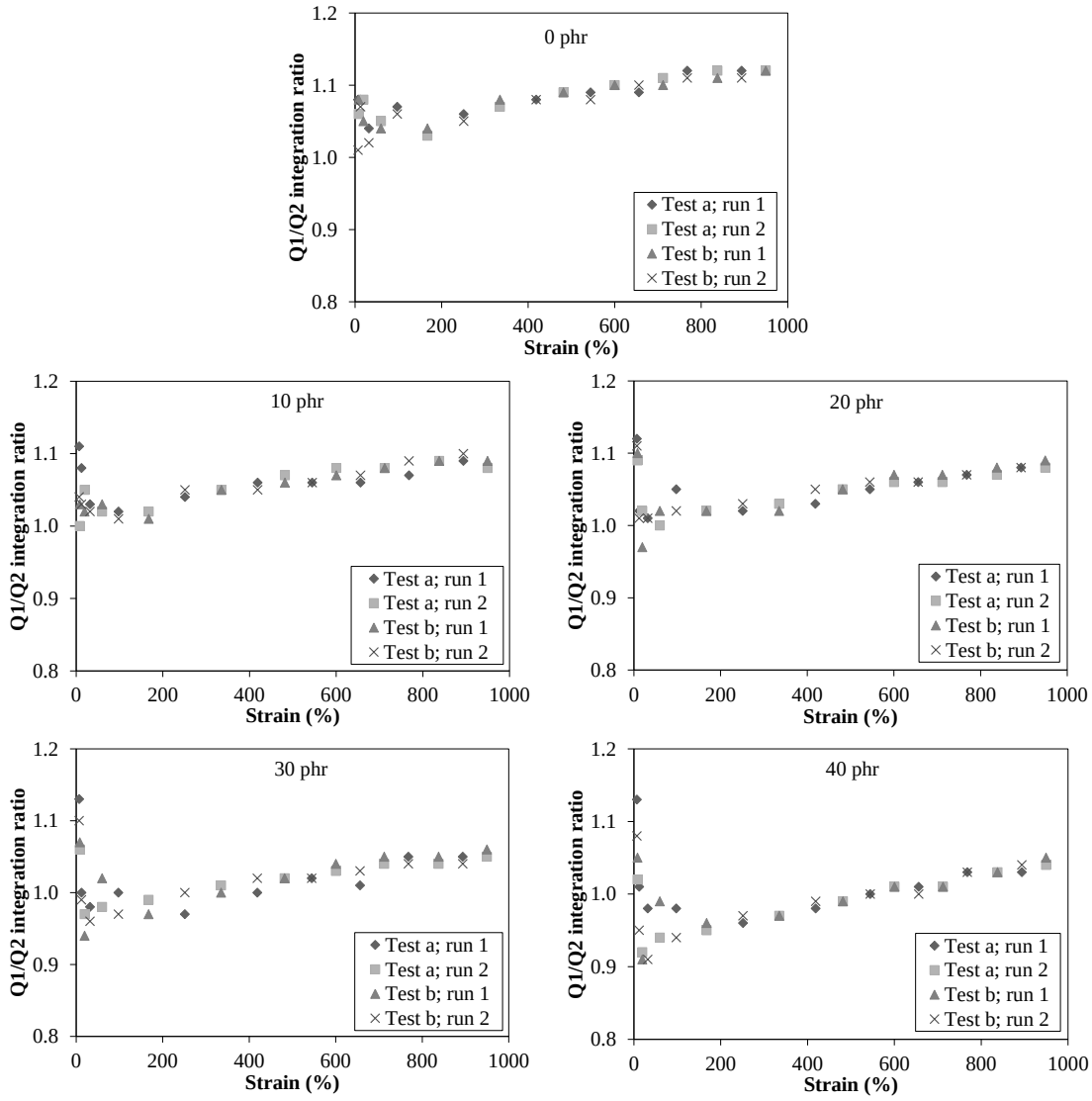

Figure 5.48 RPA-FT at 100°C on HNBR compounds filled with silica assessing extrinsic or intrinsic non-linear viscoelastic character through the quarter cycle torque integration; strain sweep tests at 3.14 rad/s

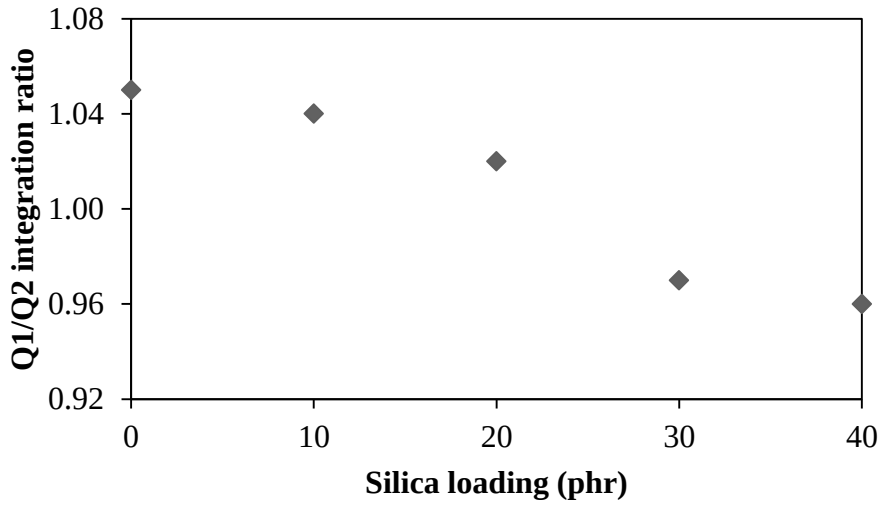

Figure 5.49 Relationship between quarter torque signal integration ratio and silica loading in HNBR compounds at strain amplitude of 167.55%

b) Cured silica filled HNBR systems

Strain sweep test

In the cases of HNBR vulcanisates, the results of G′, G″ and tanδ as a function of stain amplitude are exhibited in Figures 5.50, 5.51 and 5.52, respectively. The unfilled cured system shows lowest G′ with broadest LVE region. The G′ increases with increasing silica loading, which is in agreement with the crosslink density and reinforcing effects. It must be noted that the magnitude of Payne effect in highly silica filled compounds is relatively high which implies the fertility of filler network formation.

The strain dependence of the G″ in vulcanisates with and without silica is shown in Figure 5.51. Evidently, the incorporation of silica in HNBR substantially increases the G″ of the material regardless of strain amplitude. This result is in accordance with the crosslink density effect, hydrodynamic effect, the filler-rubber interaction and filler network formation. It is known that not only the presence of filler network, but also the process of breakdown and reformation of the filler network under dynamic strain is the necessary conditions for the hysteresis of filled rubber (21). With the result of G″ as a function of strain amplitude, the highly filled HNBR vulcanisates (i.e., HNBR filled with silica loading of 40 phr) exhibits the

noticeable strain dependence. The G″ passes its maximum, and decreases as the rate of filler reformation is lower than that of disruption (21).

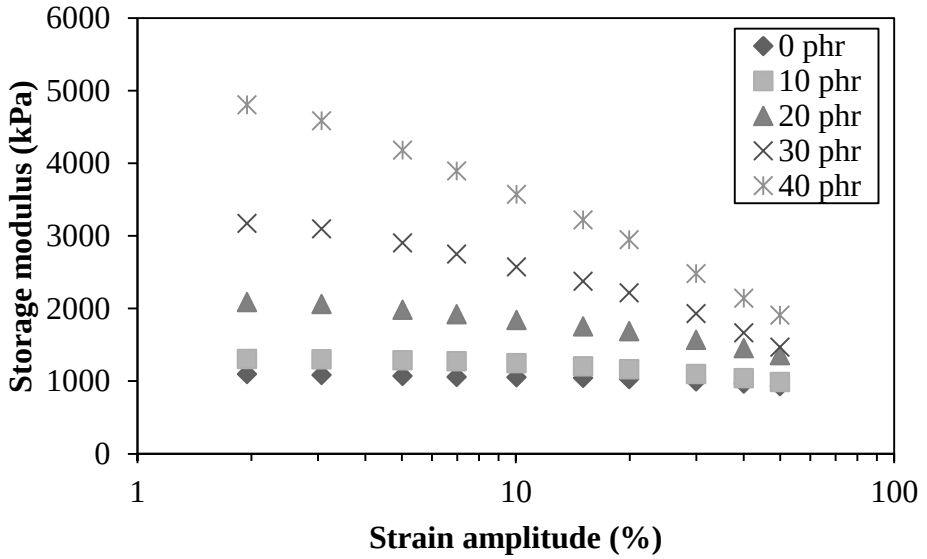

Figure 5.50 Storage modulus (G′) as a function of strain amplitude of filled HNBR vulcanisates with various silica loadings at test temperature and frequency of 60°C and 1 rad/s, respectively

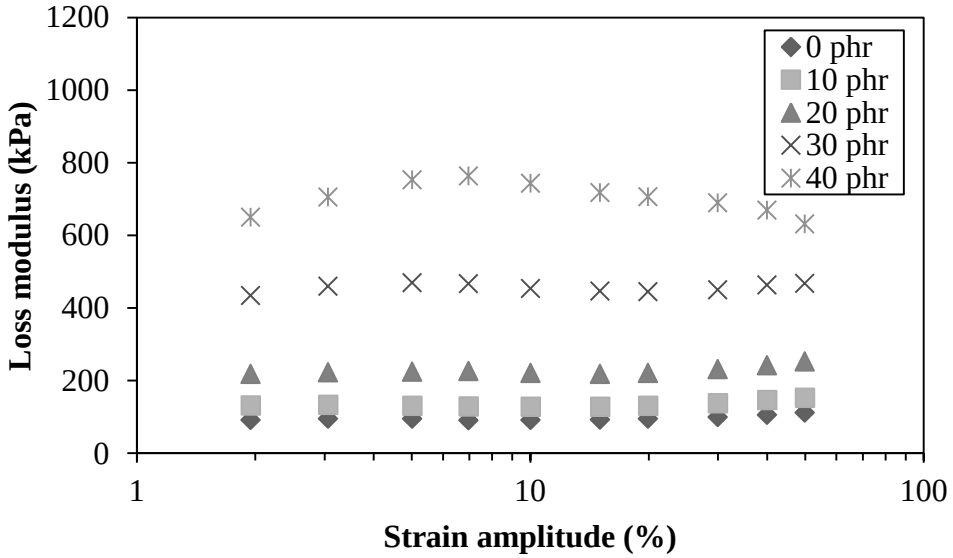

Figure 5.51 Loss modulus (G″) as a function of strain amplitude of filled HNBR vulcanisates with various silica loadings at test temperature and frequency of 60°C and 1 rad/s, respectively

Plots of tanδ of HNBR vulcanisates filled with various silica loadings as a function of strain amplitude are exhibited in Figure 5.52. The results are in good agreement with the G′ and G″ results, i.e., the tanδ increases with increasing silica loading and strain amplitude, and the highly filled vulcanisates show the high magnitude of increase in tanδ. The energy dissipation via the disruption of filler-filler networks is responsible for the results at low strain. The molecular slippage is responsible for the results at high strains.

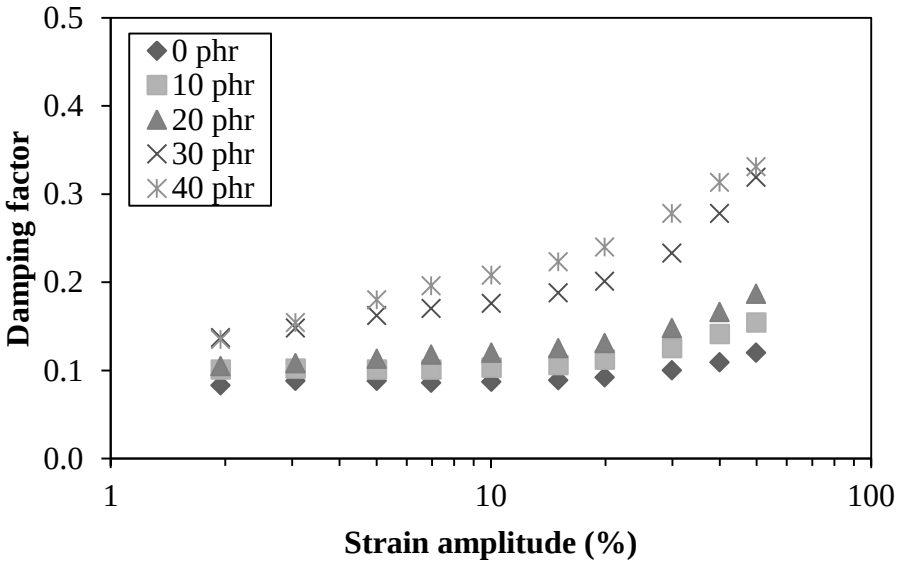

Figure 5.52 Damping factor (tanδ) as a function of strain amplitude of filled HNBR vulcanisates with various silica loadings at test temperature and frequency of 60°C and 1 rad/s, respectively

Temperature sweep test

The effect of silica loading on the G′, G″ and tanδ as a function of temperature for HNBR vulcanisates is presented in Figures 5.53 to 5.55. It can be seen that both G′ and G″ increase with increasing silica loading over the range of test temperature. The hydrodynamic effect is a major role, hence, at the glass transition temperature (T_g), the tanδ peak decreases with the loading of silica. Interestingly, the tanδ at 50°C to 70°C is still lower for the highly silica filled vulcanisates. This may be anticipated from strongly and highly constructed filler clusters. It has been well recognized that the loss factor in temperature range between 50°C and 70°C could be

used to predict the degree of rolling resistance of a tire (108). As for high performance tyre, a decrease in tanδ at this temperature range results in a reduction in the rolling resistance (21, 109, 110). In the rubbery region, it is evident that the tanδ decreases with increasing temperature. With increasing temperature, the molecular mobility and free volume of the rubber chains on the filler surface will increase, and the tanδ will decrease due to a decrease in energy dissipation (21). However, it can be seen that the temperature dependence of the tanδ is depressed by the introduction of silica. This may be anticipated from more developed filler network in the HNBR vulcanisates filled with highly silica loading.

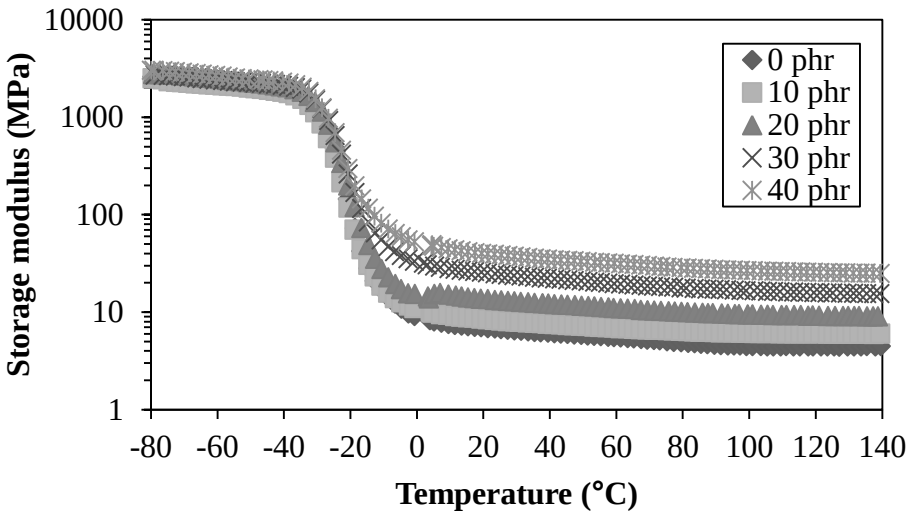

Figure 5.53 Storage modulus (G′) as a function of temperature of filled HNBR vulcanisates with various silica loadings at test static strain, dynamic strain and frequency of 2%, 0.1% and 62.8 rad/s, respectively

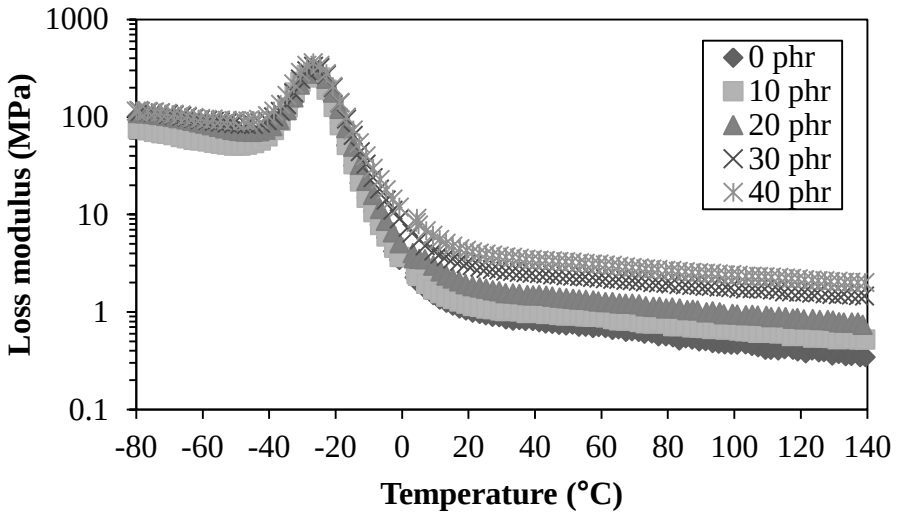

Figure 5.54 Loss modulus (G″) as a function of temperature of filled HNBR vulcanisates with various silica loadings at test static strain, dynamic strain and frequency of 2%, 0.1% and 62.8 rad/s, respectively

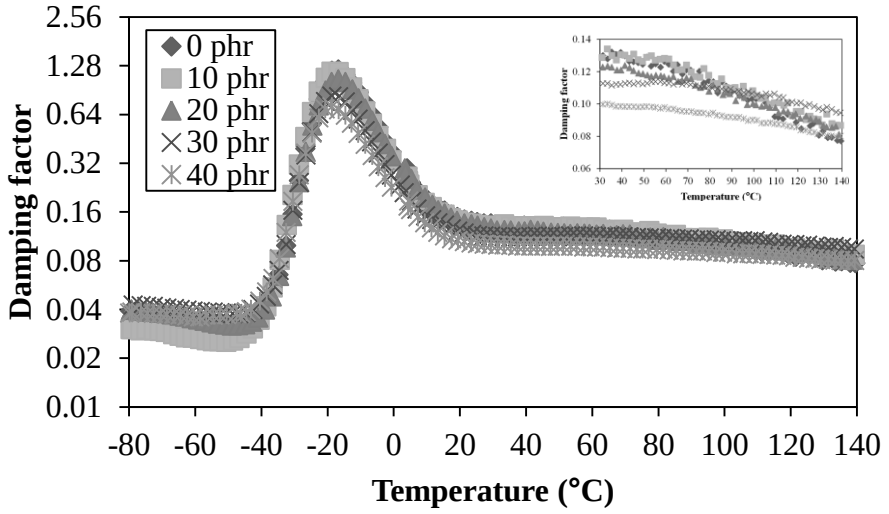

Figure 5.55 Damping factor (tanδ) as a function of temperature of filled HNBR vulcanisates with various silica loadings at test static strain, dynamic strain and frequency of 2%, 0.1% and 62.8 rad/s, respectively

5.1.2.3 Filler dispersion and distribution

SEM micrographs of silica filled HNBR vulcanisates as observed by SEM technique are shown in Figure 5.56. The degrees of dispersion and distribution of silica in HNBR matrix are characterised by the statistical processing of SEM micrographs using the quadrate method and Morishita's I_δ value (49) (as detailed in section 3.2.1 of chapter 3).

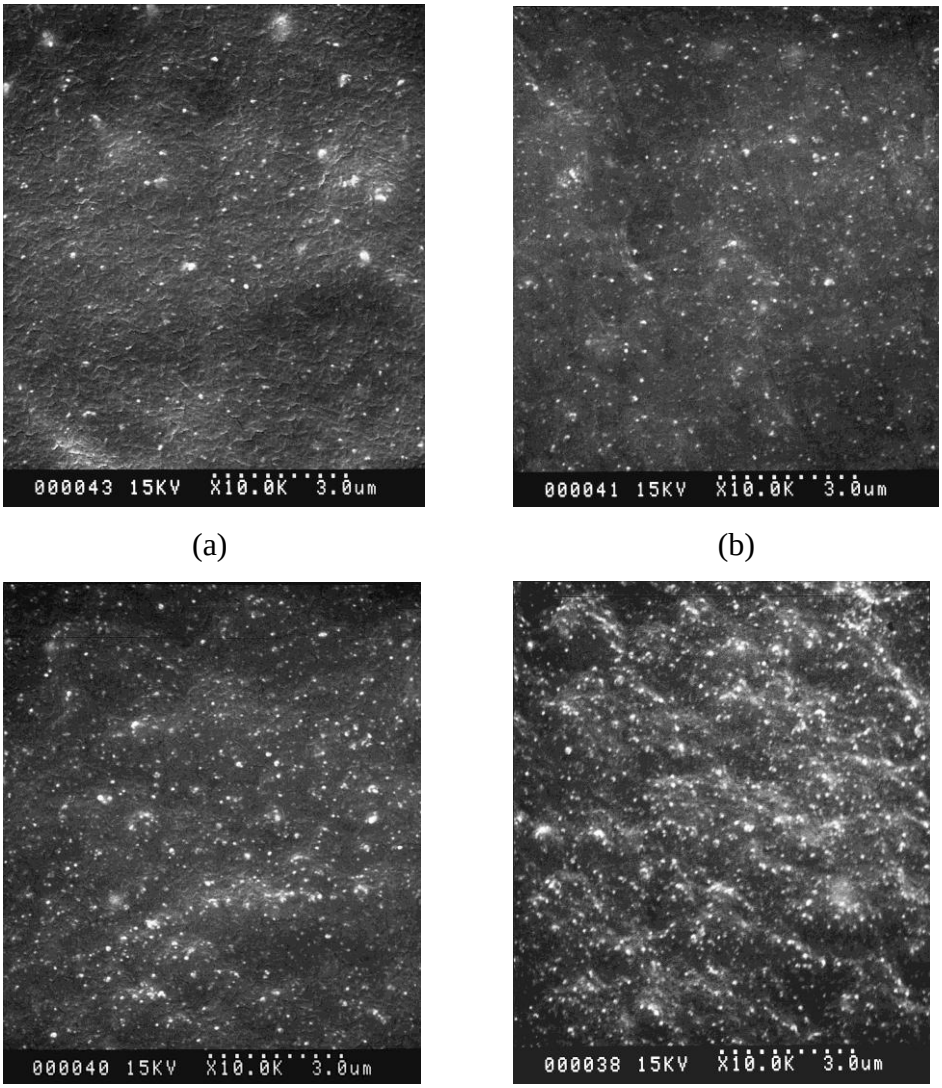

(a) (b)

(c) (d)

Figure 5.56 SEM micrographs of HNBR vulcanisates filled with various silica loadings: (a) 10 phr; (b) 20 phr; (c) 30 phr; (d) 40 phr

The plot between I_δ and q for filled vulcanisates with various silica loadings is presented in Figure 5.57. Evidently, the HNBR filled with silica loading of 10 phr shows the aggregate mode in a manner that the size of each aggregate is small, and the particles of each aggregate are distributed in Poisson's mode. Due to the stronger intermolecular hydrogen bonds between silanol groups on the silica surfaces, the tight silica clusters are formed (103, 104). This can cause a poor dispersion of silica in a rubber matrix. In this work, vinyl silane might act as dispersing aids, and thus the dispersion of silica is improved as expected. Moreover, there is the alteration of distribution mode from the aggregate mode to the Poisson's distribution with increasing silica loading (greater than 10 phr), indicating the improvement in silica dispersion. The increase in bulk viscosity with silica loading causes increased stress field available for disrupting the silica clusters. However, the plots between I_δ and q show similar pattern for the vulcanisates filled with 20, 30 and 40 phr of silica, indicating that the degree of filler dispersion is not affected by the increased silica loading. This could be explained by effect of counter-balancing between formation and disruption of silica clusters.

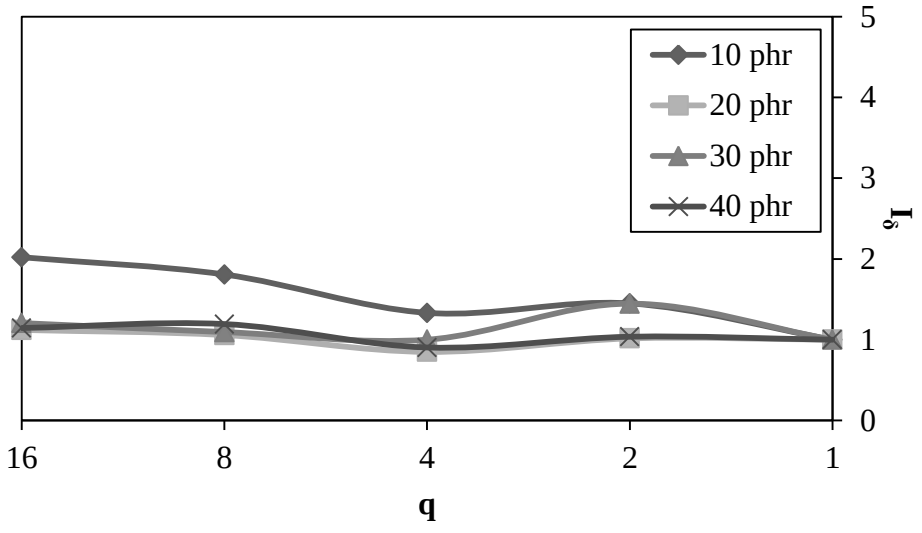

Figure 5.57 Morishita's index (I_δ) for silica filled HNBR vulcanisates filled with various silica loadings as a function of quadrat number (q)

5.1.2.4 Mechanical properties

Figure 5.58 represents the plot of M100 against silica loading. It is evident that the M100 of silica filled HNBR vulcanisates increases with increasing silica loading as expected. There are two main possible factors controlling M100, i.e., crosslink density and filler reinforcement effects. Regarding the crosslink density effect, it is known that the higher the crosslink density, the greater the M100. As shown previously in Figure 5.43, the crosslink density increases with the loading of silica. In the case of filler reinforcement effect, apart from the hydrodynamic effect, it is believed that the vinylsilane added as a coupling agent have been effective in improving interaction between filler and rubber matrix (111). The higher the amount of silica, the larger the extent of filler network formation and filler-rubber interaction, and thus the greater the M100.

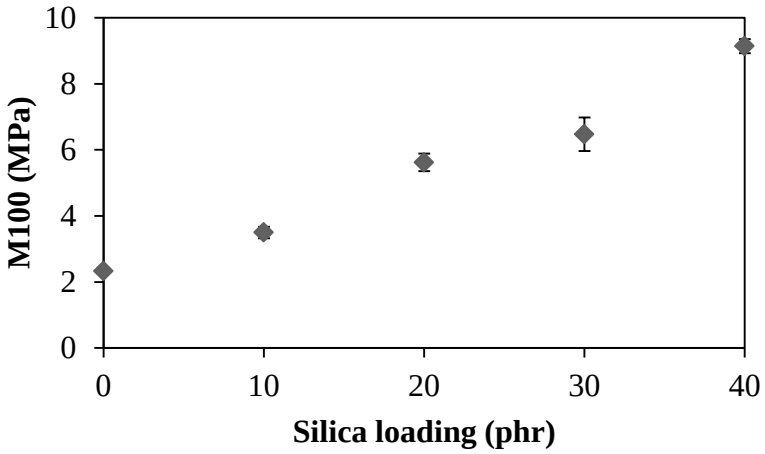

Figure 5.58 Relationship between modulus at 100% strain (M100) and silica loading in HNBR vulcanisates

The result of tensile strength is shown in Figure 5.59. As expected, the tensile strength of unfilled vulcanisate is lowest, and appears to increase with increasing silica loading, which could be explained by filler reinforcement and/or crosslink density effects as discussed earlier in the M100 results.

Figure 5.60 demonstrates the relationship between elongation at break (% EB) and silica loading. It can be seen that the % EB decreases progressively with increasing silica loading, which can be explained by an increase in crosslink density associated with a decrease in the amount of deformable phase or sometimes known as a dilution effect.

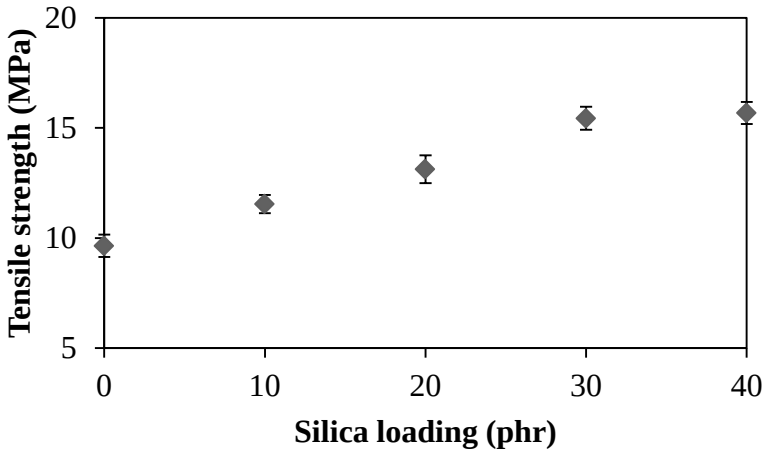

Figure 5.59 Relationship between tensile strength and silica loading in HNBR vulcanisates

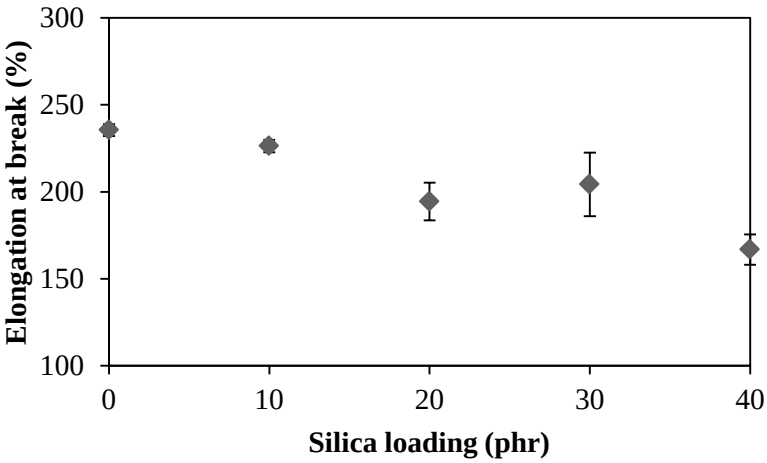

Figure 5.60 Relationship between elongation at break and silica loading in HNBR vulcanisates

Expectedly, tear strength of HNBR vulcanisates increases with increasing silica loading, as shown in Figure 5.61. Tear characteristics of vulcanisates can be related to the crosslink density as well as filler type and loading (1). With increasing silica loading, the magnitude of crosslink density and rubber-filler interaction increase, leading to the improvement in tear strength.

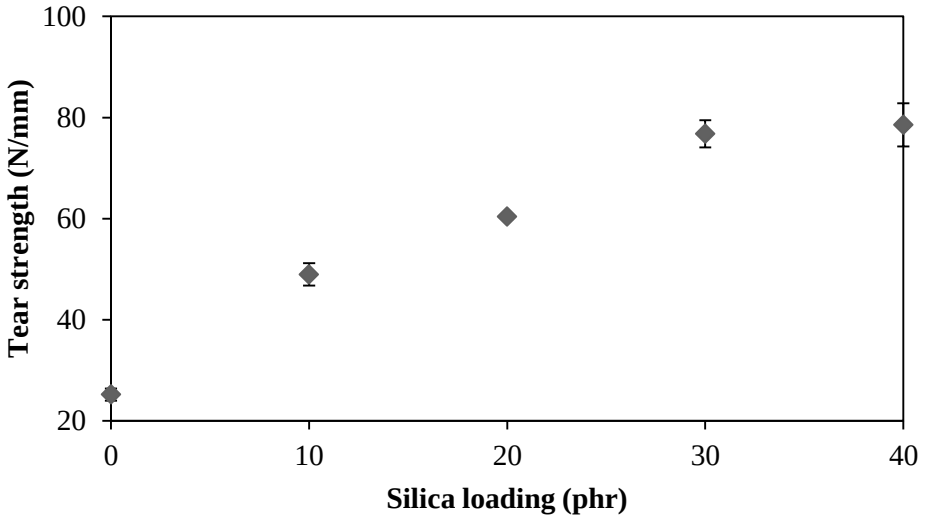

Figure 5.61 Relationship between tear strength and silica loading in HNBR vulcanisates

Regarding the hardness of silica filled HNBR vulcanisates, it is obvious from Figure 5.62 that the hardness increases continually with increasing silica loading. The results of hardness are in line with the M100 result (112). It is known that the measurement of hardness could be used to predict the modulus of vulcanisates.

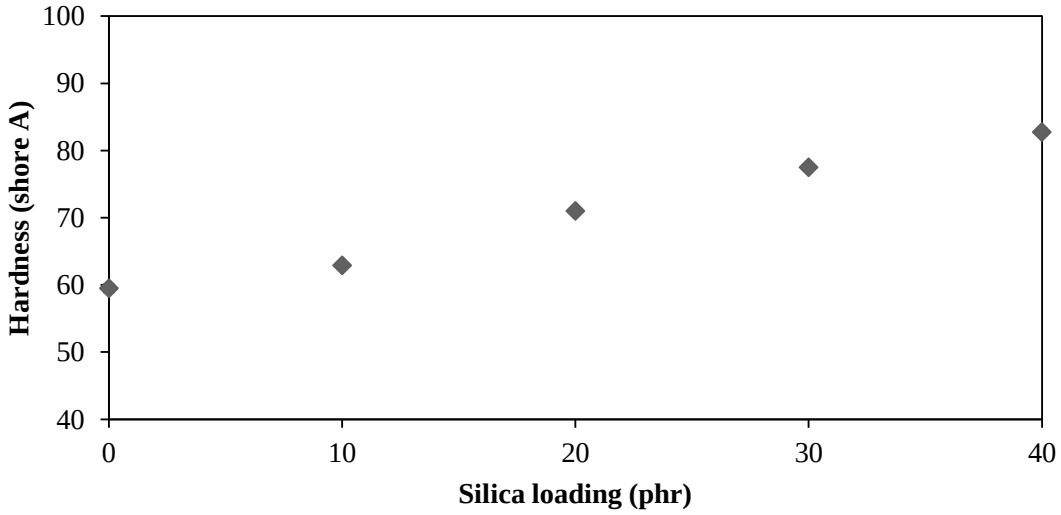

Figure 5.62 Relationship between hardness and silica loading in HNBR vulcanisates

Apparently, the abrasion resistance is diminished with increased silica loading, as illustrated in Figure 5.63, i.e., the increase in abrasion loss with the amount of silica is observed for HNBR vulcanisates filled with silica loading greater than 20 phr. As discussed previously in the G′ results (viscoelstic properties of silica filled HNBR vulcanisates section), the highly silica filled vulcanisates show the greater magnitude of Payne effect implying the more filler network formation through the filler-filler interaction. The increase in developed silica cluster or the strong silica-silica interaction results in the reduction in abrasion resistance at high silica loading (113).

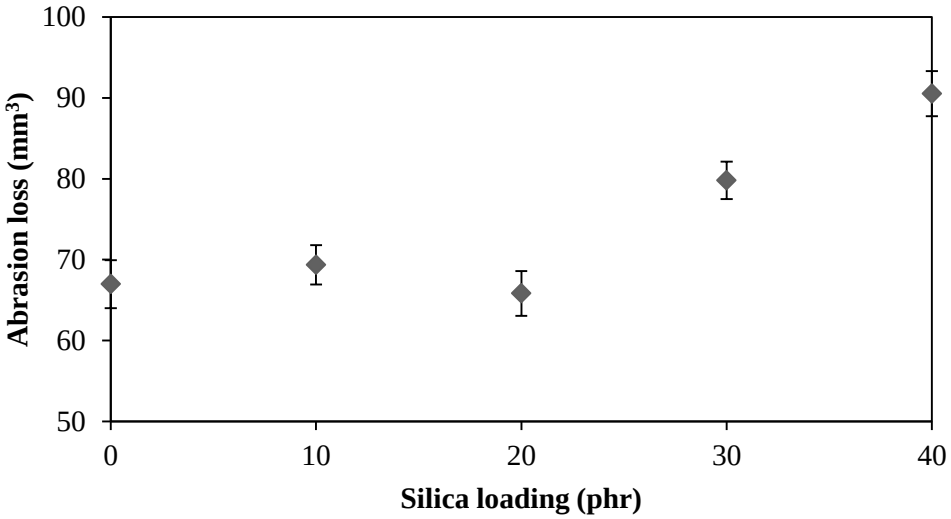

Figure 5.63 Relationship between loss and silica loading in HNBR vulcanisates

5.1.3 Influences of organoclay loading

Nano-clay is one of non-black reinforcing fillers, which is used to impart a number of desirable properties to rubber compounds. Naturally, the clay is composed of hydrated aluminum silicates. Exchangeable cations, such as, sodium ion (Na^{+}) and calcium (Ca^{2+}) ion hydrate strongly in the presence of water, result in a hydrophilic environment at the clay surfaces. As a result, a good dispersion of the clay in the hydrophobic matrix is difficult to accomplish.

In fact, the surface properties of nano-clay can change from hydrophilic to hydrophobic by a simple ion-exchange reaction. The hydrated cations of the interlayers can be exchanged with cationic surfactants such as alkylammonium or alkylphosphonium, leading to a broadened interlayer spacing. The modified clays then become more compatible with organic polymers.

Bentone® 38 is an organically modified clay where its hectorite is treated by quaternary ammonium cations. It is well known that the incorporation of organically modified clays into rubber matrix can result in performance improvement which expands the range of rubber applications (114, 115). In this study, the effect of Bentone® 38 on properties of HNBR compounds and vulcanisates is of interest.

5.1.3.1 Cure characteristics

Figures 5.64 and 5.65 show scorch time (t_{s2}) and optimum cure time (t_{c90}) of HNBR filled with various organoclay loadings, respectively. It is evident that the scorch time (t_{s2}) and optimum cure time (t_{c90}) decrease with increasing organoclay loading, associated with an increase in torque difference (or crosslink density), as illustrated in Figure 5.66. The cure promotion phenomenon is explained by the thermal history as discussed earlier. In addition, the restriction of curative migration into the immobilised rubber giving rise to the increase in curative concentration in free rubber might be responsible for the cure promotion phenomenon.

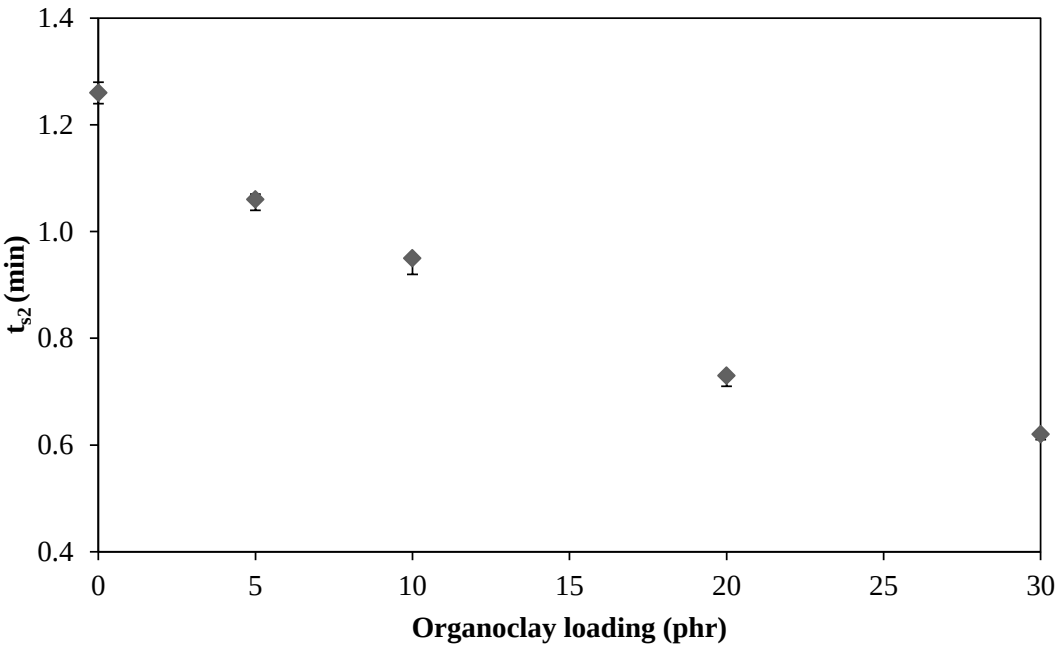

Figure 5.64 Relationship between scorch time (t_{s2}) and organoclay loading in HNBR compounds

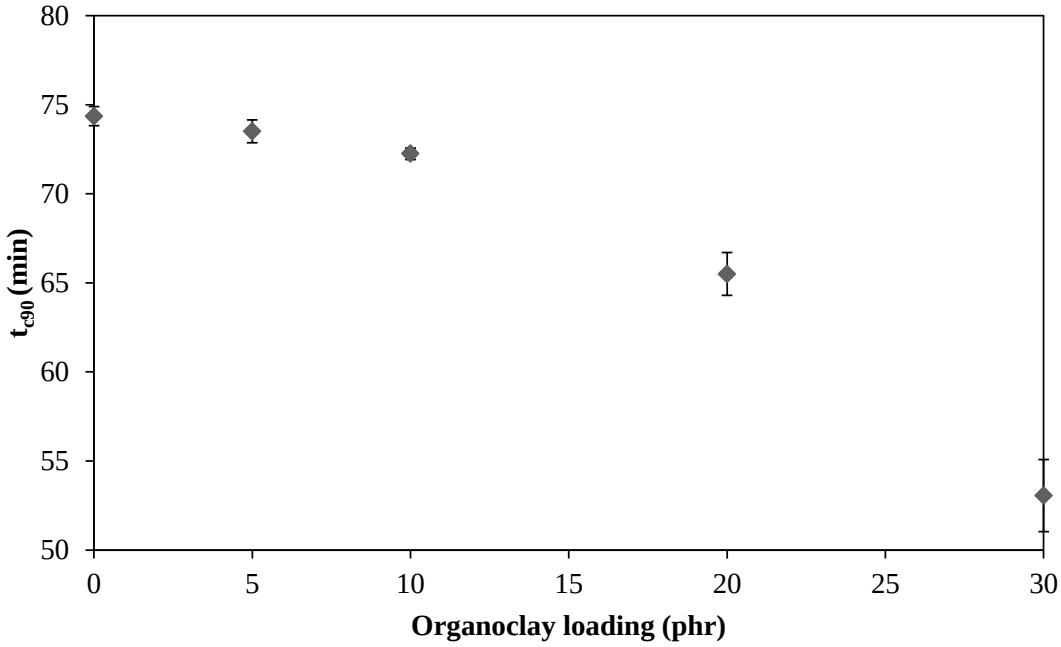

Figure 5.65 Relationship between cure time (t_{c90}) and organoclay loading in HNBR compounds

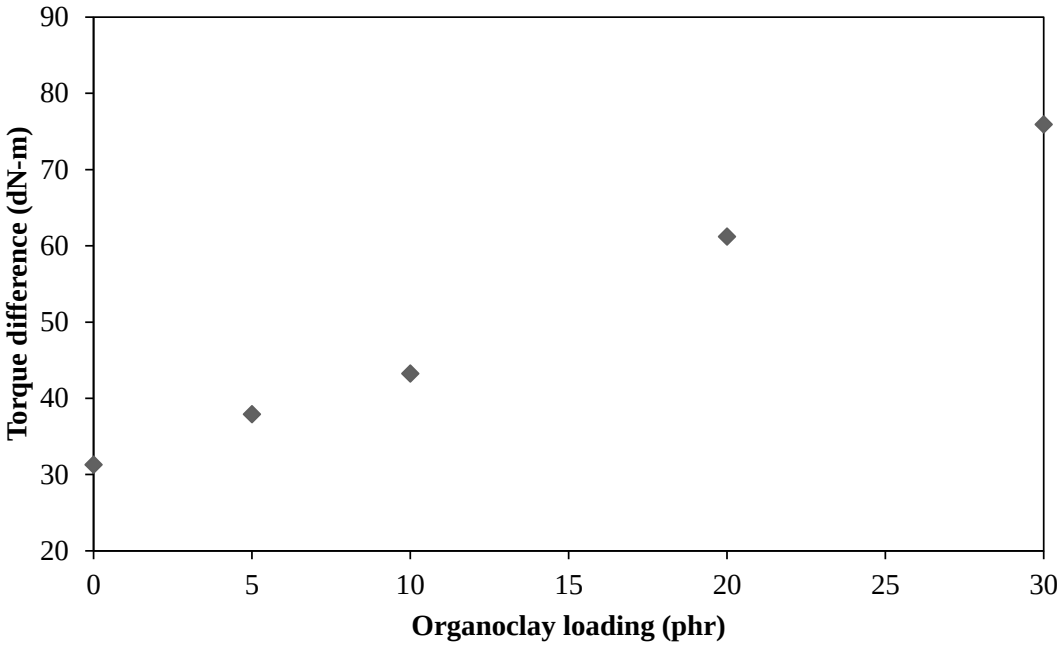

Figure 5.66 Relationship between torque difference (or crosslink density) and organoclay loading in HNBR compounds

5.1.3.2 Viscoelastic properties

a) Uncured organoclay filled HNBR systems

(RPA-FT) Complex modulus vs. Strain amplitude

Figure 5.67 shows the strain dependence detected on the G^* of organoclay filled HNBR compounds. Reproducibility is excellent and there is no strain history effect, excepting that the highly filled HNBR compounds (i.e., HNBR filled with the organoclay loadings of 20 and 30 phr) show obvious difference between run 1 and run 2 at low strain. This implies a strain history effect during the 2 minutes resting period between runs. The LVE region is observed, and decreases with the amount of organoclay.

Fitting parameters of Equation 3.16 are given in the Figure 5.68. It is evident that the G_0^* increases with organoclay content, which is due to the reinforcement of organoclay, including hydrodynamic effect, filler-rubber interaction and filler network. The 1/A related with the extent of the LVE region decreases, and the strain sensitivity parameter B decreases steadily with increasing organoclay loading. This is attributed to the filler network is destroyed at sufficient strain amplitudes, denoted as a dynamic strain softening effect (DSS) effect. The observation is in good accordance with the results of silica as discussed previously.

(RPA-FT) Torque Harmonics vs. Strain amplitude

The typical torque harmonic responses including the total torque harmonic content (TTHC), the 3^{rd} torque harmonic (T(3/1)) and the 5^{th} torque harmonic (T5/1)) components of organoclay filled HNBR compounds are shown in Figure 5.69. As expected, the T(3/1) illustrates the essential of the non-linear behaviour, i.e., the results exhibit the S-shape. It is evident that there are bad data files for test b of all filled compounds, and the strain history effect is noticed in the highly filled HNBR compounds (i.e., there is difference between run 1 and run 2 of compound filled with 20 and 30 phr of organoclay loadings).

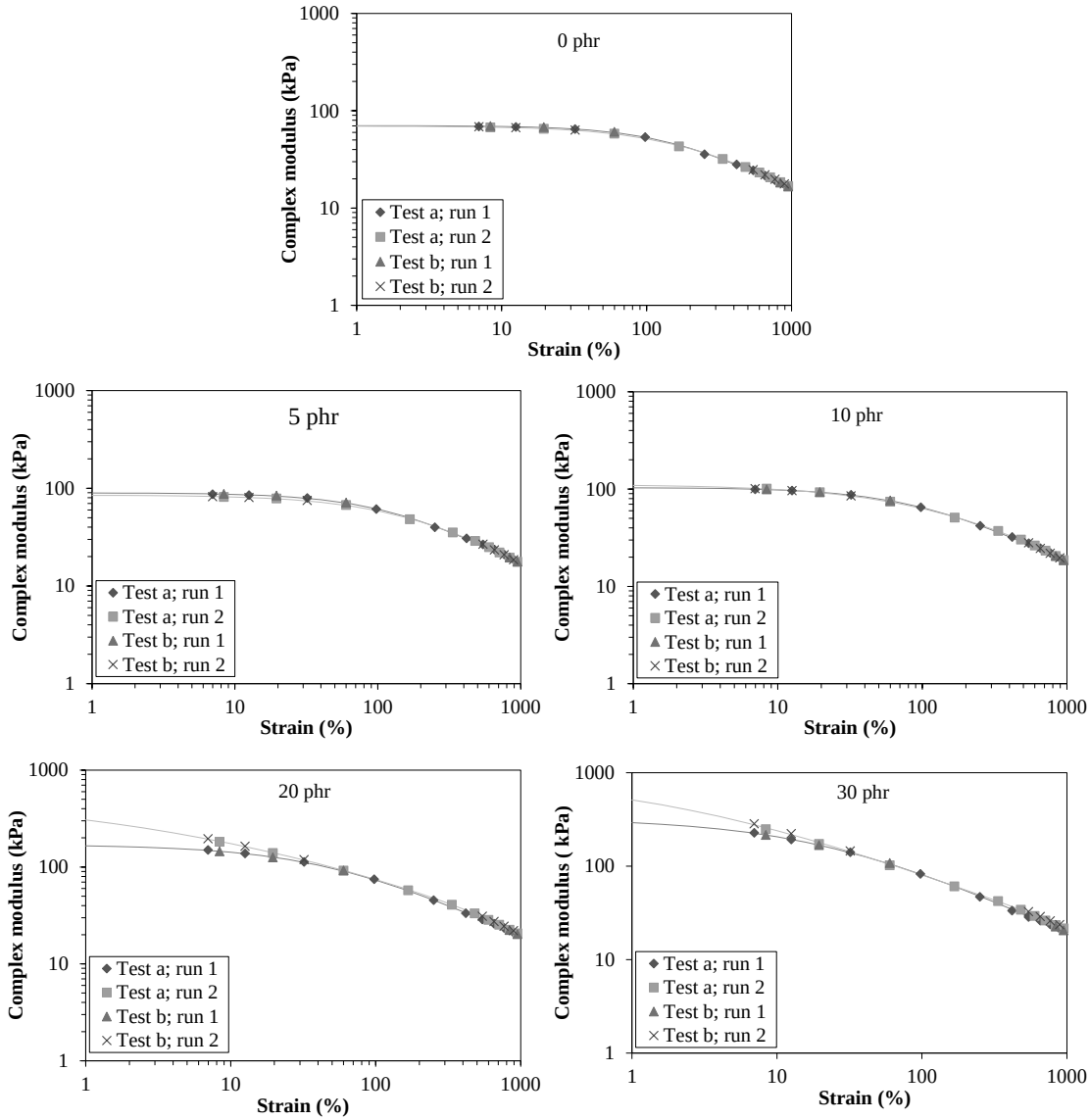

Figure 5.67 Complex modulus (G^*) as a function of strain amplitude at 3.14 rad/s and 100°C as measured by the RPA-FT of HNBR compounds filled with various organoclay loadings

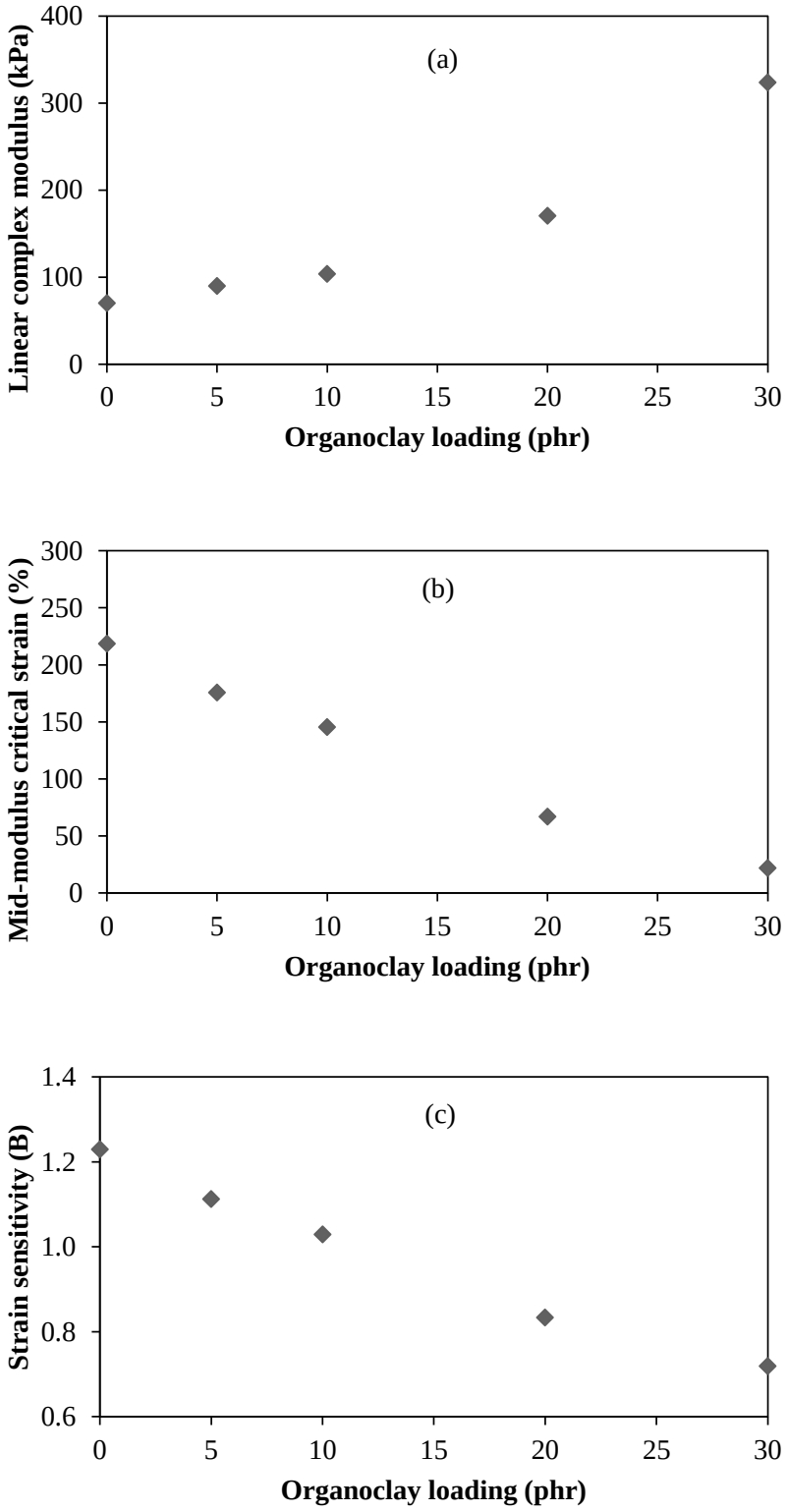

Figure 5.68 Relationship between fit parameters of Equation 3.16 and organoclay loading in HNBR compounds: (a) linear complex modulus $\left(G_0^*\right)$; (b) mid-modulus critical strain (1/A); (c) strain sensitivity (B)

The model (Equation 3.17) parameters are shown in Figure 5.69. A linear variation of harmonics in the high strain region can be expressed by the parameters TH_0 and α. There are changes in the values of TH_0 and α with increasing organoclay loading more than 20 phr. In principle, the filler-filler interaction as well as the physical interaction between filler and rubber can be fully destroyed at high strain. As a consequence, the non-linear character of filled compound depends on the stretched rubber properties resulting in the insensitivity in the parameters TH_0 and α with increasing filler loading. However, the HNBR compound filled with high loading of organoclay (i.e., 30 phr organoclay filled HNBR compound) consists of a great magnitude of rubber-filler interaction. Since the available experimental window is limited to some 1000% strain, which is obviously not enough to ensure a full destruction of the rubber-filler (78), the increase in the parameter TH_0 and the decrease in the parameter α are clearly observed for such highly filled compound.

The non-linear character of HNBR compounds is significantly affected by the high loading of organoclay. The parameters C and D using to quantify strain effect tend to decrease with organoclay content. The parameter C indicates the strain sensitivity of the non-linear response while the parameter D implies the extent of the LVE region. Interestingly, the strain sensitivity of filled compound is in line with the disruption of filler network due to a large strain amplitude, i.e., the parameter C seems insensitive to organoclay content until the organoclay loading is increased more than 20 phr, and then the decrease in parameter C is noticeable. In the case of the parameter D, there is the obvious decrease in the parameter D with increasing organoclay loading. The filler-filler interaction plays a significant role, and as a result, the DSS effect could be used to explain the non-linearity of filled compounds.

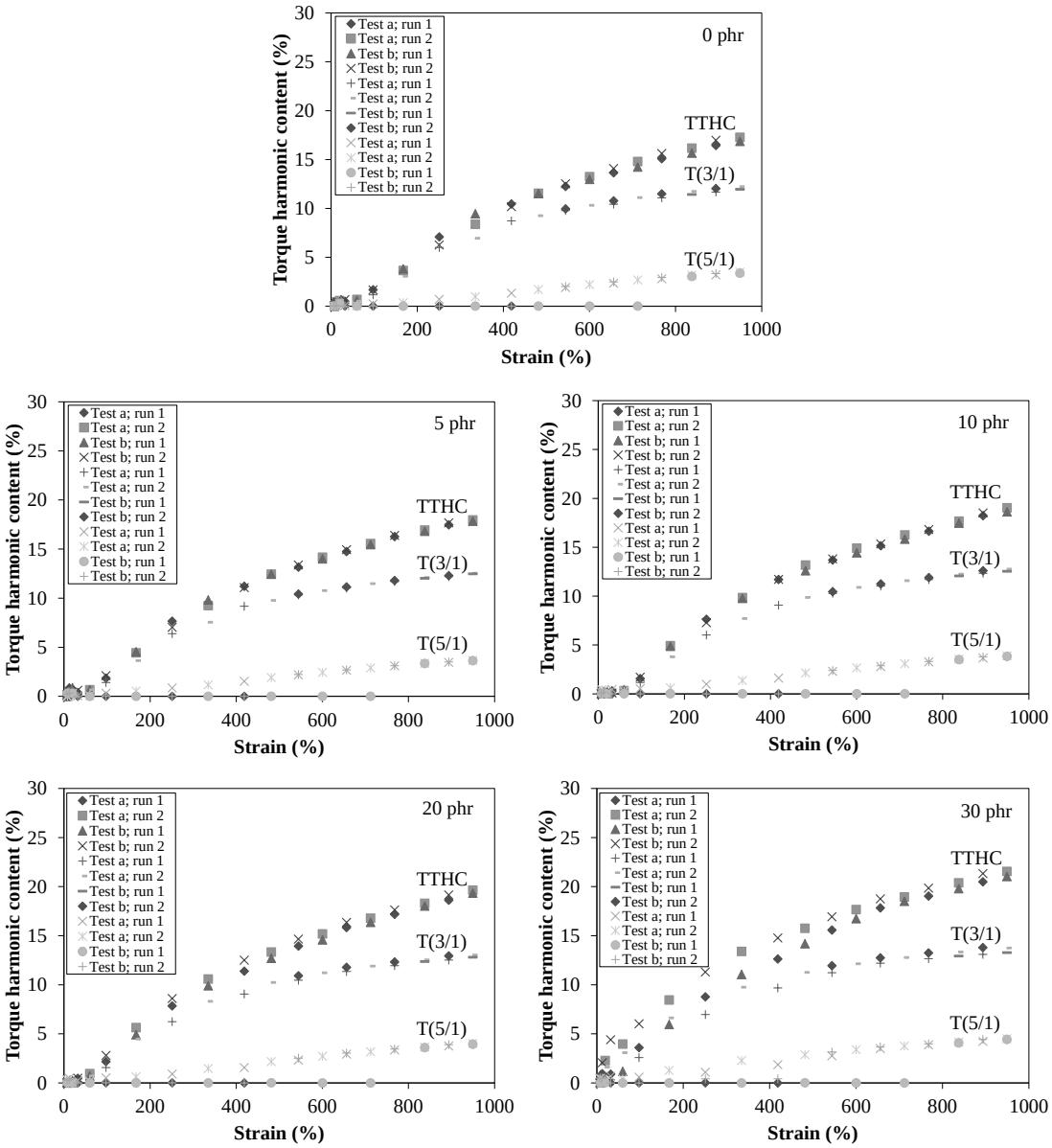

Figure 5.69 Torque harmonics as a function of strain amplitude at 3.14 rad/s and 100°C as measured by the RPA-FT of HNBR compounds filled with various organoclay loadings

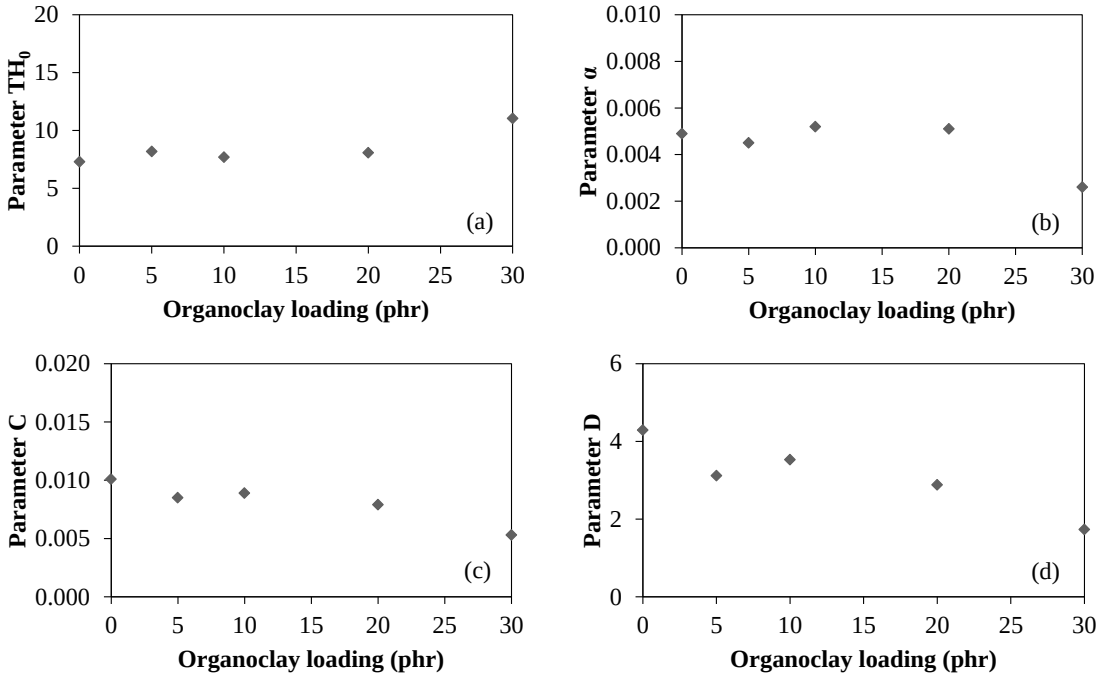

Figure 5.70 Relationship between fit parameters of Equation 3.17 and organoclay loading in HNBR compounds: (a) parameter TH_0; (b) parameter α; (c) parameter C; (d) parameter D

Quarter Torque Signal Integration

As demonstrated previously, the FT rheometry allows clearly quantifying the non-linear response of viscoelastic materials (116). The non-linear viscoelactic behaviour of filled rubber compounds can be investigated using a quarter cycle integration in terms of extrinsic and intrinsic non-linear viscoelasticity. The distortion of Q1/Q2 ratio is utilised.

Figure 5.71 shows the Q1/Q2 ratio of organoclay filled HNBR compounds as a function of strain amplitude. Expectedly, the strain history effect can be observed in the highly filled compounds, i.e., the values of run 1 and run 2 are not superimposed. The unfilled HNBR compound exhibits the extrinsic non-linearity behaviour of pure polymers, i.e., the Q1/Q2 ratio is always higher than 1, and increases with strain amplitude. The minimum Q1/Q2 ratio of filled compounds appears at strain amplitude of 167.55%. It is evident that the minimum Q1/Q2 ratio tends to decrease below 1 as the organoclay loading is increased. In other words, the

non-linear character can change from extrinsic to intrinsic as the organoclay loading increases.

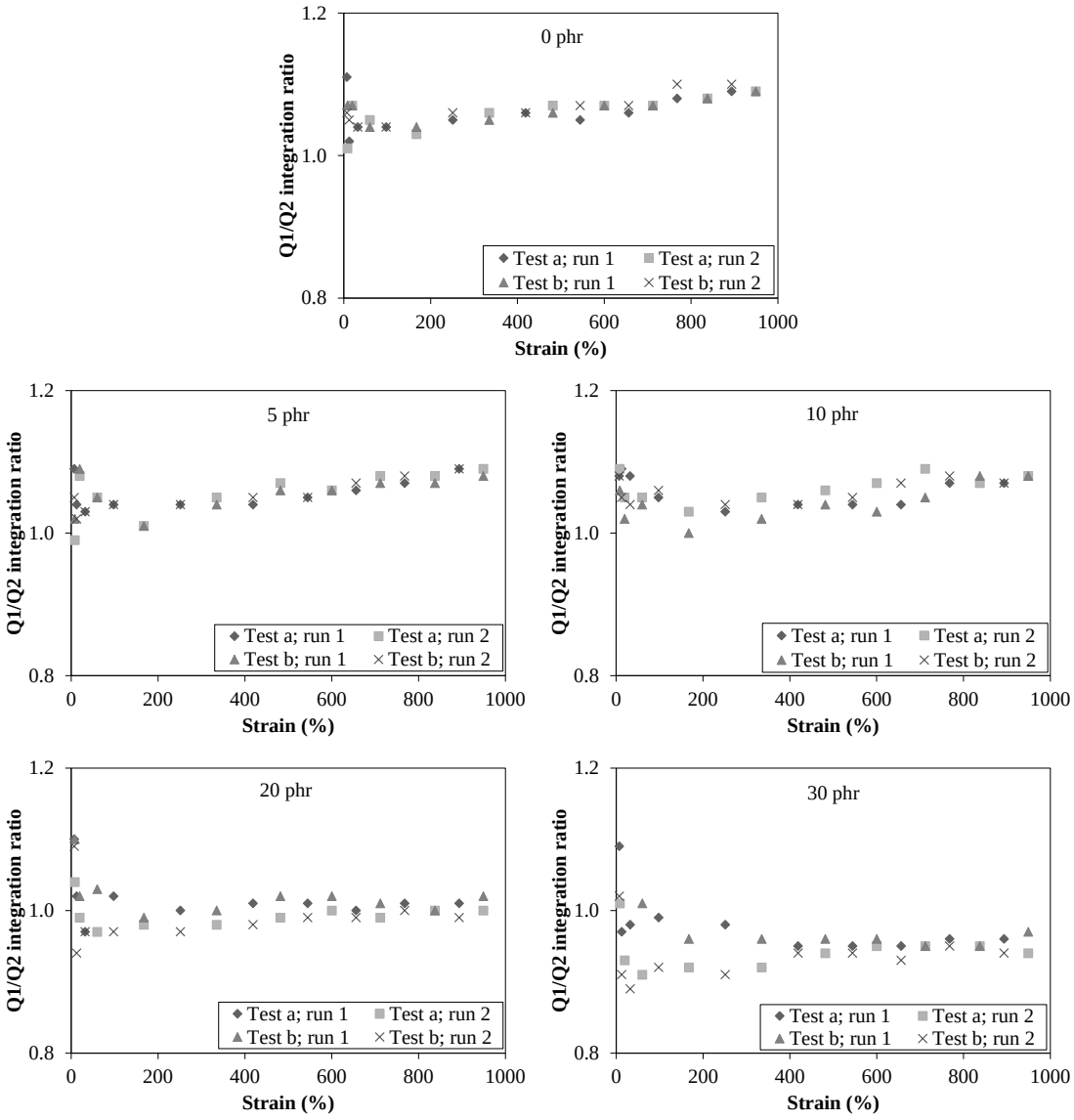

Figure 5.71 RPA-FT at 100°C on HNBR compounds filled with organoclay assessing extrinsic or intrinsic non-linear viscoelastic character through the quarter cycle torque integration; strain sweep tests at 3.14 rad/s

Besides, Figure 5.72 demonstrates that the transition occurs at organoclay loading of 10 phr. As mentioned previously, the non-linear behaviour of filled rubber compounds depends on the internal effect, such as, the filler network formation. Consequently, the result implies that the formation of filler network is significant in the HNBR compounds filled with 20 and 30 phr of organoclay loadings.

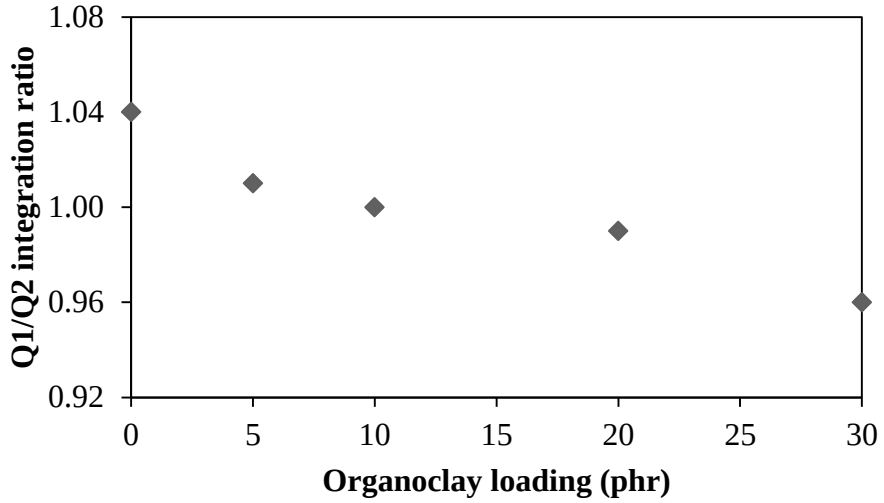

Figure 5.72 Relationship between quarter torque signal integration ratio and organoclay loading in HNBR compounds at strain amplitude of 167.55%

b) Cured organoclay filled HNBR systems

Strain sweep test

In the case of filled vulcanisates, the results of strain-dependent elastic modulus, loss modulus and damping factor are shown in Figures 5.73, 5.74 and 5.75, respectively. It can be seen from Figure 5.73 that the G′ increases, and the LVE region decreases with increasing organoclay loading, particularly in the highly filled compounds. The increase in G′ can be explained by the filler reinforcement and crosslink density effects. For the reduction in the linear behaviour, the filler network plays a major role. From Figure 5.74, it is evident that the G″ at low strain of cured compounds are similar in trend to the G′, i.e., the G″ increases with increasing organoclay loading, and the high magnitude of increase can be observed in

highly filled vulcanisates. Thus, a similar explanation could be applied. In contrast to the G′ for filled compounds, the G″ at high strain of cured specimen increases with increasing strain amplitude. Such behaviour can be explained by the energy dissipation via molecular slippage during applied dynamic strain.

As for the tanδ (Figure 5.75) which is a ratio of energy loss to energy stored, it is obvious that the tanδ increases with increasing strain amplitudes and organoclay loading, corresponding to the results of G′ and G″. The results are in line with the precipitated silica as discussed previously.

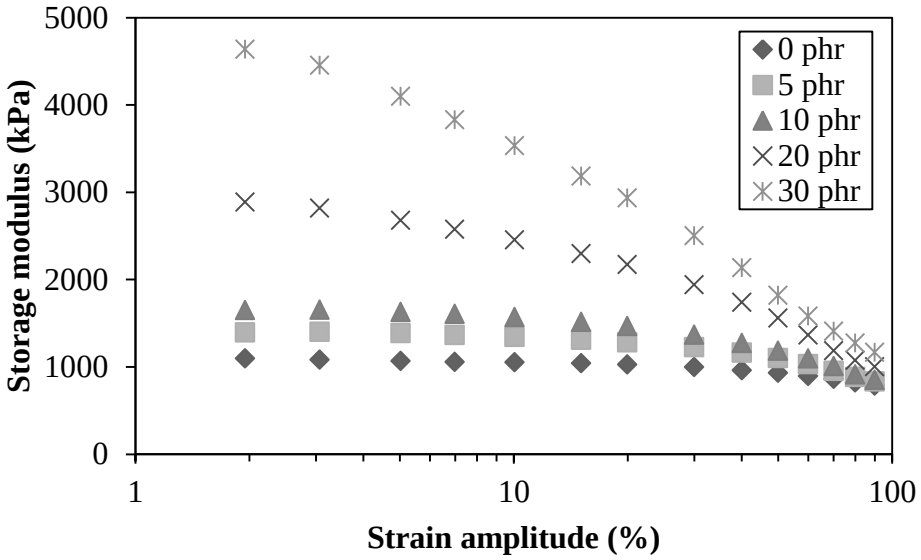

Figure 5.73 Storage modulus (G′) as a function of strain amplitude of filled HNBR vulcanisates with various organoclay loadings at test temperature and frequency of 60°C and 1 rad/s, respectively

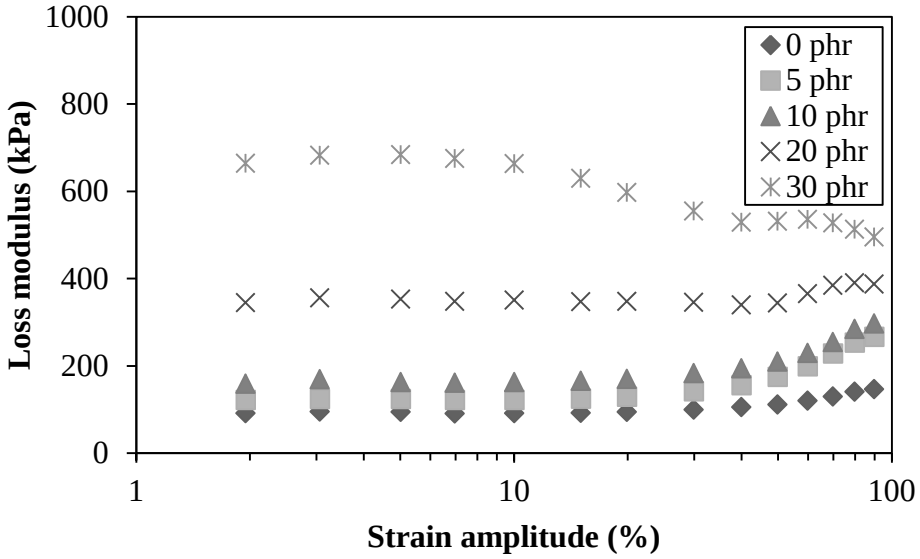

Figure 5.74 Loss modulus (G″) as a function of strain amplitude of filled HNBR vulcanisates with various organoclay loadings at test temperature and frequency of 60°C and 1 rad/s, respectively

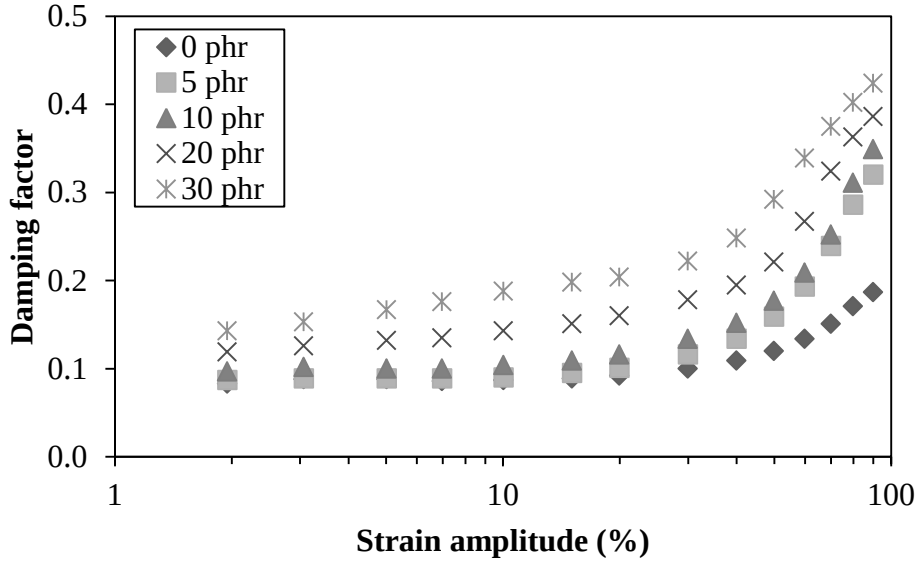

Figure 5.75 Damping factor (tanδ) as a function of strain amplitude of filled HNBR vulcanisates with various organoclay loadings at test temperature and frequency of 60°C and 1 rad/s, respectively

Temperature sweep test

Figure 5.76 represents the G′ of HNBR vulcanisates filled with various loading of organoclay. The G′ of the filled vulcanisates lies markedly higher

than the unfilled HNBR, and the significant increase in G′ with organoclay loading is noticeable above the T_g. Having in mind that the service temperature of rubbers is usually above their T_g, the plateau values of the G′ in this region is of great importance.

As shown in Figure 5.77, the hysteresis loss of the organoclay filled HNBR vulcanisates above the Tg is significantly higher than the unfilled compounds. The G″ increases with increasing organoclay loading. However, the plateau values of the G″ above the T_g is also seen for filled vulcanisates.

In the case of tanδ, it can be seen that the tanδ peak decreases with increasing organoclay loading. However, the amount of organoclay does not affect the temperature at tanδ peak (or T_g).

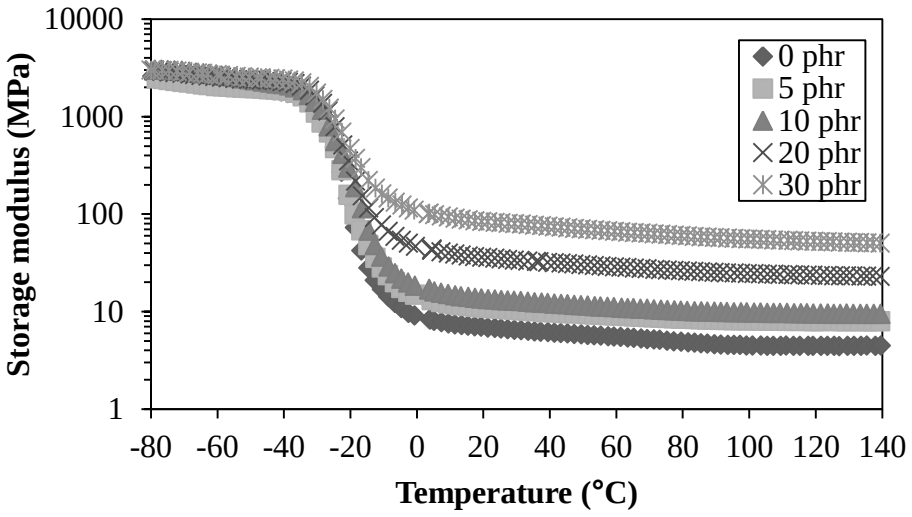

Figure 5.76 Storage modulus (G′) as a function of temperature of filled HNBR vulcanisates with various organoclay loadings at test static strain, dynamic strain and frequency of 2%, 0.1% and 62.8 rad/s, respectively

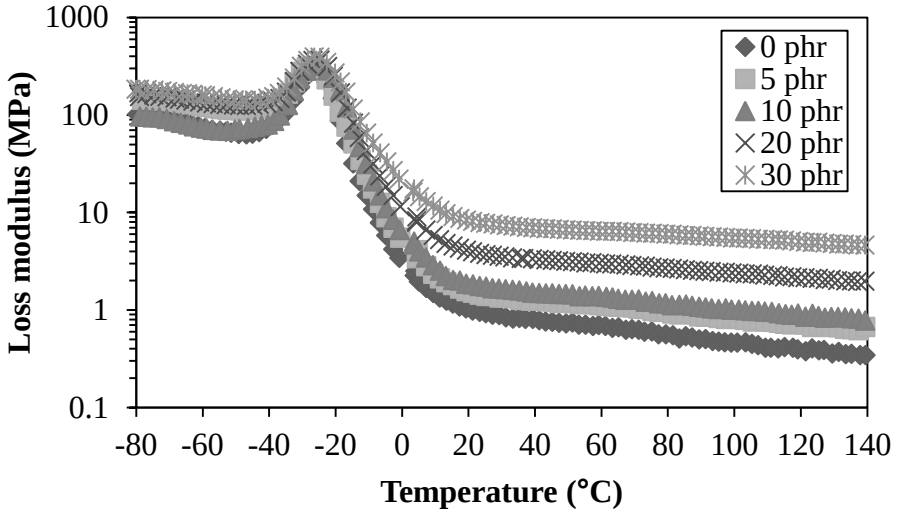

Figure 5.77 Loss modulus (G″) as a function of temperature of filled HNBR vulcanisates with various organoclay loadings at test static strain, dynamic strain and frequency of 2%, 0.1% and 62.8 rad/s, respectively

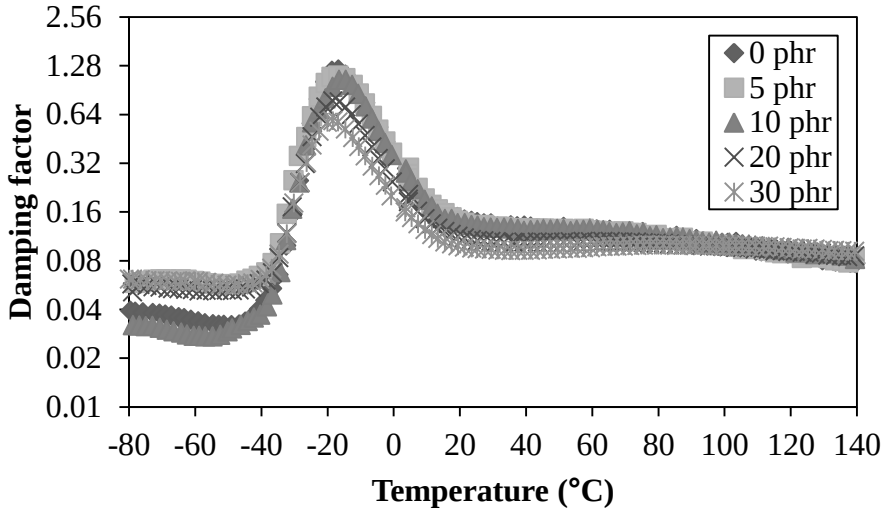

Figure 5.78 Damping factor (tanδ) as a function of temperature of filled HNBR vulcanisates with various organoclay loadings at test static strain, dynamic strain and frequency of 2%, 0.1% and 62.8 rad/s, respectively

5.1.3.3 Filler dispersion and distribution

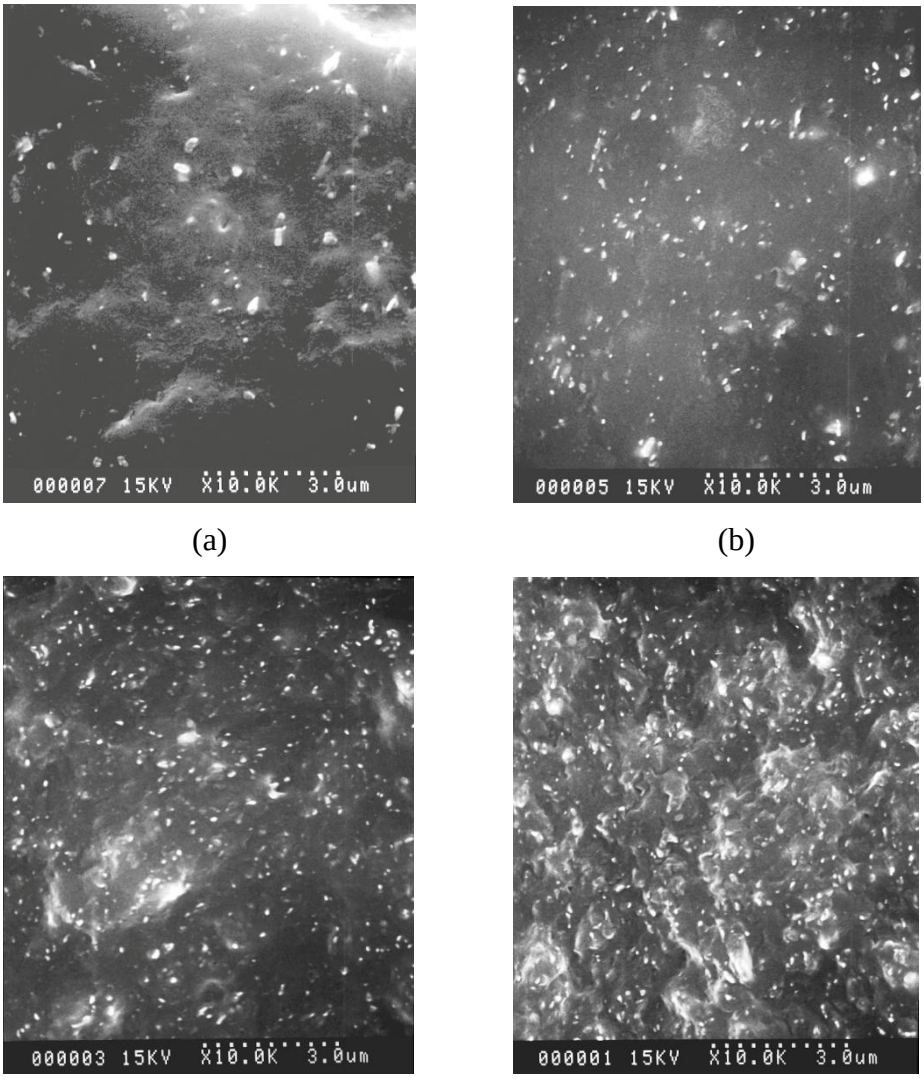

Figure 5.79 SEM micrographs of HNBR vulcanisates filled with various organoclay loadings: (a) 5 phr; (b) 10 phr; (c) 20 phr; (d) 30 phr

The organoclay dispersion in the HNBR matrix can be qualitatively determined from SEM images. As observed in Figure 5.79, the uniform distribution of the organoclays in the rubber matrix is observed in all filled vulcanisates, i.e., the organoclay particles as bright spots in micrographs distribute throughly in HNBR matrix. It is well known that the organoclays can be more easily dispersed in rubber matrix due to: (i) the presence of large alkyl hydrocarbon in the

galleries of silicate layers, (ii) the silicate surface properties changed from hydrophilic to hydrophobic and (iii) the interlayer distance increased (117-119). This leads to the excellent modulus, tensile strength and tear strength, which will be discussed in the next section.

5.1.3.4 Mechanical properties

Tensile properties including M100, tensile strength and elongation at break elongation at break are revealed in Figures 5.80 to 5.82. Results obtained show that the M100 increases with increasing organoclay loading (Figure 5.80). The increase of M100 can be explained by the filler reinforcement and crosslink density effects as discussed earlier (see the effects of CB and silica sections).

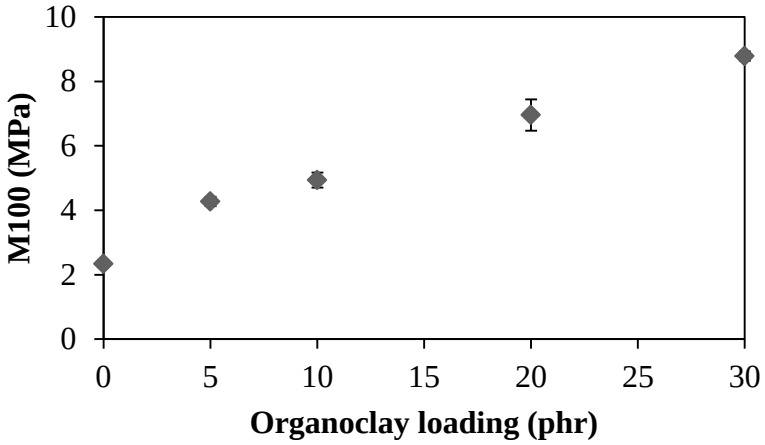

Figure 5.80 Relationship between modulus at 100% strain (M100) and organoclay loading in HNBR vulcanisates

Figure 5.81 shows the tensile strength as a function of organoclay loading. It is obvious that the tensile strength increases with organoclay loading. The explanation is similar to the results of M100, i.e., the increase in tensile strength with organoclay loading is due to the filler reinforcement effect associated with an improvement in crosslink density. Results of elongation at break as shown in Figure 5.82 reveals a slight decrease with the organoclay loading which supports the increase in interfacial interaction between polymer and organoclay layers along with the crosslink density (120, 121).

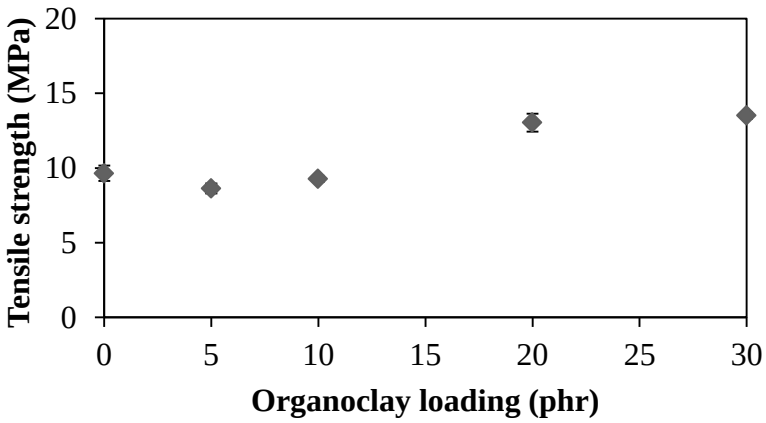

Figure 5.81 Relationship between tensile strength and organoclay loading in HNBR vulcanisates

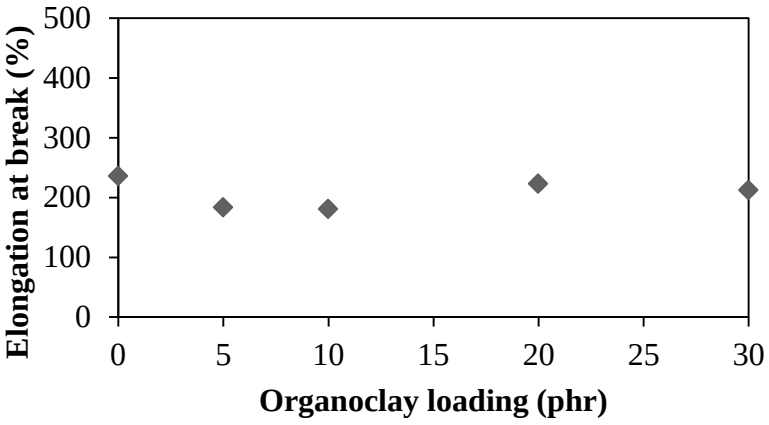

Figure 5.82 Relationship between elongation at break and organoclay loading in HNBR vulcanisates

Figure 5.83 demonstrates the tear strength of organoclay filled HNBR vulcanisates. It is evident that the tear strength increases with increasing organoclay loading. The results are in line with the tensile properties. As a consequence, the similar explanation can be applied.

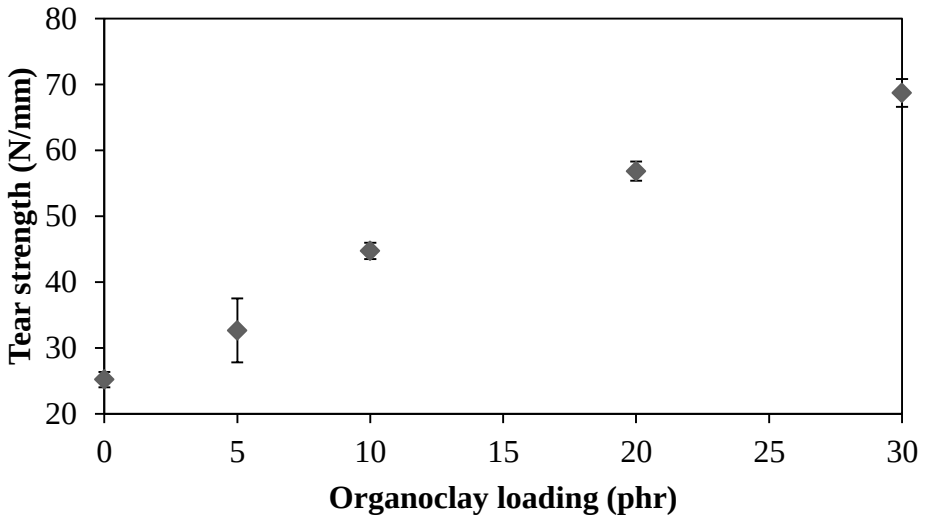

Figure 5.83 Relationship between tear strength and organoclay loading in HNBR vulcanisates

Hardness of vulcanisates as illustrated in Figure 5.84 is influenced by organoclay loading in a manner that the hardness increases continually with organoclay loading. Undoubtedly, the filled system with the high crosslink density gives the high hardness. Also, it is evident the result of hardness is in good agreement with the M100 results, and therefore, similar explanation could be applied.

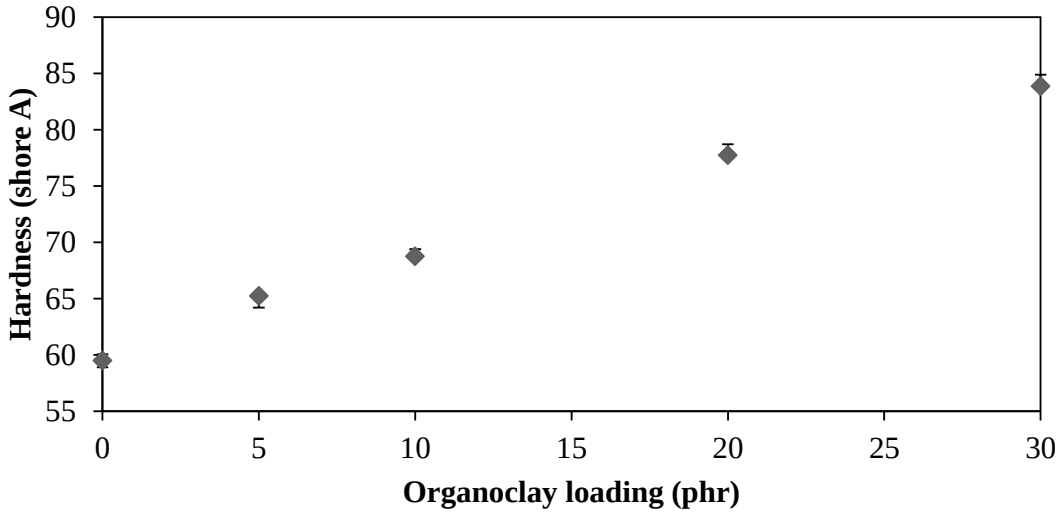

Figure 5.84 Relationship between hardness and organoclay loading in HNBR vulcanisates

Results of abrasion resistance, which is inversely proportional to abrasion loss of vulcanisates are revealed in Figure 5.85. The addition of organoclay does not significantly change abrasion resistance of vulcanisates up to the organoclay loading of 10 phr, and then abrasion resistance is impaired with increasing organoclay content. It has been reported that, during intense abrasion in sliding contact, a high temperature is developed, and such high temperature of rubber is detrimental to abrasion resistance (19, 21, 122). The increase in organoclay loading exhibits enhanced hysteresis (123, 124) due to more frictional sliding at the interface between the surface of the organoclay layer and rubber chain under deformation. It is well known that the hysteresis is proportional to the G″ (21, 125), and consequently, the deterioration in abrasion resistance of organoclay filled HNBR vulcanisates agrees well with the result of G″ as shown previously in Figure 5.74.

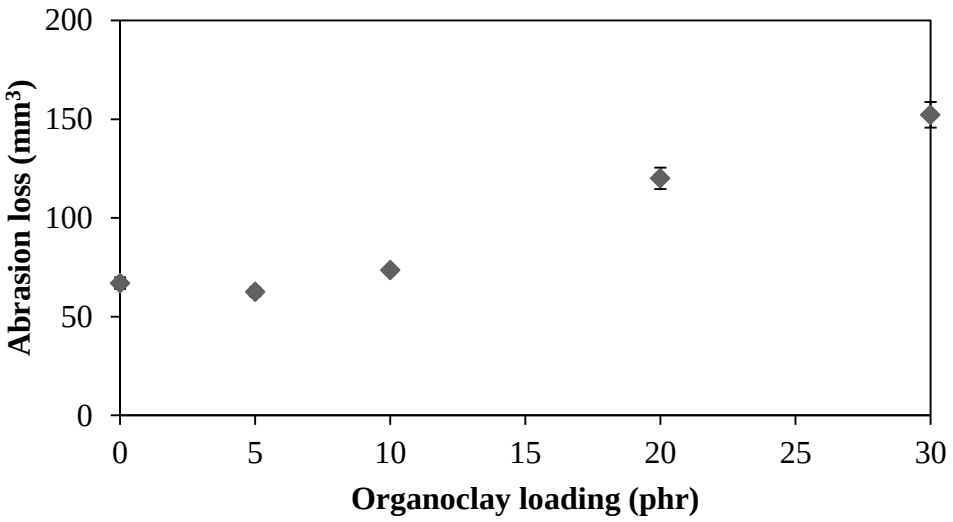

Figure 5.85 Relationship between loss and organoclay loading in HNBR vulcanisates

5.1.4 Comparative study of mechanical properties of carbon black, silica and organoclay filled HNBR systems

Basically, the rubber roll covers used in paper mill industry require good mechanical properties, such as, tensile strength abrasion and tear resistances associated with low heat build-up (HBU). However, a specific hardness is needed for the rubber covered rolls. In this section, the effect of filler types on the mechanical properties of HNBR vulcanisates at similar hardness level of 80 Shore A is focused. The CB used in this part is N550 due to its superior mechanical properties as mentioned previously in section 5.1.1.

Hardness and M100 of all vulcanisates are shown in Figures 5.86 and 5.87, respectively, where both properties increase with increasing filler loading. At filler loading of 10, 20 and 30 phr, the highest hardness and M100 are observed in the HNBR vulcanisates filled with organoclay. To achieve the hardness of 80 to 82 Shore A, the filler loadings required are 30 phr for organoclay, 40 phr for silica and 60 phr for CB. In other words, organoclay is the most effective for enhancing hardness of the HNBR vulcanisate, followed by silica and CB, respectively.

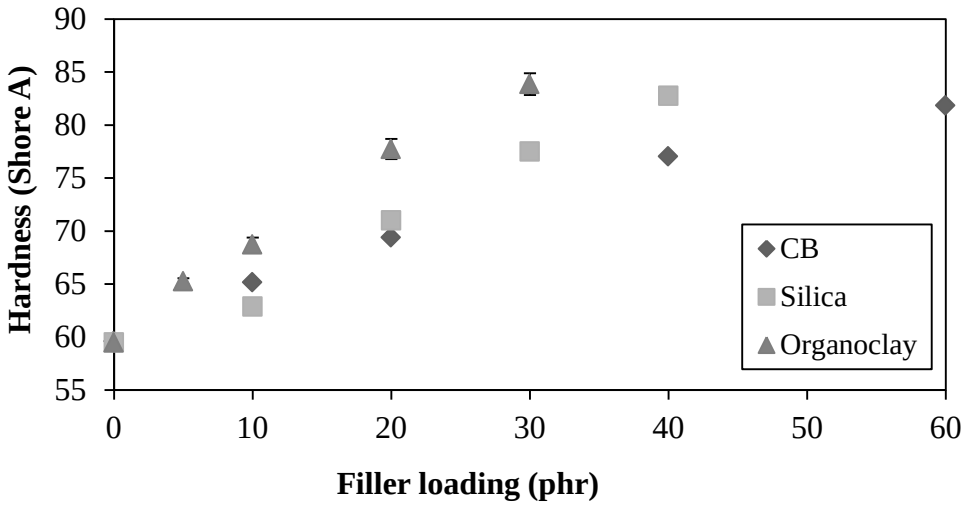

Figure 5.86 Hardness as a function of filler loading for filled HNBR vulcanisates

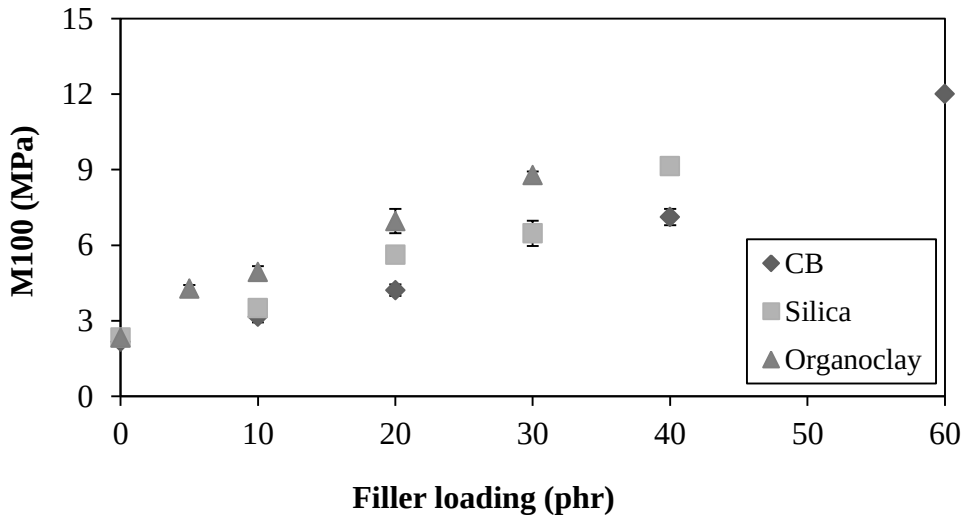

Figure 5.87 Modulus at 100% strain (M100) as a function of filler loading for filled HNBR vulcanisates

Tensile strength of filled HNBR vulcanisates having similar hardness of 80 Shore A is shown in Figure 5.88. The tensile strength of all filled vulcanisates is higher than control (i.e., unfilled vulacnisate). The CB filled vulcanisate exhibits the highest tensile strength followed by the systems with silica and organoclay. The results might be explained by the filler network formation, and by the interaction development between filler and rubber. Figure 5.89 displays the results of G′ as a function of strain amplitude of HNBR vulcanisates filled with various types of filler possessing similar hardness level. It is evident that the G′ of HNBR vulcanisate filled with CB is lower than that filled with organoclay and silica, and shows broader LVE region. The less filler network formation and more filler-rubber interaction of the CB filled vulcanisates results in the higher tensile strength.

The elongation at break of filled HNBR vulcanisates possessing similar hardness level is in line with the tensile strength results, i.e., the elongation at break of CB filled vulcanisate is lowest, followed by silica and organoclay filled ones, respectively, as illustrated in Figure 5.90.

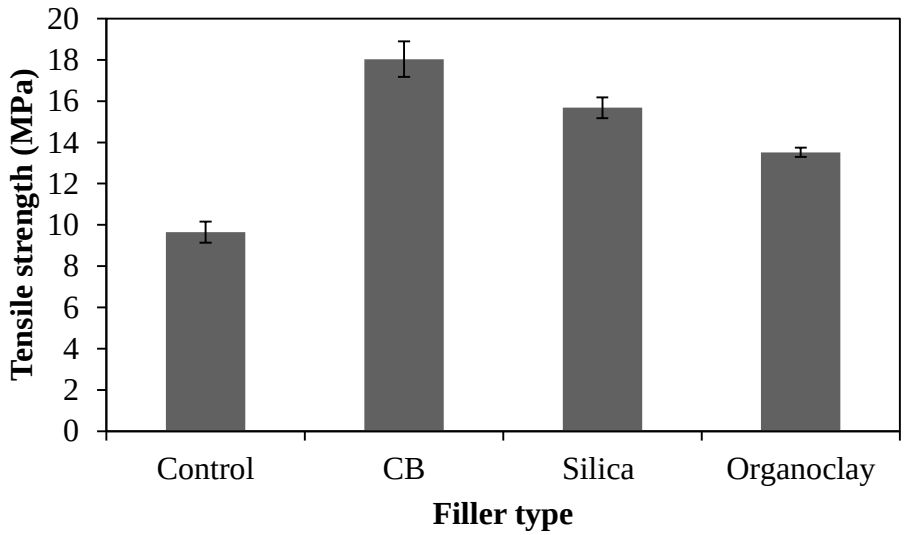

Figure 5.88 Tensile strength as a function of filler loading for filled HNBR vulcanisates having the hardness of 80 Shore A

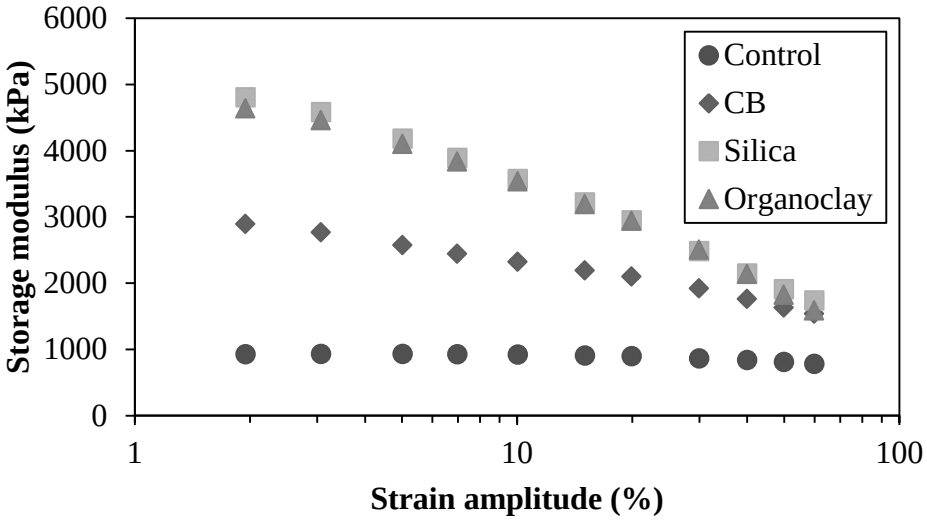

Figure 5.89 Storage modulus (G′) as a function of strain amplitude of filled HNBR vulcanisates having the hardness of 80 Shore A

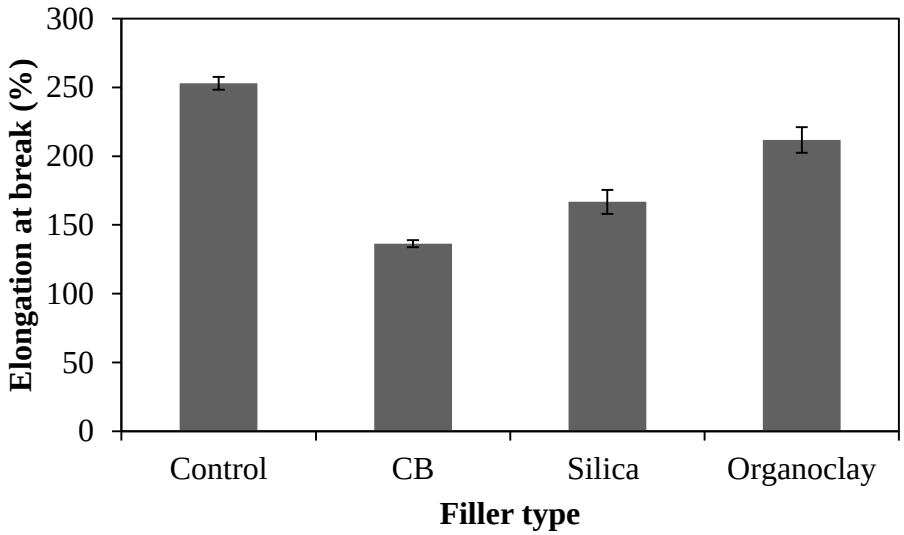

Figure 5.90 Elongation at break as a function of filler loading for filled HNBR vulcanisates having the hardness of 80 Shore A

Figure 5.91 shows tear strength at the hardness of 80 Shore A of filled HNBR vulcanisates. The CB filled valcanisate exhibits lower tear strength to that of silica and organoclay filled vulcanisates. The lower tear strength is also explained by the strong effect of filler-rubber interaction. Wang and coworkers (126) found that the higher tear energy for the vulcanisate is related mainly to the lower polymer-filler interaction with which the slippage and detachment (dewetting) of polymer molecules on the filler surfaces occurs under stress. This, while causing internal energy dissipation, will release the stress concentration in polymer network, and facilitate the orientation or crystallisation near the tear tip, resulting in higher tear resistance.

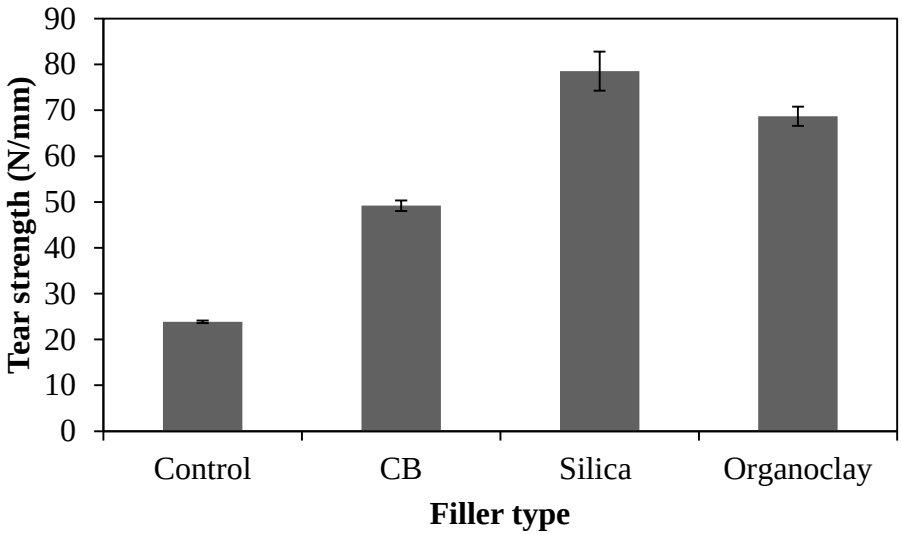

Figure 5.91 Tear strength as a function of filler loading for filled HNBR vulcanisates having the hardness of 80 Shore A

Results of abrasion resistance, as expressed by the abrasion loss, are presented in Figure 5.92. The abrasion resistance of unfilled HNBR vulcanisates is lower than all filled vulcanisates. The different wear mechanism is used to the explanation, as discussed previously in the section 5.1.1.4. Obviously, the CB filled vulcanisate possessing stronger filler-rubber interaction exhibits the lower abrasion loss and thus the higher abrasion resistance. The lower abrasion resistance of silica and organoclay results from their poor filler dispersion due to their stronger filler-filler interaction.

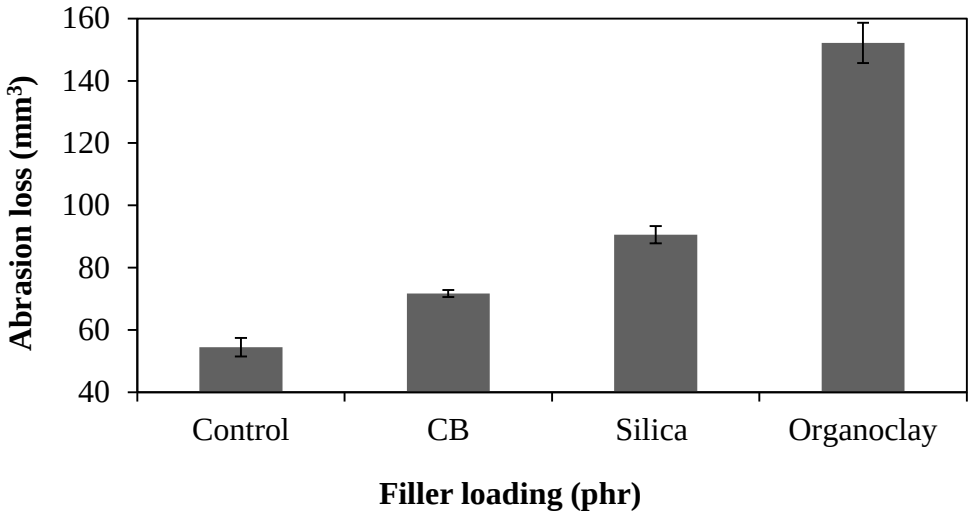

Figure 5.92 Abrasion loss as a function of filler loading for filled HNBR vulcanisates having the hardness of 80 Shore A

5.1.5 Influences of carbon black hybrid system

In this section, four types of CBs, i.e., N326, N550, N774 and N990, were utilised for preparing the CB hybrid systems. Specific surface areas of CBs used in this work are in the order as follows: N326 > N550 > N774 > N990 while degrees of structures are in the following order: N550 > N326 ~ N774 > N990, which is determined by iodine adsorption and DBP absorption, respectively (127). Three CB hybrid systems, namely, N326/N990, N326/N774 and N550/N990 were prepared. The objectives for preparing each CB hybrid system used in this work are described in Table 5.2. Influence of CB hybrid ratio in different hybrid systems on cure behaviour, viscoelastic properties and mechanical properties was investigated.

5.1.5.1 Cure characteristics

Figures 5.93 to 5.95 show scorch time (t_{s2}), cure time (t_{c90}) and crosslink density of filled HNBR system. Apparently, for the HNBR compounds with N326/N990 hybrid system, the scorch time of filled HNBR compounds decreases slightly with increasing N326 content. The cure time and crosslink density (as represented by torque difference) are not significantly affected by the increase in N326 content in hybrid ratio up to 40%. Further increase the amount of N326 in hybrid ratio beyond 40% gives a decrease in cure time in association with the increase in crosslink

density. Since the amounts of bound and occluded rubber increase with increases in surface area and structure of CB hybrid systems (i.e., N326 content), the migration of curative to rubber matrix would probably increase, promoting the cure reaction. In addition, as the content of N326 possessing relatively high surface area and structure increases, the increased bulk viscosity leads to increased shear heating via viscous dissipation. The increased bulk temperature during the mixing process is resulted, giving the shortened time required for curative dissociation and hence a cure promotion phenomenon. It is noticeable that the cure behaviour of N326/N990 filled HNBR depends on characteristics of major CB composition in the CB hybrid system, i.e., at N326/N990 ratio of 0/100, 20/80 and 40/60, the cure behaviour is dominated by N990, while at the ratio of 60/40, 80/20 and 100/0, the cure characteristics are governed by N326. This phenomenon is sometimes known as the dilution effect.

Table 5.2 Summarised objectives for preparing carbon black hybrid systems used in the present section

System	Objectives
N326/N990	To investigate surface area and structure effects in hybrid system assembling extreme characteristics of CB
N326/N774	To investigate the effect of the different CB surface area in hybrid systems on the filler reinforcement and the processability with minimal effect of CB structure
N550/N990	To monitor the effect of N550 instead of N326 on HNBR properties compared with the N326/N990 hybrid system

In the case of HNBR compounds filled with N326/N774 hybrid system, the content of N326 impacts slightly on scorch time, and the cure time is somewhat shortened with N326 loading. Crosslink density does not increase systemically with increasing N326 loading. Compared with HNBR filled with N326/N990 hybrid system, it is noticed that both scorch and cure times of N326/N774 filled HNBR vulcanisates are shorter, particularly at a hybrid ratio which N774 is main

composition. This result can be explained by predominant characteristics (i.e., CB surface area and structure) of CB composition. The higher the CB surface area and the structure, the greater the filler-polymer interaction, leading to the faster the cure reaction. As a consequence, the compounds filled with N326/N774 show the higher crosslink density.

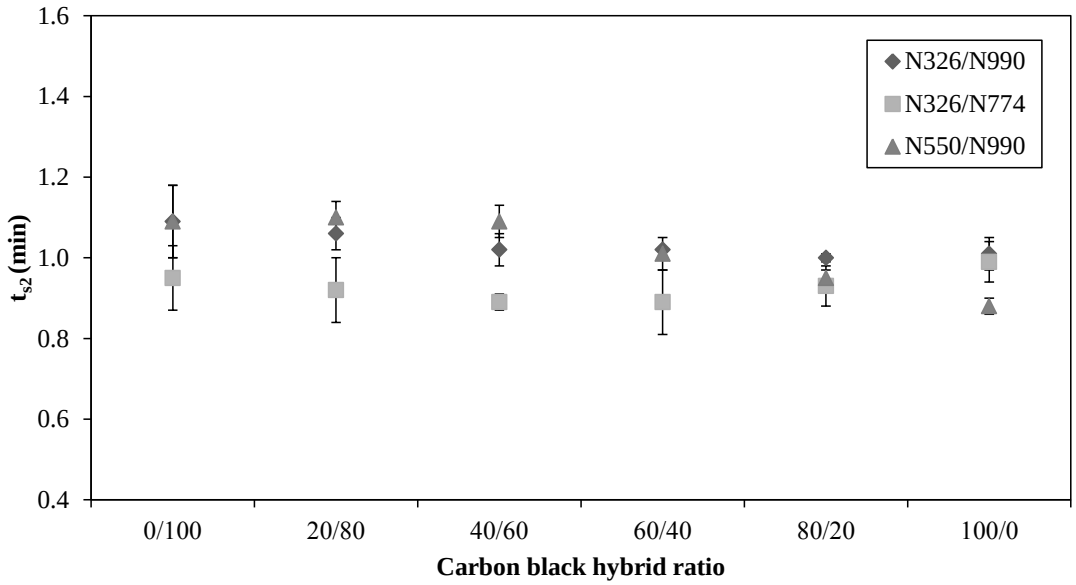

Figure 5.93 Relationship among scorch time (t_{s2}), carbon black hybrid ratio and hybrid system in HNBR compounds

In the case of HNBR compounds filled with N550/N990 hybrid system, both scorch and cure times of filled compounds decrease with increasing N550 content. Expectedly, crosslink density of HNBR vulcanisates increase with increasing N550 content, which is due to the increase of CB structure in CB hybrid ratio, as discussed previously. By comparing the cure characteristics of N550/N990 filled HNBR with N326/N990 filled HNBR, it is observed that, the crosslink density of HNBR filled with both hybrid systems are comparable, which is due probably to the bound rubber and/or crosslinking reaction effects, as discussed earlier in section 5.1.1.

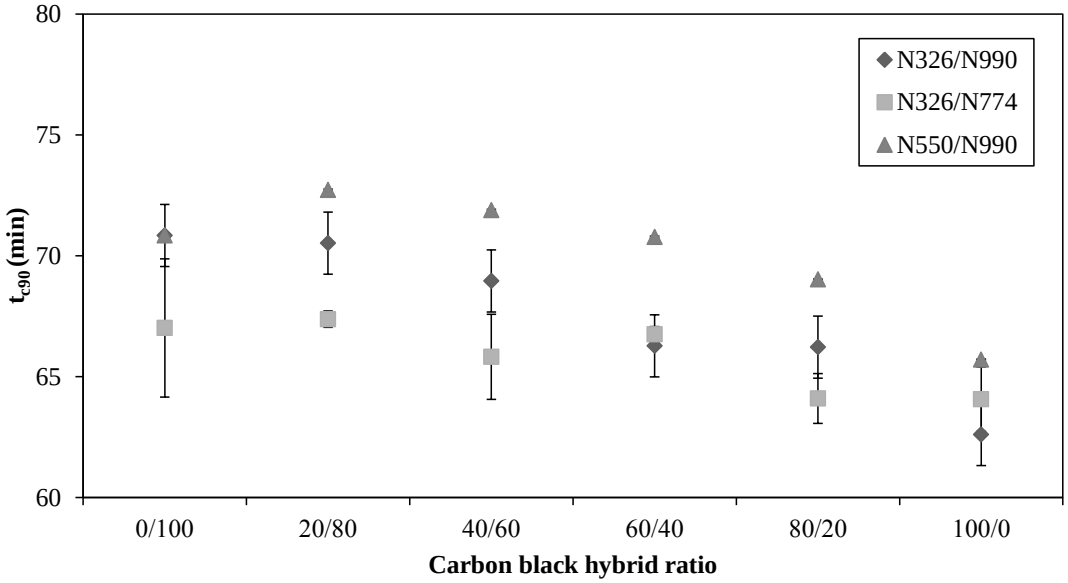

Figure 5.94 Relationship among cure time (t_{c90}), carbon black hybrid ratio and hybrid system in HNBR compounds

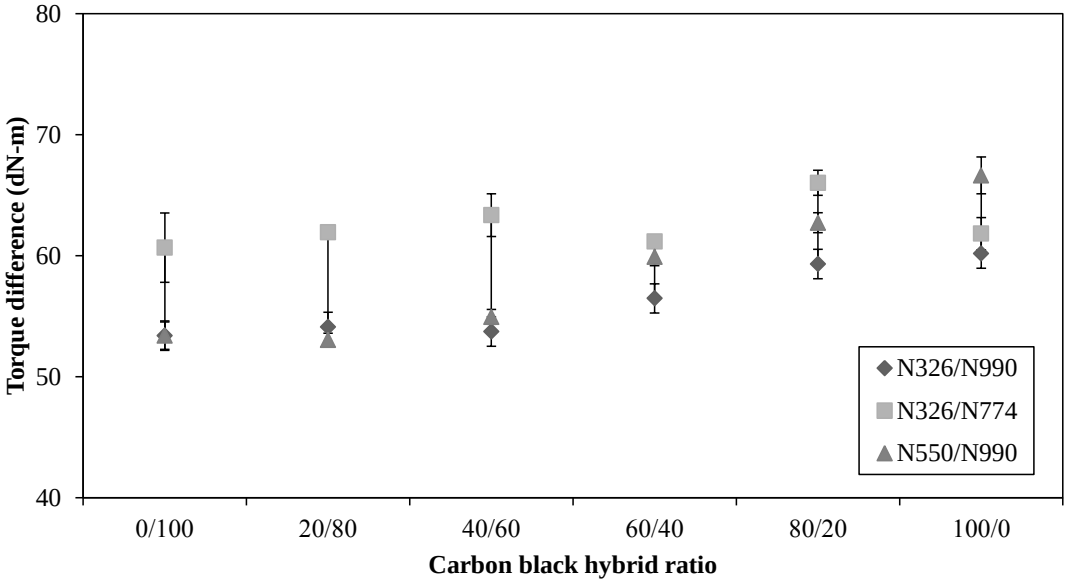

Figure 5.95 Relationship among torque difference (or crosslink density), carbon black hybrid ratio and hybrid system in HNBR compounds

5.1.5.2 Viscoelastic properties

c) Uncured CB hybrid system filled HNBR

(RPA-FT) Complex modulus vs. Strain amplitude

Figures 5.96 to 5.98 show the complex modulus (G*) of filled HNBR compounds with N326/N990, N326/N774 and N550/N990 hybrid systems as a function of strain amplitude, respectively. It is clearly seen that all compounds are homogeneous, since the results from two tests (a and b) are identical. Moreover, it is found that, in all cases, except for the HNBR compound filled with N550/N990 hybrid ratio of 100/0, the G* appears to be insensitive to strain history as observed by the superimposition between runs 1 and 2. At the N550/N990 hybrid ratio of 100/0 filled HNBR compound, a deviation of run 2 curve is observed at high strain. Referred to Figure 5.93, it is evident that this system exhibits the fastest scorch time. Consequently, such deviation result could probably be explained by the localised premature crosslink of the test compounds.

Results of complex modulus as a function of strain amplitude of filled HNBR with the three CB hybrid systems are modelled with Equation 3.16. Fit parameters of Equation 3.16 are plotted in Figure 5.99, where the relationship between G_0^* and the CB hybrid ratio of HNBR compounds filled with different CB hybrid systems is correlated.

In the case of N326/N990 filled compounds, it is evident that the G_0^* increases with increasing N326 content, which is attributed to the reinforcing effect, i.e., a combination of hydrodynamic effect, filler-filler interaction as well as filler-rubber interaction. The presence of N326 with relatively high surface area and structure is generally reported to yield a strong filler transient network and filler-rubber interaction, leading to a remarkable rise in G_0^*. The increase of G_0^* with increasing N326 and N550 content is also found in the results of N326/N774 and N550/N990 hybrid system filled HNBR compounds, respectively. The addition of CB having higher surface area and/or structure in CB hybrid system results in higher G_0^* of HNBR compounds, due likely to the greater magnitudes of a filler tri-dimensional transient network, and filler-rubber interaction through larger contacting area.

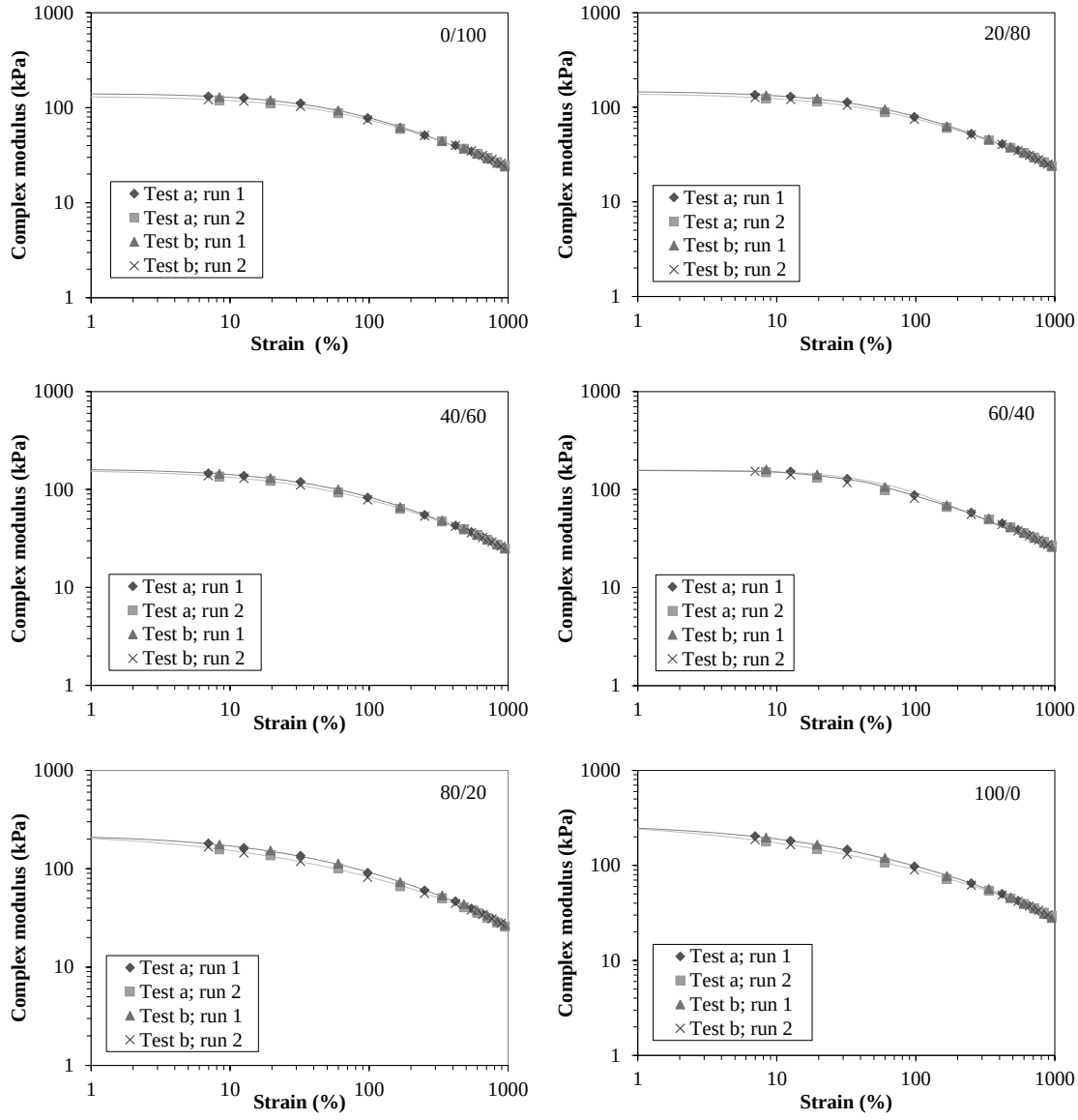

Figure 5.96 Complex modulus (G^*) as a function of strain amplitude at 3.14 rad/s and 100°C as measured by the RPA-FT of HNBR filled with various N326/N990 hybrid ratios

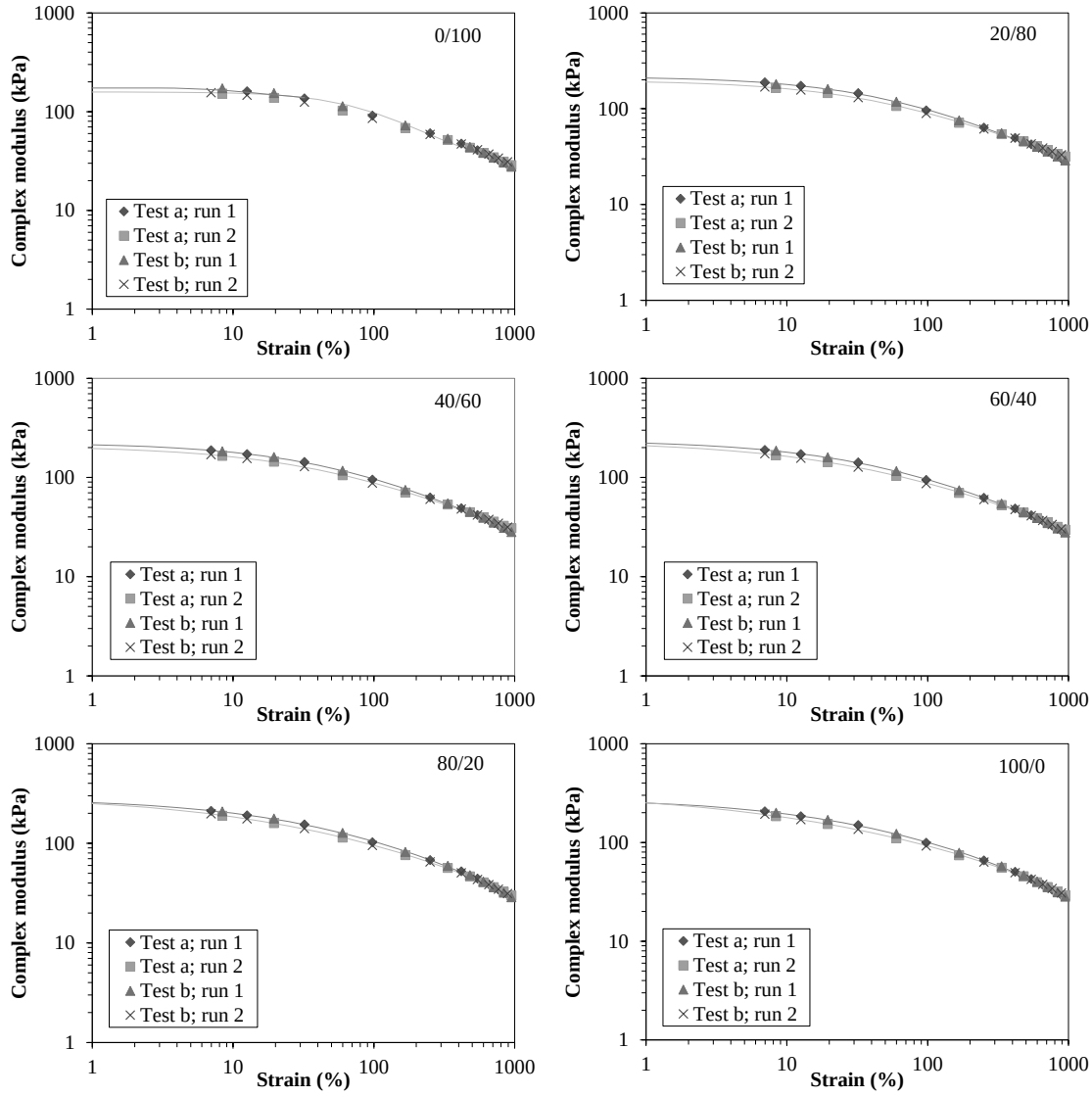

Figure 5.97 Complex modulus (G^*) as a function of strain amplitude at 3.14 rad/s and 100°C as measured by the RPA-FT of HNBR filled with various N326/N774 hybrid ratios

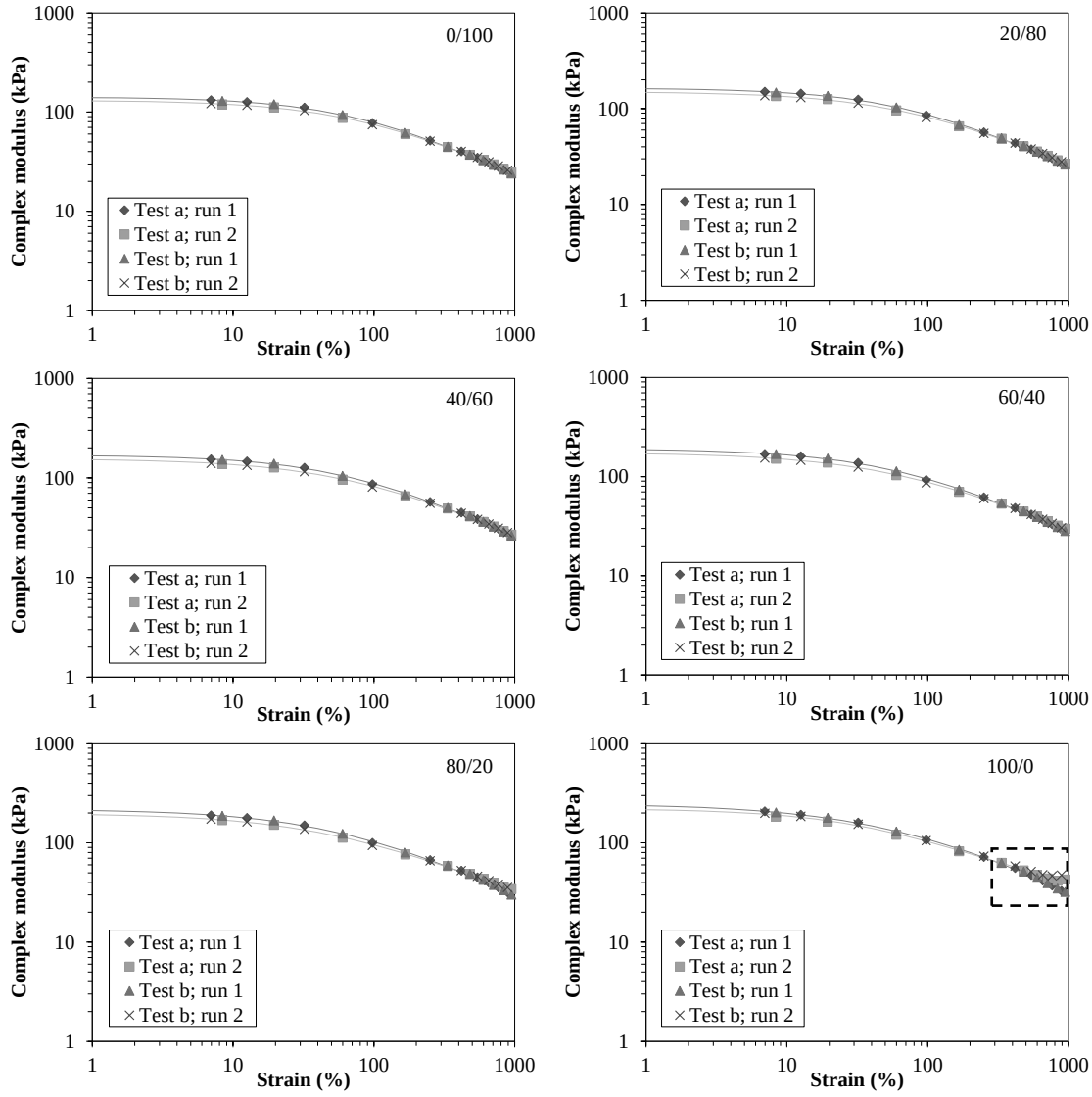

Figure 5.98 Complex modulus (G^*) as a function of strain amplitude at 3.14 rad/s and 100°C as measured by the RPA-FT of HNBR filled with various N550/N990 hybrid ratios

At a given CB hybrid ratio, it is apparent that the G_0^* of filled HNBR compounds with N326/N774 hybrid system is higher than those with N326/N990 as expected. This is due to N774 in the N326/N774 hybrid system exhibits higher surface area and structure than N990 in N326/N990 hybrid system, likely leading to greater filler-filler and filler-rubber interactions, as discussed earlier. Expectedly, the G_0^* of HNBR vulcanisates filled with N550/N990 and N326/N990 is

similar, excepting in case 100/0 hybrid ratio. The lower G_0^* of neat N550 filled HNBR compound is caused by the lower magnitudes of the filler network formation and filler-rubber interaction in filled HNBR compounds, which is in agreement with the bound rubber result (as shown in Table 5.1).

As mentioned previously, the mid modulus critical strain (1/A) is used to determine the extent of the LVE region. Figure 5.99 (b) exhibits the 1/A values which decrease with increasing CB contents having higher surface area and/or structure into hybrid ratio. This is attributed to a greater magnitude of filler network formation, leading to the narrower LVE region and hence a larger dynamic strain softening effect. Seemingly, at the CB hybrid ratios of 0/100, 20/80 and 40/60, the 1/A values of N326/N774 filled HNBR compound are lower than those of N326/N990 filled system, demonstrating that the narrower LVE region is pronounced by the incorporation of CB possessing higher surface area and structure into the hybrid system. Compared between N326/N990 and N550/N990 filled HNBR compounds, similar 1/A values are resulted, i.e., the extent of the LVE region is dominantly governed by the N990 characteristics. In the case of 60/40, 80/20 and 100/0 CB hybrid ratios, the 1/A values of N550/N990 filled HNBR compound are higher than those of N326/N990 filled HNBR compound. The greater magnitude of a CB tridimensional transient network through the CB with larger surface area is responsible for the shorter LVE region, and hence a larger dynamic strain softening effect. Accordingly, the increase in CB content having higher surface area and/or structure into hybrid ratio influences extremely the strain sensitivity of HNBR compounds, as evidenced from a decrease in parameter B in Figure 5.99 (c).

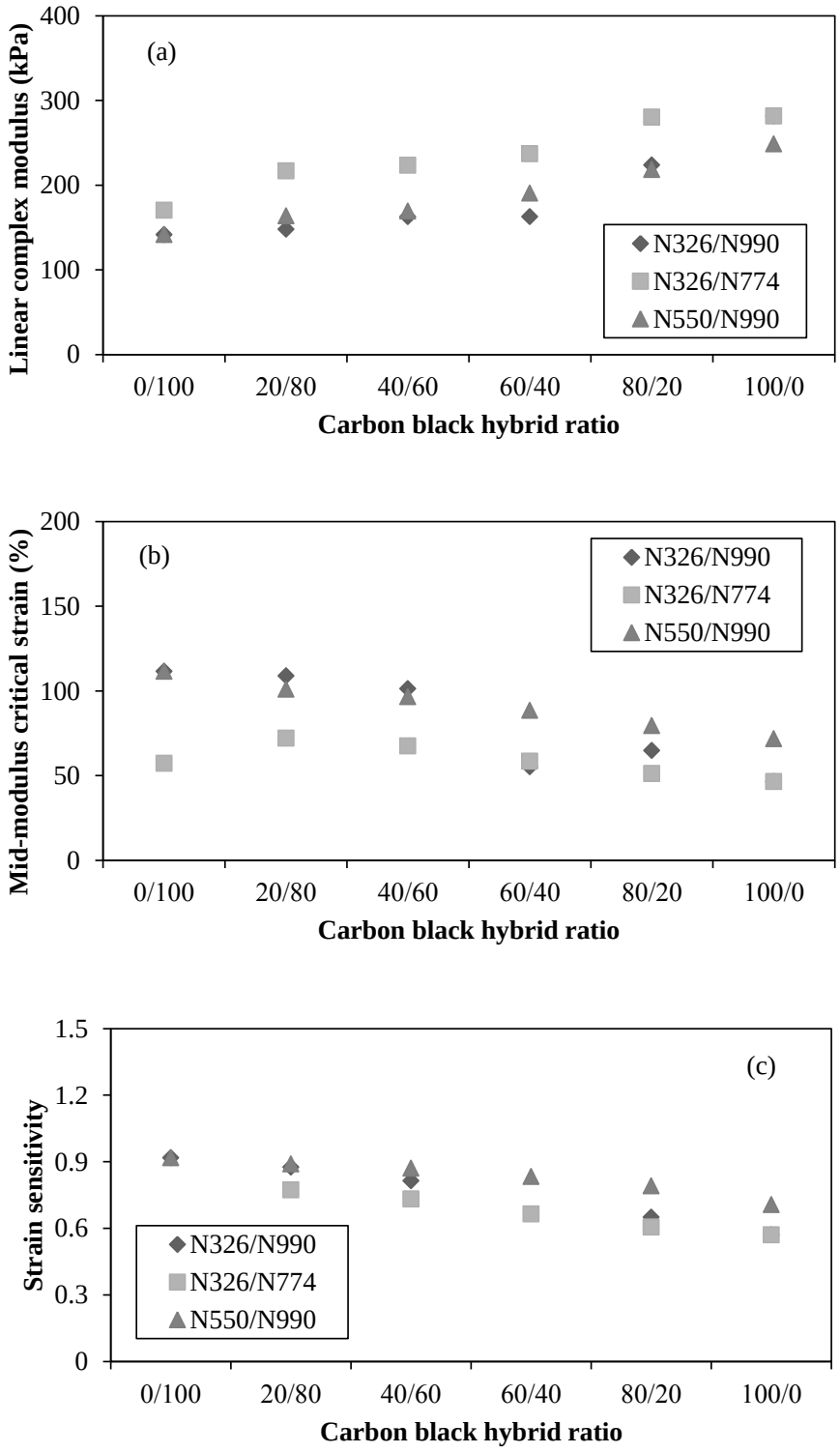

Figure 5.99 Relationship among fit parameters of Equation 3.16, carbon black hybrid ratio and hybrid system in HNBR compounds: (a) linear complex modulus $\left(G_0^*\right)$; (b) mid-modulus critical strain (1/A); (c) strain sensitivity (B)

(RPA-FT) Torque Harmonics vs. Strain amplitude

The non-linear viscoelasticity of tested compounds is described by odd torque harmonics at high strain amplitude, reported as the overall torque harmonic content, TTHC (i.e., the sum of the odd harmonics up to the 15^{th}), 3^{rd} relative torque harmonic T(3/1) and 5^{th} relative torque harmonic T(5/1).

The variations of torque harmonics, i.e., TTHC, T(3/1) and T(5/1) versus strain amplitude of filled HNBR compounds with carbon black hybrid systems are shown in Figures 5.100 to 5.102. It is clearly seen that all the tested compounds show the torque signal harmonic insensitive to the strain history and the homogeneity effects as observed from the superimposition between runs 1 and 2, and between tests a and b, respectively. The exception is found in the case of filled HNBR compound with N550/N990 hybrid ratio of 100/0, in which the difference between run 1 and 2 is clearly observed at high strain due to scorch of compound, as discussed previously. Evidently the relative torque harmonics variation with strain amplitude is conformed to S-shape curves for all tested compounds, so that, at high strain, there is a linear variation with strain. Consequently, the fit parameter of Equation 2 could successfully be used to fit the non-linear viscoelastic behaviour of filled HNBR compounds.

The T(3/1) is largest and most convenient to capture the essential of the nonlinear behaviour. The fit parameters for T(3/1) of tested compounds are presented in Figure 5.96. At high strain, the filler network could be destroyed, being in agreement with the concept of dynamic strain softening, as mentioned previously. The TH_0, parameters α, C and D are used to quantify the non-linear viscoelastic behaviour of filled HNBR compounds with different CB hybrid ratio and system. The TH_0 and parameter α describe the asymptotic non-linear behaviour at infinite strain, i.e., when all filler-rubber interaction is expectedly be destroyed, and when the viscoelastic character is maintained only by the stretched rubber phase (78). Consequently, all filled HNBR compounds should display similar TH_0 and parameter α values. However, the increase of strain is experimentally limited to 1000%, which might not be sufficient to completely demolish the filler-rubber interactions (78). The change of TH_0 and parameter α, therefore, are not systematic with increasing CB loading having high surface area and/or structure in hybrid ratio,

as noticed in Figure 5.96 (a). In addition, it is found that the TH_0 value of filled HNBR with N326/N774 is higher than that of filled HNBR with N326/N990 hybrid system up to the N326 content in hybrid ratio of 40%, and then the TH_0 values of both CB hybrid systems filled HNBR compounds are comparable. With respect to filled HNBR compounds with N550/N990 hybrid system, the TH_0 of 326/N990 is greater. It is apparent that the filler-rubber interaction of N550 is weaker than that of N326. The non-linear viscoelastic behaviour of filled HNBR compounds is dominated by characteristics of the major CB composition in the hybrid system. Evidently, the filler-rubber interaction depending strongly on CB characteristics in hybrid system is responsible. Generally, the parameter α tends to decrease when the TH_0 increases. Therefore, the parameter α is in line with the TH_0 results, i.e., at 0/100, 20/80 and 40/60 CB hybrid ratio. The parameter α of HNBR filled with N326/N774 hybrid is lower than that of HNBR filled with N326/N990 hybrid, and the parameter α of HNBR vulcanisate filled with N550/N990 is greater than that of HNBR vulcanisate filled with N326/N990 at 60/40, 80/20 and 100/0 hybrid ratios.

The most significant information of non-linear viscoelastic behaviour is provided by parameters C and D, as illustrated in Figures 5.103 (c) and 5.103 (d), respectively. The parameter D of all hybrid systems filled HNBR compounds increases with increasing CB loading which possesses higher surface area and/or structure into the hybrid ratio. This result is in agreement with the concept of filler transient network (or "Payne effect") and strain softening effect. Also, the parameter D increases systematically with the decrease in extent of linear region. The increase in CB possessing high surface area and/or structure in hybrid ratio causes the increase in magnitude of the filler network. The parameter C describing the strain sensitivity reflects the non-linear viscoelastic behaviour of HNBR compounds filled with different CB hybrid systems in the same manner as the parameter D, i.e., the strain sensitivity tends to increase with the rise in the amount of CB with high surface area and/or structure in hybrid ratio.

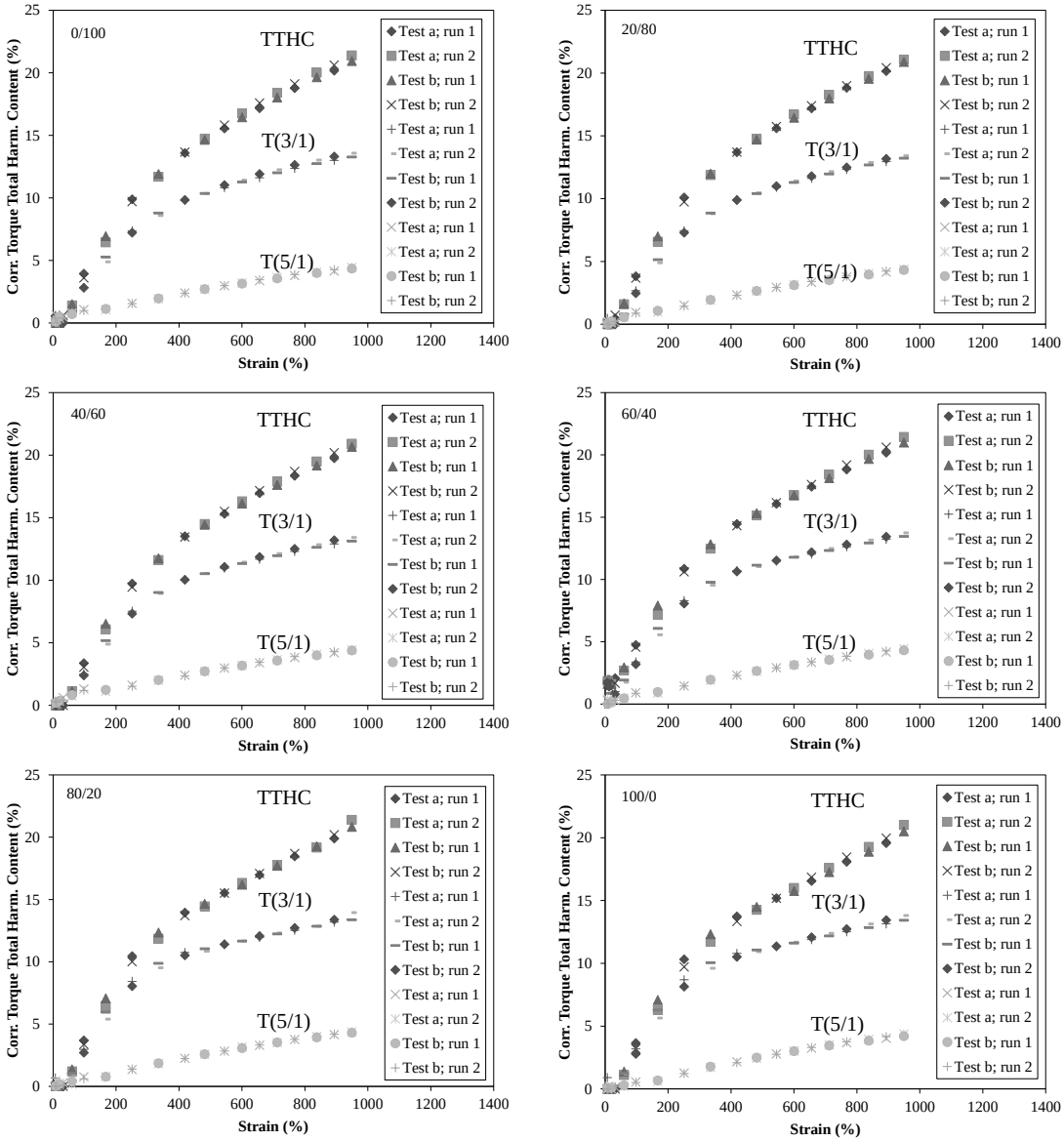

Figure 5.100 Torque harmonics as a function of strain amplitude at 3.14 rad/s and 100°C as measured by the RPA-FT of HNBR filled with various N326/N990 hybrid ratios

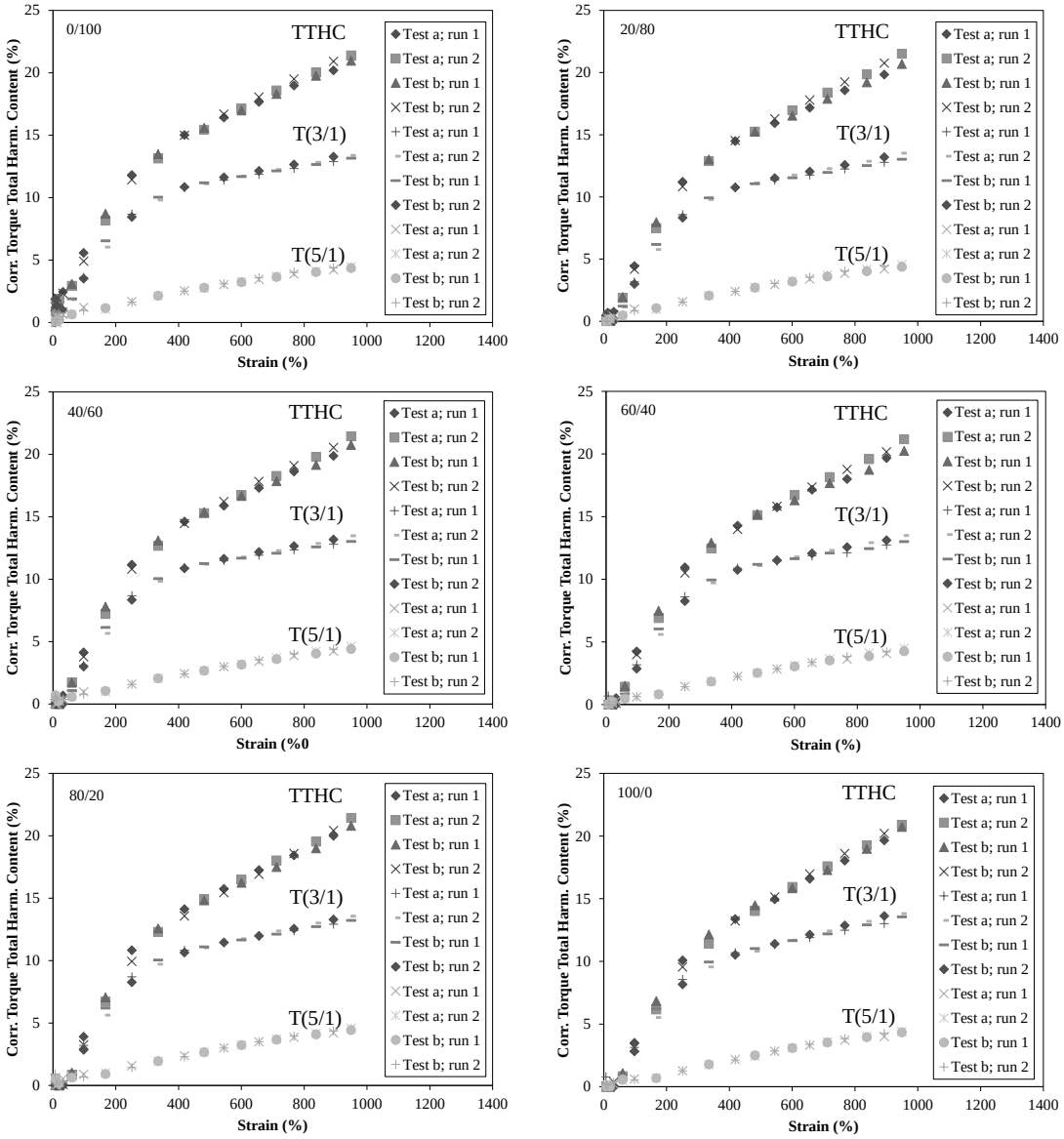

Figure 5.101 Torque harmonics as a function of strain amplitude at 3.14 rad/s and 100°C as measured by the RPA-FT of HNBR filled with various N326/N774 hybrid ratios

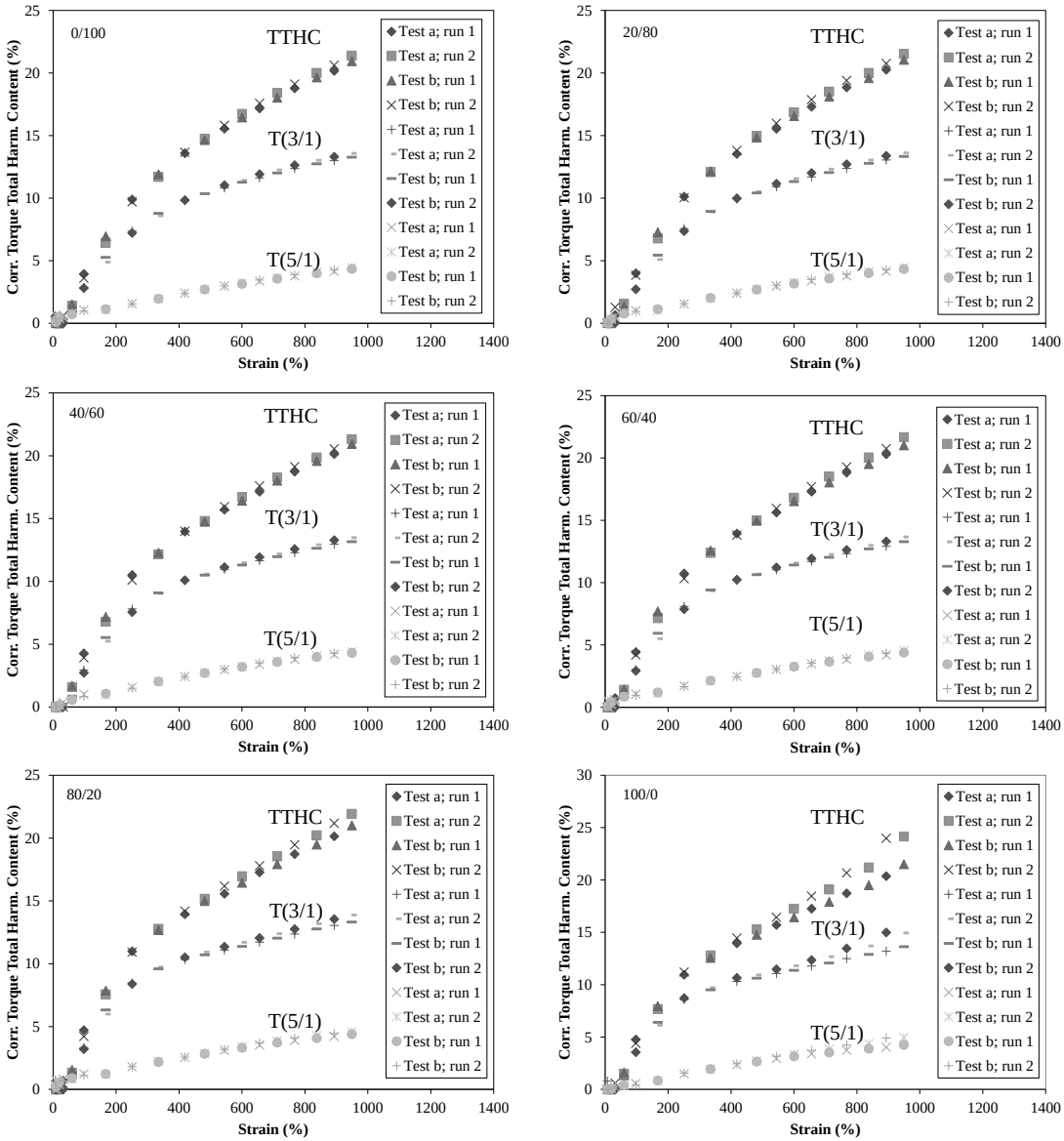

Figure 5.102 Torque harmonics as a function of strain amplitude at 3.14 rad/s and 100°C as measured by the RPA-FT of HNBR filled with various N550/N990 hybrid ratios

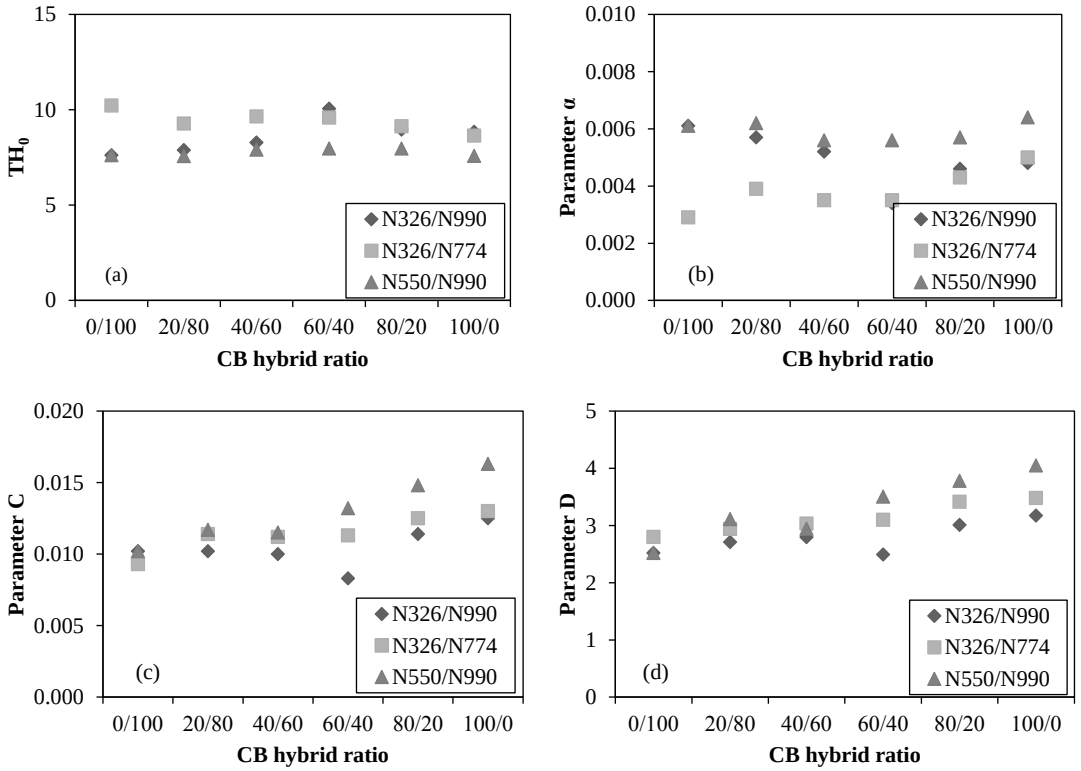

Figure 5.103 Relationship among fit parameters of Equation 3.17, carbon black hybrid ratio and hybrid system in HNBR compounds: (a) parameter TH_0; (b) parameter α; (c) parameter C; (d) parameter D

Quarter Torque Signal Integration

Quarter cycle integration of averaged torque signal is utilised to establish the distinction in non-linearity behaviour of filled HNBR compounds with different CB hybrid ratios. The extrinsic and intrinsic non-linear viscoelasticity can be indicated by the Q1/Q2 ratio. The change in non-linear character of filled HNBR compounds with various CB hybrid systems is shown in Figures 5.104 to 5.106. At low strain, the Q1/Q2 is higher than 1. As strain increases, the Q1/Q2 ratio decreases until the minimum value is reached (at approximately 250% strain), and then the Q1/Q2 increases with increasing strain.

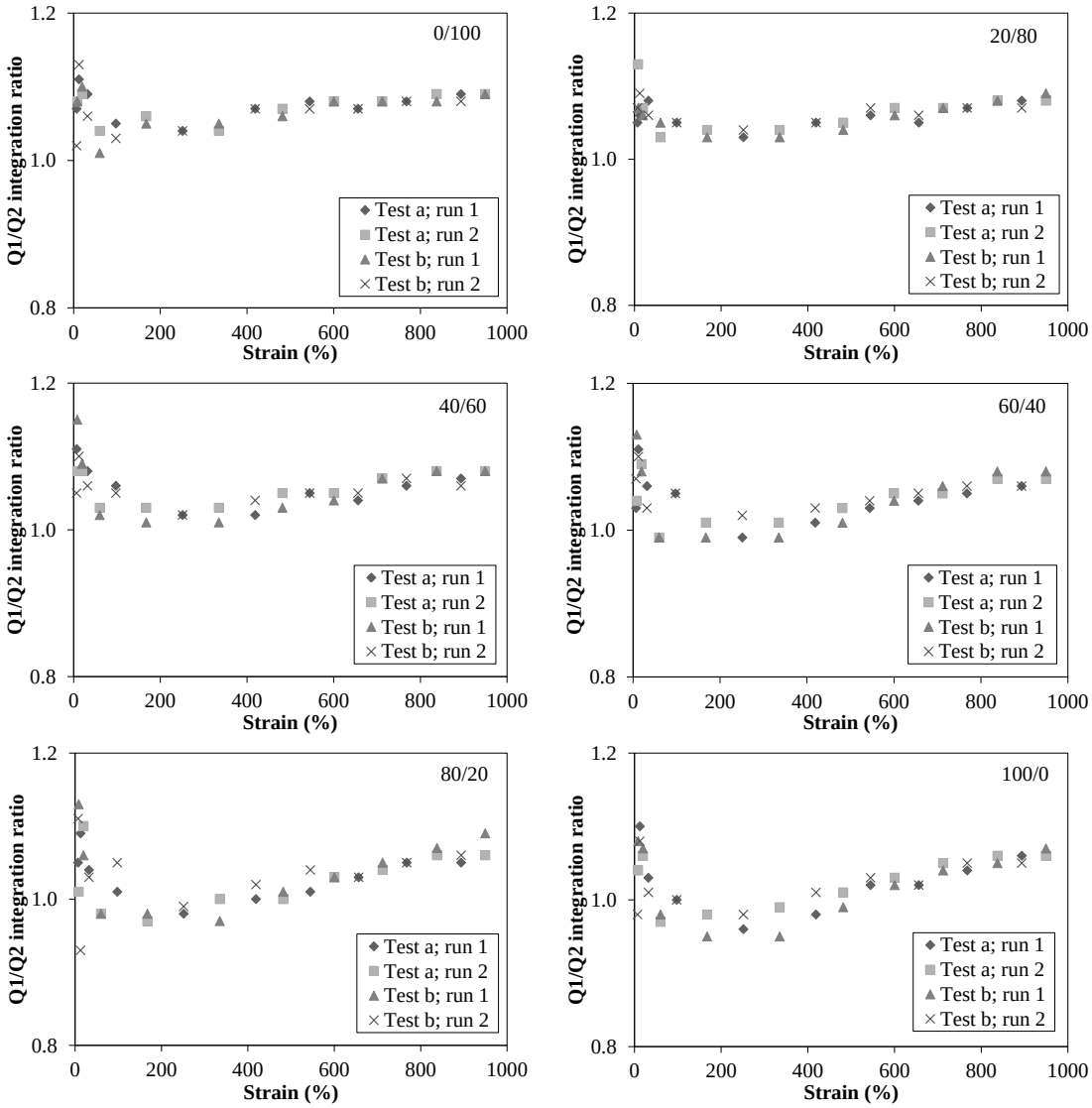

Figure 5.104 RPA-FT at 100°C on HNBR filled with N326/N990 assessing extrinsic or intrinsic non-linear viscoelastic character through the quarter cycle torque integration; strain sweep tests at 3.14 rad/s

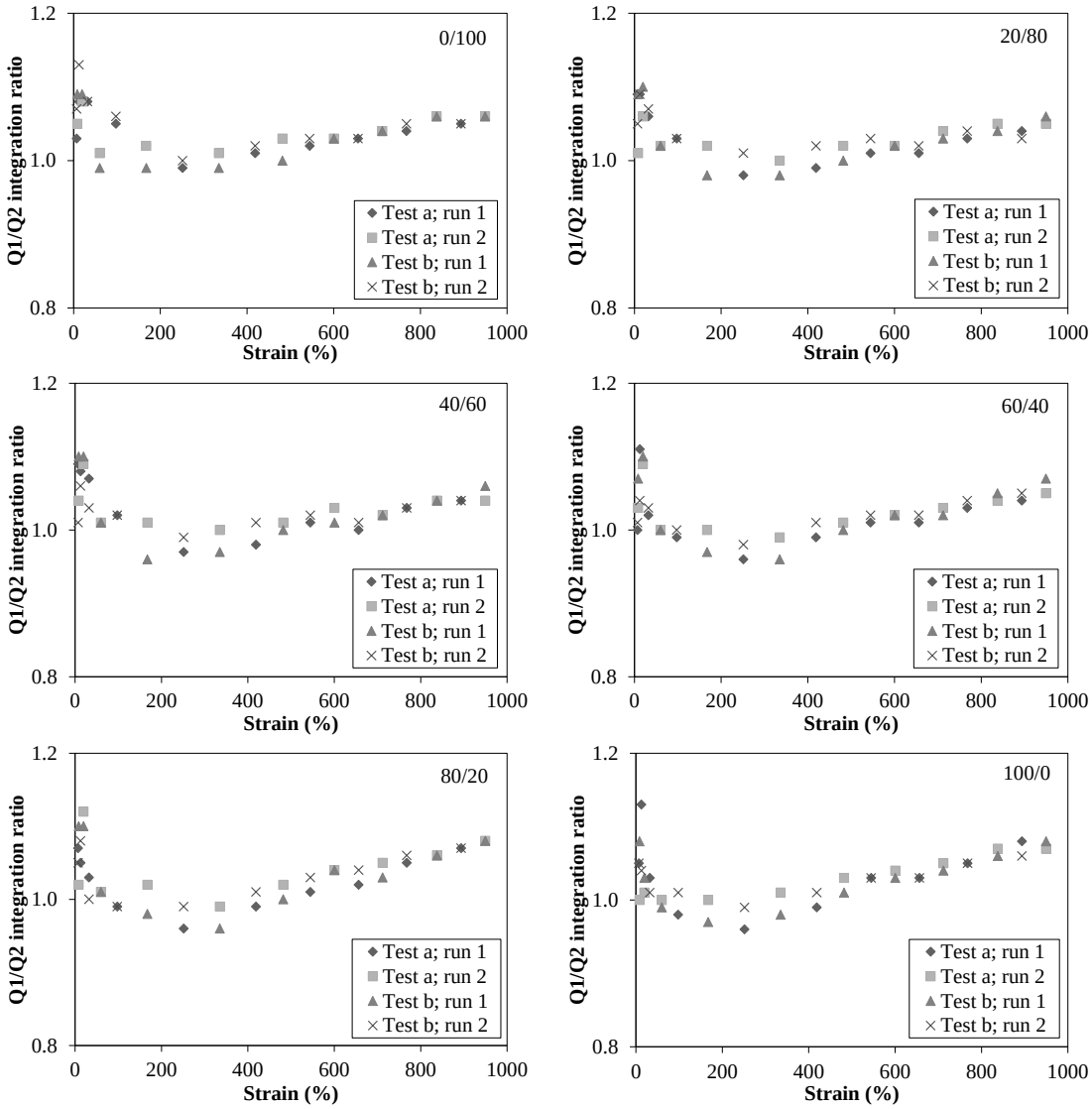

Figure 5.105 RPA-FT at 100°C on HNBR filled with N326/N774 assessing extrinsic or intrinsic non-linear viscoelastic character through the quarter cycle torque integration; strain sweep tests at 3.14 rad/s

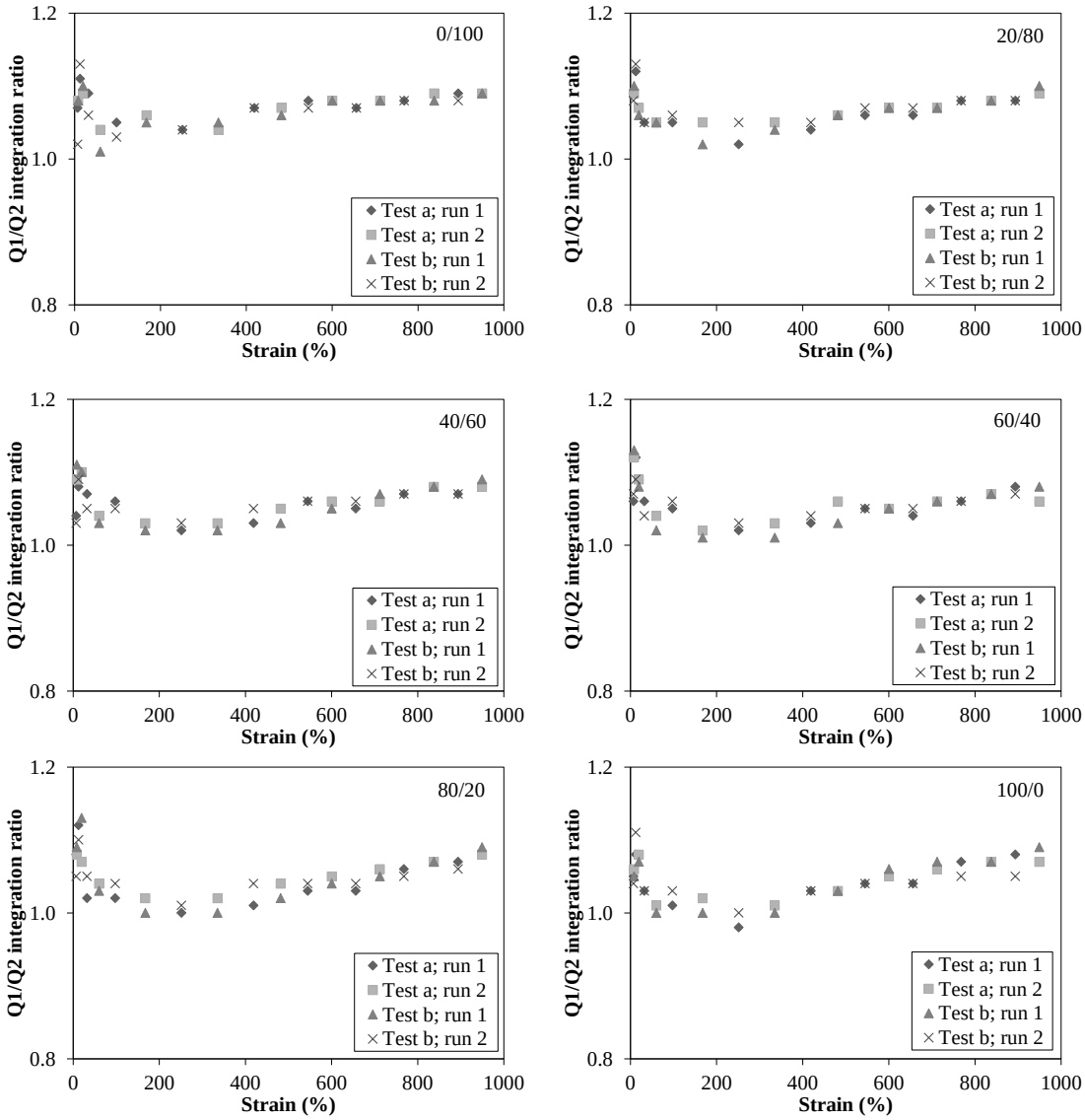

Figure 5.106 RPA-FT at 100°C on HNBR filled with N550/N990 assessing extrinsic or intrinsic non-linear viscoelastic character through the quarter cycle torque integration; strain sweep tests at 3.14 rad/s

Figure 5.107 illustrates effects of CB hybrid ratio and system on Q1/Q2 ratio of filled HNBR compounds. Apparently, the Q1/Q2 ratio of HNBR compounds decrease with increasing the amount of CB possessing larger surface area and/or greater structure in hybrid ratio. The filler-rubber interaction is a major factor on the change from extrinsic to intrinsic non-linearity behaviour of filled HNBR compounds. The intrinsic non-linear viscoelasticity is revealed, and believed to be the result of the strong interaction between filler particles and rubber matrix.

It is known that the interaction between filler and rubber plays a crucial role on the flow properties of filled compounds. The decreasing filler-rubber interaction leads to the decreased viscosity and the improved flow properties of filled compounds, and thus the advantage in processability. Consequently, the filled compound exhibiting lower Q1/Q2 ratio, such as, N326/N774 filled HNBR compound is more difficult to process. Interestingly, when the CB having large surface area and/or high structure is major component in hybrid system (i.e., 60/40, 80/20 and 100/0 hybrid ratio), the Q1/Q2 ratio of N550/N990 filled HNBR compound is greater than that of N326/N990 filled system, indicating the superior processability.

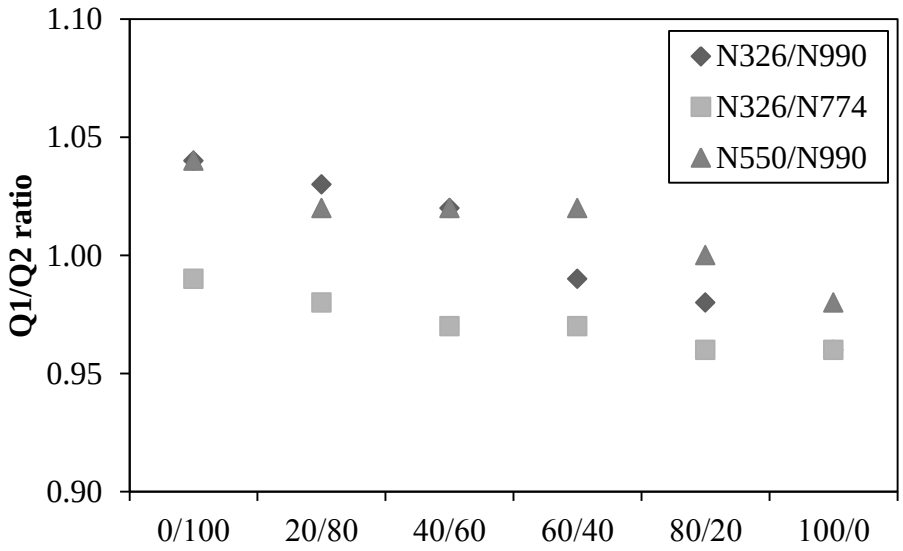

Figure 5.107 Relationship among quarter torque signal integration ratio, carbon black hybrid ratio and hybrid system in HNBR compounds

d) Cured CB hybrid system filled HNBR

Strain sweep test

Storage modulus (G′) of HNBR vulcanisates filled with different CB hybrid and CB hybrid system as a function of strain amplitude is shown in Figure 5.108.

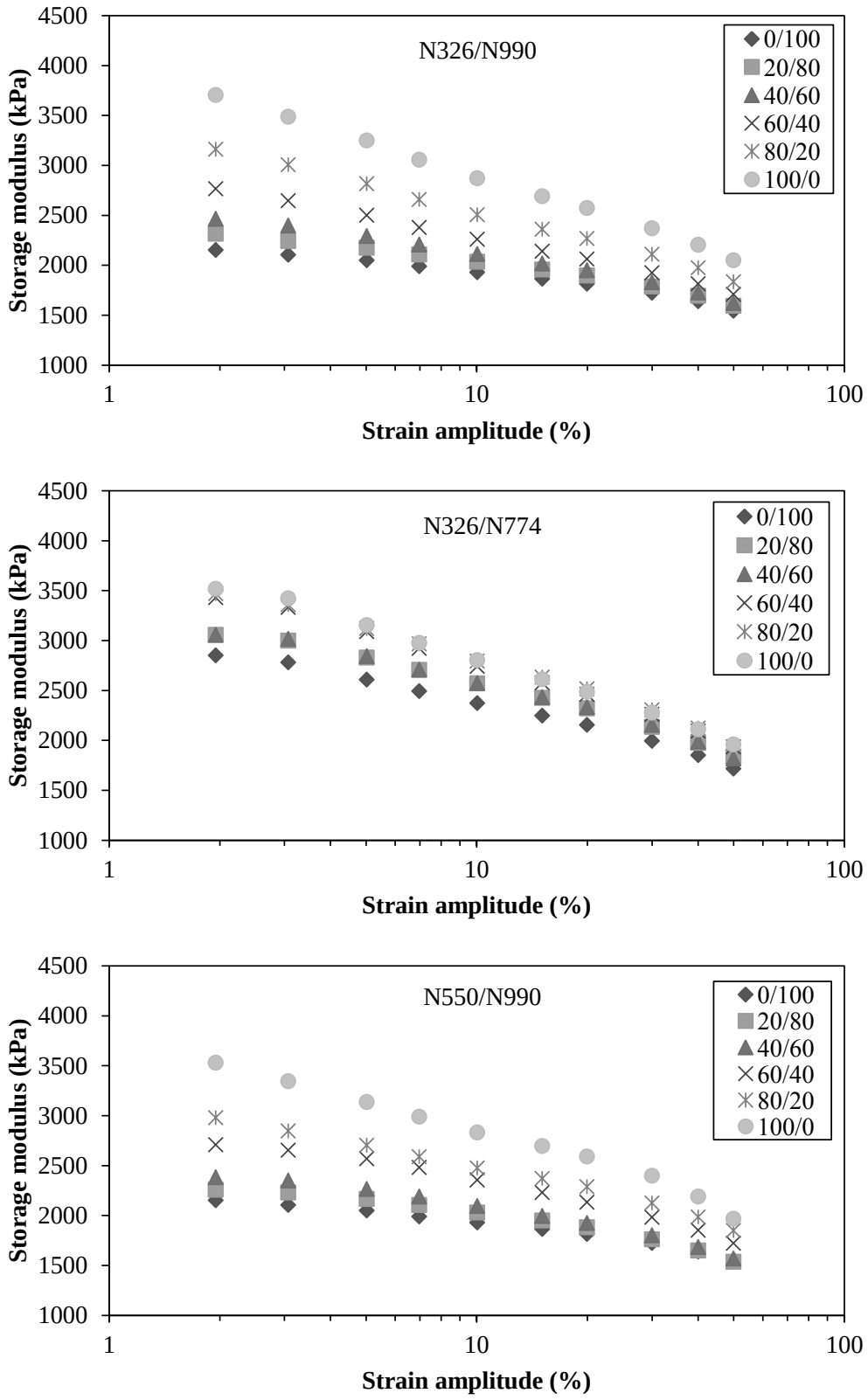

Figure 5.108 Storage modulus (G′) as a function of strain amplitude of filled HNBR vulcanisates with various carbon black hybrid ratios and hybrid systems at test temperature and frequency of 60°C and 1 rad/s, respectively

It is evident that the G′ increases with increasing the amount of CB having higher surface area and/or structure, i.e., N326 and N550 into CB hybrid ratio, which is attributed to the reinforcing effect, i.e. hydrodynamic effect, filler-filler interaction as well as filler-rubber interaction. The presence of CB with relatively high surface area and/or structure is reported to yield the strong filler transient network, leading to a remarkable rise in G′ particularly at low strain of deformation. At high strain, the G′ decreases as a result of filler transient network disruption.

Figure 5.109 illustrates the comparative G′ of cured HNBR filled with different CB hybrid systems at 10% strain amplitude. It can be seen that the G′ of filled vulcanisates is in line with the crosslink density as illustrated in Figure 5.95, thus, similar explanation could be applied.

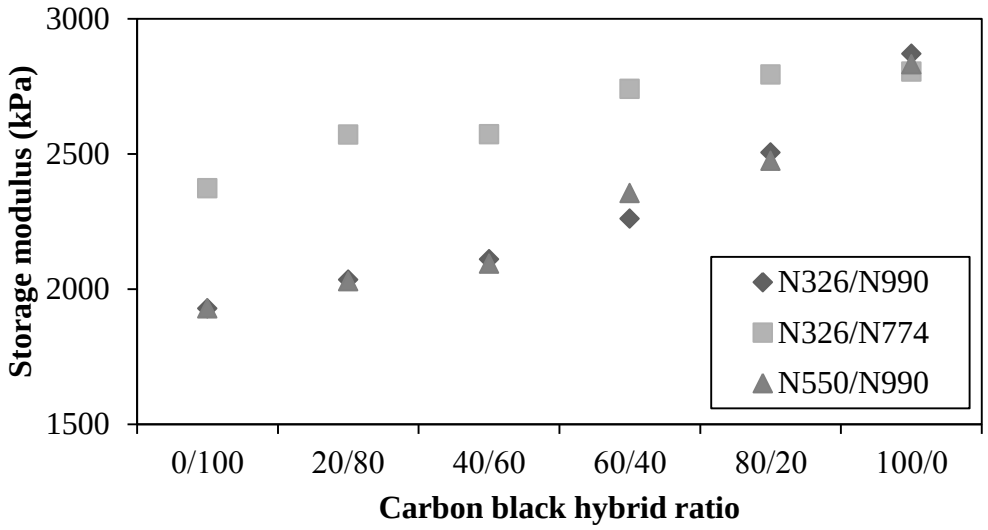

Figure 5.109 Relationship among storage modulus (G′), carbon black hybrid ratio and hybrid system in HNBR vulcanisates at test strain, temperature and frequency of 10%, 60°C and 1 rad/s, respectively

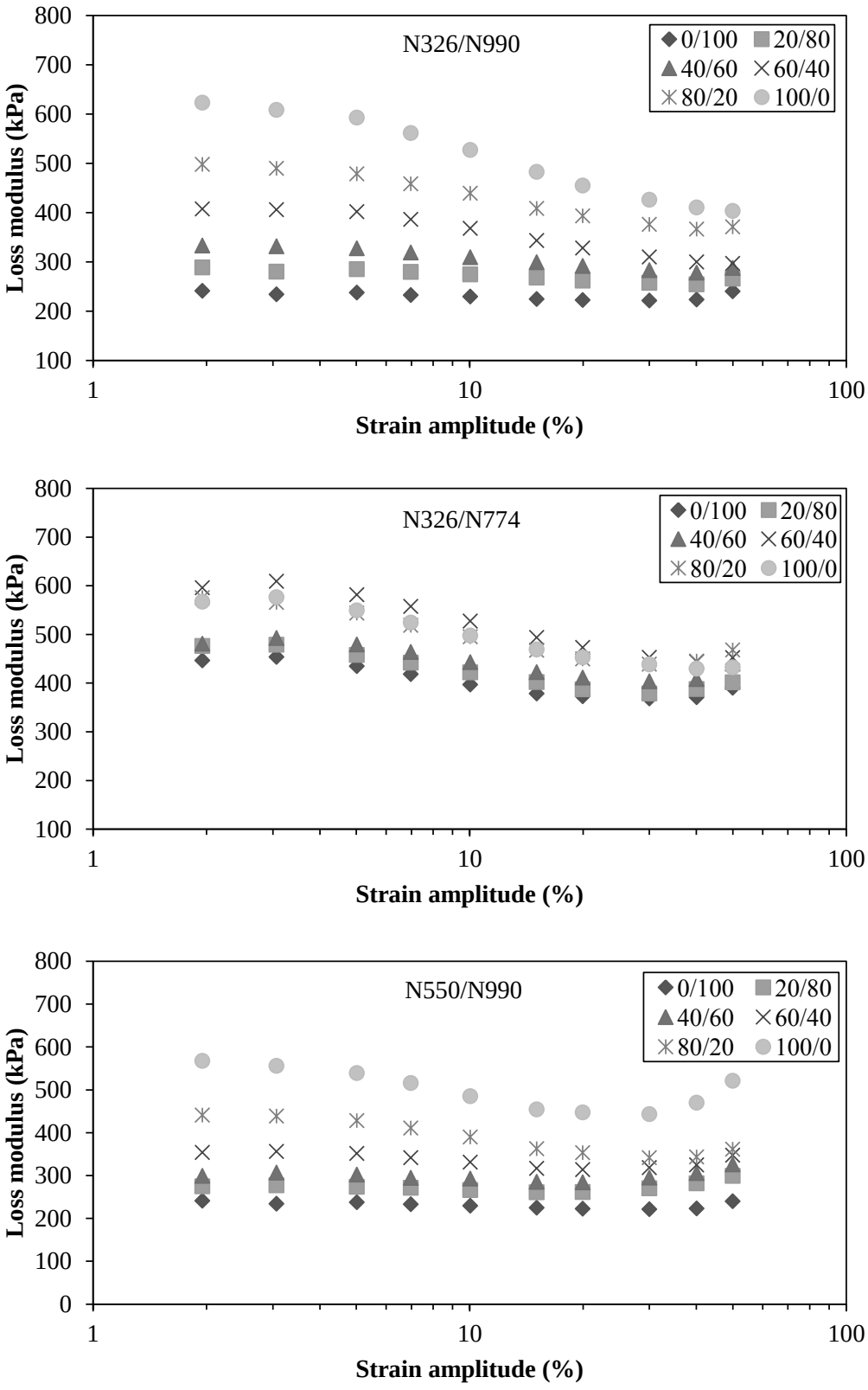

Figure 5.110 Loss modulus (G″) as a function of strain amplitude of filled HNBR vulcanisates with various carbon black hybrid ratios and hybrid systems at test temperature and frequency of 60°C and 1 rad/s, respectively

In the case of G″, it could be seen form Figures 5.110 and 5.111 that the G″ increases with increasing CB possessing relatively high surface area and structure into CB hybrid system. The hysteresis loss is expected to increase due to the greater filler network formation and the stronger filler-rubber interaction as well as crosslink density. The G″ decreases with dynamic strain due to the reduction in magnitude of filler network. The magnitude of G″ reduction with strain amplitude could be observed in the vulcanisates filled with CB hybrid ratio dominated by CB having relative high surface area and structure. However, at high strain of deformation where the filler transient network is already disrupted, the G″ increases slightly with stain amplitude, which could be explained by the viscous dissipation via molecular flow at the CB surfaces. The result trends of the G″ of HNBR vulcanisates filled with different CB hybrid systems (at 10% strain amplitude) are similar to the G′. Therefore, the reinforcing and crosslink density effects could be taken as the explanation.

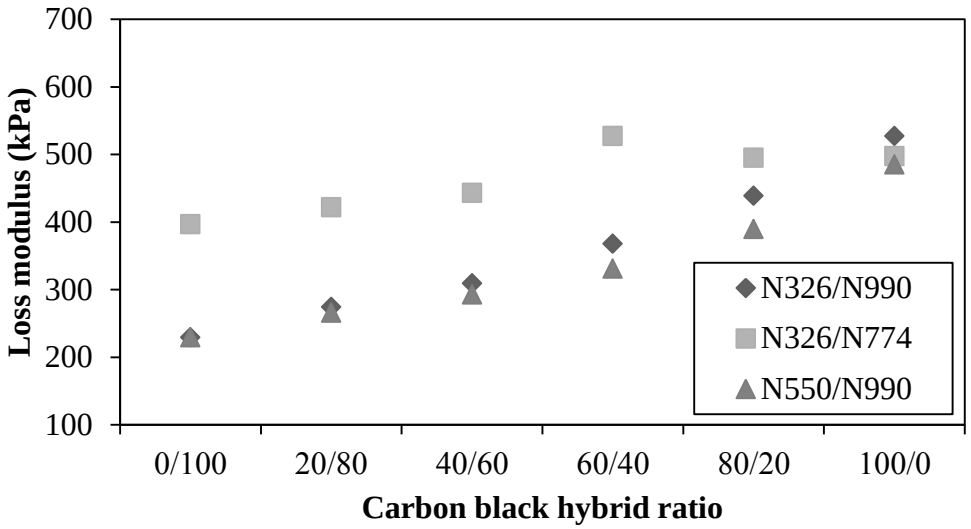

Figure 5.111 Relationship among loss modulus (G″), carbon black hybrid ratio and hybrid system in HNBR vulcanisates at test strain, temperature and frequency of 10%, 60°C and 1 rad/s, respectively

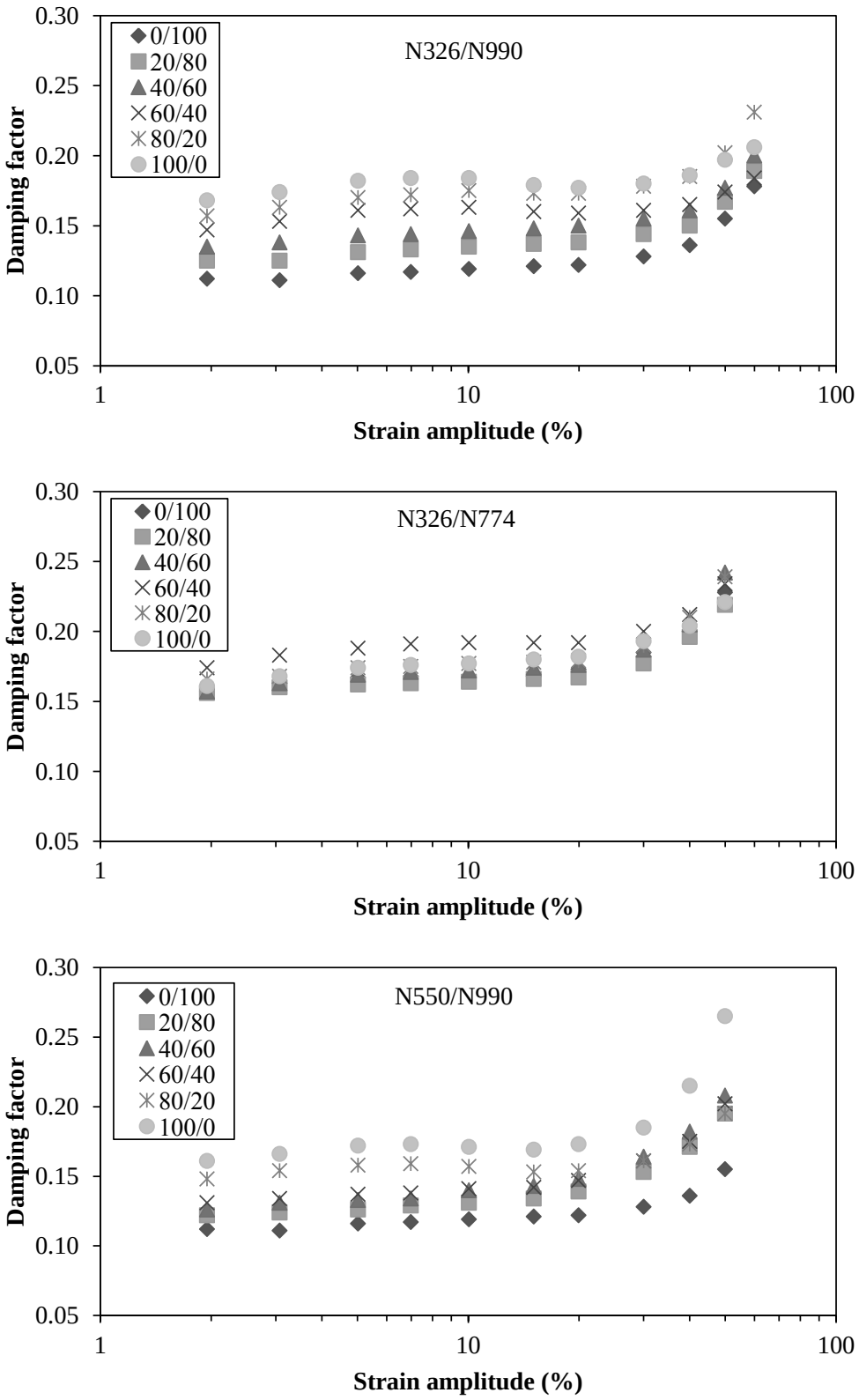

Figure 5.112 Damping factor (tanδ) as a function of strain amplitude of filled HNBR vulcanisates with various carbon black hybrid ratios and hybrid systems at test temperature and frequency of 60°C and 1 rad/s, respectively

Plots of tanδ of cured HNBR filled with various CB hybrid ratios as a function of strain amplitude and CB hybrid ratio are exhibited in Figures 5.112 and 5.113, respectively. The results of damping factor are in good agreement with the G′ and G″ results, i.e. tanδ increases with increasing CB having relatively high surface area and structure (i.e., N326 and N550) into hybrid system. This is due to the energy dissipitation via the disruption of filler-filler networks.

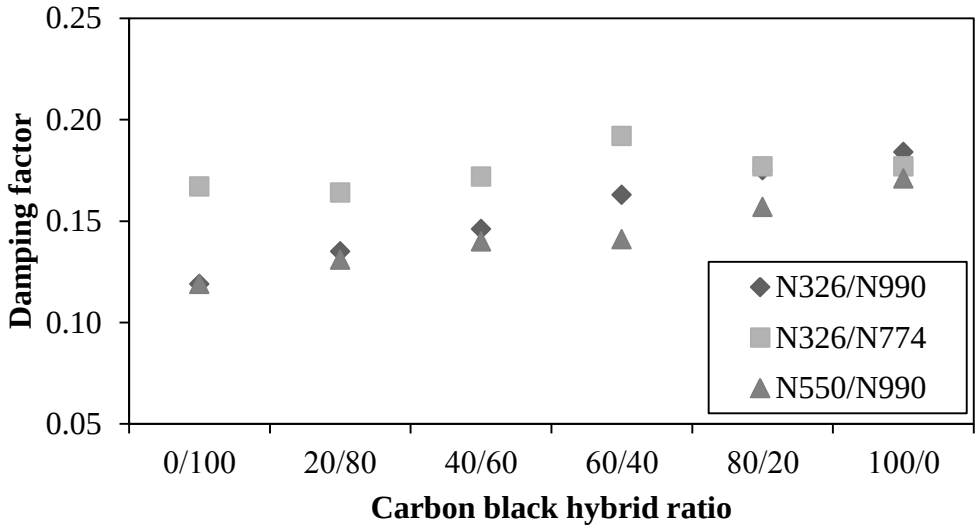

Figure 5.113 Relationship among damping factor (tanδ), carbon black hybrid ratio and hybrid system in HNBR vulcanisates at test strain, temperature and frequency of 10%, 60°C and 1 rad/s, respectively

Temperature sweep test

Figures 5.114 and 5.115 demonstrate G′ and G″ of CB hybrid system filled HNBR, respectively. The values of T_g as determined from the temperature at abrupt change in G′ or peak of G″ are not significantly affected by CB composition ratio in a hybrid system. As expected, it is evident from Figures 5.116 and 5.117 that the values of G′ and G″ at temperature of 60°C agree well with those determined from the strain sweep test, as revealed earlier in Figures 5.109 and 5.111, respectively. The vulcanisates with greater content of CB owning relatively high surface area and structure exhibit higher magnitude of reinforcement.

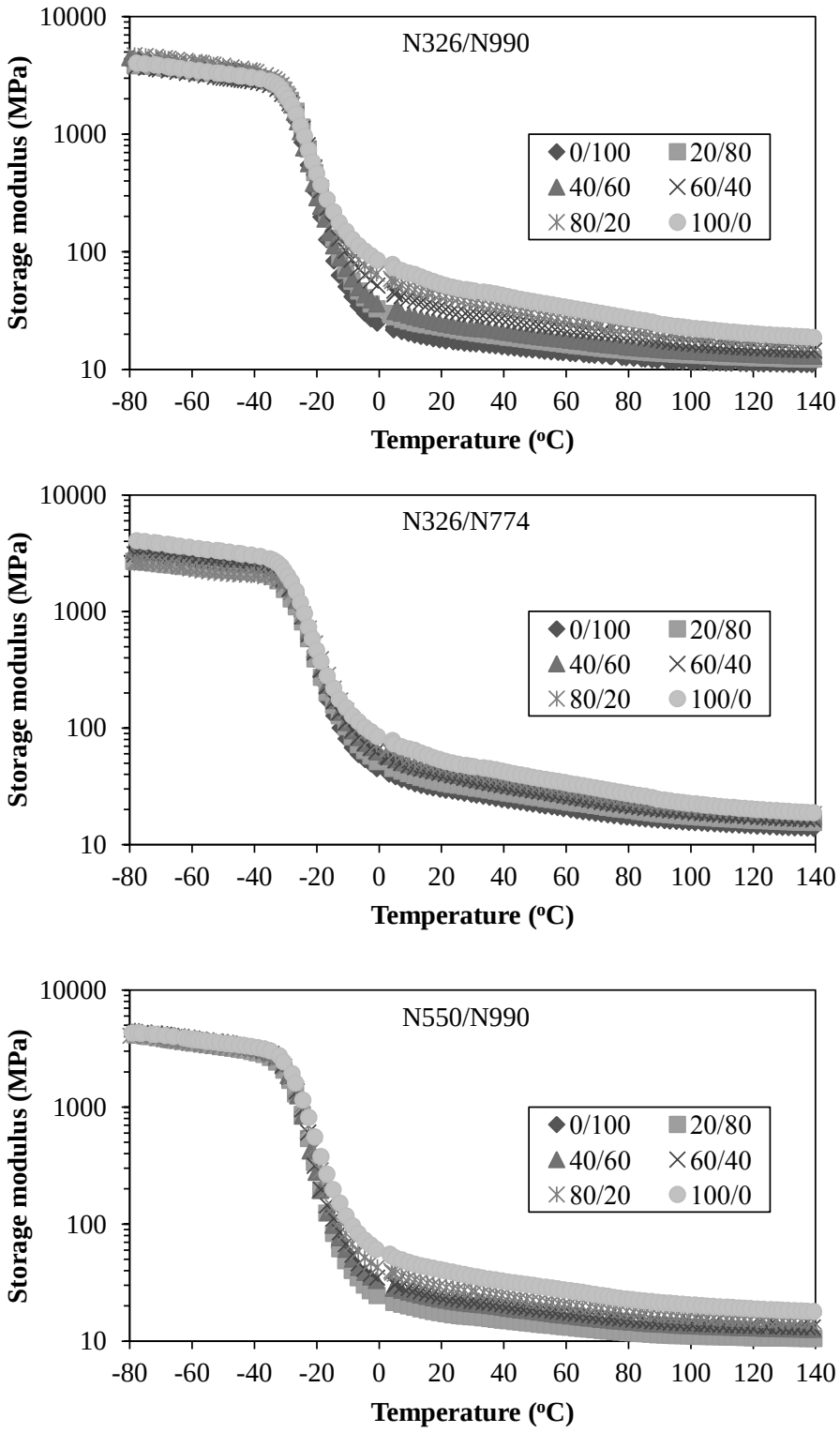

Figure 5.114 Storage modulus (G′) as a function of temperature of filled HNBR vulcanisates with various carbon black hybrid ratios and hybrid systems at test static strain, dynamic strain and frequency of 2%, 0.1% and 62.8 rad/s, respectively

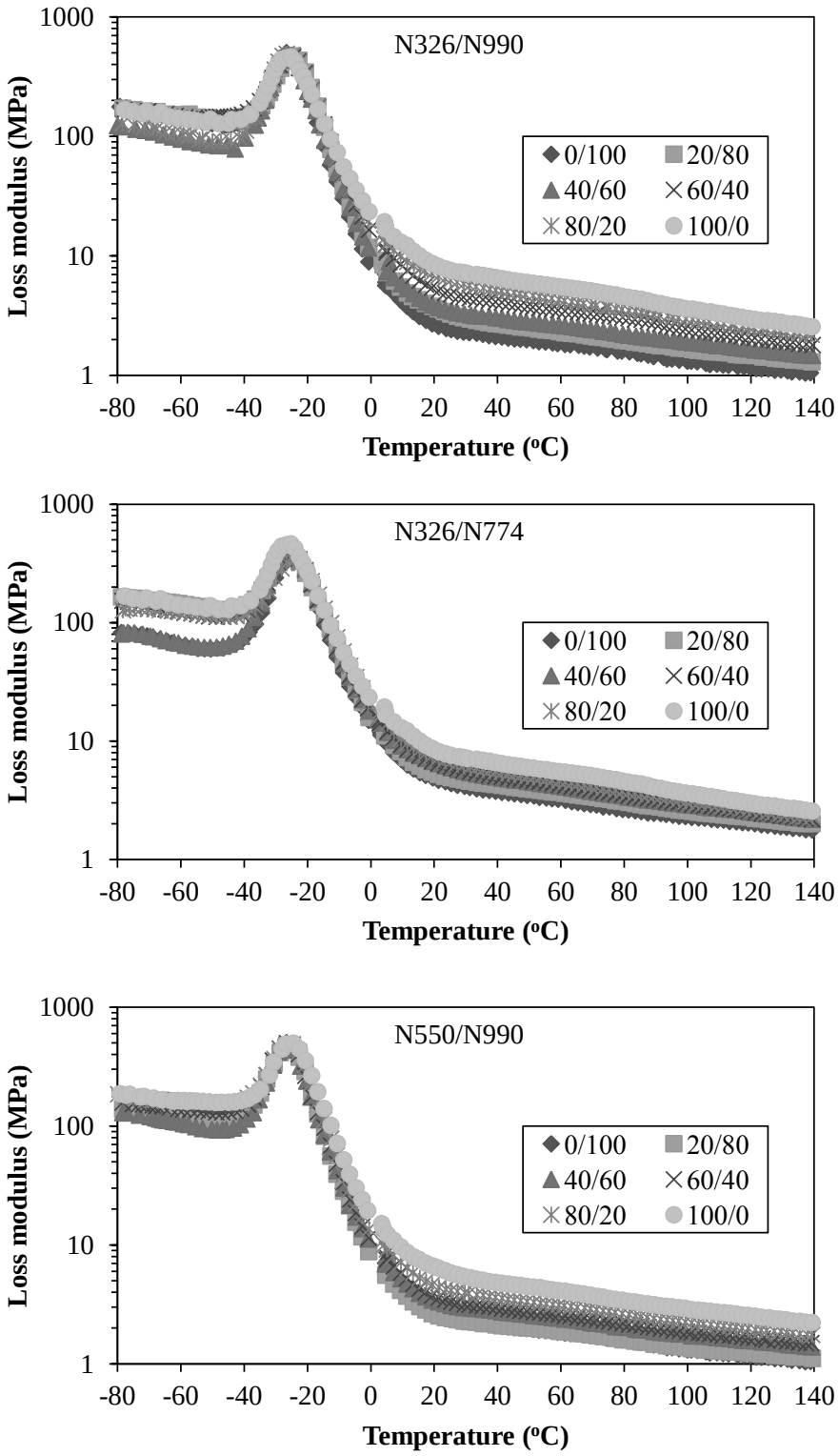

Figure 5.115 Loss modulus (G″) as a function of temperature of filled HNBR vulcanisates with various carbon black hybrid ratios and hybrid systems at test static strain, dynamic strain and frequency of 2%, 0.1% and 62.8 rad/s, respectively

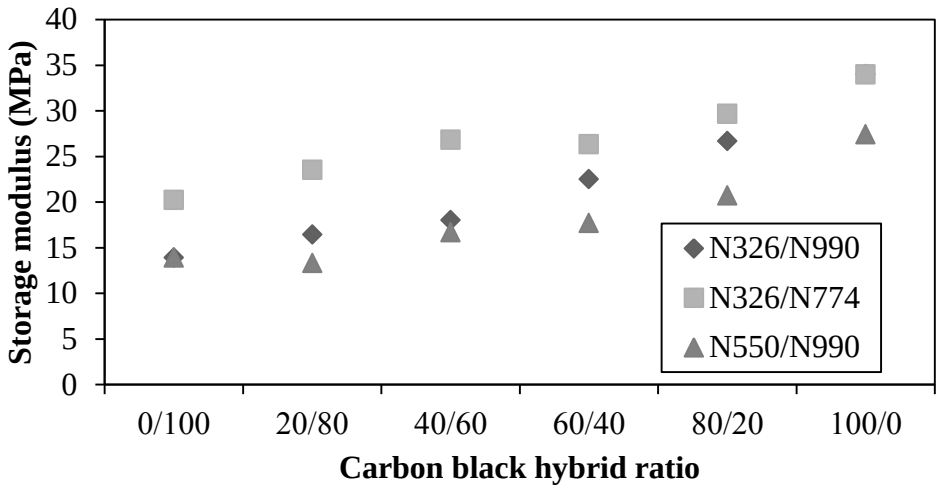

Figure 5.116 Relationship among storage modulus (G′), carbon black hybrid ratio and hybrid system in HNBR vulcanisates at test static strain, dynamic strain, frequency and temperature of 2%, 0.1%, 62.8 rad/s and 60°C, respectively

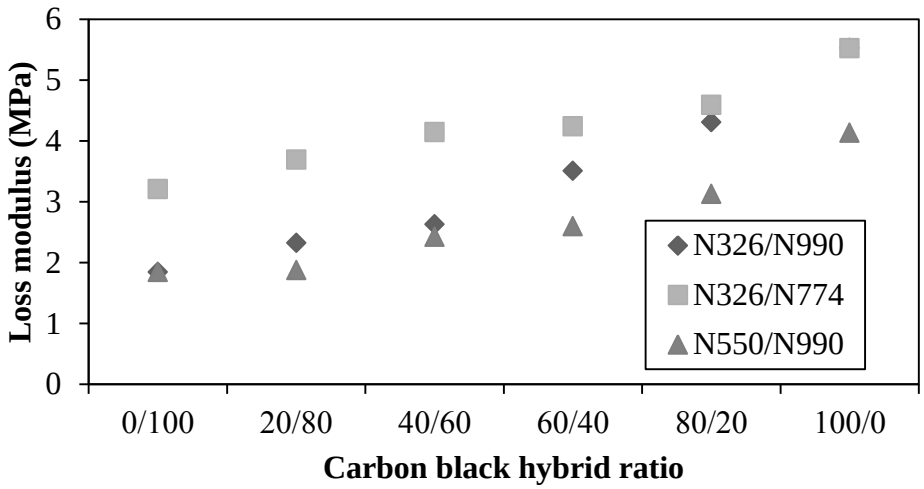

Figure 5.117 Relationship among loss modulus (G″), carbon black hybrid ratio and hybrid system in HNBR vulcanisates at test static strain, dynamic strain, frequency and temperature of 2%, 0.1%, 62.8 rad/s and 60°C, respectively

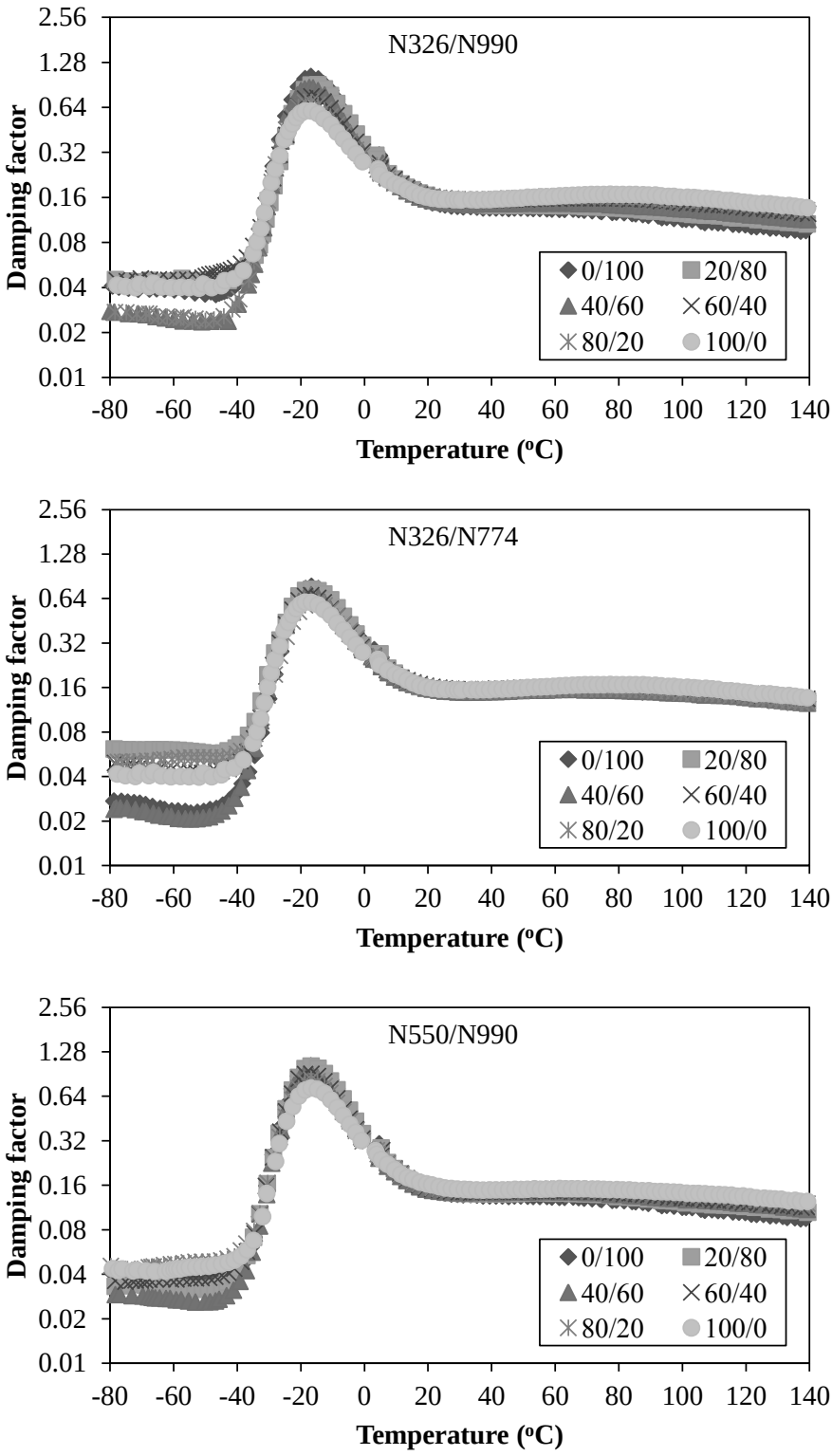

Figure 5.118 Damping factor (tanδ) as a function of temperature of filled HNBR vulcanisates with various carbon black hybrid ratios and hybrid systems at test static strain, dynamic strain and frequency of 2%, 0.1% and 62.8 rad/s, respectively

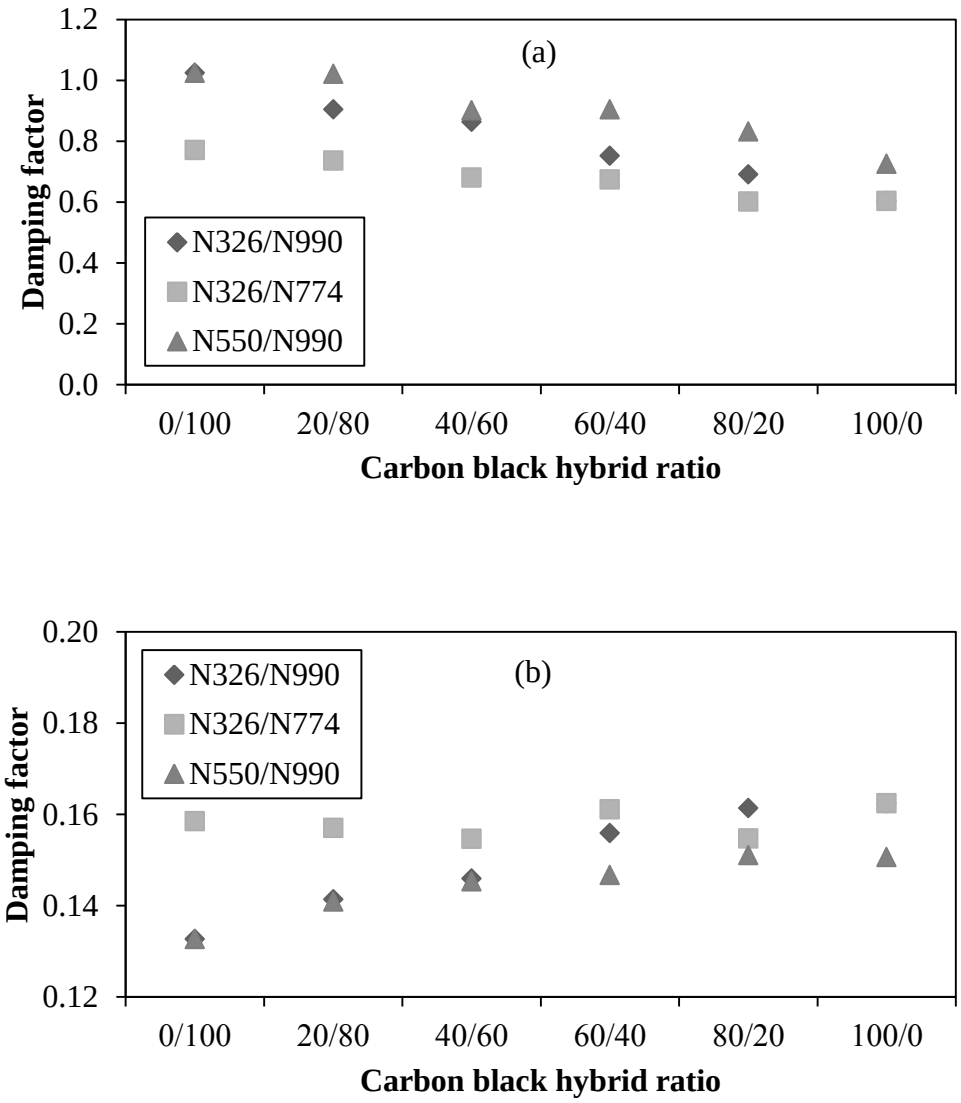

Figure 5.119 Relationship among damping factor (tanδ), carbon black hybrid ratio and hybrid system in HNBR vulcanisates at test static strain, dynamic strain and frequency of 2%, 0.1% and 62.8 rad/s, respectively: (a) the glass transition temperature; (b) 60°C

Results of tanδ over a temperature range of -80 to 140°C are given in Figures 5.118 and 5.119. The damping peaks of filled HNBR decrease with the increasing the amount of CB possessing relatively high surface area and structure into hybrid ratio, implying the restricted molecular mobility (or HNBR segmental motions) via the increased rubber-filler interaction.

On the contrary, the damping factor in the rubbery plateau appears to increase with increasing the amount of CB having relatively high surface area and structure into hybrid ratio (as shown in Figure 5.119 (b)), which is consistent with the results measured from the strain sweep test as shown previously in Figure 5.113. The higher damping factor at rubbery plateau would practically cause the higher extent of heat build-up found under sinusoidal deformation including tyre and industrial roll applications.

5.1.5.3 Filler dispersion and distribution

In this section, the effects of CB hybrid ratio and CB hybrid system on the filler dispersion and distribution of cured HNBR are investigated. The SEM images as shown in Figures 5.120 to 5.122 reveal that all types of CB aggregates (i.e., the bright phase) in hybrid system distribute uniformly in HNBR. Nevertheless, the size of the CB aggregates varies with the type of the CB. The SEM results are in agreement with the viscoelastic properties as discussed previously.

In the SEM image of HNBR filled with N326/N990 hybrid system, the difference in size of CB aggregates can be obviously distinguished. The N326 has much smaller aggregate size than the N990. The interfacial boundary between N990 aggregates and the HNBR matrix is relatively sharp. By contrast, the interfacial boundary between N326 and HNBR is not clear indicating the greater the filler-rubber interaction of N326 with HNBR, and thus the improvement in the mechanical properties of filled HNBR. Similar observation is found in the SEM images of HNBR filled with N326/N774 and N550/N990 hybrid systems.

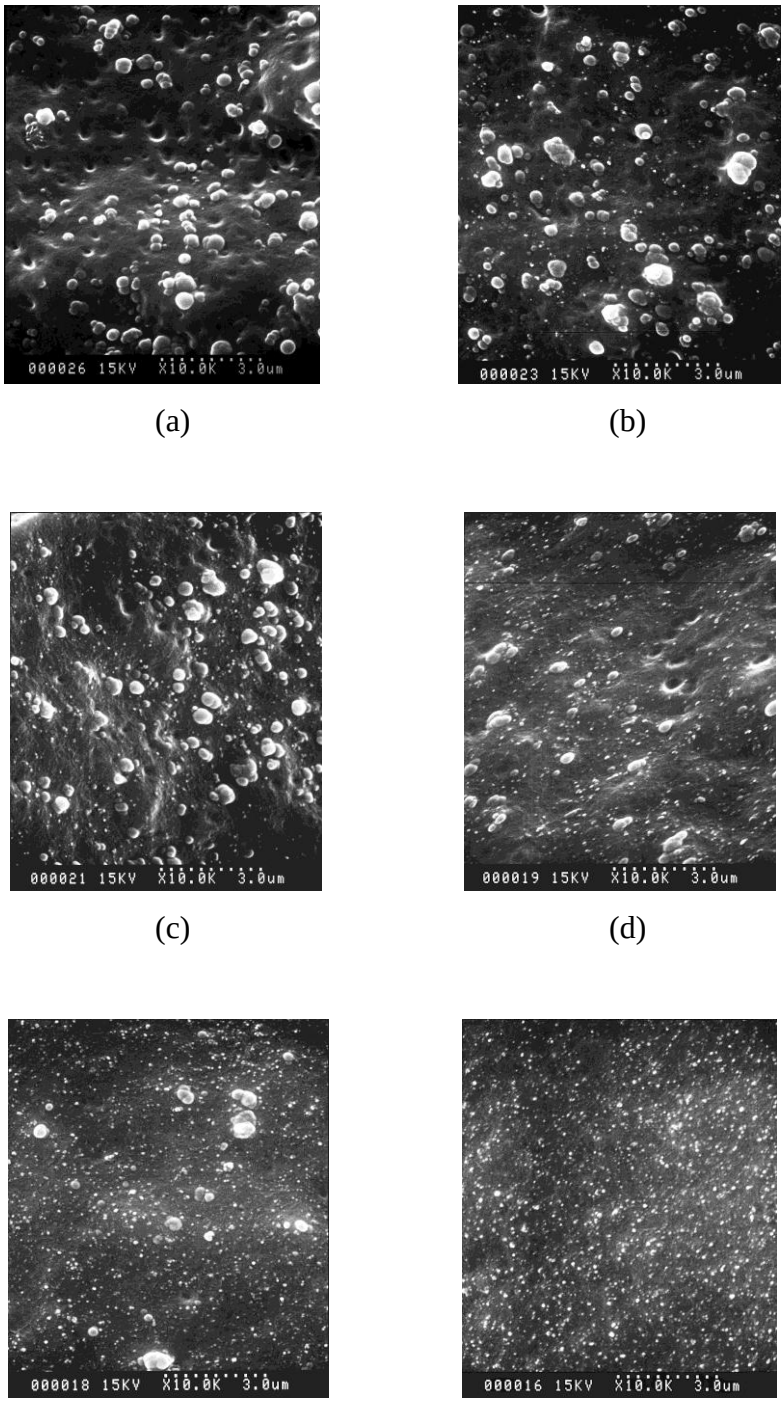

Figure 5.120 SEM micrographs of N326/N990 filled HNBR vulcanisates with various carbon black hybrid ratios: (a) 0/100; (b) 20/80; (c) 40/60; (d) 60/40; (e) 80/20; (f) 100/0

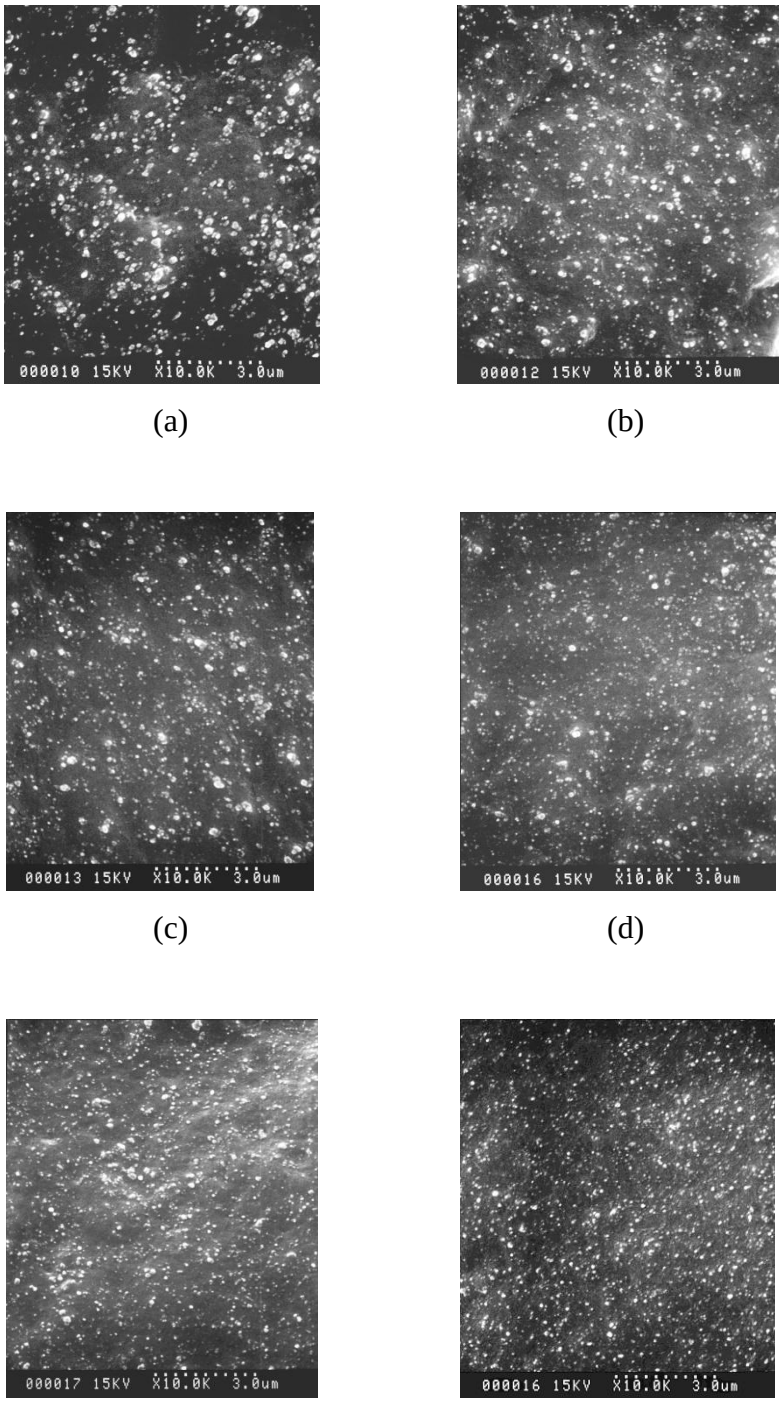

Figure 5.121 SEM micrographs of N326/N774 filled HNBR vulcanisates with various carbon black hybrid ratios: (a) 0/100; (b) 20/80; (c) 40/60; (d) 60/40; (e) 80/20; (f) 100/0

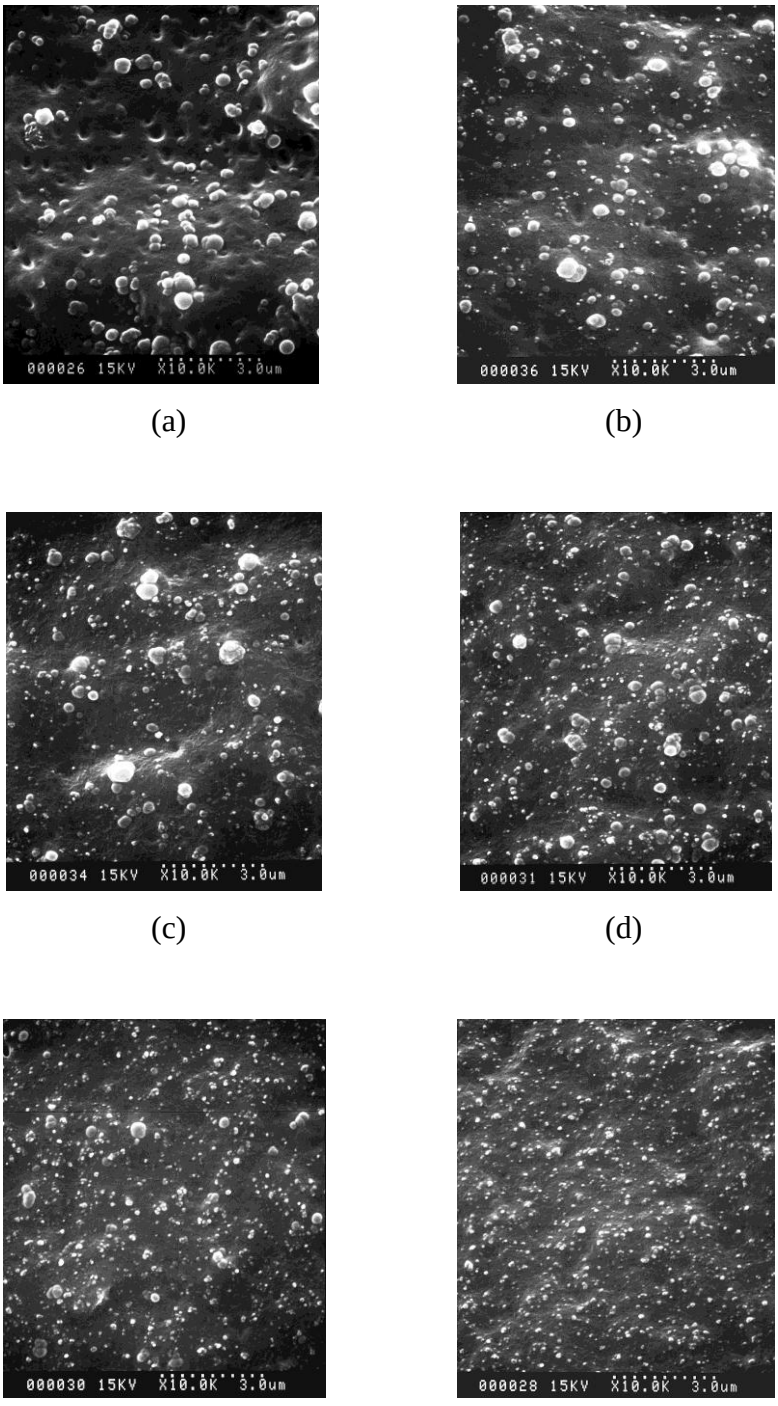

Figure 5.122 SEM micrographs of N550/N990 filled HNBR vulcanisates with various carbon black hybrid ratios: (a) 0/100; (b) 20/80; (c) 40/60; (d) 60/40; (e) 80/20; (f) 100/0

5.1.5.4 Mechanical properties

Mechanical properties of HNBR vulcanisates as a function of CB hybrid ratio and system are shown in Figures 5.123 to 5.128. Figure 5.123 shows the M100 of CB hybrid system filled HNBR vulcanisates. As expected, the M100 increases with the amount of CB having relative high specific surface area and structure in CB hybrid system. The increased M100 is controlled by crosslink density and filler reinforcement effects, as evidenced by the results of crosslink density and the viscoelastic behaviour (see Figures 5.95 and 5.108, respectively).

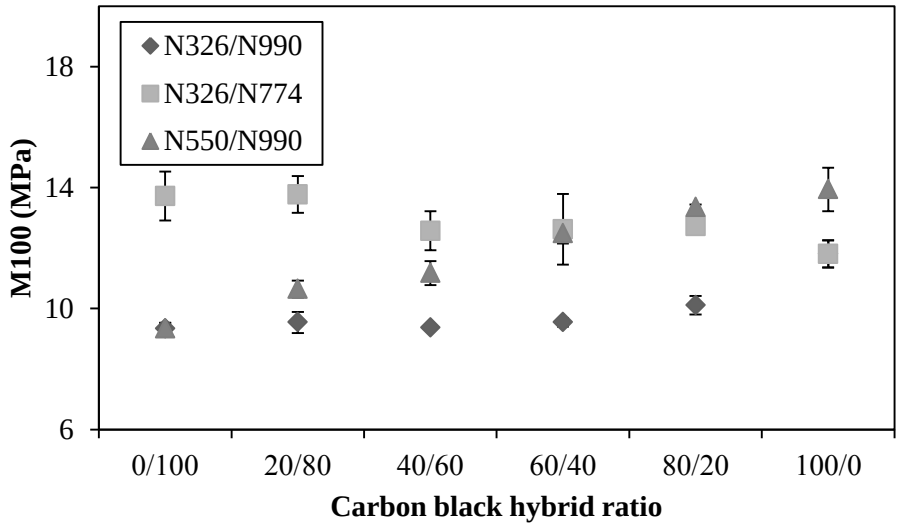

Figure 5.123 Relationship among modulus at 100% strain (M100), carbon black hybrid ratio and hybrid system in HNBR vulcanisates

The tensile strength of filled HNBR vulcanisates is shown in Figure 5.124. Similar to the M100 results, the tensile strength of filled HNBR vulcanisates increases with increasing the amount of CB possessing relatively high surface area and structure into hybrid system. Thus, similar explanation could be applied.

In the case of elongation at break, it can be seen from Figure 5.125 that the elongation at break is not significantly changed with increasing loading of CB having relatively high surface area and structure into hybrid system.

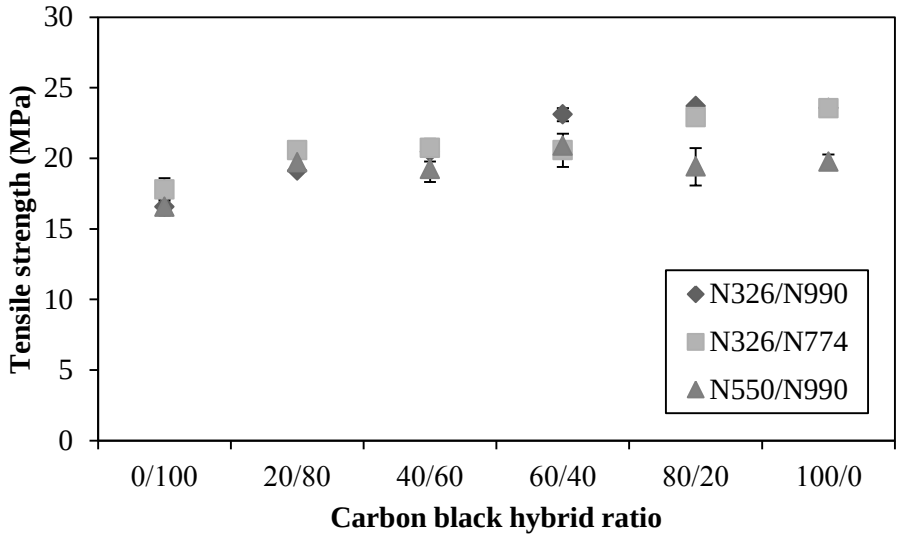

Figure 5.124 Relationship among tensile strength, carbon black hybrid ratio and hybrid system in HNBR vulcanisates

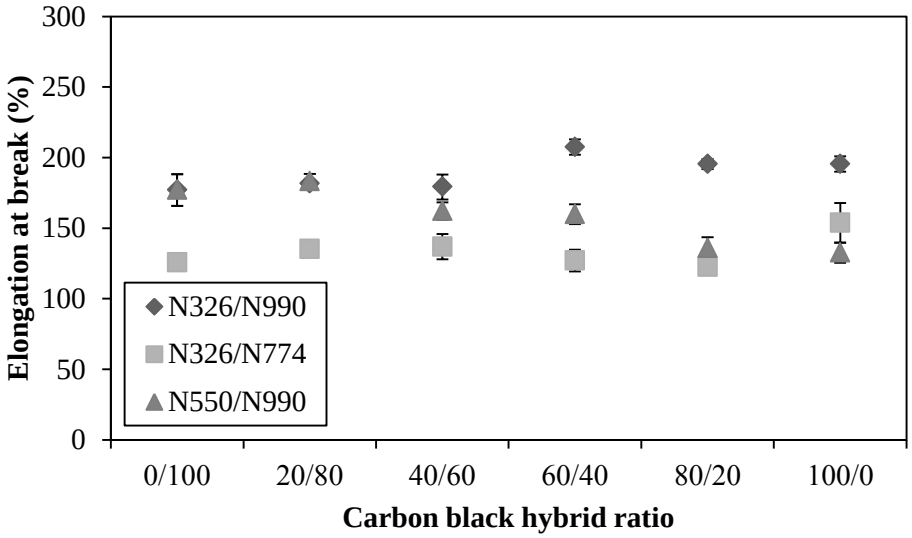

Figure 5.125 Relationship among elongation at break, carbon black hybrid ratio and hybrid system in HNBR vulcanisates

Results of tear strength as illustrated in Figure 5.126 are in line with the tensile strength results, i.e., the increase in tear strength is governed by the amount of CB owning relatively high specific surface area and structure development in hybrid system. Therefore, similar explanation could be applied.

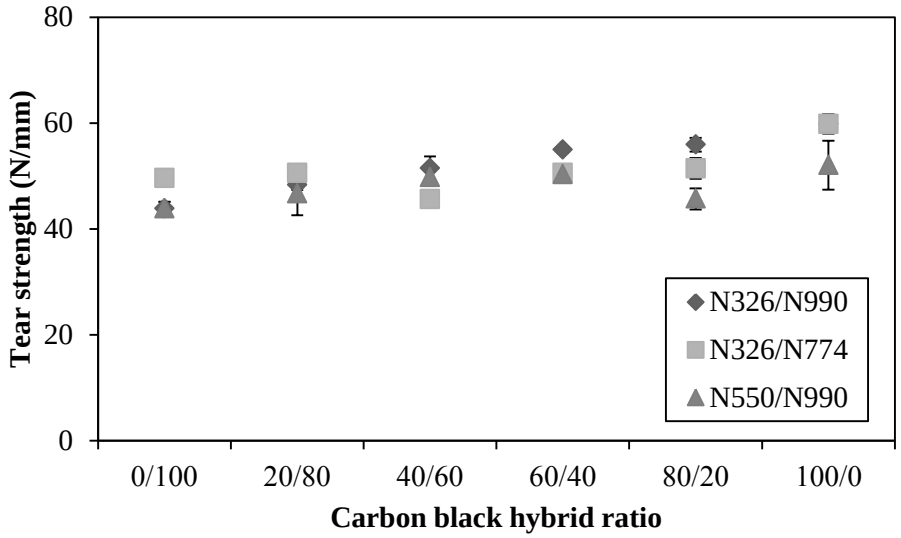

Figure 5.126 Relationship among tear strength, carbon black hybrid ratio and hybrid system in HNBR vulcanisates

For the hardness results as illustrated in Figure 5.127, the result trends agree well with those of M100, and similar explanation could be applied (i.e., based on the crosslink density and the filler network effects).

Figure 5.128 demonstrates the results of abrasion loss of HNBR vulcanisates with various CB hybrid systems. It is expected that the larger surface area and greater structure of CB would result in the improved abrasion resistance. Nevertheless, the abrasion resistance is not significantly affected by the increase of N326 content in N326/N990 and N326/N774 hybrid systems. Interestingly, it is found that the abrasion resistance of N550/N990 filled HNBR vulcanisate can be improved by the increasing N550 loading in hybrid ratio up to 40% weight, and then the abrasion resistance is independent of N550 loading. This result is due probably to the good filler dispersion of N550 as discussed previously in section 5.1.1.3. The valcanisates filled with the CB having large particle size and structure display good CB dispersion. Compared to the N326, the N550 has relatively large particle size and structure, as a consequence, the incorporation of N550 into CB hybrid system is capable of enhancing the abrasion resistance of vulcanisates.

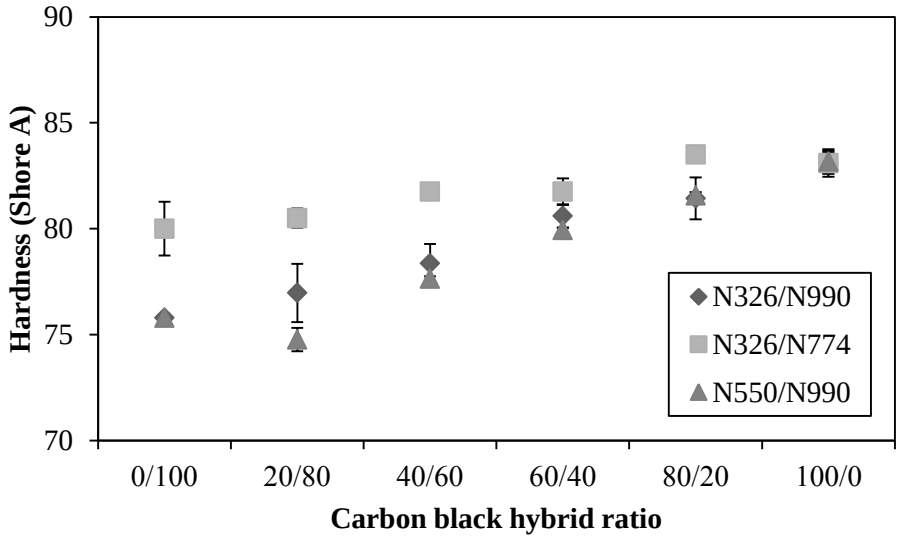

Figure 5.127 Relationship among hardness, carbon black hybrid ratio and hybrid system in HNBR compounds

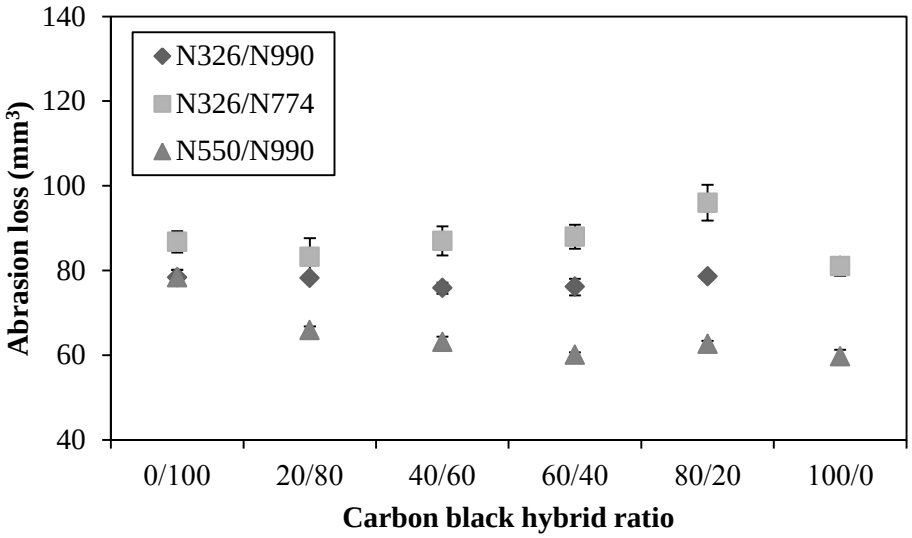

Figure 5.128 Relationship among abrasion loss, carbon black hybrid ratio and hybrid system in HNBR vulcanisates

5.2 Correlation between viscoelastic behaviour and heat build-up of carbon black filled hydrogenated nitrile rubber vulcanisates

It is known that CB is the most widely used reinforcing filler used in rubber industry and its elementary particle size and the aggregate structure are the key factor controlling the reinforcement efficiency. The reinforcement mechanism of filled rubber arises from a superimposition of several effects, namely, hydrodynamic effect, filler-filler interactions and rubber-filler interactions (19, 77, 128). Although the presence of rubber-CB interaction leads to a high extent of reinforcement, such interaction gives rise to the high magnitude of heat build-up (HBU) taking place in rubber products. This is because of the fact that the rubber-CB interaction is dominated by the physical over chemical interactions (20), allowing molecular flow at rubber-CB interfaces, and thus the greater energy dissipation via hysteretic process (21). In CB filled natural rubber (NR), the HBU increases with increasing hysteresis loss, implying a correlation of HBU to viscoelastic behaviour to some extent (22). Consequently, the present section aims to investigate the interconnection between HBU and viscoelastic properties of HNBR filled with CBs having different surface area and structure. The prediction of HBU by the routine measurement of viscoelastic properties was conducted and discussed. With the appropriate test procedure, the RPA 2000 could be used to directly measure HBU of rubber compounds and vulcanisates with excellent repeatability under moderate strain and high frequency (90).

5.2.1 Heat build-up (HBU) behaviour

In this study, a correlation between HBU results (as measured with the stress controlled flexometer equipped with high load force, i.e., the Gabometer 4000), and the viscoelastic properties as measured with the RPA 2000 is established.

5.2.1.1 Heat build-up behaviour

Generally, HBU measurement is carried out using a conventional Goodrich flexometer. However, in some industrial roll products in which high stress is applied to the rolls, the high modulus of rubber vulcanisates covering over the metal cores is required in order to prevent excessive deformation. This means

the high modulus of roll products is needed. The precise prediction of HBU behaviour of this high-modulus rubber vulcanisates is not practical with the use of conventional Goodrich flexometer under the static stress of only 0.99 MPa. Consequently, the stress-controlled flexometer equipped with high load cell (up to 4,000 N), namely, Gabometer 4000, was used to measure the HBU of rubber vulcanisates in this section.

The HBU is plotted against CB loading as shown in Figure 5.129 for filled HNBR vulcanisates with different CB characteristics. By increasing CB loading, the HBU significantly increases, and the magnitude of HBU rise is more pronounced in the specimens with high surface area and/or structure. Such increase in HBU is anticipated to be the results of hysteretic process via the disruption of transient filler network and molecular flow at the CB interfaces (21, 22, 129). Exceptionally, the HBU is found to be highest in HNBR filled with N550, which is due probably to its relatively high extent of developed structure. At a given CB loading, the increase in surface area and structure of CB would increase filler transient network. Under deformation, these transient networks are disrupted, leading to the more energy dissipated, and thus the energy loss is increased. The higher energy loss results in the higher HBU occurring in rubber vulcanisates.

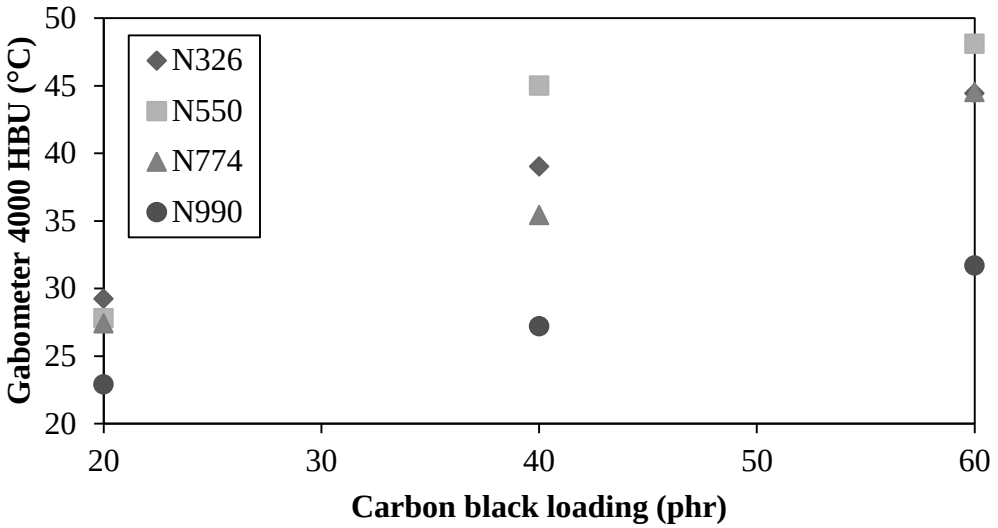

Figure 5.129 Relationship among Gabometer 4000 HBU, carbon black loading and characteristics in HNBR vulcanisates

It is clear that the HBU behaviour depends significantly on CB characteristics, and is needed to be measured for ensuring the acceptable performance of rubber product. However, the HBU measurement using the flexometer equipped with high load cell and powerful shaker is rather costly. Thus, one of objectives of the present work is to draw the correlation between viscoelastic results measured from oscillatory RPA 2000 as a routine test and the HBU monitored from the specially designed flexometer. By this means, it is possible to estimate the HBU from the RPA 2000 results.

5.2.2 A prediction of heat build-up behavior under high-load by the use of conventional viscoelastic results in CB filled HNBR vulcanisates

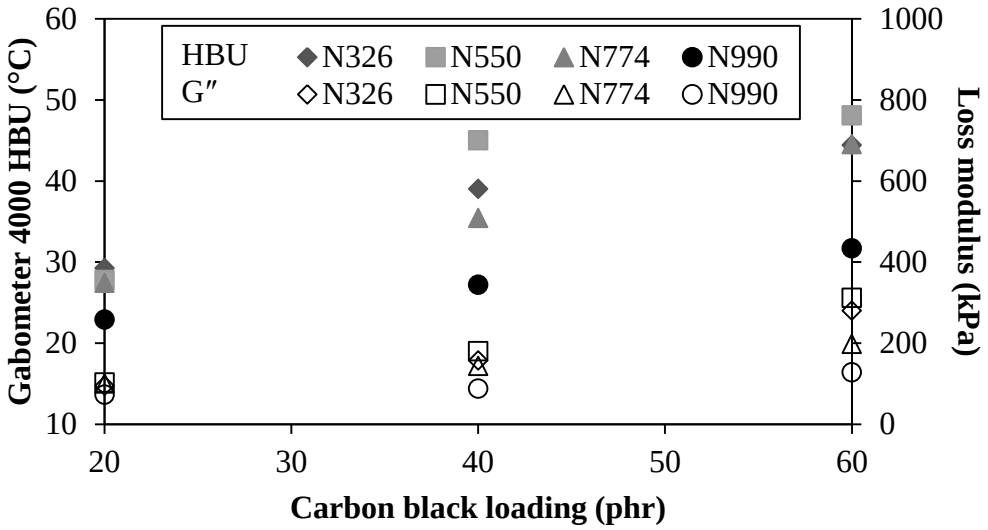

Figure 5.130 Relationship among Gabometer 4000 HBU, loss modulus (G″), carbon black loading and characteristics in HNBR vulcanisates: the G″ is measured with RPA 2000 at test strain, temperature and frequency of 2%, 100°C and 1 rad/s, respectively

Hysteresis loss is defined as the loss of energy of the rubber vulcanisate under cyclic deformation, which then this lost energy converts into heat. The HBU is measured as the temperature rise of the rubber vulcanisate resulting from the

hysteresis loss. Such hysteresis loss is proportional to the G″ (21, 125, 130). Therefore, the G″ is applied to predict the HBU in this work.

Figures 5.130 reveals the effect of CB loading on HBU and G″ of HNBR vulcanisates filled with different CB characteristics. It is observed that both HBU and G″ of filled HNBR vulcanisates increases with increasing CB loading, and increases with increasing surface area and/or structure of CB at a given loading.

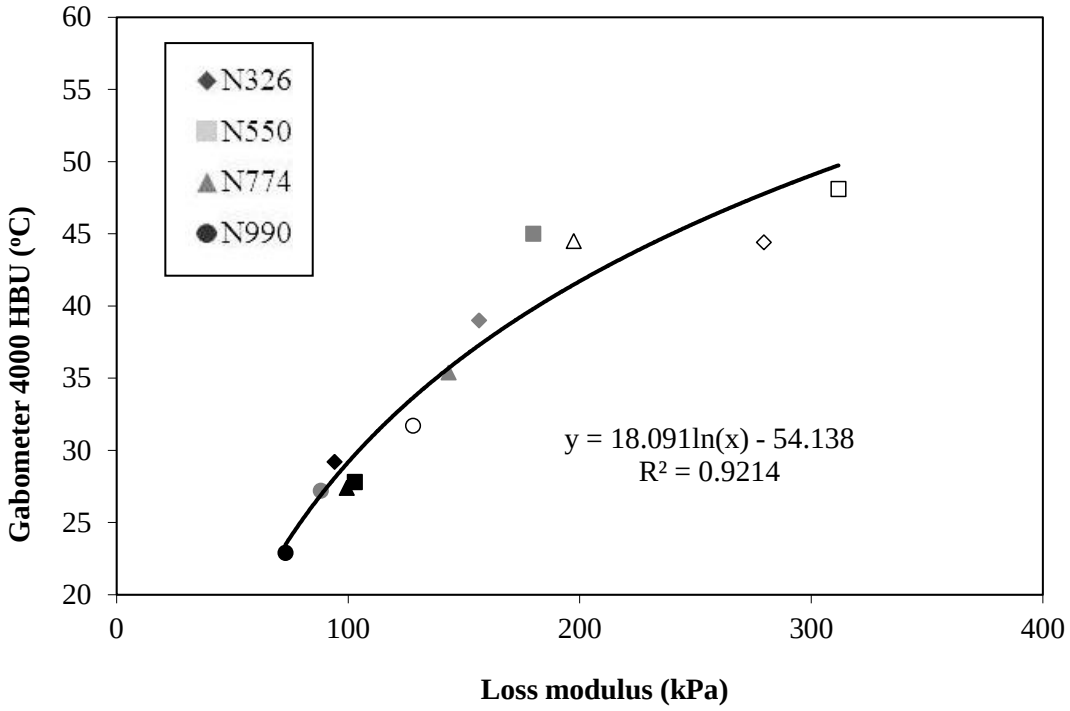

Figure 5.131 Relationship between Gabometer 4000 HBU and loss modulus (G″) in filled HNBR (vulcanisates) with various carbon black loadings and characteristics: 20 phr (black solid symbol); 40 phr (gray solid symbol); 60 phr (unfilled symbol)

The correlation of HBU with G″ for all vulcanisates filled with various CB loadings and characteristics is plotted as illustrated in Figure 5.131. Evidently, regardless of CB loading and characteristics, the HBU increases with increasing G″, and their correlation agree well with the logarithmic regression equation as shown in Equation 5.1 with R^2 = 0.9214. In other words, the G″ plays strong role on HBU of HNBR vulcanisates studied.

$$HBU_G = 18.019\ln(G'') - 54.138 \quad (5.1)$$

where HBU_G = heat build-up as determined from the Gabometer 4000
G'' = loss modulus as measured routinely from the RPA 2000

Apart from G″, one might consider the tanδ as an indication of HBU at a given G′ (or stiffness). In this case, the energy loss or dynamic hysteresis is also proportional to the tanδ (21, 85). The plot of HBU and tanδ with CB loading of HNBR vulcanisates filled with different CB characteristics is shown in Figure 5.132. As can be seen, the filled vulcanisates expressing high tanδ, will also show high HBU.

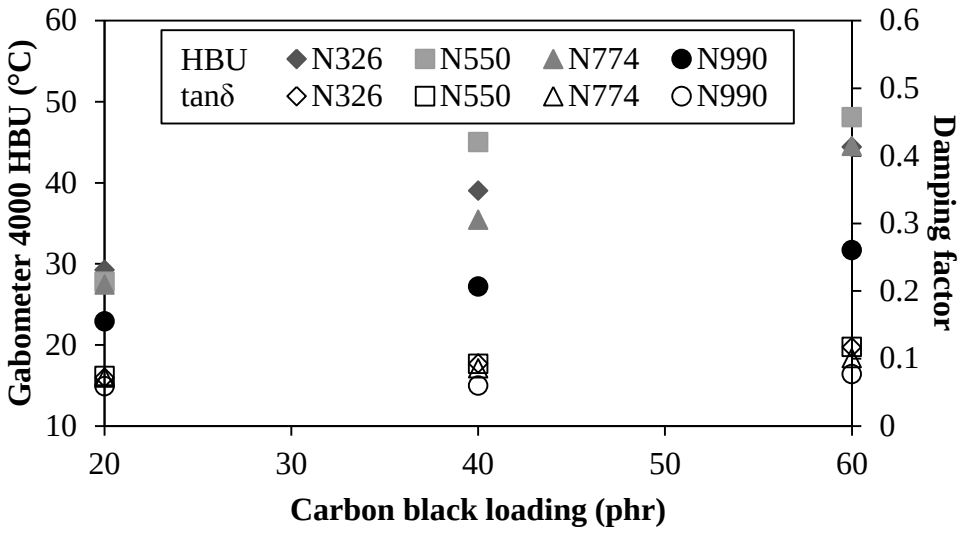

Figure 5.132 Relationship among Gabometer 4000 HBU, damping factor (tanδ), carbon black loading and characteristics in HNBR vulcanisates: the tanδ is measured with RPA 2000 at test strain, temperature and frequency of 2%, 100°C and 1 rad/s, respectively

Figure 5.133 reveals the change in HBU as a function of tanδ in a similar trend to that of HBU against G″ as illustrated in Equation 5.2, but with the lower R^2 of 0.9011. As indicated from the R^2, the tanδ is not as good as the G″ in predicting HBU under high load applied.

$$HBU_G = 35.995\ln(\tan\delta) + 125.03 \quad (5.2)$$

where HBU_G = heat build-up as determined from the Gabometer 4000
$\tan\delta$ = damping factor as measured routinely from the RPA 2000

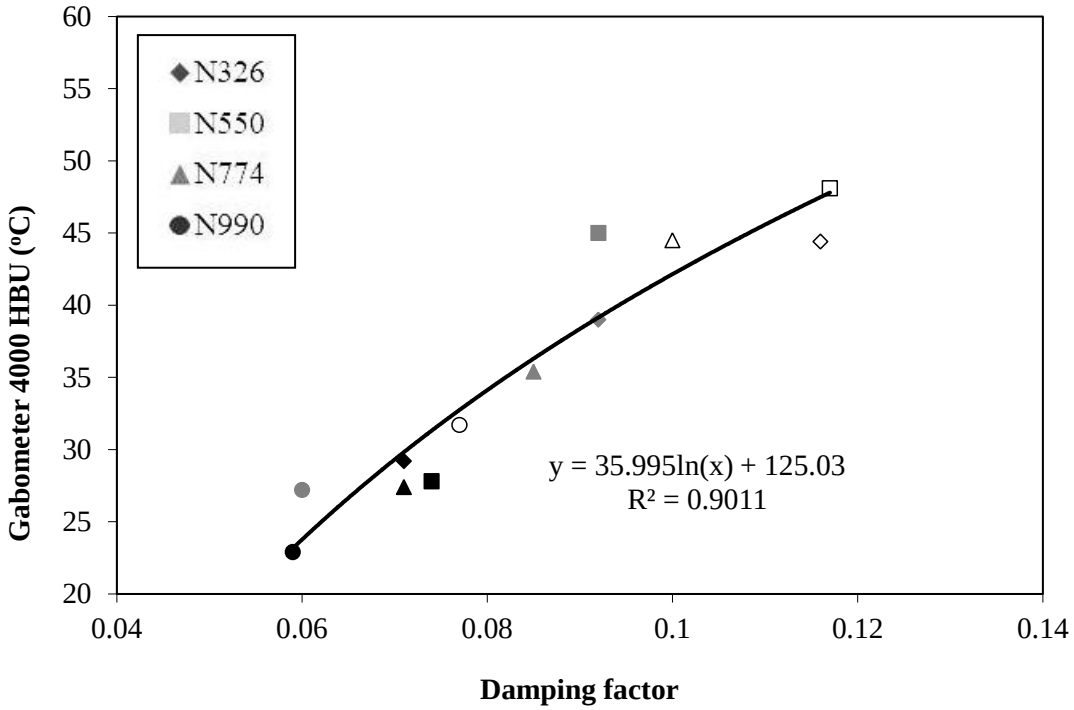

Figure 5.133 Relationship between Gabometer 4000 HBU and damping factor (tanδ) in filled HNBR vulcanisates with various carbon black loadings and characteristics: 20 phr (black solid symbol); 40 phr (gray solid symbol); 60 phr (unfilled symbol)

From the overall results, it is possible to estimate the HBU generally measured from the high-load flexometer, by the use of RPA 2000 results as a routine test.

5.2.3 A study of heat build-up behaviour of carbon black filled hydrogenated nitrile rubber vulcanisates using closed cavity torsional rheometers

The RPA 2000 has been used to directly measure HBU of rubber vulcanisate with excellent repeatability under moderate strain and high frequency (90). In this work, a correlation between HBU results as measured with the Gabometer 4000 and with the RPA 2000 is established.

Figure 5.134 shows HBU as measured from RPA 2000. Evidently, the HBU significantly increases with increasing CB loading and/or surface area, and the magnitude of HBU increment is more pronounced in specimens loaded with high surface area and/or structure of CB. Compared to Gabometer 4000 HBU, a similar trend can be observed despite the different mode of deformation, i.e., shear in RPA 2000 and compression in Gabometer 4000. Indeed, since the HBU is an overall effect reflecting the viscous dissipation of a rubber compound submitted to large dynamic strain, then a similar effect can be expected to be observed with the RPA 2000 when the temperature control of the instrument has been switched-off.

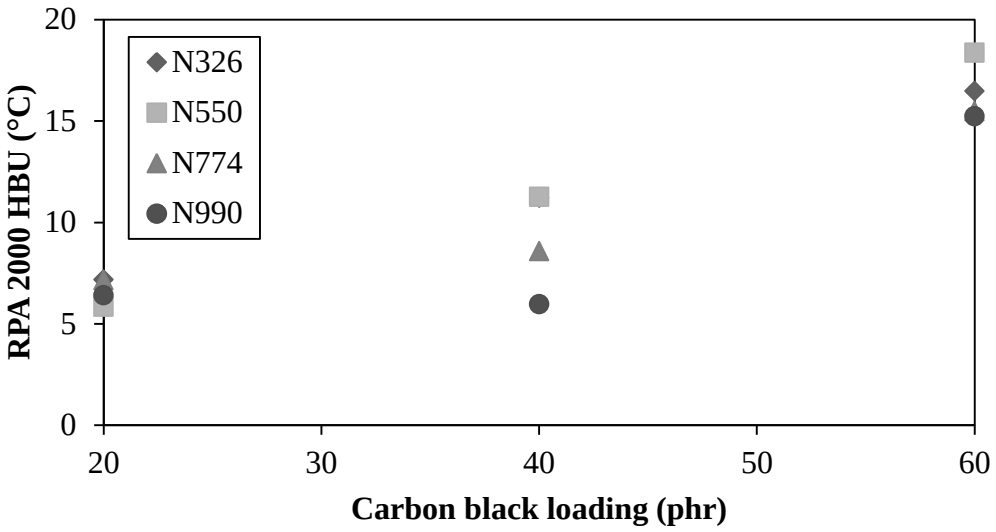

Figure 5.134 Relationship among HBU as measured from RPA 2000, carbon black loading and characteristics in HNBR vulcanisates

As discussed previously, the G″ is an effective indication of HBU. The RPA 2000 HBU versus the G″ of filled vulcanisates with different CB loadings and

characteristics is illustrated in Figure 5.135. The correlation of RPA 2000 HBU to G″ is also represented by logarithmic regression equation as displayed in Equation 5.3 with R^2 = 0.7931. Compared to the Gabometer 4000 HBU, the RPA 2000 does not correlate well to the G″ as indicated from the relatively low R^2.

$$HBU_R = 8.8541\ln(G'') - 32.977 \quad (5.3)$$

where HBU_R = heat build-up as determined from the RPA 2000
G″ = loss modulus as measured routinely from the RPA 2000

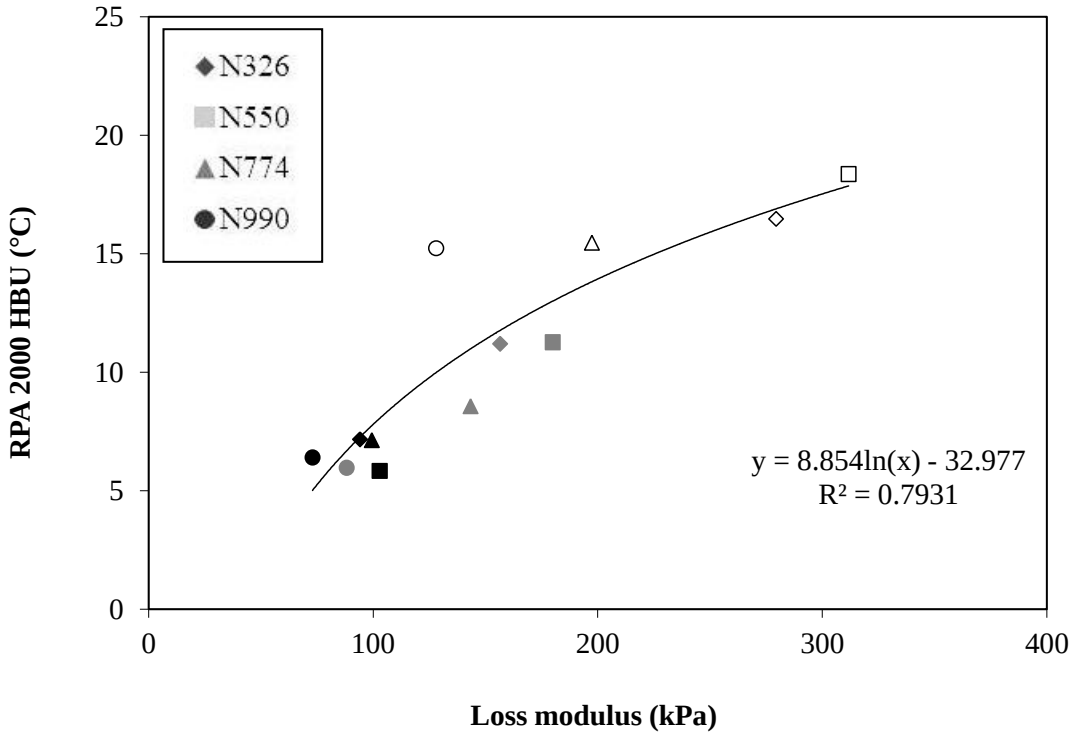

Figure 5.135 Relationship between RPA 2000 HBU and loss modulus (G″) in filled HNBR vulcanisates with various carbon black loadings and characteristics: 20 phr (black solid symbol); 40 phr (gray solid symbol); 60 phr (unfilled symbol)

Figure 5.136 illustrates the relationship between HBU measured from RPA 2000 and Gabometer 4000 of HNBR vulcanisates filled with various CB loadings and characteristics. Evidently, the change in RPA 2000 HBU and

Gabometer 4000 HBU shows a relatively poor correlation as illustrated in Equation 5.4 with R^2 = 0.7271. Such low R^2 means that the 72.71% of the total variation in HBU measured from the standard manner with the Gabometer 4000 can be explained by the relationship between RPA 2000 HBU and Gabometer 4000 HBU as Equation 5.4. In other words, the HBU measurement with RPA 2000 could not satisfactorily replace the standard HBU technique. This is due probably to the RPA 2000 is far from being an effective calorimeter, so that uncontrolled heat losses introduce an error.

$$HBU_G = 17.269\ln(HBU_R) - 4.3585 \quad (5.4)$$

where HBU_G = heat build-up as determined from the Gabometer 4000

HBU_R = heat build-up as measured directly from the RPA 2000

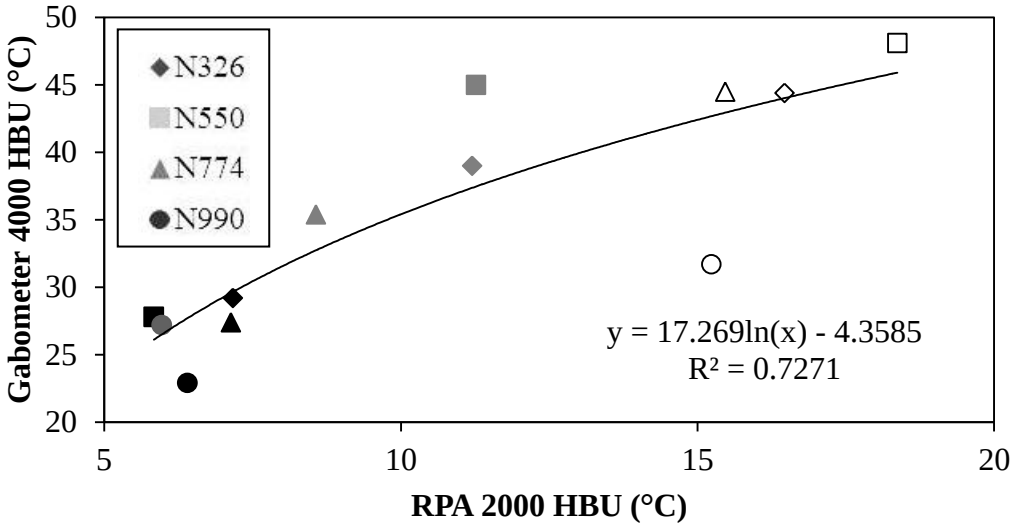

Figure 5.136 Relationship between Gabometer 4000 HBU and RPA 2000 HBU in filled HNBR vulcanisates with various carbon black loadings and characteristics: 20 phr (black solid symbol); 40 phr (gray solid symbol); 60 phr (unfilled symbol)

CHAPTER VI
CONCLUSIONS

Part 1: Effects of filler type and loading

1. Investigation of carbon black type (i.e. N326, N550, N774 and N990) and loading effects on properties of HNBR compounds and vulcanisates

A significant dependence of cure behaviour (i.e., scorch time, optimum cure time and crosslink density) on CB loading and specific surface area is observed. Interestingly, the high structure of N550 CB gives the high bound rubber content, and thus the increased magnitudes of cure rate, state-of-cure and crosslink density.

The non-linear viscoelastic behaviour of compounds was investigated at large strain amplitude through the Fourier transform technique. The results show strain history effects with 60 phr N550 filled HNBR, which is due mainly to the high magnitude of filler transient network.

Storage modulus and damping factor of vulcanisates significantly increase with increasing CB specific surface area and loading of CBs. The combined effects of hydrodynamic effect, filler transient network, molecular slippage at CB interfaces, crosslink density and filler dispersion (especially at high loading of N326 having high surface area) are proposed to be responsible for the mechanical and viscoelastic properties. The overall results imply a close correlation of viscoelastic and mechanical properties via energy dissipation process caused by molecular slippage at CB surfaces.

2. Investigation of precipitated silica (i.e. Hi-Sil 233-S) loading effect on properties of HNBR compounds and vulcanisates

Cure promotion phenomenon (i.e., decrease in scorch and cure times, and an increase in crosslink density) is explained by the interplay of thermal history and the reduced migration of curatives to tightly bound rubber (i.e., an increase in curative residing in mobilised HNBR matrix). Viscoelastic properties of silica filled HNBR are

influenced strongly by the hydrodynamic effect associated with strong silica transient network and silica-HNBR interaction. Tensile properties and tear resistance are found to be affected by the combination of filler reinforcement and crosslink density effects. However, at high silica loading (i.e., 30 and 40 phr), the degree of silica dispersion becomes the crucial factors controlling mechanical properties.

3. Investigation of organoclay (i.e. Bentone® 38) loading effect on properties of HNBR compounds and vulcanisates

Scorch and cure time decrease with increasing nanoclay loading, which could be explained by: (i) cure promotion phenomenon via the reduced magnitude of curative migration to the tightly bound rubber and (ii) high thermal history of rubber bulk during the mixing process.

Similar to CB and silica, the incorporation of nanoclay into HNBR plays role on viscoelastic properties of compounds and vulcanisates, which is due mainly to the hydrodynamic and filler network effects as well as filler-rubber interaction. Tensile and tear properties in organoclay filled vulcanisates are governed by changes in crosslink density and filler reinforcement effects. Abrasion resistance is found to depend significantly on the increased hysteresis loss, which is more pronounced in the vulcanisates with high nanoclay loading (i.e., 20 and 30 phr).

4. Property comparison of mechanical properties of carbon black, silica and nanoclay filled HNBR systems

Hardness and modulus increase noticeably with increasing filler loading. At any given loading of fillers, the nanoclay filled HNBR vulcanisates exhibit relatively high hardness and modulus. A larger amount of CB is needed to match the hardness of the vulcanisates filled with silica and nanoclay. At similar hardness of 80 Sh A, the CB filled vulcanisates gives the superiority in tensile strength and abrasion resistance, but the inferiority in tear strength to the silica and nanoclay filled vulcanisates. The explanation is proposed by good filler dispersion and strong filler-rubber interaction.

5. Investigation of carbon black hybrid system effects on properties of HBNR compounds and vulcanisates

As the loading of CB having higher surface area and/or structure in hybrid systems increases to become a major portion, a rise in crosslink density (as determined from the cure torque difference) is observed. The N326/N990 and N550/N990 filled HNBR vulcanisates show comparable crosslink density.

The non-linear viscoelastic behaviour of filled HNBR compounds at large strain amplitude through the use of Fourier transform technique is dominated by characteristics of major portion of CB in the hybrid systems. The increase in N326 or N550 in the CB hybrid system is attractive in enhancing the filler-rubber interaction and thus the mechanical properties.

Part 2: Correlation between viscoelastic behaviour and heat build-up of HNBR vulcanisates

The heat build-up (HBU) significantly increases with increasing CB loading and/or surface area, and the magnitude of HBU rise is more pronounced in specimens with high surface area and/or structure. It is found that the G″ is a more effective in predicting HBU than the loss factor (tanδ). In the present work with filler loading and characteristics used (i.e., 0 to 60 phr of N326, N550, N774, N990), it is possible to estimate the HBU generally measured from the high load flexometer from the RPA2000 results as a routine test with the logarithmic regression equation, as follows:

$$HBU_G = 18.019\ln(G'') - 54.138$$

The HBU of cured specimens, as measured with the RPA2000, shows the expected general trend with respect to CB loading and characteristics. However, there are some extent of discrepancies in HBU measured directly from Gabometer4000 and RPA2000 which could be explained by the uncontrolled heat losses in RPA2000. In other words, the RPA2000 is far from being an efficient calorimeter.

REFERENCES

1 Dick JS, editor. Rubber technology: Compounding and testing for performance. 1st ed. Munich: Hanser; 2001.

2 Baranwal KG, Stephens HL, editors. Basic elastomer technology. Akron: The Rubber Division American Chemical Society; 2001.

3 Furtado CRG, Leblanc JL, Nunes RCR. Fatigue resistance of mica-carbon black-styrene butadiene rubber (SBR) compounds. European Polymer Journal. 1999;35(7):1319-25.

4 Yatsuyanagi F, Suzuki N, Ito M, Kaidou H. Effects of secondary structure of fillers on the mechanical properties of silica filled rubber systems. Polymer. 2001;42(23):9523-9.

5 Gatos KG, Sawanis NS, Apostolov AA, Thomann R, Karger-Kocsis J. Nanocomposite formation in hydrogenated nitrile rubber (HNBR)/organo-montmorillonite as a function of the intercalant type. Macromolecular Materials and Engineering. 2004;289(12):1079-86.

6 Achten D, Wrana C. Optimisation of HNBR based formulations for dynamically used applications at elevated temperatures. KGK Kautschuk Gummi Kunststoffe. 2005;58(6):298-303.

7 Yue D, Liu Y, Shen Z, Zhang L. Study on preparation and properties of carbon nanotubes/rubber composites. Journal of Materials Science. 2006;41(8):2541-4.

8 Gatos KG, Karger-Kocsis J. Effect of the aspect ratio of silicate platelets on the mechanical and barrier properties of hydrogenated acrylonitrile butadiene rubber (HNBR)/layered silicate nanocomposites. European Polymer Journal. 2007;43(4):1097-104.

9 Wang X-p, Huang A-m, Jia D-m, Li Y-m. From exfoliation to intercalation-changes in morphology of HNBR/organoclay nanocomposites. European Polymer Journal. 2008;44(9):2784-9.

10 Felhös D, Karger-Kocsis J, Xu D. Tribological testing of peroxide cured HNBR with different MWCNT and silica contents under dry sliding and rolling conditions against steel. Journal of Applied Polymer Science. 2008;108(5):2840-51.

11 Xu D, Karger-Kocsis J, Schlarb AK. Friction and wear of HNBR with different fillers under dry rolling and sliding conditions. Express Polymer Letters. 2009;3(2):126-36.

12 Chen S, Yu H, Ren W, Zhang Y. Thermal degradation behavior of hydrogenated nitrile-butadiene rubber (HNBR)/clay nanocomposite and HNBR/clay/carbon nanotubes nanocomposites. Thermochimica Acta. 2009;491(1-2):103-8.

13 Thavamani P, Bhowmick AK. Dynamic mechanical properties of hydrogenated nitrile rubber: effect of cross-link density, curing system, filler and resin. Journal of Materials Science. 1992;27(12):3243-53.

14 Medalia AI. Filler aggregates and their effect on reinforcement. Rubber Chemistry and Technology. 1974;47(2):411-33.

15 Medalia AI. Elastic modulus of vulcanizates as related to carbon black structure. Rubber Chemistry and Technology. 1973;46(4):877-96.

16 Dutta NK, Khastgir D, Tripathy DK. The effect of carbon black concentration on the dynamic mechanical properties of bromobutyl rubber. Journal of Materials Science. 1991;26(1):177-88.

17 Sajjayanukul T, Saeoui P, Sirisinha C. Experimental analysis of viscoelastic properties in carbon black-filled natural rubber compounds. Journal of Applied Polymer Science. 2005;97(6):2197-203.

18 Demirhan E, Kandemirli F, Kandemirli M. The effects of furnace carbon blacks on the mechanical and the rheological properties of SBR1502 styrene butadiene rubber. Materials and Design. 2007;28(4):1326-9.

19 Kohls DJ, Beaucage G. Rational design of reinforced rubber. Current Opinion in Solid State and Materials Science. 2002;6(3):183-94.

20 De SK, White JR, editors. Rubber technologist's handbook. Shawbury, Shrewsbury, Shropshire, SY4 4NR, United Kingdom: Rapra Technology; 2001.

21 Wang MJ. Effect of polymer-filler and filler-filler interactions on dynamic properties of filled vulcanizates. Rubber Chemistry and Technology. 1998;71(3):520-89.

22 Park DM, Hong WH, Kim SG, Kim HJ. Heat generation of filled rubber vulcanizates and its relationship with vulcanizate network structures. European Polymer Journal. 2000;36(11):2429-36.

23 Boonstra BB, Medalia AI. Effect of carbon black dispersion on the mechanical properties of rubber vulcanizates. Rubber Chemistry and Technology. 1963;36(1):115-42.

24 Bokobza L. Multiwall carbon nanotube elastomeric composites: A review. Polymer. 2007;48(17):4907-20.

25 Pérez LD, López JF, Orozco VH, Kyu T, López BL. Effect of the chemical characteristics of mesoporous silica MCM-41 on morphological, thermal, and rheological properties of composites based on polystyrene. Journal of Applied Polymer Science. 2009;111(5):2229-37.

26 Boonstra BB. Resistivity of unvulcanized compounds of rubber and carbon black. Rubber Chemistry and Technology. 1977;50(1):194-210.

27 Cembrola RJ. The relationship of carbon black dispersion to electrical resistivity and vulcanizate physical properties. Polymer Engineering & Science. 1982;22(10):601-9.

28 Hess WM. Characterization of dispersions. Rubber Chemistry and Technology. 1991;64(3):386-449.

29 Smits V, Chevalier P, Deheunynck D, Miller S. A new filler dispersion technology. Reinforced Plastics. 2008;52(11):37-43.

30 Funt JM. Rubber mixing. Rubber Chemistry and Technology. 1980;53(3):772-9.

31 Shiga S, Furuta M. Processability of EPR in an internal mixer (II) morphological. Changes of carbon black agglomerates during mixing. Rubber Chemistry and Technology. 1985;58(1):1-22.

32 Coran AY, Donnet J-B. The dispersion of carbon black in rubber Part I. Rapid method for assessing quality of dispersion. Rubber Chemistry and Technology. 1992;65(5):973-97.

33 White JL, Liu D, Bumm SH. Development of dispersion in rubber-particle compounds in internal and continuous mixers. Journal of Applied Polymer Science. 2006;102(4):3940-3.

34 Mark JE, Erman B, Eirich FR, editors. Science and technology of rubber. 2 ed. San Diego, CA: Academic Press; 1994.

35 Rahman M, Brazel CS. The plasticizer market: an assessment of traditional plasticizers and research trends to meet new challenges. Progress in Polymer Science. 2004;29(12):1223-48.

36 Höfer R, Hinrichs K. Additives for the manufacture and processing of polymers. In: Eyerer P, Weller M, Hübner C, editors.: Springer Berlin / Heidelberg; 2010. p. 97-145.

37 Rostler FS, Pont HId. Plasticizer-filler mixtures and their dispersion in rubber. Industrial & Engineering Chemistry. 1947;39(10):1311-22.

38 Castellano M, Conzatti L, Costa G, Falqui L, Turturro A, Valenti B, et al. Surface modification of silica: 1. Thermodynamic aspects and effect on elastomer reinforcement. Polymer. 2005;46(3):695-703.

39 Ansarifar A, Shiah SF, Bennett M. Optimising the chemical bonding between silanised silica nanofiller and natural rubber and assessing its effects on the properties of the rubber. International Journal of Adhesion and Adhesives. 2006;26(6):454-63.

40 Brown DS, Warner FP, Wetton RE. Surface areas of fillers in polymers by small-angle X-ray scattering. Polymer. 1972;13(12):575-8.

41 Oono R. Distribution of carbon black in SBR. Journal of Applied Polymer Science. 1977;21(7):1743-9.

42 Vegvari PC, Hess WM, Chirico VE. Measurement of carbon black dispersion in rubber by surface analysis. Rubber Chemistry and Technology. 1978;51(4):817-39.

43 Ebell PC, Hemsley DA. A novel optical method for estimating the dispersion of carbon black in rubbers. Rubber Chemistry and Technology. 1981;54(4):698-717.

44 Tscheschel A, Lacayo J, Stoyan D. Statistical characterization of TEM images of silica-filled rubber. Journal of Microscopy. 2005;217(1):75-82.

45 Wolff S. Silanes in tire compounding after ten years - A review. Tire Science and Technology. 1987;15(4):276-94.

46 Morisita M. Measuring of the dispersion of individuals and analysis of the distributional patterns. Memoirs Faculty of Science, Kyushu University Series E Biology. 1959;2(4):215-35.

47 Morisita M. Iδ-index, a measure of dispersion. Researches on Population Ecology. 1962;4:1-7.

48 Sumita M, Sakata K, Hayakawa Y, Asai S, Miyasaka K, Tanemura M. Double percolation effect on the electrical conductivity of conductive particles filled polymer blends. Colloid & Polymer Science. 1992;270(2):134-9.

49 Karásek L, Sumita M. Characterization of dispersion state of filler and polymer-filler interactions in rubber-carbon black composites. Journal of Materials Science. 1996;31(2):281-9.

50 Azizi J, Dollimore D, Heal GR, Kneller WA, Manley P, Philip CC. An investigation of the activity of carbon blacks recovered from elastomer composites. Journal of Thermal Analysis and Calorimetry. 1996;46(6):1837-44.

51 Park S-J, Kim J-S. Role of chemically modified carbon black surfaces in enhancing interfacial adhesion between carbon black and rubber in a composite system. Journal of Colloid and Interface Science. 2000;232(2):311-6.

52 Edwards DC. Polymer-filler interactions in rubber reinforcement. Journal of Materials Science. 1990;25(10):4175-85.

53 Aso O, Eguiazábal JI, Nazábal J. The influence of surface modification on the structure and properties of a nanosilica filled thermoplastic elastomer. Composites Science and Technology. 2007;67(13):2854-63.

54 Chakraborty S, Ganguly S, Black PC, Bhattacharya P. Novel approach of rubber-filler interaction through surface modification of carbon black. Rubber World. [Article]. 2003;228(1):38.

55 Leblanc JL. Rubber-filler interactions and rheological properties in filled compounds. Progress in Polymer Science. 2002;27(4):627-87.

56 Blow CM. Polymer/particulate filler interaction-the bound rubber phenomena. Polymer. 1973;14(7):309-23.

57 Kraus G. Reinforcement of elastomers by carbon black. Fortschritte der Hochpolymeren-Forschung: Springer Berlin / Heidelberg; 1971. p. 155-237.

58 Boonstra BB. Role of particulate fillers in elastomer reinforcement: a review. Polymer. 1979;20(6):691-704.

59 Dannenberg EM. Bound rubber and carbon black reinforcement. Rubber Chemistry and Technology. 1986;59(3):512-24.

60 Sircar AK, Voet A. Immobilization of elastomers at the carbon black particle surface. Rubber Chemistry and Technology. 1970;43(5):973-80.

61 Meissner B. Theory of bound rubber. Rubber Chemistry and Technology. 1975;48(5):810-8.

62 Wolff S, Wang M-J, Tan E-H. Filler-elastomer interactions. Part VII. Study on bound rubber. Rubber Chemistry and Technology. 1993;66(2):163-77.

63 Yatsuyanagi F, Kaidou H, Ito M. Relationship between viscoelastic properties and characteristics of filler-gel in filled rubber system. Rubber Chemistry and Technology. 1999;72(4):657-72.

64 Choi S-S. Effect of bound rubber on characteristics of highly filled styrene–butadiene rubber compounds with different types of carbon black. Journal of Applied Polymer Science. 2004;93(3):1001-6.

65 Leblanc JL. Elastomer–filler interactions and the rheology of filled rubber compounds. Journal of Applied Polymer Science. 2000;78(8):1541-50.

66 O'Brien J, Cashell E, Wardell GE, McBrierty VJ. An NMR investigation of the interaction between carbon black and cis-polybutadiene. Macromolecules. 1976;9(4):653-60.

67 Kenny JC, McBrierty VJ, Rigbi Z, Douglass DC. Carbon black filled natural rubber. 1. Structural investigations. Macromolecules. 1991;24(2):436-43.

68 Legrand AP, Lecomte N, Vidal A, Haidar B, Papirer E. Application of NMR spectroscopy to the characterization of elastomer/filler interactions. Journal of Applied Polymer Science. 1992;46(12):2223-32.

69 Choi S-S. Difference in bound rubber formation of silica and carbon black with styrene-butadiene rubber. Polymers for Advanced Technologies. 2002;13(6):466-74.

70 Choi S-S, Hwang K-J, Kim B-T. Influence of bound polymer on cure characteristics of natural rubber compounds reinforced with different types of carbon blacks. Journal of Applied Polymer Science. 2005;98(5):2282-9.

71 Le HH, Ilisch S, Kasaliwal GR, Radusch HJ. Method for the characterization of phase specific filler distribution in rubber blends using thermogravimetric analysis on the rubber-filler gel. Thermogravimetrischer Analyse an Kautschuk-Fůllstoff-Gel. 2007;60(5):241-8.

72 Le HH, Ilisch S, Kasaliwal GR, Radusch HJ. Filler phase distribution in rubber blends characterized by thermogravimetric analysis of the rubber-filler gel. Rubber Chemistry and Technology. 2008;81(5):767-81.

73 Le HH, Ilisch S, Radusch HJ. Characterization of the effect of the filler dispersion on the stress relaxation behavior of carbon black filled rubber composites. Polymer. 2009;50(10):2294-303.

74 Fletcher WP, Gent AN. Apparatus for the measurement of the dynamic shear modulus and hysteresis of rubber at low frequencies. Journal of Scientific Instruments. 1952;29(6):186.

75 Payne AR. The dynamic properties of carbon black-loaded natural rubber vulcanizates. Part I. Journal of Applied Polymer Science. 1962;6(19):57-63.

76 Payne AR, Whittaker RE. Low strain dynamic properties of filled rubbers. Rubber Chemistry and Technology. 1971;44(2):440-78.

77 Fröhlich J, Niedermeier W, Luginsland HD. The effect of filler-filler and filler-elastomer interaction on rubber reinforcement. Composites Part A: Applied Science and Manufacturing. 2005;36(4):449-60.

78 Leblanc JL. Large amplitude oscillatory shear experiments to investigate the nonlinear viscoelastic properties of highly loaded carbon black rubber compounds without curatives. Journal of Applied Polymer Science. 2008;109(2):1271-93.

79 Leblanc JL, De La Chapelle C. Updating a torsional dynamic rheometer for Fourier Transform rheometry on rubber materials. Rubber Chemistry and Technology. 2003;76(2):287-98.

80 Leblanc JL. Fourier transform rheometry on carbon black filled polybutadiene compounds. Journal of Applied Polymer Science. 2006;100(6):5102-18.

81 Leblanc JL. Fourier transform rheometry : a new tool to investigate intrinsically non-linear viscoelastic materials. Annaual Transactions of the Nordic Rheology Society. 2008;13:3-21.

82 Leblanc JL, editor. Strain and morphology induced non-linearities in the viscoelastic behavior of filled polymer systems2008; Monterey, CA.

83 Leblanc J. Investigating the non-linear viscoelastic behavior of filled rubber compounds through fourier transform rheometry. Rubber Chem Technol. [10.5254/1.3547873]. 2005;78(1):54.

84 Harwood JAC, Payne AR, Smith JF. A new approach to rubber reinforcement. Rubber Chemistry and Technology. 1970;43(4):687-700.

85 Medalia AI. Heat generation in elastomer compounds: Causes and effects. Rubber Chemistry and Technology. 1991;64(3):481-92.

86 Meinecke E. Effect of carbon-black loading and crosslink density on the heat build-up in elastomers. Rubber Chemistry and Technology. 1991;64(2):269-84.

87 Caruthers J. Effect of carbon black on hysteresis of rubber vulcanizates: Equivalence of surface area and loading. Rubber Chem Technol. [10.5254/1.3534990]. 1976;49(4):1076.

88 Reed TF. Heat buildup of dynamically loaded engineered elastomeric components - I. Elastomerics. 1989;121(11):22-8.

89 Leblanc JL, Mongruel A. A thorough examination of a torsional dynamic rheometer with a closed oscillating cavity. Progress in Rubber and Plastics Technology. 2001;17(3):162-85.

90 Dick JS, Pawlowski H, Moore J. Viscous heating and reinforcement effects of fillers using the rubber process analyzer. Rubber World. [Article]. 2000;221(4):22.

91 Phewphong P, Saeoui P, Sirisinha C. The use of dynamic mechanical thermal analysis technique for determining an uneven distribution of precipitated silica in CPE/NR blends. Polymer Testing. 2008;27(7):873-80.

92 Radhakrishnan CK, Sujith A, Unnikrishnan G, Thomas S. Effects of the blend ratio and crosslinking systems on the curing behavior, morphology, and mechanical properties of styrene-butadiene rubber/poly(ethylene-co-vinyl acetate) blends. Journal of Applied Polymer Science. 2004;94(2):827-37.

93 Loan LD. Mechanism of peroxide vulcanization of elastomers. Rubber Chemistry and Technology. 1967;40(1):149-76.

94 Akiba M, Hashim AS. Vulcanization and crosslinking in elastomers. Progress in Polymer Science. 1997;22(3):475-521.

95 Dannenberg EM, Jordan ME, Cole HM. Peroxide crosslinked carbon black polyethylene compositions. Journal of Polymer Science. 1958;31(122):127-53.

96 Puri BR, Kalra KC. The decomposition of hydrogen peroxide in the presence of carbon blacks. Carbon. 1971;9(3):313-20.

97 Mark JE, editor. Physical properties of polymers handbook 2 nd ed. New York: Springer; 2007.

98 King JA, Hauser RA, Tomson AM, Wescoat IM, Keith JM. Synergistic effects of carbon fillers in thermally conductive liquid crystal polymer based resins. Journal of Composite Materials. 2008 January 1, 2008;42(1):91-107.

99 Litvinov VM, Steeman PAM. EPDM−carbon black interactions and the reinforcement mechanisms, as studied by low-resolution 1H NMR. Macromolecules. 1999 1999/12/01;32(25):8476-90.

100 Li ZH, Zhang J, Chen SJ. Effects of carbon blacks with various structures on vulcanization and reinforcement of filled ethylene-propylene-diene rubber. Express Polymer Letters. 2008;2(10):695-704.

101 Bhowmick AK, Hall MM, Benarey HA, editors. Rubber products manufacturing technology. 1st ed. New York: Marcel Dekker; 1994.

102 Hashim AS, Azahari B, Ikeda Y, Kohjiya S. The effect of bis(3-triethoxysilylpropyl) tetrasulfide on silica reinforcement of styrene-butadiene rubber. Rubber Chemistry and Technology. 1998;71(2):289-99.

103 Wolff S, Wang M-J. Filler-elastomer interactions. Part IV. The effect of the surface energies of fillers on elastomer reinforcement. Rubber Chemistry and Technology. 1992;65(2):329-42.

104 Li Y, Wang MJ, Zhang T, Zhang F, Fu X. Study on Dispersion Morphology of Silica in Rubber. Rubber Chemistry and Technology. 1994;67(4):693-9.

105 Wang M-J, Wolff S. Filler-elastomer interactions. Part V. Investigation of the surface energies of silane-modified silicas. Rubber Chemistry and Technology. 1992;65(4):715-35.

106 Hasse A, Luginsland HD. Reinforcement of silica-filled EPM compounds using vinylsilanes. KGK-Kautschuk und Gummi Kunststoffe. 2002;55(5):294-9.

107 Pattanawanidchai S, Saeoui P, Sirisinha C. Influence of precipitated silica on dynamic mechanical properties and resistance to oil and thermal aging in CPE/NR blends. Journal of Applied Polymer Science. 2005;96(6):2218-24.

108 Futamura S, Engelhardt ML. Determining characteristics. European Rubber Journal. 1986;168(9).

109 Nordsiek KH. The "integral rubber" concept–an approach to an ideal tire tread rubber. Kautschuk und Gummi, Kunststoffe. 1985;38(3):178-85.

110 Choi S-S. Improvement of properties of silica-filled styrene-butadiene rubber compounds using acrylonitrile-butadiene rubber. Journal of Applied Polymer Science. 2001;79(6):1127-33.

111 Ye X, Tian M, Zhang L-Q. Some interesting phenomena in silica-filled HNBR with the addition of silane coupling agent. Journal of Applied Polymer Science. 2012;124(2):927-34.

112 Gent AN. On the relation between indentation hardness and young's modulus. Transactions of the Institute of the Rubber Industry. 1958;34(2):46-57.

113 Rattanasom N, Saowapark T, Deeprasertkul C. Reinforcement of natural rubber with silica/carbon black hybrid filler. Polymer Testing. 2007;26(3):369-77.

114 Choudhury A, Bhowmick AK, Soddemann M. Effect of organo-modified clay on accelerated aging resistance of hydrogenated nitrile rubber nanocomposites and their life time prediction. Polymer Degradation and Stability. 2010;95(12):2555-62.

115 Samadi A, Razzaghi Kashani M. Effects of organo-clay modifier on physical–mechanical properties of butyl-based rubber nano-composites. Journal of Applied Polymer Science. 2010;116(4):2101-9.

116 Leblanc JL, Putman M, Pianhanuruk E. A thorough study on the relationships between dispersion quality and viscoelastic properties in carbon black filled SBR compounds. Journal of Applied Polymer Science. 2011;121(2):1096-117.

117 Lan T, Kaviratna PD, Pinnavaia TJ. Mechanism of Clay Tactoid Exfoliation in Epoxy-Clay Nanocomposites. Chemistry of Materials. 1995 1995/11/01;7(11):2144-50.

118 Zilg C, Thomann R, Finter J, Mülhaupt R. The influence of silicate modification and compatibilizers on mechanical properties and morphology of anhydride-cured epoxy nanocomposites. Macromolecular Materials and Engineering. 2000;280-281(1):41-6.

119 Fornes TD, Hunter DL, Paul DR. Nylon-6 Nanocomposites from Alkylammonium-Modified Clay: The Role of Alkyl Tails on Exfoliation. Macromolecules. 2004 2004/03/01;37(5):1793-8.

120 Ganter M, Gronski W, Reichert P, Mülhaupt R. Rubber Nanocomposites: Morphology and Mechanical Properties of BR and SBR Vulcanizates Reinforced by Organophilic Layered Silicates. Rubber Chemistry and Technology. 2001 2001/05/01;74(2):221-35.

121 Rooj S, Das A, Thakur V, Mahaling RN, Bhowmick AK, Heinrich G. Preparation and properties of natural nanocomposites based on natural rubber and naturally occurring halloysite nanotubes. Materials & Design. 2010;31(4):2151-6.

122 Houwink R, Decker HKd, editors. Elasticity, plasticity and structure of matter. 3 rd ed. New York: Cambridge University Press; 2009.

123 Jin J, Chen L, Song M, Yao K. An analysis on enhancement of fatigue durability of polyurethane by incorporating organoclay nanofillers. Macromolecular Materials and Engineering. 2006;291(11):1414-21.

124 Sengupta R, Chakraborty S, Bandyopadhyay S, Dasgupta S, Mukhopadhyay R, Auddy K, et al. A short review on rubber/clay nanocomposites with emphasis on mechanical properties. Polymer Engineering & Science. 2007;47(11):1956-74.

125 Ahankari SS, Kar KK. Hysteresis measurements and dynamic mechanical characterization of functionally graded natural rubber–carbon black composites. Polymer Engineering & Science. 2010;50(5):871-7.

126 Wang M-J, Zhang P, Mahmud K. Carbon-silica dual phase filler, a new generation reinforcing agent for rubber: Part IX. Application to truck tire tread compound. Rubber Chemistry and Technology. 2001 2001/03/01;74(1):124-37.

127 ASTM Standard D 1765-03. Standard classification system for carbon blacks used in rubber products. West Conshohocken, PA: ASTM International; 2003.

128 Heinrich G, Klüppel M, Vilgis TA. Reinforcement of elastomers. Current Opinion in Solid State and Materials Science. 2002;6(3):195-203.

129 Soltani S, Sourki FA. Effect of carbon black type on viscous heating, heat build-up, and relaxation behaviour of SBR compounds. Iranian Polymer Journal (English Edition). 2005;14(8):745-51.

130 Luo W, Hu X, Wang C, Li Q. Frequency- and strain-amplitude-dependent dynamical mechanical properties and hysteresis loss of CB-filled vulcanized natural rubber. International Journal of Mechanical Sciences. 2010;52(2):168-74.

APPENDICES

APPENDIX A
INFLUENCES OF CARBON BLACK LOADING AND CHARACTERISTICS ON REINFORCEMENT OF HYDROGENATED NITRILE RUBBER

Table A1 Scorch time (t_{s2}), cure time (t_c), and torque difference ($\Delta S'$) of HNBR filled with various CB characteristics and loadings

CB type	CB loading (phr)	Scorch time (min)	Cure time (min)	S'max-S'min (dN-m)
-	0	1.42 ± 0.03	74.54 ± 1.07	28.14 ± 0.19
N326	10	1.30 ± 0.03	74.73 ± 0.37	31.57 ± 0.72
	20	1.17 ± 0.01	73.94 ± 0.50	36.35 ± 0.09
	40	1.06 ± 0.01	71.94 ± 0.31	42.61 ± 0.71
	60	0.98 ± 0.03	69.22 ± 0.20	48.71 ± 1.21
N550	10	1.21 ± 0.15	74.06 ± 0.76	34.02 ± 0.18
	20	1.10 ± 0.06	73.93 ± 0.39	38.11 ± 0.55
	40	0.98 ± 0.05	72.14 ± 0.88	49.61 ± 0.60
	60	0.87 ± 0.04	69.86 ± 1.96	54.77 ± 3.21
N774	10	1.33 ± 0.03	74.25 ± 1.42	32.32 ± 1.91
	20	1.20 ± 0.02	74.07 ± 1.18	37.73 ± 0.81
	40	1.06 ± 0.03	72.65 ± 1.59	43.43 ± 2.91
	60	0.99 ± 0.02	71.44 ± 1.25	46.51 ± 2.84
N990	10	1.21 ± 0.15	75.23 ± 0.06	32.54 ± 0.80
	20	1.22 ± 0.03	75.83 ± 0.16	35.47 ± 0.20
	40	1.12 ± 0.02	75.48 ± 0.09	41.13 ± 0.44
	60	1.06 ± 0.04	75.69 ± 0.70	45.47 ± 0.77

Table A2 Complex modulus (G^*) result at 3.14 rad/s and 100°C as measured by the RPA-FT of HNBR compounds filled with various CB characteristics and loadings

CB type	CB loading (phr)	Test a				Test b			
		run 1		run 2		run 1		run 2	
		Strain (%)	G^* (kPa)	Strain (%)	G^* (kPa)	Strain (%)	G^* (kPa)	Strain (%)	G^* (kPa)
-	0	6.98	68.68	8.38	68.71	8.38	68.11	6.98	68.91
		12.57	67.64	19.55	66.90	19.55	66.26	12.57	67.66
		32.11	65.00	60.04	59.58	60.04	59.46	32.11	64.42
		97.74	53.43	167.55	43.87	167.55	43.85	97.74	52.85
		251.33	36.94	335.10	32.51	335.10	32.41	251.33	37.00
		418.88	29.16	481.71	26.86	481.71	26.97	418.88	28.93
		544.54	25.18	600.39	23.52	600.39	23.66	544.54	24.90
		656.24	22.38	712.09	21.08	712.09	21.13	656.24	22.19
		767.94	20.10	837.76	18.86	837.76	18.85	767.94	19.97
		893.61	18.00	949.46	17.32	949.46	17.19	893.61	17.94
N326	10	6.98	79.83	8.38	77.19	8.38	79.96	6.98	78.05
		12.57	77.91	19.55	73.94	19.55	77.04	12.57	75.84
		32.11	73.37	60.04	63.94	60.04	66.77	32.11	70.63
		97.74	58.14	167.55	46.39	167.55	47.67	97.74	56.12
		251.33	39.72	335.10	34.63	335.10	35.08	251.33	39.45
		418.88	31.31	481.71	28.67	481.71	29.05	418.88	30.98
		544.54	26.97	600.39	25.15	600.39	25.41	544.54	26.70
		656.24	23.93	712.09	22.51	712.09	22.68	656.24	23.74
		767.94	21.48	837.76	20.09	837.76	20.18	767.94	21.35
		893.61	19.23	949.46	18.36	949.46	18.38	893.61	19.17
	20	6.98	92.22	8.38	86.11	8.38	92.00	6.98	88.46
		12.57	89.58	19.55	81.04	19.55	87.00	12.57	84.49
		32.11	82.29	60.04	67.30	60.04	72.55	32.11	76.42
		97.74	62.43	167.55	48.21	167.55	50.39	97.74	58.50
		251.33	42.18	335.10	36.28	335.10	37.03	251.33	41.06
		418.88	33.14	481.71	30.11	481.71	30.67	418.88	32.46
		544.54	28.52	600.39	26.45	600.39	26.84	544.54	28.02
		656.24	25.27	712.09	23.67	712.09	23.95	656.24	24.93
		767.94	22.66	837.76	21.19	837.76	21.34	767.94	22.45
		893.61	20.36	949.46	19.37	949.46	19.48	893.61	20.17
	40	6.98	139.56	8.38	125.82	8.38	138.08	6.98	130.04
		12.57	129.51	19.55	110.65	19.55	122.13	12.57	118.76
		32.11	111.39	60.04	84.71	60.04	93.92	32.11	99.89
		97.74	77.88	167.55	58.35	167.55	62.07	97.74	71.54
		251.33	51.98	335.10	44.05	335.10	45.76	251.33	50.01
		418.88	40.75	481.71	36.57	481.71	37.62	418.88	39.48
		544.54	34.85	600.39	31.98	600.39	32.72	544.54	33.99
		656.24	30.81	712.09	28.58	712.09	29.14	656.24	30.18
		767.94	27.57	837.76	25.48	837.76	25.88	767.94	27.12
		893.61	24.62	949.46	23.19	949.46	23.42	893.61	24.33

Table A2 Complex modulus (G^*) result at 3.14 rad/s and 100°C as measured by the RPA-FT of HNBR compounds filled with various CB characteristics and loadings (cont.)

CB type	CB loading (phr)	Test a				Test b			
		run 1		run 2		run 1		run 2	
		Strain (%)	G^* (kPa)	Strain (%)	G^* (kPa)	Strain (%)	G^* (kPa)	Strain (%)	G^* (kPa)
N326	60	6.98	205.60	8.38	179.18	8.38	198.71	6.98	188.38
		12.57	178.34	19.55	146.35	19.55	161.19	12.57	163.54
		32.11	141.08	60.04	103.33	60.04	114.40	32.11	127.45
		97.74	92.21	167.55	69.48	167.55	73.26	97.74	85.54
		251.33	62.24	335.10	53.01	335.10	54.67	251.33	59.92
		418.88	48.62	481.71	43.80	481.71	44.62	418.88	47.35
		544.54	41.29	600.39	38.24	600.39	38.63	544.54	40.61
		656.24	36.42	712.09	34.03	712.09	34.33	656.24	35.96
		767.94	32.62	837.76	30.21	837.76	30.38	767.94	32.25
		893.61	28.98	949.46	27.65	949.46	27.79	893.61	28.78
N550	10	6.98	77.93	8.38	73.71	8.38	76.27	6.98	74.59
		12.57	75.78	19.55	70.89	19.55	73.94	12.57	72.66
		32.11	70.71	60.04	61.09	60.04	63.98	32.11	67.82
		97.74	55.67	167.55	44.39	167.55	45.54	97.74	53.79
		251.33	38.23	335.10	33.48	335.10	33.73	251.33	37.94
		418.88	30.24	481.71	27.84	481.71	28.07	418.88	30.01
		544.54	26.15	600.39	24.46	600.39	24.65	544.54	25.95
		656.24	23.23	712.09	21.93	712.09	22.05	656.24	23.14
		767.94	20.93	837.76	19.63	837.76	19.71	767.94	20.85
		893.61	18.82	949.46	18.00	949.46	18.00	893.61	18.77
	20	6.98	93.36	8.38	85.39	8.38	92.15	6.98	86.64
		12.57	90.20	19.55	81.74	19.55	87.95	12.57	84.12
		32.11	82.33	60.04	68.03	60.04	72.98	32.11	77.00
		97.74	61.43	167.55	48.10	167.55	50.14	97.74	58.87
		251.33	41.38	335.10	36.21	335.10	37.14	251.33	41.30
		418.88	32.76	481.71	30.18	481.71	30.88	418.88	32.79
		544.54	28.32	600.39	26.55	600.39	27.07	544.54	28.36
		656.24	25.23	712.09	23.85	712.09	24.21	656.24	25.29
		767.94	22.74	837.76	21.38	837.76	21.66	767.94	22.86
		893.61	20.52	949.46	19.57	949.46	19.80	893.61	20.63
	40	6.98	136.11	8.38	120.91	8.38	135.32	6.98	123.36
		12.57	129.02	19.55	110.15	19.55	122.64	12.57	116.00
		32.11	112.28	60.04	85.29	60.04	94.06	32.11	100.59
		97.74	78.12	167.55	59.54	167.55	62.60	97.74	72.34
		251.33	53.61	335.10	46.39	335.10	47.35	251.33	51.74
		418.88	42.55	481.71	39.09	481.71	39.32	418.88	41.78
		544.54	36.65	600.39	34.75	600.39	34.48	544.54	36.53
		656.24	32.60	712.09	31.42	712.09	30.85	656.24	32.83
		767.94	29.33	837.76	28.38	837.76	27.55	767.94	29.80
		893.61	26.29	949.46	26.16	949.46	25.01	893.61	27.05

Table A2 Complex modulus (G^*) result at 3.14 rad/s and 100°C as measured by the RPA-FT of HNBR compounds filled with various CB characteristics and loadings (cont.)

CB type	CB loading (phr)	Test a				Test b			
		run 1		run 2		run 1		run 2	
		Strain (%)	G^* (kPa)	Strain (%)	G^* (kPa)	Strain (%)	G^* (kPa)	Strain (%)	G^* (kPa)
N550	60	6.98	188.91	8.38	178.44	8.38	183.17	6.98	181.46
		12.57	174.79	19.55	159.23	19.55	157.77	12.57	168.97
		32.11	144.70	60.04	115.64	60.04	114.66	32.11	140.34
		97.74	96.61	167.55	78.64	167.55	75.98	97.74	95.05
		251.33	67.37	335.10	62.48	335.10	58.96	251.33	68.65
		418.88	53.86	481.71	53.55	481.71	49.15	418.88	56.52
		544.54	46.35	600.39	50.83	600.39	43.03	544.54	51.95
		656.24	41.08	712.09	53.21	712.09	38.31	656.24	52.30
		767.94	37.01	837.76	55.28	837.76	34.19	767.94	53.56
		893.61	33.50	949.46	57.29	949.46	31.33	893.61	53.20
N774	10	6.98	79.72	8.38	76.23	8.38	77.12	6.98	76.44
		12.57	77.84	19.55	73.18	19.55	74.70	12.57	74.60
		32.11	72.91	60.04	63.46	60.04	65.36	32.11	69.82
		97.74	57.56	167.55	46.01	167.55	46.72	97.74	55.51
		251.33	39.39	335.10	34.42	335.10	34.56	251.33	39.00
		418.88	31.10	481.71	28.51	481.71	28.72	418.88	30.69
		544.54	26.81	600.39	24.96	600.39	25.17	544.54	26.45
		656.24	23.80	712.09	22.33	712.09	22.45	656.24	23.53
		767.94	21.34	837.76	19.96	837.76	19.99	767.94	21.18
		893.61	19.13	949.46	18.15	949.46	18.15	893.61	19.00
	20	6.98	92.01	8.38	85.59	8.38	91.47	6.98	86.96
		12.57	89.23	19.55	81.86	19.55	87.06	12.57	84.62
		32.11	81.83	60.04	68.81	60.04	72.88	32.11	77.85
		97.74	62.19	167.55	49.14	167.55	50.79	97.74	59.89
		251.33	42.41	335.10	37.06	335.10	37.66	251.33	42.17
		418.88	33.53	481.71	30.85	481.71	31.26	418.88	33.35
		544.54	28.98	600.39	27.09	600.39	27.40	544.54	28.84
		656.24	25.80	712.09	24.30	712.09	24.49	656.24	25.69
		767.94	23.21	837.76	21.78	837.76	21.85	767.94	23.16
		893.61	20.86	949.46	19.96	949.46	19.90	893.61	20.86
	40	6.98	116.07	8.38	104.71	8.38	115.81	6.98	106.09
		12.57	111.07	19.55	96.83	19.55	107.74	12.57	101.01
		32.11	98.70	60.04	76.70	60.04	85.20	32.11	89.32
		97.74	70.31	167.55	53.47	167.55	56.81	97.74	65.39
		251.33	47.41	335.10	40.84	335.10	42.09	251.33	46.12
		418.88	37.46	481.71	34.17	481.71	34.84	418.88	36.81
		544.54	32.28	600.39	30.06	600.39	30.51	544.54	31.91
		656.24	28.75	712.09	27.00	712.09	27.33	656.24	28.50
		767.94	25.89	837.76	24.19	837.76	24.41	767.94	25.70
		893.61	23.23	949.46	22.02	949.46	22.15	893.61	23.10

Table A2 Complex modulus (G^*) result at 3.14 rad/s and 100°C as measured by the RPA-FT of HNBR compounds filled with various CB characteristics and loadings (cont.)

CB type	CB loading (phr)	Test a				Test b			
		run 1		run 2		run 1		run 2	
		Strain (%)	G^* (kPa)	Strain (%)	G^* (kPa)	Strain (%)	G^* (kPa)	Strain (%)	G^* (kPa)
N774	60	6.98	159.33	8.38	141.27	8.38	158.02	6.98	144.90
		12.57	149.04	19.55	126.38	19.55	140.58	12.57	135.04
		32.11	126.83	60.04	94.49	60.04	104.38	32.11	114.79
		97.74	85.41	167.55	64.70	167.55	67.91	97.74	79.91
		251.33	58.35	335.10	50.23	335.10	51.67	251.33	56.37
		418.88	46.40	481.71	42.28	481.71	42.92	418.88	45.48
		544.54	39.95	600.39	37.49	600.39	37.64	544.54	39.74
		656.24	35.49	712.09	33.79	712.09	33.61	656.24	35.66
		767.94	31.85	837.76	30.35	837.76	29.75	767.94	32.36
		893.61	28.37	949.46	28.19	949.46	27.12	893.61	29.32
N990	10	6.98	73.77	8.38	70.15	8.38	72.63	6.98	70.84
		12.57	72.47	19.55	68.23	19.55	71.02	12.57	69.66
		32.11	68.51	60.04	59.91	60.04	62.47	32.11	65.73
		97.74	54.74	167.55	43.64	167.55	44.80	97.74	52.81
		251.33	37.37	335.10	32.56	335.10	32.96	251.33	37.02
		418.88	29.40	481.71	27.07	481.71	27.35	418.88	29.15
		544.54	25.40	600.39	23.76	600.39	23.97	544.54	25.20
		656.24	22.63	712.09	21.31	712.09	21.48	656.24	22.48
		767.94	20.35	837.76	19.10	837.76	19.19	767.94	20.27
		893.61	18.31	949.46	17.49	949.46	17.47	893.61	18.25
	20	6.98	82.65	8.38	76.78	8.38	81.27	6.98	77.96
		12.57	80.45	19.55	73.49	19.55	78.06	12.57	75.60
		32.11	75.15	60.04	62.87	60.04	66.93	32.11	70.40
		97.74	58.05	167.55	45.19	167.55	46.90	97.74	55.27
		251.33	39.29	335.10	33.88	335.10	34.46	251.33	38.62
		418.88	30.83	481.71	28.23	481.71	28.56	418.88	30.45
		544.54	26.61	600.39	24.84	600.39	25.04	544.54	26.36
		656.24	23.67	712.09	22.26	712.09	22.40	656.24	23.50
		767.94	21.31	837.76	19.92	837.76	19.89	767.94	21.19
		893.61	19.07	949.46	18.13	949.46	18.11	893.61	18.98
	40	6.98	104.84	8.38	95.63	8.38	104.43	6.98	96.32
		12.57	101.70	19.55	90.30	19.55	98.86	12.57	93.12
		32.11	92.29	60.04	73.66	60.04	80.25	32.11	84.34
		97.74	67.37	167.55	51.62	167.55	53.94	97.74	63.14
		251.33	44.87	335.10	38.54	335.10	39.21	251.33	43.59
		418.88	35.10	481.71	32.17	481.71	32.47	418.88	34.47
		544.54	30.27	600.39	28.35	600.39	28.49	544.54	29.91
		656.24	26.95	712.09	25.40	712.09	25.48	656.24	26.71
		767.94	24.29	837.76	22.74	837.76	22.83	767.94	24.10
		893.61	21.76	949.46	20.81	949.46	20.76	893.61	21.64

Table A2 Complex modulus (G^*) result at 3.14 rad/s and 100°C as measured by the RPA-FT of HNBR compounds filled with various CB characteristics and loadings (cont.)

CB type	CB loading (phr)	Test a				Test b			
		run 1		run 2		run 1		run 2	
		Strain (%)	G^* (kPa)	Strain (%)	G^* (kPa)	Strain (%)	G^* (kPa)	Strain (%)	G^* (kPa)
N990	60	6.98	126.26	8.38	115.62	8.38	126.67	6.98	117.91
		12.57	120.93	19.55	107.10	19.55	116.68	12.57	112.74
		32.11	106.11	60.04	83.28	60.04	89.85	32.11	98.62
		97.74	73.62	167.55	56.93	167.55	58.67	97.74	70.67
		251.33	48.53	335.10	42.35	335.10	42.72	251.33	48.17
		418.88	38.29	481.71	35.46	481.71	35.61	418.88	38.14
		544.54	33.26	600.39	31.26	600.39	31.38	544.54	33.14
		656.24	29.73	712.09	28.08	712.09	28.22	656.24	29.64
		767.94	26.86	837.76	25.15	837.76	25.21	767.94	26.76
		893.61	24.12	949.46	23.11	949.46	23.23	893.61	24.04

Table A3 Fit parameters of Equation 3.16 of HNBR compounds filled with various CB characteristics and loadings

CB type	CB loading (phr)	G_0^* (kPa)	1/A (%)	B
-	0	69.86	241.6	1.137
N326	10	82.42	209.0	1.042
	20	96.87	171.3	0.954
	40	161.70	95.7	0.717
	60	359.40	16.7	0.458
N550	10	79.96	202.6	1.019
	20	97.74	157.9	0.968
	40	153.30	102.4	0.788
	60	239.90	56.8	0.634
N774	10	81.27	210.9	1.029
	20	96.53	173.1	0.949
	40	125.50	123.3	0.892
	60	185.10	79.8	0.760
N990	10	75.27	211.9	1.111
	20	85.11	187.2	1.029
	40	110.50	141.5	0.988
	60	137.00	104.5	0.934

Table A4 Total torque harmonic content (TTHC) result at 3.14 rad/s and 100°C as measured by the RPA-FT of HNBR compounds filled with various CB characteristics and loadings

CB type	CB loading (phr)	Test a				Test b			
		run 1		run 2		run 1		run 2	
		Strain (%)	TTHC (%)	Strain (%)	TTHC (%)	Strain (%)	TTHC (%)	Strain (%)	TTHC (%)
-	0	6.98	0.00	8.38	0.00	8.38	0.53	6.98	0.00
		12.57	0.00	19.55	0.15	19.55	0.79	12.57	0.00
		32.11	0.83	60.04	0.90	60.04	0.97	32.11	0.67
		97.74	2.03	167.55	4.36	167.55	4.45	97.74	2.01
		251.33	7.07	335.10	8.99	335.10	9.03	251.33	6.85
		418.88	10.89	481.71	12.05	481.71	12.00	418.88	10.78
		544.54	13.02	600.39	13.75	600.39	13.70	544.54	13.11
		656.24	14.47	712.09	15.52	712.09	15.29	656.24	14.72
		767.94	15.99	837.76	17.03	837.76	16.70	767.94	16.17
		893.61	17.38	949.46	18.33	949.46	18.13	893.61	17.54
N326	10	6.98	0.00	8.38	0.00	8.38	0.64	6.98	0.00
		12.57	0.00	19.55	0.00	19.55	0.08	12.57	0.00
		32.11	0.52	60.04	1.07	60.04	1.07	32.11	0.79
		97.74	2.29	167.55	4.70	167.55	4.87	97.74	2.28
		251.33	7.47	335.10	9.36	335.10	9.59	251.33	7.23
		418.88	11.32	481.71	12.38	481.71	12.46	418.88	11.18
		544.54	13.43	600.39	14.16	600.39	14.07	544.54	13.33
		656.24	14.77	712.09	15.75	712.09	15.56	656.24	14.92
		767.94	16.29	837.76	17.17	837.76	17.05	767.94	16.41
		893.61	17.68	949.46	18.50	949.46	18.37	893.61	17.83
	20	6.98	0.00	8.38	0.00	8.38	0.08	6.98	0.00
		12.57	0.00	19.55	0.24	19.55	0.54	12.57	0.10
		32.11	0.64	60.04	1.32	60.04	1.25	32.11	1.09
		97.74	2.51	167.55	5.05	167.55	5.46	97.74	2.41
		251.33	7.97	335.10	9.90	335.10	10.19	251.33	7.61
		418.88	11.74	481.71	12.71	481.71	12.76	418.88	11.72
		544.54	13.64	600.39	14.30	600.39	14.36	544.54	13.75
		656.24	15.01	712.09	15.95	712.09	15.89	656.24	15.20
		767.94	16.40	837.76	17.40	837.76	17.40	767.94	16.57
		893.61	17.85	949.46	18.71	949.46	18.68	893.61	17.99
	40	6.98	0.00	8.38	0.00	8.38	0.00	6.98	0.00
		12.57	0.00	19.55	0.00	19.55	0.00	12.57	0.00
		32.11	0.44	60.04	0.91	60.04	0.84	32.11	0.63
		97.74	3.18	167.55	5.94	167.55	6.35	97.74	2.75
		251.33	9.14	335.10	11.00	335.10	11.26	251.33	8.81
		418.88	12.86	481.71	13.46	481.71	13.73	418.88	12.54
		544.54	14.70	600.39	15.04	600.39	15.12	544.54	14.40
		656.24	15.85	712.09	16.57	712.09	16.63	656.24	15.89
		767.94	17.30	837.76	18.02	837.76	18.14	767.94	17.20
		893.61	18.63	949.46	19.33	949.46	19.40	893.61	18.55

Table A4 Total torque harmonic content (TTHC) result at 3.14 rad/s and 100°C as measured by the RPA-FT of HNBR compounds filled with various CB characteristics and loadings (cont.)

CB type	CB loading (phr)	Test a				Test b			
		run 1		run 2		run 1		run 2	
		Strain (%)	TTHC (%)	Strain (%)	TTHC (%)	Strain (%)	TTHC (%)	Strain (%)	TTHC (%)
N326	60	6.98	0.00	8.38	0.00	8.38	0.00	6.98	0.00
		12.57	0.17	19.55	0.00	19.55	0.56	12.57	0.00
		32.11	1.45	60.04	1.62	60.04	1.71	32.11	0.39
		97.74	4.24	167.55	7.20	167.55	7.81	97.74	3.85
		251.33	10.60	335.10	12.07	335.10	12.46	251.33	10.22
		418.88	13.93	481.71	14.34	481.71	14.83	418.88	13.46
		544.54	15.83	600.39	15.98	600.39	16.31	544.54	15.37
		656.24	17.01	712.09	17.54	712.09	17.77	656.24	16.83
		767.94	18.36	837.76	18.95	837.76	19.23	767.94	18.25
		893.61	19.60	949.46	20.52	949.46	20.63	893.61	19.66
N550	10	6.98	0.00	8.38	0.00	8.38	0.00	6.98	0.00
		12.57	0.14	19.55	0.56	19.55	0.00	12.57	0.00
		32.11	0.95	60.04	1.30	60.04	1.36	32.11	0.51
		97.74	2.54	167.55	4.78	167.55	4.90	97.74	2.50
		251.33	7.57	335.10	9.39	335.10	9.54	251.33	7.44
		418.88	11.31	481.71	12.34	481.71	12.34	418.88	11.34
		544.54	13.19	600.39	14.14	600.39	13.92	544.54	13.36
		656.24	14.65	712.09	15.72	712.09	15.50	656.24	14.96
		767.94	16.14	837.76	17.30	837.76	17.21	767.94	16.34
		893.61	17.63	949.46	18.62	949.46	18.47	893.61	17.81
	20	6.98	0.00	8.38	0.00	8.38	0.00	6.98	0.00
		12.57	0.00	19.55	0.00	19.55	0.06	12.57	0.00
		32.11	0.05	60.04	1.25	60.04	1.14	32.11	0.98
		97.74	2.91	167.55	5.13	167.55	5.38	97.74	2.54
		251.33	8.26	335.10	9.98	335.10	10.25	251.33	7.97
		418.88	11.80	481.71	12.76	481.71	12.90	418.88	11.86
		544.54	13.70	600.39	14.52	600.39	14.34	544.54	13.81
		656.24	15.16	712.09	16.08	712.09	16.00	656.24	15.26
		767.94	16.65	837.76	17.61	837.76	17.56	767.94	16.84
		893.61	18.05	949.46	19.03	949.46	18.86	893.61	18.25
	40	6.98	0.00	8.38	0.00	8.38	0.00	6.98	0.00
		12.57	0.17	19.55	0.24	19.55	0.11	12.57	0.33
		32.11	0.68	60.04	1.61	60.04	1.61	32.11	0.90
		97.74	3.73	167.55	6.67	167.55	7.18	97.74	3.62
		251.33	9.80	335.10	11.39	335.10	11.57	251.33	9.44
		418.88	12.91	481.71	13.72	481.71	13.69	418.88	12.87
		544.54	14.56	600.39	15.49	600.39	15.09	544.54	14.72
		656.24	15.97	712.09	17.17	712.09	16.71	656.24	16.34
		767.94	17.33	837.76	18.63	837.76	18.29	767.94	17.78
		893.61	18.71	949.46	20.10	949.46	19.57	893.61	19.27

Table A4 Total torque harmonic content (TTHC) result at 3.14 rad/s and 100°C as measured by the RPA-FT of HNBR compounds filled with various CB characteristics and loadings (cont.)

CB type	CB loading (phr)	Test a				Test b			
		run 1		run 2		run 1		run 2	
		Strain (%)	TTHC (%)	Strain (%)	TTHC (%)	Strain (%)	TTHC (%)	Strain (%)	TTHC (%)
N550	60	6.98	0.00	8.38	0.00	8.38	1.21	6.98	0.00
		12.57	0.00	19.55	0.00	19.55	0.61	12.57	0.00
		32.11	0.53	60.04	1.99	60.04	2.34	32.11	0.00
		97.74	4.61	167.55	7.77	167.55	8.01	97.74	4.39
		251.33	10.78	335.10	12.22	335.10	12.11	251.33	10.93
		418.88	13.35	481.71	14.60	481.71	14.16	418.88	13.84
		544.54	14.93	600.39	16.62	600.39	15.65	544.54	16.03
		656.24	16.51	712.09	19.45	712.09	17.17	656.24	18.75
		767.94	18.00	837.76	22.26	837.76	18.82	767.94	21.38
		893.61	19.61	949.46	25.38	949.46	20.44	893.61	24.07
N774	10	6.98	0.00	8.38	0.48	8.38	0.05	6.98	0.00
		12.57	0.00	19.55	0.27	19.55	0.22	12.57	0.02
		32.11	0.64	60.04	1.17	60.04	1.13	32.11	0.87
		97.74	2.58	167.55	4.87	167.55	5.04	97.74	2.38
		251.33	7.75	335.10	9.43	335.10	9.64	251.33	7.44
		418.88	11.46	481.71	12.51	481.71	12.52	418.88	11.36
		544.54	13.57	600.39	14.35	600.39	14.20	544.54	13.56
		656.24	14.97	712.09	15.96	712.09	15.78	656.24	15.07
		767.94	16.44	837.76	17.47	837.76	17.29	767.94	16.63
		893.61	17.87	949.46	18.76	949.46	18.66	893.61	18.06
	20	6.98	0.00	8.38	0.00	8.38	0.14	6.98	0.00
		12.57	0.00	19.55	1.05	19.55	0.61	12.57	0.00
		32.11	1.32	60.04	1.69	60.04	1.92	32.11	1.17
		97.74	3.12	167.55	5.45	167.55	5.91	97.74	3.20
		251.33	8.61	335.10	10.15	335.10	10.42	251.33	8.22
		418.88	12.07	481.71	13.08	481.71	13.15	418.88	12.20
		544.54	13.96	600.39	14.72	600.39	14.83	544.54	14.18
		656.24	15.39	712.09	16.39	712.09	16.37	656.24	15.69
		767.94	16.97	837.76	18.05	837.76	17.93	767.94	17.25
		893.61	18.30	949.46	19.38	949.46	19.27	893.61	18.61
	40	6.98	0.00	8.38	0.04	8.38	0.00	6.98	0.00
		12.57	0.00	19.55	0.90	19.55	0.00	12.57	0.00
		32.11	1.24	60.04	2.05	60.04	2.17	32.11	1.22
		97.74	4.19	167.55	6.36	167.55	6.81	97.74	3.89
		251.33	9.75	335.10	11.27	335.10	11.61	251.33	9.16
		418.88	13.17	481.71	13.98	481.71	14.10	418.88	12.97
		544.54	14.90	600.39	15.67	600.39	15.48	544.54	14.85
		656.24	16.29	712.09	17.15	712.09	16.98	656.24	16.32
		767.94	17.74	837.76	18.62	837.76	18.60	767.94	17.81
		893.61	19.04	949.46	19.97	949.46	19.84	893.61	19.15

Table A4 Total torque harmonic content (TTHC) result at 3.14 rad/s and 100°C as measured by the RPA-FT of HNBR compounds filled with various CB characteristics and loadings (cont.)

CB type	CB loading (phr)	Test a				Test b			
		run 1		run 2		run 1		run 2	
		Strain (%)	TTHC (%)	Strain (%)	TTHC (%)	Strain (%)	TTHC (%)	Strain (%)	TTHC (%)
N774	60	6.98	0.00	8.38	0.00	8.38	0.00	6.98	0.32
		12.57	0.00	19.55	0.63	19.55	0.63	12.57	0.32
		32.11	1.01	60.04	2.53	60.04	2.43	32.11	1.26
		97.74	4.98	167.55	7.50	167.55	7.91	97.74	4.50
		251.33	10.99	335.10	12.32	335.10	12.50	251.33	10.50
		418.88	13.97	481.71	14.70	481.71	14.63	418.88	13.92
		544.54	15.59	600.39	16.34	600.39	16.16	544.54	15.66
		656.24	16.94	712.09	17.94	712.09	17.68	656.24	17.17
		767.94	18.47	837.76	19.48	837.76	19.19	767.94	18.68
		893.61	19.77	949.46	20.96	949.46	20.63	893.61	20.15
N990	10	6.98	0.00	8.38	0.00	8.38	0.00	6.98	0.00
		12.57	0.00	19.55	0.03	19.55	0.00	12.57	0.00
		32.11	0.00	60.04	0.95	60.04	0.79	32.11	0.00
		97.74	2.19	167.55	4.22	167.55	4.40	97.74	2.22
		251.33	7.26	335.10	8.86	335.10	9.24	251.33	6.89
		418.88	11.08	481.71	11.93	481.71	12.06	418.88	10.86
		544.54	13.03	600.39	13.89	600.39	13.78	544.54	12.99
		656.24	14.50	712.09	15.53	712.09	15.32	656.24	14.62
		767.94	16.07	837.76	17.18	837.76	16.99	767.94	16.11
		893.61	17.41	949.46	18.39	949.46	18.29	893.61	17.54
	20	6.98	0.00	8.38	0.00	8.38	0.00	6.98	0.00
		12.57	0.32	19.55	0.89	19.55	0.55	12.57	0.04
		32.11	1.01	60.04	1.71	60.04	1.79	32.11	0.67
		97.74	3.25	167.55	5.31	167.55	5.62	97.74	3.12
		251.33	8.53	335.10	10.04	335.10	10.64	251.33	7.98
		418.88	12.09	481.71	12.98	481.71	13.29	418.88	11.88
		544.54	14.00	600.39	14.72	600.39	14.95	544.54	13.92
		656.24	15.50	712.09	16.34	712.09	16.32	656.24	15.54
		767.94	16.99	837.76	17.98	837.76	17.84	767.94	16.99
		893.61	18.29	949.46	19.24	949.46	19.32	893.61	18.29
	40	6.98	0.00	8.38	0.47	8.38	0.17	6.98	0.00
		12.57	0.00	19.55	0.37	19.55	0.32	12.57	0.00
		32.11	0.57	60.04	1.69	60.04	1.81	32.11	0.91
		97.74	3.79	167.55	6.15	167.55	6.43	97.74	3.45
		251.33	9.40	335.10	10.91	335.10	11.35	251.33	8.88
		418.88	13.05	481.71	13.76	481.71	13.97	418.88	12.78
		544.54	14.99	600.39	15.67	600.39	15.63	544.54	14.78
		656.24	16.45	712.09	17.30	712.09	17.24	656.24	16.46
		767.94	18.07	837.76	18.93	837.76	19.02	767.94	18.04
		893.61	19.36	949.46	20.16	949.46	20.19	893.61	19.41

Table A4 Total torque harmonic content (TTHC) result at 3.14 rad/s and 100°C as measured by the RPA-FT of HNBR compounds filled with various CB characteristics and loadings (cont.)

CB type	CB loading (phr)	Test a				Test b			
		run 1		run 2		run 1		run 2	
		Strain (%)	TTHC (%)	Strain (%)	TTHC (%)	Strain (%)	TTHC (%)	Strain (%)	TTHC (%)
N990	60	6.98	0.00	8.38	0.00	8.38	0.00	6.98	0.00
		12.57	0.00	19.55	0.26	19.55	0.00	12.57	0.00
		32.11	0.85	60.04	1.77	60.04	1.94	32.11	0.51
		97.74	4.38	167.55	6.86	167.55	7.24	97.74	3.97
		251.33	10.35	335.10	11.72	335.10	12.05	251.33	9.74
		418.88	13.86	481.71	14.52	481.71	14.71	418.88	13.67
		544.54	15.78	600.39	16.55	600.39	16.60	544.54	15.68
		656.24	17.41	712.09	18.19	712.09	18.16	656.24	17.47
		767.94	18.88	837.76	19.73	837.76	19.67	767.94	18.90
		893.61	20.22	949.46	21.05	949.46	21.04	893.61	20.18

Table A5 3rd relative torque harmonic (T(3/1)) result at 3.14 rad/s and 100°C as measured by the RPA-FT of HNBR compounds filled with various CB characteristics and loadings

CB type	CB loading (phr)	Test a				Test b			
		run 1		run 2		run 1		run 2	
		Strain (%)	T(3/1) (%)	Strain (%)	T(3/1) (%)	Strain (%)	T(3/1) (%)	Strain (%)	T(3/1) (%)
-	0	6.98	0.11	8.38	0.00	8.38	0.00	6.98	0.00
		12.57	0.00	19.55	0.00	19.55	0.00	12.57	0.00
		32.11	0.00	60.04	0.01	60.04	0.00	32.11	0.00
		97.74	0.92	167.55	2.96	167.55	2.97	97.74	0.97
		251.33	5.24	335.10	6.88	335.10	6.88	251.33	5.13
		418.88	8.20	481.71	9.04	481.71	8.95	418.88	8.21
		544.54	9.56	600.39	10.12	600.39	9.97	544.54	9.62
		656.24	10.36	712.09	10.94	712.09	10.72	656.24	10.51
		767.94	11.13	837.76	11.72	837.76	11.50	767.94	11.27
		893.61	11.83	949.46	12.34	949.46	12.14	893.61	11.98

Table A5 3rd relative torque harmonic (T(3/1)) result at 3.14 rad/s and 100°C as measured by the RPA-FT of HNBR compounds filled with various CB characteristics and loadings (cont.)

CB type	CB loading (phr)	Test a				Test b			
		run 1		run 2		run 1		run 2	
		Strain (%)	T(3/1) (%)	Strain (%)	T(3/1) (%)	Strain (%)	T(3/1) (%)	Strain (%)	T(3/1) (%)
N326	10	6.98	0.00	8.38	0.00	8.38	0.00	6.98	0.05
		12.57	0.00	19.55	0.00	19.55	0.00	12.57	0.00
		32.11	0.00	60.04	0.19	60.04	0.08	32.11	0.00
		97.74	1.16	167.55	3.22	167.55	3.32	97.74	1.21
		251.33	5.60	335.10	7.17	335.10	7.28	251.33	5.39
		418.88	8.56	481.71	9.29	481.71	9.28	418.88	8.50
		544.54	9.86	600.39	10.32	600.39	10.21	544.54	9.83
		656.24	10.60	712.09	11.09	712.09	10.92	656.24	10.65
		767.94	11.29	837.76	11.80	837.76	11.65	767.94	11.35
		893.61	11.95	949.46	12.36	949.46	12.22	893.61	12.02
	20	6.98	0.00	8.38	0.00	8.38	0.00	6.98	0.27
		12.57	0.00	19.55	0.00	19.55	0.00	12.57	0.08
		32.11	0.00	60.04	0.40	60.04	0.32	32.11	0.10
		97.74	1.43	167.55	3.55	167.55	3.78	97.74	1.41
		251.33	5.96	335.10	7.45	335.10	7.63	251.33	5.67
		418.88	8.80	481.71	9.45	481.71	9.48	418.88	8.79
		544.54	10.02	600.39	10.43	600.39	10.39	544.54	10.09
		656.24	10.72	712.09	11.11	712.09	11.08	656.24	10.82
		767.94	11.37	837.76	11.85	837.76	11.76	767.94	11.49
		893.61	12.01	949.46	12.45	949.46	12.37	893.61	12.15
	40	6.98	0.00	8.38	0.00	8.38	0.00	6.98	0.00
		12.57	0.00	19.55	0.00	19.55	0.00	12.57	0.00
		32.11	0.00	60.04	0.40	60.04	0.40	32.11	0.03
		97.74	2.13	167.55	4.35	167.55	4.77	97.74	1.98
		251.33	7.10	335.10	8.44	335.10	8.63	251.33	6.70
		418.88	9.75	481.71	10.16	481.71	10.26	418.88	9.59
		544.54	10.75	600.39	10.97	600.39	11.02	544.54	10.61
		656.24	11.31	712.09	11.59	712.09	11.58	656.24	11.27
		767.94	11.90	837.76	12.26	837.76	12.25	767.94	11.90
		893.61	12.49	949.46	12.82	949.46	12.78	893.61	12.55
	60	6.98	0.00	8.38	0.00	8.38	0.00	6.98	0.00
		12.57	0.00	19.55	0.00	19.55	0.00	12.57	0.00
		32.11	0.24	60.04	1.22	60.04	1.23	32.11	0.05
		97.74	3.57	167.55	5.91	167.55	6.36	97.74	3.27
		251.33	8.47	335.10	9.52	335.10	9.75	251.33	8.11
		418.88	10.62	481.71	10.80	481.71	11.04	418.88	10.37
		544.54	11.44	600.39	11.56	600.39	11.75	544.54	11.23
		656.24	11.98	712.09	12.18	712.09	12.29	656.24	11.89
		767.94	12.56	837.76	12.90	837.76	12.94	767.94	12.54
		893.61	13.16	949.46	13.56	949.46	13.54	893.61	13.26

Table A5 3rd relative torque harmonic (T(3/1)) result at 3.14 rad/s and 100°C as measured by the RPA-FT of HNBR compounds filled with various CB characteristics and loadings (cont.)

CB type	CB loading (phr)	Test a				Test b			
		run 1		run 2		run 1		run 2	
		Strain (%)	T(3/1) (%)	Strain (%)	T(3/1) (%)	Strain (%)	T(3/1) (%)	Strain (%)	T(3/1) (%)
N550	10	6.98	0.00	8.38	0.00	8.38	0.00	6.98	0.00
		12.57	0.00	19.55	0.00	19.55	0.00	12.57	0.14
		32.11	0.00	60.04	0.57	60.04	0.49	32.11	0.11
		97.74	1.34	167.55	3.39	167.55	3.49	97.74	1.45
		251.33	5.63	335.10	7.20	335.10	7.23	251.33	5.61
		418.88	8.46	481.71	9.22	481.71	9.18	418.88	8.57
		544.54	9.68	600.39	10.27	600.39	10.16	544.54	9.87
		656.24	10.50	712.09	11.06	712.09	10.93	656.24	10.72
		767.94	11.27	837.76	11.81	837.76	11.66	767.94	11.44
		893.61	11.96	949.46	12.41	949.46	12.28	893.61	12.11
	20	6.98	0.00	8.38	0.00	8.38	0.00	6.98	0.00
		12.57	0.00	19.55	0.00	19.55	0.00	12.57	0.00
		32.11	0.00	60.04	0.42	60.04	0.35	32.11	0.00
		97.74	1.77	167.55	3.79	167.55	3.93	97.74	1.66
		251.33	6.26	335.10	7.58	335.10	7.71	251.33	5.99
		418.88	8.89	481.71	9.48	481.71	9.49	418.88	8.88
		544.54	10.01	600.39	10.46	600.39	10.41	544.54	10.08
		656.24	10.77	712.09	11.18	712.09	11.08	656.24	10.88
		767.94	11.43	837.76	11.88	837.76	11.80	767.94	11.57
		893.61	12.10	949.46	12.49	949.46	12.39	893.61	12.24
	40	6.98	0.00	8.38	0.00	8.38	0.00	6.98	0.20
		12.57	0.00	19.55	0.00	19.55	0.00	12.57	0.01
		32.11	0.00	60.04	0.72	60.04	0.66	32.11	0.24
		97.74	2.62	167.55	4.85	167.55	5.16	97.74	2.40
		251.33	7.27	335.10	8.59	335.10	8.56	251.33	7.02
		418.88	9.52	481.71	10.03	481.71	9.94	418.88	9.53
		544.54	10.38	600.39	10.87	600.39	10.68	544.54	10.48
		656.24	11.00	712.09	11.57	712.09	11.29	656.24	11.21
		767.94	11.64	837.76	12.36	837.76	12.06	767.94	11.91
		893.61	12.34	949.46	12.99	949.46	12.65	893.61	12.66
	60	6.98	0.00	8.38	0.00	8.38	0.00	6.98	0.00
		12.57	0.00	19.55	0.00	19.55	0.00	12.57	0.00
		32.11	0.00	60.04	1.30	60.04	1.37	32.11	0.00
		97.74	3.59	167.55	6.42	167.55	6.30	97.74	3.53
		251.33	8.43	335.10	9.59	335.10	9.21	251.33	8.69
		418.88	9.93	481.71	10.54	481.71	10.17	418.88	10.28
		544.54	10.59	600.39	11.37	600.39	10.87	544.54	11.16
		656.24	11.26	712.09	12.35	712.09	11.58	656.24	12.09
		767.94	12.04	837.76	13.50	837.76	12.47	767.94	13.12
		893.61	12.83	949.46	14.67	949.46	13.18	893.61	14.38

Table A5 3rd relative torque harmonic (T(3/1)) result at 3.14 rad/s and 100°C as measured by the RPA-FT of HNBR compounds filled with various CB characteristics and loadings (cont.)

CB type	CB loading (phr)	Test a				Test b			
		run 1		run 2		run 1		run 2	
		Strain (%)	T(3/1) (%)	Strain (%)	T(3/1) (%)	Strain (%)	T(3/1) (%)	Strain (%)	T(3/1) (%)
N774	10	6.98	0.00	8.38	0.00	8.38	0.00	6.98	0.00
		12.57	0.00	19.55	0.00	19.55	0.00	12.57	0.00
		32.11	0.00	60.04	0.13	60.04	0.03	32.11	0.00
		97.74	1.10	167.55	3.22	167.55	3.30	97.74	1.22
		251.33	5.48	335.10	7.05	335.10	7.15	251.33	5.38
		418.88	8.39	481.71	9.11	481.71	9.10	418.88	8.37
		544.54	9.69	600.39	10.16	600.39	10.07	544.54	9.69
		656.24	10.46	712.09	10.95	712.09	10.81	656.24	10.57
		767.94	11.20	837.76	11.74	837.76	11.60	767.94	11.31
		893.61	11.89	949.46	12.29	949.46	12.14	893.61	11.98
	20	6.98	0.00	8.38	0.00	8.38	0.00	6.98	0.00
		12.57	0.00	19.55	0.00	19.55	0.00	12.57	0.00
		32.11	0.00	60.04	0.46	60.04	0.45	32.11	0.00
		97.74	1.75	167.55	3.65	167.55	3.89	97.74	1.69
		251.33	6.07	335.10	7.36	335.10	7.53	251.33	5.86
		418.88	8.67	481.71	9.32	481.71	9.37	418.88	8.78
		544.54	9.86	600.39	10.35	600.39	10.35	544.54	10.02
		656.24	10.66	712.09	11.11	712.09	11.08	656.24	10.87
		767.94	11.34	837.76	11.87	837.76	11.80	767.94	11.56
		893.61	12.01	949.46	12.50	949.46	12.35	893.61	12.20
	40	6.98	0.00	8.38	0.00	8.38	0.00	6.98	0.00
		12.57	0.00	19.55	0.00	19.55	0.00	12.57	0.00
		32.11	0.00	60.04	0.60	60.04	0.67	32.11	0.05
		97.74	2.24	167.55	4.28	167.55	4.68	97.74	2.00
		251.33	6.92	335.10	8.04	335.10	8.28	251.33	6.51
		418.88	9.29	481.71	9.79	481.71	9.87	418.88	9.19
		544.54	10.30	600.39	10.71	600.39	10.68	544.54	10.26
		656.24	10.99	712.09	11.38	712.09	11.31	656.24	11.02
		767.94	11.60	837.76	12.05	837.76	11.97	767.94	11.65
		893.61	12.23	949.46	12.65	949.46	12.53	893.61	12.32
	60	6.98	0.00	8.38	0.00	8.38	0.00	6.98	0.00
		12.57	0.00	19.55	0.00	19.55	0.00	12.57	0.00
		32.11	0.00	60.04	0.91	60.04	0.93	32.11	0.00
		97.74	2.90	167.55	5.28	167.55	5.69	97.74	2.59
		251.33	7.87	335.10	8.84	335.10	9.01	251.33	7.53
		418.88	9.91	481.71	10.23	481.71	10.28	418.88	9.86
		544.54	10.66	600.39	11.02	600.39	10.97	544.54	10.75
		656.24	11.25	712.09	11.69	712.09	11.59	656.24	11.44
		767.94	11.87	837.76	12.41	837.76	12.25	767.94	12.11
		893.61	12.56	949.46	13.13	949.46	12.87	893.61	12.88

Table A5 3rd relative torque harmonic (T(3/1)) result at 3.14 rad/s and 100°C as measured by the RPA-FT of HNBR compounds filled with various CB characteristics and loadings (cont.)

CB type	CB loading (phr)	Test a				Test b			
		run 1		run 2		run 1		run 2	
		Strain (%)	T(3/1) (%)	Strain (%)	T(3/1) (%)	Strain (%)	T(3/1) (%)	Strain (%)	T(3/1) (%)
N990	10	6.98	0.00	8.38	0.00	8.38	0.00	6.98	0.59
		12.57	0.00	19.55	0.00	19.55	0.00	12.57	0.00
		32.11	0.00	60.04	0.50	60.04	0.49	32.11	0.00
		97.74	1.39	167.55	3.27	167.55	3.42	97.74	1.41
		251.33	5.67	335.10	7.01	335.10	7.28	251.33	5.44
		418.88	8.42	481.71	9.05	481.71	9.10	418.88	8.35
		544.54	9.66	600.39	10.13	600.39	10.09	544.54	9.65
		656.24	10.44	712.09	10.97	712.09	10.85	656.24	10.57
		767.94	11.20	837.76	11.74	837.76	11.60	767.94	11.33
		893.61	11.91	949.46	12.37	949.46	12.24	893.61	12.05
	20	6.98	0.00	8.38	0.00	8.38	0.00	6.98	0.00
		12.57	0.00	19.55	0.00	19.55	0.00	12.57	0.00
		32.11	0.00	60.04	0.46	60.04	0.37	32.11	0.00
		97.74	1.58	167.55	3.61	167.55	3.68	97.74	1.45
		251.33	6.10	335.10	7.28	335.10	7.38	251.33	5.59
		418.88	8.71	481.71	9.21	481.71	9.14	418.88	8.44
		544.54	9.81	600.39	10.27	600.39	10.07	544.54	9.73
		656.24	10.65	712.09	11.07	712.09	10.88	656.24	10.65
		767.94	11.37	837.76	11.81	837.76	11.51	767.94	11.39
		893.61	12.05	949.46	12.40	949.46	12.10	893.61	12.07
	40	6.98	0.00	8.38	0.00	8.38	0.00	6.98	0.00
		12.57	0.00	19.55	0.00	19.55	0.00	12.57	0.00
		32.11	0.00	60.04	0.66	60.04	0.73	32.11	0.00
		97.74	2.07	167.55	4.26	167.55	4.53	97.74	1.97
		251.33	6.71	335.10	7.87	335.10	8.13	251.33	6.33
		418.88	9.23	481.71	9.68	481.71	9.78	418.88	9.03
		544.54	10.35	600.39	10.75	600.39	10.76	544.54	10.27
		656.24	11.16	712.09	11.58	712.09	11.51	656.24	11.17
		767.94	11.85	837.76	12.30	837.76	12.26	767.94	11.93
		893.61	12.51	949.46	12.88	949.46	12.76	893.61	12.58
	60	6.98	0.00	8.38	0.00	8.38	0.00	6.98	0.00
		12.57	0.00	19.55	0.00	19.55	0.00	12.57	0.00
		32.11	0.00	60.04	0.81	60.04	0.76	32.11	0.00
		97.74	2.56	167.55	4.77	167.55	5.11	97.74	2.39
		251.33	7.33	335.10	8.38	335.10	8.65	251.33	6.95
		418.88	9.71	481.71	10.13	481.71	10.27	418.88	9.60
		544.54	10.79	600.39	11.21	600.39	11.24	544.54	10.75
		656.24	11.58	712.09	11.99	712.09	11.99	656.24	11.66
		767.94	12.32	837.76	12.68	837.76	12.69	767.94	12.40
		893.61	12.92	949.46	13.27	949.46	13.26	893.61	13.02

Table A6 5^{th} relative torque harmonic (T(5/1)) result at 3.14 rad/s and 100°C as measured by the RPA-FT of HNBR compounds filled with various CB characteristics and loadings

CB type	CB loading (phr)	Test a				Test b			
		run 1		run 2		run 1		run 2	
		Strain (%)	T(5/1) (%)	Strain (%)	T(5/1) (%)	Strain (%)	T(5/1) (%)	Strain (%)	T(5/1) (%)
-	0	6.98	0.00	8.38	0.00	8.38	0.00	6.98	0.00
		12.57	0.00	19.55	0.01	19.55	0.00	12.57	0.00
		32.11	0.22	60.04	0.26	60.04	0.30	32.11	0.07
		97.74	0.34	167.55	0.46	167.55	0.54	97.74	0.35
		251.33	0.80	335.10	1.15	335.10	1.21	251.33	0.74
		418.88	1.59	481.71	1.93	481.71	1.93	418.88	1.57
		544.54	2.23	600.39	2.46	600.39	2.45	544.54	2.27
		656.24	2.65	712.09	2.89	712.09	2.86	656.24	2.72
		767.94	3.11	837.76	3.36	837.76	3.33	767.94	3.15
		893.61	3.52	949.46	3.70	949.46	3.67	893.61	3.53
N326	10	6.98	0.00	8.38	0.18	8.38	0.17	6.98	0.00
		12.57	0.21	19.55	0.13	19.55	0.01	12.57	0.00
		32.11	0.27	60.04	0.43	60.04	0.44	32.11	0.35
		97.74	0.54	167.55	0.61	167.55	0.69	97.74	0.53
		251.33	0.95	335.10	1.30	335.10	1.36	251.33	0.91
		418.88	1.70	481.71	2.02	481.71	2.04	418.88	1.68
		544.54	2.31	600.39	2.55	600.39	2.54	544.54	2.30
		656.24	2.71	712.09	2.97	712.09	2.95	656.24	2.74
		767.94	3.17	837.76	3.42	837.76	3.41	767.94	3.18
		893.61	3.58	949.46	3.76	949.46	3.76	893.61	3.60
	20	6.98	0.00	8.38	0.54	8.38	0.29	6.98	0.18
		12.57	0.00	19.55	0.35	19.55	0.41	12.57	0.41
		32.11	0.63	60.04	0.80	60.04	0.83	32.11	0.58
		97.74	0.86	167.55	0.85	167.55	0.97	97.74	0.76
		251.33	1.17	335.10	1.52	335.10	1.57	251.33	1.12
		418.88	1.87	481.71	2.15	481.71	2.19	418.88	1.89
		544.54	2.43	600.39	2.63	600.39	2.66	544.54	2.45
		656.24	2.79	712.09	3.06	712.09	3.06	656.24	2.84
		767.94	3.25	837.76	3.53	837.76	3.55	767.94	3.29
		893.61	3.66	949.46	3.88	949.46	3.88	893.61	3.69
	40	6.98	0.00	8.38	0.12	8.38	0.29	6.98	0.48
		12.57	0.15	19.55	0.17	19.55	0.26	12.57	0.13
		32.11	0.36	60.04	0.45	60.04	0.41	32.11	0.37
		97.74	0.61	167.55	0.74	167.55	0.80	97.74	0.47
		251.33	1.19	335.10	1.60	335.10	1.62	251.33	1.13
		418.88	1.97	481.71	2.19	481.71	2.24	418.88	1.90
		544.54	2.53	600.39	2.68	600.39	2.71	544.54	2.47
		656.24	2.92	712.09	3.13	712.09	3.17	656.24	2.94
		767.94	3.40	837.76	3.60	837.76	3.66	767.94	3.39
		893.61	3.80	949.46	3.94	949.46	3.99	893.61	3.78

Table A6 5th relative torque harmonic (T(5/1)) result at 3.14 rad/s and 100°C as measured by the RPA-FT of HNBR compounds filled with various CB characteristics and loadings (cont.)

CB type	CB loading (phr)	Test a				Test b			
		run 1		run 2		run 1		run 2	
		Strain (%)	T(5/1) (%)	Strain (%)	T(5/1) (%)	Strain (%)	T(5/1) (%)	Strain (%)	T(5/1) (%)
N326	60	6.98	0.00	8.38	0.16	8.38	0.00	6.98	0.00
		12.57	0.00	19.55	0.01	19.55	0.00	12.57	0.00
		32.11	0.23	60.04	0.07	60.04	0.14	32.11	0.09
		97.74	0.25	167.55	0.56	167.55	0.63	97.74	0.18
		251.33	1.23	335.10	1.65	335.10	1.75	251.33	1.16
		418.88	2.16	481.71	2.32	481.71	2.46	418.88	2.04
		544.54	2.80	600.39	2.92	600.39	3.00	544.54	2.68
		656.24	3.21	712.09	3.38	712.09	3.43	656.24	3.17
		767.94	3.63	837.76	3.82	837.76	3.86	767.94	3.60
		893.61	3.98	949.46	4.17	949.46	4.19	893.61	3.98
N550	10	6.98	0.00	8.38	0.49	8.38	0.62	6.98	0.50
		12.57	0.00	19.55	0.25	19.55	0.16	12.57	0.06
		32.11	0.52	60.04	0.58	60.04	0.64	32.11	0.44
		97.74	1.04	167.55	0.76	167.55	0.86	97.74	0.82
		251.33	1.13	335.10	1.43	335.10	1.49	251.33	1.04
		418.88	1.83	481.71	2.13	481.71	2.12	418.88	1.83
		544.54	2.39	600.39	2.61	600.39	2.57	544.54	2.40
		656.24	2.76	712.09	3.01	712.09	2.99	656.24	2.80
		767.94	3.20	837.76	3.44	837.76	3.43	767.94	3.22
		893.61	3.61	949.46	3.81	949.46	3.80	893.61	3.63
	20	6.98	0.00	8.38	0.09	8.38	0.34	6.98	0.00
		12.57	0.19	19.55	0.18	19.55	0.15	12.57	0.00
		32.11	0.40	60.04	0.57	60.04	0.58	32.11	0.43
		97.74	0.85	167.55	0.77	167.55	0.84	97.74	0.74
		251.33	1.14	335.10	1.55	335.10	1.59	251.33	1.12
		418.88	1.92	481.71	2.19	481.71	2.23	418.88	1.93
		544.54	2.49	600.39	2.65	600.39	2.65	544.54	2.48
		656.24	2.86	712.09	3.07	712.09	3.04	656.24	2.87
		767.94	3.29	837.76	3.54	837.76	3.52	767.94	3.31
		893.61	3.73	949.46	3.91	949.46	3.90	893.61	3.73
	40	6.98	0.00	8.38	0.08	8.38	0.27	6.98	0.09
		12.57	0.00	19.55	0.12	19.55	0.12	12.57	0.06
		32.11	0.24	60.04	0.58	60.04	0.53	32.11	0.42
		97.74	0.79	167.55	0.87	167.55	0.97	97.74	0.72
		251.33	1.37	335.10	1.77	335.10	1.83	251.33	1.30
		418.88	2.11	481.71	2.33	481.71	2.35	418.88	2.08
		544.54	2.61	600.39	2.89	600.39	2.80	544.54	2.62
		656.24	3.03	712.09	3.36	712.09	3.22	656.24	3.13
		767.94	3.45	837.76	3.80	837.76	3.68	767.94	3.57
		893.61	3.80	949.46	4.09	949.46	3.97	893.61	3.94

Table A6 5^{th} relative torque harmonic (T(5/1)) result at 3.14 rad/s and 100°C as measured by the RPA-FT of HNBR compounds filled with various CB characteristics and loadings (cont.)

CB type	CB loading (phr)	Test a				Test b			
		run 1		run 2		run 1		run 2	
		Strain (%)	T(5/1) (%)	Strain (%)	T(5/1) (%)	Strain (%)	T(5/1) (%)	Strain (%)	T(5/1) (%)
N550	60	6.98	0.00	8.38	0.00	8.38	0.09	6.98	0.00
		12.57	0.00	19.55	0.18	19.55	0.28	12.57	0.00
		32.11	0.24	60.04	0.38	60.04	0.67	32.11	0.24
		97.74	0.80	167.55	0.88	167.55	1.04	97.74	0.64
		251.33	1.56	335.10	1.97	335.10	2.03	251.33	1.57
		418.88	2.30	481.71	2.71	481.71	2.61	418.88	2.46
		544.54	2.89	600.39	3.44	600.39	3.10	544.54	3.28
		656.24	3.32	712.09	4.22	712.09	3.45	656.24	4.07
		767.94	3.70	837.76	4.80	837.76	3.84	767.94	4.68
		893.61	4.03	949.46	5.34	949.46	4.16	893.61	5.13
N774	10	6.98	0.00	8.38	0.43	8.38	0.16	6.98	0.28
		12.57	0.00	19.55	0.38	19.55	0.15	12.57	0.17
		32.11	0.47	60.04	0.59	60.04	0.69	32.11	0.49
		97.74	0.82	167.55	0.79	167.55	0.86	97.74	0.76
		251.33	1.14	335.10	1.40	335.10	1.47	251.33	1.03
		418.88	1.88	481.71	2.12	481.71	2.17	418.88	1.80
		544.54	2.46	600.39	2.67	600.39	2.66	544.54	2.45
		656.24	2.84	712.09	3.07	712.09	3.04	656.24	2.86
		767.94	3.25	837.76	3.52	837.76	3.48	767.94	3.29
		893.61	3.65	949.46	3.87	949.46	3.83	893.61	3.70
	20	6.98	0.00	8.38	0.54	8.38	0.50	6.98	0.68
		12.57	0.00	19.55	0.36	19.55	0.30	12.57	0.26
		32.11	0.66	60.04	0.91	60.04	0.97	32.11	0.52
		97.74	1.04	167.55	1.01	167.55	1.12	97.74	1.07
		251.33	1.32	335.10	1.68	335.10	1.74	251.33	1.29
		418.88	2.04	481.71	2.34	481.71	2.36	418.88	2.07
		544.54	2.61	600.39	2.77	600.39	2.80	544.54	2.64
		656.24	2.93	712.09	3.18	712.09	3.18	656.24	3.01
		767.94	3.36	837.76	3.64	837.76	3.63	767.94	3.42
		893.61	3.77	949.46	4.01	949.46	4.01	893.61	3.85
	40	6.98	0.00	8.38	0.08	8.38	0.13	6.98	0.33
		12.57	0.00	19.55	0.36	19.55	0.15	12.57	0.08
		32.11	0.43	60.04	0.76	60.04	0.76	32.11	0.47
		97.74	1.10	167.55	1.01	167.55	1.10	97.74	1.04
		251.33	1.45	335.10	1.83	335.10	1.86	251.33	1.36
		418.88	2.20	481.71	2.45	481.71	2.48	418.88	2.15
		544.54	2.72	600.39	2.91	600.39	2.90	544.54	2.68
		656.24	3.09	712.09	3.34	712.09	3.30	656.24	3.11
		767.94	3.52	837.76	3.72	837.76	3.72	767.94	3.52
		893.61	3.91	949.46	4.08	949.46	4.04	893.61	3.92

Table A6 5^{th} relative torque harmonic (T(5/1)) result at 3.14 rad/s and 100°C as measured by the RPA-FT of HNBR compounds filled with various CB characteristics and loadings (cont.)

CB type	CB loading (phr)	Test a				Test b			
		run 1		run 2		run 1		run 2	
		Strain (%)	T(5/1) (%)	Strain (%)	T(5/1) (%)	Strain (%)	T(5/1) (%)	Strain (%)	T(5/1) (%)
N774	60	6.98	0.00	8.38	0.00	8.38	0.11	6.98	0.00
		12.57	0.01	19.55	0.12	19.55	0.11	12.57	0.00
		32.11	0.36	60.04	0.63	60.04	0.62	32.11	0.38
		97.74	0.97	167.55	1.02	167.55	1.04	97.74	0.93
		251.33	1.54	335.10	1.95	335.10	1.97	251.33	1.53
		418.88	2.32	481.71	2.55	481.71	2.57	418.88	2.31
		544.54	2.84	600.39	3.09	600.39	3.06	544.54	2.88
		656.24	3.30	712.09	3.55	712.09	3.48	656.24	3.34
		767.94	3.69	837.76	3.90	837.76	3.82	767.94	3.74
		893.61	4.01	949.46	4.25	949.46	4.16	893.61	4.07
N990	10	6.98	0.00	8.38	0.41	8.38	0.42	6.98	0.46
		12.57	0.05	19.55	0.55	19.55	0.34	12.57	0.59
		32.11	0.48	60.04	0.86	60.04	0.84	32.11	0.73
		97.74	1.27	167.55	0.89	167.55	0.96	97.74	1.09
		251.33	1.21	335.10	1.45	335.10	1.55	251.33	1.06
		418.88	1.94	481.71	2.16	481.71	2.23	418.88	1.82
		544.54	2.50	600.39	2.67	600.39	2.67	544.54	2.45
		656.24	2.87	712.09	3.07	712.09	3.05	656.24	2.86
		767.94	3.27	837.76	3.50	837.76	3.48	767.94	3.27
		893.61	3.67	949.46	3.85	949.46	3.85	893.61	3.68
	20	6.98	0.00	8.38	0.21	8.38	0.34	6.98	0.29
		12.57	0.08	19.55	0.12	19.55	0.22	12.57	0.15
		32.11	0.57	60.04	0.62	60.04	0.66	32.11	0.43
		97.74	1.01	167.55	0.85	167.55	1.02	97.74	0.99
		251.33	1.22	335.10	1.54	335.10	1.76	251.33	1.18
		418.88	1.95	481.71	2.26	481.71	2.37	418.88	1.97
		544.54	2.55	600.39	2.75	600.39	2.85	544.54	2.56
		656.24	2.95	712.09	3.14	712.09	3.17	656.24	2.97
		767.94	3.36	837.76	3.53	837.76	3.55	767.94	3.35
		893.61	3.73	949.46	3.88	949.46	3.94	893.61	3.73
	40	6.98	0.00	8.38	0.28	8.38	0.12	6.98	0.00
		12.57	0.00	19.55	0.11	19.55	0.09	12.57	0.00
		32.11	0.45	60.04	0.55	60.04	0.52	32.11	0.38
		97.74	1.05	167.55	0.95	167.55	1.03	97.74	0.95
		251.33	1.38	335.10	1.72	335.10	1.80	251.33	1.29
		418.88	2.16	481.71	2.45	481.71	2.50	418.88	2.08
		544.54	2.72	600.39	2.92	600.39	2.93	544.54	2.68
		656.24	3.12	712.09	3.32	712.09	3.32	656.24	3.13
		767.94	3.54	837.76	3.72	837.76	3.73	767.94	3.53
		893.61	3.93	949.46	4.06	949.46	4.07	893.61	3.93

Table A6 5^{th} relative torque harmonic (T(5/1)) result at 3.14 rad/s and 100°C as measured by the RPA-FT of HNBR compounds filled with various CB characteristics and loadings (cont.)

CB type	CB loading (phr)	Test a				Test b			
		run 1		run 2		run 1		run 2	
		Strain (%)	T(5/1) (%)	Strain (%)	T(5/1) (%)	Strain (%)	T(5/1) (%)	Strain (%)	T(5/1) (%)
N990	60	6.98	0.00	8.38	0.00	8.38	0.14	6.98	0.00
		12.57	0.00	19.55	0.05	19.55	0.07	12.57	0.00
		32.11	0.52	60.04	0.72	60.04	0.83	32.11	0.34
		97.74	1.33	167.55	1.13	167.55	1.24	97.74	1.15
		251.33	1.61	335.10	1.90	335.10	2.00	251.33	1.49
		418.88	2.37	481.71	2.61	481.71	2.67	418.88	2.34
		544.54	2.94	600.39	3.13	600.39	3.16	544.54	2.93
		656.24	3.36	712.09	3.56	712.09	3.55	656.24	3.39
		767.94	3.78	837.76	3.94	837.76	3.95	767.94	3.77
		893.61	4.13	949.46	4.28	949.46	4.29	893.61	4.13

Table A7 Fit parameters of Equation 3.17 of HNBR compounds filled with various CB characteristics and loadings

CB type	CB loading (phr)	TH	α	C	D
-	0	6.700	0.0058	0.0090	3.7030
N326	10	7.200	0.0053	0.0090	3.4250
	20	7.400	0.0053	0.0090	3.1070
	40	8.100	0.0049	0.0100	3.1540
	60	8.600	0.0052	0.0120	2.7560
N550	10	7.000	0.0056	0.0080	2.8140
	20	7.200	0.0055	0.0090	2.9650
	40	7.300	0.0057	0.0120	3.2100
	60	7.200	0.0062	0.0170	3.8210
N774	10	6.800	0.0057	0.0090	3.5380
	20	7.100	0.0056	0.0080	2.6800
	40	7.500	0.0053	0.0100	2.8320
	60	7.700	0.0055	0.0130	3.3100
N990	10	6.896	0.0057	0.0082	2.8440
	20	6.954	0.0056	0.0089	2.9770
	40	7.298	0.0059	0.0094	2.6670
	60	7.507	0.0062	0.0105	2.7880

Table A8 Integrating torque signals result at 3.14 rad/s and 100°C as measured by the RPA-FT of HNBR compounds filled with various CB characteristics and loadings

CB type	CB loading (phr)	Test a				Test b			
		run 1		run 2		run 1		run 2	
		Strain (%)	Q1/Q2	Strain (%)	Q1/Q2	Strain (%)	Q1/Q2	Strain (%)	Q1/Q2
-	0	6.98	1.08	8.38	1.06	8.38	1.08	6.98	1.01
		12.57	1.08	19.55	1.08	19.55	1.05	12.57	1.07
		32.11	1.04	60.04	1.05	60.04	1.04	32.11	1.02
		97.74	1.07	167.55	1.03	167.55	1.04	97.74	1.06
		251.33	1.06	335.10	1.07	335.10	1.08	251.33	1.05
		418.88	1.08	481.71	1.09	481.71	1.09	418.88	1.08
		544.54	1.09	600.39	1.10	600.39	1.10	544.54	1.08
		656.24	1.09	712.09	1.11	712.09	1.10	656.24	1.10
		767.94	1.12	837.76	1.12	837.76	1.11	767.94	1.11
		893.61	1.12	949.46	1.12	949.46	1.12	893.61	1.11
N326	10	6.98	1.06	8.38	1.09	8.38	1.06	6.98	1.06
		12.57	1.07	19.55	1.06	19.55	1.08	12.57	1.09
		32.11	1.04	60.04	1.05	60.04	1.05	32.11	1.05
		97.74	1.05	167.55	1.04	167.55	1.03	97.74	1.06
		251.33	1.04	335.10	1.06	335.10	1.06	251.33	1.05
		418.88	1.07	481.71	1.09	481.71	1.07	418.88	1.07
		544.54	1.07	600.39	1.09	600.39	1.09	544.54	1.08
		656.24	1.09	712.09	1.10	712.09	1.10	656.24	1.08
		767.94	1.10	837.76	1.11	837.76	1.10	767.94	1.10
		893.61	1.10	949.46	1.10	949.46	1.11	893.61	1.11
	20	6.98	1.10	8.38	1.09	8.38	1.12	6.98	1.04
		12.57	1.08	19.55	1.08	19.55	1.09	12.57	1.08
		32.11	1.05	60.04	1.05	60.04	1.04	32.11	1.02
		97.74	1.07	167.55	1.04	167.55	1.03	97.74	1.06
		251.33	1.02	335.10	1.04	335.10	1.03	251.33	1.03
		418.88	1.05	481.71	1.08	481.71	1.07	418.88	1.06
		544.54	1.06	600.39	1.08	600.39	1.08	544.54	1.07
		656.24	1.07	712.09	1.09	712.09	1.08	656.24	1.07
		767.94	1.09	837.76	1.10	837.76	1.10	767.94	1.10
		893.61	1.10	949.46	1.09	949.46	1.10	893.61	1.09
	40	6.98	1.12	8.38	1.03	8.38	1.08	6.98	1.01
		12.57	1.08	19.55	1.05	19.55	1.06	12.57	1.04
		32.11	1.03	60.04	1.04	60.04	1.03	32.11	1.00
		97.74	1.01	167.55	1.02	167.55	1.00	97.74	1.02
		251.33	1.00	335.10	1.02	335.10	1.00	251.33	1.02
		418.88	1.02	481.71	1.06	481.71	1.04	418.88	1.04
		544.54	1.04	600.39	1.05	600.39	1.05	544.54	1.05
		656.24	1.04	712.09	1.07	712.09	1.06	656.24	1.04
		767.94	1.07	837.76	1.09	837.76	1.07	767.94	1.06
		893.61	1.07	949.46	1.08	949.46	1.09	893.61	1.07

Table A8 Integrating torque signals result at 3.14 rad/s and 100°C as measured by the RPA-FT of HNBR compounds filled with various CB characteristics and loadings (cont.)

CB type	CB loading (phr)	Test a				Test b			
		run 1		run 2		run 1		run 2	
		Strain (%)	Q1/Q2	Strain (%)	Q1/Q2	Strain (%)	Q1/Q2	Strain (%)	Q1/Q2
N326	60	6.98	1.03	8.38	0.98	8.38	1.02	6.98	0.97
		12.57	1.09	19.55	1.01	19.55	1.02	12.57	0.98
		32.11	1.00	60.04	1.02	60.04	1.01	32.11	1.00
		97.74	0.98	167.55	0.99	167.55	0.97	97.74	1.01
		251.33	0.95	335.10	0.99	335.10	0.97	251.33	0.98
		418.88	0.98	481.71	1.03	481.71	1.00	418.88	1.02
		544.54	1.01	600.39	1.04	600.39	1.02	544.54	1.04
		656.24	1.02	712.09	1.05	712.09	1.05	656.24	1.03
		767.94	1.05	837.76	1.07	837.76	1.06	767.94	1.06
		893.61	1.06	949.46	1.06	949.46	1.07	893.61	1.07
N550	10	6.98	1.04	8.38	1.07	8.38	1.04	6.98	1.05
		12.57	1.12	19.55	1.04	19.55	1.06	12.57	1.07
		32.11	1.09	60.04	1.02	60.04	1.04	32.11	1.04
		97.74	1.08	167.55	1.06	167.55	1.03	97.74	1.08
		251.33	1.05	335.10	1.06	335.10	1.06	251.33	1.05
		418.88	1.07	481.71	1.09	481.71	1.08	418.88	1.06
		544.54	1.09	600.39	1.10	600.39	1.10	544.54	1.09
		656.24	1.10	712.09	1.10	712.09	1.09	656.24	1.08
		767.94	1.10	837.76	1.11	837.76	1.12	767.94	1.11
		893.61	1.10	949.46	1.12	949.46	1.11	893.61	1.11
	20	6.98	1.03	8.38	1.06	8.38	1.06	6.98	1.07
		12.57	1.09	19.55	1.12	19.55	1.07	12.57	1.08
		32.11	1.03	60.04	1.05	60.04	1.04	32.11	1.04
		97.74	1.04	167.55	1.04	167.55	1.04	97.74	1.04
		251.33	1.01	335.10	1.04	335.10	1.04	251.33	1.04
		418.88	1.04	481.71	1.07	481.71	1.06	418.88	1.06
		544.54	1.07	600.39	1.08	600.39	1.08	544.54	1.08
		656.24	1.06	712.09	1.09	712.09	1.09	656.24	1.08
		767.94	1.09	837.76	1.10	837.76	1.09	767.94	1.09
		893.61	1.08	949.46	1.11	949.46	1.11	893.61	1.10
	40	6.98	1.11	8.38	1.04	8.38	1.06	6.98	1.04
		12.57	1.07	19.55	1.05	19.55	1.07	12.57	1.04
		32.11	1.08	60.04	1.06	60.04	1.04	32.11	1.05
		97.74	1.04	167.55	1.05	167.55	1.03	97.74	1.05
		251.33	1.02	335.10	1.03	335.10	1.02	251.33	1.03
		418.88	1.03	481.71	1.05	481.71	1.04	418.88	1.05
		544.54	1.06	600.39	1.05	600.39	1.06	544.54	1.06
		656.24	1.05	712.09	1.07	712.09	1.07	656.24	1.05
		767.94	1.07	837.76	1.07	837.76	1.07	767.94	1.06
		893.61	1.08	949.46	1.08	949.46	1.09	893.61	1.07

Table A8 Integrating torque signals result at 3.14 rad/s and 100°C as measured by the RPA-FT of HNBR compounds filled with various CB characteristics and loadings (cont.)

CB type	CB loading (phr)	Test a				Test b			
		run 1		run 2		run 1		run 2	
		Strain (%)	Q1/Q2	Strain (%)	Q1/Q2	Strain (%)	Q1/Q2	Strain (%)	Q1/Q2
N326	60	6.98	1.03	8.38	0.98	8.38	1.02	6.98	0.97
		12.57	1.09	19.55	1.01	19.55	1.02	12.57	0.98
		32.11	1.00	60.04	1.02	60.04	1.01	32.11	1.00
		97.74	0.98	167.55	0.99	167.55	0.97	97.74	1.01
		251.33	0.95	335.10	0.99	335.10	0.97	251.33	0.98
		418.88	0.98	481.71	1.03	481.71	1.00	418.88	1.02
		544.54	1.01	600.39	1.04	600.39	1.02	544.54	1.04
		656.24	1.02	712.09	1.05	712.09	1.05	656.24	1.03
		767.94	1.05	837.76	1.07	837.76	1.06	767.94	1.06
		893.61	1.06	949.46	1.06	949.46	1.07	893.61	1.07
N550	10	6.98	1.04	8.38	1.07	8.38	1.04	6.98	1.05
		12.57	1.12	19.55	1.04	19.55	1.06	12.57	1.07
		32.11	1.09	60.04	1.02	60.04	1.04	32.11	1.04
		97.74	1.08	167.55	1.06	167.55	1.03	97.74	1.08
		251.33	1.05	335.10	1.06	335.10	1.06	251.33	1.05
		418.88	1.07	481.71	1.09	481.71	1.08	418.88	1.06
		544.54	1.09	600.39	1.10	600.39	1.10	544.54	1.09
		656.24	1.10	712.09	1.10	712.09	1.09	656.24	1.08
		767.94	1.10	837.76	1.11	837.76	1.12	767.94	1.11
		893.61	1.10	949.46	1.12	949.46	1.11	893.61	1.11
	20	6.98	1.03	8.38	1.06	8.38	1.06	6.98	1.07
		12.57	1.09	19.55	1.12	19.55	1.07	12.57	1.08
		32.11	1.03	60.04	1.05	60.04	1.04	32.11	1.04
		97.74	1.04	167.55	1.04	167.55	1.04	97.74	1.04
		251.33	1.01	335.10	1.04	335.10	1.04	251.33	1.04
		418.88	1.04	481.71	1.07	481.71	1.06	418.88	1.06
		544.54	1.07	600.39	1.08	600.39	1.08	544.54	1.08
		656.24	1.06	712.09	1.09	712.09	1.09	656.24	1.08
		767.94	1.09	837.76	1.10	837.76	1.09	767.94	1.09
		893.61	1.08	949.46	1.11	949.46	1.11	893.61	1.10
	40	6.98	1.11	8.38	1.04	8.38	1.06	6.98	1.04
		12.57	1.07	19.55	1.05	19.55	1.07	12.57	1.04
		32.11	1.08	60.04	1.06	60.04	1.04	32.11	1.05
		97.74	1.04	167.55	1.05	167.55	1.03	97.74	1.05
		251.33	1.02	335.10	1.03	335.10	1.02	251.33	1.03
		418.88	1.03	481.71	1.05	481.71	1.04	418.88	1.05
		544.54	1.06	600.39	1.05	600.39	1.06	544.54	1.06
		656.24	1.05	712.09	1.07	712.09	1.07	656.24	1.05
		767.94	1.07	837.76	1.07	837.76	1.07	767.94	1.06
		893.61	1.08	949.46	1.08	949.46	1.09	893.61	1.07

Table A8 Integrating torque signals result at 3.14 rad/s and 100°C as measured by the RPA-FT of HNBR compounds filled with various CB characteristics and loadings (cont.)

CB type	CB loading (phr)	Test a				Test b			
		run 1		run 2		run 1		run 2	
		Strain (%)	Q1/Q2	Strain (%)	Q1/Q2	Strain (%)	Q1/Q2	Strain (%)	Q1/Q2
N550	60	6.98	1.09	8.38	1.05	8.38	1.09	6.98	1.06
		12.57	1.10	19.55	1.06	19.55	1.09	12.57	1.08
		32.11	1.06	60.04	1.01	60.04	1.02	32.11	1.05
		97.74	1.01	167.55	1.00	167.55	1.00	97.74	1.03
		251.33	0.97	335.10	1.00	335.10	1.00	251.33	0.99
		418.88	1.00	481.71	1.01	481.71	1.02	418.88	1.01
		544.54	1.02	600.39	1.02	600.39	1.04	544.54	1.02
		656.24	1.03	712.09	1.00	712.09	1.06	656.24	1.00
		767.94	1.04	837.76	1.01	837.76	1.06	767.94	1.00
		893.61	1.05	949.46	1.00	949.46	1.08	893.61	0.98
N774	10	6.98	1.08	8.38	1.07	8.38	1.11	6.98	1.12
		12.57	1.08	19.55	1.10	19.55	1.10	12.57	1.08
		32.11	1.09	60.04	1.05	60.04	1.05	32.11	1.07
		97.74	1.08	167.55	1.04	167.55	1.05	97.74	1.07
		251.33	1.07	335.10	1.06	335.10	1.06	251.33	1.05
		418.88	1.07	481.71	1.09	481.71	1.08	418.88	1.07
		544.54	1.08	600.39	1.09	600.39	1.08	544.54	1.09
		656.24	1.09	712.09	1.11	712.09	1.11	656.24	1.09
		767.94	1.10	837.76	1.12	837.76	1.11	767.94	1.12
		893.61	1.12	949.46	1.12	949.46	1.13	893.61	1.11
	20	6.98	1.09	8.38	1.09	8.38	1.08	6.98	1.08
		12.57	1.11	19.55	1.07	19.55	1.08	12.57	1.13
		32.11	1.08	60.04	1.05	60.04	1.05	32.11	1.09
		97.74	1.07	167.55	1.05	167.55	1.05	97.74	1.07
		251.33	1.04	335.10	1.06	335.10	1.05	251.33	1.04
		418.88	1.06	481.71	1.08	481.71	1.07	418.88	1.07
		544.54	1.08	600.39	1.10	600.39	1.08	544.54	1.09
		656.24	1.08	712.09	1.10	712.09	1.10	656.24	1.09
		767.94	1.10	837.76	1.12	837.76	1.12	767.94	1.10
		893.61	1.11	949.46	1.12	949.46	1.13	893.61	1.10
	40	6.98	1.11	8.38	1.09	8.38	1.11	6.98	1.10
		12.57	1.10	19.55	1.09	19.55	1.10	12.57	1.13
		32.11	1.06	60.04	1.05	60.04	1.04	32.11	1.04
		97.74	1.06	167.55	1.06	167.55	1.04	97.74	1.07
		251.33	1.03	335.10	1.05	335.10	1.03	251.33	1.04
		418.88	1.04	481.71	1.06	481.71	1.04	418.88	1.05
		544.54	1.07	600.39	1.07	600.39	1.07	544.54	1.08
		656.24	1.07	712.09	1.09	712.09	1.08	656.24	1.07
		767.94	1.08	837.76	1.10	837.76	1.10	767.94	1.08
		893.61	1.09	949.46	1.11	949.46	1.11	893.61	1.09

Table A8 Integrating torque signals result at 3.14 rad/s and 100°C as measured by the RPA-FT of HNBR compounds filled with various CB characteristics and loadings (cont.)

CB type	CB loading (phr)	Test a				Test b			
		run 1		run 2		run 1		run 2	
		Strain (%)	Q1/Q2	Strain (%)	Q1/Q2	Strain (%)	Q1/Q2	Strain (%)	Q1/Q2
N774	60	6.98	1.12	8.38	1.06	8.38	1.06	6.98	1.07
		12.57	1.09	19.55	1.10	19.55	1.09	12.57	1.09
		32.11	1.06	60.04	1.05	60.04	1.03	32.11	1.06
		97.74	1.06	167.55	1.03	167.55	1.02	97.74	1.08
		251.33	1.00	335.10	1.04	335.10	1.02	251.33	1.04
		418.88	1.03	481.71	1.05	481.71	1.03	418.88	1.05
		544.54	1.06	600.39	1.07	600.39	1.05	544.54	1.06
		656.24	1.06	712.09	1.07	712.09	1.06	656.24	1.06
		767.94	1.07	837.76	1.09	837.76	1.09	767.94	1.07
		893.61	1.08	949.46	1.09	949.46	1.10	893.61	1.08
N990	10	6.98	1.08	8.38	1.12	8.38	1.09	6.98	1.66
		12.57	1.12	19.55	1.09	19.55	1.07	12.57	1.08
		32.11	1.08	60.04	1.01	60.04	1.01	32.11	1.05
		97.74	1.08	167.55	1.05	167.55	1.06	97.74	1.07
		251.33	1.05	335.10	1.06	335.10	1.05	251.33	1.05
		418.88	1.08	481.71	1.09	481.71	1.08	418.88	1.07
		544.54	1.09	600.39	1.10	600.39	1.10	544.54	1.09
		656.24	1.09	712.09	1.09	712.09	1.10	656.24	1.09
		767.94	1.11	837.76	1.12	837.76	1.12	767.94	1.10
		893.61	1.11	949.46	1.11	949.46	1.13	893.61	1.10
	20	6.98	1.13	8.38	1.11	8.38	1.11	6.98	1.10
		12.57	1.09	19.55	1.10	19.55	1.08	12.57	1.12
		32.11	1.06	60.04	1.04	60.04	1.05	32.11	1.08
		97.74	1.09	167.55	1.05	167.55	1.05	97.74	1.09
		251.33	1.05	335.10	1.05	335.10	1.06	251.33	1.07
		418.88	1.06	481.71	1.08	481.71	1.08	418.88	1.08
		544.54	1.09	600.39	1.10	600.39	1.10	544.54	1.10
		656.24	1.09	712.09	1.10	712.09	1.10	656.24	1.09
		767.94	1.10	837.76	1.12	837.76	1.14	767.94	1.11
		893.61	1.11	949.46	1.12	949.46	1.15	893.61	1.11
	40	6.98	1.08	8.38	1.06	8.38	1.09	6.98	1.10
		12.57	1.10	19.55	1.09	19.55	1.08	12.57	1.09
		32.11	1.10	60.04	1.06	60.04	1.04	32.11	1.08
		97.74	1.08	167.55	1.07	167.55	1.06	97.74	1.09
		251.33	1.05	335.10	1.06	335.10	1.05	251.33	1.06
		418.88	1.06	481.71	1.08	481.71	1.07	418.88	1.08
		544.54	1.08	600.39	1.10	600.39	1.09	544.54	1.09
		656.24	1.08	712.09	1.10	712.09	1.10	656.24	1.08
		767.94	1.11	837.76	1.12	837.76	1.10	767.94	1.09
		893.61	1.09	949.46	1.10	949.46	1.11	893.61	1.10

Table A8 Integrating torque signals result at 3.14 rad/s and 100°C as measured by the RPA-FT of HNBR compounds filled with various CB characteristics and loadings (cont.)

CB type	CB loading (phr)	Test a				Test b			
		run 1		run 2		run 1		run 2	
		Strain (%)	Q1/Q2	Strain (%)	Q1/Q2	Strain (%)	Q1/Q2	Strain (%)	Q1/Q2
N990	60	6.98	1.14	8.38	1.09	8.38	1.06	6.98	1.08
		12.57	1.08	19.55	1.08	19.55	1.06	12.57	1.10
		32.11	1.08	60.04	1.08	60.04	1.07	32.11	1.08
		97.74	1.10	167.55	1.07	167.55	1.05	97.74	1.09
		251.33	1.06	335.10	1.08	335.10	1.06	251.33	1.07
		418.88	1.07	481.71	1.08	481.71	1.07	418.88	1.08
		544.54	1.08	600.39	1.09	600.39	1.08	544.54	1.09
		656.24	1.08	712.09	1.10	712.09	1.09	656.24	1.08
		767.94	1.09	837.76	1.10	837.76	1.09	767.94	1.09
		893.61	1.09	949.46	1.10	949.46	1.10	893.61	1.09

Table A9 Strain sweep test results at 60°C and 1 rad/s as measured by the RPA2000 of HNBR compounds filled with various CB characteristics and loadings: (a) Storage modulus (G′)

1) N326

Strain amplitude (%)	G′ (kPa)				
	0 phr	10 phr	20 phr	40 phr	60 phr
0.56	943.88	1326.80	1521.30	2211.80	27702.00
0.70	927.81	1199.30	1419.80	2143.70	3465.40
0.98	918.06	1175.70	1422.40	2068.90	3227.20
1.95	924.85	1196.40	1394.50	1977.50	2944.40
3.07	929.36	1205.80	1384.60	1933.50	2805.20
5.02	931.28	1204.10	1359.00	1858.60	2597.20
6.98	926.94	1201.20	1338.80	1796.50	2446.30
10.04	921.62	1186.70	1301.50	1710.80	2291.60
15.07	907.15	1157.90	1261.00	1624.30	2128.30
19.95	893.44	1128.40	1226.30	1562.00	2013.00
29.99	861.85	1070.90	1163.00	1453.60	1819.40
40.04	835.20	1024.00	1106.70	1363.60	1669.20
49.94	806.94	980.27	1055.70	1284.60	1545.20
59.99	780.41	940.85	1010.60	1216.70	1441.30
70.03	755.73	904.57	965.01	1147.70	1333.10
79.93	732.17	872.43	925.02	1081.90	1247.90

Table A9 Strain sweep test results at 60°C and 1 rad/s as measured by the RPA2000 of HNBR compounds filled with various CB characteristics and loadings (cont.): (a) Storage modulus (G′)

2) N550

Strain amplitude (%)	G′ (kPa)				
	0 phr	10 phr	20 phr	40 phr	60 phr
0.56	943.88	1272.90	1486.90	2381.70	3658.20
0.70	927.81	1230.80	1451.30	2223.20	3321.90
0.98	918.06	1228.40	1432.90	2179.30	3124.00
1.95	924.85	1212.30	1434.60	2079.60	2887.30
3.07	929.36	1203.70	1439.30	2042.80	2763.90
5.02	931.28	1191.10	1432.80	1979.80	2568.30
6.98	926.94	1178.30	1421.50	1923.40	2437.20
10.04	921.62	1157.60	1393.00	1852.70	2316.70
15.07	907.15	1130.10	1354.90	1750.80	2189.20
19.95	893.44	1107.00	1316.70	1682.00	2096.70
29.99	861.85	1056.10	1250.10	1565.80	1915.00
40.04	835.20	1014.10	1194.40	1464.30	1756.90
49.94	806.94	974.03	1144.70	1385.10	1626.20
59.99	780.41	936.54	1099.40	1315.70	1535.10
70.03	755.73	901.58	1056.00	1255.90	1449.70
79.93	732.17	870.37	1012.40	1190.10	1365.40

3) N774

Strain amplitude (%)	G′ (kPa)				
	0 phr	10 phr	20 phr	40 phr	60 phr
0.56	943.88	1237.80	1476.20	1967.00	2568.00
0.70	927.81	1165.20	1416.90	1853.00	2429.00
0.98	918.06	1155.70	1385.20	1814.60	2320.70
1.95	924.85	1134.30	1359.50	1739.40	2247.20
3.07	929.36	1121.40	1344.90	1719.10	2224.70
5.02	931.28	1112.00	1321.50	1674.30	2156.30
6.98	926.94	1105.70	1306.70	1647.50	2101.40
10.04	921.62	1093.20	1283.30	1598.30	2017.80
15.07	907.15	1072.20	1245.20	1536.00	1920.80
19.95	893.44	1051.60	1211.10	1482.50	1842.10
29.99	861.85	1008.50	1149.30	1388.90	1696.50
40.04	835.20	967.84	1093.60	1309.80	1571.40
49.94	806.94	930.53	1045.20	1242.00	1448.90
59.99	780.41	891.13	1000.50	1175.80	1334.80
70.03	755.73	855.79	960.35	1108.60	1270.70
79.93	732.17	817.89	919.20	1038.30	1224.40

Table A9 Strain sweep test results at 60°C and 1 rad/s as measured by the RPA2000 of HNBR compounds filled with various CB characteristics and loadings (cont.): (a) Storage modulus (G′)

4) N990

Strain amplitude (%)	G′ (kPa)				
	0 phr	10 phr	20 phr	40 phr	60 phr
0.56	943.88	1142.80	1317.30	1524.40	1896.00
0.70	927.81	1149.10	1269.20	1516.30	1760.40
0.98	918.06	1100.20	1227.30	1472.50	1767.70
1.95	924.85	1080.90	1220.80	1453.10	1736.00
3.07	929.36	1055.80	1190.50	1421.90	1742.80
5.02	931.28	1043.70	1188.80	1395.70	1720.20
6.98	926.94	1032.70	1174.90	1370.00	1697.10
10.04	921.62	1013.30	1150.40	1335.80	1643.60
15.07	907.15	992.02	1122.80	1297.60	1572.70
19.95	893.44	970.13	1095.60	1261.40	1515.20
29.99	861.85	927.97	1047.60	1193.10	1413.30
40.04	835.20	888.10	999.45	1130.30	1328.50
49.94	806.94	852.07	954.59	1073.80	1249.80
59.99	780.41	815.84	908.74	1019.00	1173.50
70.03	755.73	781.07	864.57	962.11	1090.10
79.93	732.17	747.86	821.23	906.05	1033.60

Table A9 Strain sweep test results at 60°C and 1 rad/s as measured by the RPA2000 of HNBR compounds filled with various CB characteristics and loadings (cont.): (b) Loss modulus (G″)

1) N326

Strain amplitude (%)	G″ (kPa)				
	0 phr	10 phr	20 phr	40 phr	60 phr
0.56	71.72	171.13	179.49	295.23	24773.00
0.70	79.51	125.26	158.26	289.95	558.18
0.98	78.10	106.26	168.10	298.48	545.23
1.95	82.20	119.37	158.98	294.90	546.50
3.07	82.07	118.93	155.97	292.11	543.84
5.02	82.15	121.15	163.67	288.97	526.37
6.98	80.94	122.19	161.37	284.86	497.67
10.04	81.55	121.93	161.35	279.56	469.07
15.07	82.74	121.07	162.11	271.13	433.78
19.95	84.16	125.87	162.81	265.60	411.44
29.99	89.49	133.39	165.39	261.62	388.09
40.04	91.78	136.64	166.08	256.91	371.27
49.94	94.70	140.35	167.63	255.77	363.76
59.99	97.36	142.31	170.29	258.07	361.10
70.03	101.64	149.66	177.30	268.35	373.52
79.93	104.69	158.97	187.77	281.88	379.81

2) N550

Strain amplitude (%)	G″ (kPa)				
	0 phr	10 phr	20 phr	40 phr	60 phr
0.56	71.72	105.19	159.88	291.93	588.89
0.70	79.51	124.51	142.51	288.42	526.36
0.98	78.10	118.53	143.45	284.47	520.66
1.95	82.20	125.69	145.41	285.82	548.74
3.07	82.07	124.32	152.14	283.35	535.88
5.02	82.15	128.08	151.09	281.30	516.68
6.98	80.94	125.72	152.09	272.21	490.70
10.04	81.55	125.76	151.79	266.65	458.13
15.07	82.74	127.49	153.19	260.64	419.04
19.95	84.16	129.17	155.37	260.19	395.05
29.99	89.49	134.70	162.42	257.93	377.83
40.04	91.78	135.04	164.50	256.62	382.35
49.94	94.70	135.55	168.88	255.32	396.85
59.99	97.36	135.24	172.05	257.91	400.60
70.03	101.64	136.13	179.75	263.58	401.29
79.93	104.69	137.46	190.38	272.61	396.67

Table A9 Strain sweep test results at 60°C and 1 rad/s as measured by the RPA2000 of HNBR compounds filled with various CB characteristics and loadings (cont.): (b) Loss modulus (G″)

3) N774

Strain amplitude (%)	G″ (kPa)				
	0 phr	10 phr	20 phr	40 phr	60 phr
0.56	71.72	116.72	163.80	233.54	322.13
0.70	79.51	133.12	133.88	221.87	326.68
0.98	78.10	113.68	144.39	228.98	314.52
1.95	82.20	113.67	150.57	226.82	330.80
3.07	82.07	113.37	150.93	228.82	329.49
5.02	82.15	110.72	146.32	225.80	327.97
6.98	80.94	109.56	146.28	222.92	322.43
10.04	81.55	109.98	144.78	218.84	311.23
15.07	82.74	110.68	145.92	216.65	301.13
19.95	84.16	112.67	147.90	216.91	296.38
29.99	89.49	116.41	149.31	215.00	302.04
40.04	91.78	118.86	151.26	215.27	315.91
49.94	94.70	120.41	152.45	218.19	338.58
59.99	97.36	122.10	156.44	224.42	376.06
70.03	101.64	126.32	165.98	242.78	392.56
79.93	104.69	134.80	182.74	264.55	389.65

4) N990

Strain amplitude (%)	G″ (kPa)				
	0 phr	10 phr	20 phr	40 phr	60 phr
0.56	71.72	114.76	142.22	161.62	186.36
0.70	79.51	103.28	126.23	143.06	178.51
0.98	78.10	110.45	116.91	149.24	186.95
1.95	82.20	110.66	126.51	157.11	190.72
3.07	82.07	110.43	124.75	151.80	193.52
5.02	82.15	108.59	122.00	153.22	192.11
6.98	80.94	106.86	118.28	149.33	192.87
10.04	81.55	105.94	115.87	147.22	194.82
15.07	82.74	106.89	115.40	147.48	199.42
19.95	84.16	109.40	118.45	148.97	201.44
29.99	89.49	112.32	120.81	153.37	205.76
40.04	91.78	114.36	124.67	156.73	210.02
49.94	94.70	117.19	128.39	162.13	218.08
59.99	97.36	118.89	131.78	172.20	237.57
70.03	101.64	120.85	136.96	187.22	271.15
79.93	104.69	126.11	148.47	203.79	281.02

Table A10 Temperature sweep test results at 62.8 rad/s as measured by the DMA of HNBR compounds filled with various CB characteristics and loadings: (a) Storage modulus (G′)

1) N326

0 phr		10 phr		20 phr		40 phr		60 phr	
Temp.(C°)	G′ (MPa)	Temp.(C°)	G′ (MPa)	Temp.(C°)	G′ (MPa)	Temp.(C°)	G′ (MPa)	Temp.(C°)	G′ (MPa)
-80.1	2590.50	-82.1	2917.08	-81.1	3371.53	-81.0	3858.72	-79.8	3955.01
-79.6	2594.41	-79.8	2937.01	-79.3	3229.65	-78.6	3830.05	-77.2	3973.79
-78.1	2571.16	-77.2	2924.39	-77.3	3209.81	-76.9	3786.74	-74.0	3935.63
-75.8	2534.68	-74.7	2893.92	-75.2	3176.67	-75.3	3749.35	-70.9	3877.07
-72.8	2480.94	-72.7	2870.00	-73.0	3137.57	-73.4	3709.35	-69.9	3845.69
-70.8	2443.93	-70.7	2838.04	-71.0	3100.09	-71.4	3661.24	-67.0	3776.73
-69.0	2403.53	-69.1	2810.32	-69.2	3060.09	-69.1	3603.47	-63.9	3710.78
-67.2	2364.91	-67.2	2765.93	-67.2	3013.66	-67.2	3564.97	-61.5	3644.07
-65.0	2319.63	-65.1	2732.62	-65.4	2966.00	-65.4	3525.49	-58.6	3568.65
-63.3	2278.99	-63.3	2690.71	-63.2	2922.45	-63.2	3463.40	-55.4	3513.91
-61.3	2234.60	-61.1	2646.09	-60.9	2875.75	-61.3	3418.69	-54.3	3493.08
-59.1	2189.45	-58.9	2602.53	-59.3	2842.42	-59.0	3357.72	-53.5	3477.56
-57.0	2145.52	-57.1	2558.44	-57.0	2800.76	-57.1	3299.28	-52.5	3454.05
-54.6	2110.26	-55.1	2510.27	-55.2	2766.78	-55.2	3244.64	-51.6	3435.57
-52.9	2087.62	-52.9	2461.39	-53.1	2715.71	-52.9	3182.21	-50.3	3411.97
-51.3	2043.89	-50.8	2409.64	-51.0	2676.59	-51.0	3131.64	-49.3	3384.86
-49.0	1990.56	-48.7	2366.60	-49.3	2635.87	-48.8	3069.66	-48.2	3361.04
-46.7	1954.07	-46.8	2327.92	-47.2	2589.21	-46.7	3017.79	-46.7	3325.02
-44.9	1914.04	-44.9	2276.31	-44.7	2537.09	-45.0	2973.09	-44.8	3268.72
-42.9	1862.60	-42.7	2205.07	-43.2	2485.15	-42.9	2911.42	-42.9	3220.38
-40.7	1802.77	-40.5	2137.58	-41.2	2423.35	-41.0	2843.61	-40.9	3160.35
-38.8	1746.78	-38.6	2057.67	-38.8	2335.52	-39.0	2766.96	-38.8	3084.31
-36.7	1681.55	-36.5	1967.27	-37.0	2235.93	-36.9	2657.86	-36.8	2973.97
-34.8	1611.48	-34.6	1842.68	-34.8	2101.16	-35.1	2543.70	-34.7	2824.70
-32.5	1445.58	-32.7	1670.61	-32.8	1853.30	-32.8	2331.97	-32.7	2591.66
-30.5	1245.11	-30.5	1403.29	-30.7	1525.53	-30.8	2010.36	-30.7	2248.33
-28.6	997.53	-28.6	1122.00	-28.5	1221.83	-28.6	1646.01	-28.5	1812.87
-26.7	718.17	-26.6	807.84	-26.4	887.91	-26.6	1266.09	-26.6	1424.29
-24.7	485.73	-24.6	534.37	-24.7	619.25	-24.8	864.91	-24.5	1051.65
-22.6	270.80	-22.6	326.17	-22.6	387.20	-22.7	523.12	-22.6	747.13
-20.7	145.21	-20.5	181.23	-20.4	227.18	-20.7	349.05	-20.6	516.44
-18.6	72.77	-18.6	107.34	-18.7	150.80	-18.4	233.91	-18.6	365.35
-16.7	42.27	-16.5	66.43	-16.6	97.01	-16.7	169.05	-16.5	271.29
-14.6	28.14	-14.7	47.06	-14.5	67.18	-14.6	125.66	-14.5	211.07
-12.6	20.94	-12.7	34.17	-12.6	49.34	-12.7	97.29	-12.6	172.98
-10.5	16.97	-10.6	26.34	-10.6	37.91	-10.6	78.33	-10.6	146.05
-8.6	14.23	-8.6	21.72	-8.7	31.31	-8.6	67.72	-8.6	126.67
-6.6	12.26	-6.6	18.62	-6.6	26.59	-6.7	59.79	-6.6	112.75
-4.6	10.86	-4.6	16.53	-4.7	23.38	-4.6	53.46	-4.5	101.25

Table A10 Temperature sweep test results at 62.8 rad/s as measured by the DMA of HNBR compounds filled with various CB characteristics and loadings (cont.): (a) Storage modulus (G′)

0 phr		10 phr		20 phr		40 phr		60 phr	
Temp.(C°)	G′ (MPa)	Temp.(C°)	G′ (MPa)	Temp.(C°)	G′ (MPa)	Temp.(C°)	G′ (MPa)	Temp.(C°)	G′ (MPa)
-2.5	9.66	-2.5	14.92	-2.6	21.17	-2.6	48.79	-2.5	92.38
-0.7	9.09	-0.7	13.86	-0.7	19.22	-0.6	45.25	-0.6	85.18
4.1	8.41	4.0	12.79	5.0	17.50	5.3	40.79	3.5	78.36
3.9	8.24	3.9	12.19	4.6	16.85	5.0	39.00	3.5	74.87
5.2	8.00	5.3	12.00	4.5	16.63	4.6	38.50	5.3	71.63
7.4	7.77	7.5	11.59	7.3	15.99	7.3	36.69	7.5	68.10
9.5	7.56	9.4	11.25	9.4	15.43	9.4	35.13	9.6	65.06
11.4	7.40	11.4	11.00	11.5	14.92	11.3	33.77	11.5	62.90
13.5	7.28	13.5	10.77	13.7	14.51	13.6	32.39	13.4	61.16
15.4	7.14	15.2	10.64	15.4	14.21	15.5	31.33	15.4	59.24
17.4	7.05	17.4	10.49	17.4	13.96	17.3	30.50	17.4	57.29
19.3	6.97	19.3	10.29	19.4	13.69	19.4	29.69	19.4	55.24
21.4	6.86	21.4	10.10	21.3	13.49	21.4	28.94	21.2	53.43
23.5	6.77	23.3	9.91	23.3	13.31	23.5	28.29	23.4	51.65
25.3	6.69	25.3	9.74	25.5	13.04	25.4	27.60	25.4	49.97
27.3	6.57	27.4	9.58	27.7	12.80	27.5	26.85	27.6	48.47
29.4	6.49	29.4	9.41	29.3	12.57	29.7	26.16	29.4	47.12
31.4	6.43	31.5	9.26	31.3	12.37	31.2	25.75	31.6	45.74
33.5	6.34	33.5	9.09	33.5	12.16	33.2	25.22	33.4	44.55
35.4	6.26	35.3	8.95	35.5	11.96	35.5	24.60	35.3	43.39
37.3	6.20	37.5	8.82	37.4	11.79	37.4	24.06	37.4	42.22
39.5	6.13	39.4	8.70	39.3	11.62	39.3	23.60	39.4	41.13
41.4	6.06	41.5	8.57	41.2	11.42	41.6	23.02	41.6	39.94
43.3	6.02	43.7	8.45	43.4	11.29	43.7	22.52	43.5	38.91
45.3	5.96	45.4	8.35	45.0	11.10	45.4	22.07	45.5	37.81
47.4	5.89	47.7	8.23	47.1	10.96	47.7	21.53	47.6	36.58
49.5	5.84	49.7	8.13	49.3	10.83	49.6	21.13	49.4	35.67
51.4	5.76	51.3	8.01	51.3	10.67	51.5	20.72	51.3	34.69
53.3	5.72	53.0	7.91	53.4	10.50	53.3	20.26	53.3	33.78
55.4	5.65	55.4	7.77	55.6	10.34	55.5	19.82	55.7	32.82
57.6	5.58	57.0	7.72	57.4	10.19	57.5	19.40	57.5	31.94
59.3	5.54	59.4	7.53	59.4	10.04	59.3	18.96	59.6	31.03
61.3	5.49	61.3	7.46	61.4	9.87	61.4	18.54	61.4	30.20
63.4	5.42	63.5	7.29	63.5	9.71	63.6	18.03	63.4	29.37
65.3	5.35	65.0	7.25	65.5	9.52	65.2	17.65	65.3	28.68
67.5	5.28	67.3	7.10	67.5	9.34	67.3	17.20	67.4	27.85
69.3	5.22	69.0	7.00	69.5	9.19	69.5	16.81	69.8	27.03
71.3	5.17	71.8	6.82	71.6	8.99	71.1	16.46	71.5	26.34
73.1	5.12	73.0	6.83	73.4	8.86	73.4	16.04	73.6	25.70
75.3	5.02	75.7	6.60	75.4	8.69	75.4	15.69	75.6	25.03
77.3	4.96	77.4	6.52	77.5	8.50	77.4	15.33	77.4	24.48

Table A10 Temperature sweep test results at 62.8 rad/s as measured by the DMA of HNBR compounds filled with various CB characteristics and loadings (cont.): (a) Storage modulus (G′)

0 phr		10 phr		20 phr		40 phr		60 phr	
Temp.(C°)	G′ (MPa)	Temp.(C°)	G′ (MPa)	Temp.(C°)	G′ (MPa)	Temp.(C°)	G′ (MPa)	Temp.(C°)	G′ (MPa)
79.5	4.90	79.3	6.42	79.3	8.38	79.2	15.05	79.4	23.90
81.6	4.83	81.6	6.30	81.4	8.24	81.4	14.73	81.6	23.29
83.6	4.78	83.5	6.23	83.7	8.09	83.6	14.44	83.5	22.82
85.5	4.73	85.0	6.19	85.5	7.97	85.4	14.14	85.5	22.29
87.4	4.68	87.8	6.08	87.4	7.86	87.5	13.91	87.4	21.84
89.5	4.63	89.2	6.00	89.3	7.77	89.5	13.67	89.6	21.34
91.5	4.59	91.0	5.95	91.5	7.67	91.4	13.48	91.5	20.92
93.6	4.55	93.1	5.89	93.5	7.57	93.5	13.28	93.4	20.59
95.4	4.54	95.7	5.83	95.2	7.51	95.5	13.15	95.1	20.26
97.2	4.53	97.1	5.79	97.5	7.43	97.7	12.97	97.4	19.96
99.2	4.48	99.0	5.82	99.4	7.41	99.5	12.82	99.3	19.72
101.0	4.49	101.1	5.73	101.7	7.37	101.4	12.76	101.6	19.42
103.5	4.46	103.5	5.70	103.6	7.34	103.5	12.64	103.6	19.16
105.4	4.44	105.4	5.71	105.3	7.28	105.5	12.51	105.3	18.92
107.3	4.44	107.2	5.70	107.7	7.25	107.2	12.41	107.4	18.69
109.5	4.45	109.4	5.66	109.5	7.23	109.1	12.32	109.3	18.50
111.1	4.46	111.2	5.65	111.4	7.21	111.2	12.21	111.4	18.27
113.3	4.44	113.7	5.63	113.4	7.20	113.5	12.11	113.7	18.05
115.3	4.43	115.2	5.69	115.4	7.17	115.6	12.01	115.6	17.85
117.8	4.43	117.5	5.59	117.4	7.13	117.5	11.91	117.7	17.67
119.2	4.45	119.4	5.59	119.6	7.08	119.1	11.85	119.5	17.49
121.6	4.43	121.3	5.58	121.5	7.07	121.3	11.79	121.5	17.34
123.5	4.44	123.3	5.56	123.5	7.07	123.4	11.72	123.4	17.18
125.6	4.45	125.7	5.55	125.5	7.05	125.7	11.61	125.8	17.00
127.1	4.42	127.2	5.53	127.4	7.04	127.3	11.55	127.8	16.86
129.6	4.43	129.3	5.53	129.5	7.02	129.7	11.49	129.5	16.74
131.5	4.44	131.2	5.52	131.6	6.99	131.4	11.44	131.6	16.59
133.6	4.44	133.0	5.52	133.6	6.99	133.5	11.38	133.4	16.41
135.4	4.46	135.1	5.51	135.6	7.00	135.5	11.31	135.1	16.31
138.0	4.43	137.7	5.51	137.8	6.98	137.8	11.23	137.6	16.35
139.6	4.47	139.9	5.52	139.6	6.96	139.4	11.14	140.4	16.31
141.5	4.46	141.2	5.59	141.2	6.96	141.5	11.14	141.5	15.93
143.3	4.46	143.4	5.49	143.2	6.95	143.4	11.10	144.0	16.08
145.1	4.48	145.3	5.49	145.3	6.93	145.2	11.04	145.2	15.87
147.5	4.46	147.5	5.50	147.1	6.92	147.4	10.99	146.5	15.93
149.1	4.48	149.3	5.50	149.4	6.91	149.5	10.92	149.5	15.82

Table A10 Temperature sweep test results at 62.8 rad/s as measured by the DMA of HNBR compounds filled with various CB characteristics and loadings (cont.): (a) Storage modulus (G′)

2) N550

0 phr		10 phr		20 phr		40 phr		60 phr	
Temp.(C°)	G′ (MPa)	Temp.(C°)	G′ (MPa)	Temp.(C°)	G′ (MPa)	Temp.(C°)	G′ (MPa)	Temp.(C°)	G′ (MPa)
-80.1	2590.50	-79.3	2752.87	-80.2	3345.97	-80.3	3908.55	-80.0	4467.16
-79.6	2594.41	-79.3	2774.61	-79.5	3333.88	-77.0	3910.74	-77.7	4356.46
-78.1	2571.16	-77.2	2766.09	-77.7	3252.30	-73.2	3831.08	-74.6	4298.48
-75.8	2534.68	-74.9	2746.17	-75.6	3168.69	-72.2	3658.76	-71.5	4226.24
-72.8	2480.94	-73.1	2720.31	-73.6	3119.18	-71.3	3629.21	-68.8	4152.39
-70.8	2443.93	-70.9	2685.91	-71.3	3069.23	-70.3	3607.64	-67.6	4122.69
-69.0	2403.53	-68.9	2650.94	-69.2	3026.29	-68.8	3563.51	-64.9	4051.37
-67.2	2364.91	-67.1	2610.59	-67.0	2978.69	-66.9	3506.63	-62.1	3974.75
-65.0	2319.63	-64.7	2564.27	-65.5	2937.16	-65.1	3457.68	-59.3	3897.65
-63.3	2278.99	-63.0	2532.83	-63.2	2883.09	-63.0	3393.22	-56.3	3819.83
-61.3	2234.60	-61.0	2492.59	-61.1	2831.65	-61.0	3343.30	-55.2	3781.91
-59.1	2189.45	-59.1	2458.18	-59.1	2789.23	-58.9	3287.91	-52.5	3720.20
-57.0	2145.52	-57.1	2416.40	-57.4	2744.33	-56.9	3239.59	-49.6	3640.58
-54.6	2110.26	-55.0	2376.05	-55.2	2679.24	-55.0	3187.02	-48.4	3610.95
-52.9	2087.62	-53.1	2335.94	-53.0	2633.25	-53.1	3129.94	-47.5	3580.17
-51.3	2043.89	-50.9	2291.01	-50.9	2592.53	-51.0	3064.18	-46.3	3550.47
-49.0	1990.56	-48.9	2253.23	-48.9	2552.61	-48.9	3002.10	-45.4	3523.06
-46.7	1954.07	-47.0	2213.35	-46.9	2516.42	-46.9	2958.18	-44.3	3488.55
-44.9	1914.04	-44.9	2169.51	-45.1	2477.71	-44.9	2909.17	-43.3	3450.30
-42.9	1862.60	-42.8	2122.68	-43.0	2427.42	-42.8	2853.08	-42.2	3410.74
-40.7	1802.77	-40.9	2075.50	-40.8	2355.94	-40.8	2792.18	-40.9	3357.60
-38.8	1746.78	-38.9	2017.25	-38.9	2237.82	-38.7	2731.21	-38.8	3266.24
-36.7	1681.55	-36.8	1935.90	-36.6	2091.95	-36.8	2644.91	-36.9	3138.92
-34.8	1611.48	-34.6	1818.51	-34.8	1948.57	-34.7	2520.20	-34.8	2970.78
-32.5	1445.58	-32.6	1646.76	-32.4	1705.37	-32.6	2321.30	-32.8	2715.01
-30.5	1245.11	-30.6	1424.93	-30.5	1499.72	-30.4	1985.50	-30.6	2329.71
-28.6	997.53	-28.5	1136.66	-29.1	1260.89	-28.4	1622.55	-28.5	1849.61
-26.7	718.17	-26.6	835.83	-26.3	769.25	-26.5	1258.07	-26.5	1433.64
-24.7	485.73	-24.5	552.10	-24.7	555.31	-24.5	892.41	-24.6	1044.21
-22.6	270.80	-22.6	338.89	-22.3	323.01	-22.6	602.19	-22.7	723.71
-20.7	145.21	-20.6	198.88	-20.5	208.44	-20.6	376.49	-20.7	488.62
-18.6	72.77	-18.7	119.51	-18.8	130.95	-18.6	241.10	-18.6	338.96
-16.7	42.27	-16.7	72.94	-16.5	85.31	-16.7	163.99	-16.6	252.19
-14.6	28.14	-14.6	48.85	-14.8	59.16	-14.6	115.57	-14.6	194.10
-12.6	20.94	-12.5	35.23	-12.8	39.31	-12.7	86.95	-12.6	156.65
-10.5	16.97	-10.6	27.58	-10.5	31.07	-10.6	68.88	-10.6	131.69
-8.6	14.23	-8.6	22.80	-8.6	26.74	-8.6	57.20	-8.6	113.81
-6.6	12.26	-6.5	19.39	-6.6	23.57	-6.6	49.66	-6.6	100.44
-4.6	10.86	-4.7	17.24	-4.6	21.27	-4.6	44.40	-4.6	91.06

Table A10 Temperature sweep test results at 62.8 rad/s as measured by the DMA of HNBR compounds filled with various CB characteristics and loadings (cont.): (a) Storage modulus (G′)

0 phr		10 phr		20 phr		40 phr		60 phr	
Temp.(C°)	G′ (MPa)	Temp.(C°)	G′ (MPa)	Temp.(C°)	G′ (MPa)	Temp.(C°)	G′ (MPa)	Temp.(C°)	G′ (MPa)
-2.5	9.66	-2.6	15.58	-2.6	19.80	-2.6	39.99	-2.6	82.75
-0.7	9.09	-0.6	14.39	-0.7	18.46	-0.6	37.00	-0.7	77.09
4.1	8.41	3.4	13.43	4.8	16.99	3.7	34.25	3.1	71.67
3.9	8.24	3.6	12.82	4.5	16.21	3.9	33.01	3.4	68.91
5.2	8.00	5.3	12.60	4.4	16.03	5.2	31.89	5.3	66.09
7.4	7.77	7.0	12.19	7.4	15.55	7.5	30.45	7.5	63.30
9.5	7.56	9.5	11.81	9.4	15.04	9.5	29.33	9.5	61.24
11.4	7.40	11.7	11.52	11.4	14.63	11.5	28.41	11.4	59.51
13.5	7.28	13.5	11.35	13.4	14.26	13.5	27.77	13.4	57.91
15.4	7.14	15.4	11.21	15.4	13.94	15.3	27.32	15.4	56.10
17.4	7.05	17.3	11.02	17.4	13.68	17.4	26.71	17.3	54.28
19.3	6.97	19.2	10.82	19.5	13.43	19.3	26.12	19.2	52.42
21.4	6.86	21.4	10.62	21.6	13.25	21.4	25.49	21.2	50.89
23.5	6.77	23.5	10.43	23.4	13.09	23.4	24.83	23.5	49.51
25.3	6.69	25.4	10.27	25.4	12.88	25.4	24.30	25.2	48.31
27.3	6.57	27.4	10.10	28.1	12.73	27.4	23.77	27.3	47.05
29.4	6.49	29.4	9.93	29.1	12.61	29.4	23.26	29.4	45.76
31.4	6.43	31.3	9.79	31.4	12.39	31.6	22.77	31.4	44.66
33.5	6.34	33.5	9.66	33.4	12.21	33.5	22.33	33.5	43.58
35.4	6.26	35.4	9.53	35.4	12.01	35.6	21.91	35.5	42.60
37.3	6.20	37.8	9.34	37.5	11.82	37.4	21.53	37.3	41.64
39.5	6.13	39.6	9.20	39.4	11.67	39.3	21.10	39.4	40.70
41.4	6.06	41.4	9.11	41.6	11.45	41.3	20.74	41.6	39.60
43.3	6.02	43.5	8.99	43.5	11.31	43.5	20.39	43.4	38.65
45.3	5.96	45.3	8.88	45.2	11.15	45.7	19.97	45.4	37.72
47.4	5.89	47.6	8.75	47.1	10.99	47.2	19.66	47.6	36.81
49.5	5.84	49.6	8.65	49.4	10.83	49.2	19.32	49.2	36.06
51.4	5.76	51.6	8.52	51.5	10.69	50.9	19.02	51.2	35.21
53.3	5.72	53.4	8.42	53.3	10.59	53.5	18.64	53.0	34.48
55.4	5.65	55.5	8.31	55.5	10.40	55.6	18.28	55.3	33.58
57.6	5.58	57.7	8.21	57.4	10.27	57.4	17.97	57.1	32.89
59.3	5.54	59.2	8.10	59.5	10.13	59.5	17.62	59.7	31.94
61.3	5.49	61.3	8.01	61.5	9.98	61.1	17.33	61.5	31.26
63.4	5.42	63.4	7.88	63.4	9.83	63.0	17.07	63.3	30.63
65.3	5.35	65.6	7.76	65.5	9.70	65.3	16.70	65.4	29.93
67.5	5.28	67.4	7.67	67.5	9.54	67.1	16.41	67.6	29.20
69.3	5.22	69.4	7.54	69.5	9.38	69.2	16.10	69.4	28.55
71.3	5.17	71.4	7.41	71.4	9.23	71.1	15.80	71.7	27.85
73.1	5.12	73.5	7.30	73.4	9.04	73.2	15.45	73.5	27.22
75.3	5.02	75.8	7.13	75.6	8.89	75.1	15.23	75.4	26.70
77.3	4.96	77.6	7.03	77.3	8.78	77.2	14.94	77.5	26.07

Table A10 Temperature sweep test results at 62.8 rad/s as measured by the DMA of HNBR compounds filled with various CB characteristics and loadings (cont.): (a) Storage modulus (G′)

0 phr		10 phr		20 phr		40 phr		60 phr	
Temp.(C°)	G′ (MPa)	Temp.(C°)	G′ (MPa)	Temp.(C°)	G′ (MPa)	Temp.(C°)	G′ (MPa)	Temp.(C°)	G′ (MPa)
79.5	4.90	79.6	6.90	79.5	8.57	79.6	14.63	79.5	25.51
81.6	4.83	81.5	6.81	81.3	8.47	81.6	14.37	81.2	25.02
83.6	4.78	83.7	6.71	83.6	8.31	83.9	14.14	83.4	24.50
85.5	4.73	86.0	6.59	85.2	8.29	86.1	13.89	85.5	24.02
87.4	4.68	87.6	6.52	87.3	8.09	87.0	13.73	87.4	23.54
89.5	4.63	89.1	6.48	89.4	7.98	89.1	13.51	89.5	23.09
91.5	4.59	91.8	6.36	91.4	7.92	91.5	13.33	91.7	22.67
93.6	4.55	93.6	6.30	93.5	7.83	93.7	13.17	93.7	22.22
95.4	4.54	95.7	6.23	95.5	7.74	95.3	13.03	95.6	21.87
97.2	4.53	97.0	6.21	97.4	7.72	97.2	12.86	97.7	21.55
99.2	4.48	99.6	6.14	99.7	7.64	99.1	12.75	99.8	21.27
101.0	4.49	101.0	6.13	101.5	7.62	101.7	12.64	101.8	20.97
103.5	4.46	103.6	6.11	103.4	7.61	103.6	12.54	103.5	20.74
105.4	4.44	105.5	6.07	105.3	7.57	105.2	12.44	105.3	20.51
107.3	4.44	107.2	6.07	107.5	7.55	107.1	12.36	107.4	20.30
109.5	4.45	109.8	6.05	109.4	7.53	109.0	12.29	109.3	20.06
111.1	4.46	111.2	6.08	111.4	7.49	111.3	12.21	111.5	19.86
113.3	4.44	113.5	6.00	113.4	7.50	112.9	12.10	113.4	19.69
115.3	4.43	115.5	6.00	115.4	7.46	115.9	12.04	115.8	19.44
117.8	4.43	117.8	5.97	117.5	7.42	118.2	12.00	117.4	19.23
119.2	4.45	119.1	5.99	119.3	7.42	119.5	11.92	119.6	19.08
121.6	4.43	121.0	5.98	121.6	7.39	121.5	11.85	121.6	18.89
123.5	4.44	123.7	5.95	123.8	7.39	123.4	11.78	123.4	18.72
125.6	4.45	125.8	5.95	125.6	7.38	125.9	11.72	125.4	18.60
127.1	4.42	128.3	5.93	127.3	7.40	127.7	11.69	127.2	18.45
129.6	4.43	129.8	5.93	129.5	7.37	129.8	11.65	129.2	18.30
131.5	4.44	131.6	5.93	131.5	7.37	131.1	11.60	131.4	18.12
133.6	4.44	133.1	5.94	133.3	7.35	133.2	11.55	133.4	17.99
135.4	4.46	135.5	5.93	135.2	7.32	135.3	11.51	135.7	17.82
138.0	4.43	137.3	5.90	137.2	7.38	137.4	11.47	137.5	17.70
139.6	4.47	138.7	5.98	139.4	7.33	139.4	11.43	139.4	17.58
141.5	4.46	141.3	5.88	141.5	7.31	141.3	11.39	141.5	17.46
143.3	4.46	143.1	5.90	143.6	7.28	143.6	11.34	143.6	17.30
145.1	4.48	145.2	5.92	145.8	7.30	145.4	11.29	145.7	17.17
147.5	4.46	147.1	5.92	147.8	7.28	147.4	11.26	147.8	17.05
149.1	4.48	149.3	5.93	149.3	7.25	149.5	11.23	149.6	16.96

Table A10 Temperature sweep test results at 62.8 rad/s as measured by the DMA of HNBR compounds filled with various CB characteristics and loadings (cont.): (a) Storage modulus (G′)

3) N774

0 phr		10 phr		20 phr		40 phr		60 phr	
Temp.(C°)	G′ (MPa)	Temp.(C°)	G′ (MPa)	Temp.(C°)	G′ (MPa)	Temp.(C°)	G′ (MPa)	Temp.(C°)	G′ (MPa)
-80.1	2590.50	-81.6	2846.47	-80.2	3365.32	-80.6	3674.76	-80.4	4474.25
-79.6	2594.41	-80.2	2854.59	-80.0	3362.98	-79.3	3679.52	-78.3	4487.77
-78.1	2571.16	-76.9	2814.85	-77.9	3323.06	-78.2	3665.42	-74.4	4422.95
-75.8	2534.68	-74.5	2781.02	-75.7	3285.52	-74.5	3601.73	-71.5	4350.96
-72.8	2480.94	-72.6	2749.50	-73.8	3236.70	-72.6	3560.36	-68.5	4264.95
-70.8	2443.93	-71.4	2722.90	-71.3	3180.67	-70.6	3509.14	-65.8	4187.61
-69.0	2403.53	-69.3	2677.15	-69.1	3131.06	-69.4	3467.04	-64.5	4147.83
-67.2	2364.91	-67.1	2645.91	-67.0	3083.52	-66.8	3409.18	-61.8	4063.19
-65.0	2319.63	-65.2	2605.91	-64.7	3032.41	-65.0	3363.91	-60.6	4033.03
-63.3	2278.99	-63.3	2563.02	-62.9	2984.57	-63.0	3299.33	-57.7	3939.95
-61.3	2234.60	-61.4	2519.68	-61.2	2942.92	-61.3	3239.83	-55.0	3860.68
-59.1	2189.45	-58.8	2473.45	-59.4	2895.82	-59.2	3176.41	-52.2	3764.88
-57.0	2145.52	-57.1	2434.03	-57.2	2854.98	-56.2	3111.72	-49.2	3670.76
-54.6	2110.26	-55.4	2387.10	-55.5	2813.40	-54.6	3066.38	-46.3	3575.66
-52.9	2087.62	-53.3	2348.82	-53.1	2763.21	-53.2	3006.63	-43.4	3473.31
-51.3	2043.89	-50.9	2310.95	-50.8	2721.21	-50.5	2943.25	-42.3	3435.41
-49.0	1990.56	-49.2	2281.29	-49.1	2675.46	-48.9	2912.76	-41.4	3390.24
-46.7	1954.07	-46.7	2239.30	-47.2	2626.21	-46.9	2859.29	-40.3	3340.52
-44.9	1914.04	-45.3	2206.42	-45.4	2572.16	-45.1	2826.09	-39.1	3282.39
-42.9	1862.60	-43.2	2162.12	-43.1	2498.66	-43.3	2770.57	-38.1	3222.25
-40.7	1802.77	-41.2	2109.78	-41.1	2431.82	-40.8	2691.21	-36.9	3152.06
-38.8	1746.78	-39.1	2031.37	-38.8	2349.52	-38.6	2595.19	-35.9	3073.12
-36.7	1681.55	-36.8	1925.51	-37.0	2261.17	-36.9	2504.98	-34.7	2975.73
-34.8	1611.48	-34.8	1766.14	-34.9	2126.74	-34.9	2357.94	-33.7	2862.61
-32.5	1445.58	-32.6	1593.46	-32.9	1930.08	-33.1	2178.98	-32.6	2709.77
-30.5	1245.11	-30.9	1436.02	-30.7	1656.26	-30.6	1833.62	-30.7	2384.15
-28.6	997.53	-28.6	1204.70	-28.6	1368.85	-28.4	1483.60	-28.4	1921.91
-26.7	718.17	-26.8	906.76	-26.2	995.42	-26.6	1208.83	-26.5	1481.54
-24.7	485.73	-24.5	499.81	-24.9	749.62	-24.9	878.47	-24.6	1047.83
-22.6	270.80	-22.6	265.25	-22.5	409.28	-22.5	529.09	-22.5	710.52
-20.7	145.21	-20.5	135.67	-20.6	237.78	-20.5	315.59	-20.8	492.19
-18.6	72.77	-18.5	70.58	-18.5	137.26	-19.0	210.87	-18.7	320.77
-16.7	42.27	-16.9	46.88	-16.5	80.64	-16.3	117.52	-16.7	220.45
-14.6	28.14	-14.6	32.38	-14.7	57.62	-14.6	82.68	-14.6	161.41
-12.6	20.94	-12.6	24.75	-12.6	42.90	-12.8	64.43	-12.6	122.35
-10.5	16.97	-10.5	20.54	-10.7	34.26	-10.6	52.07	-10.6	99.07
-8.6	14.23	-8.7	19.21	-8.6	28.19	-8.5	44.18	-8.6	82.93
-6.6	12.26	-6.6	16.70	-6.6	23.83	-6.5	38.91	-6.6	71.75
-4.6	10.86	-4.6	14.72	-4.6	21.16	-4.6	35.34	-4.5	63.23

Table A10 Temperature sweep test results at 62.8 rad/s as measured by the DMA of HNBR compounds filled with various CB characteristics and loadings (cont.): (a) Storage modulus (G′)

0 phr		10 phr		20 phr		40 phr		60 phr	
Temp.(C°)	G′ (MPa)	Temp.(C°)	G′ (MPa)	Temp.(C°)	G′ (MPa)	Temp.(C°)	G′ (MPa)	Temp.(C°)	G′ (MPa)
-2.5	9.66	-2.6	13.42	-2.7	19.24	-2.6	32.16	-2.7	56.14
-0.7	9.09	-0.8	12.27	-0.7	17.70	-0.8	30.04	-0.8	51.73
4.1	8.41	5.2	11.23	5.6	15.88	5.2	27.11	3.9	47.37
3.9	8.24	4.9	10.69	5.1	15.28	4.8	25.93	3.9	45.47
5.2	8.00	4.5	10.55	4.7	15.16	4.6	25.63	5.2	43.80
7.4	7.77	7.0	10.28	7.2	14.75	7.3	24.55	7.6	41.81
9.5	7.56	9.5	9.95	9.4	14.30	9.5	23.69	9.5	40.15
11.4	7.40	11.4	9.71	11.5	13.92	11.4	22.95	11.6	38.70
13.5	7.28	13.5	9.44	13.3	13.56	13.3	22.24	13.4	37.66
15.4	7.14	15.5	9.26	15.3	13.29	15.3	21.54	15.4	36.70
17.4	7.05	17.4	9.08	17.4	13.08	17.6	20.92	17.4	35.82
19.3	6.97	19.4	8.89	19.2	12.90	19.4	20.52	19.4	34.84
21.4	6.86	21.7	8.74	21.2	12.73	21.5	20.17	21.5	33.86
23.5	6.77	23.5	8.67	23.4	12.52	23.2	19.85	23.3	33.05
25.3	6.69	25.3	8.49	25.3	12.36	25.1	19.53	25.2	32.19
27.3	6.57	27.3	8.41	27.2	12.19	27.5	19.10	27.2	31.42
29.4	6.49	29.7	8.28	29.1	11.99	29.8	18.69	29.4	30.66
31.4	6.43	31.5	8.19	31.5	11.79	31.3	18.36	31.3	29.96
33.5	6.34	33.5	8.06	33.6	11.57	32.8	18.12	33.4	29.28
35.4	6.26	35.4	7.95	35.5	11.37	35.3	17.75	35.3	28.65
37.3	6.20	37.2	7.86	37.5	11.21	37.3	17.44	37.3	28.03
39.5	6.13	39.2	7.78	39.4	11.05	39.4	17.14	39.5	27.40
41.4	6.06	41.4	7.67	41.3	10.89	41.6	16.85	41.2	26.87
43.3	6.02	43.6	7.57	43.8	10.78	43.5	16.56	43.1	26.32
45.3	5.96	45.3	7.49	45.3	10.62	45.5	16.31	45.6	25.72
47.4	5.89	47.5	7.40	47.3	10.53	47.5	16.06	47.3	25.19
49.5	5.84	49.5	7.33	49.3	10.41	49.5	15.81	49.5	24.69
51.4	5.76	51.3	7.23	51.3	10.29	51.3	15.56	51.6	24.13
53.3	5.72	53.4	7.16	53.3	10.18	53.2	15.35	54.0	23.54
55.4	5.65	55.5	7.09	55.4	10.05	55.2	15.11	55.5	23.11
57.6	5.58	57.3	7.01	57.4	9.92	57.4	14.80	58.1	22.59
59.3	5.54	59.4	6.95	59.6	9.79	59.6	14.56	59.3	22.16
61.3	5.49	61.2	6.86	61.6	9.64	61.3	14.33	61.1	21.75
63.4	5.42	63.4	6.81	63.4	9.52	63.4	14.09	63.1	21.27
65.3	5.35	65.4	6.69	65.3	9.38	65.6	13.83	65.4	20.79
67.5	5.28	67.6	6.60	67.2	9.24	67.5	13.59	67.2	20.32
69.3	5.22	69.4	6.52	69.1	9.12	69.2	13.35	69.3	19.90
71.3	5.17	71.4	6.42	71.5	8.90	71.4	13.10	71.4	19.50
73.1	5.12	73.6	6.31	73.4	8.75	73.5	12.87	73.2	19.08
75.3	5.02	75.6	6.23	75.5	8.61	75.7	12.64	74.9	18.68
77.3	4.96	77.6	6.16	77.6	8.46	77.5	12.43	76.8	18.35

Table A10 Temperature sweep test results at 62.8 rad/s as measured by the DMA of HNBR compounds filled with various CB characteristics and loadings (cont.): (a) Storage modulus (G′)

0 phr		10 phr		20 phr		40 phr		60 phr	
Temp.(C°)	G′ (MPa)	Temp.(C°)	G′ (MPa)	Temp.(C°)	G′ (MPa)	Temp.(C°)	G′ (MPa)	Temp.(C°)	G′ (MPa)
79.5	4.90	79.3	6.05	79.5	8.34	79.4	12.21	79.4	17.89
81.6	4.83	81.5	5.99	81.6	8.19	81.5	12.02	81.4	17.48
83.6	4.78	83.5	5.91	83.6	8.07	83.5	11.82	83.3	17.17
85.5	4.73	85.4	5.84	85.5	7.96	85.6	11.63	85.7	16.80
87.4	4.68	87.3	5.80	87.5	7.85	87.4	11.44	87.3	16.53
89.5	4.63	89.4	5.74	89.5	7.76	89.4	11.30	89.5	16.21
91.5	4.59	91.4	5.67	91.4	7.64	91.2	11.16	91.7	15.95
93.6	4.55	93.7	5.62	93.3	7.58	93.7	11.00	93.3	15.74
95.4	4.54	95.6	5.61	95.3	7.54	95.6	10.88	95.4	15.52
97.2	4.53	97.5	5.55	97.5	7.47	97.1	10.78	97.5	15.32
99.2	4.48	99.6	5.56	99.5	7.43	99.7	10.71	99.5	15.12
101.0	4.49	101.6	5.51	101.4	7.38	101.5	10.63	101.4	14.95
103.5	4.46	103.3	5.46	103.5	7.36	103.6	10.54	103.6	14.83
105.4	4.44	105.5	5.49	105.4	7.33	105.6	10.47	105.5	14.68
107.3	4.44	107.5	5.47	107.4	7.29	107.4	10.43	107.5	14.59
109.5	4.45	109.4	5.47	109.2	7.29	109.2	10.38	109.6	14.45
111.1	4.46	111.5	5.45	111.4	7.26	111.4	10.33	111.5	14.35
113.3	4.44	113.2	5.43	113.5	7.25	113.8	10.24	113.5	14.23
115.3	4.43	115.3	5.40	115.4	7.26	115.5	10.20	115.3	14.14
117.8	4.43	117.2	5.40	117.4	7.20	117.6	10.16	117.3	14.04
119.2	4.45	119.5	5.39	119.5	7.19	119.6	10.13	119.4	13.93
121.6	4.43	121.5	5.39	121.5	7.19	121.4	10.10	121.5	13.83
123.5	4.44	123.4	5.39	123.6	7.18	123.4	10.04	122.8	13.74
125.6	4.45	125.5	5.38	125.3	7.16	125.4	10.00	125.6	13.63
127.1	4.42	127.5	5.36	127.1	7.15	127.7	9.95	127.2	13.57
129.6	4.43	129.7	5.37	129.3	7.12	129.7	9.93	129.0	13.50
131.5	4.44	131.4	5.37	131.5	7.12	131.6	9.90	131.5	13.41
133.6	4.44	133.4	5.37	133.6	7.14	133.6	9.86	133.4	13.35
135.4	4.46	135.5	5.37	135.5	7.12	135.4	9.83	135.3	13.26
138.0	4.43	137.4	5.36	137.4	7.11	137.5	9.81	137.2	13.17
139.6	4.47	139.7	5.35	139.6	7.12	139.3	9.77	139.3	13.12
141.5	4.46	141.6	5.36	141.4	7.09	141.4	9.76	141.3	13.05
143.3	4.46	143.5	5.37	143.4	7.09	143.4	9.73	143.5	12.97
145.1	4.48	145.6	5.36	145.4	7.10	145.3	9.69	145.5	12.92
147.5	4.46	147.6	5.36	147.6	7.07	147.2	9.68	147.6	12.85
149.1	4.48	149.6	5.34	149.6	7.07	149.3	9.66	149.2	12.79

Table A10 Temperature sweep test results at 62.8 rad/s as measured by the DMA of HNBR compounds filled with various CB characteristics and loadings (cont.): (a) Storage modulus (G′)

4) N990

0 phr		10 phr		20 phr		40 phr		60 phr	
Temp.(C°)	G′ (MPa)	Temp.(C°)	G′ (MPa)	Temp.(C°)	G′ (MPa)	Temp.(C°)	G′ (MPa)	Temp.(C°)	G′ (MPa)
-80.1	2590.50	-81.6	2846.47	-81.4	3174.53	-80.8	3770.98	-79.9	3973.89
-79.6	2594.41	-80.2	2854.59	-79.6	3101.33	-79.8	3758.82	-79.4	3934.34
-78.1	2571.16	-76.9	2814.85	-77.7	3074.09	-77.9	3725.24	-77.1	3924.05
-75.8	2534.68	-74.5	2781.02	-75.1	3029.43	-75.7	3689.73	-75.0	3888.14
-72.8	2480.94	-72.6	2749.50	-72.8	2981.27	-73.2	3629.35	-73.2	3840.67
-70.8	2443.93	-71.4	2722.90	-71.0	2945.12	-71.3	3579.18	-71.2	3812.50
-69.0	2403.53	-69.3	2677.15	-69.3	2897.43	-69.3	3526.74	-69.2	3764.57
-67.2	2364.91	-67.1	2645.91	-67.0	2849.02	-67.5	3468.50	-67.1	3707.16
-65.0	2319.63	-65.2	2605.91	-64.9	2797.76	-65.4	3407.07	-65.2	3663.02
-63.3	2278.99	-63.3	2563.02	-63.1	2760.25	-63.1	3346.69	-63.1	3607.49
-61.3	2234.60	-61.4	2519.68	-60.9	2703.04	-60.9	3288.68	-61.1	3550.86
-59.1	2189.45	-58.8	2473.45	-58.8	2662.00	-58.8	3235.89	-59.0	3490.96
-57.0	2145.52	-57.1	2434.03	-57.2	2614.48	-57.1	3187.45	-56.9	3445.00
-54.6	2110.26	-55.4	2387.10	-54.9	2569.96	-55.2	3135.09	-55.3	3389.22
-52.9	2087.62	-53.3	2348.82	-53.5	2494.30	-53.4	3082.12	-53.1	3328.40
-51.3	2043.89	-50.9	2310.95	-50.9	2438.13	-51.8	3027.97	-50.9	3269.04
-49.0	1990.56	-49.2	2281.29	-48.9	2392.86	-49.4	2969.75	-49.0	3213.68
-46.7	1954.07	-46.7	2239.30	-46.7	2342.03	-47.0	2916.70	-46.7	3147.95
-44.9	1914.04	-45.3	2206.42	-44.9	2303.94	-45.1	2863.17	-44.8	3092.17
-42.9	1862.60	-43.2	2162.12	-43.0	2268.24	-43.1	2799.02	-42.7	3031.19
-40.7	1802.77	-41.2	2109.78	-40.9	2216.61	-41.1	2731.74	-40.8	2960.27
-38.8	1746.78	-39.1	2031.37	-38.9	2145.00	-39.0	2653.42	-38.7	2881.16
-36.7	1681.55	-36.8	1925.51	-36.8	2039.50	-37.1	2552.60	-36.7	2772.13
-34.8	1611.48	-34.4	1786.46	-34.9	1909.55	-34.6	2392.47	-34.7	2615.57
-32.5	1445.58	-32.6	1629.17	-32.7	1688.30	-32.6	2209.67	-32.8	2397.73
-30.5	1245.11	-30.9	1425.85	-30.2	1395.12	-31.0	1958.86	-30.6	2009.24
-28.6	997.53	-28.3	1098.03	-28.9	1218.08	-28.7	1390.16	-28.7	1612.64
-26.7	718.17	-26.4	734.56	-26.1	790.34	-26.3	906.83	-26.6	1155.92
-24.7	485.73	-24.9	550.20	-24.7	559.38	-24.5	530.71	-24.7	764.85
-22.6	270.80	-22.1	283.95	-22.8	324.95	-22.9	381.71	-22.6	463.92
-20.7	145.21	-21.1	178.91	-20.5	155.68	-20.7	213.51	-20.6	275.52
-18.6	72.77	-18.5	76.16	-18.6	97.84	-18.7	126.37	-18.6	165.52
-16.7	42.27	-16.5	48.36	-16.7	57.14	-16.6	72.92	-16.5	102.40
-14.6	28.14	-14.5	35.62	-14.5	39.65	-14.7	50.29	-14.6	71.80
-12.6	20.94	-12.7	27.21	-12.6	30.26	-12.6	38.94	-12.7	53.16
-10.5	16.97	-10.5	20.88	-10.4	23.11	-10.6	31.23	-10.6	41.48
-8.6	14.23	-8.7	17.53	-8.7	19.26	-8.6	25.38	-8.6	34.13
-6.6	12.26	-6.7	15.23	-6.7	16.72	-6.6	21.86	-6.6	29.22
-4.6	10.86	-4.6	13.41	-4.6	15.07	-4.6	19.35	-4.6	25.99

Table A10 Temperature sweep test results at 62.8 rad/s as measured by the DMA of HNBR compounds filled with various CB characteristics and loadings (cont.): (a) Storage modulus (G′)

0 phr		10 phr		20 phr		40 phr		60 phr	
Temp.(C°)	G′ (MPa)	Temp.(C°)	G′ (MPa)	Temp.(C°)	G′ (MPa)	Temp.(C°)	G′ (MPa)	Temp.(C°)	G′ (MPa)
-2.5	9.66	-2.6	12.07	-2.6	13.80	-2.6	17.62	-2.6	23.62
-0.7	9.09	-0.6	10.92	-0.7	12.97	-0.6	16.26	-0.6	21.79
4.1	8.41	5.5	9.96	5.7	11.83	5.2	15.03	3.9	20.03
3.9	8.24	5.0	9.61	5.3	11.37	4.8	14.34	3.9	19.38
5.2	8.00	4.7	9.46	4.9	11.26	4.6	14.21	5.2	18.76
7.4	7.77	7.3	9.18	7.4	10.87	7.3	13.91	7.4	18.06
9.5	7.56	9.4	8.92	9.5	10.55	9.5	13.48	9.5	17.50
11.4	7.40	11.3	8.72	11.3	10.31	11.4	13.14	11.6	17.04
13.5	7.28	13.3	8.45	13.4	10.01	13.3	12.83	13.5	16.72
15.4	7.14	15.3	8.25	15.5	9.80	15.3	12.54	15.3	16.44
17.4	7.05	17.4	8.10	17.3	9.60	17.4	12.29	17.3	16.11
19.3	6.97	19.4	7.99	19.4	9.41	19.5	12.05	19.4	15.76
21.4	6.86	21.4	7.82	21.3	9.27	21.5	11.85	21.5	15.44
23.5	6.77	23.5	7.70	23.3	9.13	23.5	11.67	23.4	15.19
25.3	6.69	25.8	7.64	25.4	9.00	25.3	11.51	25.4	14.90
27.3	6.57	26.8	7.60	27.4	8.87	27.9	11.41	27.5	14.67
29.4	6.49	29.4	7.47	29.3	8.77	28.9	11.34	29.4	14.43
31.4	6.43	31.4	7.38	31.3	8.66	31.4	11.14	31.2	14.26
33.5	6.34	33.5	7.26	33.6	8.56	33.3	10.98	33.5	14.03
35.4	6.26	35.4	7.17	35.5	8.45	35.4	10.83	35.3	13.82
37.3	6.20	37.3	7.10	37.4	8.34	37.4	10.64	37.2	13.65
39.5	6.13	39.1	7.01	39.5	8.25	39.3	10.53	39.4	13.47
41.4	6.06	41.3	6.93	41.4	8.14	41.4	10.37	41.4	13.27
43.3	6.02	43.5	6.87	43.4	8.05	43.6	10.21	43.6	13.10
45.3	5.96	45.4	6.81	45.4	7.96	45.5	10.10	45.3	12.91
47.4	5.89	47.3	6.72	47.4	7.88	47.5	9.99	47.6	12.71
49.5	5.84	49.0	6.64	49.4	7.79	49.5	9.85	49.5	12.55
51.4	5.76	51.4	6.60	51.4	7.71	51.5	9.76	51.4	12.38
53.3	5.72	53.7	6.52	53.5	7.62	53.0	9.64	53.5	12.21
55.4	5.65	55.1	6.45	55.4	7.54	55.2	9.53	55.5	12.03
57.6	5.58	57.2	6.39	57.2	7.45	57.3	9.42	57.3	11.93
59.3	5.54	59.4	6.34	59.3	7.39	59.3	9.29	59.2	11.74
61.3	5.49	61.7	6.25	61.3	7.30	61.1	9.19	61.2	11.59
63.4	5.42	63.4	6.18	63.3	7.21	63.4	9.04	63.5	11.42
65.3	5.35	65.4	6.11	65.5	7.14	65.4	8.95	65.5	11.26
67.5	5.28	67.4	6.05	67.4	7.04	67.4	8.79	67.5	11.10
69.3	5.22	69.3	5.94	69.2	6.95	69.6	8.63	69.4	10.93
71.3	5.17	71.4	5.87	71.6	6.85	71.3	8.50	71.3	10.75
73.1	5.12	73.6	5.79	73.3	6.75	73.3	8.35	73.6	10.61
75.3	5.02	75.6	5.71	75.5	6.67	75.4	8.22	75.4	10.45
77.3	4.96	77.4	5.62	77.5	6.58	77.5	8.08	77.4	10.31

Table A10 Temperature sweep test results at 62.8 rad/s as measured by the DMA of HNBR compounds filled with various CB characteristics and loadings (cont.): (a) Storage modulus (G′)

0 phr		10 phr		20 phr		40 phr		60 phr	
Temp.(C°)	G′ (MPa)	Temp.(C°)	G′ (MPa)	Temp.(C°)	G′ (MPa)	Temp.(C°)	G′ (MPa)	Temp.(C°)	G′ (MPa)
79.5	4.90	79.7	5.60	79.3	6.51	79.3	8.03	79.4	10.18
81.6	4.83	81.6	5.50	81.4	6.45	81.5	7.87	81.4	10.05
83.6	4.78	83.7	5.45	83.6	6.37	83.7	7.78	83.5	9.93
85.5	4.73	85.6	5.38	85.3	6.29	85.6	7.68	85.2	9.81
87.4	4.68	87.1	5.34	87.4	6.26	87.4	7.60	87.7	9.69
89.5	4.63	89.2	5.29	89.1	6.19	89.3	7.52	89.5	9.55
91.5	4.59	91.4	5.26	91.5	6.14	91.2	7.45	91.4	9.51
93.6	4.55	93.6	5.21	93.4	6.08	93.5	7.41	93.2	9.42
95.4	4.54	95.4	5.18	95.5	6.06	95.4	7.33	95.6	9.37
97.2	4.53	97.6	5.15	97.5	6.02	97.6	7.29	97.5	9.29
99.2	4.48	99.2	5.12	99.7	6.01	99.7	7.27	99.5	9.24
101.0	4.49	101.3	5.12	101.4	5.98	101.4	7.23	101.6	9.20
103.5	4.46	103.4	5.10	103.5	5.94	103.1	7.26	103.5	9.18
105.4	4.44	105.4	5.08	105.3	5.93	105.6	7.19	105.5	9.15
107.3	4.44	107.4	5.09	106.8	5.91	107.8	7.17	107.6	9.10
109.5	4.45	109.9	5.08	109.5	5.94	109.3	7.17	109.7	9.09
111.1	4.46	111.6	5.06	111.4	5.90	111.0	7.21	111.8	9.04
113.3	4.44	113.4	5.04	113.9	5.91	113.6	7.13	113.5	9.02
115.3	4.43	115.3	5.05	115.9	5.88	115.5	7.13	115.5	8.99
117.8	4.43	117.4	5.06	118.2	5.88	118.0	7.15	117.6	8.98
119.2	4.45	119.4	5.04	118.7	5.95	119.9	7.10	119.4	8.96
121.6	4.43	121.4	5.03	122.0	5.88	121.5	7.13	121.2	8.94
123.5	4.44	123.5	5.03	123.8	5.86	123.6	7.08	123.2	8.90
125.6	4.45	125.3	5.02	125.4	5.86	124.8	7.12	125.4	8.88
127.1	4.42	127.2	5.05	127.2	5.87	127.0	7.10	127.4	8.90
129.6	4.43	129.2	5.05	129.6	5.87	129.6	7.07	129.7	8.87
131.5	4.44	131.6	5.04	131.4	5.84	131.3	7.08	131.5	8.86
133.6	4.44	133.6	5.03	133.2	5.82	133.4	7.05	133.3	8.83
135.4	4.46	135.5	5.02	135.5	5.85	135.8	7.08	135.7	8.82
138.0	4.43	137.2	5.03	137.3	5.82	136.9	7.12	137.3	8.81
139.6	4.47	139.3	5.04	139.4	5.85	139.9	7.09	139.5	8.81
141.5	4.46	141.2	5.04	141.6	5.84	141.4	7.06	141.6	8.81
143.3	4.46	143.2	5.05	143.5	5.85	143.3	7.11	143.6	8.72
145.1	4.48	145.6	5.04	145.5	5.81	145.9	7.05	145.6	8.79
147.5	4.46	147.4	5.03	147.3	5.85	147.8	7.09	147.6	8.76
149.1	4.48	149.4	5.05	149.1	5.80	149.4	7.08	149.6	8.73

Table A10 Temperature sweep test results at 62.8 rad/s as measured by the DMA of HNBR compounds filled with various CB characteristics and loadings (cont.): (b) Loss modulus (G″)

1) N326

0 phr		10 phr		20 phr		40 phr		60 phr	
Temp.(C°)	G″ (MPa)	Temp.(C°)	G″ (MPa)	Temp.(C°)	G″ (MPa)	Temp.(C°)	G″ (MPa)	Temp.(C°)	G″ (MPa)
-80.1	100.58	-82.1	101.11	-81.1	110.45	-81.0	110.47	-79.8	187.50
-79.6	101.53	-79.8	102.72	-79.3	129.74	-78.6	108.21	-77.2	174.63
-78.1	99.39	-77.2	101.14	-77.3	125.10	-76.9	106.02	-74.0	166.94
-75.8	97.33	-74.7	98.66	-75.2	121.84	-75.3	105.19	-70.9	159.92
-72.8	94.32	-72.7	97.01	-73.0	118.26	-73.4	103.00	-69.9	162.91
-70.8	92.15	-70.7	94.72	-71.0	115.54	-71.4	99.33	-67.0	151.02
-69.0	89.42	-69.1	92.87	-69.2	112.32	-69.1	96.39	-63.9	145.94
-67.2	86.63	-67.2	89.69	-67.2	110.16	-67.2	93.30	-61.5	141.96
-65.0	82.96	-65.1	86.57	-65.4	106.32	-65.4	91.03	-58.6	138.07
-63.3	80.45	-63.3	83.60	-63.2	102.85	-63.2	87.31	-55.4	135.40
-61.3	77.00	-61.1	79.11	-60.9	99.56	-61.3	84.59	-54.3	139.95
-59.1	73.75	-58.9	76.26	-59.3	96.16	-59.0	81.15	-53.5	139.44
-57.0	70.30	-57.1	72.87	-57.0	92.84	-57.1	77.88	-52.5	140.00
-54.6	68.44	-55.1	69.76	-55.2	90.32	-55.2	74.80	-51.6	138.96
-52.9	66.99	-52.9	67.08	-53.1	86.91	-52.9	72.51	-50.3	137.73
-51.3	65.46	-50.8	64.95	-51.0	85.83	-51.0	71.48	-49.3	138.51
-49.0	63.66	-48.7	64.06	-49.3	83.88	-48.8	70.74	-48.2	137.64
-46.7	63.08	-46.8	63.11	-47.2	82.62	-46.7	71.05	-46.7	138.23
-44.9	64.20	-44.9	63.64	-44.7	81.99	-45.0	71.96	-44.8	140.62
-42.9	66.55	-42.7	65.93	-43.2	83.62	-42.9	73.44	-42.9	144.14
-40.7	72.16	-40.5	70.12	-41.2	87.65	-41.0	78.98	-40.9	148.33
-38.8	79.57	-38.6	79.75	-38.8	98.40	-39.0	88.41	-38.8	158.40
-36.7	90.72	-36.5	93.16	-37.0	115.14	-36.9	106.06	-36.8	177.34
-34.8	105.53	-34.6	117.91	-34.8	145.07	-35.1	132.92	-34.7	212.15
-32.5	143.22	-32.7	157.52	-32.8	205.04	-32.8	189.49	-32.7	270.95
-30.5	193.27	-30.5	221.58	-30.7	284.20	-30.8	278.22	-30.7	356.07
-28.6	248.80	-28.6	284.12	-28.5	341.81	-28.6	359.76	-28.5	437.03
-26.7	283.17	-26.6	319.45	-26.4	364.34	-26.6	407.51	-26.6	471.87
-24.7	273.78	-24.6	302.84	-24.7	341.14	-24.8	397.93	-24.5	454.35
-22.6	216.43	-22.6	244.82	-22.6	276.95	-22.7	319.11	-22.6	389.04
-20.7	148.17	-20.5	169.08	-20.4	196.48	-20.7	242.04	-20.6	301.43
-18.6	86.68	-18.6	111.73	-18.7	142.02	-18.4	171.23	-18.6	220.81
-16.7	51.26	-16.5	70.84	-16.6	94.16	-16.7	122.51	-16.5	159.89
-14.6	31.74	-14.7	48.20	-14.5	62.93	-14.6	85.91	-14.5	116.26
-12.6	20.96	-12.7	31.77	-12.6	42.38	-12.7	60.28	-12.6	87.23
-10.5	14.89	-10.6	21.31	-10.6	28.72	-10.6	42.66	-10.6	66.16
-8.6	10.76	-8.6	15.16	-8.7	20.62	-8.6	32.89	-8.6	51.14
-6.6	7.84	-6.6	11.09	-6.6	14.97	-6.7	25.71	-6.6	40.77
-4.6	5.80	-4.6	8.35	-4.7	11.22	-4.6	20.14	-4.5	32.52

Table A10 Temperature sweep test results at 62.8 rad/s as measured by the DMA of HNBR compounds filled with various CB characteristics and loadings (cont.): (b) Loss modulus (G″)

0 phr		10 phr		20 phr		40 phr		60 phr	
Temp.(C°)	G″ (MPa)	Temp.(C°)	G″ (MPa)	Temp.(C°)	G″ (MPa)	Temp.(C°)	G″ (MPa)	Temp.(C°)	G″ (MPa)
-2.5	4.18	-2.5	6.34	-2.6	8.71	-2.6	16.17	-2.5	26.61
-0.7	3.42	-0.7	5.09	-0.7	6.60	-0.6	13.33	-0.6	22.15
4.1	2.50	4.0	3.82	5.0	4.85	5.3	10.09	3.5	18.34
3.9	2.25	3.9	3.35	4.6	4.32	5.0	9.06	3.5	16.94
5.2	1.95	5.3	2.97	4.5	4.16	4.6	8.73	5.3	15.00
7.4	1.68	7.5	2.57	7.3	3.49	7.3	7.55	7.5	13.48
9.5	1.49	9.4	2.26	9.4	3.07	9.4	6.70	9.6	12.32
11.4	1.34	11.4	2.04	11.5	2.76	11.3	6.07	11.5	11.55
13.5	1.24	13.5	1.89	13.7	2.52	13.6	5.50	13.4	10.95
15.4	1.16	15.2	1.81	15.4	2.37	15.5	5.13	15.4	10.33
17.4	1.09	17.4	1.69	17.4	2.25	17.3	4.89	17.4	9.77
19.3	1.04	19.3	1.61	19.4	2.15	19.4	4.63	19.4	9.26
21.4	0.98	21.4	1.53	21.3	2.08	21.4	4.43	21.2	8.84
23.5	0.95	23.3	1.47	23.3	2.02	23.5	4.30	23.4	8.43
25.3	0.92	25.3	1.42	25.5	1.95	25.4	4.16	25.4	8.13
27.3	0.89	27.4	1.37	27.7	1.88	27.5	4.03	27.6	7.81
29.4	0.88	29.4	1.34	29.3	1.82	29.7	3.89	29.4	7.61
31.4	0.84	31.5	1.30	31.3	1.79	31.2	3.84	31.6	7.35
33.5	0.81	33.5	1.27	33.5	1.76	33.2	3.73	33.4	7.16
35.4	0.83	35.3	1.25	35.5	1.72	35.5	3.67	35.3	7.00
37.3	0.81	37.5	1.23	37.4	1.69	37.4	3.56	37.4	6.83
39.5	0.81	39.4	1.21	39.3	1.66	39.3	3.51	39.4	6.69
41.4	0.79	41.5	1.19	41.2	1.65	41.6	3.45	41.6	6.53
43.3	0.76	43.7	1.17	43.4	1.61	43.7	3.38	43.5	6.38
45.3	0.75	45.4	1.17	45.0	1.57	45.4	3.32	45.5	6.24
47.4	0.74	47.7	1.12	47.1	1.57	47.7	3.26	47.6	6.10
49.5	0.73	49.7	1.12	49.3	1.56	49.6	3.20	49.4	5.96
51.4	0.74	51.3	1.09	51.3	1.53	51.5	3.16	51.3	5.84
53.3	0.70	53.0	1.09	53.4	1.51	53.3	3.11	53.3	5.73
55.4	0.71	55.4	1.06	55.6	1.49	55.5	3.04	55.7	5.62
57.6	0.69	57.0	1.05	57.4	1.45	57.5	2.98	57.5	5.50
59.3	0.70	59.4	1.02	59.4	1.43	59.3	2.91	59.6	5.39
61.3	0.68	61.3	1.01	61.4	1.41	61.4	2.88	61.4	5.28
63.4	0.65	63.5	0.98	63.5	1.37	63.6	2.80	63.4	5.15
65.3	0.66	65.0	0.99	65.5	1.35	65.2	2.76	65.3	5.04
67.5	0.63	67.3	0.95	67.5	1.32	67.3	2.69	67.4	4.94
69.3	0.63	69.0	0.94	69.5	1.28	69.5	2.62	69.8	4.81
71.3	0.62	71.8	0.89	71.6	1.25	71.1	2.56	71.5	4.71
73.1	0.60	73.0	0.90	73.4	1.22	73.4	2.51	73.6	4.60
75.3	0.60	75.7	0.86	75.4	1.21	75.4	2.45	75.6	4.46
77.3	0.56	77.4	0.84	77.5	1.17	77.4	2.39	77.4	4.38

Table A10 Temperature sweep test results at 62.8 rad/s as measured by the DMA of HNBR compounds filled with various CB characteristics and loadings (cont.): (b) Loss modulus (G″)

0 phr		10 phr		20 phr		40 phr		60 phr	
Temp.(C°)	G″ (MPa)	Temp.(C°)	G″ (MPa)	Temp.(C°)	G″ (MPa)	Temp.(C°)	G″ (MPa)	Temp.(C°)	G″ (MPa)
79.5	0.56	79.3	0.83	79.3	1.16	79.2	2.34	79.4	4.28
81.6	0.55	81.6	0.82	81.4	1.13	81.4	2.29	81.6	4.18
83.6	0.51	83.5	0.80	83.7	1.09	83.6	2.22	83.5	4.10
85.5	0.54	85.0	0.80	85.5	1.05	85.4	2.17	85.5	4.01
87.4	0.52	87.8	0.76	87.4	1.04	87.5	2.13	87.4	3.92
89.5	0.50	89.2	0.75	89.3	1.02	89.5	2.08	89.6	3.82
91.5	0.50	91.0	0.75	91.5	0.99	91.4	2.05	91.5	3.73
93.6	0.48	93.1	0.72	93.5	0.99	93.5	2.01	93.4	3.65
95.4	0.47	95.7	0.71	95.2	0.97	95.5	1.97	95.1	3.59
97.2	0.46	97.1	0.70	97.5	0.95	97.7	1.92	97.4	3.52
99.2	0.46	99.0	0.69	99.4	0.93	99.5	1.89	99.3	3.45
101.0	0.46	101.1	0.68	101.7	0.92	101.4	1.86	101.6	3.39
103.5	0.46	103.5	0.67	103.6	0.93	103.5	1.84	103.6	3.33
105.4	0.45	105.4	0.65	105.3	0.91	105.5	1.79	105.3	3.28
107.3	0.43	107.2	0.65	107.7	0.89	107.2	1.79	107.4	3.22
109.5	0.41	109.4	0.66	109.5	0.86	109.1	1.75	109.3	3.16
111.1	0.41	111.2	0.64	111.4	0.86	111.2	1.73	111.4	3.12
113.3	0.40	113.7	0.62	113.4	0.83	113.5	1.69	113.7	3.07
115.3	0.41	115.2	0.63	115.4	0.83	115.6	1.66	115.6	3.01
117.8	0.41	117.5	0.61	117.4	0.82	117.5	1.65	117.7	2.95
119.2	0.39	119.4	0.60	119.6	0.83	119.1	1.61	119.5	2.90
121.6	0.38	121.3	0.58	121.5	0.81	121.3	1.58	121.5	2.83
123.5	0.40	123.3	0.58	123.5	0.80	123.4	1.57	123.4	2.78
125.6	0.38	125.7	0.57	125.5	0.78	125.7	1.53	125.8	2.74
127.1	0.39	127.2	0.57	127.4	0.77	127.3	1.51	127.8	2.69
129.6	0.36	129.3	0.57	129.5	0.75	129.7	1.47	129.5	2.65
131.5	0.37	131.2	0.57	131.6	0.75	131.4	1.49	131.6	2.60
133.6	0.35	133.0	0.55	133.6	0.74	133.5	1.45	133.4	2.56
135.4	0.35	135.1	0.53	135.6	0.72	135.5	1.43	135.1	2.52
138.0	0.34	137.7	0.53	137.8	0.71	137.8	1.40	137.6	2.53
139.6	0.34	139.9	0.52	139.6	0.71	139.4	1.39	140.4	2.49
141.5	0.36	141.2	0.51	141.2	0.71	141.5	1.36	141.5	2.46
143.3	0.34	143.4	0.52	143.2	0.70	143.4	1.35	144.0	2.44
145.1	0.33	145.3	0.52	145.3	0.68	145.2	1.32	145.2	2.40
147.5	0.34	147.5	0.49	147.1	0.69	147.4	1.31	146.5	2.39
149.1	0.34	149.3	0.51	149.4	0.68	149.5	1.29	149.5	2.37

Table A10 Temperature sweep test results at 62.8 rad/s as measured by the DMA of HNBR compounds filled with various CB characteristics and loadings (cont.): (b) Loss modulus (G″)

2) N550

0 phr		10 phr		20 phr		40 phr		60 phr	
Temp.(C°)	G″ (MPa)	Temp.(C°)	G″ (MPa)	Temp.(C°)	G″ (MPa)	Temp.(C°)	G″ (MPa)	Temp.(C°)	G″ (MPa)
-80.1	100.58	-79.3	109.53	-80.2	110.48	-80.3	144.95	-80.0	4467.16
-79.6	101.53	-79.3	111.04	-79.5	109.67	-77.0	140.39	-77.7	4356.46
-78.1	99.39	-77.2	108.95	-77.7	109.07	-73.2	135.49	-74.6	4298.48
-75.8	97.33	-74.9	107.17	-75.6	106.11	-72.2	149.13	-71.5	4226.24
-72.8	94.32	-73.1	105.20	-73.6	103.57	-71.3	149.53	-68.8	4152.39
-70.8	92.15	-70.9	102.55	-71.3	100.38	-70.3	147.92	-67.6	4122.69
-69.0	89.42	-68.9	100.46	-69.2	97.66	-68.8	145.82	-64.9	4051.37
-67.2	86.63	-67.1	97.51	-67.0	93.99	-66.9	143.43	-62.1	3974.75
-65.0	82.96	-64.7	94.05	-65.5	92.30	-65.1	140.88	-59.3	3897.65
-63.3	80.45	-63.0	91.40	-63.2	87.75	-63.0	138.91	-56.3	3819.83
-61.3	77.00	-61.0	88.17	-61.1	84.76	-61.0	135.65	-55.2	3781.91
-59.1	73.75	-59.1	85.37	-59.1	81.62	-58.9	132.78	-52.5	3720.20
-57.0	70.30	-57.1	82.21	-57.4	78.64	-56.9	130.41	-49.6	3640.58
-54.6	68.44	-55.0	79.26	-55.2	75.39	-55.0	126.35	-48.4	3610.95
-52.9	66.99	-53.1	76.43	-53.0	74.24	-53.1	125.74	-47.5	3580.17
-51.3	65.46	-50.9	73.80	-50.9	72.37	-51.0	125.73	-46.3	3550.47
-49.0	63.66	-48.9	71.70	-48.9	72.10	-48.9	125.41	-45.4	3523.06
-46.7	63.08	-47.0	70.57	-46.9	71.68	-46.9	123.49	-44.3	3488.55
-44.9	64.20	-44.9	70.30	-45.1	71.46	-44.9	122.75	-43.3	3450.30
-42.9	66.55	-42.8	71.41	-43.0	74.90	-42.8	124.31	-42.2	3410.74
-40.7	72.16	-40.9	73.85	-40.8	78.10	-40.8	127.66	-40.9	3357.60
-38.8	79.57	-38.9	80.40	-38.9	93.50	-38.7	134.95	-38.8	3266.24
-36.7	90.72	-36.8	93.33	-36.6	127.15	-36.8	148.56	-36.9	3138.92
-34.8	105.53	-34.6	117.14	-34.8	163.26	-34.7	175.49	-34.8	206.96
-32.5	143.22	-32.6	158.86	-32.4	224.47	-32.6	224.98	-32.8	268.87
-30.5	193.27	-30.6	214.92	-30.5	271.94	-30.4	304.75	-30.6	359.00
-28.6	248.80	-28.5	278.18	-29.1	323.65	-28.4	379.67	-28.5	449.38
-26.7	283.17	-26.6	313.90	-26.3	357.40	-26.5	427.79	-26.5	489.27
-24.7	273.78	-24.5	301.08	-24.7	328.23	-24.5	425.69	-24.6	471.06
-22.6	216.43	-22.6	246.67	-22.3	251.52	-22.6	369.48	-22.7	399.96
-20.7	148.17	-20.6	178.49	-20.5	187.44	-20.6	278.91	-20.7	305.99
-18.6	86.68	-18.7	121.08	-18.8	128.41	-18.6	196.93	-18.6	221.44
-16.7	51.26	-16.7	76.91	-16.5	84.62	-16.7	136.85	-16.6	161.31
-14.6	31.74	-14.6	49.48	-14.8	55.78	-14.6	92.46	-14.6	116.12
-12.6	20.96	-12.5	32.27	-12.8	31.63	-12.7	63.61	-12.6	84.96
-10.5	14.89	-10.6	22.15	-10.5	21.28	-10.6	44.55	-10.6	63.78
-8.6	10.76	-8.6	15.86	-8.6	16.02	-8.6	32.14	-8.6	48.63
-6.6	7.84	-6.5	11.36	-6.6	12.14	-6.6	24.26	-6.6	37.58
-4.6	5.80	-4.7	8.58	-4.6	9.47	-4.6	18.85	-4.6	30.24

Table A10 Temperature sweep test results at 62.8 rad/s as measured by the DMA of HNBR compounds filled with various CB characteristics and loadings (cont.): (b) Loss modulus (G″)

0 phr		10 phr		20 phr		40 phr		60 phr	
Temp.(C°)	G″ (MPa)	Temp.(C°)	G″ (MPa)	Temp.(C°)	G″ (MPa)	Temp.(C°)	G″ (MPa)	Temp.(C°)	G″ (MPa)
-2.5	4.18	-2.6	6.55	-2.6	7.80	-2.6	14.51	-2.6	24.05
-0.7	3.42	-0.6	5.08	-0.7	6.23	-0.6	11.73	-0.7	20.11
4.1	2.50	3.4	3.99	4.8	4.69	3.7	9.33	3.1	16.61
3.9	2.25	3.6	3.54	4.5	4.08	3.9	8.47	3.4	15.33
5.2	1.95	5.3	3.07	4.4	3.91	5.2	7.43	5.3	13.46
7.4	1.68	7.0	2.67	7.4	3.29	7.5	6.41	7.5	12.09
9.5	1.49	9.5	2.33	9.4	2.92	9.5	5.69	9.5	11.19
11.4	1.34	11.7	2.12	11.4	2.61	11.5	5.18	11.4	10.49
13.5	1.24	13.5	2.00	13.4	2.37	13.5	4.86	13.4	9.88
15.4	1.16	15.4	1.88	15.4	2.18	15.3	4.64	15.4	9.28
17.4	1.09	17.3	1.76	17.4	2.07	17.4	4.38	17.3	8.71
19.3	1.04	19.2	1.64	19.5	1.98	19.3	4.15	19.2	8.24
21.4	0.98	21.4	1.57	21.6	1.91	21.4	3.94	21.2	7.86
23.5	0.95	23.5	1.50	23.4	1.85	23.4	3.76	23.5	7.54
25.3	0.92	25.4	1.44	25.4	1.79	25.4	3.59	25.2	7.29
27.3	0.89	27.4	1.39	28.1	1.75	27.4	3.48	27.3	7.05
29.4	0.88	29.4	1.39	29.1	1.73	29.4	3.36	29.4	6.83
31.4	0.84	31.3	1.35	31.4	1.68	31.6	3.29	31.4	6.68
33.5	0.81	33.5	1.30	33.4	1.65	33.5	3.21	33.5	6.51
35.4	0.83	35.4	1.28	35.4	1.61	35.6	3.14	35.5	6.37
37.3	0.81	37.8	1.26	37.5	1.60	37.4	3.06	37.3	6.24
39.5	0.81	39.6	1.24	39.4	1.55	39.3	3.01	39.4	6.14
41.4	0.79	41.4	1.21	41.6	1.53	41.3	2.98	41.6	5.98
43.3	0.76	43.5	1.19	43.5	1.51	43.5	2.91	43.4	5.87
45.3	0.75	45.3	1.18	45.2	1.47	45.7	2.86	45.4	5.75
47.4	0.74	47.6	1.17	47.1	1.49	47.2	2.81	47.6	5.65
49.5	0.73	49.6	1.12	49.4	1.43	49.2	2.77	49.2	5.54
51.4	0.74	51.6	1.12	51.5	1.40	50.9	2.73	51.2	5.44
53.3	0.70	53.4	1.13	53.3	1.39	53.5	2.68	53.0	5.35
55.4	0.71	55.5	1.09	55.5	1.37	55.6	2.63	55.3	5.23
57.6	0.69	57.7	1.08	57.4	1.36	57.4	2.59	57.1	5.14
59.3	0.70	59.2	1.05	59.5	1.33	59.5	2.53	59.7	5.03
61.3	0.68	61.3	1.03	61.5	1.33	61.1	2.50	61.5	4.94
63.4	0.65	63.4	1.03	63.4	1.29	63.0	2.43	63.3	4.86
65.3	0.66	65.6	0.98	65.5	1.27	65.3	2.38	65.4	4.75
67.5	0.63	67.4	0.97	67.5	1.26	67.1	2.34	67.6	4.65
69.3	0.63	69.4	0.95	69.5	1.22	69.2	2.30	69.4	4.57
71.3	0.62	71.4	0.92	71.4	1.18	71.1	2.23	71.7	4.46
73.1	0.60	73.5	0.92	73.4	1.16	73.2	2.21	73.5	4.37
75.3	0.60	75.8	0.90	75.6	1.14	75.1	2.14	75.4	4.28
77.3	0.56	77.6	0.89	77.3	1.10	77.2	2.10	77.5	4.19

Table A10 Temperature sweep test results at 62.8 rad/s as measured by the DMA of HNBR compounds filled with various CB characteristics and loadings (cont.): (b) Loss modulus (G″)

0 phr		10 phr		20 phr		40 phr		60 phr	
Temp.(C°)	G″ (MPa)	Temp.(C°)	G″ (MPa)	Temp.(C°)	G″ (MPa)	Temp.(C°)	G″ (MPa)	Temp.(C°)	G″ (MPa)
79.5	0.56	79.6	0.86	79.5	1.08	79.6	2.05	79.5	4.10
81.6	0.55	81.5	0.84	81.3	1.06	81.6	2.03	81.2	4.00
83.6	0.51	83.7	0.80	83.6	1.01	83.9	1.97	83.4	3.93
85.5	0.54	86.0	0.80	85.2	1.03	86.1	1.94	85.5	3.86
87.4	0.52	87.6	0.79	87.3	0.99	87.0	1.88	87.4	3.77
89.5	0.50	89.1	0.77	89.4	0.97	89.1	1.87	89.5	3.69
91.5	0.50	91.8	0.73	91.4	0.94	91.5	1.83	91.7	3.61
93.6	0.48	93.6	0.76	93.5	0.93	93.7	1.79	93.7	3.53
95.4	0.47	95.7	0.73	95.5	0.91	95.3	1.75	95.6	3.47
97.2	0.46	97.0	0.72	97.4	0.89	97.2	1.72	97.7	3.42
99.2	0.46	99.6	0.70	99.7	0.89	99.1	1.73	99.8	3.35
101.0	0.46	101.0	0.70	101.5	0.89	101.7	1.68	101.8	3.30
103.5	0.46	103.6	0.69	103.4	0.87	103.6	1.65	103.5	3.26
105.4	0.45	105.5	0.65	105.3	0.86	105.2	1.63	105.3	3.19
107.3	0.43	107.2	0.67	107.5	0.83	107.1	1.62	107.4	3.16
109.5	4.45	109.8	0.64	109.4	0.81	109.0	1.60	109.3	3.12
111.1	4.46	111.2	0.64	111.4	0.81	111.3	1.57	111.5	3.07
113.3	4.44	113.5	0.63	113.4	0.81	112.9	1.56	113.4	3.02
115.3	4.43	115.5	0.64	115.4	0.79	115.9	1.52	115.8	2.99
117.8	4.43	117.8	0.63	117.5	0.80	118.2	1.51	117.4	2.93
119.2	4.45	119.1	0.59	119.3	0.79	119.5	1.49	119.6	2.89
121.6	4.43	121.0	0.60	121.6	0.78	121.5	1.48	121.6	2.84
123.5	4.44	123.7	0.58	123.8	0.76	123.4	1.46	123.4	2.81
125.6	4.45	125.8	0.57	125.6	0.75	125.9	1.46	125.4	2.77
127.1	4.42	128.3	0.59	127.3	0.74	127.7	1.41	127.2	2.73
129.6	4.43	129.8	0.58	129.5	0.74	129.8	1.41	129.2	2.69
131.5	4.44	131.6	0.55	131.5	0.73	131.1	1.38	131.4	2.64
133.6	4.44	133.1	0.54	133.3	0.72	133.2	1.37	133.4	2.61
135.4	4.46	135.5	0.55	135.2	0.69	135.3	1.37	135.7	2.57
138.0	4.43	137.3	0.54	137.2	0.71	137.4	1.35	137.5	2.53
139.6	4.47	138.7	0.54	139.4	0.70	139.4	1.32	139.4	2.50
141.5	4.46	141.3	0.54	141.5	0.69	141.3	1.31	141.5	2.46
143.3	4.46	143.1	0.52	143.6	0.68	143.6	1.31	143.6	2.42
145.1	4.48	145.2	0.51	145.8	0.66	145.4	1.29	145.7	2.40
147.5	4.46	147.1	0.51	147.8	0.68	147.4	1.27	147.8	2.35
149.1	4.48	149.3	0.51	149.3	0.67	149.5	1.25	149.6	2.32

Table A10 Temperature sweep test results at 62.8 rad/s as measured by the DMA of HNBR compounds filled with various CB characteristics and loadings (cont.): (b) Loss modulus (G″)

3) N774

0 phr		10 phr		20 phr		40 phr		60 phr	
Temp.(C°)	G″ (MPa)	Temp.(C°)	G″ (MPa)	Temp.(C°)	G″ (MPa)	Temp.(C°)	G″ (MPa)	Temp.(C°)	G″ (MPa)
-80.1	100.58	-81.6	99.33	-80.2	109.48	-80.6	130.51	-80.4	151.68
-79.6	101.53	-80.2	99.81	-80.0	109.59	-79.3	130.09	-78.3	147.37
-78.1	99.39	-76.9	97.56	-77.9	107.66	-78.2	128.07	-74.4	142.96
-75.8	97.33	-74.5	95.10	-75.7	106.12	-74.5	124.68	-71.5	139.04
-72.8	94.32	-72.6	92.89	-73.8	103.24	-72.6	121.56	-68.5	134.48
-70.8	92.15	-71.4	91.06	-71.3	99.87	-70.6	119.22	-65.8	130.44
-69.0	89.42	-69.3	87.81	-69.1	96.63	-69.4	116.81	-64.5	131.01
-67.2	86.63	-67.1	85.22	-67.0	93.45	-66.8	114.27	-61.8	123.06
-65.0	82.96	-65.2	82.30	-64.7	89.37	-65.0	111.04	-60.6	124.00
-63.3	80.45	-63.3	79.24	-62.9	86.03	-63.0	107.65	-57.7	116.75
-61.3	77.00	-61.4	75.24	-61.2	82.76	-61.3	103.55	-55.0	112.70
-59.1	73.75	-58.8	72.02	-59.4	79.08	-59.2	99.97	-52.2	109.01
-57.0	70.30	-57.1	68.89	-57.2	75.87	-56.2	96.33	-49.2	106.50
-54.6	68.44	-55.4	66.01	-55.5	72.29	-54.6	94.16	-46.3	105.78
-52.9	66.99	-53.3	63.95	-53.1	70.30	-53.2	92.19	-43.4	108.98
-51.3	65.46	-50.9	61.79	-50.8	68.38	-50.5	90.87	-42.3	112.56
-49.0	63.66	-49.2	61.48	-49.1	65.92	-48.9	91.02	-41.4	115.46
-46.7	63.08	-46.7	60.68	-47.2	64.35	-46.9	88.48	-40.3	119.39
-44.9	64.20	-45.3	61.57	-45.4	66.61	-45.1	92.66	-39.1	124.97
-42.9	66.55	-43.2	63.71	-43.1	68.59	-43.3	96.90	-38.1	133.07
-40.7	72.16	-41.2	67.64	-41.1	72.60	-40.8	104.12	-36.9	143.00
-38.8	79.57	-39.1	77.83	-38.8	81.12	-38.6	119.33	-35.9	157.83
-36.7	90.72	-36.8	97.25	-37.0	93.86	-36.9	137.52	-34.7	178.05
-34.8	105.53	-34.8	133.60	-34.9	121.45	-34.9	172.20	-33.7	203.29
-32.5	143.22	-32.6	178.06	-32.9	168.45	-33.1	220.06	-32.6	241.60
-30.5	193.27	-30.9	220.22	-30.7	239.21	-30.6	303.79	-30.7	321.95
-28.6	248.80	-28.6	274.20	-28.6	306.12	-28.4	376.10	-28.4	421.16
-26.7	283.17	-26.8	316.68	-26.2	359.22	-26.6	410.94	-26.5	480.89
-24.7	273.78	-24.5	297.85	-24.9	359.72	-24.9	413.08	-24.6	481.33
-22.6	216.43	-22.6	222.50	-22.5	290.45	-22.5	342.99	-22.5	417.97
-20.7	148.17	-20.5	141.68	-20.6	209.25	-20.5	249.61	-20.8	336.28
-18.6	86.68	-18.5	80.47	-18.5	136.79	-19.0	182.00	-18.7	241.97
-16.7	51.26	-16.9	52.16	-16.5	82.52	-16.3	102.99	-16.7	169.61
-14.6	31.74	-14.6	32.58	-14.7	56.35	-14.6	67.38	-14.6	119.24
-12.6	20.96	-12.6	21.69	-12.6	38.12	-12.8	47.50	-12.6	82.85
-10.5	14.89	-10.5	15.70	-10.7	27.01	-10.6	33.71	-10.6	60.27
-8.6	10.76	-8.7	13.93	-8.6	19.18	-8.5	24.94	-8.6	44.50
-6.6	7.84	-6.6	10.37	-6.6	13.59	-6.5	19.12	-6.6	33.75
-4.6	5.80	-4.6	7.65	-4.6	10.35	-4.6	15.31	-4.5	25.79

Table A10 Temperature sweep test results at 62.8 rad/s as measured by the DMA of HNBR compounds filled with various CB characteristics and loadings (cont.): (b) Loss modulus (G″)

0 phr		10 phr		20 phr		40 phr		60 phr	
Temp.(C°)	G″ (MPa)	Temp.(C°)	G″ (MPa)	Temp.(C°)	G″ (MPa)	Temp.(C°)	G″ (MPa)	Temp.(C°)	G″ (MPa)
-2.5	4.18	-2.6	5.93	-2.7	8.09	-2.6	12.06	-2.7	19.47
-0.7	3.42	-0.8	4.45	-0.7	6.28	-0.8	9.95	-0.8	15.76
4.1	2.50	5.2	3.22	5.6	4.33	5.2	7.27	3.9	12.44
3.9	2.25	4.9	2.74	5.1	3.82	4.8	6.38	3.9	11.29
5.2	1.95	4.5	2.65	4.7	3.75	4.6	6.14	5.2	9.98
7.4	1.68	7.0	2.28	7.2	3.24	7.3	5.24	7.6	8.73
9.5	1.49	9.5	1.95	9.4	2.85	9.5	4.65	9.5	7.87
11.4	1.34	11.4	1.76	11.5	2.54	11.4	4.23	11.6	7.12
13.5	1.24	13.5	1.58	13.3	2.35	13.3	3.84	13.4	6.67
15.4	1.16	15.5	1.45	15.3	2.17	15.3	3.53	15.4	6.29
17.4	1.09	17.4	1.36	17.4	2.05	17.6	3.31	17.4	5.95
19.3	1.04	19.4	1.31	19.2	1.96	19.4	3.17	19.4	5.64
21.4	0.98	21.7	1.23	21.2	1.88	21.5	3.04	21.5	5.36
23.5	0.95	23.5	1.20	23.4	1.83	23.2	2.96	23.3	5.15
25.3	0.92	25.3	1.17	25.3	1.78	25.1	2.90	25.2	4.98
27.3	0.89	27.3	1.17	27.2	1.72	27.5	2.77	27.2	4.80
29.4	0.88	29.7	1.13	29.1	1.68	29.8	2.70	29.4	4.63
31.4	0.84	31.5	1.11	31.5	1.62	31.3	2.64	31.3	4.52
33.5	0.81	33.5	1.08	33.6	1.58	32.8	2.62	33.4	4.39
35.4	0.83	35.4	1.06	35.5	1.55	35.3	2.53	35.3	4.30
37.3	0.81	37.2	1.04	37.5	1.52	37.3	2.50	37.3	4.23
39.5	0.81	39.2	1.03	39.4	1.49	39.4	2.45	39.5	4.13
41.4	0.79	41.4	1.01	41.3	1.47	41.6	2.40	41.2	4.04
43.3	0.76	43.6	1.00	43.8	1.45	43.5	2.37	43.1	3.99
45.3	0.75	45.3	0.97	45.3	1.42	45.5	2.34	45.6	3.89
47.4	0.74	47.5	0.98	47.3	1.41	47.5	2.31	47.3	3.82
49.5	0.73	49.5	0.96	49.3	1.42	49.5	2.26	49.5	3.74
51.4	0.74	51.3	0.96	51.3	1.39	51.3	2.24	51.6	3.66
53.3	0.70	53.4	0.95	53.3	1.33	53.2	2.20	54.0	3.59
55.4	0.71	55.5	0.92	55.4	1.34	55.2	2.17	55.5	3.54
57.6	0.69	57.3	0.92	57.4	1.30	57.4	2.14	58.1	3.45
59.3	0.70	59.4	0.89	59.6	1.30	59.6	2.08	59.3	3.39
61.3	0.68	61.2	0.88	61.6	1.27	61.3	2.06	61.1	3.33
63.4	0.65	63.4	0.86	63.4	1.23	63.4	2.02	63.1	3.27
65.3	0.66	65.4	0.85	65.3	1.21	65.6	1.97	65.4	3.18
67.5	0.63	67.6	0.84	67.2	1.20	67.5	1.92	67.2	3.12
69.3	0.63	69.4	0.80	69.1	1.16	69.2	1.90	69.3	3.03
71.3	0.62	71.4	0.82	71.5	1.13	71.4	1.85	71.4	2.95
73.1	0.60	73.6	0.79	73.4	1.10	73.5	1.82	73.2	2.91
75.3	0.60	75.6	0.77	75.5	1.08	75.7	1.78	74.9	2.86
77.3	0.56	77.6	0.75	77.6	1.07	77.5	1.74	76.8	2.78

Table A10 Temperature sweep test results at 62.8 rad/s as measured by the DMA of HNBR compounds filled with various CB characteristics and loadings (cont.): (b) Loss modulus (G″)

0 phr		10 phr		20 phr		40 phr		60 phr	
Temp.(C°)	G″ (MPa)	Temp.(C°)	G″ (MPa)	Temp.(C°)	G″ (MPa)	Temp.(C°)	G″ (MPa)	Temp.(C°)	G″ (MPa)
79.5	0.56	79.3	0.75	79.5	1.02	79.4	1.70	79.4	2.70
81.6	0.55	81.5	0.73	81.6	1.00	81.5	1.66	81.4	2.64
83.6	0.51	83.5	0.69	83.6	0.98	83.5	1.63	83.3	2.58
85.5	0.54	85.4	0.68	85.5	0.97	85.6	1.60	85.7	2.52
87.4	0.52	87.3	0.68	87.5	0.94	87.4	1.55	87.3	2.48
89.5	0.50	89.4	0.67	89.5	0.93	89.4	1.52	89.5	2.41
91.5	0.50	91.4	0.66	91.4	0.92	91.2	1.52	91.7	2.35
93.6	0.48	93.7	0.62	93.3	0.89	93.7	1.48	93.3	2.30
95.4	0.47	95.6	0.61	95.3	0.87	95.6	1.44	95.4	2.27
97.2	0.46	97.5	0.62	97.5	0.87	97.1	1.43	97.5	2.21
99.2	0.46	99.6	0.60	99.5	0.85	99.7	1.40	99.5	2.20
101.0	0.46	101.6	0.61	101.4	0.84	101.5	1.38	101.4	2.17
103.5	0.46	103.3	0.58	103.5	0.82	103.6	1.35	103.6	2.13
105.4	0.45	105.5	0.57	105.4	0.82	105.6	1.35	105.5	2.11
107.3	0.43	107.5	0.58	107.4	0.81	107.4	1.31	107.5	2.07
109.5	0.41	109.4	0.55	109.2	0.80	109.2	1.31	109.6	2.04
111.1	0.41	111.5	0.56	111.4	0.78	111.4	1.28	111.5	2.01
113.3	0.40	113.2	0.55	113.5	0.77	113.8	1.29	113.5	1.97
115.3	0.41	115.3	0.56	115.4	0.76	115.5	1.26	115.3	1.98
117.8	0.41	117.2	0.56	117.4	0.74	117.6	1.25	117.3	1.93
119.2	0.39	119.5	0.53	119.5	0.74	119.6	1.22	119.4	1.89
121.6	0.38	121.5	0.51	121.5	0.73	121.4	1.21	121.5	1.88
123.5	0.40	123.4	0.48	123.6	0.72	123.4	1.20	122.8	1.87
125.6	0.38	125.5	0.52	125.3	0.72	125.4	1.17	125.6	1.83
127.1	0.39	127.5	0.50	127.1	0.71	127.7	1.17	127.2	1.80
129.6	0.36	129.7	0.50	129.3	0.70	129.7	1.14	129.0	1.77
131.5	0.37	131.4	0.50	131.5	0.69	131.6	1.14	131.5	1.75
133.6	0.35	133.4	0.48	133.6	0.68	133.6	1.12	133.4	1.75
135.4	0.35	135.5	0.48	135.5	0.67	135.4	1.12	135.3	1.72
138.0	0.34	137.4	0.46	137.4	0.69	137.5	1.11	137.2	1.69
139.6	0.34	139.7	0.47	139.6	0.68	139.3	1.10	139.3	1.69
141.5	0.36	141.6	0.47	141.4	0.67	141.4	1.10	141.3	1.65
143.3	0.34	143.5	0.46	143.4	0.67	143.4	1.06	143.5	1.63
145.1	0.33	145.6	0.44	145.4	0.63	145.3	1.03	145.5	1.61
147.5	0.34	147.6	0.45	147.6	0.67	147.2	1.04	147.6	1.59
149.1	0.34	149.6	0.45	149.6	0.62	149.3	1.03	149.2	1.58

Table A10 Temperature sweep test results at 62.8 rad/s as measured by the DMA of HNBR compounds filled with various CB characteristics and loadings (cont.): (b) Loss modulus (G″)

4) N990

0 phr		10 phr		20 phr		40 phr		60 phr	
Temp.(C°)	G″ (MPa)	Temp.(C°)	G″ (MPa)	Temp.(C°)	G″ (MPa)	Temp.(C°)	G″ (MPa)	Temp.(C°)	G″ (MPa)
-80.1	100.58	-81.6	99.35	-81.4	110.36	-80.8	135.99	-79.9	126.58
-79.6	101.53	-80.2	100.55	-79.6	115.08	-79.8	135.11	-79.4	136.45
-78.1	99.39	-76.9	99.36	-77.7	113.05	-77.9	132.90	-77.1	134.66
-75.8	97.33	-74.5	96.51	-75.1	110.92	-75.7	130.50	-75.0	132.90
-72.8	94.32	-72.6	95.28	-72.8	108.29	-73.2	128.16	-73.2	128.52
-70.8	92.15	-71.4	92.73	-71.0	105.85	-71.3	126.26	-71.2	127.60
-69.0	89.42	-69.3	90.64	-69.3	103.03	-69.3	122.59	-69.2	124.53
-67.2	86.63	-67.1	87.93	-67.0	99.38	-67.5	119.90	-67.1	122.11
-65.0	82.96	-65.2	84.72	-64.9	95.64	-65.4	115.89	-65.2	118.80
-63.3	80.45	-63.3	81.24	-63.1	93.31	-63.1	111.82	-63.1	115.60
-61.3	77.00	-61.4	77.31	-60.9	88.77	-60.9	108.08	-61.1	112.08
-59.1	73.75	-58.8	73.75	-58.8	85.62	-58.8	104.17	-59.0	108.04
-57.0	70.30	-57.1	70.70	-57.2	82.22	-57.1	102.21	-56.9	105.27
-54.6	68.44	-55.4	68.27	-54.9	79.28	-55.2	98.40	-55.3	101.69
-52.9	66.99	-53.3	66.72	-53.5	75.40	-53.4	95.74	-53.1	98.30
-51.3	65.46	-50.9	64.18	-50.9	73.64	-51.8	92.20	-50.9	95.64
-49.0	63.66	-49.2	63.42	-48.9	73.08	-49.4	89.57	-49.0	94.66
-46.7	63.08	-46.7	62.90	-46.7	73.71	-47.0	76.69	-46.7	92.64
-44.9	64.20	-45.3	63.00	-44.9	72.64	-45.1	90.00	-44.8	93.68
-42.9	66.55	-43.2	64.85	-43.0	77.27	-43.1	90.14	-42.7	95.64
-40.7	72.16	-41.2	65.86	-40.9	83.34	-41.1	94.39	-40.8	101.85
-38.8	79.57	-39.1	69.97	-38.9	91.27	-39.0	102.06	-38.7	112.09
-36.7	90.72	-36.8	94.47	-36.8	105.49	-37.1	118.41	-36.7	132.58
-34.8	105.53	-34.4	127.48	-34.9	138.68	-34.6	152.04	-34.7	169.39
-32.5	143.22	-32.6	166.01	-32.7	191.34	-32.6	195.61	-32.8	227.69
-30.5	193.27	-30.9	217.12	-30.2	263.17	-31.0	255.30	-30.6	323.46
-28.6	248.80	-28.3	288.27	-28.9	301.38	-28.7	376.44	-28.7	407.21
-26.7	283.17	-26.4	321.56	-26.1	342.05	-26.3	414.28	-26.6	460.00
-24.7	273.78	-24.9	310.63	-24.7	322.72	-24.5	358.14	-24.7	436.13
-22.6	216.43	-22.1	233.39	-22.8	256.02	-22.9	304.38	-22.6	350.74
-20.7	148.17	-21.1	175.33	-20.5	158.71	-20.7	209.18	-20.6	252.48
-18.6	86.68	-18.5	88.90	-18.6	108.42	-18.7	137.48	-18.6	169.01
-16.7	51.26	-16.5	56.33	-16.7	63.83	-16.6	80.31	-16.5	107.14
-14.6	31.74	-14.5	39.30	-14.5	41.36	-14.7	51.77	-14.6	71.73
-12.6	20.96	-12.7	27.43	-12.6	28.41	-12.6	36.48	-12.7	48.28
-10.5	14.89	-10.5	18.07	-10.4	18.30	-10.6	25.90	-10.6	32.96
-8.6	10.76	-8.7	13.14	-8.7	12.90	-8.6	17.79	-8.6	23.37
-6.6	7.84	-6.7	9.78	-6.7	9.38	-6.6	12.98	-6.6	16.97
-4.6	5.80	-4.6	7.25	-4.6	7.18	-4.6	9.64	-4.6	12.91

Table A10 Temperature sweep test results at 62.8 rad/s as measured by the DMA of HNBR compounds filled with various CB characteristics and loadings (cont.): (b) Loss modulus (G″)

0 phr		10 phr		20 phr		40 phr		60 phr	
Temp.(C°)	G″ (MPa)	Temp.(C°)	G″ (MPa)	Temp.(C°)	G″ (MPa)	Temp.(C°)	G″ (MPa)	Temp.(C°)	G″ (MPa)
-2.5	4.18	-2.6	5.48	-2.6	5.54	-2.6	7.43	-2.6	10.03
-0.7	3.42	-0.6	4.02	-0.7	4.52	-0.6	5.70	-0.6	7.86
4.1	2.50	5.5	2.86	5.7	3.27	5.2	4.29	3.9	5.91
3.9	2.25	5.0	2.51	5.3	2.84	4.8	3.76	3.9	5.29
5.2	1.95	4.7	2.43	4.9	2.74	4.6	3.64	5.2	4.63
7.4	1.68	7.3	2.04	7.4	2.32	7.3	3.11	7.4	3.99
9.5	1.49	9.4	1.76	9.5	2.06	9.5	2.71	9.5	3.52
11.4	1.34	11.3	1.63	11.3	1.86	11.4	2.43	11.6	3.20
13.5	1.24	13.3	1.43	13.4	1.68	13.3	2.21	13.5	2.98
15.4	1.16	15.3	1.34	15.5	1.56	15.3	2.03	15.3	2.79
17.4	1.09	17.4	1.23	17.3	1.46	17.4	1.89	17.3	2.62
19.3	1.04	19.4	1.18	19.4	1.39	19.5	1.82	19.4	2.47
21.4	0.98	21.4	1.13	21.3	1.32	21.5	1.72	21.5	2.35
23.5	0.95	23.5	1.08	23.3	1.30	23.5	1.66	23.4	2.24
25.3	0.92	25.8	1.05	25.4	1.26	25.3	1.62	25.4	2.16
27.3	0.89	26.8	1.04	27.4	1.22	27.9	1.60	27.5	2.10
29.4	0.88	29.4	1.01	29.3	1.20	28.9	1.58	29.4	2.05
31.4	0.84	31.4	1.01	31.3	1.17	31.4	1.55	31.2	1.99
33.5	0.81	33.5	0.99	33.6	1.13	33.3	1.49	33.5	1.96
35.4	0.83	35.4	0.98	35.5	1.12	35.4	1.47	35.3	1.92
37.3	0.81	37.3	0.96	37.4	1.12	37.4	1.44	37.2	1.90
39.5	0.81	39.1	0.95	39.5	1.10	39.3	1.41	39.4	1.86
41.4	0.79	41.3	0.92	41.4	1.09	41.4	1.40	41.4	1.84
43.3	0.76	43.5	0.89	43.4	1.07	43.6	1.38	43.6	1.78
45.3	0.75	45.4	0.88	45.4	1.06	45.5	1.35	45.3	1.77
47.4	0.74	47.3	0.88	47.4	1.03	47.5	1.33	47.6	1.75
49.5	0.73	49.0	0.88	49.4	1.03	49.5	1.32	49.5	1.72
51.4	0.74	51.4	0.85	51.4	1.02	51.5	1.28	51.4	1.69
53.3	0.70	53.7	0.84	53.5	1.00	53.0	1.26	53.5	1.66
55.4	0.71	55.1	0.85	55.4	0.97	55.2	1.24	55.5	1.63
57.6	0.69	57.2	0.83	57.2	0.97	57.3	1.22	57.3	1.60
59.3	0.70	59.4	0.80	59.3	0.96	59.3	1.19	59.2	1.58
61.3	0.68	61.7	0.78	61.3	0.94	61.1	1.18	61.2	1.55
63.4	0.65	63.4	0.78	63.3	0.93	63.4	1.17	63.5	1.51
65.3	0.66	65.4	0.75	65.5	0.91	65.4	1.14	65.5	1.47
67.5	0.63	67.4	0.74	67.4	0.88	67.4	1.11	67.5	1.45
69.3	0.63	69.3	0.74	69.2	0.85	69.6	1.10	69.4	1.43
71.3	0.62	71.4	0.72	71.6	0.87	71.3	1.06	71.3	1.41
73.1	0.60	73.6	0.71	73.3	0.82	73.3	1.04	73.6	1.36
75.3	0.60	75.6	0.68	75.5	0.81	75.4	1.01	75.4	1.33
77.3	0.56	77.4	0.68	77.5	0.79	77.5	0.99	77.4	1.29

Table A10 Temperature sweep test results at 62.8 rad/s as measured by the DMA of HNBR compounds filled with various CB characteristics and loadings (cont.): (b) Loss modulus (G″)

0 phr		10 phr		20 phr		40 phr		60 phr	
Temp.(C°)	G″ (MPa)	Temp.(C°)	G″ (MPa)	Temp.(C°)	G″ (MPa)	Temp.(C°)	G″ (MPa)	Temp.(C°)	G″ (MPa)
79.5	0.56	79.7	0.64	79.3	0.77	79.3	0.96	79.4	1.27
81.6	0.55	81.6	0.65	81.4	0.76	81.5	0.93	81.4	1.26
83.6	0.51	83.7	0.64	83.6	0.75	83.7	0.92	83.5	1.24
85.5	0.54	85.6	0.63	85.3	0.73	85.6	0.89	85.2	1.20
87.4	0.52	87.1	0.61	87.4	0.71	87.4	0.88	87.7	1.18
89.5	0.50	89.2	0.59	89.1	0.71	89.3	0.87	89.5	1.15
91.5	0.50	91.4	0.59	91.5	0.68	91.2	0.84	91.4	1.12
93.6	0.48	93.6	0.55	93.4	0.68	93.5	0.85	93.2	1.12
95.4	0.47	95.4	0.54	95.5	0.65	95.4	0.82	95.6	1.09
97.2	0.46	97.6	0.56	97.5	0.64	97.6	0.81	97.5	1.06
99.2	0.46	99.2	0.53	99.7	0.63	99.7	0.80	99.5	1.07
101.0	0.46	101.3	0.52	101.4	0.63	101.4	0.79	101.6	1.06
103.5	0.46	103.4	0.53	103.5	0.62	103.1	0.76	103.5	1.02
105.4	0.45	105.4	0.51	105.3	0.61	105.6	0.78	105.5	1.02
107.3	0.43	107.4	0.50	106.8	0.59	107.8	0.77	107.6	1.02
109.5	0.41	109.9	0.51	109.5	0.60	109.3	0.75	109.7	1.00
111.1	0.41	111.6	0.51	111.4	0.59	111.0	0.74	111.8	0.99
113.3	0.40	113.4	0.48	113.9	0.60	113.6	0.73	113.5	0.98
115.3	0.41	115.3	0.47	115.9	0.59	115.5	0.71	115.5	0.95
117.8	0.41	117.4	0.47	118.2	0.56	118.0	0.70	117.6	0.94
119.2	0.39	119.4	0.47	118.7	0.57	119.9	0.70	119.4	0.94
121.6	0.38	121.4	0.48	122.0	0.55	121.5	0.72	121.2	0.93
123.5	0.40	123.5	0.45	123.8	0.56	123.6	0.68	123.2	0.92
125.6	0.38	125.3	0.47	125.4	0.54	124.8	0.67	125.4	0.91
127.1	0.39	127.2	0.44	127.2	0.54	127.0	0.68	127.4	0.89
129.6	0.36	129.2	0.45	129.6	0.52	129.6	0.67	129.7	0.89
131.5	0.37	131.6	0.45	131.4	0.51	131.3	0.66	131.5	0.86
133.6	0.35	133.6	0.42	133.2	0.51	133.4	0.65	133.3	0.88
135.4	0.35	135.5	0.44	135.5	0.53	135.8	0.63	135.7	0.87
138.0	0.34	137.2	0.43	137.3	0.50	136.9	0.62	137.3	0.87
139.6	0.34	139.3	0.41	139.4	0.51	139.9	0.65	139.5	0.83
141.5	0.36	141.2	0.40	141.6	0.50	141.4	0.63	141.6	0.84
143.3	0.34	143.2	0.40	143.5	0.49	143.3	0.62	143.6	0.84
145.1	0.33	145.6	0.39	145.5	0.49	145.9	0.62	145.6	0.83
147.5	0.34	147.4	0.40	147.3	0.49	147.8	0.60	147.6	0.82
149.1	0.34	149.4	0.40	149.1	0.48	149.4	0.62	149.6	0.81

Table A11 Mechanical properties of HNBR compounds filled with various CB characteristics and loadings

M100 (MPa)				
CB loading (phr)	CB type			
	N326	N550	N774	N990
0	2.16 ± 0.05			
10	3.13 ± 0.23	3.16 ± 0.19	2.73 ± 0.13	2.52 ± 0.18
20	3.77 ± 0.23	4.21 ± 0.16	4.04 ± 0.28	3.08 ± 0.21
40	7.00 ± 0.32	7.12 ± 0.06	6.14 ± 0.34	4.23 ± 0.61
60	10.13 ± 0.11	12.00 ± 0.83	10.08 ± 0.70	5.48 ± 0.28
Tensile strength (MPa)				
CB loading (phr)	CB type			
	N326	N550	N774	N990
0	9.48 ± 0.21			
10	13.92 ± 0.79	14.45 ± 0.16	9.62 ± 0.46	10.62 ± 0.25
20	16.39 ± 0.34	16.15 ± 0.62	15.69 ± 0.16	11.19 ± 0.51
40	18.96 ± 1.49	17.55 ± 0.36	18.11 ± 0.55	13.44 ± 0.10
60	19.30 ± 0.34	18.04 ± 0.86	20.92 ± 1.11	17.35 ± 0.31
Elongation at break (%)				
CB loading (phr)	CB type			
	N326	N550	N774	N990
0	252.98 ± 4.54			
10	259.08 ± 13.08	259.36 ± 6.92	219.18 ± 8.18	244.63 ± 9.66
20	250.08 ± 8.82	227.55 ± 3.11	232.93 ± 7.97	220.84 ± 10.08
40	205.10 ± 17.56	165.47 ± 11.79	204.44 ± 9.36	206.25 ± 18.66
60	168.20 ± 3.01	136.27 ± 2.57	182.79 ± 9.96	218.73 ± 7.94
Tear strength (N/mm)				
CB loading (phr)	CB type			
	N326	N550	N774	N990
0	23.89 ± 0.27			
10	30.82 ± 0.96	32.58 ± 0.84	29.87 ± 0.59	29.12 ± 0.36
20	40.61 ± 0.85	36.75 ± 0.29	37.25 ± 1.03	32.24 ± 0.10
40	48.43 ± 0.32	44.50 ± 1.10	44.54 ± 0.28	36.59 ± 1.02
60	54.38 ± 0.56	49.18 ± 1.12	51.01 ± 2.14	41.44 ± 0.01
Hardness (Shore A)				
CB loading (phr)	CB type			
	N326	N550	N774	N990
0	59.6 ± 0.200			
10	63.7 ± 0.173	65.2 ± 0.252	63.5 ± 0.321	62.2 ± 0.379
20	68.5 ± 0.100	69.4 ± 0.300	68.2 ± 0.100	64.4 ± 0.115
40	76.0 ± 0.231	77.0 ± 0.252	74.4 ± 0.404	68.8 ± 0.153
60	81.7 ± 0.462	81.9 ± 0.416	78.7 ± 0.458	72.8 ± 0.551
Abrasion loss (mm^3)				
CB loading (phr)	CB type			
	N326	N550	N774	N990
0	54.43 ± 2.966			
10	62.08 ± 1.728	57.33 ± 2.121	67.75 ± 3.515	60.82 ± 1.270
20	64.96 ± 1.477	58.14 ± 1.739	68.51 ± 4.574	67.53 ± 1.787
40	67.77 ± 1.580	61.90 ± 1.129	64.11 ± 0.582	72.50 ± 1.438
60	86.16 ± 1.180	71.66 ± 1.105	70.99 ± 0.751	81.84 ± 0.671

APPENDIX B
INFLUENCES OF PRECIPITATED SILICA LOADING ON REINFORCEMENT OF HYDROGENATED NITRILE RUBBER

Table B1 Scorch time (t_{s2}), cure time (t_c), and torque difference ($\Delta S'$) of HNBR filled with various silica loadings

Silica loading (phr)	Scorch time (min)	Cure time (min)	S'max-S'min (dN-m)
0	1.26 ± 0.02	74.36 ± 0.54	31.29 ± 0.38
10	1.19 ± 0.01	74.10 ± 1.22	34.77 ± 0.95
20	0.86 ± 0.05	73.41 ± 0.53	50.43 ± 1.39
30	0.80 ± 0.02	70.62 ± 1.14	65.41 ± 1.21
40	0.68 ± 0.02	64.78 ± 0.81	89.59 ± 2.74

Table B2 Complex modulus (G^*) result at 3.14 rad/s and 100°C as measured by the RPA-FT of HNBR compounds filled with various silica loadings

Silica loading (phr)	Test a				Test b			
	run 1		run 2		run 1		run 2	
	Strain (%)	G^* (kPa)	Strain (%)	G^* (kPa)	Strain (%)	G^* (kPa)	Strain (%)	G^* (kPa)
0	6.98	68.68	8.38	68.71	8.38	68.11	6.98	68.91
	12.57	67.64	19.55	66.90	19.55	66.26	12.57	67.66
	32.11	65.00	60.04	59.58	60.04	59.46	32.11	64.42
	97.74	53.43	167.55	43.87	167.55	43.85	97.74	52.85
	251.33	36.94	335.10	32.51	335.10	32.41	251.33	37.00
	418.88	29.16	481.71	26.86	481.71	26.97	418.88	28.93
	544.54	25.18	600.39	23.52	600.39	23.66	544.54	24.90
	656.24	22.38	712.09	21.08	712.09	21.13	656.24	22.19
	767.94	20.10	837.76	18.86	837.76	18.85	767.94	19.97
	893.61	18.00	949.46	17.32	949.46	17.19	893.61	17.94

Table B2 Complex modulus (G^*) result at 3.14 rad/s and 100°C as measured by the RPA-FT of HNBR compounds filled with various silica loadings (cont.)

Silica loading (phr)	Test a				Test b			
	run 1		run 2		run 1		run 2	
	Strain (%)	G^* (kPa)	Strain (%)	G^* (kPa)	Strain (%)	G^* (kPa)	Strain (%)	G^* (kPa)
10	6.98	79.83	8.38	77.19	8.38	79.96	6.98	78.05
	12.57	77.91	19.55	73.94	19.55	77.04	12.57	75.84
	32.11	73.37	60.04	63.94	60.04	66.77	32.11	70.63
	97.74	58.14	167.55	46.39	167.55	47.67	97.74	56.12
	251.33	39.72	335.10	34.63	335.10	35.08	251.33	39.45
	418.88	31.31	481.71	28.67	481.71	29.05	418.88	30.98
	544.54	26.97	600.39	25.15	600.39	25.41	544.54	26.70
	656.24	23.93	712.09	22.51	712.09	22.68	656.24	23.74
	767.94	21.48	837.76	20.09	837.76	20.18	767.94	21.35
	893.61	19.23	949.46	18.36	949.46	18.38	893.61	19.17
20	6.98	92.22	8.38	86.11	8.38	92.00	6.98	88.46
	12.57	89.58	19.55	81.04	19.55	87.00	12.57	84.49
	32.11	82.29	60.04	67.30	60.04	72.55	32.11	76.42
	97.74	62.43	167.55	48.21	167.55	50.39	97.74	58.50
	251.33	42.18	335.10	36.28	335.10	37.03	251.33	41.06
	418.88	33.14	481.71	30.11	481.71	30.67	418.88	32.46
	544.54	28.52	600.39	26.45	600.39	26.84	544.54	28.02
	656.24	25.27	712.09	23.67	712.09	23.95	656.24	24.93
	767.94	22.66	837.76	21.19	837.76	21.34	767.94	22.45
	893.61	20.36	949.46	19.37	949.46	19.48	893.61	20.17
30	6.98	139.56	8.38	125.82	8.38	138.08	6.98	130.04
	12.57	129.51	19.55	110.65	19.55	122.13	12.57	118.76
	32.11	111.39	60.04	84.71	60.04	93.92	32.11	99.89
	97.74	77.88	167.55	58.35	167.55	62.07	97.74	71.54
	251.33	51.98	335.10	44.05	335.10	45.76	251.33	50.01
	418.88	40.75	481.71	36.57	481.71	37.62	418.88	39.48
	544.54	34.85	600.39	31.98	600.39	32.72	544.54	33.99
	656.24	30.81	712.09	28.58	712.09	29.14	656.24	30.18
	767.94	27.57	837.76	25.48	837.76	25.88	767.94	27.12
	893.61	24.62	949.46	23.19	949.46	23.42	893.61	24.33
40	6.98	139.56	8.38	125.82	8.38	138.08	6.98	130.04
	12.57	129.51	19.55	110.65	19.55	122.13	12.57	118.76
	32.11	111.39	60.04	84.71	60.04	93.92	32.11	99.89
	97.74	77.88	167.55	58.35	167.55	62.07	97.74	71.54
	251.33	51.98	335.10	44.05	335.10	45.76	251.33	50.01
	418.88	40.75	481.71	36.57	481.71	37.62	418.88	39.48
	544.54	34.85	600.39	31.98	600.39	32.72	544.54	33.99
	656.24	30.81	712.09	28.58	712.09	29.14	656.24	30.18
	767.94	27.57	837.76	25.48	837.76	25.88	767.94	27.12
	893.61	24.62	949.46	23.19	949.46	23.42	893.61	24.33

Table B3 Fit parameters of Equation 3.16 of HNBR compounds filled with various silica loadings

Silica loading (phr)	G_0^* (kPa)	1/A (%)	B
0	69.86	241.6	1.137
10	91.14	214.8	0.9434
20	110.6	211.6	0.6674
30	271.6	43.5	0.2932
40	886.5	0.1	0.2201

Table B4 Total torque harmonic content (TTHC) result at 3.14 rad/s and 100°C as measured by the RPA-FT of HNBR compounds filled with various silica loadings

Silica loading (phr)	Test a				Test b			
	run 1		run 2		run 1		run 2	
	Strain (%)	TTHC (%)	Strain (%)	TTHC (%)	Strain (%)	TTHC (%)	Strain (%)	TTHC (%)
0	6.98	0.00	8.38	0.00	8.38	0.53	6.98	0.00
	12.57	0.00	19.55	0.15	19.55	0.79	12.57	0.00
	32.11	0.83	60.04	0.90	60.04	0.97	32.11	0.67
	97.74	2.03	167.55	4.36	167.55	4.45	97.74	2.01
	251.33	7.07	335.10	8.99	335.10	9.03	251.33	6.85
	418.88	10.89	481.71	12.05	481.71	12.00	418.88	10.78
	544.54	13.02	600.39	13.75	600.39	13.70	544.54	13.11
	656.24	14.47	712.09	15.52	712.09	15.29	656.24	14.72
	767.94	15.99	837.76	17.03	837.76	16.70	767.94	16.17
	893.61	17.38	949.46	18.33	949.46	18.13	893.61	17.54
10	6.98	0.00	8.38	0.00	8.38	0.00	6.98	0.00
	12.57	0.00	19.55	0.55	19.55	0.73	12.57	0.59
	32.11	0.55	60.04	0.51	60.04	0.70	32.11	0.38
	97.74	1.75	167.55	4.39	167.55	4.39	97.74	1.68
	251.33	6.60	335.10	9.00	335.10	9.28	251.33	6.73
	418.88	10.65	481.71	11.87	481.71	12.02	418.88	10.76
	544.54	12.66	600.39	13.35	600.39	13.51	544.54	12.88
	656.24	13.90	712.09	14.69	712.09	14.76	656.24	14.01
	767.94	15.26	837.76	16.19	837.76	16.13	767.94	15.46
	893.61	16.79	949.46	17.49	949.46	17.64	893.61	16.96

Table B4 Total torque harmonic content (TTHC) result at 3.14 rad/s and 100°C as measured by the RPA-FT of HNBR compounds filled with various silica loadings (cont.)

Silica loading (phr)	Test a				Test b			
	run 1		run 2		run 1		run 2	
	Strain (%)	TTHC (%)	Strain (%)	TTHC (%)	Strain (%)	TTHC (%)	Strain (%)	TTHC (%)
20	6.98	0.00	8.38	0.32	8.38	0.15	6.98	0.00
	12.57	0.91	19.55	0.45	19.55	1.02	12.57	1.11
	32.11	0.71	60.04	0.53	60.04	0.67	32.11	0.49
	97.74	2.21	167.55	5.16	167.55	4.86	97.74	2.20
	251.33	7.74	335.10	9.81	335.10	9.61	251.33	7.85
	418.88	10.92	481.71	12.29	481.71	11.98	418.88	11.56
	544.54	12.96	600.39	13.77	600.39	13.53	544.54	13.42
	656.24	14.32	712.09	15.23	712.09	14.99	656.24	14.63
	767.94	15.62	837.76	16.93	837.76	16.62	767.94	16.06
	893.61	17.20	949.46	18.34	949.46	18.11	893.61	17.65
30	6.98	0.00	8.38	0.00	8.38	0.80	6.98	0.00
	12.57	1.29	19.55	0.60	19.55	0.81	12.57	0.85
	32.11	0.82	60.04	1.00	60.04	0.76	32.11	0.98
	97.74	2.92	167.55	5.82	167.55	5.45	97.74	2.89
	251.33	8.39	335.10	10.25	335.10	10.12	251.33	8.44
	418.88	11.32	481.71	12.50	481.71	12.27	418.88	11.79
	544.54	13.08	600.39	14.04	600.39	13.70	544.54	13.52
	656.24	14.59	712.09	15.45	712.09	15.26	656.24	14.81
	767.94	15.92	837.76	17.23	837.76	16.80	767.94	16.25
	893.61	17.41	949.46	18.51	949.46	18.12	893.61	17.81
40	6.98	0.00	8.38	0.00	8.38	0.00	6.98	0.00
	12.57	1.05	19.55	1.16	19.55	2.23	12.57	0.13
	32.11	1.37	60.04	1.57	60.04	1.20	32.11	1.59
	97.74	3.39	167.55	6.09	167.55	5.70	97.74	3.38
	251.33	8.67	335.10	10.49	335.10	10.34	251.33	8.63
	418.88	11.40	481.71	12.62	481.71	12.34	418.88	11.80
	544.54	13.13	600.39	14.03	600.39	13.77	544.54	13.47
	656.24	14.57	712.09	15.44	712.09	15.18	656.24	14.78
	767.94	15.88	837.76	17.15	837.76	16.69	767.94	16.07
	893.61	17.36	949.46	18.39	949.46	17.98	893.61	17.68

Table B5 3rd relative torque harmonic (T(3/1)) result at 3.14 rad/s and 100°C as measured by the RPA-FT of HNBR compounds filled with various silica loadings

Silica loading (phr)	Test a				Test b			
	run 1		run 2		run 1		run 2	
	Strain (%)	T(3/1) (%)	Strain (%)	T(3/1) (%)	Strain (%)	T(3/1) (%)	Strain (%)	T(3/1) (%)
0	6.98	0.11	8.38	0.00	8.38	0.00	6.98	0.00
	12.57	0.00	19.55	0.00	19.55	0.00	12.57	0.00
	32.11	0.00	60.04	0.01	60.04	0.00	32.11	0.00
	97.74	0.92	167.55	2.96	167.55	2.97	97.74	0.97
	251.33	5.24	335.10	6.88	335.10	6.88	251.33	5.13
	418.88	8.20	481.71	9.04	481.71	8.95	418.88	8.21
	544.54	9.56	600.39	10.12	600.39	9.97	544.54	9.62
	656.24	10.36	712.09	10.94	712.09	10.72	656.24	10.51
	767.94	11.13	837.76	11.72	837.76	11.50	767.94	11.27
	893.61	11.83	949.46	12.34	949.46	12.14	893.61	11.98
10	6.98	0.00	8.38	0.00	8.38	0.00	6.98	0.00
	12.57	0.00	19.55	0.00	19.55	0.00	12.57	0.00
	32.11	0.00	60.04	0.01	60.04	0.31	32.11	0.00
	97.74	1.16	167.55	2.96	167.55	3.58	97.74	1.30
	251.33	5.61	335.10	6.88	335.10	7.62	251.33	5.61
	418.88	8.82	481.71	9.04	481.71	9.61	418.88	8.78
	544.54	10.04	600.39	10.12	600.39	10.42	544.54	10.10
	656.24	10.68	712.09	10.94	712.09	11.03	656.24	10.71
	767.94	11.27	837.76	11.72	837.76	11.63	767.94	11.33
	893.61	11.92	949.46	12.34	949.46	12.20	893.61	11.99
20	6.98	0.00	8.38	0.00	8.38	0.00	6.98	0.00
	12.57	0.00	19.55	0.00	19.55	0.00	12.57	0.00
	32.11	0.00	60.04	0.00	60.04	0.00	32.11	0.00
	97.74	1.23	167.55	3.91	167.55	3.51	97.74	1.40
	251.33	6.09	335.10	7.71	335.10	7.59	251.33	6.14
	418.88	8.64	481.71	9.58	481.71	9.32	418.88	9.01
	544.54	9.76	600.39	10.41	600.39	10.14	544.54	10.13
	656.24	10.50	712.09	11.02	712.09	10.85	656.24	10.82
	767.94	11.13	837.76	11.78	837.76	11.61	767.94	11.43
	893.61	11.83	949.46	12.43	949.46	12.25	893.61	12.18
30	6.98	1.93	8.38	0.00	8.38	0.00	6.98	1.01
	12.57	0.62	19.55	0.00	19.55	0.00	12.57	0.16
	32.11	0.24	60.04	1.12	60.04	0.72	32.11	0.43
	97.74	2.57	167.55	5.04	167.55	4.79	97.74	2.71
	251.33	7.07	335.10	8.46	335.10	8.45	251.33	7.08
	418.88	9.27	481.71	9.98	481.71	9.78	418.88	9.45
	544.54	10.14	600.39	10.71	600.39	10.50	544.54	10.38
	656.24	10.82	712.09	11.29	712.09	11.11	656.24	11.02
	767.94	11.46	837.76	12.05	837.76	11.84	767.94	11.62
	893.61	12.14	949.46	12.65	949.46	12.45	893.61	12.39

Table B5 3rd relative torque harmonic (T(3/1)) result at 3.14 rad/s and 100°C as measured by the RPA-FT of HNBR compounds filled with various silica loadings (cont.)

Silica loading (phr)	Test a				Test b			
	run 1		run 2		run 1		run 2	
	Strain (%)	T(3/1) (%)	Strain (%)	T(3/1) (%)	Strain (%)	T(3/1) (%)	Strain (%)	T(3/1) (%)
40	6.98	0.00	8.38	0.00	8.38	0.21	6.98	0.00
	12.57	0.00	19.55	0.42	19.55	0.57	12.57	0.00
	32.11	0.38	60.04	1.73	60.04	0.98	32.11	1.22
	97.74	3.21	167.55	5.53	167.55	5.27	97.74	3.43
	251.33	7.44	335.10	8.71	335.10	8.66	251.33	7.43
	418.88	9.39	481.71	9.95	481.71	9.81	418.88	9.47
	544.54	10.15	600.39	10.60	600.39	10.42	544.54	10.29
	656.24	10.73	712.09	11.15	712.09	11.01	656.24	10.86
	767.94	11.33	837.76	11.91	837.76	11.71	767.94	11.47
	893.61	12.03	949.46	12.53	949.46	12.33	893.61	12.23

Table B6 5th relative torque harmonic (T(5/1)) result at 3.14 rad/s and 100°C as measured by the RPA-FT of HNBR compounds filled with various silica loadings

Silica loading (phr)	Test a				Test b			
	run 1		run 2		run 1		run 2	
	Strain (%)	T(5/1) (%)	Strain (%)	T(5/1) (%)	Strain (%)	T(5/1) (%)	Strain (%)	T(5/1) (%)
0	6.98	0.00	8.38	0.00	8.38	0.00	6.98	0.00
	12.57	0.00	19.55	0.01	19.55	0.00	12.57	0.00
	32.11	0.22	60.04	0.26	60.04	0.30	32.11	0.07
	97.74	0.34	167.55	0.46	167.55	0.54	97.74	0.35
	251.33	0.80	335.10	1.15	335.10	1.21	251.33	0.74
	418.88	1.59	481.71	1.93	481.71	1.93	418.88	1.57
	544.54	2.23	600.39	2.46	600.39	2.45	544.54	2.27
	656.24	2.65	712.09	2.89	712.09	2.86	656.24	2.72
	767.94	3.11	837.76	3.36	837.76	3.33	767.94	3.15
	893.61	3.52	949.46	3.70	949.46	3.67	893.61	3.53

Table B6 5th relative torque harmonic (T(5/1)) result at 3.14 rad/s and 100°C as measured by the RPA-FT of HNBR compounds filled with various silica loadings (cont.)

Silica loading (phr)	Test a				Test b			
	run 1		run 2		run 1		run 2	
	Strain (%)	T(5/1) (%)	Strain (%)	T(5/1) (%)	Strain (%)	T(5/1) (%)	Strain (%)	T(5/1) (%)
10	6.98	0.00	8.38	0.00	8.38	0.01	6.98	0.00
	12.57	0.00	19.55	0.00	19.55	0.03	12.57	0.05
	32.11	0.10	60.04	0.00	60.04	0.01	32.11	0.07
	97.74	0.14	167.55	0.32	167.55	0.37	97.74	0.07
	251.33	0.60	335.10	1.02	335.10	1.02	251.33	0.67
	418.88	1.36	481.71	1.69	481.71	1.70	418.88	1.41
	544.54	1.94	600.39	2.17	600.39	2.20	544.54	1.99
	656.24	2.33	712.09	2.60	712.09	2.62	656.24	2.37
	767.94	2.80	837.76	3.08	837.76	3.08	767.94	2.83
	893.61	3.24	949.46	3.42	949.46	3.43	893.61	3.28
20	6.98	0.00	8.38	0.00	8.38	0.00	6.98	0.00
	12.57	0.43	19.55	0.00	19.55	0.00	12.57	0.23
	32.11	0.28	60.04	0.10	60.04	0.17	32.11	0.09
	97.74	0.43	167.55	0.43	167.55	0.53	97.74	0.30
	251.33	0.74	335.10	1.22	335.10	1.14	251.33	0.85
	418.88	1.45	481.71	1.89	481.71	1.80	418.88	1.65
	544.54	2.09	600.39	2.41	600.39	2.34	544.54	2.21
	656.24	2.57	712.09	2.82	712.09	2.78	656.24	2.60
	767.94	3.00	837.76	3.37	837.76	3.29	767.94	3.07
	893.61	3.41	949.46	3.69	949.46	3.65	893.61	3.55
30	6.98	0.00	8.38	0.00	8.38	0.65	6.98	0.23
	12.57	0.31	19.55	0.00	19.55	0.08	12.57	0.46
	32.11	0.35	60.04	0.00	60.04	0.07	32.11	0.24
	97.74	0.31	167.55	0.38	167.55	0.43	97.74	0.19
	251.33	0.78	335.10	1.20	335.10	1.08	251.33	0.81
	418.88	1.46	481.71	1.90	481.71	1.80	418.88	1.61
	544.54	2.10	600.39	2.46	600.39	2.37	544.54	2.21
	656.24	2.65	712.09	2.90	712.09	2.87	656.24	2.66
	767.94	3.09	837.76	3.47	837.76	3.35	767.94	3.15
	893.61	3.49	949.46	3.78	949.46	3.69	893.61	3.62
40	6.98	0.00	8.38	0.51	8.38	0.93	6.98	0.46
	12.57	0.52	19.55	0.00	19.55	0.00	12.57	0.31
	32.11	0.40	60.04	0.00	60.04	0.00	32.11	0.12
	97.74	0.05	167.55	0.31	167.55	0.35	97.74	0.02
	251.33	0.73	335.10	1.17	335.10	1.10	251.33	0.77
	418.88	1.43	481.71	1.90	481.71	1.81	418.88	1.59
	544.54	2.14	600.39	2.46	600.39	2.41	544.54	2.23
	656.24	2.70	712.09	2.92	712.09	2.89	656.24	2.69
	767.94	3.12	837.76	3.46	837.76	3.35	767.94	3.16
	893.61	3.51	949.46	3.77	949.46	3.66	893.61	3.61

Table B7 Fit parameters of Equation 3.17 of HNBR compounds filled with various silica loadings

Silica loading (phr)	TH	α	C	D
0	6.7	0.0058	0.009	3.7030
10	8.1	0.0043	0.008	3.1790
20	7.3	0.0055	0.010	3.3720
40	7.5	0.0052	0.010	2.4890
60	7.5	0.0050	0.010	2.2650

Table B8 Integrating torque signals result at 3.14 rad/s and 100°C as measured by the RPA-FT of HNBR compounds filled with various silica loadings

Silica loading (phr)	Test a				Test b			
	run 1		run 2		run 1		run 2	
	Strain (%)	Q1/Q2	Strain (%)	Q1/Q2	Strain (%)	Q1/Q2	Strain (%)	Q1/Q2
0	6.98	1.08	8.38	1.06	8.38	1.08	6.98	1.01
	12.57	1.08	19.55	1.08	19.55	1.05	12.57	1.07
	32.11	1.04	60.04	1.05	60.04	1.04	32.11	1.02
	97.74	1.07	167.55	1.03	167.55	1.04	97.74	1.06
	251.33	1.06	335.10	1.07	335.10	1.08	251.33	1.05
	418.88	1.08	481.71	1.09	481.71	1.09	418.88	1.08
	544.54	1.09	600.39	1.10	600.39	1.10	544.54	1.08
	656.24	1.09	712.09	1.11	712.09	1.10	656.24	1.10
	767.94	1.12	837.76	1.12	837.76	1.11	767.94	1.11
	893.61	1.12	949.46	1.12	949.46	1.12	893.61	1.11
10	6.98	1.11	8.38	1.00	8.38	1.03	6.98	1.04
	12.57	1.08	19.55	1.05	19.55	1.02	12.57	1.03
	32.11	1.03	60.04	1.02	60.04	1.03	32.11	1.02
	97.74	1.02	167.55	1.02	167.55	1.01	97.74	1.01
	251.33	1.04	335.10	1.05	335.10	1.05	251.33	1.05
	418.88	1.06	481.71	1.07	481.71	1.06	418.88	1.05
	544.54	1.06	600.39	1.08	600.39	1.07	544.54	1.06
	656.24	1.06	712.09	1.08	712.09	1.08	656.24	1.07
	767.94	1.07	837.76	1.09	837.76	1.09	767.94	1.09
	893.61	1.09	949.46	1.08	949.46	1.09	893.61	1.10

Table B8 Integrating torque signals result at 3.14 rad/s and 100°C as measured by the RPA-FT of HNBR compounds filled with various silica loadings (cont.)

Silica loading (phr)	Test a				Test b			
	run 1		run 2		run 1		run 2	
	Strain (%)	Q1/Q2	Strain (%)	Q1/Q2	Strain (%)	Q1/Q2	Strain (%)	Q1/Q2
20	6.98	1.12	8.38	1.09	8.38	1.10	6.98	1.11
	12.57	1.02	19.55	1.02	19.55	0.97	12.57	1.01
	32.11	1.01	60.04	1.00	60.04	1.02	32.11	1.01
	97.74	1.05	167.55	1.02	167.55	1.02	97.74	1.02
	251.33	1.02	335.10	1.03	335.10	1.02	251.33	1.03
	418.88	1.03	481.71	1.05	481.71	1.05	418.88	1.05
	544.54	1.05	600.39	1.06	600.39	1.07	544.54	1.06
	656.24	1.06	712.09	1.06	712.09	1.07	656.24	1.06
	767.94	1.07	837.76	1.07	837.76	1.08	767.94	1.07
	893.61	1.08	949.46	1.08	949.46	1.09	893.61	1.08
30	6.98	1.13	8.38	1.06	8.38	1.07	6.98	1.10
	12.57	1.00	19.55	0.97	19.55	0.94	12.57	0.99
	32.11	0.98	60.04	0.98	60.04	1.02	32.11	0.96
	97.74	1.00	167.55	0.99	167.55	0.97	97.74	0.97
	251.33	0.97	335.10	1.01	335.10	1.00	251.33	1.00
	418.88	1.00	481.71	1.02	481.71	1.02	418.88	1.02
	544.54	1.02	600.39	1.03	600.39	1.04	544.54	1.02
	656.24	1.01	712.09	1.04	712.09	1.05	656.24	1.03
	767.94	1.05	837.76	1.04	837.76	1.05	767.94	1.04
	893.61	1.05	949.46	1.05	949.46	1.06	893.61	1.04
40	6.98	1.13	8.38	1.02	8.38	1.05	6.98	1.08
	12.57	1.01	19.55	0.92	19.55	0.91	12.57	0.95
	32.11	0.98	60.04	0.94	60.04	0.99	32.11	0.91
	97.74	0.98	167.55	0.95	167.55	0.96	97.74	0.94
	251.33	0.96	335.10	0.97	335.10	0.97	251.33	0.97
	418.88	0.98	481.71	0.99	481.71	0.99	418.88	0.99
	544.54	1.00	600.39	1.01	600.39	1.01	544.54	1.00
	656.24	1.01	712.09	1.01	712.09	1.01	656.24	1.00
	767.94	1.03	837.76	1.03	837.76	1.03	767.94	1.03
	893.61	1.03	949.46	1.04	949.46	1.05	893.61	1.04

Table B9 Strain sweep test results at 60°C and 1 rad/s as measured by the RPA2000 of HNBR compounds filled with various silica loadings:

(a) Storage modulus (G′)

Strain amplitude (%)	G′ (kPa)				
	0 phr	10 phr	20 phr	30 phr	40 phr
0.56	1136.40	1421.20	2244.50	3700.70	5600.20
0.70	1141.60	1313.30	2167.60	3523.10	5517.60
0.98	1127.10	1293.70	2152.40	3388.90	5293.90
1.95	1097.10	1301.70	2086.90	3171.20	4801.60
3.07	1083.20	1299.90	2062.70	3097.10	4582.70
5.02	1069.30	1285.20	1981.00	2900.70	4179.60
6.98	1057.70	1271.00	1921.60	2748.40	3891.30
10.04	1053.80	1244.50	1841.00	2570.40	3569.30
15.07	1042.20	1200.80	1754.10	2374.90	3217.30
19.95	1027.00	1162.20	1688.40	2213.30	2944.50
29.99	997.09	1097.50	1567.10	1926.80	2480.30
40.04	963.21	1039.40	1453.60	1664.50	2141.10
49.94	931.20	984.71	1355.10	1466.20	1907.20
59.99	897.29	933.10	1260.50	1323.90	1739.10

(b) Loss modulus (G″)

Strain amplitude (%)	G″ (kPa)				
	0 phr	10 phr	20 phr	30 phr	40 phr
0.56	88.63	163.80	218.04	460.99	597.70
0.70	93.76	129.01	213.01	391.71	573.02
0.98	95.36	127.51	211.20	410.54	584.03
1.95	91.43	131.04	218.47	433.62	649.49
3.07	95.28	132.49	222.39	459.73	705.59
5.02	94.62	130.21	224.20	469.37	753.22
6.98	90.69	128.56	225.99	466.47	763.52
10.04	91.54	127.61	221.28	453.67	743.38
15.07	92.27	127.82	218.58	446.53	717.52
19.95	94.71	130.41	220.61	444.68	706.51
29.99	99.76	137.09	231.31	449.45	688.97
40.04	105.40	146.44	241.88	462.80	669.25
49.94	111.57	151.93	253.02	467.84	631.40
59.99	120.46	156.05	266.03	455.32	593.85

Table B10 Temperature sweep test results at 62.8 rad/s as measured by the DMA of HNBR compounds filled with various silica loadings: (a) Storage modulus (G′)

0 phr		10 phr		20 phr		30 phr		40 phr	
Temp.(°C)	G′ (MPa)	Temp.(°C)	G′ (MPa)	Temp.(°C)	G′ (MPa)	Temp.(°C)	G′ (MPa)	Temp.(°C)	G′ (MPa)
-80.1	2590.50	-79.5	2499.78	-80.4	1452.83	-80.4	2684.61	-79.8	3028.86
-79.6	2594.41	-79.1	2493.13	-78.0	1413.78	-78.7	2692.06	-79.1	3023.09
-78.1	2571.16	-76.5	2453.59	-75.6	1410.20	-76.3	2674.89	-76.4	2992.21
-75.8	2534.68	-74.6	2332.77	-73.5	1384.68	-74.6	2658.79	-74.4	2963.70
-72.8	2480.94	-72.4	2293.67	-71.6	1327.47	-72.6	2633.16	-72.6	2932.76
-70.8	2443.93	-70.7	2277.70	-69.1	1310.36	-70.2	2601.59	-70.5	2894.46
-69.0	2403.53	-68.8	2250.55	-67.7	1276.08	-68.5	2569.34	-68.5	2852.27
-67.2	2364.91	-66.6	2218.22	-65.7	1228.61	-66.2	2523.58	-66.4	2805.84
-65.0	2319.63	-64.7	2192.87	-63.7	1202.43	-64.5	2489.42	-64.5	2762.74
-63.3	2278.99	-62.7	2165.36	-61.6	1175.29	-62.5	2444.04	-62.5	2717.76
-61.3	2234.60	-60.7	2149.46	-59.3	1154.11	-60.6	2407.31	-60.5	2670.92
-59.1	2189.45	-58.5	2125.88	-57.6	1133.87	-58.4	2369.94	-58.6	2634.29
-57.0	2145.52	-56.5	2104.27	-56.0	1111.56	-56.3	2339.25	-56.7	2572.22
-54.6	2110.26	-54.6	2081.42	-53.3	1088.44	-54.5	2308.64	-54.5	2527.39
-52.9	2087.62	-52.7	2048.64	-51.3	1085.80	-52.5	2281.96	-52.5	2491.12
-51.3	2043.89	-50.6	2016.30	-49.3	1081.02	-50.6	2259.84	-50.5	2462.61
-49.0	1990.56	-48.5	1980.04	-47.2	1075.56	-48.6	2234.94	-47.5	2423.62
-46.7	1954.07	-46.6	1943.34	-45.2	1073.60	-46.7	2211.91	-46.2	2404.47
-44.9	1914.04	-44.5	1902.93	-43.0	1077.02	-44.6	2190.57	-44.5	2375.51
-42.9	1862.60	-42.5	1868.68	-41.0	1063.48	-42.5	2160.28	-43.1	2350.83
-40.7	1802.77	-40.5	1824.88	-38.8	1061.36	-40.5	2124.54	-40.4	2292.68
-38.8	1746.78	-38.5	1767.53	-36.6	1052.78	-38.5	2078.07	-38.4	2238.05
-36.7	1681.55	-36.5	1682.13	-34.4	1038.44	-36.5	2011.62	-36.4	2156.13
-34.8	1611.48	-34.4	1543.52	-32.1	998.45	-34.6	1928.34	-34.5	2028.36
-32.5	1445.58	-32.3	1340.05	-29.7	944.18	-32.5	1762.45	-32.5	1833.02
-30.5	1245.11	-30.5	1120.53	-27.8	849.83	-30.4	1495.97	-30.4	1547.04
-28.6	997.53	-28.6	860.68	-26.1	735.75	-28.5	1226.60	-28.5	1246.75
-26.7	718.17	-26.7	610.76	-24.5	614.93	-26.5	922.39	-26.6	970.50
-24.7	485.73	-24.6	382.70	-23.2	484.05	-24.6	646.31	-24.6	691.09
-22.6	270.80	-22.6	214.59	-21.9	386.94	-22.6	417.26	-22.6	458.34
-20.7	145.21	-20.5	117.86	-20.5	310.61	-20.6	260.14	-20.7	297.84
-18.6	72.77	-18.7	69.95	-18.5	224.80	-18.6	168.53	-18.6	197.62
-16.7	42.27	-16.6	44.05	-16.5	145.19	-16.6	115.02	-16.6	145.33
-14.6	28.14	-14.6	30.58	-14.5	95.77	-14.6	84.18	-14.6	116.50
-12.6	20.94	-12.6	23.21	-12.5	64.89	-12.4	64.99	-12.7	96.17
-10.5	16.97	-10.6	18.65	-10.5	46.85	-10.7	54.84	-10.7	81.49
-8.6	14.23	-8.6	15.85	-8.5	35.68	-8.6	46.85	-8.6	71.30
-6.6	12.26	-6.6	13.92	-6.5	28.71	-6.7	41.75	-6.5	64.24
-4.6	10.86	-4.6	12.61	-4.4	24.51	-4.6	38.03	-4.6	59.13

Table B10 Temperature sweep test results at 62.8 rad/s as measured by the DMA of HNBR compounds filled with various silica loadings (cont.): (a) Storage modulus (G′)

0 phr		10 phr		20 phr		30 phr		40 phr	
Temp.(°C)	G′ (MPa)	Temp.(°C)	G′ (MPa)	Temp.(°C)	G′ (MPa)	Temp.(°C)	G′ (MPa)	Temp.(°C)	G′ (MPa)
-2.5	9.66	-2.3	11.65	-2.4	21.29	-2.6	35.23	-2.6	55.16
-0.7	9.09	-0.7	11.01	-0.5	19.10	-0.7	33.17	-0.7	52.43
4.1	8.41	4.2	10.27	2.8	17.69	2.0	31.61	4.6	49.05
3.9	8.24	4.4	9.94	3.0	17.24	3.2	30.56	4.4	47.88
5.2	8.00	4.8	9.90	5.4	16.40	5.4	29.50	5.1	47.25
7.4	7.77	7.3	9.55	7.6	15.73	7.1	28.63	7.4	45.77
9.5	7.56	9.4	9.36	9.7	15.15	9.7	27.81	9.4	44.62
11.4	7.40	11.5	9.13	11.5	14.77	11.5	27.35	11.4	43.48
13.5	7.28	13.4	9.00	13.6	14.41	13.4	26.92	13.4	42.46
15.4	7.14	15.4	8.84	15.5	14.12	15.4	26.47	15.4	41.58
17.4	7.05	17.3	8.74	17.3	13.93	17.4	26.04	17.5	40.82
19.3	6.97	19.4	8.58	19.5	13.74	19.4	25.62	19.5	40.18
21.4	6.86	21.4	8.44	21.5	13.56	21.3	25.20	21.4	39.61
23.5	6.77	23.5	8.31	23.8	13.31	23.6	24.74	23.4	39.02
25.3	6.69	25.4	8.21	25.6	13.18	25.4	24.38	25.4	38.46
27.3	6.57	27.4	8.09	27.5	13.01	27.3	24.00	27.4	37.93
29.4	6.49	29.6	8.00	29.6	12.87	29.3	23.69	29.4	37.36
31.4	6.43	31.0	7.94	31.5	12.71	31.4	23.35	31.4	36.78
33.5	6.34	33.4	7.84	33.6	12.56	33.4	23.04	33.4	36.25
35.4	6.26	35.5	7.76	35.5	12.44	35.4	22.76	35.4	35.76
37.3	6.20	37.5	7.69	37.6	12.35	37.4	22.44	37.4	35.25
39.5	6.13	39.4	7.61	39.5	12.21	39.3	22.21	39.4	34.84
41.4	6.06	41.4	7.53	41.5	12.06	41.5	21.91	41.4	34.56
43.3	6.02	43.4	7.46	43.5	11.96	43.4	21.67	43.3	34.28
45.3	5.96	45.4	7.38	45.4	11.85	45.4	21.39	45.4	33.90
47.4	5.89	47.4	7.33	47.5	11.75	47.4	21.12	47.4	33.56
49.5	5.84	49.4	7.24	49.5	11.63	49.5	20.85	49.4	33.21
51.4	5.76	51.3	7.19	51.5	11.50	51.5	20.56	51.3	32.89
53.3	5.72	53.4	7.12	53.4	11.41	53.5	20.32	53.5	32.51
55.4	5.65	55.2	7.06	55.6	11.29	55.3	20.07	55.3	32.21
57.6	5.58	57.4	6.98	57.6	11.14	57.5	19.83	57.5	31.89
59.3	5.54	59.4	6.94	59.5	10.99	59.4	19.60	59.4	31.59
61.3	5.49	61.3	6.86	61.6	10.91	61.3	19.39	61.3	31.27
63.4	5.42	63.5	6.81	63.4	10.81	63.5	19.19	63.4	30.97
65.3	5.35	65.4	6.75	65.5	10.74	65.4	18.98	65.4	30.68
67.5	5.28	67.4	6.69	67.6	10.55	67.5	18.77	67.4	30.37
69.3	5.22	69.4	6.63	69.6	10.46	69.4	18.58	69.4	30.04
71.3	5.17	71.5	6.60	71.6	10.37	71.2	18.41	71.5	29.67
73.1	5.12	73.4	6.56	73.6	10.27	73.4	18.26	73.5	29.31
75.3	5.02	75.5	6.51	75.3	10.21	75.6	18.06	75.3	29.02
77.3	4.96	77.3	6.46	77.5	10.12	77.3	17.92	77.1	28.78

Table B10 Temperature sweep test results at 62.8 rad/s as measured by the DMA of HNBR compounds filled with various silica loadings (cont.): (a) Storage modulus (G′)

0 phr		10 phr		20 phr		30 phr		40 phr	
Temp.(°C)	G′ (MPa)	Temp.(°C)	G′ (MPa)	Temp.(°C)	G′ (MPa)	Temp.(°C)	G′ (MPa)	Temp.(°C)	G′ (MPa)
79.5	4.90	79.5	6.44	79.5	10.06	79.5	17.75	79.5	28.49
81.6	4.83	81.6	6.37	81.4	9.97	81.1	17.64	81.4	28.24
83.6	4.78	83.5	6.36	83.6	9.90	83.5	17.48	83.3	28.01
85.5	4.73	85.3	6.30	85.7	9.84	85.4	17.35	85.4	27.80
87.4	4.68	87.4	6.28	87.6	9.78	87.3	17.24	87.4	27.62
89.5	4.63	89.5	6.26	89.5	9.73	89.4	17.12	89.4	27.43
91.5	4.59	91.5	6.21	91.5	9.67	91.3	17.02	91.5	27.25
93.6	4.55	93.4	6.22	93.6	9.60	93.2	16.91	93.3	27.10
95.4	4.54	95.2	6.18	95.6	9.54	95.5	16.83	95.3	26.95
97.2	4.53	97.4	6.17	97.5	9.52	97.5	16.69	97.4	26.83
99.2	4.48	99.5	6.14	99.6	9.49	99.1	16.60	99.4	26.67
101.0	4.49	101.5	6.12	101.7	9.45	101.5	16.52	101.3	26.55
103.5	4.46	103.3	6.11	103.5	9.39	103.5	16.44	103.6	26.42
105.4	4.44	105.3	6.09	105.3	9.39	105.5	16.34	105.5	26.30
107.3	4.44	107.3	6.10	107.3	9.35	107.4	16.26	107.5	26.18
109.5	4.45	109.4	6.08	109.5	9.33	109.3	16.17	109.4	26.07
111.1	4.46	111.4	6.05	111.5	9.32	111.6	16.08	111.3	25.97
113.3	4.44	113.6	6.04	113.5	9.29	113.4	16.03	113.5	25.84
115.3	4.43	115.4	6.04	115.4	9.31	115.3	15.96	115.5	25.75
117.8	4.43	117.4	6.06	117.4	9.21	117.4	15.90	117.4	25.65
119.2	4.45	119.3	6.04	119.6	9.22	119.5	15.85	119.4	25.57
121.6	4.43	121.4	6.04	121.6	9.18	121.3	15.81	121.3	25.49
123.5	4.44	123.7	6.03	123.5	9.12	123.4	15.74	123.5	25.42
125.6	4.45	125.5	6.01	125.4	9.12	125.2	15.68	125.4	25.34
127.1	4.42	127.4	6.00	127.6	9.12	127.5	15.64	127.4	25.28
129.6	4.43	129.3	6.00	129.6	9.12	129.5	15.60	129.1	25.22
131.5	4.44	131.1	6.02	131.6	9.08	131.4	15.56	131.3	25.15
133.6	4.44	133.2	6.00	133.5	9.08	133.2	15.52	133.4	25.09
135.4	4.46	135.5	6.01	135.6	9.07	135.4	15.46	135.2	25.06
138.0	4.43	137.5	5.98	137.5	9.05	137.5	15.43	137.3	25.00
139.6	4.47	139.4	5.99	139.5	9.07	139.3	15.41	139.4	24.93
141.5	4.46	141.3	6.01	141.6	9.02	141.6	15.38	141.5	24.88
143.3	4.46	143.2	6.02	143.6	9.03	143.3	15.34	143.3	24.85
145.1	4.48	145.3	6.01	145.4	9.02	145.3	15.31	145.6	24.80
147.5	4.46	147.2	6.00	147.5	9.01	147.7	15.25	147.5	24.76
149.1	4.48	149.5	6.03	149.7	8.99	149.5	15.23	149.3	24.73

Table B10 Temperature sweep test results at 62.8 rad/s as measured by the DMA of HNBR compounds filled with various silica loadings (cont.): (b) Loss modulus (G″)

0 phr		10 phr		20 phr		30 phr		40 phr	
Temp.(°C)	G″ (MPa)	Temp.(°C)	G″ (MPa)	Temp.(°C)	G″ (MPa)	Temp.(°C)	G″ (MPa)	Temp.(°C)	G″ (MPa)
-80.1	101.53	-79.5	75.55	-80.4	81.79	-80.4	114.23	-79.8	115.18
-79.6	99.39	-79.1	75.26	-78.0	83.23	-78.7	114.35	-79.1	116.24
-78.1	97.33	-76.5	72.96	-75.6	82.59	-76.3	112.97	-76.4	113.98
-75.8	94.32	-74.6	70.38	-73.5	81.43	-74.6	111.12	-74.4	112.60
-72.8	92.15	-72.4	68.05	-71.6	79.57	-72.6	109.96	-72.6	110.80
-70.8	89.42	-70.7	67.20	-69.1	79.39	-70.2	106.67	-70.5	108.98
-69.0	86.63	-68.8	65.33	-67.7	77.74	-68.5	104.39	-68.5	106.31
-67.2	82.96	-66.6	62.48	-65.7	77.29	-66.2	101.96	-66.4	104.51
-65.0	80.45	-64.7	60.41	-63.7	75.79	-64.5	99.29	-64.5	101.93
-63.3	77.00	-62.7	58.16	-61.6	73.09	-62.5	96.85	-62.5	99.01
-61.3	73.75	-60.7	57.42	-59.3	71.96	-60.6	93.90	-60.5	96.20
-59.1	70.30	-58.5	55.96	-57.6	68.03	-58.4	91.95	-58.6	94.72
-57.0	68.44	-56.5	54.28	-56.0	64.47	-56.3	90.22	-56.7	94.94
-54.6	66.99	-54.6	52.96	-53.3	61.23	-54.5	89.04	-54.5	92.98
-52.9	65.46	-52.7	52.05	-51.3	59.33	-52.5	86.90	-52.5	92.11
-51.3	63.66	-50.6	50.75	-49.3	57.56	-50.6	85.85	-50.5	91.27
-49.0	63.08	-48.5	50.77	-47.2	56.22	-48.6	84.28	-47.5	91.41
-46.7	64.20	-46.6	51.86	-45.2	57.79	-46.7	83.33	-46.2	90.85
-44.9	66.55	-44.5	54.05	-43.0	58.67	-44.6	83.55	-44.5	91.70
-42.9	72.16	-42.5	57.13	-41.0	58.96	-42.5	86.15	-43.1	94.43
-40.7	79.57	-40.5	63.12	-38.8	60.63	-40.5	91.56	-40.4	103.22
-38.8	90.72	-38.5	73.72	-36.6	65.21	-38.5	99.98	-38.4	114.77
-36.7	105.53	-36.5	91.75	-34.4	70.79	-36.5	114.01	-36.4	134.16
-34.8	101.53	-34.4	124.96	-32.1	81.35	-34.6	134.06	-34.5	166.68
-32.5	143.22	-32.3	177.51	-29.7	102.12	-32.5	177.23	-32.5	219.17
-30.5	193.27	-30.5	227.85	-27.8	128.80	-30.4	245.27	-30.4	287.63
-28.6	248.80	-28.6	269.48	-26.1	152.59	-28.5	298.01	-28.5	338.22
-26.7	283.17	-26.7	283.67	-24.5	168.59	-26.5	330.96	-26.6	359.02
-24.7	273.78	-24.6	253.03	-23.2	177.51	-24.6	321.30	-24.6	339.19
-22.6	216.43	-22.6	190.01	-21.9	178.09	-22.6	270.02	-22.6	279.12
-20.7	148.17	-20.5	126.86	-20.5	173.38	-20.6	200.24	-20.7	205.97
-18.6	86.68	-18.7	82.12	-18.5	153.77	-18.6	139.81	-18.6	141.08
-16.7	51.26	-16.6	51.41	-16.5	116.26	-16.6	94.77	-16.6	99.35
-14.6	31.74	-14.6	32.71	-14.5	82.47	-14.6	64.51	-14.6	73.51
-12.6	20.96	-12.6	21.82	-12.5	56.01	-12.4	43.99	-12.7	54.19
-10.5	14.89	-10.6	14.82	-10.5	38.19	-10.7	32.76	-10.7	39.79
-8.6	10.76	-8.6	10.58	-8.5	26.28	-8.6	23.78	-8.6	29.75
-6.6	7.84	-6.6	7.80	-6.5	18.36	-6.7	18.10	-6.5	22.87
-4.6	5.80	-4.6	5.92	-4.4	13.46	-4.6	14.06	-4.6	17.94

Table B10 Temperature sweep test results at 62.8 rad/s as measured by the DMA of HNBR compounds filled with various silica loadings (cont.): (b) Loss modulus (G″)

0 phr		10 phr		20 phr		30 phr		40 phr	
Temp.(°C)	G″ (MPa)	Temp.(°C)	G″ (MPa)	Temp.(°C)	G″ (MPa)	Temp.(°C)	G″ (MPa)	Temp.(°C)	G″ (MPa)
-2.5	4.18	-2.3	4.57	-2.4	9.71	-2.6	11.05	-2.6	14.33
-0.7	3.42	-0.7	3.67	-0.5	7.23	-0.7	8.97	-0.7	11.90
4.1	2.50	4.2	2.72	2.8	5.67	2.0	7.41	4.6	9.16
3.9	2.25	4.4	2.46	3.0	5.14	3.2	6.43	4.4	8.31
5.2	1.95	4.8	2.34	5.4	4.19	5.4	5.49	5.1	7.79
7.4	1.68	7.3	1.94	7.6	3.46	7.1	4.78	7.4	6.79
9.5	1.49	9.4	1.70	9.7	2.97	9.7	4.21	9.4	6.10
11.4	1.34	11.5	1.56	11.5	2.61	11.5	3.92	11.4	5.53
13.5	1.24	13.4	1.43	13.6	2.36	13.4	3.68	13.4	5.07
15.4	1.16	15.4	1.36	15.5	2.21	15.4	3.51	15.4	4.72
17.4	1.09	17.3	1.28	17.3	2.06	17.4	3.28	17.5	4.47
19.3	1.04	19.4	1.22	19.5	1.93	19.4	3.12	19.5	4.29
21.4	0.98	21.4	1.16	21.5	1.84	21.3	2.99	21.4	4.14
23.5	0.95	23.5	1.12	23.8	1.78	23.6	2.88	23.4	4.01
25.3	0.92	25.4	1.09	25.6	1.74	25.4	2.79	25.4	3.93
27.3	0.89	27.4	1.07	27.5	1.67	27.3	2.73	27.4	3.83
29.4	0.88	29.6	1.04	29.6	1.63	29.3	2.68	29.4	3.75
31.4	0.84	31.0	1.02	31.5	1.56	31.4	2.63	31.4	3.67
33.5	0.81	33.4	1.05	33.6	1.55	33.4	2.60	33.4	3.62
35.4	0.83	35.5	1.01	35.5	1.53	35.4	2.54	35.4	3.55
37.3	0.81	37.5	0.98	37.6	1.49	37.4	2.52	37.4	3.47
39.5	0.81	39.4	0.99	39.5	1.48	39.3	2.49	39.4	3.43
41.4	0.79	41.4	0.98	41.5	1.49	41.5	2.47	41.4	3.40
43.3	0.76	43.4	0.96	43.5	1.46	43.4	2.45	43.3	3.37
45.3	0.75	45.4	0.97	45.4	1.43	45.4	2.40	45.4	3.33
47.4	0.74	47.4	0.93	47.5	1.40	47.4	2.39	47.4	3.29
49.5	0.73	49.4	0.91	49.5	1.38	49.5	2.34	49.4	3.26
51.4	0.74	51.3	0.93	51.5	1.36	51.5	2.32	51.3	3.24
53.3	0.70	53.4	0.92	53.4	1.34	53.5	2.31	53.5	3.19
55.4	0.71	55.2	0.90	55.6	1.33	55.3	2.28	55.3	3.15
57.6	0.69	57.4	0.89	57.6	1.31	57.5	2.26	57.5	3.10
59.3	0.70	59.4	0.89	59.5	1.28	59.4	2.22	59.4	3.09
61.3	0.68	61.3	0.88	61.6	1.27	61.3	2.19	61.3	3.03
63.4	0.65	63.5	0.85	63.4	1.26	63.5	2.15	63.4	3.00
65.3	0.66	65.4	0.82	65.5	1.22	65.4	2.15	65.4	2.95
67.5	0.63	67.4	0.81	67.6	1.21	67.5	2.11	67.4	2.90
69.3	0.63	69.4	0.82	69.6	1.21	69.4	2.09	69.4	2.86
71.3	0.62	71.5	0.79	71.6	1.20	71.2	2.06	71.5	2.83
73.1	0.60	73.4	0.77	73.6	1.15	73.4	2.03	73.5	2.77
75.3	0.60	75.5	0.76	75.3	1.13	75.6	2.00	75.3	2.74
77.3	0.56	77.3	0.79	77.5	1.12	77.3	1.98	77.1	2.72

Table B10 Temperature sweep test results at 62.8 rad/s as measured by the DMA of HNBR compounds filled with various silica loadings (cont.): (b) Loss modulus (G″)

0 phr		10 phr		20 phr		30 phr		40 phr	
Temp.(°C)	G″ (MPa)	Temp.(°C)	G″ (MPa)	Temp.(°C)	G″ (MPa)	Temp.(°C)	G″ (MPa)	Temp.(°C)	G″ (MPa)
79.5	0.56	79.5	0.76	79.5	1.09	79.5	1.97	79.5	2.67
81.6	0.55	81.6	0.72	81.4	1.11	81.1	1.94	81.4	2.67
83.6	0.51	83.5	0.72	83.6	1.08	83.5	1.91	83.3	2.61
85.5	0.54	85.3	0.73	85.7	1.04	85.4	1.90	85.4	2.58
87.4	0.52	87.4	0.69	87.6	1.05	87.3	1.87	87.4	2.54
89.5	0.50	89.5	0.69	89.5	1.03	89.4	1.87	89.4	2.52
91.5	0.50	91.5	0.68	91.5	0.99	91.3	1.83	91.5	2.50
93.6	0.48	93.4	0.67	93.6	1.01	93.2	1.82	93.3	2.49
95.4	0.47	95.2	0.69	95.6	0.99	95.5	1.80	95.3	2.45
97.2	0.46	97.4	0.66	97.5	0.95	97.5	1.80	97.4	2.40
99.2	0.46	99.5	0.66	99.6	0.95	99.1	1.77	99.4	2.41
101.0	0.46	101.5	0.64	101.7	0.94	101.5	1.74	101.3	2.38
103.5	0.46	103.3	0.63	103.5	0.93	103.5	1.72	103.6	2.33
105.4	0.45	105.3	0.63	105.3	0.93	105.5	1.74	105.5	2.32
107.3	0.43	107.3	0.61	107.3	0.92	107.4	1.71	107.5	2.31
109.5	0.41	109.4	0.61	109.5	0.91	109.3	1.72	109.4	2.29
111.1	3.00	111.4	0.61	111.5	0.88	111.6	1.68	111.3	2.27
113.3	2.95	113.6	0.60	113.5	0.89	113.4	1.67	113.5	2.25
115.3	2.90	115.4	0.61	115.4	0.89	115.3	1.61	115.5	2.22
117.8	2.86	117.4	0.56	117.4	0.85	117.4	1.61	117.4	2.21
119.2	2.83	119.3	0.58	119.6	0.87	119.5	1.59	119.4	2.19
121.6	2.77	121.4	0.58	121.6	0.84	121.3	1.59	121.3	2.13
123.5	2.74	123.7	0.54	123.5	0.84	123.4	1.55	123.5	2.13
125.6	2.72	125.5	0.56	125.4	0.83	125.2	1.56	125.4	2.09
127.1	2.67	127.4	0.54	127.6	0.82	127.5	1.54	127.4	2.09
129.6	2.67	129.3	0.54	129.6	0.81	129.5	1.52	129.1	2.05
131.5	2.61	131.1	0.52	131.6	0.79	131.4	1.50	131.3	2.05
133.6	2.58	133.2	0.56	133.5	0.78	133.2	1.52	133.4	2.01
135.4	2.54	135.5	0.53	135.6	0.77	135.4	1.49	135.2	2.01
138.0	2.52	137.5	0.52	137.5	0.78	137.5	1.47	137.3	1.99
139.6	2.50	139.4	0.52	139.5	0.74	139.3	1.46	139.4	2.00
141.5	2.49	141.3	0.50	141.6	0.77	141.6	1.45	141.5	1.95
143.3	2.45	143.2	0.47	143.6	0.73	143.3	1.44	143.3	1.94
145.1	2.40	145.3	0.49	145.4	0.75	145.3	1.43	145.6	1.94
147.5	2.41	147.2	0.50	147.5	0.74	147.7	1.42	147.5	1.91
149.1	2.38	149.5	0.50	149.7	0.76	149.5	1.41	149.3	1.94

Table B11 Mechanical properties of HNBR compounds filled with various silica loadings

Silica loading (phr)	M100 (MPa)	Tensile strength (MPa)	Elongation at break (%)
0	2.33 ± 0.08	9.65 ± 0.51	235.48 ± 3.47
10	3.50 ± 0.17	11.54 ± 0.41	226.34 ± 3.56
20	5.62 ± 0.27	13.13 ± 0.63	194.39 ± 10.91
30	6.47 ± 0.51	15.44 ± 0.52	204.17 ± 18.29
40	9.14 ± 0.21	15.68 ± 0.50	166.77 ± 8.79

Silica loading (phr)	Tear strength (N/mm)	Hardness (Shore A)	Abrasion loss (mm^3)
0	25.19 ± 1.18	59.5 ± 0.577	66.98 ± 2.968
10	48.97 ± 2.24	62.9 ± 0.250	69.36 ± 2.426
20	60.38 ± 0.63	71.0 ± 0.000	65.83 ± 2.778
30	76.76 ± 2.69	77.5 ± 0.408	79.81 ± 2.302
40	78.53 ± 4.27	82.8 ± 0.500	90.53 ± 2.778

APPENDIX C
INFLUENCES OF ORGANOCLAY LOADING ON REINFORCEMENT OF HYDROGENATED NITRILE RUBBER

Table C1 Scorch time (t_{s2}), cure time (t_c), and torque difference ($\Delta S'$) of HNBR filled with various organoclay loadings

Organoclay loading (phr)	Scorch time (min)	Cure time (min)	S'max-S'min (dN-m)
0	1.26 ± 0.02	74.36 ± 0.54	31.29 ± 0.38
5	1.06 ± 0.02	73.51 ± 0.64	37.89 ± 0.65
10	0.95 ± 0.03	72.25 ± 0.32	43.22 ± 0.26
20	0.73 ± 0.02	65.50 ± 1.20	61.20 ± 1.52
30	0.62 ± 0.01	53.06 ± 2.03	75.91 ± 4.72

Table C2 Complex modulus (G^*) result at 3.14 rad/s and 100°C as measured by the RPA-FT of HNBR compounds filled with various organoclay loadings

Organoclay loading (phr)	Test a				Test b			
	run 1		run 2		run 1		run 2	
	Strain (%)	G^* (kPa)	Strain (%)	G^* (kPa)	Strain (%)	G^* (kPa)	Strain (%)	G^* (kPa)
0	6.98	68.93	8.38	67.44	8.38	69.57	6.98	68.30
	12.57	68.03	19.55	65.31	19.55	67.72	12.57	66.81
	32.11	64.84	60.04	58.03	60.04	60.72	32.11	63.46
	97.74	53.54	167.55	42.98	167.55	44.06	97.74	52.15
	251.33	35.69	335.10	31.93	335.10	31.09	251.33	36.48
	418.88	28.03	481.71	26.43	481.71	26.22	418.88	28.52
	544.54	24.40	600.39	23.16	600.39	22.85	544.54	24.77
	656.24	21.53	712.09	20.68	712.09	20.37	656.24	21.91
	767.94	19.30	837.76	18.45	837.76	18.23	767.94	19.76
	893.61	17.38	949.46	16.87	949.46	16.58	893.61	17.69

Table C2 Complex modulus (G^*) result at 3.14 rad/s and 100°C as measured by the RPA-FT of HNBR compounds filled with various organoclay loadings (cont.)

Organoclay loading (phr)	Test a				Test b			
	run 1		run 2		run 1		run 2	
	Strain (%)	G^* (kPa)	Strain (%)	G^* (kPa)	Strain (%)	G^* (kPa)	Strain (%)	G^* (kPa)
5	6.98	86.79	8.38	81.50	8.38	87.34	6.98	81.92
	12.57	85.08	19.55	78.57	19.55	83.96	12.57	80.51
	32.11	79.24	60.04	67.39	60.04	71.27	32.11	74.92
	97.74	61.23	167.55	48.06	167.55	49.12	97.74	58.82
	251.33	39.87	335.10	35.22	335.10	34.41	251.33	40.32
	418.88	30.72	481.71	28.85	481.71	28.46	418.88	31.19
	544.54	26.56	600.39	24.96	600.39	24.90	544.54	26.72
	656.24	23.52	712.09	22.02	712.09	22.16	656.24	23.35
	767.94	21.02	837.76	19.47	837.76	19.59	767.94	20.84
	893.61	18.66	949.46	17.66	949.46	17.69	893.61	18.50
10	6.98	99.29	8.38	100.97	8.38	99.12	6.98	101.19
	12.57	96.44	19.55	92.64	19.55	93.15	12.57	96.48
	32.11	87.15	60.04	74.24	60.04	76.41	32.11	85.03
	97.74	64.89	167.55	50.97	167.55	51.21	97.74	63.18
	251.33	41.91	335.10	37.10	335.10	35.32	251.33	42.52
	418.88	32.11	481.71	30.29	481.71	28.95	418.88	32.88
	544.54	27.73	600.39	26.26	600.39	25.35	544.54	28.02
	656.24	24.65	712.09	23.29	712.09	22.49	656.24	24.57
	767.94	22.05	837.76	20.49	837.76	20.54	767.94	21.87
	893.61	19.53	949.46	18.63	949.46	18.55	893.61	19.56
20	6.98	226.38	8.38	248.57	8.38	214.24	6.98	282.84
	12.57	191.95	19.55	172.67	19.55	166.90	12.57	221.45
	32.11	140.27	60.04	101.99	60.04	107.27	32.11	144.28
	97.74	82.22	167.55	60.74	167.55	60.75	97.74	83.65
	251.33	46.62	335.10	42.17	335.10	38.69	251.33	51.05
	418.88	33.20	481.71	34.07	481.71	30.62	418.88	38.26
	544.54	28.43	600.39	29.30	600.39	27.13	544.54	32.41
	656.24	25.99	712.09	26.13	712.09	25.03	656.24	28.71
	767.94	23.68	837.76	23.36	837.76	22.46	767.94	25.91
	893.61	21.29	949.46	21.55	949.46	20.46	893.61	23.54
30	6.98	149.21	8.38	182.29	8.38	144.75	6.98	195.13
	12.57	137.60	19.55	139.63	19.55	125.11	12.57	163.64
	32.11	112.28	60.04	91.77	60.04	91.60	32.11	118.65
	97.74	74.34	167.55	57.51	167.55	56.63	97.74	75.36
	251.33	45.22	335.10	40.73	335.10	38.06	251.33	47.96
	418.88	33.23	481.71	33.14	481.71	30.93	418.88	36.43
	544.54	28.59	600.39	28.47	600.39	27.29	544.54	30.87
	656.24	25.91	712.09	25.31	712.09	24.79	656.24	27.24
	767.94	23.37	837.76	22.45	837.76	22.24	767.94	24.34
	893.61	20.99	949.46	20.61	949.46	20.18	893.61	21.89

Table C3 Fit parameters of Equation 3.16 of HNBR compounds filled with various organoclay loadings

Organoclay loading (phr)	G_0^* (kPa)	1/A (%)	B
0	70.3	218.53	1.229
5	89.7	175.72	1.112
10	103.8	145.26	1.029
20	170.4	66.84	0.833
30	323.6	21.81	0.7186

Table C4 Total torque harmonic content (TTHC) result at 3.14 rad/s and 100°C as measured by the RPA-FT of HNBR compounds filled with various organoclay loadings

Organoclay loading (phr)	Test a				Test b			
	run 1		run 2		run 1		run 2	
	Strain (%)	TTHC (%)	Strain (%)	TTHC (%)	Strain (%)	TTHC (%)	Strain (%)	TTHC (%)
0	6.98	0.00	8.38	0.00	8.38	0.00	6.98	0.00
	12.57	0.13	19.55	0.57	19.55	0.42	12.57	0.45
	32.11	0.49	60.04	0.69	60.04	0.60	32.11	0.68
	97.74	1.67	167.55	3.65	167.55	3.82	97.74	1.65
	251.33	7.08	335.10	8.36	335.10	9.45	251.33	6.26
	418.88	10.46	481.71	11.55	481.71	11.51	418.88	10.18
	544.54	12.23	600.39	13.25	600.39	12.97	544.54	12.52
	656.24	13.65	712.09	14.79	712.09	14.23	656.24	14.07
	767.94	15.08	837.76	16.16	837.76	15.66	767.94	15.61
	893.61	16.43	949.46	17.26	949.46	16.86	893.61	16.96
5	6.98	0.00	8.38	0.04	8.38	0.00	6.98	0.15
	12.57	0.84	19.55	0.40	19.55	0.87	12.57	0.31
	32.11	0.37	60.04	0.67	60.04	0.66	32.11	0.60
	97.74	1.84	167.55	4.43	167.55	4.52	97.74	2.09
	251.33	7.65	335.10	9.23	335.10	9.81	251.33	7.03
	418.88	11.20	481.71	12.44	481.71	12.45	418.88	11.07
	544.54	13.16	600.39	14.16	600.39	13.99	544.54	13.37
	656.24	14.74	712.09	15.56	712.09	15.45	656.24	14.93
	767.94	16.26	837.76	16.92	837.76	16.81	767.94	16.38
	893.61	17.47	949.46	17.96	949.46	17.84	893.61	17.66

Table C4 Total torque harmonic content (TTHC) result at 3.14 rad/s and 100°C as measured by the RPA-FT of HNBR compounds filled with various organoclay loadings (cont.)

Organoclay loading (phr)	Test a				Test b			
	run 1		run 2		run 1		run 2	
	Strain (%)	TTHC (%)	Strain (%)	TTHC (%)	Strain (%)	TTHC (%)	Strain (%)	TTHC (%)
10	6.98	0.00	8.38	0.00	8.38	0.00	6.98	0.00
	12.57	0.24	19.55	0.00	19.55	0.08	12.57	0.19
	32.11	0.29	60.04	0.32	60.04	0.43	32.11	0.08
	97.74	1.56	167.55	4.93	167.55	4.87	97.74	1.71
	251.33	7.63	335.10	9.85	335.10	9.77	251.33	7.28
	418.88	11.70	481.71	13.17	481.71	12.60	418.88	11.72
	544.54	13.68	600.39	14.90	600.39	14.43	544.54	13.79
	656.24	15.14	712.09	16.25	712.09	15.83	656.24	15.34
	767.94	16.63	837.76	17.67	837.76	17.46	767.94	16.82
	893.61	18.22	949.46	19.03	949.46	18.62	893.61	18.49
20	6.98	0.00	8.38	0.00	8.38	0.81	6.98	0.00
	12.57	0.00	19.55	2.28	19.55	0.38	12.57	2.06
	32.11	0.89	60.04	3.95	60.04	1.18	32.11	4.39
	97.74	3.58	167.55	8.45	167.55	5.95	97.74	6.00
	251.33	8.76	335.10	13.39	335.10	11.04	251.33	11.29
	418.88	12.62	481.71	15.75	481.71	14.17	418.88	14.76
	544.54	15.56	600.39	17.65	600.39	16.73	544.54	16.93
	656.24	17.82	712.09	18.93	712.09	18.49	656.24	18.74
	767.94	19.03	837.76	20.38	837.76	19.79	767.94	19.84
	893.61	20.48	949.46	21.54	949.46	21.02	893.61	21.32
30	6.98	0.00	8.38	0.00	8.38	0.00	6.98	0.00
	12.57	0.09	19.55	0.00	19.55	0.21	12.57	0.00
	32.11	0.46	60.04	0.94	60.04	0.71	32.11	0.48
	97.74	2.17	167.55	5.63	167.55	4.91	97.74	2.80
	251.33	7.84	335.10	10.57	335.10	9.89	251.33	8.60
	418.88	11.38	481.71	13.32	481.71	12.69	418.88	12.50
	544.54	13.93	600.39	15.18	600.39	14.57	544.54	14.64
	656.24	15.82	712.09	16.78	712.09	16.36	656.24	16.35
	767.94	17.16	837.76	18.28	837.76	18.01	767.94	17.62
	893.61	18.61	949.46	19.64	949.46	19.34	893.61	19.15

Table C5 3rd relative torque harmonic (T(3/1)) result at 3.14 rad/s and 100°C as measured by the RPA-FT of HNBR compounds filled with various organoclay loadings

Organoclay loading (phr)	Test a				Test b			
	run 1		run 2		run 1		run 2	
	Strain (%)	T(3/1) (%)	Strain (%)	T(3/1) (%)	Strain (%)	T(3/1) (%)	Strain (%)	T(3/1) (%)
0	6.98	0.00	8.38	0.00	8.38	0.00	6.98	0.43
	12.57	0.00	19.55	0.07	19.55	0.00	12.57	0.00
	32.11	0.07	60.04	0.51	60.04	0.40	32.11	0.14
	97.74	1.16	167.55	3.05	167.55	3.20	97.74	1.24
	251.33	6.00	335.10	6.94	335.10	7.98	251.33	5.23
	418.88	8.72	481.71	9.24	481.71	9.28	418.88	8.42
	544.54	9.78	600.39	10.31	600.39	10.07	544.54	9.95
	656.24	10.44	712.09	11.10	712.09	10.75	656.24	10.77
	767.94	11.08	837.76	11.74	837.76	11.43	767.94	11.48
	893.61	11.66	949.46	12.23	949.46	11.95	893.61	12.02
5	6.98	0.33	8.38	0.14	8.38	0.00	6.98	0.00
	12.57	0.24	19.55	0.04	19.55	0.19	12.57	0.00
	32.11	0.20	60.04	0.66	60.04	0.57	32.11	0.20
	97.74	1.40	167.55	3.63	167.55	3.64	97.74	1.60
	251.33	6.37	335.10	7.54	335.10	8.12	251.33	5.81
	418.88	9.18	481.71	9.77	481.71	9.80	418.88	8.98
	544.54	10.33	600.39	10.76	600.39	10.66	544.54	10.42
	656.24	11.02	712.09	11.47	712.09	11.37	656.24	11.14
	767.94	11.68	837.76	12.09	837.76	12.01	767.94	11.79
	893.61	12.20	949.46	12.53	949.46	12.47	893.61	12.29
10	6.98	0.00	8.38	0.00	8.38	0.00	6.98	0.00
	12.57	0.00	19.55	0.00	19.55	0.06	12.57	0.00
	32.11	0.00	60.04	0.27	60.04	0.29	32.11	0.00
	97.74	1.16	167.55	3.79	167.55	3.54	97.74	1.27
	251.33	6.01	335.10	7.70	335.10	7.76	251.33	5.85
	418.88	9.07	481.71	9.86	481.71	9.67	418.88	9.04
	544.54	10.28	600.39	10.88	600.39	10.53	544.54	10.44
	656.24	11.03	712.09	11.57	712.09	11.33	656.24	11.24
	767.94	11.70	837.76	12.24	837.76	12.06	767.94	11.90
	893.61	12.33	949.46	12.76	949.46	12.53	893.61	12.59
20	6.98	0.00	8.38	0.00	8.38	0.00	6.98	0.00
	12.57	0.00	19.55	1.61	19.55	0.00	12.57	0.93
	32.11	0.32	60.04	3.08	60.04	0.73	32.11	3.17
	97.74	2.59	167.55	6.62	167.55	4.67	97.74	4.88
	251.33	6.96	335.10	9.75	335.10	8.53	251.33	8.49
	418.88	9.67	481.71	11.25	481.71	10.53	418.88	10.81
	544.54	11.23	600.39	12.13	600.39	11.76	544.54	11.94
	656.24	12.19	712.09	12.77	712.09	12.45	656.24	12.73
	767.94	12.65	837.76	13.33	837.76	12.92	767.94	13.23
	893.61	13.08	949.46	13.74	949.46	13.26	893.61	13.78

Table C5 3rd relative torque harmonic (T(3/1)) result at 3.14 rad/s and 100°C as measured by the RPA-FT of HNBR compounds filled with various organoclay loadings (cont.)

Organoclay loading (phr)	Test a				Test b			
	run 1		run 2		run 1		run 2	
	Strain (%)	T(3/1) (%)	Strain (%)	T(3/1) (%)	Strain (%)	T(3/1) (%)	Strain (%)	T(3/1) (%)
30	6.98	0.00	8.38	0.00	8.38	0.00	6.98	0.00
	12.57	0.00	19.55	0.00	19.55	0.00	12.57	0.00
	32.11	0.13	60.04	0.72	60.04	0.24	32.11	0.27
	97.74	1.56	167.55	4.48	167.55	3.69	97.74	2.43
	251.33	6.24	335.10	8.31	335.10	7.87	251.33	6.75
	418.88	9.06	481.71	10.23	481.71	9.81	418.88	9.61
	544.54	10.46	600.39	11.21	600.39	10.86	544.54	10.92
	656.24	11.34	712.09	11.90	712.09	11.63	656.24	11.76
	767.94	11.94	837.76	12.53	837.76	12.36	767.94	12.32
	893.61	12.52	949.46	13.02	949.46	12.80	893.61	12.93

Table C6 5th relative torque harmonic (T(5/1)) result at 3.14 rad/s and 100°C as measured by the RPA-FT of HNBR compounds filled with various organoclay loadings

Organoclay loading (phr)	Test a				Test b			
	run 1		run 2		run 1		run 2	
	Strain (%)	T(5/1) (%)	Strain (%)	T(5/1) (%)	Strain (%)	T(5/1) (%)	Strain (%)	T(5/1) (%)
0	6.98	0.00	8.38	0.00	8.38	0.00	6.98	0.00
	12.57	0.08	19.55	0.27	19.55	0.29	12.57	0.06
	32.11	0.07	60.04	0.04	60.04	0.05	32.11	0.07
	97.74	0.23	167.55	0.35	167.55	0.37	97.74	0.18
	251.33	0.68	335.10	0.98	335.10	1.01	251.33	0.63
	418.88	1.33	481.71	1.70	481.71	1.63	418.88	1.37
	544.54	1.90	600.39	2.21	600.39	2.12	544.54	2.01
	656.24	2.35	712.09	2.68	712.09	2.55	656.24	2.47
	767.94	2.79	837.76	3.16	837.76	3.03	767.94	2.93
	893.61	3.20	949.46	3.47	949.46	3.38	893.61	3.33

Table C6 5th relative torque harmonic (T(5/1)) result at 3.14 rad/s and 100°C as measured by the RPA-FT of HNBR compounds filled with various organoclay loadings (cont.)

Organoclay loading (phr)	Test a				Test b			
	run 1		run 2		run 1		run 2	
	Strain (%)	T(5/1) (%)	Strain (%)	T(5/1) (%)	Strain (%)	T(5/1) (%)	Strain (%)	T(5/1) (%)
5	6.98	0.00	8.38	0.00	8.38	0.31	6.98	0.20
	12.57	0.16	19.55	0.30	19.55	0.31	12.57	0.34
	32.11	0.04	60.04	0.06	60.04	0.06	32.11	0.02
	97.74	0.31	167.55	0.52	167.55	0.59	97.74	0.31
	251.33	0.84	335.10	1.16	335.10	1.15	251.33	0.82
	418.88	1.52	481.71	1.90	481.71	1.86	418.88	1.56
	544.54	2.17	600.39	2.43	600.39	2.39	544.54	2.22
	656.24	2.65	712.09	2.89	712.09	2.87	656.24	2.68
	767.94	3.10	837.76	3.35	837.76	3.33	767.94	3.12
	893.61	3.45	949.46	3.65	949.46	3.62	893.61	3.49
10	6.98	0.24	8.38	0.43	8.38	0.00	6.98	0.04
	12.57	0.34	19.55	0.03	19.55	0.00	12.57	0.19
	32.11	0.44	60.04	0.27	60.04	0.31	32.11	0.35
	97.74	0.53	167.55	0.62	167.55	0.69	97.74	0.48
	251.33	0.97	335.10	1.35	335.10	1.26	251.33	0.93
	418.88	1.61	481.71	2.13	481.71	2.01	418.88	1.74
	544.54	2.30	600.39	2.65	600.39	2.60	544.54	2.39
	656.24	2.79	712.09	3.09	712.09	2.92	656.24	2.87
	767.94	3.27	837.76	3.55	837.76	3.49	767.94	3.32
	893.61	3.67	949.46	3.88	949.46	3.83	893.61	3.77
20	6.98	0.46	8.38	0.44	8.38	0.00	6.98	0.47
	12.57	0.37	19.55	0.24	19.55	0.03	12.57	0.48
	32.11	0.67	60.04	0.41	60.04	0.29	32.11	0.48
	97.74	0.58	167.55	1.27	167.55	0.82	97.74	0.75
	251.33	1.08	335.10	2.27	335.10	1.42	251.33	1.83
	418.88	1.86	481.71	2.87	481.71	2.32	418.88	2.62
	544.54	2.77	600.39	3.38	600.39	3.13	544.54	3.14
	656.24	3.49	712.09	3.76	712.09	3.70	656.24	3.65
	767.94	3.87	837.76	4.16	837.76	4.07	767.94	3.97
	893.61	4.23	949.46	4.50	949.46	4.43	893.61	4.42
30	6.98	0.32	8.38	0.30	8.38	0.00	6.98	0.29
	12.57	0.46	19.55	0.00	19.55	0.00	12.57	0.32
	32.11	0.24	60.04	0.16	60.04	0.11	32.11	0.16
	97.74	0.52	167.55	0.63	167.55	0.72	97.74	0.26
	251.33	0.90	335.10	1.47	335.10	1.22	251.33	1.06
	418.88	1.56	481.71	2.17	481.71	1.96	418.88	1.92
	544.54	2.30	600.39	2.70	600.39	2.59	544.54	2.52
	656.24	2.93	712.09	3.16	712.09	3.11	656.24	3.04
	767.94	3.36	837.76	3.66	837.76	3.59	767.94	3.44
	893.61	3.76	949.46	4.02	949.46	3.94	893.61	3.90

Table C7 Fit parameters of Equation 3.17 of HNBR compounds filled with various organoclay loadings

Organoclay loading (phr)	TH	α	C	D
0	7.307	0.0049	0.0101	4.2900
5	8.194	0.0045	0.0085	3.1190
10	7.700	0.0052	0.0090	3.5310
20	8.076	0.0051	0.0079	2.8820
30	11.040	0.0026	0.0053	1.7300

Table C8 Integrating torque signals result at 3.14 rad/s and 100°C as measured by the RPA-FT of HNBR compounds filled with various organoclay loadings

Organoclay loading (phr)	Test a				Test b			
	run 1		run 2		run 1		run 2	
	Strain (%)	Q1/Q2	Strain (%)	Q1/Q2	Strain (%)	Q1/Q2	Strain (%)	Q1/Q2
0	6.98	1.11	8.38	1.01	8.38	1.07	6.98	1.06
	12.57	1.02	19.55	1.07	19.55	1.07	12.57	1.05
	32.11	1.04	60.04	1.05	60.04	1.04	32.11	1.04
	97.74	1.04	167.55	1.03	167.55	1.04	97.74	1.04
	251.33	1.05	335.10	1.06	335.10	1.05	251.33	1.06
	418.88	1.06	481.71	1.07	481.71	1.06	418.88	1.06
	544.54	1.05	600.39	1.07	600.39	1.07	544.54	1.07
	656.24	1.06	712.09	1.07	712.09	1.07	656.24	1.07
	767.94	1.08	837.76	1.08	837.76	1.08	767.94	1.10
	893.61	1.09	949.46	1.09	949.46	1.09	893.61	1.10
5	6.98	1.09	8.38	0.99	8.38	1.02	6.98	1.05
	12.57	1.04	19.55	1.08	19.55	1.09	12.57	1.02
	32.11	1.03	60.04	1.05	60.04	1.05	32.11	1.03
	97.74	1.04	167.55	1.01	167.55	1.01	97.74	1.04
	251.33	1.04	335.10	1.05	335.10	1.04	251.33	1.04
	418.88	1.04	481.71	1.07	481.71	1.06	418.88	1.05
	544.54	1.05	600.39	1.06	600.39	1.06	544.54	1.05
	656.24	1.06	712.09	1.08	712.09	1.07	656.24	1.07
	767.94	1.07	837.76	1.08	837.76	1.07	767.94	1.08
	893.61	1.09	949.46	1.09	949.46	1.08	893.61	1.09

Table C8 Integrating torque signals result at 3.14 rad/s and 100°C as measured by the RPA-FT of HNBR compounds filled with various organoclay loadings (cont.)

Organoclay loading (phr)	Test a				Test b			
	run 1		run 2		run 1		run 2	
	Strain (%)	Q1/Q2	Strain (%)	Q1/Q2	Strain (%)	Q1/Q2	Strain (%)	Q1/Q2
10	6.98	1.08	8.38	1.09	8.38	1.06	6.98	1.08
	12.57	1.09	19.55	1.05	19.55	1.02	12.57	1.05
	32.11	1.08	60.04	1.05	60.04	1.04	32.11	1.04
	97.74	1.05	167.55	1.03	167.55	1.00	97.74	1.06
	251.33	1.03	335.10	1.05	335.10	1.02	251.33	1.04
	418.88	1.04	481.71	1.06	481.71	1.04	418.88	1.04
	544.54	1.04	600.39	1.07	600.39	1.03	544.54	1.05
	656.24	1.04	712.09	1.09	712.09	1.05	656.24	1.07
	767.94	1.07	837.76	1.07	837.76	1.08	767.94	1.08
	893.61	1.07	949.46	1.08	949.46	1.08	893.61	1.07
20	6.98	1.09	8.38	1.01	8.38	1.28	6.98	1.02
	12.57	0.97	19.55	0.93	19.55	1.31	12.57	0.91
	32.11	0.98	60.04	0.91	60.04	1.01	32.11	0.89
	97.74	0.99	167.55	0.92	167.55	0.96	97.74	0.92
	251.33	0.98	335.10	0.92	335.10	0.96	251.33	0.91
	418.88	0.95	481.71	0.94	481.71	0.96	418.88	0.94
	544.54	0.95	600.39	0.95	600.39	0.96	544.54	0.94
	656.24	0.95	712.09	0.95	712.09	0.95	656.24	0.93
	767.94	0.96	837.76	0.95	837.76	0.95	767.94	0.95
	893.61	0.96	949.46	0.94	949.46	0.97	893.61	0.94
30	6.98	1.10	8.38	1.04	8.38	1.10	6.98	1.09
	12.57	1.02	19.55	0.99	19.55	1.02	12.57	0.94
	32.11	0.97	60.04	0.97	60.04	1.03	32.11	0.97
	97.74	1.02	167.55	0.98	167.55	0.99	97.74	0.97
	251.33	1.00	335.10	0.98	335.10	1.00	251.33	0.97
	418.88	1.01	481.71	0.99	481.71	1.02	418.88	0.98
	544.54	1.01	600.39	1.00	600.39	1.02	544.54	0.99
	656.24	1.00	712.09	0.99	712.09	1.01	656.24	0.99
	767.94	1.01	837.76	1.00	837.76	1.00	767.94	1.00
	893.61	1.01	949.46	1.00	949.46	1.02	893.61	0.99

Table C9 Strain sweep test results at 60°C and 1 rad/s as measured by the RPA2000 of HNBR compounds filled with various organoclay loadings:

(a) Storage modulus (G′)

Strain amplitude (%)	G′ (kPa)				
	0 phr	5phr	10 phr	20 phr	30 phr
0.56	1136.40	1449.80	1775.30	3242.60	29524.00
0.70	1141.60	1433.30	1725.20	3113.80	5363.20
0.98	1127.10	1393.60	1661.90	3035.40	4967.50
1.95	1097.10	1394.10	1650.50	2886.70	4636.30
3.07	1083.20	1402.30	1655.50	2816.80	4454.70
5.02	1069.30	1386.70	1629.80	2679.30	4096.70
6.98	1057.70	1366.80	1605.50	2575.00	3831.50
10.04	1053.80	1343.20	1569.00	2455.30	3531.30
15.07	1042.20	1310.30	1514.60	2297.90	3186.20
19.95	1027.00	1281.60	1466.40	2172.10	2935.20
29.99	997.09	1224.50	1368.10	1941.20	2502.30
40.04	963.21	1162.90	1274.60	1739.60	2135.50
49.94	931.20	1099.90	1184.80	1559.20	1818.60
59.99	897.29	1031.60	1097.10	1366.50	1581.10
70.03	861.83	956.05	1007.90	1186.60	1408.90
79.93	821.65	884.90	915.40	1075.90	1275.00
89.98	786.55	833.55	852.39	1003.20	1167.90
100.02	759.23	794.06	810.85	949.82	1079.20

Table C9 Strain sweep test results at 60°C and 1 rad/s as measured by the RPA2000 of HNBR compounds filled with various organoclay loadings (cont.):

(b) Loss modulus (G″)

Strain amplitude (%)	G″ (kPa)				
	0 phr	5phr	10 phr	20 phr	30 phr
0.56	88.63	118.58	173.61	371.74	24868.00
0.70	93.76	140.26	165.25	328.21	634.68
0.98	95.36	107.32	151.42	323.80	631.70
1.95	91.43	121.76	159.48	344.81	663.67
3.07	95.28	124.15	169.53	355.92	682.46
5.02	94.62	123.71	162.49	352.90	684.07
6.98	90.69	121.89	161.14	347.42	674.98
10.04	91.54	121.40	163.16	350.45	662.99
15.07	92.27	124.82	165.83	347.29	629.47
19.95	94.71	129.06	170.15	348.07	597.42
29.99	99.76	141.63	183.62	345.29	554.90
40.04	105.40	155.64	194.33	339.58	528.82
49.94	111.57	174.62	209.80	344.17	531.53
59.99	120.46	198.63	229.29	365.25	535.67
70.03	130.02	228.49	254.28	384.56	527.72
79.93	140.52	253.44	284.53	390.51	512.54
89.98	147.05	266.64	297.07	387.23	495.52
100.02	150.59	266.35	297.34	383.77	481.64

Table C10 Temperature sweep test results at 62.8 rad/s as measured by the DMA of HNBR compounds filled with various organoclay loadings: (a) Storage modulus (G′)

0 phr		5 phr		10 phr		20 phr		30 phr	
Temp.(°C)	G′ (MPa)	Temp.(°C)	G′ (MPa)	Temp.(°C)	G′ (MPa)	Temp.(°C)	G′ (MPa)	Temp.(°C)	G′ (MPa)
-80.1	2590.50	-81.2	2483.62	-80.4	2981.04	-78.9	3009.03	-79.9	2991.91
-79.6	2594.41	-78.2	2455.38	-78.8	3021.55	-79.1	2930.98	-78.9	2992.62
-78.1	2571.16	-76.3	2419.57	-76.9	3024.99	-76.7	2900.25	-76.6	2985.39
-75.8	2534.68	-74.6	2377.68	-74.9	3007.06	-74.5	2861.34	-74.5	2968.68
-72.8	2480.94	-72.6	2320.40	-72.9	2975.68	-72.7	2822.22	-72.1	2927.62
-70.8	2443.93	-70.5	2275.08	-70.7	2944.42	-70.6	2783.99	-70.4	2891.60
-69.0	2403.53	-68.6	2227.73	-68.5	2885.97	-68.2	2739.89	-68.4	2848.29
-67.2	2364.91	-66.4	2187.49	-66.5	2832.98	-66.8	2702.76	-66.0	2802.40
-65.0	2319.63	-64.3	2141.32	-64.2	2781.03	-64.9	2642.44	-64.4	2775.26
-63.3	2278.99	-62.6	2098.59	-62.5	2740.16	-62.8	2608.97	-62.9	2723.06
-61.3	2234.60	-60.4	2060.91	-60.4	2693.14	-60.8	2570.70	-60.0	2690.21
-59.1	2189.45	-58.4	2040.60	-58.8	2645.17	-58.8	2538.75	-59.0	2659.77
-57.0	2145.52	-56.5	2021.97	-56.9	2588.76	-56.7	2498.28	-56.6	2633.48
-54.6	2110.26	-54.5	1994.72	-54.7	2534.77	-54.7	2459.84	-54.3	2574.45
-52.9	2087.62	-52.5	1982.15	-52.4	2469.18	-52.8	2432.19	-52.4	2552.74
-51.3	2043.89	-50.5	1958.30	-50.2	2406.91	-50.6	2406.36	-50.4	2537.57
-49.0	1990.56	-48.6	1948.97	-48.8	2358.02	-48.7	2392.65	-48.0	2506.71
-46.7	1954.07	-46.6	1934.39	-46.2	2287.72	-46.7	2374.56	-46.8	2497.33
-44.9	1914.04	-44.5	1904.59	-44.1	2236.41	-44.8	2355.61	-44.2	2467.61
-42.9	1862.60	-42.6	1887.87	-42.2	2190.42	-42.9	2332.76	-42.5	2453.66
-40.7	1802.77	-40.7	1863.78	-40.3	2145.84	-40.6	2286.85	-40.3	2418.91
-38.8	1746.78	-38.5	1829.68	-38.3	2084.66	-38.6	2248.71	-38.5	2376.43
-36.7	1681.55	-36.5	1755.90	-36.6	1999.29	-36.6	2177.36	-36.8	2321.44
-34.8	1611.48	-34.3	1611.94	-34.2	1866.02	-34.7	2060.10	-34.6	2211.06
-32.5	1445.58	-32.3	1393.07	-32.5	1659.37	-32.3	1859.20	-32.3	2033.64
-30.5	1245.11	-30.3	1095.66	-30.6	1414.53	-30.6	1622.84	-30.2	1735.30
-28.6	997.53	-28.6	869.08	-28.5	1173.45	-28.3	1364.50	-28.2	1492.13
-26.7	718.17	-26.4	688.77	-26.5	795.53	-26.7	1138.44	-26.3	1220.79
-24.7	485.73	-24.6	475.02	-24.6	558.26	-24.6	786.17	-24.6	943.63
-22.6	270.80	-22.6	281.31	-22.4	414.81	-22.3	509.80	-22.5	689.97
-20.7	145.21	-20.5	157.57	-20.6	299.90	-20.5	351.91	-20.0	470.97
-18.6	72.77	-18.7	99.41	-18.5	189.20	-18.4	218.08	-18.4	373.35
-16.7	42.27	-16.7	68.15	-16.5	114.95	-16.4	153.59	-16.8	298.07
-14.6	28.14	-14.6	47.91	-14.5	67.50	-14.5	115.26	-14.6	221.09
-12.6	20.94	-12.4	35.56	-12.6	48.09	-12.7	91.74	-12.4	184.28
-10.5	16.97	-10.5	28.35	-10.7	36.63	-10.6	77.22	-10.5	161.53
-8.6	14.23	-8.7	23.60	-8.5	29.04	-8.6	66.46	-8.6	145.46
-6.6	12.26	-6.6	19.99	-6.6	24.67	-6.6	58.91	-6.5	132.55
-4.6	10.86	-4.6	17.41	-4.6	21.75	-4.6	53.74	-4.4	123.16

Table C10 Temperature sweep test results at 62.8 rad/s as measured by the DMA of HNBR compounds filled with various organoclay loadings (cont.): (a) Storage modulus (G′)

0 phr		5 phr		10 phr		20 phr		30 phr	
Temp.(°C)	G′ (MPa)	Temp.(°C)	G′ (MPa)	Temp.(°C)	G′ (MPa)	Temp.(°C)	G′ (MPa)	Temp.(°C)	G′ (MPa)
-2.5	9.66	-2.5	15.92	-2.6	19.82	-2.5	50.26	-2.5	115.75
-0.7	9.09	-0.5	14.87	-0.6	18.33	-0.4	46.73	-0.8	109.19
4.1	8.41	4.7	13.70	3.7	17.11	4.6	43.93	3.7	102.64
3.9	8.24	4.6	13.34	3.7	16.78	4.5	42.95	3.5	101.06
5.2	8.00	4.5	13.14	5.3	16.08	4.5	42.65	5.4	98.30
7.4	7.77	7.3	12.53	7.3	15.61	7.3	40.90	7.4	95.70
9.5	7.56	9.4	12.14	9.4	15.12	9.5	39.77	9.5	93.17
11.4	7.40	11.4	11.88	11.5	14.61	11.4	38.84	11.5	90.89
13.5	7.28	13.4	11.58	13.3	14.31	13.4	38.01	13.4	88.80
15.4	7.14	15.4	11.41	15.5	14.08	15.5	37.26	15.5	87.00
17.4	7.05	17.5	11.19	17.5	13.81	17.4	36.68	17.5	85.61
19.3	6.97	19.4	11.03	19.4	13.62	19.5	36.15	19.5	84.27
21.4	6.86	21.4	10.91	21.5	13.41	21.4	35.64	21.4	83.36
23.5	6.77	23.4	10.77	23.5	13.27	23.5	35.18	23.6	82.18
25.3	6.69	25.4	10.65	25.4	13.13	25.4	34.72	25.3	81.61
27.3	6.57	27.4	10.50	27.3	12.98	27.3	34.30	27.5	80.57
29.4	6.49	29.4	10.40	29.3	12.87	29.4	33.76	29.5	79.70
31.4	6.43	31.4	10.30	31.3	12.76	31.1	33.37	31.5	78.81
33.5	6.34	33.4	10.18	33.4	12.58	33.4	32.91	33.5	77.77
35.4	6.26	35.5	10.06	35.4	12.45	36.0	32.57	35.4	76.86
37.3	6.20	37.9	9.95	37.5	12.32	36.8	32.47	37.5	75.89
39.5	6.13	38.9	9.84	39.4	12.21	39.4	32.02	39.5	74.99
41.4	6.06	41.3	9.81	41.4	12.07	41.4	31.70	41.4	74.08
43.3	6.02	43.6	9.69	43.4	11.94	43.4	31.35	43.4	73.13
45.3	5.96	45.5	9.63	45.3	11.84	45.3	31.01	45.4	72.18
47.4	5.89	47.4	9.57	47.4	11.71	47.3	30.68	47.5	71.30
49.5	5.84	49.4	9.51	49.4	11.57	49.4	30.34	49.5	70.49
51.4	5.76	51.4	9.41	51.4	11.48	51.4	30.00	51.4	69.67
53.3	5.72	53.4	9.33	53.5	11.35	53.4	29.65	53.5	68.85
55.4	5.65	55.5	9.24	55.3	11.25	55.5	29.35	55.5	68.14
57.6	5.58	57.5	9.16	57.4	11.17	57.3	29.04	57.5	67.38
59.3	5.54	59.4	9.09	59.3	11.07	59.5	28.74	59.5	66.65
61.3	5.49	61.4	9.02	61.6	10.94	61.4	28.49	61.4	65.93
63.4	5.42	63.4	8.99	63.4	10.85	63.3	28.22	63.4	65.23
65.3	5.35	65.4	8.90	65.2	10.81	65.5	27.95	65.5	64.68
67.5	5.28	67.4	8.84	67.3	10.71	67.5	27.64	67.5	64.07
69.3	5.22	69.5	8.75	69.3	10.65	69.3	27.40	69.5	63.37
71.3	5.17	71.2	8.69	71.3	10.54	71.6	27.11	71.4	62.66
73.1	5.12	73.4	8.61	73.5	10.44	73.4	26.87	73.5	61.99
75.3	5.02	75.4	8.56	75.4	10.35	75.4	26.62	75.5	61.43
77.3	4.96	77.4	8.51	77.5	10.29	77.4	26.44	77.5	60.80

Table C10 Temperature sweep test results at 62.8 rad/s as measured by the DMA of HNBR compounds filled with various organoclay loadings (cont.): (a) Storage modulus (G′)

0 phr		5 phr		10 phr		20 phr		30 phr	
Temp.(°C)	G′ (MPa)	Temp.(°C)	G′ (MPa)	Temp.(°C)	G′ (MPa)	Temp.(°C)	G′ (MPa)	Temp.(°C)	G′ (MPa)
79.5	4.90	79.5	8.43	79.4	10.19	79.3	26.25	79.5	60.21
81.6	4.83	81.4	8.42	81.4	10.13	81.5	26.00	81.5	59.60
83.6	4.78	83.5	8.35	83.6	10.07	83.4	25.77	83.5	59.09
85.5	4.73	85.3	8.31	85.6	10.06	85.4	25.60	85.5	58.53
87.4	4.68	87.4	8.28	87.4	9.99	87.5	25.41	87.4	58.11
89.5	4.63	89.4	8.24	89.5	9.94	89.4	25.23	89.5	57.56
91.5	4.59	91.4	8.21	91.5	9.92	91.3	25.08	91.3	57.21
93.6	4.55	93.4	8.18	93.3	9.90	93.2	24.95	93.5	56.76
95.4	4.54	95.3	8.14	95.4	9.84	95.5	24.80	95.4	56.36
97.2	4.53	97.5	8.14	97.5	9.80	97.4	24.69	97.5	55.97
99.2	4.48	99.5	8.11	99.3	9.79	99.5	24.57	99.6	55.59
101.0	4.49	101.5	8.10	101.5	9.75	101.5	24.46	101.4	55.28
103.5	4.46	103.3	8.08	103.4	9.75	103.4	24.36	103.4	54.95
105.4	4.44	105.6	8.07	105.4	9.68	105.5	24.21	105.3	54.59
107.3	4.44	107.4	8.05	107.4	9.68	107.5	24.12	107.4	54.31
109.5	4.45	109.3	8.06	109.3	9.65	109.3	24.03	109.4	53.95
111.1	4.46	111.4	8.02	111.4	9.65	111.7	23.90	111.7	53.60
113.3	4.44	113.4	8.02	113.5	9.61	113.3	23.83	113.4	53.36
115.3	4.43	115.3	8.00	115.5	9.62	115.3	23.75	115.3	53.05
117.8	4.43	117.4	7.99	117.4	9.58	117.5	23.68	117.4	52.78
119.2	4.45	119.4	7.97	119.3	9.54	119.2	23.62	119.5	52.49
121.6	4.43	121.3	7.98	121.5	9.51	121.4	23.45	121.5	52.25
123.5	4.44	123.4	8.05	123.6	9.56	123.5	23.40	123.5	52.00
125.6	4.45	125.4	7.99	125.5	9.46	125.5	23.30	125.3	51.80
127.1	4.42	127.5	7.95	127.4	9.47	127.5	23.30	127.4	51.58
129.6	4.43	129.2	7.97	129.3	9.50	129.3	23.21	129.6	51.35
131.5	4.44	131.4	7.99	131.3	9.49	131.2	23.18	131.5	51.19
133.6	4.44	133.4	7.96	133.5	9.47	133.6	23.11	133.3	50.97
135.4	4.46	135.5	7.96	135.4	9.49	135.4	23.04	135.5	50.75
138.0	4.43	137.4	7.95	137.5	9.45	137.2	23.01	137.3	50.59
139.6	4.47	139.4	7.96	139.5	9.48	139.4	22.92	139.4	50.38
141.5	4.46	141.5	7.96	141.6	9.46	141.4	22.88	141.4	50.20
143.3	4.46	143.3	7.95	143.5	9.48	143.4	22.83	143.5	50.02
145.1	4.48	145.4	7.94	145.6	9.49	145.3	22.80	145.4	49.77
147.5	4.46	147.4	7.92	147.6	9.45	147.3	22.72	147.5	49.58
149.1	4.48	149.5	7.99	149.4	9.41	149.5	22.66	149.4	49.38

Table C10 Temperature sweep test results at 62.8 rad/s as measured by the DMA of HNBR compounds filled with various organoclay loadings (cont.): (b) Loss modulus (G″)

0 phr		5 phr		10 phr		20 phr		30 phr	
Temp.(°C)	G″ (MPa)	Temp.(°C)	G″ (MPa)	Temp.(°C)	G″ (MPa)	Temp.(°C)	G″ (MPa)	Temp.(°C)	G″ (MPa)
-80.1	100.58	-81.2	145.66	-80.4	94.10	-78.9	154.59	-79.9	184.00
-79.6	101.53	-78.2	143.11	-78.8	96.40	-79.1	168.49	-78.9	184.09
-78.1	99.39	-76.3	142.28	-76.9	96.05	-76.7	164.81	-76.6	181.71
-75.8	97.33	-74.6	141.65	-74.9	94.72	-74.5	160.68	-74.5	178.90
-72.8	94.32	-72.6	141.51	-72.9	94.24	-72.7	155.58	-72.1	176.24
-70.8	92.15	-70.5	139.14	-70.7	90.90	-70.6	153.01	-70.4	173.54
-69.0	89.42	-68.6	136.34	-68.5	86.34	-68.2	148.66	-68.4	170.66
-67.2	86.63	-66.4	133.08	-66.5	82.96	-66.8	144.97	-66.0	166.81
-65.0	82.96	-64.3	131.04	-64.2	80.14	-64.9	142.01	-64.4	165.63
-63.3	80.45	-62.6	128.17	-62.5	76.64	-62.8	138.91	-62.9	162.84
-61.3	77.00	-60.4	123.28	-60.4	73.92	-60.8	135.83	-60.0	160.76
-59.1	73.75	-58.4	120.97	-58.8	72.68	-58.8	132.29	-59.0	157.68
-57.0	70.30	-56.5	117.41	-56.9	70.49	-56.7	130.92	-56.6	154.54
-54.6	68.44	-54.5	114.68	-54.7	69.09	-54.7	128.72	-54.3	149.11
-52.9	66.99	-52.5	113.41	-52.4	68.82	-52.8	127.80	-52.4	145.32
-51.3	65.46	-50.5	112.19	-50.2	70.64	-50.6	126.87	-50.4	142.89
-49.0	63.66	-48.6	111.71	-48.8	72.01	-48.7	125.00	-48.0	141.32
-46.7	63.08	-46.6	111.53	-46.2	73.29	-46.7	125.10	-46.8	141.36
-44.9	64.20	-44.5	114.76	-44.1	75.71	-44.8	126.08	-44.2	142.23
-42.9	66.55	-42.6	116.53	-42.2	78.06	-42.9	128.19	-42.5	143.20
-40.7	72.16	-40.7	119.90	-40.3	79.77	-40.6	132.01	-40.3	148.02
-38.8	79.57	-38.5	123.66	-38.3	87.07	-38.6	136.64	-38.5	154.74
-36.7	90.72	-36.5	135.57	-36.6	99.07	-36.6	147.04	-36.8	166.86
-34.8	105.53	-34.3	165.30	-34.2	126.73	-34.7	171.57	-34.6	193.91
-32.5	143.22	-32.3	216.75	-32.5	177.59	-32.3	220.27	-32.3	238.27
-30.5	193.27	-30.3	275.43	-30.6	236.44	-30.6	279.54	-30.2	315.63
-28.6	248.80	-28.6	308.12	-28.5	284.84	-28.3	331.97	-28.2	363.23
-26.7	283.17	-26.4	319.66	-26.5	328.45	-26.7	362.36	-26.3	393.87
-24.7	273.78	-24.6	295.82	-24.6	319.21	-24.6	366.27	-24.6	390.59
-22.6	216.43	-22.6	231.31	-22.4	285.98	-22.3	313.70	-22.5	347.54
-20.7	148.17	-20.5	157.74	-20.6	241.63	-20.5	250.22	-20.0	268.99
-18.6	86.68	-18.7	108.48	-18.5	179.00	-18.4	169.28	-18.4	218.08
-16.7	51.26	-16.7	75.78	-16.5	120.20	-16.4	117.81	-16.8	171.40
-14.6	31.74	-14.6	51.26	-14.5	70.81	-14.5	82.11	-14.6	114.83
-12.6	20.96	-12.4	34.64	-12.6	46.76	-12.7	58.41	-12.4	84.68
-10.5	14.89	-10.5	24.44	-10.7	31.40	-10.6	43.11	-10.5	65.33
-8.6	10.76	-8.7	17.63	-8.5	20.87	-8.6	31.60	-8.6	51.65
-6.6	7.84	-6.6	12.52	-6.6	14.90	-6.6	23.69	-6.5	40.64
-4.6	5.80	-4.6	8.95	-4.6	11.02	-4.6	18.40	-4.4	32.91

Table C10 Temperature sweep test results at 62.8 rad/s as measured by the DMA of HNBR compounds filled with various organoclay loadings (cont.): (b) Loss modulus (G″)

0 phr		5 phr		10 phr		20 phr		30 phr	
Temp.(°C)	G″ (MPa)	Temp.(°C)	G″ (MPa)	Temp.(°C)	G″ (MPa)	Temp.(°C)	G″ (MPa)	Temp.(°C)	G″ (MPa)
-2.5	4.18	-2.5	6.94	-2.6	8.43	-2.5	14.88	-2.5	27.01
-0.7	3.42	-0.5	5.52	-0.6	6.59	-0.4	11.49	-0.8	21.96
4.1	2.50	4.7	4.11	3.7	5.02	4.6	9.03	3.7	17.44
3.9	2.25	4.6	3.65	3.7	4.69	4.5	8.23	3.5	16.17
5.2	1.95	4.5	3.39	5.3	3.98	4.5	7.89	5.4	14.46
7.4	1.68	7.3	2.82	7.3	3.45	7.3	6.59	7.4	12.94
9.5	1.49	9.4	2.35	9.4	2.88	9.5	5.79	9.5	11.61
11.4	1.34	11.4	2.10	11.5	2.52	11.4	5.26	11.5	10.54
13.5	1.24	13.4	1.92	13.3	2.22	13.4	4.82	13.4	9.72
15.4	1.16	15.4	1.79	15.5	2.04	15.5	4.52	15.5	9.08
17.4	1.09	17.5	1.66	17.5	2.00	17.4	4.28	17.5	8.67
19.3	1.04	19.4	1.55	19.4	1.86	19.5	4.09	19.5	8.33
21.4	0.98	21.4	1.50	21.5	1.83	21.4	3.94	21.4	8.10
23.5	0.95	23.4	1.43	23.5	1.76	23.5	3.80	23.6	7.85
25.3	0.92	25.4	1.39	25.4	1.73	25.4	3.70	25.3	7.75
27.3	0.89	27.4	1.39	27.3	1.67	27.3	3.64	27.5	7.60
29.4	0.88	29.4	1.34	29.3	1.65	29.4	3.55	29.5	7.47
31.4	0.84	31.4	1.33	31.3	1.63	31.1	3.49	31.5	7.35
33.5	0.81	33.4	1.32	33.4	1.61	33.4	3.41	33.5	7.21
35.4	0.83	35.5	1.27	35.4	1.59	36.0	3.38	35.4	7.10
37.3	0.81	37.9	1.26	37.5	1.55	36.8	3.36	37.5	7.02
39.5	0.81	38.9	1.24	39.4	1.49	39.4	3.33	39.5	6.94
41.4	0.79	41.3	1.24	41.4	1.49	41.4	3.29	41.4	6.87
43.3	0.76	43.6	1.22	43.4	1.48	43.4	3.27	43.4	6.81
45.3	0.75	45.5	1.22	45.3	1.48	45.3	3.22	45.4	6.78
47.4	0.74	47.4	1.18	47.4	1.46	47.3	3.20	47.5	6.70
49.5	0.73	49.4	1.19	49.4	1.45	49.4	3.14	49.5	6.65
51.4	0.74	51.4	1.18	51.4	1.44	51.4	3.13	51.4	6.62
53.3	0.70	53.4	1.15	53.5	1.38	53.4	3.11	53.5	6.55
55.4	0.71	55.5	1.14	55.3	1.40	55.5	3.04	55.5	6.50
57.6	0.69	57.5	1.15	57.4	1.38	57.3	3.05	57.5	6.48
59.3	0.70	59.4	1.12	59.3	1.39	59.5	3.01	59.5	6.41
61.3	0.68	61.4	1.10	61.6	1.35	61.4	2.97	61.4	6.42
63.4	0.65	63.4	1.08	63.4	1.34	63.3	2.97	63.4	6.39
65.3	0.66	65.4	1.07	65.2	1.30	65.5	2.94	65.5	6.33
67.5	0.63	67.4	1.06	67.3	1.27	67.5	2.89	67.5	6.31
69.3	0.63	69.5	1.06	69.3	1.27	69.3	2.86	69.5	6.22
71.3	0.62	71.2	1.03	71.3	1.28	71.6	2.82	71.4	6.22
73.1	0.60	73.4	1.02	73.5	1.22	73.4	2.80	73.5	6.14
75.3	0.60	75.4	0.98	75.4	1.23	75.4	2.76	75.5	6.11
77.3	0.56	77.4	0.95	77.5	1.17	77.4	2.71	77.5	6.08

Table C10 Temperature sweep test results at 62.8 rad/s as measured by the DMA of HNBR compounds filled with various organoclay loadings (cont.): (b) Loss modulus (G″)

0 phr		5 phr		10 phr		20 phr		30 phr	
Temp.(°C)	G″ (MPa)	Temp.(°C)	G″ (MPa)	Temp.(°C)	G″ (MPa)	Temp.(°C)	G″ (MPa)	Temp.(°C)	G″ (MPa)
79.5	0.56	79.5	0.97	79.4	1.17	79.3	2.68	79.5	5.99
81.6	0.55	81.4	0.92	81.4	1.12	81.5	2.66	81.5	5.96
83.6	0.51	83.5	0.90	83.6	1.12	83.4	2.62	83.5	5.90
85.5	0.54	85.3	0.92	85.6	1.13	85.4	2.58	85.5	5.81
87.4	0.52	87.4	0.92	87.4	1.10	87.5	2.54	87.4	5.78
89.5	0.50	89.4	0.86	89.5	1.08	89.4	2.53	89.5	5.75
91.5	0.50	91.4	0.85	91.5	1.06	91.3	2.49	91.3	5.67
93.6	0.48	93.4	0.86	93.3	1.04	93.2	2.48	93.5	5.63
95.4	0.47	95.3	0.83	95.4	1.02	95.5	2.44	95.4	5.58
97.2	0.46	97.5	0.81	97.5	1.04	97.4	2.43	97.5	5.54
99.2	0.46	99.5	0.81	99.3	1.01	99.5	2.40	99.6	5.46
101.0	0.46	101.5	0.80	101.5	1.01	101.5	2.38	101.4	5.44
103.5	0.46	103.3	0.79	103.4	0.99	103.4	2.35	103.4	5.40
105.4	0.45	105.6	0.76	105.4	0.97	105.5	2.34	105.3	5.39
107.3	0.43	107.4	0.78	107.4	0.97	107.5	2.32	107.4	5.31
109.5	0.41	109.3	0.77	109.3	0.96	109.3	2.27	109.4	5.30
111.1	0.41	111.4	0.76	111.4	0.95	111.7	2.26	111.7	5.25
113.3	0.40	113.4	0.74	113.5	0.92	113.3	2.24	113.4	5.24
115.3	0.41	115.3	0.72	115.5	0.91	115.3	2.18	115.3	5.17
117.8	0.41	117.4	0.71	117.4	0.89	117.5	2.19	117.4	5.09
119.2	0.39	119.4	0.73	119.3	0.91	119.2	2.15	119.5	5.04
121.6	0.38	121.3	0.71	121.5	0.85	121.4	2.14	121.5	4.97
123.5	0.40	123.4	0.67	123.6	0.91	123.5	2.11	123.5	4.91
125.6	0.38	125.4	0.70	125.5	0.87	125.5	2.10	125.3	4.93
127.1	0.39	127.5	0.69	127.4	0.83	127.5	2.04	127.4	4.86
129.6	0.36	129.2	0.67	129.3	0.85	129.3	2.07	129.6	4.82
131.5	0.37	131.4	0.66	131.3	0.84	131.2	2.00	131.5	4.72
133.6	0.35	133.4	0.64	133.5	0.84	133.6	1.99	133.3	4.72
135.4	0.35	135.5	0.64	135.4	0.82	135.4	1.98	135.5	4.69
138.0	0.34	137.4	0.62	137.5	0.82	137.2	1.95	137.3	4.63
139.6	0.34	139.4	0.67	139.5	0.78	139.4	1.97	139.4	4.61
141.5	0.36	141.5	0.63	141.6	0.79	141.4	1.96	141.4	4.57
143.3	0.34	143.3	0.63	143.5	0.79	143.4	1.94	143.5	4.55
145.1	0.33	145.4	0.60	145.6	0.77	145.3	1.89	145.4	4.52
147.5	0.34	147.4	0.62	147.6	0.76	147.3	1.91	147.5	4.52
149.1	0.34	149.5	0.60	149.4	0.77	149.5	1.89	149.4	4.44

Table C11 Mechanical properties of HNBR compounds filled with various organoclay loadings

Organoclay loading (phr)	M100 (MPa)	Tensile strength (MPa)	Elongation at break (%)
0	2.33 ± 0.08	9.65 ± 0.51	235.48 ± 3.47
5	4.27 ± 0.15	8.64 ± 0.33	182.92 ± 6.98
10	4.94 ± 0.23	9.28 ± 0.21	180.07 ± 1.35
20	6.96 ± 0.49	13.04 ± 0.60	222.30 ± 17.52
30	8.79 ± 0.15	13.52 ± 0.22	211.73 ± 9.27

Organoclay loading (phr)	Tear strength (N/mm)	Hardness (Shore A)	Abrasion loss (mm^3)
0	25.19 ± 1.18	59.5 ± 0.577	66.98 ± 2.968
5	32.65 ± 4.87	65.3 ± 0.289	62.51 ± 2.204
10	44.74 ± 1.24	68.8 ± 0.645	73.54 ± 1.325
20	56.84 ± 1.48	77.8 ± 0.957	120.02 ± 5.415
30	68.71 ± 2.11	83.9 ± 1.031	152.19 ± 6.475

APPENDIX D
INFLUENCES OF CARBON BLACK HYBRID SYSTEM ON REINFORCEMENT OF HYDROGENATED NITRILE RUBBER

Table D1 Scorch time (t_{s2}), cure time (t_c), and torque difference ($\Delta S'$) of HNBR filled with various CB hybrid systems and hybrid ratios

CB	CB	Scorch time	Cure time	S'max-S'min
N326/N990	0/100	1.09 ± 0.09	70.84 ± 1.13	53.40 ± 2.58
	20/80	1.06 ± 0.04	70.53 ± 0.78	54.12 ± 2.35
	40/60	1.02 ± 0.04	68.96 ± 1.35	53.74 ± 2.74
	60/40	1.02 ± 0.00	66.28 ± 1.81	56.48 ± 3.61
	80/20	1.00 ± 0.01	66.22 ± 1.49	59.32 ± 1.14
	100/0	1.01 ± 0.04	62.61 ± 2.50	60.19 ± 0.04
N326/N774	0/100	0.95 ± 0.08	67.02 ± 2.86	60.67 ± 1.53
	20/80	0.92 ± 0.08	67.38 ± 0.34	61.94 ± 1.49
	40/60	0.89 ± 0.02	65.82 ± 1.76	63.36 ± 0.85
	60/40	0.89 ± 0.08	66.75 ± 0.32	61.17 ± 1.85
	80/20	0.93 ± 0.05	64.10 ± 1.03	66.03 ± 2.13
	100/0	0.99 ± 0.05	64.07 ± 1.33	61.83 ± 1.94
N550/N990	0/100	1.09 ± 0.09	70.84 ± 1.13	53.40 ± 2.58
	20/80	1.10 ± 0.04	72.72 ± 0.55	53.04 ± 0.63
	40/60	1.09 ± 0.04	71.89 ± 0.62	54.95 ± 0.99
	60/40	1.01 ± 0.04	70.78 ± 0.74	59.92 ± 1.70
	80/20	0.95 ± 0.02	69.02 ± 0.83	62.73 ± 2.17
	100/0	0.88 ± 0.02	65.71 ± 1.52	66.64 ± 1.27

Table D2 Complex modulus (G^*) result at 3.14 rad/s and 100°C as measured by the RPA-FT of HNBR compounds filled with various CB hybrid systems and hybrid ratios

CB hybrid system	CB hybrid ratio	Test a				Test b			
		run 1		run 2		run 1		run 2	
		Strain (%)	G^* (kPa)	Strain (%)	G^* (kPa)	Strain (%)	G^* (kPa)	Strain (%)	G^* (kPa)
N326/N990	0/100	6.98	131.53	8.38	119.73	8.38	129.39	6.98	121.57
		12.57	126.26	19.55	111.67	19.55	120.16	12.57	117.09
		32.11	110.97	60.04	87.10	60.04	93.32	32.11	103.25
		97.74	77.64	167.55	59.74	167.55	61.78	97.74	74.23
		251.33	51.39	335.10	44.24	335.10	44.79	251.33	50.70
		418.88	40.07	481.71	37.00	481.71	37.18	418.88	40.07
		544.54	34.62	600.39	32.76	600.39	32.68	544.54	34.99
		656.24	30.84	712.09	29.64	712.09	29.28	656.24	31.45
		767.94	27.83	837.76	26.77	837.76	26.23	767.94	28.57
		893.61	25.04	949.46	24.61	949.46	23.92	893.61	25.94
	20/80	6.98	135.54	8.38	124.02	8.38	133.96	6.98	126.75
		12.57	129.41	19.55	114.58	19.55	123.33	12.57	120.64
		32.11	113.21	60.04	88.47	60.04	95.13	32.11	104.99
		97.74	78.90	167.55	60.48	167.55	62.99	97.74	74.70
		251.33	52.48	335.10	44.87	335.10	45.87	251.33	51.14
		418.88	40.87	481.71	37.31	481.71	37.90	418.88	40.24
		544.54	35.15	600.39	32.76	600.39	33.16	544.54	34.76
		656.24	31.22	712.09	29.38	712.09	29.61	656.24	30.98
		767.94	28.07	837.76	26.31	837.76	26.46	767.94	27.89
		893.61	25.22	949.46	24.02	949.46	24.03	893.61	25.12
	40/60	6.98	146.00	8.38	135.50	8.38	144.42	6.98	137.96
		12.57	138.00	19.55	122.32	19.55	130.88	12.57	129.61
		32.11	119.35	60.04	92.82	60.04	100.07	32.11	110.78
		97.74	82.69	167.55	63.20	167.55	66.04	97.74	78.16
		251.33	55.09	335.10	46.98	335.10	48.16	251.33	53.41
		418.88	42.91	481.71	38.96	481.71	39.63	418.88	41.96
		544.54	36.78	600.39	34.13	600.39	34.56	544.54	36.17
		656.24	32.62	712.09	30.55	712.09	30.81	656.24	32.24
		767.94	29.23	837.76	27.39	837.76	27.43	767.94	29.10
		893.61	26.15	949.46	25.05	949.46	24.86	893.61	26.26
	60/40	6.98	10.05	8.38	150.03	8.38	160.68	6.98	153.35
		12.57	152.79	19.55	131.96	19.55	142.42	12.57	141.05
		32.11	128.76	60.04	98.17	60.04	106.49	32.11	117.42
		97.74	87.67	167.55	66.29	167.55	69.49	97.74	81.58
		251.33	58.25	335.10	49.46	335.10	50.64	251.33	55.83
		418.88	45.22	481.71	40.99	481.71	41.51	418.88	43.94
		544.54	38.65	600.39	36.01	600.39	36.09	544.54	37.90
		656.24	34.19	712.09	32.45	712.09	32.12	656.24	33.79
		767.94	30.64	837.76	29.18	837.76	28.51	767.94	30.52
		893.61	27.41	949.46	26.87	949.46	25.89	893.61	27.56

Table D2 Complex modulus (G^*) result at 3.14 rad/s and 100°C as measured by the RPA-FT of HNBR compounds filled with various CB hybrid systems and hybrid ratios (cont.)

CB hybrid system	CB hybrid ratio	Test a				Test b			
		run 1		run 2		run 1		run 2	
		Strain (%)	G^* (kPa)	Strain (%)	G^* (kPa)	Strain (%)	G^* (kPa)	Strain (%)	G^* (kPa)
N326/N990	80/20	6.98	180.39	8.38	156.98	8.38	175.33	6.98	165.69
		12.57	162.56	19.55	136.71	19.55	152.50	12.57	143.91
		32.11	135.21	60.04	101.04	60.04	112.25	32.11	117.88
		97.74	90.88	167.55	66.18	167.55	72.74	97.74	81.27
		251.33	60.17	335.10	50.27	335.10	53.15	251.33	56.03
		418.88	46.52	481.71	40.45	481.71	43.41	418.88	44.09
		544.54	39.38	600.39	35.45	600.39	37.60	544.54	37.90
		656.24	34.79	712.09	31.51	712.09	33.32	656.24	33.98
		767.94	31.07	837.76	28.51	837.76	29.50	767.94	30.76
		893.61	27.95	949.46	25.65	949.46	26.58	893.61	27.76
	100/0	6.98	202.23	8.38	177.99	8.38	195.01	6.98	185.72
		12.57	180.51	19.55	148.70	19.55	164.74	12.57	164.04
		32.11	146.60	60.04	107.05	60.04	119.43	32.11	130.77
		97.74	97.30	167.55	72.04	167.55	77.01	97.74	89.00
		251.33	64.71	335.10	54.26	335.10	56.37	251.33	61.45
		418.88	50.04	481.71	44.77	481.71	45.88	418.88	48.35
		544.54	42.43	600.39	39.25	600.39	39.64	544.54	41.57
		656.24	37.29	712.09	35.28	712.09	35.06	656.24	37.04
		767.94	33.15	837.76	31.78	837.76	30.91	767.94	33.46
		893.61	29.37	949.46	29.31	949.46	27.83	893.61	30.14
N326/N774	0/100	6.98	9.99	8.38	152.25	8.38	171.93	6.98	155.34
		12.57	160.49	19.55	137.60	19.55	154.03	12.57	146.58
		32.11	136.17	60.04	102.30	60.04	113.59	32.11	124.63
		97.74	91.15	167.55	68.11	167.55	72.59	97.74	85.53
		251.33	60.37	335.10	51.53	335.10	53.15	251.33	58.54
		418.88	47.44	481.71	43.13	481.71	43.82	418.88	46.96
		544.54	40.68	600.39	38.13	600.39	38.30	544.54	41.04
		656.24	36.13	712.09	34.50	712.09	34.17	656.24	37.00
		767.94	32.41	837.76	31.15	837.76	30.45	767.94	33.77
		893.61	28.99	949.46	28.72	949.46	27.59	893.61	30.93
	20/80	6.98	187.85	8.38	163.94	8.38	180.95	6.98	168.64
		12.57	173.70	19.55	145.15	19.55	160.56	12.57	156.15
		32.11	145.36	60.04	106.63	60.04	117.91	32.11	130.46
		97.74	96.13	167.55	71.16	167.55	75.53	97.74	88.99
		251.33	63.38	335.10	54.08	335.10	55.45	251.33	61.30
		418.88	49.48	481.71	45.42	481.71	45.67	418.88	49.09
		544.54	42.43	600.39	40.36	600.39	39.89	544.54	42.91
		656.24	37.64	712.09	36.68	712.09	35.61	656.24	38.74
		767.94	33.72	837.76	33.42	837.76	31.62	767.94	35.59
		893.61	30.04	949.46	31.75	949.46	28.72	893.61	32.92

Table D2 Complex modulus (G^*) result at 3.14 rad/s and 100°C as measured by the RPA-FT of HNBR compounds filled with various CB hybrid systems and hybrid ratios (cont.)

CB hybrid system	CB hybrid ratio	Test a				Test b			
		run 1		run 2		run 1		run 2	
		Strain (%)	G^* (kPa)	Strain (%)	G^* (kPa)	Strain (%)	G^* (kPa)	Strain (%)	G^* (kPa)
N326/N774	40/60	6.98	187.85	8.38	164.68	8.38	183.62	6.98	169.58
		12.57	172.22	19.55	143.94	19.55	160.56	12.57	155.06
		32.11	143.55	60.04	105.23	60.04	117.14	32.11	128.22
		97.74	95.21	167.55	70.32	167.55	74.94	97.74	87.46
		251.33	62.73	335.10	53.30	335.10	54.86	251.33	60.17
		418.88	48.92	481.71	44.67	481.71	45.08	418.88	48.03
		544.54	41.84	600.39	39.60	600.39	39.27	544.54	41.88
		656.24	37.02	712.09	35.91	712.09	34.95	656.24	37.72
		767.94	33.11	837.76	32.63	837.76	30.97	767.94	34.51
		893.61	29.42	949.46	30.80	949.46	28.17	893.61	31.57
	60/40	6.98	189.45	8.38	167.34	8.38	185.84	6.98	173.17
		12.57	172.03	19.55	143.18	19.55	159.48	12.57	156.34
		32.11	141.77	60.04	104.03	60.04	115.84	32.11	127.10
		97.74	94.27	167.55	69.78	167.55	74.42	97.74	86.64
		251.33	62.34	335.10	52.82	335.10	54.56	251.33	59.73
		418.88	48.56	481.71	44.05	481.71	44.75	418.88	47.41
		544.54	41.45	600.39	38.92	600.39	38.90	544.54	41.11
		656.24	36.62	712.09	35.14	712.09	34.55	656.24	36.83
		767.94	32.70	837.76	31.72	837.76	30.52	767.94	33.48
		893.61	28.99	949.46	29.77	949.46	27.85	893.61	30.31
	80/20	6.98	211.64	8.38	189.09	8.38	208.62	6.98	197.97
		12.57	190.57	19.55	159.35	19.55	176.92	12.57	175.97
		32.11	154.93	60.04	113.98	60.04	127.34	32.11	140.50
		97.74	102.57	167.55	76.05	167.55	81.90	97.74	95.05
		251.33	67.81	335.10	56.52	335.10	59.33	251.33	64.86
		418.88	52.23	481.71	46.45	481.71	47.89	418.88	50.54
		544.54	44.18	600.39	40.51	600.39	41.25	544.54	43.32
		656.24	38.78	712.09	36.26	712.09	36.28	656.24	38.40
		767.94	34.28	837.76	32.60	837.76	31.86	767.94	34.57
		893.61	30.47	949.46	29.84	949.46	28.64	893.61	31.24
	100/0	6.98	206.31	8.38	183.91	8.38	200.19	6.98	192.82
		12.57	184.26	19.55	153.45	19.55	168.93	12.57	170.35
		32.11	149.84	60.04	109.98	60.04	122.24	32.11	135.63
		97.74	99.40	167.55	73.94	167.55	78.79	97.74	92.12
		251.33	65.74	335.10	55.34	335.10	57.37	251.33	63.28
		418.88	50.51	481.71	45.47	481.71	46.52	418.88	49.45
		544.54	42.66	600.39	39.56	600.39	40.18	544.54	42.32
		656.24	37.32	712.09	35.41	712.09	35.37	656.24	37.55
		767.94	33.12	837.76	31.65	837.76	31.18	767.94	34.06
		893.61	29.38	949.46	29.17	949.46	28.19	893.61	30.79

Table D2 Complex modulus (G^*) result at 3.14 rad/s and 100°C as measured by the RPA-FT of HNBR compounds filled with various CB hybrid systems and hybrid ratios (cont.)

CB hybrid system	CB hybrid ratio	Test a				Test b			
		run 1		run 2		run 1		run 2	
		Strain (%)	G^* (kPa)	Strain (%)	G^* (kPa)	Strain (%)	G^* (kPa)	Strain (%)	G^* (kPa)
N550/N990	0/100	6.98	131.53	8.38	119.73	8.38	129.39	6.98	121.57
		12.57	126.26	19.55	111.67	19.55	120.16	12.57	117.09
		32.11	110.97	60.04	87.10	60.04	93.32	32.11	103.25
		97.74	77.64	167.55	59.74	167.55	61.78	97.74	74.23
		251.33	51.39	335.10	44.24	335.10	44.79	251.33	50.70
		418.88	40.07	481.71	37.00	481.71	37.18	418.88	40.07
		544.54	34.62	600.39	32.76	600.39	32.68	544.54	34.99
		656.24	30.84	712.09	29.64	712.09	29.28	656.24	31.45
		767.94	27.83	837.76	26.77	837.76	26.23	767.94	28.57
		893.61	25.04	949.46	24.61	949.46	23.92	893.61	25.94
	20/80	6.98	150.00	8.38	135.07	8.38	147.41	6.98	136.48
		12.57	143.52	19.55	125.11	19.55	135.76	12.57	130.60
		32.11	124.40	60.04	95.94	60.04	103.12	32.11	113.90
		97.74	85.43	167.55	65.31	167.55	67.79	97.74	80.63
		251.33	56.47	335.10	48.57	335.10	49.34	251.33	55.19
		418.88	43.83	481.71	40.48	481.71	40.71	418.88	43.62
		544.54	37.70	600.39	35.78	600.39	35.68	544.54	37.90
		656.24	33.55	712.09	32.26	712.09	31.92	656.24	34.04
		767.94	30.23	837.76	28.97	837.76	28.56	767.94	30.85
		893.61	27.22	949.46	26.59	949.46	26.01	893.61	27.96
	40/60	6.98	153.48	8.38	137.71	8.38	151.95	6.98	139.43
		12.57	146.38	19.55	126.89	19.55	139.00	12.57	133.06
		32.11	126.45	60.04	96.15	60.04	104.78	32.11	115.14
		97.74	86.19	167.55	65.42	167.55	68.43	97.74	80.73
		251.33	57.31	335.10	49.16	335.10	50.16	251.33	55.53
		418.88	44.83	481.71	40.97	481.71	41.43	418.88	44.06
		544.54	38.56	600.39	36.09	600.39	36.29	544.54	38.29
		656.24	34.28	712.09	32.52	712.09	32.45	656.24	34.36
		767.94	30.78	837.76	29.25	837.76	28.90	767.94	31.14
		893.61	27.62	949.46	26.85	949.46	26.21	893.61	28.19
	60/40	6.98	169.22	8.38	150.92	8.38	168.23	6.98	153.71
		12.57	160.19	19.55	137.79	19.55	151.87	12.57	145.30
		32.11	137.25	60.04	103.06	60.04	112.93	32.11	124.29
		97.74	92.45	167.55	70.02	167.55	73.48	97.74	86.28
		251.33	61.65	335.10	53.08	335.10	54.08	251.33	59.78
		418.88	48.29	481.71	44.41	481.71	44.67	418.88	47.55
		544.54	41.45	600.39	39.31	600.39	39.04	544.54	41.34
		656.24	36.78	712.09	35.53	712.09	34.80	656.24	37.06
		767.94	32.94	837.76	32.02	837.76	30.88	767.94	33.65
		893.61	29.31	949.46	29.78	949.46	28.16	893.61	30.42

Table D2 Complex modulus (G^*) result at 3.14 rad/s and 100°C as measured by the RPA-FT of HNBR compounds filled with various CB hybrid systems and hybrid ratios (cont.)

CB hybrid system	CB hybrid ratio	Test a				Test b			
		run 1		run 2		run 1		run 2	
		Strain (%)	G^* (kPa)	Strain (%)	G^* (kPa)	Strain (%)	G^* (kPa)	Strain (%)	G^* (kPa)
N550/N990	80/20	6.98	189.80	8.38	168.97	8.38	187.61	6.98	173.04
		12.57	178.14	19.55	152.12	19.55	168.23	12.57	162.56
		32.11	150.11	60.04	112.39	60.04	123.23	32.11	137.06
		97.74	99.99	167.55	76.20	167.55	79.75	97.74	94.22
		251.33	67.03	335.10	58.26	335.10	59.07	251.33	65.79
		418.88	52.35	481.71	48.84	481.71	48.58	418.88	52.64
		544.54	44.84	600.39	43.46	600.39	42.30	544.54	46.03
		656.24	39.70	712.09	39.51	712.09	37.58	656.24	41.59
		767.94	35.49	837.76	36.15	837.76	33.28	767.94	38.22
		893.61	31.67	949.46	34.23	949.46	30.03	893.61	35.45
	100/0	6.98	207.73	8.38	184.36	8.38	202.70	6.98	198.86
		12.57	192.35	19.55	164.30	19.55	178.69	12.57	184.75
		32.11	160.26	60.04	120.53	60.04	130.25	32.11	153.89
		97.74	106.82	167.55	82.12	167.55	85.08	97.74	105.02
		251.33	71.96	335.10	62.85	335.10	62.66	251.33	73.24
		418.88	55.72	481.71	52.72	481.71	51.23	418.88	58.38
		544.54	47.37	600.39	47.36	600.39	44.37	544.54	51.51
		656.24	41.63	712.09	43.87	712.09	39.22	656.24	47.71
		767.94	37.04	837.76	41.49	837.76	34.62	767.94	46.45
		893.61	32.82	949.46	42.80	949.46	31.97	893.61	47.15

Table D3 Fit parameters of Equation 3.16 of HNBR compounds filled with various CB hybrid systems and hybrid ratios

CB hybrid system	CB hybrid ratio	G_0^* (kPa)	1/A (%)	B
N326/N990	0/100	141.6	111.6	0.918
	20/80	147.9	109.0	0.875
	40/60	162.9	101.3	0.814
	60/40	162.8	55.2	1.804
	80/20	223.7	64.9	0.650
	100/0	281.5	46.4	0.571
N326/N774	0/100	170.5	57.3	1.978
	20/80	216.9	72.1	0.774
	40/60	223.4	67.4	0.732
	60/40	237.2	58.5	0.664
	80/20	280.4	51.2	0.606
	100/0	281.5	46.4	0.571
N550/N990	0/100	141.6	111.6	0.918
	20/80	163.8	100.9	0.890
	40/60	169.5	96.5	0.871
	60/40	190.5	88.5	0.834
	80/20	218.3	79.6	0.791
	100/0	248.8	71.7	0.706

Table D4 Total torque harmonic content (TTHC) result at 3.14 rad/s and 100°C as measured by the RPA-FT of HNBR compounds filled with various CB hybrid systems and hybrid ratios

CB hybrid system	CB hybrid ratio	Test a				Test b			
		run 1		run 2		run 1		run 2	
		Strain (%)	TTHC (%)	Strain (%)	TTHC (%)	Strain (%)	TTHC (%)	Strain (%)	TTHC (%)
N326/N990	0/100	6.98	0.00	8.38	0.00	8.38	0.00	6.98	0.00
		12.57	0.00	19.55	0.00	19.55	0.00	12.57	0.00
		32.11	0.00	60.04	1.41	60.04	1.50	32.11	0.61
		97.74	3.94	167.55	6.45	167.55	6.94	97.74	3.60
		251.33	9.88	335.10	11.69	335.10	11.91	251.33	9.70
		418.88	13.59	481.71	14.74	481.71	14.64	418.88	13.65
		544.54	15.54	600.39	16.73	600.39	16.44	544.54	15.81
		656.24	17.16	712.09	18.40	712.09	18.02	656.24	17.58
		767.94	18.76	837.76	20.00	837.76	19.64	767.94	19.11
		893.61	20.17	949.46	21.39	949.46	20.94	893.61	20.62
	20/80	6.98	0.00	8.38	0.00	8.38	0.00	6.98	0.00
		12.57	0.00	19.55	0.00	19.55	0.21	12.57	0.04
		32.11	0.46	60.04	1.60	60.04	1.66	32.11	0.73
		97.74	3.82	167.55	6.58	167.55	6.99	97.74	3.67
		251.33	10.09	335.10	11.87	335.10	11.99	251.33	9.74
		418.88	13.69	481.71	14.75	481.71	14.70	418.88	13.71
		544.54	15.60	600.39	16.69	600.39	16.44	544.54	15.74
		656.24	17.18	712.09	18.25	712.09	17.97	656.24	17.39
		767.94	18.81	837.76	19.75	837.76	19.54	767.94	18.99
		893.61	20.15	949.46	21.07	949.46	20.88	893.61	20.42
	40/60	6.98	0.00	8.38	0.00	8.38	0.00	6.98	0.00
		12.57	0.00	19.55	0.00	19.55	0.00	12.57	0.00
		32.11	0.00	60.04	1.13	60.04	1.13	32.11	0.00
		97.74	3.36	167.55	6.07	167.55	6.52	97.74	3.05
		251.33	9.72	335.10	11.61	335.10	11.75	251.33	9.44
		418.88	13.52	481.71	14.49	481.71	14.44	418.88	13.45
		544.54	15.30	600.39	16.31	600.39	16.12	544.54	15.49
		656.24	16.95	712.09	17.88	712.09	17.61	656.24	17.16
		767.94	18.33	837.76	19.49	837.76	19.16	767.94	18.69
		893.61	19.75	949.46	20.91	949.46	20.65	893.61	20.19
	60/40	6.98	0.00	8.38	1.77	8.38	1.95	6.98	1.58
		12.57	1.95	19.55	1.60	19.55	1.58	12.57	1.37
		32.11	2.08	60.04	2.69	60.04	2.95	32.11	1.66
		97.74	4.74	167.55	7.18	167.55	7.90	97.74	4.56
		251.33	10.86	335.10	12.47	335.10	12.82	251.33	10.61
		418.88	14.45	481.71	15.14	481.71	15.30	418.88	14.32
		544.54	16.06	600.39	16.75	600.39	16.74	544.54	16.16
		656.24	17.44	712.09	18.40	712.09	18.13	656.24	17.61
		767.94	18.82	837.76	20.02	837.76	19.67	767.94	19.18
		893.61	20.16	949.46	21.44	949.46	20.98	893.61	20.61

Table D4 Total torque harmonic content (TTHC) result at 3.14 rad/s and 100°C as measured by the RPA-FT of HNBR compounds filled with various CB hybrid systems and hybrid ratios (cont.)

CB hybrid system	CB hybrid ratio	Test a				Test b			
		run 1		run 2		run 1		run 2	
		Strain (%)	TTHC (%)	Strain (%)	TTHC (%)	Strain (%)	TTHC (%)	Strain (%)	TTHC (%)
N326/N990	80/20	6.98	0.00	8.38	0.00	8.38	0.00	6.98	0.00
		12.57	0.00	19.55	0.00	19.55	0.00	12.57	0.00
		32.11	0.00	60.04	1.21	60.04	1.36	32.11	0.00
		97.74	3.69	167.55	6.41	167.55	7.06	97.74	3.36
		251.33	10.45	335.10	11.85	335.10	12.34	251.33	9.99
		418.88	13.94	481.71	14.45	481.71	14.64	418.88	13.70
		544.54	15.52	600.39	16.33	600.39	16.18	544.54	15.51
		656.24	16.97	712.09	17.77	712.09	17.70	656.24	17.09
		767.94	18.46	837.76	19.17	837.76	19.26	767.94	18.68
		893.61	19.88	949.46	21.39	949.46	20.83	893.61	20.20
	100/0	6.98	0.00	8.38	0.00	8.38	0.00	6.98	0.00
		12.57	0.00	19.55	0.00	19.55	0.00	12.57	0.00
		32.11	0.00	60.04	1.09	60.04	1.38	32.11	0.00
		97.74	3.65	167.55	6.29	167.55	7.07	97.74	3.20
		251.33	10.31	335.10	11.70	335.10	12.31	251.33	9.72
		418.88	13.72	481.71	14.25	481.71	14.48	418.88	13.33
		544.54	15.18	600.39	16.00	600.39	15.75	544.54	15.17
		656.24	16.55	712.09	17.58	712.09	17.26	656.24	16.85
		767.94	18.08	837.76	19.27	837.76	18.88	767.94	18.45
		893.61	19.56	949.46	21.01	949.46	20.51	893.61	19.97
N326/N774	0/100	6.98	0.00	8.38	0.86	8.38	1.53	6.98	1.26
		12.57	1.27	19.55	1.87	19.55	1.57	12.57	2.04
		32.11	2.45	60.04	2.94	60.04	3.09	32.11	2.34
		97.74	5.57	167.55	8.15	167.55	8.70	97.74	4.91
		251.33	11.81	335.10	13.13	335.10	13.49	251.33	11.43
		418.88	15.02	481.71	15.43	481.71	15.59	418.88	14.99
		544.54	16.42	600.39	17.15	600.39	16.98	544.54	16.69
		656.24	17.66	712.09	18.59	712.09	18.30	656.24	18.04
		767.94	18.97	837.76	20.02	837.76	19.76	767.94	19.50
		893.61	20.18	949.46	21.39	949.46	20.96	893.61	20.91
	20/80	6.98	0.00	8.38	0.00	8.38	0.56	6.98	0.00
		12.57	0.68	19.55	0.00	19.55	0.60	12.57	0.14
		32.11	0.76	60.04	1.86	60.04	1.95	32.11	0.54
		97.74	4.43	167.55	7.49	167.55	7.96	97.74	4.18
		251.33	11.21	335.10	12.88	335.10	13.01	251.33	10.82
		418.88	14.49	481.71	15.25	481.71	15.23	418.88	14.52
		544.54	15.93	600.39	16.95	600.39	16.53	544.54	16.28
		656.24	17.17	712.09	18.39	712.09	17.88	656.24	17.79
		767.94	18.57	837.76	19.86	837.76	19.21	767.94	19.25
		893.61	19.84	949.46	21.51	949.46	20.69	893.61	20.75

Table D4 Total torque harmonic content (TTHC) result at 3.14 rad/s and 100°C as measured by the RPA-FT of HNBR compounds filled with various CB hybrid systems and hybrid ratios (cont.)

CB hybrid system	CB hybrid ratio	Test a				Test b			
		run 1		run 2		run 1		run 2	
		Strain (%)	TTHC (%)	Strain (%)	TTHC (%)	Strain (%)	TTHC (%)	Strain (%)	TTHC (%)
N326/774	40/60	6.98	0.00	8.38	0.00	8.38	0.00	6.98	0.00
		12.57	0.00	19.55	0.00	19.55	0.00	12.57	0.00
		32.11	0.67	60.04	1.71	60.04	1.70	32.11	0.36
		97.74	4.13	167.55	7.22	167.55	7.79	97.74	3.77
		251.33	11.15	335.10	12.67	335.10	13.08	251.33	10.79
		418.88	14.60	481.71	15.28	481.71	15.36	418.88	14.44
		544.54	15.87	600.39	16.74	600.39	16.65	544.54	16.20
		656.24	17.29	712.09	18.27	712.09	17.84	656.24	17.81
		767.94	18.61	837.76	19.79	837.76	19.14	767.94	19.09
		893.61	19.86	949.46	21.44	949.46	20.74	893.61	20.53
	60/40	6.98	0.00	8.38	0.00	8.38	0.00	6.98	0.00
		12.57	0.00	19.55	0.00	19.55	0.00	12.57	0.00
		32.11	0.51	60.04	1.42	60.04	1.49	32.11	0.10
		97.74	4.24	167.55	6.90	167.55	7.48	97.74	3.99
		251.33	10.95	335.10	12.45	335.10	12.91	251.33	10.49
		418.88	14.27	481.71	15.12	481.71	15.20	418.88	13.97
		544.54	15.73	600.39	16.70	600.39	16.29	544.54	15.82
		656.24	17.15	712.09	18.15	712.09	17.67	656.24	17.36
		767.94	17.99	837.76	19.58	837.76	18.73	767.94	18.76
		893.61	19.66	949.46	21.17	949.46	20.25	893.61	20.17
	80/20	6.98	0.00	8.38	0.00	8.38	0.00	6.98	0.00
		12.57	0.00	19.55	0.00	19.55	0.00	12.57	0.00
		32.11	0.06	60.04	0.85	60.04	1.04	32.11	0.06
		97.74	3.91	167.55	6.69	167.55	7.06	97.74	3.25
		251.33	10.82	335.10	12.30	335.10	12.57	251.33	9.93
		418.88	14.12	481.71	14.92	481.71	14.82	418.88	13.57
		544.54	15.75	600.39	16.46	600.39	16.23	544.54	15.45
		656.24	17.25	712.09	18.02	712.09	17.49	656.24	16.92
		767.94	18.42	837.76	19.52	837.76	18.99	767.94	18.57
		893.61	19.99	949.46	21.43	949.46	20.78	893.61	20.42
	100/0	6.98	0.00	8.38	0.00	8.38	0.00	6.98	0.00
		12.57	0.00	19.55	0.00	19.55	0.00	12.57	0.00
		32.11	0.00	60.04	0.84	60.04	1.08	32.11	0.38
		97.74	3.50	167.55	6.17	167.55	6.83	97.74	3.12
		251.33	10.08	335.10	11.43	335.10	12.14	251.33	9.56
		418.88	13.37	481.71	14.01	481.71	14.47	418.88	13.23
		544.54	14.94	600.39	15.94	600.39	15.83	544.54	15.13
		656.24	16.59	712.09	17.59	712.09	17.29	656.24	16.97
		767.94	18.04	837.76	19.25	837.76	18.97	767.94	18.60
		893.61	19.65	949.46	20.87	949.46	20.72	893.61	20.19

Table D4 Total torque harmonic content (TTHC) result at 3.14 rad/s and 100°C as measured by the RPA-FT of HNBR compounds filled with various CB hybrid systems and hybrid ratios

CB hybrid system	CB hybrid ratio	Test a				Test b			
		run 1		run 2		run 1		run 2	
		Strain (%)	TTHC (%)	Strain (%)	TTHC (%)	Strain (%)	TTHC (%)	Strain (%)	TTHC (%)
N550/N990	0/100	6.98	0.00	8.38	0.00	8.38	0.00	6.98	0.00
		12.57	0.00	19.55	0.00	19.55	0.00	12.57	0.00
		32.11	0.00	60.04	1.41	60.04	1.50	32.11	0.61
		97.74	3.94	167.55	6.45	167.55	6.94	97.74	3.60
		251.33	9.88	335.10	11.69	335.10	11.91	251.33	9.70
		418.88	13.59	481.71	14.74	481.71	14.64	418.88	13.65
		544.54	15.54	600.39	16.73	600.39	16.44	544.54	15.81
		656.24	17.16	712.09	18.40	712.09	18.02	656.24	17.58
		767.94	18.76	837.76	20.00	837.76	19.64	767.94	19.11
		893.61	20.17	949.46	21.39	949.46	20.94	893.61	20.62
	20/80	6.98	0.00	8.38	0.00	8.38	0.15	6.98	0.00
		12.57	0.00	19.55	0.00	19.55	0.19	12.57	0.00
		32.11	0.66	60.04	1.57	60.04	1.38	32.11	1.28
		97.74	3.99	167.55	6.78	167.55	7.28	97.74	3.83
		251.33	10.11	335.10	12.06	335.10	12.14	251.33	10.03
		418.88	13.52	481.71	14.95	481.71	14.84	418.88	13.81
		544.54	15.53	600.39	16.83	600.39	16.55	544.54	15.97
		656.24	17.30	712.09	18.51	712.09	18.09	656.24	17.86
		767.94	18.84	837.76	20.01	837.76	19.58	767.94	19.39
		893.61	20.24	949.46	21.50	949.46	21.05	893.61	20.75
	40/60	6.98	0.00	8.38	0.00	8.38	0.00	6.98	0.00
		12.57	0.00	19.55	0.00	19.55	0.00	12.57	0.00
		32.11	0.04	60.04	1.58	60.04	1.68	32.11	0.00
		97.74	4.26	167.55	6.78	167.55	7.16	97.74	3.90
		251.33	10.49	335.10	12.16	335.10	12.26	251.33	10.08
		418.88	13.95	481.71	14.80	481.71	14.73	418.88	13.97
		544.54	15.69	600.39	16.70	600.39	16.40	544.54	15.94
		656.24	17.12	712.09	18.27	712.09	18.00	656.24	17.59
		767.94	18.72	837.76	19.86	837.76	19.56	767.94	19.12
		893.61	20.11	949.46	21.31	949.46	20.92	893.61	20.54
	60/40	6.98	0.00	8.38	0.00	8.38	0.10	6.98	0.00
		12.57	0.00	19.55	0.00	19.55	0.08	12.57	0.00
		32.11	0.73	60.04	1.41	60.04	1.43	32.11	0.57
		97.74	4.42	167.55	7.14	167.55	7.69	97.74	4.18
		251.33	10.73	335.10	12.38	335.10	12.56	251.33	10.32
		418.88	13.93	481.71	14.98	481.71	14.97	418.88	13.81
		544.54	15.62	600.39	16.81	600.39	16.53	544.54	15.94
		656.24	17.29	712.09	18.50	712.09	18.03	656.24	17.69
		767.94	18.82	837.76	20.05	837.76	19.51	767.94	19.27
		893.61	20.30	949.46	21.67	949.46	21.00	893.61	20.75

Table D4 Total torque harmonic content (TTHC) result at 3.14 rad/s and 100°C as measured by the RPA-FT of HNBR compounds filled with various CB hybrid systems and hybrid ratios (cont.)

CB hybrid system	CB hybrid ratio	Test a				Test b			
		run 1		run 2		run 1		run 2	
		Strain (%)	TTHC (%)	Strain (%)	TTHC (%)	Strain (%)	TTHC (%)	Strain (%)	TTHC (%)
N550/N990	80/20	6.98	0.00	8.38	0.00	8.38	0.00	6.98	0.00
		12.57	0.00	19.55	0.00	19.55	0.00	12.57	0.00
		32.11	0.70	60.04	1.32	60.04	1.54	32.11	0.47
		97.74	4.71	167.55	7.57	167.55	7.86	97.74	4.21
		251.33	10.98	335.10	12.77	335.10	12.67	251.33	10.93
		418.88	13.93	481.71	15.17	481.71	14.99	418.88	14.17
		544.54	15.55	600.39	16.96	600.39	16.44	544.54	16.17
		656.24	17.27	712.09	18.54	712.09	17.91	656.24	17.79
		767.94	18.72	837.76	20.23	837.76	19.48	767.94	19.46
		893.61	20.13	949.46	21.93	949.46	21.00	893.61	21.17
	100/0	6.98	0.00	8.38	0.00	8.38	0.00	6.98	0.00
		12.57	0.00	19.55	0.00	19.55	0.00	12.57	0.00
		32.11	0.06	60.04	1.49	60.04	1.63	32.11	0.59
		97.74	4.76	167.55	7.67	167.55	7.95	97.74	4.40
		251.33	10.94	335.10	12.79	335.10	12.55	251.33	11.20
		418.88	13.94	481.71	15.27	481.71	14.76	418.88	14.45
		544.54	15.69	600.39	17.25	600.39	16.44	544.54	16.42
		656.24	17.24	712.09	19.08	712.09	17.90	656.24	18.45
		767.94	18.72	837.76	21.18	837.76	19.49	767.94	20.66
		893.61	20.35	949.46	24.15	949.46	21.49	893.61	23.97

Table D5 3rd relative torque harmonic (T(3/1)) result at 3.14 rad/s and 100°C as measured by the RPA-FT of HNBR compounds filled with various CB hybrid systems and hybrid ratios

CB hybrid system	CB hybrid ratio	Test a				Test b			
		run 1		run 2		run 1		run 2	
		Strain (%)	T(3/1) (%)	Strain (%)	T(3/1) (%)	Strain (%)	T(3/1) (%)	Strain (%)	T(3/1) (%)
N326/N990	0/100	6.98	0.00	8.38	0.00	8.38	0.00	6.98	0.55
		12.57	0.00	19.55	0.00	19.55	0.00	12.57	0.03
		32.11	0.00	60.04	0.87	60.04	0.96	32.11	0.07
		97.74	2.83	167.55	4.89	167.55	5.26	97.74	2.81
		251.33	7.36	335.10	8.59	335.10	8.78	251.33	7.21
		418.88	9.78	481.71	10.35	481.71	10.35	418.88	9.83
		544.54	10.81	600.39	11.42	600.39	11.27	544.54	11.02
		656.24	11.61	712.09	12.25	712.09	12.01	656.24	11.90
		767.94	12.36	837.76	13.02	837.76	12.74	767.94	12.63
		893.61	13.00	949.46	13.57	949.46	13.27	893.61	13.30
	20/80	6.98	0.46	8.38	0.00	8.38	0.00	6.98	0.00
		12.57	0.00	19.55	0.00	19.55	0.00	12.57	0.00
		32.11	0.00	60.04	0.75	60.04	0.81	32.11	0.00
		97.74	2.67	167.55	4.89	167.55	5.13	97.74	2.47
		251.33	7.44	335.10	8.80	335.10	8.84	251.33	7.29
		418.88	9.90	481.71	10.46	481.71	10.39	418.88	9.89
		544.54	10.89	600.39	11.41	600.39	11.29	544.54	10.99
		656.24	11.62	712.09	12.15	712.09	11.95	656.24	11.78
		767.94	12.33	837.76	12.87	837.76	12.68	767.94	12.48
		893.61	12.94	949.46	13.41	949.46	13.21	893.61	13.17
	40/60	6.98	0.00	8.38	0.00	8.38	0.00	6.98	0.00
		12.57	0.00	19.55	0.00	19.55	0.00	12.57	0.00
		32.11	0.00	60.04	0.86	60.04	0.85	32.11	0.00
		97.74	2.51	167.55	4.88	167.55	5.16	97.74	2.38
		251.33	7.51	335.10	8.94	335.10	9.02	251.33	7.32
		418.88	10.04	481.71	10.53	481.71	10.51	418.88	10.03
		544.54	10.97	600.39	11.44	600.39	11.33	544.54	11.06
		656.24	11.68	712.09	12.13	712.09	11.96	656.24	11.85
		767.94	12.30	837.76	12.84	837.76	12.63	767.94	12.50
		893.61	12.89	949.46	13.41	949.46	13.11	893.61	13.19
	60/40	6.98	0.00	8.38	1.54	8.38	2.15	6.98	1.70
		12.57	1.51	19.55	0.74	19.55	0.85	12.57	1.40
		32.11	1.00	60.04	1.75	60.04	1.92	32.11	0.80
		97.74	3.37	167.55	5.55	167.55	6.07	97.74	3.19
		251.33	8.30	335.10	9.53	335.10	9.78	251.33	8.07
		418.88	10.71	481.71	11.03	481.71	11.14	418.88	10.63
		544.54	11.47	600.39	11.81	600.39	11.78	544.54	11.52
		656.24	12.02	712.09	12.48	712.09	12.33	656.24	12.18
		767.94	12.61	837.76	13.15	837.76	12.92	767.94	12.80
		893.61	13.21	949.46	13.74	949.46	13.45	893.61	13.43

Table D5 3rd relative torque harmonic (T(3/1)) result at 3.14 rad/s and 100°C as measured by the RPA-FT of HNBR compounds filled with various CB hybrid systems and hybrid ratios (cont.)

CB hybrid system	CB hybrid ratio	Test a				Test b			
		run 1		run 2		run 1		run 2	
		Strain (%)	T(3/1) (%)	Strain (%)	T(3/1) (%)	Strain (%)	T(3/1) (%)	Strain (%)	T(3/1) (%)
N326/N990	80/20	6.98	0.67	8.38	0.00	8.38	0.00	6.98	0.27
		12.57	0.00	19.55	0.00	19.55	0.00	12.57	0.00
		32.11	0.00	60.04	0.98	60.04	1.04	32.11	0.00
		97.74	2.97	167.55	5.39	167.55	5.94	97.74	2.70
		251.33	8.42	335.10	9.51	335.10	9.87	251.33	8.04
		418.88	10.74	481.71	10.84	481.71	11.04	418.88	10.51
		544.54	11.41	600.39	11.67	600.39	11.66	544.54	11.39
		656.24	11.95	712.09	12.31	712.09	12.23	656.24	12.07
		767.94	12.53	837.76	12.85	837.76	12.85	767.94	12.71
		893.61	13.18	949.46	13.95	949.46	13.36	893.61	13.37
	100/0	6.98	0.91	8.38	0.00	8.38	0.00	6.98	0.00
		12.57	0.00	19.55	0.00	19.55	0.00	12.57	0.00
		32.11	0.00	60.04	1.18	60.04	1.23	32.11	0.00
		97.74	3.18	167.55	5.63	167.55	6.28	97.74	2.78
		251.33	8.69	335.10	9.60	335.10	10.04	251.33	8.14
		418.88	10.78	481.71	10.92	481.71	11.06	418.88	10.50
		544.54	11.35	600.39	11.68	600.39	11.60	544.54	11.35
		656.24	11.88	712.09	12.38	712.09	12.18	656.24	12.06
		767.94	12.50	837.76	13.13	837.76	12.84	767.94	12.73
		893.61	13.14	949.46	13.80	949.46	13.42	893.61	13.43
N326/N774	0/100	6.98	0.00	8.38	1.34	8.38	1.59	6.98	1.87
		12.57	1.37	19.55	0.88	19.55	0.94	12.57	1.36
		32.11	1.15	60.04	1.83	60.04	1.89	32.11	0.95
		97.74	3.61	167.55	6.03	167.55	6.54	97.74	3.52
		251.33	8.67	335.10	9.81	335.10	10.03	251.33	8.45
		418.88	10.82	481.71	11.11	481.71	11.18	418.88	10.86
		544.54	11.40	600.39	11.72	600.39	11.68	544.54	11.62
		656.24	11.87	712.09	12.25	712.09	12.14	656.24	12.14
		767.94	12.34	837.76	12.82	837.76	12.66	767.94	12.66
		893.61	12.89	949.46	13.37	949.46	13.15	893.61	13.28
	20/80	6.98	0.00	8.38	0.00	8.38	0.00	6.98	0.45
		12.57	0.00	19.55	0.00	19.55	0.00	12.57	0.00
		32.11	0.00	60.04	1.14	60.04	1.21	32.11	0.00
		97.74	3.16	167.55	5.76	167.55	6.16	97.74	3.00
		251.33	8.57	335.10	9.78	335.10	9.92	251.33	8.32
		418.88	10.78	481.71	11.12	481.71	11.06	418.88	10.75
		544.54	11.35	600.39	11.76	600.39	11.53	544.54	11.50
		656.24	11.76	712.09	12.27	712.09	11.97	656.24	12.04
		767.94	12.24	837.76	12.87	837.76	12.52	767.94	12.56
		893.61	12.78	949.46	13.51	949.46	13.02	893.61	13.20

Table D5 3rd relative torque harmonic (T(3/1)) result at 3.14 rad/s and 100°C as measured by the RPA-FT of HNBR compounds filled with various CB hybrid systems and hybrid ratios (cont.)

CB hybrid system	CB hybrid ratio	Test a				Test b			
		run 1		run 2		run 1		run 2	
		Strain (%)	T(3/1) (%)	Strain (%)	T(3/1) (%)	Strain (%)	T(3/1) (%)	Strain (%)	T(3/1) (%)
N326/774	40/60	6.98	0.00	8.38	0.00	8.38	0.00	6.98	0.00
		12.57	0.00	19.55	0.00	19.55	0.00	12.57	0.00
		32.11	0.00	60.04	1.04	60.04	1.08	32.11	0.00
		97.74	3.07	167.55	5.65	167.55	6.13	97.74	2.98
		251.33	8.66	335.10	9.83	335.10	10.05	251.33	8.33
		418.88	10.92	481.71	11.19	481.71	11.25	418.88	10.85
		544.54	11.47	600.39	11.77	600.39	11.69	544.54	11.62
		656.24	11.90	712.09	12.28	712.09	12.07	656.24	12.17
		767.94	12.34	837.76	12.86	837.76	12.58	767.94	12.64
		893.61	12.79	949.46	13.47	949.46	13.02	893.61	13.17
	60/40	6.98	0.68	8.38	0.00	8.38	0.00	6.98	0.00
		12.57	0.00	19.55	0.00	19.55	0.00	12.57	0.00
		32.11	0.00	60.04	0.85	60.04	0.84	32.11	0.00
		97.74	3.17	167.55	5.59	167.55	6.03	97.74	2.85
		251.33	8.60	335.10	9.71	335.10	9.93	251.33	8.25
		418.88	10.88	481.71	11.09	481.71	11.18	418.88	10.74
		544.54	11.44	600.39	11.77	600.39	11.63	544.54	11.51
		656.24	11.87	712.09	12.31	712.09	12.08	656.24	12.07
		767.94	12.10	837.76	12.91	837.76	12.44	767.94	12.57
		893.61	12.73	949.46	13.49	949.46	13.00	893.61	13.11
	80/20	6.98	0.80	8.38	0.00	8.38	0.00	6.98	0.00
		12.57	0.00	19.55	0.00	19.55	0.00	12.57	0.00
		32.11	0.00	60.04	0.69	60.04	0.82	32.11	0.00
		97.74	3.20	167.55	5.64	167.55	6.19	97.74	2.85
		251.33	8.69	335.10	9.71	335.10	10.04	251.33	8.27
		418.88	10.83	481.71	11.03	481.71	11.10	418.88	10.64
		544.54	11.42	600.39	11.75	600.39	11.65	544.54	11.45
		656.24	11.96	712.09	12.37	712.09	12.11	656.24	11.98
		767.94	12.40	837.76	13.01	837.76	12.72	767.94	12.56
		893.61	12.91	949.46	13.56	949.46	13.22	893.61	13.29
	100/0	6.98	0.77	8.38	0.00	8.38	0.00	6.98	0.00
		12.57	0.00	19.55	0.00	19.55	0.00	12.57	0.00
		32.11	0.00	60.04	0.83	60.04	0.91	32.11	0.00
		97.74	3.13	167.55	5.52	167.55	6.21	97.74	2.82
		251.33	8.55	335.10	9.55	335.10	9.95	251.33	8.16
		418.88	10.69	481.71	10.81	481.71	11.01	418.88	10.52
		544.54	11.33	600.39	11.69	600.39	11.65	544.54	11.40
		656.24	11.90	712.09	12.42	712.09	12.19	656.24	12.13
		767.94	12.48	837.76	13.19	837.76	12.92	767.94	12.86
		893.61	13.01	949.46	13.80	949.46	13.55	893.61	13.62

Table D5 3rd relative torque harmonic (T(3/1)) result at 3.14 rad/s and 100°C as measured by the RPA-FT of HNBR compounds filled with various CB hybrid systems and hybrid ratios

CB hybrid system	CB hybrid ratio	Test a				Test b			
		run 1		run 2		run 1		run 2	
		Strain (%)	T(3/1) (%)	Strain (%)	T(3/1) (%)	Strain (%)	T(3/1) (%)	Strain (%)	T(3/1) (%)
N550/N990	0/100	6.98	0.00	8.38	0.00	8.38	0.00	6.98	0.55
		12.57	0.00	19.55	0.00	19.55	0.00	12.57	0.03
		32.11	0.00	60.04	0.87	60.04	0.96	32.11	0.07
		97.74	2.83	167.55	4.89	167.55	5.26	97.74	2.81
		251.33	7.36	335.10	8.59	335.10	8.78	251.33	7.21
		418.88	9.78	481.71	10.35	481.71	10.35	418.88	9.83
		544.54	10.81	600.39	11.42	600.39	11.27	544.54	11.02
		656.24	11.61	712.09	12.25	712.09	12.01	656.24	11.90
		767.94	12.36	837.76	13.02	837.76	12.74	767.94	12.63
		893.61	13.00	949.46	13.57	949.46	13.27	893.61	13.30
	20/80	6.98	0.00	8.38	0.00	8.38	0.00	6.98	0.00
		12.57	0.00	19.55	0.00	19.55	0.00	12.57	0.00
		32.11	0.01	60.04	0.71	60.04	0.72	32.11	0.04
		97.74	2.70	167.55	5.10	167.55	5.44	97.74	2.71
		251.33	7.57	335.10	8.89	335.10	8.94	251.33	7.35
		418.88	9.93	481.71	10.51	481.71	10.41	418.88	9.98
		544.54	10.91	600.39	11.55	600.39	11.32	544.54	11.14
		656.24	11.69	712.09	12.31	712.09	12.04	656.24	12.01
		767.94	12.38	837.76	13.05	837.76	12.77	767.94	12.70
		893.61	13.05	949.46	13.61	949.46	13.32	893.61	13.37
	40/60	6.98	0.00	8.38	0.00	8.38	0.00	6.98	0.00
		12.57	0.00	19.55	0.00	19.55	0.00	12.57	0.00
		32.11	0.00	60.04	0.79	60.04	0.87	32.11	0.00
		97.74	2.92	167.55	5.24	167.55	5.53	97.74	2.71
		251.33	7.78	335.10	9.05	335.10	9.08	251.33	7.54
		418.88	10.05	481.71	10.58	481.71	10.50	418.88	10.08
		544.54	10.95	600.39	11.48	600.39	11.30	544.54	11.12
		656.24	11.63	712.09	12.18	712.09	11.96	656.24	11.91
		767.94	12.26	837.76	12.91	837.76	12.62	767.94	12.56
		893.61	12.94	949.46	13.48	949.46	13.16	893.61	13.27
	60/40	6.98	0.00	8.38	0.00	8.38	0.00	6.98	0.00
		12.57	0.00	19.55	0.00	19.55	0.00	12.57	0.00
		32.11	0.00	60.04	0.77	60.04	0.78	32.11	0.00
		97.74	3.02	167.55	5.49	167.55	5.94	97.74	2.91
		251.33	8.08	335.10	9.34	335.10	9.40	251.33	7.87
		418.88	10.21	481.71	10.69	481.71	10.63	418.88	10.23
		544.54	11.02	600.39	11.57	600.39	11.41	544.54	11.21
		656.24	11.71	712.09	12.26	712.09	12.02	656.24	11.93
		767.94	12.33	837.76	12.98	837.76	12.70	767.94	12.61
		893.61	12.91	949.46	13.66	949.46	13.28	893.61	13.30

Table D5 3rd relative torque harmonic (T(3/1)) result at 3.14 rad/s and 100°C as measured by the RPA-FT of HNBR compounds filled with various CB hybrid systems and hybrid ratios (cont.)

CB hybrid system	CB hybrid ratio	Test a				Test b			
		run 1		run 2		run 1		run 2	
		Strain (%)	T(3/1) (%)	Strain (%)	T(3/1) (%)	Strain (%)	T(3/1) (%)	Strain (%)	T(3/1) (%)
N550/N990	80/20	6.98	0.70	8.38	0.00	8.38	0.00	6.98	0.00
		12.57	0.00	19.55	0.00	19.55	0.00	12.57	0.00
		32.11	0.00	60.04	0.93	60.04	0.95	32.11	0.00
		97.74	3.33	167.55	5.99	167.55	6.32	97.74	3.20
		251.33	8.46	335.10	9.72	335.10	9.59	251.33	8.38
		418.88	10.34	481.71	10.92	481.71	10.70	418.88	10.50
		544.54	11.09	600.39	11.70	600.39	11.37	544.54	11.35
		656.24	11.71	712.09	12.39	712.09	12.03	656.24	12.05
		767.94	12.36	837.76	13.19	837.76	12.76	767.94	12.75
		893.61	13.04	949.46	13.88	949.46	13.32	893.61	13.54
	100/0	6.98	0.79	8.38	0.00	8.38	0.00	6.98	0.00
		12.57	0.00	19.55	0.00	19.55	0.00	12.57	0.00
		32.11	0.00	60.04	0.98	60.04	1.00	32.11	0.00
		97.74	3.58	167.55	6.12	167.55	6.39	97.74	3.54
		251.33	8.56	335.10	9.71	335.10	9.50	251.33	8.70
		418.88	10.31	481.71	10.92	481.71	10.62	418.88	10.65
		544.54	11.06	600.39	11.80	600.39	11.36	544.54	11.47
		656.24	11.77	712.09	12.66	712.09	12.06	656.24	12.35
		767.94	12.49	837.76	13.69	837.76	12.89	767.94	13.45
		893.61	13.20	949.46	14.94	949.46	13.62	893.61	14.98

Table D6 5^{th} relative torque harmonic (T(5/1)) result at 3.14 rad/s and 100°C as measured by the RPA-FT of HNBR compounds filled with various CB hybrid systems and hybrid ratios

CB hybrid system	CB hybrid ratio	Test a				Test b			
		run 1		run 2		run 1		run 2	
		Strain (%)	T(5/1) (%)	Strain (%)	T(5/1) (%)	Strain (%)	T(5/1) (%)	Strain (%)	T(5/1) (%)
N326/N990	0/100	6.98	0.00	8.38	0.63	8.38	0.09	6.98	0.39
		12.57	0.25	19.55	0.37	19.55	0.49	12.57	0.01
		32.11	0.45	60.04	0.80	60.04	0.70	32.11	0.40
		97.74	1.06	167.55	1.06	167.55	1.13	97.74	0.98
		251.33	1.56	335.10	1.93	335.10	1.95	251.33	1.55
		418.88	2.40	481.71	2.69	481.71	2.70	418.88	2.39
		544.54	2.97	600.39	3.19	600.39	3.15	544.54	2.99
		656.24	3.38	712.09	3.64	712.09	3.56	656.24	3.45
		767.94	3.78	837.76	4.08	837.76	3.99	767.94	3.87
		893.61	4.14	949.46	4.44	949.46	4.34	893.61	4.26
	20/80	6.98	0.01	8.38	0.20	8.38	0.00	6.98	0.00
		12.57	0.15	19.55	0.12	19.55	0.23	12.57	0.00
		32.11	0.14	60.04	0.57	60.04	0.55	32.11	0.21
		97.74	0.95	167.55	0.96	167.55	1.07	97.74	0.88
		251.33	1.51	335.10	1.91	335.10	1.94	251.33	1.43
		418.88	2.33	481.71	2.64	481.71	2.65	418.88	2.31
		544.54	2.92	600.39	3.15	600.39	3.11	544.54	2.93
		656.24	3.33	712.09	3.59	712.09	3.52	656.24	3.40
		767.94	3.76	837.76	4.02	837.76	3.96	767.94	3.83
		893.61	4.15	949.46	4.36	949.46	4.32	893.61	4.22
	40/60	6.98	0.00	8.38	0.17	8.38	0.20	6.98	0.30
		12.57	0.06	19.55	0.34	19.55	0.36	12.57	0.24
		32.11	0.61	60.04	0.73	60.04	0.81	32.11	0.41
		97.74	1.30	167.55	1.11	167.55	1.23	97.74	1.19
		251.33	1.60	335.10	1.99	335.10	2.02	251.33	1.53
		418.88	2.41	481.71	2.71	481.71	2.72	418.88	2.35
		544.54	2.97	600.39	3.18	600.39	3.17	544.54	2.98
		656.24	3.38	712.09	3.63	712.09	3.57	656.24	3.44
		767.94	3.81	837.76	4.08	837.76	3.99	767.94	3.89
		893.61	4.19	949.46	4.44	949.46	4.38	893.61	4.28
	60/40	6.98	0.30	8.38	0.39	8.38	0.00	6.98	0.00
		12.57	0.11	19.55	0.18	19.55	0.15	12.57	0.00
		32.11	0.26	60.04	0.46	60.04	0.45	32.11	0.30
		97.74	0.92	167.55	0.86	167.55	0.96	97.74	0.86
		251.33	1.45	335.10	1.90	335.10	1.95	251.33	1.44
		418.88	2.32	481.71	2.62	481.71	2.65	418.88	2.29
		544.54	2.90	600.39	3.14	600.39	3.13	544.54	2.91
		656.24	3.33	712.09	3.61	712.09	3.54	656.24	3.37
		767.94	3.77	837.76	4.06	837.76	3.95	767.94	3.83
		893.61	4.16	949.46	4.44	949.46	4.31	893.61	4.26

Table D6 5^{th} relative torque harmonic (T(5/1)) result at 3.14 rad/s and 100°C as measured by the RPA-FT of HNBR compounds filled with various CB hybrid systems and hybrid ratios (cont.)

CB hybrid system	CB hybrid ratio	Test a				Test b			
		run 1		run 2		run 1		run 2	
		Strain (%)	T(5/1) (%)	Strain (%)	T(5/1) (%)	Strain (%)	T(5/1) (%)	Strain (%)	T(5/1) (%)
N326/N990	80/20	6.98	0.00	8.38	0.46	8.38	0.00	6.98	0.00
		12.57	0.00	19.55	0.25	19.55	0.17	12.57	0.00
		32.11	0.29	60.04	0.17	60.04	0.41	32.11	0.08
		97.74	0.75	167.55	0.79	167.55	0.77	97.74	0.61
		251.33	1.34	335.10	1.81	335.10	1.85	251.33	1.38
		418.88	2.25	481.71	2.58	481.71	2.57	418.88	2.22
		544.54	2.82	600.39	3.15	600.39	3.07	544.54	2.84
		656.24	3.29	712.09	3.50	712.09	3.52	656.24	3.31
		767.94	3.76	837.76	4.01	837.76	3.93	767.94	3.77
		893.61	4.16	949.46	4.37	949.46	4.30	893.61	4.18
	100/0	6.98	0.00	8.38	0.00	8.38	0.10	6.98	0.00
		12.57	0.20	19.55	0.00	19.55	0.08	12.57	0.00
		32.11	0.13	60.04	0.20	60.04	0.28	32.11	0.18
		97.74	0.55	167.55	0.60	167.55	0.67	97.74	0.52
		251.33	1.25	335.10	1.69	335.10	1.76	251.33	1.22
		418.88	2.16	481.71	2.43	481.71	2.49	418.88	2.09
		544.54	2.78	600.39	3.01	600.39	3.00	544.54	2.76
		656.24	3.23	712.09	3.50	712.09	3.45	656.24	3.30
		767.94	3.67	837.76	3.96	837.76	3.83	767.94	3.75
		893.61	4.02	949.46	4.36	949.46	4.20	893.61	4.15
N326/N774	0/100	6.98	0.00	8.38	0.14	8.38	0.10	6.98	0.00
		12.57	0.00	19.55	0.36	19.55	0.18	12.57	0.24
		32.11	0.62	60.04	0.68	60.04	0.65	32.11	0.46
		97.74	1.21	167.55	1.06	167.55	1.15	97.74	0.97
		251.33	1.68	335.10	2.12	335.10	2.14	251.33	1.62
		418.88	2.54	481.71	2.73	481.71	2.78	418.88	2.52
		544.54	3.04	600.39	3.25	600.39	3.23	544.54	3.10
		656.24	3.45	712.09	3.71	712.09	3.65	656.24	3.57
		767.94	3.88	837.76	4.11	837.76	4.03	767.94	4.02
		893.61	4.22	949.46	4.46	949.46	4.35	893.61	4.39
	20/80	6.98	0.00	8.38	0.01	8.38	0.00	6.98	0.00
		12.57	0.24	19.55	0.19	19.55	0.18	12.57	0.00
		32.11	0.36	60.04	0.45	60.04	0.46	32.11	0.24
		97.74	0.97	167.55	0.94	167.55	1.05	97.74	0.85
		251.33	1.56	335.10	2.06	335.10	2.06	251.33	1.54
		418.88	2.40	481.71	2.72	481.71	2.69	418.88	2.39
		544.54	2.95	600.39	3.26	600.39	3.17	544.54	3.03
		656.24	3.40	712.09	3.72	712.09	3.60	656.24	3.53
		767.94	3.84	837.76	4.17	837.76	4.01	767.94	4.02
		893.61	4.20	949.46	4.55	949.46	4.37	893.61	4.43

Table D6 5^{th} relative torque harmonic (T(5/1)) result at 3.14 rad/s and 100°C as measured by the RPA-FT of HNBR compounds filled with various CB hybrid systems and hybrid ratios (cont.)

CB hybrid system	CB hybrid ratio	Test a				Test b			
		run 1		run 2		run 1		run 2	
		Strain (%)	T(5/1) (%)	Strain (%)	T(5/1) (%)	Strain (%)	T(5/1) (%)	Strain (%)	T(5/1) (%)
N326/774	40/60	6.98	0.00	8.38	0.57	8.38	0.71	6.98	0.56
		12.57	0.00	19.55	0.25	19.55	0.24	12.57	0.39
		32.11	0.37	60.04	0.60	60.04	0.58	32.11	0.36
		97.74	0.96	167.55	0.98	167.55	1.05	97.74	0.78
		251.33	1.59	335.10	2.01	335.10	2.05	251.33	1.56
		418.88	2.42	481.71	2.67	481.71	2.67	418.88	2.40
		544.54	2.97	600.39	3.19	600.39	3.16	544.54	3.00
		656.24	3.42	712.09	3.70	712.09	3.60	656.24	3.53
		767.94	3.86	837.76	4.19	837.76	4.04	767.94	4.00
		893.61	4.21	949.46	4.61	949.46	4.40	893.61	4.38
	60/40	6.98	0.00	8.38	0.08	8.38	0.00	6.98	0.00
		12.57	0.00	19.55	0.12	19.55	0.24	12.57	0.00
		32.11	0.28	60.04	0.44	60.04	0.46	32.11	0.21
		97.74	0.59	167.55	0.77	167.55	0.81	97.74	0.63
		251.33	1.45	335.10	1.83	335.10	1.83	251.33	1.42
		418.88	2.26	481.71	2.52	481.71	2.52	418.88	2.24
		544.54	2.83	600.39	3.11	600.39	3.04	544.54	2.85
		656.24	3.33	712.09	3.64	712.09	3.52	656.24	3.36
		767.94	3.61	837.76	4.11	837.76	3.85	767.94	3.82
		893.61	4.08	949.46	4.49	949.46	4.25	893.61	4.21
	80/20	6.98	0.00	8.38	0.64	8.38	0.56	6.98	0.91
		12.57	0.00	19.55	0.24	19.55	0.16	12.57	0.10
		32.11	0.55	60.04	0.67	60.04	0.63	32.11	0.27
		97.74	0.89	167.55	0.98	167.55	0.92	97.74	0.68
		251.33	1.57	335.10	1.95	335.10	1.95	251.33	1.44
		418.88	2.37	481.71	2.66	481.71	2.66	418.88	2.29
		544.54	3.00	600.39	3.25	600.39	3.23	544.54	2.99
		656.24	3.49	712.09	3.73	712.09	3.67	656.24	3.50
		767.94	3.85	837.76	4.18	837.76	4.09	767.94	3.94
		893.61	4.19	949.46	4.58	949.46	4.43	893.61	4.37
	100/0	6.98	0.00	8.38	0.23	8.38	0.00	6.98	0.21
		12.57	0.00	19.55	0.10	19.55	0.00	12.57	0.15
		32.11	0.19	60.04	0.49	60.04	0.56	32.11	0.35
		97.74	0.62	167.55	0.71	167.55	0.68	97.74	0.54
		251.33	1.27	335.10	1.73	335.10	1.78	251.33	1.27
		418.88	2.17	481.71	2.42	481.71	2.50	418.88	2.13
		544.54	2.82	600.39	3.09	600.39	3.08	544.54	2.84
		656.24	3.31	712.09	3.57	712.09	3.52	656.24	3.38
		767.94	3.72	837.76	4.02	837.76	3.95	767.94	3.83
		893.61	4.00	949.46	4.40	949.46	4.33	893.61	4.24

Table D6 5^{th} relative torque harmonic (T(5/1)) result at 3.14 rad/s and 100°C as measured by the RPA-FT of HNBR compounds filled with various CB hybrid systems and hybrid ratios

CB hybrid system	CB hybrid ratio	Test a				Test b			
		run 1		run 2		run 1		run 2	
		Strain (%)	T(5/1) (%)	Strain (%)	T(5/1) (%)	Strain (%)	T(5/1) (%)	Strain (%)	T(5/1) (%)
N550/N990	0/100	6.98	0.00	8.38	0.63	8.38	0.09	6.98	0.39
		12.57	0.25	19.55	0.37	19.55	0.49	12.57	0.01
		32.11	0.45	60.04	0.80	60.04	0.70	32.11	0.40
		97.74	1.06	167.55	1.06	167.55	1.13	97.74	0.98
		251.33	1.56	335.10	1.93	335.10	1.95	251.33	1.55
		418.88	2.40	481.71	2.69	481.71	2.70	418.88	2.39
		544.54	2.97	600.39	3.19	600.39	3.15	544.54	2.99
		656.24	3.38	712.09	3.64	712.09	3.56	656.24	3.45
		767.94	3.78	837.76	4.08	837.76	3.99	767.94	3.87
		893.61	4.14	949.46	4.44	949.46	4.34	893.61	4.26
	20/80	6.98	0.00	8.38	0.08	8.38	0.00	6.98	0.00
		12.57	0.07	19.55	0.34	19.55	0.34	12.57	0.00
		32.11	0.56	60.04	0.83	60.04	0.76	32.11	0.44
		97.74	1.00	167.55	1.02	167.55	1.13	97.74	0.95
		251.33	1.55	335.10	2.00	335.10	2.02	251.33	1.56
		418.88	2.40	481.71	2.70	481.71	2.69	418.88	2.40
		544.54	2.97	600.39	3.24	600.39	3.17	544.54	3.03
		656.24	3.39	712.09	3.67	712.09	3.58	656.24	3.50
		767.94	3.78	837.76	4.11	837.76	4.00	767.94	3.90
		893.61	4.16	949.46	4.44	949.46	4.34	893.61	4.27
	40/60	6.98	0.00	8.38	0.00	8.38	0.00	6.98	0.00
		12.57	0.00	19.55	0.10	19.55	0.17	12.57	0.00
		32.11	0.35	60.04	0.56	60.04	0.56	32.11	0.14
		97.74	0.98	167.55	0.97	167.55	1.06	97.74	0.83
		251.33	1.54	335.10	2.02	335.10	2.03	251.33	1.49
		418.88	2.40	481.71	2.70	481.71	2.71	418.88	2.41
		544.54	2.95	600.39	3.21	600.39	3.18	544.54	3.02
		656.24	3.38	712.09	3.65	712.09	3.58	656.24	3.49
		767.94	3.78	837.76	4.06	837.76	3.98	767.94	3.90
		893.61	4.17	949.46	4.40	949.46	4.31	893.61	4.27
	60/40	6.98	0.00	8.38	0.52	8.38	0.07	6.98	0.00
		12.57	0.00	19.55	0.25	19.55	0.42	12.57	0.00
		32.11	0.57	60.04	0.86	60.04	0.86	32.11	0.49
		97.74	1.05	167.55	1.11	167.55	1.19	97.74	0.97
		251.33	1.71	335.10	2.10	335.10	2.13	251.33	1.65
		418.88	2.47	481.71	2.73	481.71	2.76	418.88	2.44
		544.54	3.03	600.39	3.30	600.39	3.25	544.54	3.05
		656.24	3.48	712.09	3.75	712.09	3.65	656.24	3.54
		767.94	3.84	837.76	4.18	837.76	4.05	767.94	3.96
		893.61	4.18	949.46	4.53	949.46	4.38	893.61	4.34

Table D6 5^{th} relative torque harmonic (T(5/1)) result at 3.14 rad/s and 100°C as measured by the RPA-FT of HNBR compounds filled with various CB hybrid systems and hybrid ratios (cont.)

CB hybrid system	CB hybrid ratio	Test a				Test b			
		run 1		run 2		run 1		run 2	
		Strain (%)	T(5/1) (%)	Strain (%)	T(5/1) (%)	Strain (%)	T(5/1) (%)	Strain (%)	T(5/1) (%)
N550/N990	80/20	6.98	0.00	8.38	0.72	8.38	0.17	6.98	0.55
		12.57	0.00	19.55	0.41	19.55	0.53	12.57	0.07
		32.11	0.82	60.04	0.81	60.04	0.89	32.11	0.68
		97.74	1.22	167.55	1.21	167.55	1.22	97.74	1.12
		251.33	1.79	335.10	2.22	335.10	2.19	251.33	1.80
		418.88	2.54	481.71	2.85	481.71	2.82	418.88	2.57
		544.54	3.11	600.39	3.41	600.39	3.31	544.54	3.19
		656.24	3.54	712.09	3.85	712.09	3.72	656.24	3.69
		767.94	3.90	837.76	4.26	837.76	4.08	767.94	4.09
		893.61	4.20	949.46	4.57	949.46	4.39	893.61	4.44
	100/0	6.98	0.00	8.38	0.00	8.38	0.00	6.98	0.00
		12.57	0.00	19.55	0.07	19.55	0.09	12.57	0.00
		32.11	0.22	60.04	0.35	60.04	0.38	32.11	0.24
		97.74	0.55	167.55	0.82	167.55	0.83	97.74	0.44
		251.33	1.47	335.10	1.94	335.10	1.93	251.33	1.55
		418.88	2.36	481.71	2.72	481.71	2.65	418.88	2.45
		544.54	2.96	600.39	3.34	600.39	3.14	544.54	3.16
		656.24	3.40	712.09	3.85	712.09	3.51	656.24	3.72
		767.94	3.73	837.76	4.34	837.76	3.87	767.94	4.24
		893.61	4.02	949.46	4.94	949.46	4.25	893.61	4.91

Table D7 Fit parameters of Equation 3.17 of HNBR compounds filled with various CB hybrid systems and hybrid ratios

CB hybrid system	CB hybrid ratio	TH	α	C	D
N326/N990	0/100	7.6	0.0061	0.010	2.5180
	20/80	7.9	0.0057	0.010	2.7090
	40/60	8.3	0.0052	0.010	2.7960
	60/40	10.1	0.0034	0.008	2.4920
	80/20	9.0	0.0046	0.011	3.0080
	100/0	8.8	0.0048	0.013	3.1710
N326/N990	0/100	10.2	0.0029	0.009	2.7970
	20/80	9.3	0.0039	0.011	2.9400
	40/60	9.7	0.0035	0.011	3.0320
	60/40	9.6	0.0035	0.011	3.0970
	80/20	9.1	0.0043	0.013	3.4150
	100/0	8.6	0.0050	0.013	3.4790
N326/N990	0/100	7.6	0.0061	0.010	2.5180
	20/80	7.6	0.0062	0.012	3.1090
	40/60	7.9	0.0056	0.012	2.9430
	60/40	8.0	0.0056	0.013	3.5020
	80/20	8.0	0.0057	0.015	3.7810
	100/0	7.6	0.0064	0.016	4.0480

Table D8 Integrating torque signals result at 3.14 rad/s and 100°C as measured by the RPA-FT of HNBR compounds filled with various CB hybrid systems and hybrid ratios

CB hybrid system	CB hybrid ratio	Test a				Test b			
		run 1		run 2		run 1		run 2	
		Strain (%)	Q1/Q2	Strain (%)	Q1/Q2	Strain (%)	Q1/Q2	Strain (%)	Q1/Q2
N326/N990	0/100	6.98	1.07	8.38	1.08	8.38	1.08	6.98	1.02
		12.57	1.11	19.55	1.09	19.55	1.10	12.57	1.13
		32.11	1.09	60.04	1.04	60.04	1.01	32.11	1.06
		97.74	1.05	167.55	1.06	167.55	1.05	97.74	1.03
		251.33	1.04	335.10	1.04	335.10	1.05	251.33	1.04
		418.88	1.07	481.71	1.07	481.71	1.06	418.88	1.07
		544.54	1.08	600.39	1.08	600.39	1.08	544.54	1.07
		656.24	1.07	712.09	1.08	712.09	1.08	656.24	1.07
		767.94	1.08	837.76	1.09	837.76	1.08	767.94	1.08
		893.61	1.09	949.46	1.09	949.46	1.09	893.61	1.08
	20/80	6.98	1.05	8.38	1.13	8.38	1.07	6.98	1.07
		12.57	1.06	19.55	1.07	19.55	1.06	12.57	1.09
		32.11	1.08	60.04	1.03	60.04	1.05	32.11	1.06
		97.74	1.05	167.55	1.04	167.55	1.03	97.74	1.05
		251.33	1.03	335.10	1.04	335.10	1.03	251.33	1.04
		418.88	1.05	481.71	1.05	481.71	1.04	418.88	1.05
		544.54	1.06	600.39	1.07	600.39	1.06	544.54	1.07
		656.24	1.05	712.09	1.07	712.09	1.07	656.24	1.06
		767.94	1.07	837.76	1.08	837.76	1.08	767.94	1.07
		893.61	1.10	949.46	1.10	949.46	1.09	893.61	1.07
	40/60	6.98	1.11	8.38	1.08	8.38	1.15	6.98	1.05
		12.57	1.08	19.55	1.08	19.55	1.09	12.57	1.10
		32.11	1.08	60.04	1.03	60.04	1.02	32.11	1.06
		97.74	1.06	167.55	1.03	167.55	1.01	97.74	1.05
		251.33	1.02	335.10	1.03	335.10	1.01	251.33	1.02
		418.88	1.02	481.71	1.05	481.71	1.03	418.88	1.04
		544.54	1.05	600.39	1.05	600.39	1.04	544.54	1.05
		656.24	1.04	712.09	1.07	712.09	1.07	656.24	1.05
		767.94	1.06	837.76	1.08	837.76	1.08	767.94	1.07
		893.61	1.07	949.46	1.08	949.46	1.08	893.61	1.06
	60/40	6.98	1.03	8.38	1.04	8.38	1.13	6.98	1.07
		12.57	1.11	19.55	1.09	19.55	1.08	12.57	1.10
		32.11	1.06	60.04	0.99	60.04	0.99	32.11	1.03
		97.74	1.05	167.55	1.01	167.55	0.99	97.74	1.05
		251.33	0.99	335.10	1.01	335.10	0.99	251.33	1.02
		418.88	1.01	481.71	1.03	481.71	1.01	418.88	1.03
		544.54	1.03	600.39	1.05	600.39	1.04	544.54	1.04
		656.24	1.04	712.09	1.05	712.09	1.06	656.24	1.05
		767.94	1.05	837.76	1.07	837.76	1.08	767.94	1.06
		893.61	1.06	949.46	1.07	949.46	1.08	893.61	1.06

Table D8 Integrating torque signals result at 3.14 rad/s and 100°C as measured by the RPA-FT of HNBR compounds filled with various CB hybrid systems and hybrid ratios (cont.)

CB hybrid system	CB hybrid ratio	Test a				Test b			
		run 1		run 2		run 1		run 2	
		Strain (%)	Q1/Q2	Strain (%)	Q1/Q2	Strain (%)	Q1/Q2	Strain (%)	Q1/Q2
N326/N990	80/20	6.98	1.05	8.38	1.01	8.38	1.13	6.98	1.11
		12.57	1.09	19.55	1.10	19.55	1.06	12.57	0.93
		32.11	1.04	60.04	0.98	60.04	0.98	32.11	1.03
		97.74	1.01	167.55	0.97	167.55	0.98	97.74	1.05
		251.33	0.98	335.10	1.00	335.10	0.97	251.33	0.99
		418.88	1.00	481.71	1.00	481.71	1.01	418.88	1.02
		544.54	1.01	600.39	1.03	600.39	1.03	544.54	1.04
		656.24	1.03	712.09	1.04	712.09	1.05	656.24	1.03
		767.94	1.05	837.76	1.06	837.76	1.07	767.94	1.05
		893.61	1.05	949.46	1.06	949.46	1.09	893.61	1.06
	100/0	6.98	1.04	8.38	1.04	8.38	1.08	6.98	0.98
		12.57	1.10	19.55	1.06	19.55	1.07	12.57	1.08
		32.11	1.03	60.04	0.97	60.04	0.98	32.11	1.01
		97.74	1.00	167.55	0.98	167.55	0.95	97.74	1.00
		251.33	0.96	335.10	0.99	335.10	0.95	251.33	0.98
		418.88	0.98	481.71	1.01	481.71	0.99	418.88	1.01
		544.54	1.02	600.39	1.03	600.39	1.02	544.54	1.03
		656.24	1.02	712.09	1.05	712.09	1.04	656.24	1.02
		767.94	1.04	837.76	1.06	837.76	1.05	767.94	1.05
		893.61	1.06	949.46	1.06	949.46	1.07	893.61	1.05
N326/N774	0/100	6.98	1.03	8.38	1.05	8.38	1.09	6.98	1.07
		12.57	1.08	19.55	1.08	19.55	1.09	12.57	1.13
		32.11	1.08	60.04	1.01	60.04	0.99	32.11	1.08
		97.74	1.05	167.55	1.02	167.55	0.99	97.74	1.06
		251.33	0.99	335.10	1.01	335.10	0.99	251.33	1.00
		418.88	1.01	481.71	1.03	481.71	1.00	418.88	1.02
		544.54	1.02	600.39	1.03	600.39	1.03	544.54	1.03
		656.24	1.03	712.09	1.04	712.09	1.04	656.24	1.03
		767.94	1.04	837.76	1.06	837.76	1.06	767.94	1.05
		893.61	1.05	949.46	1.06	949.46	1.06	893.61	1.05
	20/80	6.98	1.09	8.38	1.01	8.38	1.09	6.98	1.05
		12.57	1.09	19.55	1.06	19.55	1.10	12.57	1.09
		32.11	1.06	60.04	1.02	60.04	1.02	32.11	1.07
		97.74	1.03	167.55	1.02	167.55	0.98	97.74	1.03
		251.33	0.98	335.10	1.00	335.10	0.98	251.33	1.01
		418.88	0.99	481.71	1.02	481.71	1.00	418.88	1.02
		544.54	1.01	600.39	1.02	600.39	1.02	544.54	1.03
		656.24	1.01	712.09	1.04	712.09	1.03	656.24	1.02
		767.94	1.03	837.76	1.05	837.76	1.04	767.94	1.04
		893.61	1.04	949.46	1.05	949.46	1.06	893.61	1.03

Table D8 Integrating torque signals result at 3.14 rad/s and 100°C as measured by the RPA-FT of HNBR compounds filled with various CB hybrid systems and hybrid ratios (cont.)

CB hybrid system	CB hybrid ratio	Test a				Test b			
		run 1		run 2		run 1		run 2	
		Strain (%)	Q1/Q2	Strain (%)	Q1/Q2	Strain (%)	Q1/Q2	Strain (%)	Q1/Q2
N326/N774	40/60	6.98	1.09	8.38	1.04	8.38	1.10	6.98	1.01
		12.57	1.08	19.55	1.09	19.55	1.10	12.57	1.06
		32.11	1.07	60.04	1.01	60.04	1.01	32.11	1.03
		97.74	1.02	167.55	1.01	167.55	0.96	97.74	1.02
		251.33	0.97	335.10	1.00	335.10	0.97	251.33	0.99
		418.88	0.98	481.71	1.01	481.71	1.00	418.88	1.01
		544.54	1.01	600.39	1.03	600.39	1.01	544.54	1.02
		656.24	1.00	712.09	1.02	712.09	1.02	656.24	1.01
		767.94	1.03	837.76	1.04	837.76	1.04	767.94	1.03
		893.61	1.04	949.46	1.04	949.46	1.06	893.61	1.04
	60/40	6.98	1.00	8.38	1.03	8.38	1.07	6.98	1.01
		12.57	1.11	19.55	1.09	19.55	1.10	12.57	1.04
		32.11	1.02	60.04	1.00	60.04	1.00	32.11	1.03
		97.74	0.99	167.55	1.00	167.55	0.97	97.74	1.00
		251.33	0.96	335.10	0.99	335.10	0.96	251.33	0.98
		418.88	0.99	481.71	1.01	481.71	1.00	418.88	1.01
		544.54	1.01	600.39	1.02	600.39	1.02	544.54	1.02
		656.24	1.01	712.09	1.03	712.09	1.02	656.24	1.02
		767.94	1.03	837.76	1.04	837.76	1.05	767.94	1.04
		893.61	1.04	949.46	1.05	949.46	1.07	893.61	1.05
	80/20	6.98	1.07	8.38	1.02	8.38	1.10	6.98	1.05
		12.57	1.05	19.55	1.12	19.55	1.10	12.57	1.08
		32.11	1.03	60.04	1.01	60.04	1.01	32.11	1.00
		97.74	0.99	167.55	1.02	167.55	0.98	97.74	0.99
		251.33	0.96	335.10	0.99	335.10	0.96	251.33	0.99
		418.88	0.99	481.71	1.02	481.71	1.00	418.88	1.01
		544.54	1.01	600.39	1.04	600.39	1.04	544.54	1.03
		656.24	1.02	712.09	1.05	712.09	1.03	656.24	1.04
		767.94	1.05	837.76	1.06	837.76	1.06	767.94	1.06
		893.61	1.07	949.46	1.08	949.46	1.08	893.61	1.07
	100/0	6.98	1.05	8.38	1.00	8.38	1.08	6.98	1.05
		12.57	1.13	19.55	1.01	19.55	1.03	12.57	1.04
		32.11	1.03	60.04	1.00	60.04	0.99	32.11	1.01
		97.74	0.98	167.55	1.00	167.55	0.97	97.74	1.01
		251.33	0.96	335.10	1.01	335.10	0.98	251.33	0.99
		418.88	0.99	481.71	1.03	481.71	1.01	418.88	1.01
		544.54	1.03	600.39	1.04	600.39	1.03	544.54	1.03
		656.24	1.03	712.09	1.05	712.09	1.04	656.24	1.03
		767.94	1.05	837.76	1.07	837.76	1.06	767.94	1.05
		893.61	1.08	949.46	1.07	949.46	1.08	893.61	1.06

Table D8 Integrating torque signals result at 3.14 rad/s and 100°C as measured by the RPA-FT of HNBR compounds filled with various CB hybrid systems and hybrid ratios (cont.)

CB hybrid system	CB hybrid ratio	Test a				Test b			
		run 1		run 2		run 1		run 2	
		Strain (%)	Q1/Q2	Strain (%)	Q1/Q2	Strain (%)	Q1/Q2	Strain (%)	Q1/Q2
N550/N990	0/100	6.98	1.07	8.38	1.08	8.38	1.08	6.98	1.02
		12.57	1.11	19.55	1.09	19.55	1.10	12.57	1.13
		32.11	1.09	60.04	1.04	60.04	1.01	32.11	1.06
		97.74	1.05	167.55	1.06	167.55	1.05	97.74	1.03
		251.33	1.04	335.10	1.04	335.10	1.05	251.33	1.04
		418.88	1.07	481.71	1.07	481.71	1.06	418.88	1.07
		544.54	1.08	600.39	1.08	600.39	1.08	544.54	1.07
		656.24	1.07	712.09	1.08	712.09	1.08	656.24	1.07
		767.94	1.08	837.76	1.09	837.76	1.08	767.94	1.08
		893.61	1.09	949.46	1.09	949.46	1.09	893.61	1.08
	20/80	6.98	1.09	8.38	1.09	8.38	1.10	6.98	1.08
		12.57	1.12	19.55	1.07	19.55	1.06	12.57	1.13
		32.11	1.05	60.04	1.05	60.04	1.05	32.11	1.05
		97.74	1.05	167.55	1.05	167.55	1.02	97.74	1.06
		251.33	1.02	335.10	1.05	335.10	1.04	251.33	1.05
		418.88	1.04	481.71	1.06	481.71	1.06	418.88	1.05
		544.54	1.06	600.39	1.07	600.39	1.07	544.54	1.07
		656.24	1.06	712.09	1.07	712.09	1.07	656.24	1.07
		767.94	1.08	837.76	1.08	837.76	1.08	767.94	1.08
		893.61	1.08	949.46	1.09	949.46	1.10	893.61	1.08
	40/60	6.98	1.04	8.38	1.09	8.38	1.11	6.98	1.03
		12.57	1.08	19.55	1.10	19.55	1.10	12.57	1.09
		32.11	1.07	60.04	1.04	60.04	1.03	32.11	1.05
		97.74	1.06	167.55	1.03	167.55	1.02	97.74	1.05
		251.33	1.02	335.10	1.03	335.10	1.02	251.33	1.03
		418.88	1.03	481.71	1.05	481.71	1.03	418.88	1.05
		544.54	1.06	600.39	1.06	600.39	1.05	544.54	1.06
		656.24	1.05	712.09	1.06	712.09	1.07	656.24	1.06
		767.94	1.07	837.76	1.08	837.76	1.08	767.94	1.07
		893.61	1.07	949.46	1.08	949.46	1.09	893.61	1.07
	60/40	6.98	1.06	8.38	1.12	8.38	1.13	6.98	1.07
		12.57	1.12	19.55	1.09	19.55	1.08	12.57	1.09
		32.11	1.06	60.04	1.04	60.04	1.02	32.11	1.04
		97.74	1.05	167.55	1.02	167.55	1.01	97.74	1.06
		251.33	1.02	335.10	1.03	335.10	1.01	251.33	1.03
		418.88	1.03	481.71	1.06	481.71	1.03	418.88	1.04
		544.54	1.05	600.39	1.05	600.39	1.05	544.54	1.05
		656.24	1.04	712.09	1.06	712.09	1.06	656.24	1.05
		767.94	1.06	837.76	1.07	837.76	1.07	767.94	1.06
		893.61	1.08	949.46	1.06	949.46	1.08	893.61	1.07

Table D8 Integrating torque signals result at 3.14 rad/s and 100°C as measured by the RPA-FT of HNBR compounds filled with various CB hybrid systems and hybrid ratios (cont.)

CB hybrid system	CB hybrid ratio	Test a				Test b			
		run 1		run 2		run 1		run 2	
		Strain (%)	Q1/Q2	Strain (%)	Q1/Q2	Strain (%)	Q1/Q2	Strain (%)	Q1/Q2
N550/N990	80/20	6.98	1.08	8.38	1.08	8.38	1.09	6.98	1.05
		12.57	1.12	19.55	1.07	19.55	1.13	12.57	1.10
		32.11	1.02	60.04	1.04	60.04	1.03	32.11	1.05
		97.74	1.02	167.55	1.02	167.55	1.00	97.74	1.04
		251.33	1.00	335.10	1.02	335.10	1.00	251.33	1.01
		418.88	1.01	481.71	1.04	481.71	1.02	418.88	1.04
		544.54	1.03	600.39	1.05	600.39	1.04	544.54	1.04
		656.24	1.03	712.09	1.06	712.09	1.05	656.24	1.04
		767.94	1.06	837.76	1.07	837.76	1.07	767.94	1.05
		893.61	1.07	949.46	1.08	949.46	1.09	893.61	1.06
	100/0	6.98	1.05	8.38	1.06	8.38	1.05	6.98	1.04
		12.57	1.08	19.55	1.08	19.55	1.07	12.57	1.11
		32.11	1.03	60.04	1.01	60.04	1.00	32.11	1.03
		97.74	1.01	167.55	1.02	167.55	1.00	97.74	1.03
		251.33	0.98	335.10	1.01	335.10	1.00	251.33	1.00
		418.88	1.03	481.71	1.03	481.71	1.03	418.88	1.03
		544.54	1.04	600.39	1.05	600.39	1.06	544.54	1.04
		656.24	1.04	712.09	1.06	712.09	1.07	656.24	1.04
		767.94	1.07	837.76	1.07	837.76	1.07	767.94	1.05
		893.61	1.08	949.46	1.07	949.46	1.09	893.61	1.05

Table D9 Strain sweep test results at 60°C and 1 rad/s as measured by the RPA2000 of HNBR compounds filled with various CB hybrid systems and hybrid ratios: (a) Storage modulus (G′)

1) N326/N990

Strain amplitude (%)	G′ (kPa)					
	0/100	20/80	40/60	60/40	80/20	100/0
0.28	209580.00	210320.00	241680.00	210570.00	195980.00	280370.00
0.42	38372.00	74224.00	37320.00	39341.00	78491.00	79350.00
0.56	2374.70	2672.50	2846.80	3491.30	27777.00	29401.00
0.70	2304.50	2488.00	2709.70	3099.20	3697.80	4572.40
0.98	2205.70	2375.40	2572.60	2936.30	3406.10	4082.30
1.95	2152.70	2316.00	2464.40	2765.80	3160.40	3703.50
3.07	2103.40	2242.60	2397.30	2645.80	3006.80	3486.60
5.02	2050.60	2175.50	2292.00	2500.80	2816.30	3248.50
6.98	1988.90	2107.10	2206.80	2378.30	2657.30	3056.40
10.04	1928.20	2035.10	2110.90	2261.00	2505.50	2870.70
15.07	1863.50	1955.70	2018.10	2140.80	2360.20	2690.90
19.95	1814.80	1896.80	1949.30	2062.90	2268.00	2572.00
29.99	1724.60	1786.90	1828.90	1924.80	2110.40	2371.00
40.04	1638.60	1693.70	1726.60	1813.80	1974.50	2204.70
49.94	1544.10	1594.50	1622.20	1708.60	1834.70	2049.20

2) N326/N774

Strain amplitude (%)	G′ (kPa)					
	0/100	20/80	40/60	60/40	80/20	100/0
0.28	142460.00	87682.00	168240.00	229530.00	69267.00	143050.00
0.42	72006.00	74995.00	78517.00	111210.00	35957.00	75835.00
0.56	3461.90	28557.00	28573.00	28299.00	4097.00	4506.60
0.70	3333.40	3792.80	3786.20	4207.80	3924.70	4285.90
0.98	3067.60	3337.70	3412.70	3831.20	3769.20	3915.20
1.95	2851.10	3055.40	3056.30	3428.50	3468.90	3517.10
3.07	2781.30	2999.20	3016.20	3330.90	3358.70	3421.90
5.02	2607.60	2828.60	2843.20	3087.80	3119.30	3154.80
6.98	2492.70	2706.70	2707.80	2920.90	2965.30	2977.20
10.04	2373.30	2571.30	2573.10	2740.70	2793.30	2804.20
15.07	2246.50	2424.40	2431.60	2575.60	2632.80	2611.10
19.95	2154.70	2320.80	2333.40	2461.20	2514.20	2485.40
29.99	1994.10	2135.20	2153.60	2259.30	2304.60	2277.70
40.04	1852.10	1974.30	1987.50	2093.00	2123.00	2110.10
49.94	1715.30	1837.60	1820.20	1934.10	1955.50	1959.20

Table D9 Strain sweep test results at 60°C and 1 rad/s as measured by the RPA2000 of HNBR compounds filled with various CB hybrid systems and hybrid ratios (cont.): (a) Storage modulus (G′)

3) N550/N990

Strain amplitude (%)	G′ (kPa)					
	0/100	20/80	40/60	60/40	80/20	100/0
0.28	209580.00	62910.00	63336.00	142030.00	64014.00	70565.00
0.42	38372.00	2791.00	2963.90	39105.00	3921.60	5223.00
0.56	2374.70	2569.00	2587.40	3248.40	3550.40	4502.40
0.70	2304.50	2439.60	2559.10	3048.30	3413.90	4262.00
0.98	2205.70	2330.20	2461.10	2844.70	3178.70	3837.10
1.95	2152.70	2257.40	2382.70	2707.10	2978.60	3529.50
3.07	2103.40	2229.40	2348.80	2653.90	2845.20	3344.00
5.02	2050.60	2163.90	2266.00	2568.30	2702.70	3135.70
6.98	1988.90	2105.60	2189.50	2479.20	2588.20	2988.50
10.04	1928.20	2029.40	2093.90	2355.00	2474.20	2831.20
15.07	1863.50	1949.90	1994.30	2231.00	2370.60	2695.40
19.95	1814.80	1881.00	1924.10	2132.30	2287.00	2589.30
29.99	1724.60	1762.70	1800.50	1981.20	2125.00	2396.90
40.04	1638.60	1650.00	1683.80	1852.50	1984.80	2188.50
49.94	1544.10	1536.40	1568.00	1720.50	1850.40	1965.90

Table D9 Strain sweep test results at 60°C and 1 rad/s as measured by the RPA2000 of HNBR compounds filled with various CB hybrid systems and hybrid ratios (cont.): (b) Loss modulus (G″)

1) N326/N990

Strain amplitude (%)	G″ (kPa)					
	0/100	20/80	40/60	60/40	80/20	100/0
0.28	206930.00	206780.00	239100.00	207230.00	192590.00	275880.00
0.42	36384.00	71968.00	34829.00	36374.00	75166.00	75362.00
0.56	275.82	289.48	324.14	486.95	24686.00	25589.00
0.70	227.95	284.94	329.44	413.75	530.76	686.11
0.98	243.52	282.85	318.41	420.24	507.52	614.20
1.95	241.18	288.66	333.15	407.04	497.55	623.01
3.07	233.82	280.00	331.47	405.96	489.36	608.27
5.02	237.61	285.24	327.54	401.60	478.32	592.65
6.98	232.73	279.50	318.67	386.13	458.03	561.52
10.04	229.52	274.47	309.10	367.70	438.84	527.14
15.07	224.66	267.66	299.31	342.96	408.41	482.75
19.95	222.23	261.85	291.61	328.01	392.89	454.53
29.99	221.23	257.35	282.97	310.02	375.90	425.81
40.04	223.20	254.04	277.76	299.79	366.23	410.39
49.94	240.07	265.98	287.54	296.57	370.91	403.01

2) N326/N774

Strain amplitude (%)	G″ (kPa)					
	0/100	20/80	40/60	60/40	80/20	100/0
0.28	138260.00	82650.00	163520.00	224920.00	64857.00	138620.00
0.42	69374.00	72192.00	75278.00	107880.00	32567.00	72247.00
0.56	491.24	25398.00	25459.00	24846.00	561.04	649.26
0.70	452.79	526.39	553.44	624.00	573.79	601.68
0.98	438.31	467.11	469.41	599.11	525.84	566.79
1.95	446.28	476.03	480.52	595.95	575.14	567.19
3.07	453.64	478.68	492.44	609.09	565.41	576.40
5.02	434.52	457.65	479.17	581.25	543.63	549.14
6.98	418.25	441.71	463.85	557.31	518.44	524.37
10.04	396.87	421.95	442.85	527.05	495.11	497.39
15.07	378.53	402.24	422.73	493.53	467.32	468.87
19.95	372.98	387.13	411.35	473.16	449.68	452.67
29.99	368.08	378.29	403.68	452.60	438.79	438.51
40.04	371.00	387.76	408.36	444.10	445.22	429.72
49.94	390.53	401.56	439.79	452.07	468.14	432.13

Table D9 Strain sweep test results at 60°C and 1 rad/s as measured by the RPA2000 of HNBR compounds filled with various CB hybrid systems and hybrid ratios (cont.): (b) Loss modulus (G″)

3) N550/N990

Strain amplitude (%)	G″ (kPa)					
	0/100	20/80	40/60	60/40	80/20	100/0
0.28	206930.00	60031.00	59934.00	138720.00	60299.00	64652.00
0.42	36384.00	325.86	344.27	36262.00	532.70	812.13
0.56	275.82	286.89	316.81	442.49	476.14	635.82
0.70	227.95	278.70	319.03	381.73	429.37	569.01
0.98	243.52	260.23	294.17	364.21	441.79	545.77
1.95	241.18	274.50	299.29	353.90	440.98	567.59
3.07	233.82	276.94	306.71	356.16	438.53	555.70
5.02	237.61	273.61	301.77	351.39	428.22	539.04
6.98	232.73	271.37	294.47	341.67	410.74	515.68
10.04	229.52	265.75	292.58	331.10	389.49	485.10
15.07	224.66	260.88	285.19	316.74	362.58	454.34
19.95	222.23	261.13	283.99	313.81	353.33	447.27
29.99	221.23	270.04	294.95	318.36	341.55	443.26
40.04	223.20	281.79	305.78	324.47	343.25	469.98
49.94	240.07	299.00	325.80	347.07	361.17	520.77

Table D10 Temperature sweep test results at 62.8 rad/s as measured by the DMA of HNBR compounds filled with various CB hybrid systems and hybrid ratios: (a) Storage modulus (G′)

1) N326/N990

0/100		20/80		40/60		60/40		80/20		100/0	
Temp.(°C)	G′ (MPa)	Temp.(°C)	G′ (MPa)	Temp.(°C)	G′ (MPa)	Temp.(°C)	G′ (MPa)	Temp.(°C)	G′ (MPa)	Temp.(°C)	G′ (MPa)
-79.2	4353.21	-80.6	4046.18	-80.0	4462.96	-80.1	3749.73	-80.7	4732.37	-80.3	4078.37
-77.2	4325.24	-78.2	3800.55	-78.7	4424.23	-77.8	3735.46	-78.4	4696.06	-77.7	4028.29
-74.2	4254.48	-74.8	3772.76	-74.2	4315.03	-74.7	3671.53	-74.9	4617.98	-75.1	3963.73
-71.1	4169.75	-71.5	3719.49	-71.2	4237.04	-71.4	3597.57	-71.6	4525.91	-72.0	3884.65
-67.6	4059.24	-68.5	3642.46	-68.6	4152.29	-70.3	3555.22	-68.7	4423.72	-70.8	3847.31
-65.3	3967.40	-67.5	3612.06	-65.5	4058.77	-67.4	3479.08	-67.6	4381.88	-67.8	3758.63
-62.8	3881.46	-64.3	3534.08	-62.6	3963.89	-64.6	3400.71	-64.8	4285.58	-66.4	3714.04
-59.8	3796.27	-61.7	3455.49	-59.9	3886.40	-61.6	3322.48	-62.0	4189.66	-63.9	3634.70
-56.5	3699.25	-58.7	3381.31	-57.0	3795.63	-58.6	3237.58	-59.2	4094.05	-60.8	3547.39
-53.3	3617.60	-57.4	3333.99	-54.0	3706.02	-55.6	3168.70	-57.7	4050.81	-57.8	3461.37
-50.1	3537.66	-54.7	3281.55	-51.1	3611.64	-52.6	3089.13	-56.8	4014.03	-55.1	3387.48
-48.3	3474.93	-51.7	3222.92	-48.3	3535.58	-50.9	3046.88	-54.1	3933.25	-52.0	3323.34
-46.7	3438.49	-48.6	3167.52	-45.3	3432.29	-49.8	3024.28	-53.1	3894.42	-50.7	3287.13
-45.7	3413.82	-45.8	3116.96	-42.8	3312.90	-48.7	2998.24	-50.0	3803.98	-48.0	3223.86
-44.9	3384.61	-42.8	3053.44	-39.7	3145.20	-47.6	2966.32	-47.3	3699.33	-45.0	3138.28
-44.1	3355.41	-41.6	3022.14	-36.5	2991.34	-46.4	2953.70	-44.2	3597.88	-43.9	3108.77
-43.2	3328.21	-39.9	2982.81	-35.5	2937.74	-45.1	2926.96	-41.5	3474.44	-41.0	3035.81
-41.9	3287.30	-38.7	2944.20	-34.5	2873.25	-44.0	2889.53	-40.5	3426.46	-38.0	2956.45
-40.7	3242.18	-37.8	2914.06	-33.2	2734.85	-43.0	2878.82	-39.3	3365.44	-35.0	2815.53
-39.6	3194.98	-36.5	2869.09	-31.6	2562.93	-41.9	2856.69	-36.3	3171.64	-33.8	2734.58
-38.3	3128.56	-35.4	2815.54	-30.5	2351.18	-40.6	2822.19	-34.7	3028.37	-32.6	2608.00
-36.9	3048.80	-34.4	2755.50	-29.2	2039.51	-38.7	2778.56	-33.5	2918.40	-31.4	2428.39
-35.6	2957.57	-33.0	2653.46	-28.0	1769.87	-36.9	2717.93	-32.6	2792.98	-30.4	2229.17
-34.7	2857.88	-32.0	2539.91	-27.1	1536.58	-34.9	2616.60	-31.3	2620.51	-29.3	2013.70
-32.9	2634.17	-30.9	2378.68	-26.2	1276.72	-32.6	2426.00	-30.3	2382.11	-28.1	1788.44
-30.7	2230.32	-29.7	2178.17	-25.2	1050.18	-31.0	2199.05	-29.1	2093.22	-26.6	1492.92
-28.7	1747.31	-28.4	1940.60	-24.2	762.96	-28.7	1836.90	-27.8	1774.73	-25.2	1186.25
-26.6	1288.06	-26.6	1564.88	-22.6	560.62	-26.6	1462.66	-26.5	1452.65	-23.9	961.63
-24.7	852.40	-24.7	1147.99	-21.1	380.50	-24.5	1111.23	-24.6	1059.38	-22.6	733.35
-22.7	547.80	-22.7	748.25	-19.9	288.58	-22.9	802.50	-22.6	753.25	-21.4	583.76
-20.7	329.03	-20.6	471.81	-18.7	242.70	-20.8	520.46	-20.7	510.16	-20.0	464.33
-18.6	197.98	-18.8	305.41	-17.3	190.12	-18.6	334.67	-18.6	349.30	-18.6	371.97
-16.8	126.72	-16.7	198.74	-16.1	145.21	-16.6	233.71	-16.7	255.50	-16.6	279.18
-14.5	83.37	-14.6	131.24	-14.6	112.46	-14.7	170.76	-14.6	187.76	-14.6	219.27
-12.7	63.06	-12.6	91.06	-12.5	89.06	-12.8	129.74	-12.6	145.14	-12.7	176.66
-10.6	50.61	-10.7	69.43	-10.6	71.96	-10.7	102.34	-10.7	118.07	-10.6	149.67
-8.7	41.56	-8.7	56.07	-8.7	58.78	-8.8	85.54	-8.6	98.42	-8.6	127.24
-6.7	34.69	-6.5	46.39	-6.6	49.47	-6.7	72.74	-6.5	85.12	-6.6	113.18
-4.6	30.02	-4.6	40.62	-4.5	43.15	-4.5	63.41	-4.6	76.20	-4.6	101.53

Table D10 Temperature sweep test results at 62.8 rad/s as measured by the DMA of HNBR compounds filled with various CB hybrid systems and hybrid ratios (cont.): (a) Storage modulus (G′)

0/100		20/80		40/60		60/40		80/20		100/0	0/100
Temp.(°C)	G′ (MPa)	Temp.(°C)	G′ (MPa)	Temp.(°C)	G′ (MPa)	Temp.(°C)	G′ (MPa)	Temp.(°C)	G′ (MPa)	Temp.(°C)	G′ (MPa)
-2.6	26.85	-2.5	35.91	-2.5	38.92	-2.6	57.04	-2.6	69.08	-2.6	92.79
-0.6	24.68	-0.6	32.66	-0.7	36.06	-0.5	51.53	-0.8	64.97	-0.5	84.65
4.7	23.00	3.6	29.98	5.8	33.06	4.9	46.58	3.9	59.02	4.3	78.00
4.8	22.03	3.9	29.10	5.5	31.46	5.1	44.30	4.2	56.49	4.7	74.88
4.7	21.67	5.1	27.97	5.1	31.04	5.0	43.51	5.1	54.59	4.8	73.14
7.3	20.94	7.5	26.69	7.1	30.10	7.3	42.04	7.3	52.07	7.3	69.12
9.4	20.21	9.4	25.76	9.6	28.99	9.4	40.37	9.4	49.70	9.6	65.97
11.4	19.63	11.6	24.96	11.4	28.13	11.5	38.56	11.5	47.73	11.4	64.16
13.4	19.12	13.2	24.43	15.4	26.41	13.4	37.15	13.6	46.18	13.4	61.11
15.3	18.65	15.1	23.95	17.4	25.68	15.5	35.69	15.6	45.03	15.4	58.31
17.4	18.19	17.3	23.44	19.4	25.00	17.5	34.48	17.1	44.24	17.4	55.79
19.4	17.84	19.6	22.93	21.4	24.37	19.3	33.37	19.3	43.00	19.4	53.62
21.4	17.48	21.3	22.54	23.5	23.82	21.4	32.35	21.4	41.83	21.4	51.68
23.8	17.16	23.4	22.08	25.5	23.34	23.5	31.41	23.5	40.65	23.6	49.97
25.4	16.95	25.3	21.59	27.3	22.93	25.3	30.63	25.2	39.71	25.5	48.62
27.4	16.74	27.4	21.13	29.5	22.52	27.7	29.97	27.3	38.56	28.0	47.57
29.3	16.57	29.3	20.73	31.6	22.25	29.3	29.49	29.4	37.52	29.4	46.91
31.1	16.44	31.4	20.34	32.9	22.08	31.3	29.07	31.2	36.66	30.6	46.49
33.4	16.23	33.4	20.03	35.1	21.83	33.3	28.66	33.3	35.83	33.5	45.33
35.4	16.03	35.3	19.71	37.4	21.43	35.4	28.16	35.6	34.92	35.4	44.63
37.3	15.85	37.2	19.42	39.5	21.02	37.3	27.68	37.6	34.11	37.5	43.70
39.4	15.61	39.4	19.13	41.4	20.64	39.4	27.17	39.5	33.38	39.4	42.58
41.4	15.38	41.4	18.80	43.3	20.27	41.4	26.56	41.3	32.74	41.4	41.44
43.4	15.15	43.4	18.56	45.3	19.90	43.5	25.97	43.1	32.12	43.4	40.42
45.4	14.98	45.4	18.28	47.3	19.58	45.5	25.40	45.3	31.33	45.4	39.47
47.2	14.80	47.4	18.02	49.1	19.29	47.4	24.85	47.1	30.71	47.4	38.62
49.2	14.61	49.4	17.75	51.4	19.00	49.5	24.40	48.9	30.03	49.4	37.75
51.4	14.45	51.3	17.47	53.2	18.73	51.2	24.00	51.3	29.27	51.4	36.89
53.1	14.28	53.1	17.21	55.1	18.49	53.2	23.59	53.3	28.60	53.5	36.11
55.2	14.12	55.3	16.94	57.4	18.23	55.4	23.17	55.1	27.99	55.5	35.36
57.4	13.99	57.3	16.69	59.4	17.99	57.3	22.81	57.2	27.34	57.4	34.70
59.0	13.87	59.5	16.42	15.4	26.41	59.2	22.48	59.4	26.66	59.5	34.00
61.3	13.68	61.3	16.19	61.3	17.73	61.3	22.13	61.2	26.10	61.4	33.21
63.0	13.57	63.3	15.96	63.5	17.45	63.5	21.80	63.5	25.58	63.4	32.60
65.7	13.40	65.3	15.76	65.5	17.21	65.4	21.42	65.4	25.05	65.5	31.89
67.4	13.26	67.5	15.51	67.5	16.98	67.3	21.15	67.1	24.64	67.4	31.25
69.1	13.16	69.6	15.32	69.5	16.67	69.4	20.88	69.7	24.07	69.4	30.60
71.6	13.01	71.5	15.14	71.4	16.45	71.4	20.66	71.1	23.75	71.4	29.93
74.1	12.87	73.3	14.94	73.5	16.21	73.4	20.38	74.3	23.15	73.3	29.34
74.6	12.82	75.3	14.77	75.7	16.00	75.4	20.09	75.0	22.87	75.3	28.70
78.0	12.63	77.3	14.62	77.3	15.84	77.3	19.82	77.4	22.49	77.4	28.09

Table D10 Temperature sweep test results at 62.8 rad/s as measured by the DMA of HNBR compounds filled with various CB hybrid systems and hybrid ratios (cont.): (a) Storage modulus (G′)

0/100		20/80		40/60		60/40		80/20		100/0	
Temp.(°C)	G′ (MPa)	Temp.(°C)	G′ (MPa)	Temp.(°C)	G′ (MPa)	Temp.(°C)	G′ (MPa)	Temp.(°C)	G′ (MPa)	Temp.(°C)	G′ (MPa)
79.3	12.54	79.5	14.46	79.6	15.54	79.5	19.53	79.3	22.12	79.3	27.48
81.7	12.44	81.4	14.30	81.4	15.36	81.4	19.27	81.5	21.78	81.3	26.93
84.2	12.30	83.3	14.16	83.8	15.19	83.4	18.98	83.6	21.42	83.4	26.37
85.3	12.22	85.3	14.03	85.7	15.04	85.5	18.61	85.4	21.10	85.4	25.97
87.6	12.02	87.3	13.90	87.6	14.94	87.5	18.31	87.1	20.83	87.7	25.24
89.3	11.92	89.4	13.78	89.6	14.81	89.6	17.94	89.2	20.58	89.4	24.52
92.4	11.78	91.3	13.70	91.6	14.67	91.4	17.55	91.1	20.34	91.6	24.01
93.6	11.72	93.4	13.58	93.4	14.57	93.3	17.20	93.9	20.04	93.4	23.63
95.1	11.66	95.5	13.49	95.7	14.47	95.3	16.94	95.5	19.81	95.6	23.20
97.4	11.60	97.3	13.39	97.7	14.35	97.4	16.76	97.2	19.67	97.4	22.91
100.0	11.53	99.5	13.29	99.5	14.25	99.4	16.58	99.5	19.40	99.3	22.61
101.2	11.50	101.7	13.21	101.6	14.16	101.4	16.41	101.6	19.21	101.6	22.29
103.1	11.46	103.3	13.15	103.9	14.06	103.6	16.23	103.4	19.03	103.7	21.99
105.9	11.41	105.4	13.08	105.5	13.99	105.5	16.11	105.2	18.87	105.2	21.77
107.1	11.38	107.4	13.00	107.1	13.94	107.6	15.96	106.9	18.69	107.4	21.49
109.3	11.34	109.6	12.91	109.3	13.82	109.5	15.83	109.4	18.49	109.4	21.23
111.2	11.30	111.6	12.85	111.2	13.76	111.5	15.69	111.5	18.35	111.3	20.99
113.0	11.27	113.3	12.79	113.5	13.67	113.3	15.59	113.9	18.16	113.7	20.79
115.9	11.24	115.4	12.73	115.2	13.61	115.4	15.44	114.9	18.05	115.3	20.52
117.8	11.20	117.4	12.69	117.6	13.50	117.1	15.34	117.5	17.91	117.3	20.34
119.8	11.17	119.3	12.62	119.3	13.44	119.3	15.24	119.3	17.80	119.4	20.19
121.7	11.16	121.1	12.58	121.4	13.38	121.3	15.15	120.9	17.69	121.2	19.99
123.4	11.14	123.8	12.52	123.5	13.32	123.4	15.07	123.6	17.58	123.1	19.84
125.5	11.11	125.3	12.48	125.4	13.27	125.8	14.94	125.1	17.45	125.4	19.66
127.6	11.09	127.8	12.45	127.5	13.23	127.4	14.89	127.4	17.33	127.5	19.52
129.5	11.08	129.7	12.39	129.4	13.17	129.4	14.80	129.3	17.26	129.5	19.36
131.6	11.06	131.3	12.36	131.7	13.13	131.5	14.75	131.2	17.17	131.4	19.23
133.0	11.03	133.3	12.34	133.2	13.05	133.3	14.69	133.8	17.05	133.6	19.08
135.4	11.03	135.5	12.30	135.6	13.01	135.3	14.58	135.4	16.98	135.5	18.96
137.2	11.02	137.2	12.26	137.6	12.98	137.6	14.53	137.7	16.88	137.3	18.85
138.9	10.99	139.3	12.24	139.5	12.94	139.6	14.45	139.2	16.79	139.4	18.70
141.2	11.00	141.1	12.22	141.6	12.90	141.3	14.40	141.0	16.70	141.3	18.62
143.7	10.99	143.4	12.17	143.4	12.87	143.5	14.32	143.8	16.62	143.3	18.48
145.8	10.97	145.5	12.15	145.2	12.82	146.0	14.28	145.4	16.55	145.6	18.35
147.7	10.98	147.4	12.12	147.6	12.79	147.7	14.22	147.2	16.48	147.4	18.25
149.2	10.96	149.3	12.11	149.6	12.76	149.3	14.16	149.6	16.39	149.0	18.18

Table D10 Temperature sweep test results at 62.8 rad/s as measured by the DMA of HNBR compounds filled with various CB hybrid systems and hybrid ratios (cont.): (a) Storage modulus (G′)

2) N326/N774

0/100		20/80		40/60		60/40		80/20		100/0	
Temp.(°C)	G′ (MPa)	Temp.(°C)	G′ (MPa)	Temp.(°C)	G′ (MPa)	Temp.(°C)	G′ (MPa)	Temp.(°C)	G′ (MPa)	Temp.(°C)	G′ (MPa)
-80.5	2970.24	-80.7	2696.51	-78.7	3329.21	-80.4	3130.20	-78.2	2641.19	-80.3	4078.37
-78.8	3005.25	-78.7	2689.84	-78.1	3346.54	-78.4	3097.30	-77.5	2617.79	-77.7	4028.29
-76.4	2991.34	-76.8	2670.92	-76.8	3358.76	-76.7	3111.20	-76.2	2620.28	-75.1	3963.73
-74.4	2976.36	-74.5	2644.55	-74.7	3356.03	-74.4	3092.75	-74.5	2613.40	-72.0	3884.65
-72.4	2953.70	-72.6	2607.16	-72	3332.98	-72.5	3067.72	-72.5	2593.82	-70.8	3847.31
-70.6	2931.03	-70.6	2563.52	-69.7	3298.86	-70.5	3042.97	-70.4	2568.22	-67.8	3758.63
-68.8	2897.36	-68.6	2522.82	-68.7	3282.72	-68.5	3000.44	-68.3	2532.74	-66.4	3714.04
-66.6	2867.79	-66.4	2490.08	-66.4	3245.46	-66.8	2974.37	-66.6	2491.32	-63.9	3634.70
-64.2	2833.66	-64.2	2461.72	-64.6	3204.51	-64.8	2920.95	-64.0	2442.17	-60.8	3547.39
-62.8	2805.93	-62.8	2431.94	-62.1	3166.88	-62.6	2884.64	-62.8	2402.30	-57.8	3461.37
-60.6	2763.79	-60.6	2400.66	-60.7	3133.87	-60.9	2847.24	-60.5	2341.77	-55.1	3387.48
-58.6	2733.92	-58.5	2362.73	-58.5	3089.45	-58.8	2806.75	-58.5	2293.58	-52.0	3323.34
-56.3	2711.47	-56.5	2328.08	-56.3	3054.18	-56.6	2773.65	-56.6	2248.55	-50.7	3287.13
-54.6	2676.75	-54.7	2307.98	-54.6	3020.83	-54.8	2738.96	-54.4	2205.28	-48.0	3223.86
-52.5	2628.78	-52.6	2281.52	-52.6	2970.70	-52.8	2697.86	-52.5	2164.99	-45.0	3138.28
-50.5	2580.03	-50.8	2262.89	-50.7	2927.70	-51	2666.50	-50.5	2133.89	-43.9	3108.77
-48.5	2544.26	-48.7	2247.65	-48.7	2895.64	-48.7	2639.50	-48.4	2109.84	-41.0	3035.81
-46.5	2511.72	-46.1	2220.21	-46.7	2854.09	-46.6	2613.08	-46.5	2096.16	-38.0	2956.45
-44.5	2477.48	-44.4	2199.26	-44.8	2813.51	-44.9	2597.29	-44.5	2085.63	-35.0	2815.53
-42.4	2427.49	-42.8	2179.69	-42.6	2756.36	-42.6	2568.67	-42.4	2075.36	-33.8	2734.58
-40.5	2376.81	-40.3	2162.08	-40.7	2701.10	-41	2541.77	-40.0	2067.20	-32.6	2608.00
-38.4	2320.12	-39.1	2147.62	-38.7	2624.45	-39	2497.09	-38.7	2044.26	-31.4	2428.39
-36.4	2256.81	-36.4	2084.76	-36.7	2510.79	-36.7	2427.59	-36.5	2005.00	-30.4	2229.17
-34.5	2168.76	-34.3	1997.51	-34.5	2367.90	-34.7	2332.01	-34.3	1959.34	-29.3	2013.70
-32.4	2043.29	-32.4	1835.58	-32.6	2168.98	-32.6	2155.58	-32.3	1854.01	-28.1	1788.44
-30.1	1783.59	-30.3	1542.26	-30.5	1862.90	-30.8	1900.60	-30.4	1697.29	-26.6	1492.92
-28.2	1519.99	-28.2	1280.95	-28.4	1586.54	-28.7	1563.25	-28.2	1466.92	-25.2	1186.25
-26.3	1227.73	-26.5	1096.53	-26.5	1244.03	-26.5	1224.92	-26.5	1220.82	-23.9	961.63
-24.7	910.29	-24.5	813.53	-24.5	916.67	-24.6	911.04	-24.4	945.86	-22.6	733.35
-22.6	598.43	-22.6	584.00	-22.6	674.65	-22.5	636.95	-22.5	711.35	-21.4	583.76
-20.5	389.30	-20.5	391.97	-20.6	465.70	-20.6	444.81	-20.5	530.64	-20.0	464.33
-18.5	253.32	-18.5	271.97	-18.6	321.98	-18.6	314.26	-18.6	388.32	-18.6	371.97
-16.6	173.34	-16.6	202.07	-16.7	233.38	-16.7	227.64	-16.4	285.28	-16.6	279.18
-14.5	127.31	-14.6	156.76	-14.5	171.89	-14.5	170.25	-14.6	217.90	-14.6	219.27
-12.5	100.21	-12.7	127.73	-12.6	136.64	-12.7	136.25	-12.5	172.08	-12.7	176.66
-10.6	80.76	-10.6	102.61	-10.6	111.24	-10.6	111.93	-10.6	140.52	-10.6	149.67
-8.6	67.93	-8.6	83.98	-8.6	94.47	-8.5	95.76	-8.6	117.43	-8.6	127.24
-6.6	59.13	-6.6	72.04	-6.6	82.74	-6.6	83.29	-6.5	100.10	-6.6	113.18
-4.5	53.57	-4.6	63.84	-4.5	74.08	-4.5	74.07	-4.6	89.36	-4.6	101.53

Table D10 Temperature sweep test results at 62.8 rad/s as measured by the DMA of HNBR compounds filled with various CB hybrid systems and hybrid ratios (cont.): (a) Storage modulus (G′)

0/100		20/80		40/60		60/40		80/20		100/0	0/100
Temp.(°C)	G′ (MPa)	Temp.(°C)	G′ (MPa)	Temp.(°C)	G′ (MPa)	Temp.(°C)	G′ (MPa)	Temp.(°C)	G′ (MPa)	Temp.(°C)	G′ (MPa)
-2.6	49.16	-2.6	57.43	-2.6	67.87	-2.5	67.43	-2.6	80.71	-2.6	92.79
-0.7	44.72	-0.5	51.28	-0.5	62.25	-0.9	63.01	-0.8	71.82	-0.5	84.65
3.1	41.10	4.9	47.56	2.3	58.16	2.9	57.61	2.8	66.47	4.3	78.00
3.2	40.24	4.5	45.89	2.9	56.90	3	56.05	3.0	64.85	4.7	74.88
5.3	38.04	4.4	44.97	5.4	53.33	5.4	52.84	5.3	61.09	4.8	73.14
7.3	36.08	7.4	42.59	7.5	50.41	7.1	50.40	7.4	57.46	7.3	69.12
9.5	34.52	9.4	40.69	9.5	48.39	9.6	47.91	9.6	54.55	9.6	65.97
11.5	33.23	11.5	39.04	11.6	46.89	11.6	46.20	11.5	52.48	11.4	64.16
13.5	32.17	13.4	37.67	13.4	45.69	13.6	44.69	13.5	50.70	13.4	61.11
15.5	31.30	15.5	36.45	15.5	44.49	15.4	43.53	15.3	49.28	15.4	58.31
17.3	30.62	17.4	35.35	17.4	43.38	17.4	42.35	17.4	48.07	17.4	55.79
19.6	29.87	19.4	34.42	19.4	42.29	19.4	41.24	19.4	46.77	19.4	53.62
21.4	29.25	21.4	33.56	21.4	41.18	21.4	40.15	21.4	45.61	21.4	51.68
23.6	28.64	23.4	32.84	23.5	40.16	23.6	39.15	23.5	44.52	23.6	49.97
25.4	28.09	25.4	32.21	25.4	39.14	25.3	38.31	25.5	43.50	25.5	48.62
27.4	27.54	27.6	31.54	27.5	38.02	27.4	37.29	27.3	42.47	28.0	47.57
29.6	26.94	29.5	31.02	29.4	37.05	29.3	36.36	29.4	41.49	29.4	46.91
31.3	26.43	31.3	30.51	31.3	36.19	31.4	35.41	31.4	40.45	30.6	46.49
33.4	25.89	33.5	29.95	33.4	35.26	33.4	34.58	33.4	39.46	33.5	45.33
35.4	25.35	35.4	29.36	35.4	34.49	35.5	33.74	35.5	38.51	35.4	44.63
37.4	24.86	37.6	28.78	37.5	33.70	37.4	32.98	37.5	37.64	37.5	43.70
39.4	24.34	39.3	28.27	39.4	33.00	39.4	32.26	39.4	36.79	39.4	42.58
41.4	23.87	41.5	27.72	41.4	32.30	41.4	31.61	41.4	36.05	41.4	41.44
43.5	23.41	43.4	27.22	43.4	31.67	43.4	30.94	43.5	35.29	43.4	40.42
45.4	23.01	45.4	26.71	45.5	30.98	45.5	30.31	45.4	34.58	45.4	39.47
47.5	22.57	47.4	26.20	47.4	30.42	47.4	29.75	47.4	33.89	47.4	38.62
49.4	22.20	49.4	25.71	49.5	29.82	49.4	29.13	49.4	33.23	49.4	37.75
51.5	21.78	51.4	25.20	51.3	29.26	51.4	28.59	51.4	32.53	51.4	36.89
53.3	21.41	53.5	24.77	53.4	28.68	53.3	28.10	53.4	31.83	53.5	36.11
55.4	21.05	55.4	24.32	55.4	28.00	55.4	27.54	55.5	31.10	55.5	35.36
57.3	20.68	57.4	23.91	57.3	27.46	57.4	26.87	57.3	30.41	57.4	34.70
59.2	20.25	59.4	23.52	59.5	26.82	59.5	26.33	59.5	29.67	59.5	34.00
61.5	19.86	63.4	22.71	63.4	25.78	63.4	25.21	63.4	28.37	63.4	32.60
63.5	19.47	65.4	22.44	65.4	25.24	65.3	24.69	65.4	27.74	65.5	31.89
65.4	19.15	67.4	22.09	67.5	24.78	67.5	24.21	67.5	27.09	67.4	31.25
67.4	18.82	69.4	21.67	69.3	24.39	69.3	23.73	69.5	26.55	69.4	30.60
69.4	18.51	71.5	21.26	71.4	23.89	71.5	23.20	71.3	26.03	71.4	29.93
71.3	18.20	73.3	20.88	73.5	23.50	73.4	22.76	73.5	25.47	73.3	29.34
73.4	17.96	75.5	20.54	75.4	23.12	75.3	22.37	75.3	25.01	75.3	28.70
75.4	17.66	77.4	20.22	77.4	22.77	77.4	21.94	77.4	24.51	77.4	28.09
77.6	17.42	79.3	19.92	79.4	22.41	79.4	21.58	79.4	24.07	79.3	27.48

Table D10 Temperature sweep test results at 62.8 rad/s as measured by the DMA of HNBR compounds filled with various CB hybrid systems and hybrid ratios (cont.): (a) Storage modulus (G′)

0/100		20/80		40/60		60/40		80/20		100/0	
Temp.(°C)	G′ (MPa)	Temp.(°C)	G′ (MPa)	Temp.(°C)	G′ (MPa)	Temp.(°C)	G′ (MPa)	Temp.(°C)	G′ (MPa)	Temp.(°C)	G′ (MPa)
79.5	17.18	81.4	19.61	81.3	22.07	81.4	21.24	81.4	23.67	81.3	26.93
81.4	17.00	83.6	19.28	83.6	21.73	83.5	20.92	83.5	23.29	83.4	26.37
83.5	16.76	85.4	18.99	85.3	21.47	85.4	20.63	85.4	23.01	85.4	25.97
85.4	16.57	87.3	18.71	87.4	21.18	87.5	20.35	87.3	22.66	87.7	25.24
87.5	16.41	89.4	18.46	89.5	20.89	89.5	20.09	89.3	22.39	89.4	24.52
89.4	16.24	91.4	18.23	91.4	20.67	91.3	19.86	91.4	22.08	91.6	24.01
91.6	16.04	93.4	18.06	93.3	20.46	93.4	19.65	93.4	21.80	93.4	23.63
93.3	15.91	95.4	17.86	95.4	20.22	95.3	19.39	95.4	21.52	95.6	23.20
95.4	15.79	97.4	17.69	97.3	20.02	97.3	19.20	97.4	21.28	97.4	22.91
97.4	15.62	99.5	17.52	99.3	19.83	99.5	18.98	99.5	21.05	99.3	22.61
99.4	15.48	101.6	17.35	101.4	19.62	101.5	18.77	101.3	20.83	101.6	22.29
101.4	15.36	103.4	17.21	103.6	19.44	103.6	18.58	103.4	20.65	103.7	21.99
103.5	15.25	105.5	17.07	105.5	19.29	105.3	18.44	105.5	20.42	105.2	21.77
105.4	15.15	107.5	16.93	107.2	19.17	107.6	18.25	107.3	20.24	107.4	21.49
107.6	15.02	63.4	22.71	63.4	25.78	63.4	25.21	63.4	28.37	63.4	32.60
109.5	14.93	109.4	16.78	109.2	19.04	109.4	18.06	109.5	20.04	109.4	21.23
111.4	14.82	111.6	16.67	111.4	18.87	111.4	17.91	111.4	19.84	111.3	20.99
113.3	14.72	113.5	16.54	113.3	18.70	113.4	17.78	113.5	19.71	113.7	20.79
115.5	14.67	115.4	16.43	115.3	18.60	115.1	17.65	115.4	19.56	115.3	20.52
117.4	14.54	117.5	16.32	117.4	18.44	117.5	17.52	117.7	19.41	117.3	20.34
119.2	14.47	119.5	16.22	119.7	18.30	119.3	17.39	119.6	19.22	119.4	20.19
121.3	14.35	121.4	16.16	121.5	18.17	121.6	17.26	121.3	19.18	121.2	19.99
123.4	14.31	123.4	16.00	123.5	18.06	123.5	17.15	123.4	19.01	123.1	19.84
125.4	14.22	125.5	15.94	125.2	18.00	125.2	17.02	125.6	18.91	125.4	19.66
127.6	14.12	127.5	15.87	127.3	17.92	127.4	16.92	127.3	18.77	127.5	19.52
129.4	14.05	129.4	15.79	129.3	17.76	129.5	16.82	129.6	18.69	129.5	19.36
131.3	13.98	131.3	15.71	131.4	17.68	131.3	16.73	131.4	18.59	131.4	19.23
133.3	13.92	133.5	15.60	133.5	17.57	133.4	16.61	133.2	18.50	133.6	19.08
135.4	13.86	135.4	15.57	135.3	17.53	135.2	16.56	135.5	18.40	135.5	18.96
137.4	13.80	137.4	15.51	137.4	17.42	137.3	16.44	137.4	18.32	137.3	18.85
139.4	13.73	139.4	15.46	139.4	17.36	139.3	16.36	139.5	18.21	139.4	18.70
141.5	13.67	141.4	15.38	141.4	17.25	141.6	16.25	141.3	18.15	141.3	18.62
143.4	13.61	143.4	15.31	143.6	17.19	143.3	16.19	143.6	18.08	143.3	18.48
145.4	13.58	145.5	15.23	145.3	17.11	145.2	16.12	145.3	18.00	145.6	18.35
147.6	13.52	147.6	15.18	147.6	17.01	147.5	16.06	147.2	17.89	147.4	18.25
149.5	13.44	149.5	15.16	149.1	16.97	149.3	15.99	149.3	17.83	149.0	18.18

Table D10 Temperature sweep test results at 62.8 rad/s as measured by the DMA of HNBR compounds filled with various CB hybrid systems and hybrid ratios (cont.): (a) Storage modulus (G′)

3) N550/N990

0/100		20/80		40/60		60/40		80/20		100/0	
Temp.(°C)	G′ (MPa)	Temp.(°C)	G′ (MPa)	Temp.(°C)	G′ (MPa)	Temp.(°C)	G′ (MPa)	Temp.(°C)	G′ (MPa)	Temp.(°C)	G′ (MPa)
-79.2	4353.21	-80.9	4204.14	-80.7	4460.65	-81.2	4424.77	-79.7	4064.99	-79.2	4287.06
-77.2	4325.24	-78.3	4151.21	-78.3	4449.41	-78.3	4367.90	-77.5	4053.15	-77.4	4291.65
-74.2	4254.48	-76.7	4101.65	-77.0	4410.09	-75.1	4275.53	-74.5	3987.36	-76.2	4262.61
-71.1	4169.75	-75.1	4053.37	-73.0	4310.70	-73.1	4221.19	-70.8	3879.81	-72.8	4199.79
-67.6	4059.24	-73.7	3992.85	-69.7	4224.17	-71.9	4184.53	-69.0	3808.24	-71.6	4156.01
-65.3	3967.40	-71.1	3913.83	-67.9	4163.17	-70.4	4145.05	-67.8	3769.86	-68.6	4081.40
-62.8	3881.46	-68.9	3847.73	-66.7	4122.40	-68.9	4097.51	-66.9	3730.68	-65.9	3986.32
-59.8	3796.27	-67.4	3785.71	-65.8	4081.41	-67.6	4031.60	-66.2	3698.91	-62.6	3879.31
-56.5	3699.25	-65.5	3710.74	-64.4	4039.26	-65.7	3945.42	-64.5	3640.89	-61.1	3823.88
-53.3	3617.60	-63.0	3633.46	-62.4	3991.81	-63.4	3871.90	-63.0	3586.92	-59.9	3790.83
-50.1	3537.66	-60.8	3575.14	-61.1	3946.67	-60.8	3799.92	-60.8	3532.83	-59.0	3758.79
-48.3	3474.93	-58.8	3514.84	-59.2	3886.77	-59.1	3746.95	-59.4	3483.62	-58.0	3722.80
-46.7	3438.49	-56.9	3463.48	-57.6	3831.52	-56.9	3678.55	-56.8	3422.52	-56.5	3686.31
-45.7	3413.82	-55.1	3409.13	-55.3	3755.97	-54.7	3621.23	-55.2	3371.45	-55.0	3633.58
-44.9	3384.61	-53.2	3343.84	-53.1	3680.68	-52.9	3573.53	-53.1	3320.46	-53.0	3582.19
-44.1	3355.41	-50.9	3276.11	-50.2	3606.94	-51.2	3512.65	-51.0	3276.05	-51.1	3531.32
-43.2	3328.21	-49.0	3222.35	-48.5	3562.04	-48.8	3449.50	-48.8	3234.45	-49.0	3479.57
-41.9	3287.30	-47.0	3173.12	-46.8	3516.84	-46.9	3391.59	-47.0	3189.83	-47.2	3432.94
-40.7	3242.18	-44.8	3113.53	-45.7	3460.49	-44.8	3338.29	-45.0	3147.36	-44.9	3379.96
-39.6	3194.98	-43.1	3059.62	-43.3	3370.97	-42.8	3278.62	-43.0	3104.75	-42.8	3324.91
-38.3	3128.56	-40.8	2981.15	-41.2	3285.81	-40.9	3216.33	-40.8	3060.74	-40.9	3280.61
-36.9	3048.80	-39.1	2907.13	-39.1	3197.11	-38.7	3136.13	-38.8	2990.88	-38.8	3207.28
-35.6	2957.57	-36.9	2808.84	-37.1	3074.62	-36.9	3020.59	-37.1	2919.61	-36.8	3121.41
-34.7	2857.88	-34.8	2656.33	-35.3	2937.90	-34.5	2834.20	-34.7	2780.18	-34.8	3012.97
-32.9	2634.17	-32.8	2427.07	-32.9	2705.08	-32.8	2620.13	-32.8	2594.39	-32.0	2731.13
-30.7	2230.32	-30.5	2065.52	-30.7	2350.13	-30.9	2251.23	-30.4	2204.53	-30.7	2436.59
-28.7	1747.31	-28.6	1687.47	-29.1	1854.25	-28.7	1806.92	-28.5	1821.26	-27.9	1926.97
-26.6	1288.06	-26.8	1292.50	-26.1	1243.49	-26.4	1353.69	-26.6	1425.21	-26.8	1600.87
-24.7	852.40	-24.6	862.46	-24.6	835.66	-24.6	957.14	-24.6	1038.24	-24.4	1146.62
-22.7	547.80	-22.6	536.58	-22.1	420.77	-22.7	604.65	-22.6	690.47	-22.5	815.09
-20.7	329.03	-20.7	334.64	-20.2	276.33	-20.6	314.21	-20.7	446.70	-20.6	555.09
-18.6	197.98	-18.6	194.92	-18.9	194.16	-18.6	196.59	-18.7	286.52	-18.6	375.85
-16.8	126.72	-16.7	124.10	-16.4	126.10	-16.6	144.83	-16.7	194.88	-16.7	266.27
-14.5	83.37	-14.6	82.98	-14.7	97.50	-14.6	111.21	-14.7	138.61	-14.7	196.96
-12.7	63.06	-12.6	61.35	-12.7	76.41	-12.6	84.88	-12.5	104.33	-12.6	150.71
-10.6	50.61	-10.7	48.50	-10.6	60.62	-10.7	67.07	-10.7	83.78	-10.6	117.39
-8.7	41.56	-8.6	40.05	-8.5	50.14	-8.5	54.63	-8.6	67.48	-8.5	96.48
-6.7	34.69	-6.7	34.67	-6.6	42.59	-6.5	46.19	-6.7	58.18	-6.7	83.09
-4.6	30.02	-4.7	30.10	-4.5	38.62	-4.7	41.39	-4.6	51.59	-4.6	72.98

Table D10 Temperature sweep test results at 62.8 rad/s as measured by the DMA of HNBR compounds filled with various CB hybrid systems and hybrid ratios (cont.): (a) Storage modulus (G′)

0/100		20/80		40/60		60/40		80/20		100/0	0/100
Temp.(°C)	G′ (MPa)	Temp.(°C)	G′ (MPa)	Temp.(°C)	G′ (MPa)	Temp.(°C)	G′ (MPa)	Temp.(°C)	G′ (MPa)	Temp.(°C)	G′ (MPa)
-2.6	26.85	-2.8	26.98	-2.7	35.39	-2.6	37.48	-2.6	46.83	-2.7	66.22
-0.6	24.68	-0.6	24.51	-0.9	32.97	-0.6	34.68	-0.5	42.74	-1.0	60.65
4.7	23.00	5.3	22.30	5.1	29.92	5.6	31.86	4.0	39.77	3.5	55.19
4.8	22.03	5.0	21.56	4.8	28.66	5.4	30.57	4.2	38.52	3.9	53.47
4.7	21.67	4.8	21.43	4.6	28.30	5.0	30.27	5.1	37.61	5.3	51.34
7.3	20.94	7.3	20.62	7.3	27.21	7.3	29.34	7.3	36.25	7.3	49.28
9.4	20.21	9.4	20.00	9.5	26.24	9.5	28.34	9.5	34.78	9.5	47.11
11.4	19.63	11.4	19.42	11.4	25.49	11.4	27.44	11.5	33.54	11.5	45.31
13.4	19.12	13.4	18.86	13.3	24.80	13.4	26.47	13.3	32.48	13.5	43.88
15.3	18.65	15.5	18.34	15.3	24.07	15.4	25.66	15.5	31.31	15.3	42.90
17.4	18.19	17.4	17.90	17.4	23.41	17.3	25.01	17.5	30.40	17.4	41.83
19.4	17.84	19.4	17.50	19.4	22.85	19.4	24.38	19.4	29.53	19.6	40.78
21.4	17.48	21.5	17.12	21.5	22.35	21.4	23.78	21.6	28.76	21.2	39.95
23.8	17.16	23.6	16.82	23.5	21.93	23.6	23.21	23.7	28.16	23.5	38.84
25.4	16.95	25.7	16.55	25.4	21.51	25.5	22.79	25.4	27.70	25.4	37.87
27.4	16.74	27.3	16.34	27.4	21.15	27.3	22.40	27.4	27.26	27.4	36.96
29.3	16.57	29.4	16.18	29.4	20.85	29.7	21.99	29.7	26.83	29.3	36.13
31.1	16.44	31.2	16.05	31.6	20.59	31.3	21.82	30.9	26.54	31.4	35.36
33.4	16.23	33.3	15.85	33.3	20.38	33.6	21.58	33.5	26.03	33.2	34.63
35.4	16.03	35.5	15.59	35.4	20.08	35.4	21.31	35.5	25.57	35.3	33.91
37.3	15.85	37.5	15.31	37.4	19.76	37.4	20.97	37.5	25.10	37.3	33.24
39.4	15.61	39.5	15.10	39.4	19.42	39.5	20.62	39.4	24.59	39.4	32.57
41.4	15.38	41.4	14.90	41.4	19.11	41.5	20.24	41.5	24.10	41.4	32.01
43.4	15.15	43.6	14.71	43.5	18.79	43.5	19.90	43.4	23.62	43.5	31.49
45.4	14.98	45.5	14.52	45.4	18.50	45.4	19.59	45.3	23.19	45.4	30.94
47.2	14.80	47.4	14.33	47.3	18.24	47.2	19.31	47.4	22.79	47.4	30.43
49.2	14.61	49.4	14.16	49.5	17.95	49.3	18.97	49.4	22.41	49.4	29.91
51.4	14.45	51.4	13.95	51.4	17.69	51.5	18.70	51.5	21.99	51.3	29.39
53.1	14.28	53.3	13.78	53.6	17.40	53.5	18.42	53.6	21.63	53.5	28.87
55.2	14.12	55.3	13.61	55.4	17.12	55.6	18.15	55.4	21.35	55.4	28.39
57.4	13.99	57.5	13.44	57.3	16.89	57.3	17.90	57.5	20.99	57.3	27.88
59.0	13.87	59.4	13.28	59.1	16.66	59.3	17.67	59.4	20.68	59.3	27.41
61.3	13.68	61.2	13.14	61.3	16.45	61.3	17.40	61.1	20.42	61.4	26.90
63.0	13.57	63.4	12.96	63.8	16.18	63.1	17.15	63.2	20.18	63.3	26.47
65.7	13.40	65.4	12.78	65.3	15.98	65.3	16.92	65.2	19.93	65.2	26.04
67.4	13.26	67.2	12.65	67.2	15.77	67.5	16.71	67.6	19.60	67.1	25.58
69.1	13.16	69.2	12.51	69.6	15.53	69.3	16.45	69.4	19.29	69.3	25.06
71.6	13.01	71.5	12.35	71.0	15.30	71.5	16.23	71.3	19.07	71.6	24.52
74.1	12.87	73.5	12.22	73.5	15.16	73.6	15.99	73.4	18.75	73.5	24.02
74.6	12.82	75.5	12.08	75.4	14.96	75.3	15.81	75.3	18.51	75.3	23.62
78.0	12.63	77.5	11.94	77.3	14.81	77.4	15.65	77.2	18.26	77.2	23.25

Table D10 Temperature sweep test results at 62.8 rad/s as measured by the DMA of HNBR compounds filled with various CB hybrid systems and hybrid ratios (cont.): (a) Storage modulus (G′)

0/100		20/80		40/60		60/40		80/20		100/0	
Temp.(°C)	G′ (MPa)	Temp.(°C)	G′ (MPa)	Temp.(°C)	G′ (MPa)	Temp.(°C)	G′ (MPa)	Temp.(°C)	G′ (MPa)	Temp.(°C)	G′ (MPa)
79.3	12.54	79.6	11.83	79.0	14.66	79.6	15.43	79.4	17.99	79.4	22.89
81.7	12.44	81.4	11.74	80.9	14.53	81.6	15.27	81.6	17.70	81.3	22.55
84.2	12.30	83.3	11.65	83.7	14.35	83.5	15.08	83.6	17.43	83.3	22.28
85.3	12.22	85.3	11.54	84.9	14.23	85.5	14.95	85.2	17.22	85.2	22.01
87.6	12.02	87.1	11.44	87.3	14.10	87.7	14.78	87.2	17.04	87.4	21.72
89.3	11.92	89.4	11.34	89.5	14.01	89.4	14.64	89.4	16.83	89.5	21.46
92.4	11.78	91.7	11.28	91.6	13.89	91.6	14.52	91.6	16.66	91.3	21.24
93.6	11.72	93.4	11.22	93.6	13.82	93.6	14.39	93.6	16.53	93.2	21.06
95.1	11.66	95.2	11.16	95.4	13.71	95.6	14.32	95.4	16.37	95.1	20.83
97.4	11.60	97.4	11.11	97.4	13.65	97.6	14.22	97.3	16.27	97.3	20.64
100.0	11.53	99.2	11.09	99.0	13.59	99.9	14.13	99.4	16.13	99.2	20.46
101.2	11.50	101.1	11.02	101.4	13.50	101.3	14.05	101.4	16.03	101.4	20.28
103.1	11.46	103.1	10.98	103.1	13.42	103.6	13.95	103.4	15.93	103.4	20.08
105.9	11.41	105.4	10.96	105.3	13.38	105.2	13.90	105.1	15.84	105.2	19.94
107.1	11.38	107.3	10.91	107.5	13.31	107.1	13.86	107.4	15.70	107.2	19.77
109.3	11.34	109.6	10.89	109.2	13.23	109.6	13.77	109.6	15.62	109.3	19.62
111.2	11.30	111.4	10.84	111.3	13.17	111.2	13.73	111.5	15.52	111.6	19.46
113.0	11.27	113.3	10.82	113.2	13.13	113.4	13.68	113.5	15.45	113.4	19.32
115.9	11.24	115.4	10.79	115.4	13.05	115.2	13.63	115.3	15.37	115.5	19.17
117.8	11.20	117.3	10.74	117.6	13.03	117.2	13.57	117.2	15.29	117.2	19.04
119.8	11.17	119.7	10.70	119.2	12.98	119.1	13.51	119.2	15.20	119.1	18.91
121.7	11.16	121.0	10.71	121.3	12.90	121.1	13.47	121.5	15.15	121.3	18.79
123.4	11.14	123.0	10.66	123.6	12.87	123.8	13.40	123.3	15.05	123.4	18.68
125.5	11.11	124.9	10.63	125.6	12.84	124.9	13.36	125.0	15.01	125.8	18.60
127.6	11.09	127.4	10.64	127.7	12.81	127.6	13.33	127.4	14.94	127.6	18.45
129.5	11.08	129.6	10.59	129.8	12.73	129.7	13.30	129.5	14.87	129.2	18.37
131.6	11.06	131.1	10.59	131.9	12.71	131.4	13.24	131.3	14.81	131.2	18.28
133.0	11.03	133.5	10.55	133.4	12.69	133.3	13.20	133.2	14.77	133.3	18.20
135.4	11.03	135.3	10.55	135.4	12.66	135.2	13.13	135.5	14.72	135.5	18.06
137.2	11.02	137.4	10.50	137.2	12.63	137.5	13.13	137.8	14.65	137.2	18.01
138.9	10.99	139.5	10.52	139.3	12.60	139.1	13.09	139.4	14.60	139.4	17.90
141.2	11.00	141.5	10.50	141.1	12.57	140.9	13.05	141.4	14.55	141.1	17.82
143.7	10.99	143.4	10.48	143.9	12.53	143.1	13.02	143.6	14.49	143.1	17.75
145.8	10.97	145.4	10.44	145.4	12.49	145.0	13.00	145.6	14.45	145.3	17.68
147.7	10.98	147.2	10.43	147.5	12.49	147.6	12.96	147.3	14.40	147.1	17.59
149.2	10.96	149.6	10.42	149.3	12.42	149.1	12.93	148.9	14.36	149.0	17.53

Table D10 Temperature sweep test results at 62.8 rad/s as measured by the DMA of HNBR compounds filled with various CB hybrid systems and hybrid ratios (cont.): (b) Loss modulus (G″)

1) N326/N990

0/100		20/80		40/60		60/40		80/20		100/0	
Temp.(°C)	G″ (MPa)	Temp.(°C)	G″ (MPa)	Temp.(°C)	G″ (MPa)	Temp.(°C)	G″ (MPa)	Temp.(°C)	G″ (MPa)	Temp.(°C)	G″ (MPa)
-79.2	177.06	-80.6	145.62	-80.0	122.73	-80.1	172.75	-80.7	131.15	-80.3	177.38
-77.2	173.02	-78.2	170.99	-78.7	120.40	-77.8	165.79	-78.4	128.03	-77.7	167.04
-74.2	167.33	-74.8	166.62	-74.2	114.93	-74.7	160.83	-74.9	124.87	-75.1	160.47
-71.1	161.60	-71.5	162.33	-71.2	112.30	-71.4	158.10	-71.6	119.39	-72.0	155.15
-67.6	157.99	-68.5	158.03	-68.6	108.59	-70.3	162.60	-68.7	117.73	-70.8	161.51
-65.3	154.67	-67.5	160.94	-65.5	103.15	-67.4	155.61	-67.6	116.12	-67.8	152.08
-62.8	150.21	-64.3	153.56	-62.6	98.61	-64.6	153.17	-64.8	108.78	-66.4	158.44
-59.8	145.53	-61.7	151.54	-59.9	94.72	-61.6	148.68	-62.0	106.38	-63.9	146.17
-56.5	138.83	-58.7	148.93	-57.0	90.32	-58.6	144.78	-59.2	102.31	-60.8	141.28
-53.3	132.30	-57.4	153.04	-54.0	87.97	-55.6	142.52	-57.7	101.05	-57.8	138.38
-50.1	127.16	-54.7	144.99	-51.1	84.60	-52.6	139.79	-56.8	101.24	-55.1	134.80
-48.3	129.42	-51.7	142.79	-48.3	83.46	-50.9	140.79	-54.1	93.65	-52.0	131.46
-46.7	122.90	-48.6	139.30	-45.3	83.64	-49.8	143.73	-53.1	95.87	-50.7	138.40
-45.7	124.36	-45.8	136.40	-42.8	78.34	-48.7	145.17	-50.0	90.64	-48.0	128.40
-44.9	125.25	-42.8	136.13	-39.7	96.79	-47.6	145.48	-47.3	90.29	-45.0	128.90
-44.1	125.47	-41.6	143.47	-36.5	123.90	-46.4	144.73	-44.2	91.99	-43.9	138.07
-43.2	126.43	-39.9	141.68	-35.5	142.77	-45.1	145.49	-41.5	98.54	-41.0	138.39
-41.9	129.10	-38.7	147.06	-34.5	163.76	-44.0	146.54	-40.5	105.50	-38.0	152.66
-40.7	133.19	-37.8	152.95	-33.2	200.80	-43.0	146.67	-39.3	111.63	-35.0	189.30
-39.6	137.77	-36.5	158.96	-31.6	255.45	-41.9	148.43	-36.3	141.86	-33.8	219.40
-38.3	147.12	-35.4	168.93	-30.5	324.80	-40.6	151.62	-34.7	178.78	-32.6	257.16
-36.9	161.00	-34.4	180.85	-29.2	394.60	-38.7	159.04	-33.5	212.59	-31.4	306.67
-35.6	180.12	-33.0	203.86	-28.0	442.43	-36.9	170.94	-32.6	247.54	-30.4	357.23
-34.7	203.54	-32.0	232.50	-27.1	468.80	-34.9	197.01	-31.3	297.61	-29.3	404.14
-32.9	258.38	-30.9	272.74	-26.2	483.05	-32.6	244.14	-30.3	361.08	-28.1	441.00
-30.7	353.04	-29.7	322.27	-25.2	476.51	-31.0	309.07	-29.1	421.39	-26.6	454.73
-28.7	449.66	-28.4	372.02	-24.2	436.49	-28.7	393.43	-27.8	469.79	-25.2	461.88
-26.6	501.03	-26.6	436.10	-22.6	374.07	-26.6	448.60	-26.5	491.79	-23.9	423.96
-24.7	474.63	-24.7	471.20	-21.1	293.11	-24.5	461.77	-24.6	478.38	-22.6	362.53
-22.7	393.20	-22.7	432.80	-19.9	237.60	-22.9	424.50	-22.6	417.49	-21.4	319.26
-20.7	288.19	-20.6	344.26	-18.7	205.07	-20.8	337.65	-20.7	326.85	-20.0	270.92
-18.6	195.42	-18.8	255.94	-17.3	164.17	-18.6	243.83	-18.6	239.94	-18.6	224.70
-16.8	129.90	-16.7	178.98	-16.1	124.61	-16.6	175.86	-16.7	176.76	-16.6	168.56
-14.5	82.27	-14.6	118.77	-14.6	92.74	-14.7	125.89	-14.6	124.70	-14.6	127.02
-12.7	57.56	-12.6	77.34	-12.5	68.51	-12.8	89.84	-12.6	88.93	-12.7	95.00
-10.6	41.74	-10.7	53.30	-10.6	50.01	-10.7	64.23	-10.7	65.31	-10.6	73.56
-8.7	30.00	-8.7	37.95	-8.7	35.56	-8.8	48.19	-8.6	47.84	-8.6	55.55
-6.7	21.15	-6.5	26.86	-6.6	25.42	-6.7	35.87	-6.5	36.23	-6.6	44.38
-4.6	15.26	-4.6	20.34	-4.5	18.69	-4.5	27.07	-4.6	28.66	-4.6	35.42

Table D10 Temperature sweep test results at 62.8 rad/s as measured by the DMA of HNBR compounds filled with various CB hybrid systems and hybrid ratios (cont.): (b) Loss modulus (G″)

0/100		20/80		40/60		60/40		80/20		100/0	0/100
Temp.(°C)	G″ (MPa)	Temp.(°C)	G″ (MPa)	Temp.(°C)	G″ (MPa)	Temp.(°C)	G″ (MPa)	Temp.(°C)	G″ (MPa)	Temp.(°C)	G″ (MPa)
-2.6	11.42	-2.5	15.23	-2.5	14.42	-2.6	21.34	-2.6	22.89	-2.6	29.01
-0.6	8.88	-0.6	11.78	-0.7	11.67	-0.5	16.52	-0.8	19.69	-0.5	23.47
4.7	7.01	3.6	9.14	5.8	8.93	4.9	12.53	3.9	15.38	4.3	19.29
4.8	6.01	3.9	8.38	5.5	7.69	5.1	11.13	4.2	13.86	4.7	17.70
4.7	5.66	5.1	7.23	5.1	7.36	5.0	10.64	5.1	12.54	4.8	16.67
7.3	4.91	7.5	6.14	7.1	6.58	7.3	9.47	7.3	11.08	7.3	14.50
9.4	4.26	9.4	5.46	9.6	5.83	9.4	8.48	9.4	9.82	9.6	12.97
11.4	3.78	11.6	4.90	11.4	5.29	11.5	7.50	11.5	8.91	11.4	12.20
13.4	3.40	13.2	4.56	15.4	4.80	13.4	6.82	13.6	8.25	13.4	10.96
15.3	3.10	15.1	4.30	17.4	4.43	15.5	6.22	15.6	7.80	15.4	9.99
17.4	2.88	17.3	4.00	19.4	4.11	17.5	5.75	17.1	7.53	17.4	9.21
19.4	2.69	19.6	3.78	21.4	3.89	19.3	5.40	19.3	7.11	19.4	8.62
21.4	2.56	21.3	3.59	23.5	3.69	21.4	5.11	21.4	6.77	21.4	8.16
23.8	2.46	23.4	3.41	25.5	3.54	23.5	4.87	23.5	6.44	23.6	7.79
25.4	2.40	25.3	3.25	27.3	3.44	25.3	4.73	25.2	6.25	25.5	7.53
27.4	2.33	27.4	3.12	29.5	3.35	27.7	4.58	27.3	6.01	28.0	7.33
29.3	2.29	29.3	3.04	31.6	3.27	29.3	4.49	29.4	5.82	29.4	7.23
31.1	2.27	31.4	2.96	32.9	3.20	31.3	4.42	31.2	5.66	30.6	7.14
33.4	2.24	33.4	2.87	35.1	3.15	33.3	4.34	33.3	5.53	33.5	6.99
35.4	2.20	35.3	2.82	37.4	3.13	35.4	4.28	35.6	5.37	35.4	6.85
37.3	2.14	37.2	2.77	39.5	3.11	37.3	4.21	37.6	5.27	37.5	6.74
39.4	2.11	39.4	2.71	41.4	3.04	39.4	4.12	39.5	5.17	39.4	6.58
41.4	2.08	41.4	2.67	43.3	3.00	41.4	4.07	41.3	5.07	41.4	6.45
43.4	2.05	43.4	2.63	45.3	2.93	43.5	3.98	43.1	4.99	43.4	6.30
45.4	2.01	45.4	2.59	47.3	2.89	45.5	3.89	45.3	4.92	45.4	6.19
47.2	2.00	47.4	2.54	49.1	2.84	47.4	3.83	47.1	4.82	47.4	6.08
49.2	1.98	49.4	2.52	51.4	2.81	49.5	3.77	48.9	4.73	49.4	5.98
51.4	1.95	51.3	2.49	53.2	2.78	51.2	3.71	51.3	4.63	51.4	5.90
53.1	1.91	53.1	2.44	55.1	2.74	53.2	3.67	53.3	4.56	53.5	5.79
55.2	1.90	55.3	2.39	57.4	2.69	55.4	3.61	55.1	4.47	55.5	5.71
57.4	1.87	57.3	2.37	59.4	2.66	57.3	3.58	57.2	4.40	57.4	5.61
59.0	1.84	59.5	2.32	15.4	2.63	59.2	3.51	59.4	4.30	59.5	5.52
61.3	1.81	61.3	2.27	61.3	2.59	61.3	3.46	61.2	4.23	61.4	5.44
63.0	1.80	63.3	2.25	63.5	2.55	63.5	3.42	63.5	4.13	63.4	5.36
65.7	1.78	65.3	2.22	65.5	2.51	65.4	3.37	65.4	4.05	65.5	5.27
67.4	1.75	67.5	2.17	67.5	2.46	67.3	3.33	67.1	4.00	67.4	5.19
69.1	1.72	69.6	2.13	69.5	2.42	69.4	3.27	69.7	3.91	69.4	5.10
71.6	1.69	71.5	2.09	71.4	2.39	71.4	3.24	71.1	3.85	71.4	5.00
74.1	1.67	73.3	2.07	73.5	2.34	73.4	3.19	74.3	3.76	73.3	4.90
74.6	1.64	75.3	2.03	75.7	2.31	75.4	3.15	75.0	3.73	75.3	4.80
78.0	1.59	77.3	2.00	77.3	2.26	77.3	3.11	77.4	3.62	77.4	4.71

Table D10 Temperature sweep test results at 62.8 rad/s as measured by the DMA of HNBR compounds filled with various CB hybrid systems and hybrid ratios (cont.): (b) Loss modulus (G″)

0/100		20/80		40/60		60/40		80/20		100/0	
Temp.(°C)	G″ (MPa)	Temp.(°C)	G″ (MPa)	Temp.(°C)	G″ (MPa)	Temp.(°C)	G″ (MPa)	Temp.(°C)	G″ (MPa)	Temp.(°C)	G″ (MPa)
79.3	1.59	79.5	1.96	79.6	2.20	79.5	3.06	79.3	3.57	79.3	4.59
81.7	1.56	81.4	1.94	81.4	2.16	81.4	3.01	81.5	3.49	81.3	4.50
84.2	1.53	83.3	1.90	83.8	2.13	83.4	2.94	83.6	3.44	83.4	4.40
85.3	1.51	85.3	1.88	85.7	2.10	85.5	2.91	85.4	3.38	85.4	4.34
87.6	1.47	87.3	1.84	87.6	2.06	87.5	2.83	87.1	3.32	87.7	4.21
89.3	1.43	89.4	1.80	89.6	2.05	89.6	2.77	89.2	3.25	89.4	4.06
92.4	1.41	91.3	1.77	91.6	2.01	91.4	2.69	91.1	3.20	91.6	3.97
93.6	1.36	93.4	1.76	93.4	1.99	93.3	2.59	93.9	3.13	93.4	3.87
95.1	1.36	95.5	1.72	95.7	1.96	95.3	2.56	95.5	3.06	95.6	3.77
97.4	1.34	97.3	1.69	97.7	1.93	97.4	2.50	97.2	3.03	97.4	3.72
100.0	1.31	99.5	1.68	99.5	1.90	99.4	2.44	99.5	2.98	99.3	3.63
101.2	1.31	101.7	1.65	101.6	1.88	101.4	2.39	101.6	2.94	101.6	3.57
103.1	1.30	103.3	1.62	103.9	1.86	103.6	2.37	103.4	2.90	103.7	3.50
105.9	1.26	105.4	1.60	105.5	1.84	105.5	2.32	105.2	2.85	105.2	3.44
107.1	1.23	107.4	1.58	107.1	1.80	107.6	2.28	106.9	2.82	107.4	3.39
109.3	1.24	109.6	1.57	109.3	1.78	109.5	2.26	109.4	2.76	109.4	3.32
111.2	1.22	111.6	1.55	111.2	1.78	111.5	2.22	111.5	2.72	111.3	3.25
113.0	1.21	113.3	1.54	113.5	1.74	113.3	2.20	113.9	2.67	113.7	3.16
115.9	1.18	115.4	1.50	115.2	1.71	115.4	2.16	114.9	2.63	115.3	3.12
117.8	1.18	117.4	1.48	117.6	1.68	117.1	2.11	117.5	2.58	117.3	3.06
119.8	1.17	119.3	1.48	119.3	1.66	119.3	2.08	119.3	2.54	119.4	3.00
121.7	1.14	121.1	1.46	121.4	1.63	121.3	2.05	120.9	2.52	121.2	2.94
123.4	1.13	123.8	1.42	123.5	1.61	123.4	2.02	123.6	2.47	123.1	2.88
125.5	1.13	125.3	1.42	125.4	1.60	125.8	1.99	125.1	2.44	125.4	2.86
127.6	1.10	127.8	1.39	127.5	1.57	127.4	1.95	127.4	2.40	127.5	2.82
129.5	1.10	129.7	1.37	129.4	1.55	129.4	1.93	129.3	2.35	129.5	2.77
131.6	1.09	131.3	1.37	131.7	1.53	131.5	1.90	131.2	2.32	131.4	2.71
133.0	1.07	133.3	1.35	133.2	1.51	133.3	1.88	133.8	2.27	133.6	2.69
135.4	1.06	135.5	1.34	135.6	1.49	135.3	1.83	135.4	2.24	135.5	2.64
137.2	1.04	137.2	1.32	137.6	1.48	137.6	1.82	137.7	2.22	137.3	2.60
138.9	1.05	139.3	1.30	139.5	1.46	139.6	1.79	139.2	2.19	139.4	2.55
141.2	1.04	141.1	1.28	141.6	1.45	141.3	1.76	141.0	2.14	141.3	2.50
143.7	1.02	143.4	1.28	143.4	1.44	143.5	1.74	143.8	2.12	143.3	2.47
145.8	1.02	145.5	1.27	145.2	1.42	146.0	1.72	145.4	2.09	145.6	2.43
147.7	1.00	147.4	1.26	147.6	1.41	147.7	1.70	147.2	2.04	147.4	2.39
149.2	1.01	149.3	1.25	149.6	1.38	149.3	1.69	149.6	2.04	149.0	2.36

Table D10 Temperature sweep test results at 62.8 rad/s as measured by the DMA of HNBR compounds filled with various CB hybrid systems and hybrid ratios (cont.): (b) Loss modulus (G″)

2) N326/N774

0/100		20/80		40/60		60/40		80/20		100/0	
Temp.(°C)	G″ (MPa)	Temp.(°C)	G″ (MPa)	Temp.(°C)	G″ (MPa)	Temp.(°C)	G″ (MPa)	Temp.(°C)	G″ (MPa)	Temp.(°C)	G″ (MPa)
-80.5	78.08	-80.7	165.96	-78.7	79.90	-80.4	152.80	-78.2	126.81	-80.3	177.38
-78.8	82.05	-78.7	164.70	-78.1	81.92	-78.4	152.49	-77.5	131.31	-77.7	167.04
-76.4	81.03	-76.8	161.55	-76.8	82.15	-76.7	150.24	-76.2	131.53	-75.1	160.47
-74.4	79.77	-74.5	160.02	-74.7	81.75	-74.4	146.84	-74.5	131.35	-72.0	155.15
-72.4	78.55	-72.6	157.35	-72	79.46	-72.5	144.66	-72.5	130.73	-70.8	161.51
-70.6	77.12	-70.6	154.48	-69.7	76.48	-70.5	140.99	-70.4	130.07	-67.8	152.08
-68.8	74.81	-68.6	152.24	-68.7	76.01	-68.5	137.06	-68.3	129.25	-66.4	158.44
-66.6	71.62	-66.4	151.09	-66.4	72.94	-66.8	133.95	-66.6	127.06	-63.9	146.17
-64.2	68.92	-64.2	148.96	-64.6	70.22	-64.8	129.55	-64.0	125.96	-60.8	141.28
-62.8	67.07	-62.8	146.96	-62.1	68.02	-62.6	125.97	-62.8	125.26	-57.8	138.38
-60.6	64.64	-60.6	145.03	-60.7	67.11	-60.9	124.86	-60.5	122.52	-55.1	134.80
-58.6	63.84	-58.5	141.87	-58.5	64.14	-58.8	120.78	-58.5	122.05	-52.0	131.46
-56.3	62.67	-56.5	138.69	-56.3	63.14	-56.6	119.21	-56.6	120.68	-50.7	138.40
-54.6	60.44	-54.7	136.15	-54.6	62.31	-54.8	117.24	-54.4	118.28	-48.0	128.40
-52.5	60.10	-52.6	133.28	-52.6	61.52	-52.8	114.25	-52.5	116.46	-45.0	128.90
-50.5	59.69	-50.8	130.63	-50.7	61.48	-51	112.49	-50.5	114.99	-43.9	138.07
-48.5	60.75	-48.7	128.68	-48.7	61.67	-48.7	111.16	-48.4	113.21	-41.0	138.39
-46.5	60.94	-46.1	125.13	-46.7	63.24	-46.6	112.76	-46.5	111.65	-38.0	152.66
-44.5	63.27	-44.4	126.35	-44.8	65.81	-44.9	113.13	-44.5	112.04	-35.0	189.30
-42.4	67.13	-42.8	129.67	-42.6	69.72	-42.6	114.99	-42.4	113.17	-33.8	219.40
-40.5	72.22	-40.3	134.14	-40.7	76.86	-41	118.53	-40.0	117.59	-32.6	257.16
-38.4	82.92	-39.1	141.09	-38.7	88.67	-39	126.95	-38.7	121.48	-31.4	306.67
-36.4	97.07	-36.4	157.69	-36.7	110.36	-36.7	142.18	-36.5	135.77	-30.4	357.23
-34.5	120.50	-34.3	187.22	-34.5	146.57	-34.7	168.44	-34.3	152.27	-29.3	404.14
-32.4	161.37	-32.4	237.68	-32.6	206.36	-32.6	215.14	-32.3	186.53	-28.1	441.00
-30.1	238.86	-30.3	300.98	-30.5	292.61	-30.8	286.36	-30.4	239.23	-26.6	454.73
-28.2	299.13	-28.2	349.50	-28.4	345.55	-28.7	353.93	-28.2	287.34	-25.2	461.88
-26.3	345.05	-26.5	367.03	-26.5	387.40	-26.5	393.27	-26.5	319.39	-23.9	423.96
-24.7	359.89	-24.5	358.04	-24.5	385.96	-24.6	389.69	-24.4	333.65	-22.6	362.53
-22.6	324.15	-22.6	329.99	-22.6	350.32	-22.5	342.32	-22.5	316.69	-21.4	319.26
-20.5	259.95	-20.5	260.74	-20.6	285.26	-20.6	275.68	-20.5	276.52	-20.0	270.92
-18.5	189.54	-18.5	196.89	-18.6	215.18	-18.6	209.40	-18.6	223.33	-18.6	224.70
-16.6	133.73	-16.6	148.91	-16.7	158.84	-16.7	153.46	-16.4	171.82	-16.6	168.56
-14.5	95.18	-14.6	112.93	-14.5	112.15	-14.5	110.11	-14.6	130.70	-14.6	127.02
-12.5	69.97	-12.7	87.68	-12.6	82.67	-12.7	81.92	-12.5	98.96	-12.7	95.00
-10.6	50.76	-10.6	64.39	-10.6	60.28	-10.6	60.75	-10.6	75.20	-10.6	73.56
-8.6	37.70	-8.6	46.49	-8.6	45.26	-8.5	46.47	-8.6	56.95	-8.6	55.55
-6.6	28.91	-6.6	34.82	-6.6	34.79	-6.6	35.66	-6.5	43.14	-6.6	44.38
-4.5	23.32	-4.6	27.08	-4.5	27.42	-4.5	27.78	-4.6	34.51	-4.6	35.42

Table D10 Temperature sweep test results at 62.8 rad/s as measured by the DMA of HNBR compounds filled with various CB hybrid systems and hybrid ratios (cont.): (b) Loss modulus (G″)

0/100		20/80		40/60		60/40		80/20		100/0	0/100
Temp.(°C)	G″ (MPa)	Temp.(°C)	G″ (MPa)	Temp.(°C)	G″ (MPa)	Temp.(°C)	G″ (MPa)	Temp.(°C)	G″ (MPa)	Temp.(°C)	G″ (MPa)
-2.6	19.08	-2.6	21.11	-2.6	22.36	-2.5	22.41	-2.6	27.72	-2.6	29.01
-0.7	14.95	-0.5	15.81	-0.5	17.95	-0.9	18.96	-0.8	21.11	-0.5	23.47
3.1	11.81	4.9	12.83	2.3	15.03	2.9	15.08	2.8	17.43	4.3	19.29
3.2	11.23	4.5	11.67	2.9	14.16	3	14.24	3.0	16.57	4.7	17.70
5.3	9.38	4.4	11.03	5.4	11.82	5.4	12.00	5.3	13.99	4.8	16.67
7.3	7.96	7.4	9.21	7.5	10.15	7.1	10.55	7.4	11.96	7.3	14.50
9.5	7.00	9.4	8.12	9.5	9.10	9.6	9.29	9.6	10.52	9.6	12.97
11.5	6.26	11.5	7.23	11.6	8.44	11.6	8.53	11.5	9.57	11.4	12.20
13.5	5.79	13.4	6.59	13.4	7.90	13.6	7.98	13.5	8.86	13.4	10.96
15.5	5.40	15.5	6.12	15.5	7.49	15.4	7.53	15.3	8.35	15.4	9.99
17.3	5.10	17.4	5.73	17.4	7.10	17.4	7.11	17.4	7.92	17.4	9.21
19.6	4.86	19.4	5.46	19.4	6.71	19.4	6.76	19.4	7.57	19.4	8.62
21.4	4.64	21.4	5.23	21.4	6.45	21.4	6.48	21.4	7.20	21.4	8.16
23.6	4.53	23.4	5.04	23.5	6.18	23.6	6.24	23.5	6.91	23.6	7.79
25.4	4.36	25.4	4.90	25.4	5.92	25.3	6.04	25.5	6.70	25.5	7.53
27.4	4.22	27.6	4.77	27.5	5.73	27.4	5.83	27.3	6.50	28.0	7.33
29.6	4.13	29.5	4.66	29.4	5.52	29.3	5.66	29.4	6.30	29.4	7.23
31.3	4.04	31.3	4.57	31.3	5.38	31.4	5.51	31.4	6.07	30.6	7.14
33.4	3.94	33.5	4.48	33.4	5.24	33.4	5.39	33.4	5.90	33.5	6.99
35.4	3.85	35.4	4.39	35.4	5.15	35.5	5.24	35.5	5.76	35.4	6.85
37.4	3.81	37.6	4.35	37.5	5.03	37.4	5.13	37.5	5.64	37.5	6.74
39.4	3.75	39.3	4.27	39.4	4.94	39.4	5.02	39.4	5.55	39.4	6.58
41.4	3.68	41.5	4.21	41.4	4.84	41.4	4.96	41.4	5.47	41.4	6.45
43.5	3.63	43.4	4.14	43.4	4.76	43.4	4.87	43.5	5.34	43.4	6.30
45.4	3.58	45.4	4.06	45.5	4.68	45.5	4.77	45.4	5.27	45.4	6.19
47.5	3.52	47.4	4.02	47.4	4.63	47.4	4.72	47.4	5.17	47.4	6.08
49.4	3.45	49.4	3.93	49.5	4.56	49.4	4.64	49.4	5.04	49.4	5.98
51.5	3.42	51.4	3.90	51.3	4.47	51.4	4.57	51.4	4.97	51.4	5.90
53.3	3.34	53.5	3.82	53.4	4.39	53.3	4.50	53.4	4.89	53.5	5.79
55.4	3.31	55.4	3.78	55.4	4.30	55.4	4.42	55.5	4.80	55.5	5.71
57.3	3.25	57.4	3.70	57.3	4.23	57.4	4.34	57.3	4.67	57.4	5.61
59.2	3.21	59.4	3.69	59.5	4.15	59.5	4.24	59.5	4.59	59.5	5.52
61.5	3.14	63.4	3.61	63.4	4.08	63.4	4.17	63.4	4.50	63.4	5.44
63.5	3.07	65.4	3.56	65.4	3.99	65.3	4.11	65.4	4.42	65.5	5.36
65.4	3.01	67.4	3.50	67.5	3.91	67.5	4.04	67.5	4.32	67.4	5.27
67.4	2.95	69.4	3.44	69.3	3.86	69.3	3.97	69.5	4.26	69.4	5.19
69.4	2.90	71.5	3.38	71.4	3.75	71.5	3.87	71.3	4.14	71.4	5.10
71.3	2.87	73.3	3.34	73.5	3.69	73.4	3.80	73.5	4.08	73.3	5.00
73.4	2.76	75.5	3.26	75.4	3.61	75.3	3.70	75.3	3.97	75.3	4.90
75.4	2.77	77.4	3.21	77.4	3.56	77.4	3.66	77.4	3.91	77.4	4.80
77.6	2.68	79.3	3.13	79.4	3.50	79.4	3.58	79.4	3.83	79.3	4.71

Table D10 Temperature sweep test results at 62.8 rad/s as measured by the DMA of HNBR compounds filled with various CB hybrid systems and hybrid ratios (cont.): (b) Loss modulus (G″)

0/100		20/80		40/60		60/40		80/20		100/0	
Temp.(°C)	G″ (MPa)	Temp.(°C)	G″ (MPa)	Temp.(°C)	G″ (MPa)	Temp.(°C)	G″ (MPa)	Temp.(°C)	G″ (MPa)	Temp.(°C)	G″ (MPa)
79.5	2.64	81.4	3.09	81.3	3.43	81.4	3.52	81.4	3.75	81.3	4.59
81.4	2.61	83.6	3.03	83.6	3.36	83.5	3.44	83.5	3.67	83.4	4.50
83.5	2.57	85.4	2.96	85.3	3.31	85.4	3.38	85.4	3.62	85.4	4.40
85.4	2.53	87.3	2.91	87.4	3.24	87.5	3.32	87.3	3.53	87.7	4.34
87.5	2.45	89.4	2.84	89.5	3.18	89.5	3.27	89.3	3.50	89.4	4.21
89.4	2.45	91.4	2.81	91.4	3.14	91.3	3.22	91.4	3.40	91.6	4.06
91.6	2.44	93.4	2.77	93.3	3.09	93.4	3.18	93.4	3.34	93.4	3.97
93.3	2.40	95.4	2.71	95.4	3.05	95.3	3.09	95.4	3.30	95.6	3.87
95.4	2.35	97.4	2.66	97.3	2.98	97.3	3.05	97.4	3.25	97.4	3.77
97.4	2.31	99.5	2.60	99.3	2.97	99.5	3.03	99.5	3.19	99.3	3.72
99.4	2.30	101.6	2.58	101.4	2.90	101.5	2.96	101.3	3.08	101.6	3.63
101.4	2.25	103.4	2.54	103.6	2.87	103.6	2.90	103.4	3.09	103.7	3.57
103.5	2.24	105.5	2.50	105.5	2.84	105.3	2.85	105.5	3.01	105.2	3.50
105.4	2.22	107.5	2.46	107.2	2.78	107.6	2.82	107.3	3.00	107.4	3.44
107.6	2.18	63.4	2.43	63.4	2.73	63.4	2.79	63.4	2.95	63.4	3.39
109.5	2.15	109.4	2.41	109.2	2.72	109.4	2.75	109.5	2.89	109.4	3.32
111.4	2.14	111.6	2.37	111.4	2.68	111.4	2.69	111.4	2.85	111.3	3.25
113.3	2.09	113.5	2.35	113.3	2.66	113.4	2.67	113.5	2.82	113.7	3.16
115.5	2.07	115.4	2.31	115.3	2.62	115.1	2.64	115.4	2.76	115.3	3.12
117.4	2.04	117.5	2.30	117.4	2.57	117.5	2.60	117.7	2.73	117.3	3.06
119.2	2.03	119.5	2.28	119.7	2.52	119.3	2.53	119.6	2.67	119.4	3.00
121.3	2.00	121.4	2.22	121.5	2.49	121.6	2.50	121.3	2.66	121.2	2.94
123.4	1.96	123.4	2.19	123.5	2.43	123.5	2.44	123.4	2.58	123.1	2.88
125.4	1.93	125.5	2.16	125.2	2.42	125.2	2.42	125.6	2.51	125.4	2.86
127.6	1.91	127.5	2.14	127.3	2.39	127.4	2.39	127.3	2.50	127.5	2.82
129.4	1.89	129.4	2.10	129.3	2.34	129.5	2.34	129.6	2.43	129.5	2.77
131.3	1.86	131.3	2.07	131.4	2.31	131.3	2.32	131.4	2.43	131.4	2.71
133.3	1.82	133.5	2.07	133.5	2.26	133.4	2.28	133.2	2.37	133.6	2.69
135.4	1.82	135.4	2.02	135.3	2.24	135.2	2.25	135.5	2.32	135.5	2.64
137.4	1.78	137.4	2.00	137.4	2.21	137.3	2.21	137.4	2.30	137.3	2.60
139.4	1.76	139.4	2.00	139.4	2.18	139.3	2.19	139.5	2.29	139.4	2.55
141.5	1.75	141.4	1.95	141.4	2.16	141.6	2.16	141.3	2.23	141.3	2.50
143.4	1.73	143.4	1.96	143.6	2.13	143.3	2.13	143.6	2.20	143.3	2.47
145.4	1.70	145.5	1.91	145.3	2.12	145.2	2.11	145.3	2.17	145.6	2.43
147.6	1.69	147.6	1.88	147.6	2.09	147.5	2.06	147.2	2.16	147.4	2.39
149.5	1.68	149.5	1.85	149.1	2.04	149.3	2.05	149.3	2.14	149.0	2.36

Table D10 Temperature sweep test results at 62.8 rad/s as measured by the DMA of HNBR compounds filled with various CB hybrid systems and hybrid ratios (cont.): (b) Loss modulus (G″)

3) N550/N990

0/100		20/80		40/60		60/40		80/20		100/0	
Temp.(°C)	G″ (MPa)	Temp.(°C)	G″ (MPa)	Temp.(°C)	G″ (MPa)	Temp.(°C)	G″ (MPa)	Temp.(°C)	G″ (MPa)	Temp.(°C)	G″ (MPa)
-79.2	177.06	-80.9	138.57	-80.7	130.05	-81.2	156.50	-79.7	184.42	-79.2	186.31
-77.2	173.02	-78.3	137.52	-78.3	129.38	-78.3	157.21	-77.5	175.72	-77.4	181.59
-74.2	167.33	-76.7	138.55	-77.0	128.59	-75.1	152.25	-74.5	172.52	-76.2	184.45
-71.1	161.60	-75.1	135.46	-73.0	123.20	-73.1	152.69	-70.8	165.24	-72.8	176.29
-67.6	157.99	-73.7	136.46	-69.7	120.22	-71.9	151.83	-69.0	165.28	-71.6	177.13
-65.3	154.67	-71.1	133.54	-67.9	116.90	-70.4	149.94	-67.8	167.45	-68.6	171.57
-62.8	150.21	-68.9	129.75	-66.7	114.70	-68.9	148.16	-66.9	166.46	-65.9	166.21
-59.8	145.53	-67.4	127.84	-65.8	112.51	-67.6	148.06	-66.2	166.31	-62.6	162.11
-56.5	138.83	-65.5	125.17	-64.4	111.62	-65.7	145.88	-64.5	163.89	-61.1	163.04
-53.3	132.30	-63.0	120.26	-62.4	109.18	-63.4	143.42	-63.0	165.32	-59.9	162.66
-50.1	127.16	-60.8	118.21	-61.1	107.84	-60.8	139.62	-60.8	164.65	-59.0	163.32
-48.3	129.42	-58.8	113.99	-59.2	104.29	-59.1	137.80	-59.4	163.29	-58.0	161.19
-46.7	122.90	-56.9	111.02	-57.6	102.66	-56.9	136.94	-56.8	162.09	-56.5	162.43
-45.7	124.36	-55.1	108.01	-55.3	98.75	-54.7	135.73	-55.2	162.25	-55.0	161.43
-44.9	125.25	-53.2	105.63	-53.1	95.12	-52.9	133.64	-53.1	160.90	-53.0	160.28
-44.1	125.47	-50.9	104.38	-50.2	93.68	-51.2	132.18	-51.0	158.76	-51.1	158.97
-43.2	126.43	-49.0	102.70	-48.5	92.44	-48.8	130.29	-48.8	157.04	-49.0	157.57
-41.9	129.10	-47.0	102.76	-46.8	92.58	-46.9	130.21	-47.0	155.08	-47.2	158.02
-40.7	133.19	-44.8	104.20	-45.7	93.60	-44.8	131.34	-45.0	155.48	-44.9	158.09
-39.6	137.77	-43.1	108.58	-43.3	96.15	-42.8	134.44	-43.0	157.45	-42.8	160.05
-38.3	147.12	-40.8	116.21	-41.2	102.38	-40.9	139.83	-40.8	161.54	-40.9	163.04
-36.9	161.00	-39.1	128.97	-39.1	114.21	-38.7	151.83	-38.8	172.48	-38.8	169.45
-35.6	180.12	-36.9	150.12	-37.1	129.62	-36.9	171.73	-37.1	187.54	-36.8	182.12
-34.7	203.54	-34.8	188.43	-35.3	165.76	-34.5	213.36	-34.7	217.85	-34.8	202.78
-32.9	258.38	-32.8	247.95	-32.9	229.16	-32.8	267.10	-32.8	267.61	-32.0	267.85
-30.7	353.04	-30.5	337.42	-30.7	324.28	-30.9	354.53	-30.4	364.83	-30.7	342.50
-28.7	449.66	-28.6	414.53	-29.1	418.32	-28.7	446.42	-28.5	438.12	-27.9	444.93
-26.6	501.03	-26.8	463.02	-26.1	469.64	-26.4	497.55	-26.6	483.43	-26.8	489.36
-24.7	474.63	-24.6	453.29	-24.6	435.45	-24.6	482.91	-24.6	481.07	-24.4	497.41
-22.7	393.20	-22.6	378.10	-22.1	319.18	-22.7	401.82	-22.6	418.08	-22.5	443.13
-20.7	288.19	-20.7	286.79	-20.2	238.20	-20.6	263.78	-20.7	324.57	-20.6	355.85
-18.6	195.42	-18.6	191.31	-18.9	175.10	-18.6	177.55	-18.7	231.52	-18.6	264.87
-16.8	129.90	-16.7	126.86	-16.4	112.64	-16.6	131.00	-16.7	162.29	-16.7	193.41
-14.5	82.27	-14.6	82.03	-14.7	83.41	-14.6	97.19	-14.7	112.05	-14.7	140.28
-12.7	57.56	-12.6	55.73	-12.7	60.35	-12.6	68.43	-12.5	78.11	-12.6	101.03
-10.6	41.74	-10.7	39.26	-10.6	42.20	-10.7	48.20	-10.7	56.55	-10.6	71.14
-8.7	30.00	-8.6	28.25	-8.5	30.05	-8.5	33.71	-8.6	38.98	-8.5	51.76
-6.7	21.15	-6.7	21.29	-6.6	21.49	-6.5	24.08	-6.7	29.13	-6.7	39.37
-4.6	15.26	-4.7	15.49	-4.5	17.18	-4.7	18.60	-4.6	22.29	-4.6	30.12

Table D10 Temperature sweep test results at 62.8 rad/s as measured by the DMA of HNBR compounds filled with various CB hybrid systems and hybrid ratios (cont.): (b) Loss modulus (G″)

0/100		20/80		40/60		60/40		80/20		100/0	0/100
Temp.(°C)	G″ (MPa)	Temp.(°C)	G″ (MPa)	Temp.(°C)	G″ (MPa)	Temp.(°C)	G″ (MPa)	Temp.(°C)	G″ (MPa)	Temp.(°C)	G″ (MPa)
-2.6	11.42	-2.8	11.69	-2.7	13.72	-2.6	14.30	-2.6	17.47	-2.7	24.14
-0.6	8.88	-0.6	8.76	-0.9	11.20	-0.6	11.44	-0.5	13.54	-1.0	19.46
4.7	7.01	5.3	6.36	5.1	8.23	5.6	8.77	4.0	10.97	3.5	15.06
4.8	6.01	5.0	5.72	4.8	7.18	5.4	7.71	4.2	10.01	3.9	13.90
4.7	5.66	4.8	5.54	4.6	6.89	5.0	7.46	5.1	9.16	5.3	12.25
7.3	4.91	7.3	4.69	7.3	5.86	7.3	6.60	7.3	8.14	7.3	10.93
9.4	4.26	9.4	4.14	9.5	5.17	9.5	5.83	9.5	7.13	9.5	9.61
11.4	3.78	11.4	3.70	11.4	4.68	11.4	5.25	11.5	6.38	11.5	8.62
13.4	3.40	13.4	3.32	13.3	4.27	13.4	4.68	13.3	5.81	13.5	7.92
15.3	3.10	15.5	3.02	15.3	3.91	15.4	4.28	15.5	5.25	15.3	7.50
17.4	2.88	17.4	2.83	17.4	3.65	17.3	3.99	17.5	4.94	17.4	7.01
19.4	2.69	19.4	2.64	19.4	3.44	19.4	3.75	19.4	4.64	19.6	6.65
21.4	2.56	21.5	2.52	21.5	3.31	21.4	3.59	21.6	4.40	21.2	6.40
23.8	2.46	23.6	2.45	23.5	3.21	23.6	3.45	23.7	4.24	23.5	6.08
25.4	2.40	25.7	2.39	25.4	3.10	25.5	3.33	25.4	4.15	25.4	5.80
27.4	2.33	27.3	2.34	27.4	3.03	27.3	3.25	27.4	4.07	27.4	5.61
29.3	2.29	29.4	2.29	29.4	2.97	29.7	3.16	29.7	3.97	29.3	5.44
31.1	2.27	31.2	2.26	31.6	2.93	31.3	3.15	30.9	3.90	31.4	5.29
33.4	2.24	33.3	2.24	33.3	2.91	33.6	3.09	33.5	3.81	33.2	5.16
35.4	2.20	35.5	2.18	35.4	2.87	35.4	3.06	35.5	3.78	35.3	5.03
37.3	2.14	37.5	2.18	37.4	2.84	37.4	3.03	37.5	3.68	37.3	4.92
39.4	2.11	39.5	2.12	39.4	2.79	39.5	2.98	39.4	3.63	39.4	4.83
41.4	2.08	41.4	2.09	41.4	2.72	41.5	2.92	41.5	3.56	41.4	4.76
43.4	2.05	43.6	2.06	43.5	2.69	43.5	2.87	43.4	3.50	43.5	4.69
45.4	2.01	45.5	2.05	45.4	2.67	45.4	2.84	45.3	3.44	45.4	4.60
47.2	2.00	47.4	2.02	47.3	2.63	47.2	2.78	47.4	3.40	47.4	4.55
49.2	1.98	49.4	2.00	49.5	2.60	49.3	2.76	49.4	3.34	49.4	4.46
51.4	1.95	51.4	1.98	51.4	2.54	51.5	2.71	51.5	3.30	51.3	4.41
53.1	1.91	53.3	1.97	53.6	2.52	53.5	2.69	53.6	3.24	53.5	4.36
55.2	1.90	55.3	1.94	55.4	2.49	55.6	2.65	55.4	3.19	55.4	4.25
57.4	1.87	57.5	1.91	57.3	2.44	57.3	2.60	57.5	3.15	57.3	4.19
59.0	1.84	59.4	1.87	59.1	2.42	59.3	2.59	59.4	3.12	59.3	4.13
61.3	1.81	61.2	1.86	61.3	2.38	61.3	2.53	61.1	3.08	61.4	4.08
63.0	1.80	63.4	1.84	63.8	2.35	63.1	2.51	63.2	3.04	63.3	4.00
65.7	1.78	65.4	1.80	65.3	2.31	65.3	2.45	65.2	2.99	65.2	3.93
67.4	1.75	67.2	1.79	67.2	2.27	67.5	2.42	67.6	2.95	67.1	3.87
69.1	1.72	69.2	1.75	69.6	2.22	69.3	2.38	69.4	2.91	69.3	3.78
71.6	1.69	71.5	1.73	71.0	2.18	71.5	2.34	71.3	2.86	71.6	3.69
74.1	1.67	73.5	1.69	73.5	2.17	73.6	2.31	73.4	2.80	73.5	3.62
74.6	1.64	75.5	1.67	75.4	2.13	75.3	2.26	75.3	2.76	75.3	3.54
78.0	1.59	77.5	1.64	77.3	2.06	77.4	2.23	77.2	2.70	77.2	3.48

Table D10 Temperature sweep test results at 62.8 rad/s as measured by the DMA of HNBR compounds filled with various CB hybrid systems and hybrid ratios (cont.): (b) Loss modulus (G″)

0/100		20/80		40/60		60/40		80/20		100/0	
Temp.(°C)	G″ (MPa)	Temp.(°C)	G″ (MPa)	Temp.(°C)	G″ (MPa)	Temp.(°C)	G″ (MPa)	Temp.(°C)	G″ (MPa)	Temp.(°C)	G″ (MPa)
79.3	1.59	79.6	1.59	79.0	2.04	79.6	2.19	79.4	2.65	79.4	3.42
81.7	1.56	81.4	1.59	80.9	2.02	81.6	2.13	81.6	2.60	81.3	3.34
84.2	1.53	83.3	1.54	83.7	1.96	83.5	2.13	83.6	2.54	83.3	3.32
85.3	1.51	85.3	1.52	84.9	1.94	85.5	2.08	85.2	2.49	85.2	3.24
87.6	1.47	87.1	1.52	87.3	1.92	87.7	2.04	87.2	2.45	87.4	3.19
89.3	1.43	89.4	1.46	89.5	1.87	89.4	2.02	89.4	2.40	89.5	3.15
92.4	1.41	91.7	1.46	91.6	1.84	91.6	1.97	91.6	2.37	91.3	3.08
93.6	1.36	93.4	1.42	93.6	1.82	93.6	1.96	93.6	2.34	93.2	3.05
95.1	1.36	95.2	1.41	95.4	1.80	95.6	1.90	95.4	2.31	95.1	3.01
97.4	1.34	97.4	1.39	97.4	1.78	97.6	1.89	97.3	2.29	97.3	2.96
100.0	1.31	99.2	1.38	99.0	1.79	99.9	1.85	99.4	2.25	99.2	2.93
101.2	1.31	101.1	1.34	101.4	1.72	101.3	1.83	101.4	2.22	101.4	2.86
103.1	1.30	103.1	1.36	103.1	1.74	103.6	1.82	103.4	2.18	103.4	2.83
105.9	1.26	105.4	1.31	105.3	1.70	105.2	1.80	105.1	2.16	105.2	2.80
107.1	1.23	107.3	1.33	107.5	1.68	107.1	1.76	107.4	2.14	107.2	2.77
109.3	11.34	109.6	10.89	109.2	13.23	109.6	13.77	109.6	15.62	109.3	19.62
111.2	11.30	111.4	10.84	111.3	13.17	111.2	13.73	111.5	15.52	111.6	19.46
113.0	11.27	113.3	10.82	113.2	13.13	113.4	13.68	113.5	15.45	113.4	19.32
115.9	11.24	115.4	10.79	115.4	13.05	115.2	13.63	115.3	15.37	115.5	19.17
117.8	11.20	117.3	10.74	117.6	13.03	117.2	13.57	117.2	15.29	117.2	19.04
119.8	11.17	119.7	10.70	119.2	12.98	119.1	13.51	119.2	15.20	119.1	18.91
121.7	11.16	121.0	10.71	121.3	12.90	121.1	13.47	121.5	15.15	121.3	18.79
123.4	11.14	123.0	10.66	123.6	12.87	123.8	13.40	123.3	15.05	123.4	18.68
125.5	11.11	124.9	10.63	125.6	12.84	124.9	13.36	125.0	15.01	125.8	18.60
127.6	11.09	127.4	10.64	127.7	12.81	127.6	13.33	127.4	14.94	127.6	18.45
129.5	11.08	129.6	10.59	129.8	12.73	129.7	13.30	129.5	14.87	129.2	18.37
131.6	11.06	131.1	10.59	131.9	12.71	131.4	13.24	131.3	14.81	131.2	18.28
133.0	11.03	133.5	10.55	133.4	12.69	133.3	13.20	133.2	14.77	133.3	18.20
135.4	11.03	135.3	10.55	135.4	12.66	135.2	13.13	135.5	14.72	135.5	18.06
137.2	11.02	137.4	10.50	137.2	12.63	137.5	13.13	137.8	14.65	137.2	18.01
138.9	10.99	139.5	10.52	139.3	12.60	139.1	13.09	139.4	14.60	139.4	17.90
141.2	11.00	141.5	10.50	141.1	12.57	140.9	13.05	141.4	14.55	141.1	17.82
143.7	10.99	143.4	10.48	143.9	12.53	143.1	13.02	143.6	14.49	143.1	17.75
145.8	10.97	145.4	10.44	145.4	12.49	145.0	13.00	145.6	14.45	145.3	17.68
147.7	10.98	147.2	10.43	147.5	12.49	147.6	12.96	147.3	14.40	147.1	17.59
149.2	10.96	149.6	10.42	149.3	12.42	149.1	12.93	148.9	14.36	149.0	17.53

Table D11 Mechanical properties of HNBR compounds filled with various CB hybrid systems and hybrid ratios

CB hybrid system	CB hybrid ratio	M100 (MPa)	Tensile strength (MPa)	Elongation at break (%)
N326/N990	0/100	9.33 ± 0.19	16.54 ± 0.56	177.01 ± 11.25
	20/80	9.54 ± 0.35	19.10 ± 0.16	181.57 ± 1.98
	40/60	9.36 ± 0.03	20.43 ± 0.66	179.21 ± 8.86
	60/40	9.54 ± 0.15	23.10 ± 0.46	207.46 ± 5.34
	80/20	10.11 ± 0.31	23.68 ± 0.19	195.33 ± 3.54
	100/0	11.81 ± 0.45	23.54 ± 0.52	195.42 ± 5.42
N326/N990	0/100	13.72 ± 0.81	17.79 ± 1.27	125.82 ± 1.77
	20/80	13.77 ± 0.61	20.58 ± 0.45	135.38 ± 5.91
	40/60	12.57 ± 0.64	20.73 ± 0.14	136.85 ± 8.92
	60/40	12.62 ± 1.17	20.57 ± 0.62	127.05 ± 7.60
	80/20	12.72 ± 0.03	22.91 ± 0.10	122.53 ± 4.32
	100/0	11.81 ± 0.45	23.54 ± 0.52	153.85 ± 14.07
N326/N990	0/100	9.33 ± 0.19	16.54 ± 0.56	177.01 ± 11.25
	20/80	10.64 ± 0.28	19.70 ± 0.27	183.18 ± 5.21
	40/60	11.18 ± 0.40	19.22 ± 0.90	161.99 ± 6.21
	60/40	12.48 ± 0.33	20.87 ± 0.27	159.84 ± 7.03
	80/20	13.35 ± 0.09	19.40 ± 1.32	135.66 ± 8.00
	100/0	13.94 ± 0.72	19.74 ± 0.52	132.66 ± 7.15

Table D11 Mechanical properties of HNBR compounds filled with various CB characteristics and loadings (cont.)

CB hybrid system	CB hybrid ratio	Tear strength (N/mm)	Hardness (Shore A)	Abrasion loss (mm^3)
N326/N990	0/100	43.82 ± 1.27	75.8 ± 0.408	78.27 ± 1.889
	20/80	48.31 ± 0.98	77.0 ± 0.000	78.19 ± 0.530
	40/60	51.44 ± 2.26	78.4 ± 0.289	75.83 ± 1.334
	60/40	54.91 ± 0.53	80.6 ± 0.500	76.10 ± 1.968
	80/20	55.89 ± 1.31	81.4 ± 0.000	78.55 ± 0.731
	100/0	59.82 ± 1.77	83.1 ± 0.656	81.00 ± 2.172
N326/N990	0/100	49.62 ± 0.80	80.0 ± 0.408	86.77 ± 2.547
	20/80	50.60 ± 0.91	80.5 ± 0.000	83.18 ± 4.481
	40/60	45.65 ± 0.89	81.8 ± 0.289	87.02 ± 3.439
	60/40	50.56 ± 0.78	81.8 ± 0.500	87.97 ± 2.844
	80/20	51.40 ± 1.96	83.5 ± 0.000	96.01 ± 4.212
	100/0	59.82 ± 1.77	83.1 ± 0.656	81.00 ± 2.172
N326/N990	0/100	43.82 ± 1.27	75.8 ± 0.100	78.27 ± 1.889
	20/80	46.68 ± 4.11	74.8 ± 0.551	65.84 ± 0.921
	40/60	49.72 ± 1.14	77.6 ± 0.115	63.04 ± 1.342
	60/40	50.28 ± 0.71	79.9 ± 0.115	60.03 ± 0.624
	80/20	45.66 ± 2.01	81.6 ± 0.153	62.60 ± 0.771
	100/0	52.04 ± 4.61	83.2 ± 0.503	59.62 ± 1.633

APPENDIX E

CORRELATION BETWEEN VISCOELASTIC BEHAVIOUR AND HEAT BUILD-UP OF CARBON BLACK FILLED HYDROGENATED NITRILE RUBBER VULCANISATES

Table E1 Loss modulus (G'') and damping factor (tanδ) results at test strain, temperature and frequency of 2%, 100°C and 1 rad/s, respectively as measured by the RPA2000 of HNBR compounds filled with various CB characteristics and loadings

CB type	CB loading (phr)	G″ (kPa)	tanδ
N326	20	94.14	0.071
	40	156.54	0.092
	60	279.54	0.116
N550	20	102.90	0.074
	40	179.95	0.092
	60	311.72	0.117
N774	20	99.40	0.071
	40	143.38	0.085
	60	197.42	0.100
N990	20	72.98	0.059
	40	88.17	0.060
	60	128.05	0.077

Table E2 Heat build-up (HBU) results as measured by the Gabometer4000 and the RPA2000 of HNBR compounds filled with various CB characteristics and loadings

CB type	CB loading (phr)	Gabometer 4000 HBU	RPA2000 HBU
N326	20	29.2	7.2
	40	39.0	11.2
	60	44.4	16.5
N550	20	27.8	5.8
	40	45.0	11.3
	60	48.1	18.4

Table E2 Heat build-up (HBU) results as measured by the Gabometer4000 and the RPA2000 of HNBR compounds filled with various CB characteristics and loadings (cont.)

CB type	CB loading (phr)	Gabometer 4000 HBU	RPA2000 HBU
N774	20	27.4	7.1
	40	35.4	8.6
	60	44.5	15.5
N990	20	22.9	6.4
	40	27.2	6.0
	60	31.7	15.2

APPENDIX F

PUBLICATION

CURE AND VISCOELASTIC PROPERTIES OF HNBR

ELASTOMERE UND KUNSTSTOFFE
ELASTOMERS AND PLASTICS

Reinforcement · Viscoelastic properties · Carbon black · Dynamic mechanical properties · Hydrogenated acrylonitrile butadiene rubber

Cure, viscoelastic and mechanical properties of HNBR filled with various types of carbon black were investigated. By increasing carbon black loading and specific surface area, cure promotion was observed which could be explained by a combination of thermal history, surface chemistry and thermal conductivity. Viscoelastic behaviour of both uncured and cured specimens filled with carbon black exhibits a strain-dependent behaviour. Storage modulus (G') and damping factor (tanδ) significantly increase with increasing carbon black loading and/or specific surface area. Mechanical properties are found to be governed by combined effects of hydrodynamic effect, filler transient network, molecular slippage and crosslink density, associated probably with black dispersion particularly at high black loading. The overall results imply a close correlation of viscoelastic and mechanical properties via energy dissipation process (or hysteretic process) caused by molecular slippage.

Vernetzung und viskoelastische Eigenschaften von HNBR: Einfluss von Ruß

Verstärkung · viskoelastische Eigenschaften · Ruß · dynamisch-mechanische Eigenschaften · hydrierter Acrylnitril-Butadien Kautschuk

Das Vernetzungsverhalten und mechanische Eigenschaften von rußgefülltem HNBR wurden untersucht. Durch die Erhöhung der Dosierung sowie der spezifischen Oberfläche des Rußes wurde eine Verkürzung der Heizzeit hervorgerufen, die der thermischen Vorgeschichte, der Oberflächenchemie und der thermischen Leitfähigkeit zugeordnet wird. Die viskoelastischen Eigenschaften sowohl der nichtvernetzten als auch der vernetzten Proben zeigen eine ausgeprägte Amplitudenabhängigkeit. Der Speichermodul (G') und der Dämpfungsfaktor (tanδ) steigen signifikant mit der Dosierung und der spezifischen Oberfläche der Ruße an. Es wird gezeigt, dass die mechanischen Eigenschaften der Vulkanisate von der Rußdispersion beeinflusst werden und eine Korrelation zwischen viskoelastischen und mechanischen Eigenschaften besteht, die durch dissipatorische Prozesse erklärt wird.

Cure and Viscoelastic Properties of HNBR

Effects of Carbon Black Loading and Characteristics

Hydrogenated acrylonitrile butadiene rubber (HNBR), as a synthetic rubber produced by the hydrogenation reaction of nitrile rubber (NBR), possesses excellent oil and thermal resistance. Typically, HNBR has widely been employed in automotive and industrial applications [1, 2]. HNBR is known to be curable with either peroxide or sulfur/sulfur-donor cure systems, depending on its degree of unsaturation on the backbone as well as on product properties required. Laboratory comparisons of sulfur/sulfur-donor and peroxide cured HNBR compounds reveal that the peroxide vulcanisation provides superior compression set and heat resistance [1]. Although HNBR offers relatively good mechanical properties due to its highly saturated structure facilitating the molecular packing, an incorporation of filler into HNBR is still necessary for further enhancing mechanical and dynamic properties and well as performance per cost of the final products [3, 4]. The reinforcement performance of filler has been reported to depend typically on filler characteristics including specific surface area, surface chemistry and structure (or degree of aggregation) [5-7]. In general, the greater loading of reinforcing filler will result in the higher hardness and modulus [8-11]. Simultaneously, property improvement and processability are found to reach its maxima at certain filler loading relying on the mixing efficiency for filler dispersion and distribution (i.e., state-of-mix) [2]. There are numerous works on enhancement in mechanical properties of HNBR vulcanisates by reinforcing fillers including carbon black [12-14], silica [13-15], carbon nanotubes [14-17] and organoclay [18-20]. Nonetheless, published work on viscoelastic properties of carbon black filled HNBR is still limited. It is reported that storage modulus (G') increases and damping factor peak ($\tan\delta_{max}$) decreases with carbon black loading which is attributed to the changes in occluded rubber, bound rubber and shell rubber [21, 22]. By increasing carbon black specific surface area, the tanδ appears to decrease in the transition zone and then increase in the plateau zone (rubber plateau). The magnitude of G' enhancement is more obvious with increasing specific surface area of carbon black. However, the comparison of viscoelastic properties between uncured and cured HNBR filled with carbon black has not yet been reported. Therefore, the present work aims to investigate viscoelastic behaviour and mechanical properties of HNBR filled with carbon black having different specific surface areas and structures.

Experimental

Materials

Raw HNBR (Therban VP KA 8837) having acrylonitrile and unsaturation contents of 34 % and 18 %, respectively, used in this study was supplied by Lanxess Co., Ltd. (Bangkok, Thailand). Four grades of carbon blacks (CBs) (i.e., N326, N550, N774 and N990) were supplied by Loxley Public Co., Ltd. (Bangkok, Thailand) and Siam Luck Trading Co., Ltd. (Bangkok, Thailand). The characteristics are given in Table 1. [23]. Tri-2-ethylhexyl trimellitate (TOTM) as plasticizer was purchased from Behn Meyer Chemical (Thailand) Co., Ltd. (Bangkok Thailand). Dicumyl peroxide or DCP (98 % active) as curing agent was supplied by Petchthai Chemical Co., Ltd (Bangkok, Thailand).

Authors

P. Wongwitthayakool, C. Sirisinha, Bangkok (Thailand), P. Saeoui, Pathumthani (Thailand)

Corresponding author:
Chakrit Sirisinha
Mahidol University
Salaya Campus
RDCTRI , Faculty of Science
Phutthamonthon 4 Rd
Salaya, Nakhon Pathom, 73170,
Thailand
Tel: +662/441/0511
Fax: +662/441/9816
E-mail: sccsr@mahidol.ac.th

Sample Preparation

Mixing was performed on a laboratory size two roll mill (LabTech Co., Ltd., Bangkok, Thailand) at set temperature of 40 °C. HNBR and compounding ingredients as shown in Table 2 were mixed for 20 minutes. HNBR vulcanisate sheets were prepared using a hot-press at a temperature of 145 °C under moulding pressure of 150 kg/cm^2 for 120 minutes.

Test procedures

Cure characteristics Cure characteristics were monitored at 145°C using the Rubber Process Analyser (RPA2000, Alpha Technologies, USA) with test frequency and strain of 6.28 rad/s and 15 %, respectively. Scorch time (t_{s2}) was determined from time to achieve torque rise of 2 units above the minimum torque. Cure time used in the present work was the time to reach 90 % complete cure state (t_{c90}). Torque difference between the maximum and minimum storage torques ($\Delta S'$) was used as an indication of crosslink density [24].

Viscoelastic properties Rubber Process Analyser (RPA2000, Alpha Technologies, USA) was used for viscoelastic behaviour measurement of HNBR compounds and vulcanisates. Strain sweep test was performed at test temperatures of 100 °C and 60 °C for measuring dynamic properties of uncured and cured HNBR, respectively.

Mechanical properties The universal tensile tester (Instron model 5566, USA) was used for measuring the tensile properties as per ASTM D412-98 at a crosshead speed of 500 mm/min [25]. Test specimens for tensile were punched out from the moulded sheets using ASTM die C. Hardness test was performed on 6-mm-thick specimen using with a hardness durometer (Wallace H177A, UK) at room temperature as per ASTM D2240-97 [26]. Abrasion resistance of HNBR vulcanisates was measured using the DIN-type abrasion tester (Zwick model 6120, Germany) in accordance with DIN 53516 [27].

Result and Discussion

Cure characteristics

Results of scorch time (t_{s2}), time for 90 % of cure completion (t_{c90}) and the difference between the maximum and minimum torques ($\Delta S'$) -an indication of crosslink density [24]- are presented in Table 3. It becomes evident that both the scorch time (t_{s2}) and the cure time (t_{c90}) decrease while torque difference increases as a function of CB loading. These results imply clearly a cure promotion phenomenon by the incorporation of CB. The explanations are postulated by: (i) the thermal history, (ii) the alkalinity of CB and (iii) the high thermal conductivity of CB.

It has been known that, as filler loading increases, bulk viscosity increases with the magnitude depending on filler specific surface area and filler-rubber interaction. This would lead to a rise in bulk temperature via shear heating and thus to an influence on the thermal history applied to the rubber bulk. By this means, the high magnitude of thermal history experienced in compound leads to an acceleration of curative dissociation in compounds and eventually in formation of crosslink precursors.

Regarding the pH of CB surfaces it is known that to some degree alkalinity is present and can promote the functioning of curatives [28]. In terms of thermal conductivity effect, compared with raw rubber, carbon black as solid particles possesses much higher thermal conductivity (0.1-0.6 W/mK for rubber [29] and ~2 W/mK for CB [30]) which helps transferring heat from mould surface to rubber, if a three-dimensional filler network is formed.

However, it is evident that, at any given carbon black loading, the specific surface area of carbon black affects cure behaviour to some extent, but with the lower magnitude than the carbon black loading. Exceptionally, the crosslink density appears to be highest in HNBR with CB N550 [31]. It is proposed that the tightly bound rubber in CB N550 with more developed structure obstructs curative absorption on carbon black surfaces, leading to the increase in free curatives migrating to the free rubber matrix a migration of, and the crosslinking reaction in rubber bulk is thus promoted [31].

1 Carbon black properties [23]

Properties	N326	N550	N774	N990
Iodine Adsorption No. D 1510 (g/kg)	82	43	29	-
DBP No. D 2414 (10^{-5} m^3/kg)	72	121	72	43

2 Compounding formulation used

Chemical name	Amount (phr)
HNBR	100
Carbon black	varied: 0-60
TMQ[a]	1
Zinc Oxide (ZnO)	5
Stearic acid	1
TOTM[b]	5
Dicumyl peroxide (DCP)	2

[a] 2, 2, 4-trimethyl-1, 2-dihydroquinoline
[b] tri-2-ethylhexyl trimellitate

Viscoelastic properties

Effect of carbon black loading Uncured HNBR compounds The effect of carbon black loading on dynamic mechanical properties of uncured compounds with various carbon black loadings is shown in Figures 1 to 3. Figure 1 shows plots of G' measured at

3 Cure characteristics of HNBR and filled HNBR

Carbon black	Loading (phr)	t_{s2} (min)	t_{c90} (min)	S'max-S'min[a] (dNm)
Control	0	1.42±0.03	74.54±1.07	28.14±0.19
CB N326	10	1.30±0.03	74.73±0.37	31.57±0.72
	20	1.17±0.01	73.94±0.50	36.35±0.09
	40	1.06±0.01	71.94±0.31	42.61±0.71
	60	0.98±0.03	69.22±0.20	48.71±1.21
CB N550	10	1.21±0.15	74.06±0.76	34.02±0.18
	20	1.10±0.06	73.93±0.39	38.11±0.55
	40	0.98±0.05	72.14±0.88	49.61±0.60
	60	0.87±0.04	69.86±1.96	54.77±3.21
CB N774	10	1.33±0.03	74.25±1.42	32.32±1.91
	20	1.20±0.02	74.07±1.18	37.73±0.81
	40	1.06±0.03	72.65±1.59	43.43±2.91
	60	0.99±0.02	71.44±1.25	46.51±2.84
CB N990	10	1.21±0.15	75.23±0.06	32.54±0.80
	20	1.22±0.03	75.83±0.16	35.47±0.20
	40	1.12±0.02	75.48±0.09	41.13±0.44
	60	1.06±0.04	75.69±0.70	45.47±0.77

a = Torque difference between maximum (S'max) and minimum torques (S'min) as determined from cure curves

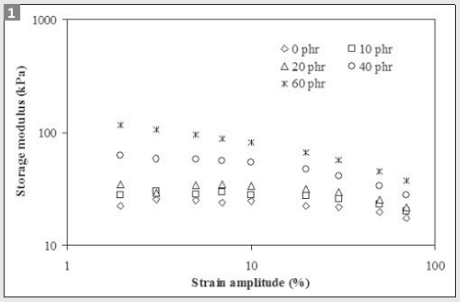

1 Storage modulus (G') as a function of strain amplitude of uncured HNBR compounds with various CB N326 loadings (measured at 1 rad/s and 100 °C)

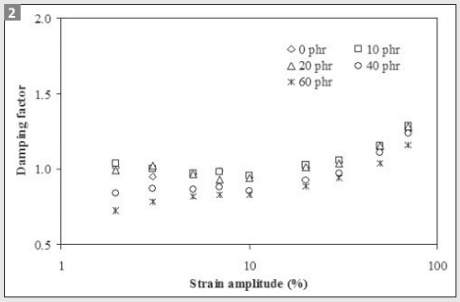

2 Damping factor (tanδ) as a function of strain amplitude of uncured HNBR compounds with various CB N326 loadings (measured at 1 rad/s and 100 °C)

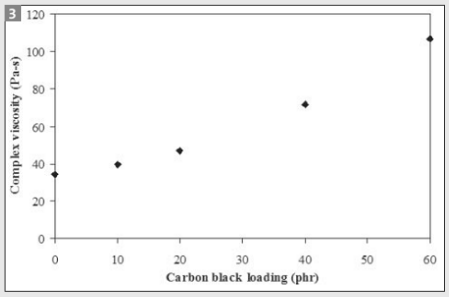

3 Complex viscosity (η^*) of uncured HNBR compounds as a function of CB N326 loading (measured at 1 rad/s, 10 % strain and 100 °C)

60 °C against strain amplitude (%) of HNBR compounds filled with different loadings of CB N326 carbon black. Clearly, at low strain, G' of unfilled compound is lowest, while the G' of filled compound with CB of 60 phr is highest. The G' of filled blend increases with increasing CB loading, which is due mainly to filler reinforcing effect, i.e., the hydrodynamic effect, the filler-filler interaction as well as the CB -HNBR interaction [32,33]. Moreover, it is evident that the compounds show relatively broad linear viscoelastic (LVE) region until the CB loading up to 20 phr, and the blends with CB loading of 40 phr show narrow LVE region. The compound with CB loading of 60 phr shows no significant LVE region. The decrease in LVE region is associated with an increase in G', indicating an increase in magnitude of filler network formation (Payne effect) [33]. At high CB loading, the magnitude of filler network is high, which would be disrupted at high shear strain. This is the reason why the LVE of highly filled blends could not be observed.

Results of damping factor (tanδ) are shown in Figure 2. It is obvious that the damping factor of all compounds increases with increasing strain amplitude. This is due to the energy dissipation through a molecular slippage associated with the breakdown of the three-dimensional filler transient network. This phenomenon is sometimes interpreted as a hysteretic process [32]. Notably, the damping factor of unfilled compounds is highest, and decreases with increasing carbon black loading particularly at low shear strain. The low values for tan δ is related to the fact that the storage modulus of the compound increases more than the loss modulus. Furthermore, the formation of three-dimensional transient filler network is responsible for the rise in elastic contribution. From another perspective, the damping behaviour of highly filled compounds at low strain could be explained by the dilution of the viscoelastic contribution of rubber matrix by as a fully elastic component

4 Mechanical properties of filled HNBR vulcanisates

Carbon black	Loading (phr)	M100 (MPa)	Tensile strength (MPa)	Elongation at break (%)	Hardness (shore A)	Abrasion loss (mm^3)
Control	0	2.16±0.05	9.48±0.21	252.98±5.54	59.6±0.2	54.43±2.97
CB N326	10	3.13±0.23	13.92±0.79	259.08±13.08	63.7±0.17	62.08±1.73
	20	3.77±0.23	16.39±0.34	250.08±8.82	68.5±0.1	64.96±1.48
	40	7.00±0.72	18.96±1.49	205.10±17.56	76.0±0.23	67.77±1.58
	60	10.13±0.11	19.30±0.34	168.20±3.01	81.7±0.46	86.16±1.18
CB N774	10	3.16±0.19	14.45±0.16	259.36±6.92	65.2±0.25	57.33±2.12
	20	4.21±0.16	16.15±0.62	227.55±3.11	69.4±0.30	58.14±1.74
	40	7.12±0.06	17.55±0.36	165.47±11.79	77.0±0.25	61.90±1.13
	60	12.00±0.83	18.04±0.86	136.27±2.57	81.9±0.42	71.66±1.11
CB N550	10	2.73±0.13	9.62±0.46	219.18±8.18	63.5±0.32	67.75±3.52
	20	4.04±0.28	15.69±0.16	232.93±7.97	68.2±0.10	68.51±4.57
	40	6.14±0.34	18.11±0.55	204.44±9.36	74.4±0.40	64.11±0.58
	60	10.08±0.70	20.92±1.11	182.79±9.96	78.7±0.46	70.99±0.75
CB N990	10	2.52±0.18	10.62±0.25	244.63±9.66	62.2±0.38	60.82±1.27
	20	3.08±0.21	11.19±0.51	220.84±10.08	64.4±0.12	67.53±1.79
	40	4.23±0.61	13.44±0.10	206.25±18.66	68.8±0.15	72.50±1.44
	60	5.48±0.28	17.35±0.31	218.73±7.94	72.8±0.55	81.84±0.67

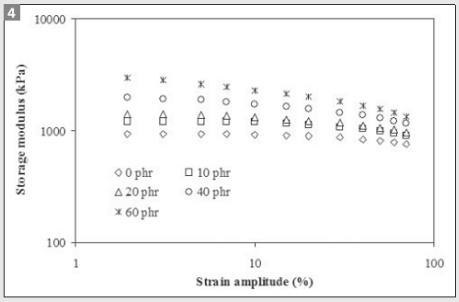

4 Storage modulus (G') as a function of strain amplitude of cured HNBR specimens (vulcanisates) with various CB N326 loadings (measured at 1 rad/s and 60 °C)

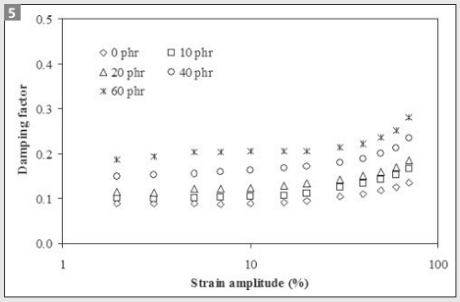

5 Damping factor (tanδ) as a function of strain amplitude of cured HNBR specimens (vulcanisates) with various CB N326 loadings (measured at 1 rad/s and 60 °C)

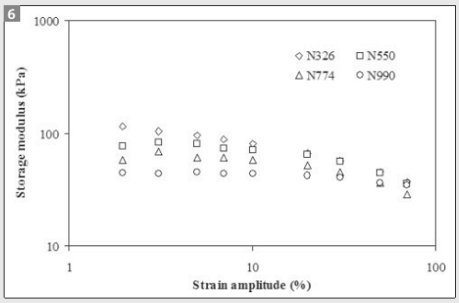

6 Storage modulus (G') as a function of strain amplitude of uncured HNBR compounds with various carbon black specific surface area (measured at 1 rad/s and 100 °C)

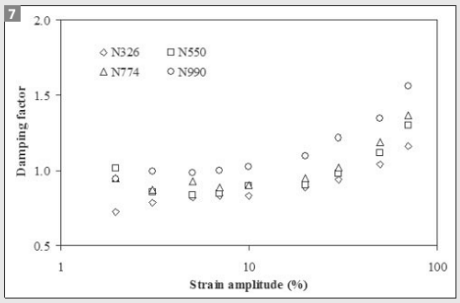

7 Damping factor (tanδ) as a function of strain amplitude of uncured HNBR compounds with various carbon black specific surface area (measured at 1 rad/s and 100 °C)

by carbon black particles having a damping factor approaching zero.

The processability of HNBR was monitored in terms of complex viscosity (η^*), as shown in Figure 3. It is obvious that η^* increases with carbon black loading which is in good agreement with the filler reinforcement effect. In other words, the processability appears to decrease due to the hydrodynamic reinforcement, i.e. (i) flow obstruction caused by solid filler particles, (ii) strong rubber-filler interactions and (iii) a formation of three-dimensional transient filler network.

Cured HNBR vulcanisates

Storage modulus (G') of cured HNBR vulcanisates with various carbon black loadings is illustrated in Figure 4. Similar to uncured compounds without filler, unfilled vulcanisates reveals broader LVE region with insignificant magnitude of strain-dependent behaviour. By contrast, filled vulcanisates show significant strain-dependent modulus which is more pronounced in highly filled vulcanisates. Such insignificant magnitude of strain dependency is caused by the presence of chemical crosslink acting as spring component with elastic contribution. Additionally, the formation of rubber network via chemical crosslink leads to a rise in elastic modulus compared with the uncured compounds at a given carbon black loading.

Results of the damping factor (tanδ) as a function of shear strain in filled HNBR vulcanisates are depicted in Figure 5. By contrast to the uncured compounds, the filled vulcanisates exhibit an increase the in damping factor with carbon black loading, especially in highly filled vulcanisates. The increased damping factor can be attributed to the molecular slippage at interfaces between rubber and carbon black particles. It is known that the rubber-carbon black interaction is dominated by the physical over chemical interactions [34], unlike rubber-silane treated silica interaction. Thus, such relatively weak interactions would allow molecular flow at rubber-carbon black interfaces, and thus the rise in dissipated energy dissipation supports the hysteretic process. The higher the carbon black loading, the higher the positions available for hysteretic processes. Also, the swing-up of the damping behavior at high strain could be explained by the disruption of the carbon black transient network [32, 33]. From the overall results, it could be summarised that the damping behaviour of carbon black filled rubber compounds and vulcanisates is governed mainly by dilution effect and interfacial molecular flow, respectively.

Effect of carbon black specific surface area (particle size)

Uncured HNBR compounds. In this part, the carbon black loading in compounds was kept constant at 60 phr in order to monitor the effects of the surface specific area on dynamic mechanical properties of uncured HNBR compounds. Figure 6 shows G' as a

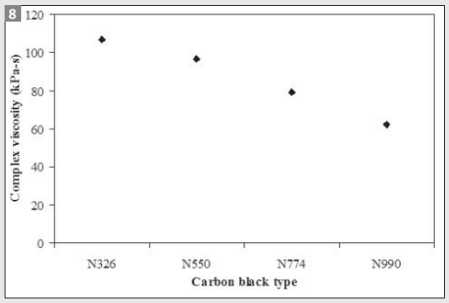

8 Complex viscosity (η*) of uncured HNBR compounds as a function of carbon black specific surface area (measured at 1 rad/s, 10 % strain and 100 °C)

function of the strain amplitude. It is evident that the strain-dependency of G' takes place in all uncured compounds with the greater magnitude found in compounds filled with carbon black having higher specific surface area. Also, at low strain amplitude, the magnitude of G' rise is more pronounced in HNBR filled with higher specific surface area (or smaller particle size) carbon black. This can be attributed mainly to the greater possibility for a formation of the filler network and the lower percolation threshold of the particles. [32].

Figure 7 illustrates results of tanδ in HNBR compounds which appear to decrease with increasing carbon black specific surface area, indicating an increase in elastic contribution. Referring to the discussion of G', the tridimensional transient filler network of carbon black which is more profound in carbon black with higher specific surface area is believed to be responsible for a rise in elastic behaviour.

Complex viscosity (η*) results as indication of processability in uncured compounds with carbon black having different specific surface areas (or particle sizes) at 100 °C are shown in Figure 8. Expectedly, the specific surface area of carbon black plays profound effect on processability of uncured HNBR compounds, i.e., η* increases with increasing specific surface area of carbon black (N326 > N550 > N774 > N990). As discussed previously, the combination of hydrodynamic effect, rubber-filler and filler-filler interactions is responsible for molecular restriction, and so an increase in bulk viscosity. The carbon black with high specific surface area (i.e., small particle size) would possess greater contacting area between rubber and carbon black, and between carbon black aggregates, leading to a decrease in molecular mobility.

Cured HNBR vulcanisates

In the case of cured HNBR filled with 60 phr carbon black having various specific surface areas, results of G' as a function of deformation strain are shown in Figure 9. The magnitude of G' rise appears to increase with increasing carbon black specific surface area, which could be explained by the greater contacting positions available for interaction between rubber and carbon black as well as between filler particles (or tridimensional transient filler network). It must be noted that, although N550 carbon black possesses smaller specific surface area than N326 carbon black, the vulcanisate with N550 shows comparable G' to that with N326. This is probably because of the high structure and crosslink density given by N550, as illustrated previously in Tables 1 and 3. Also, this phenomenon is not observed in uncured compounds, implying that such unexpected result of high G" found in specimen filled N550 must be a vulcanisation-related phenomenon.

Figure 10 shows results of tanδ of filled HNBR vulcanisates. Clearly, tanδ increases with increasing carbon black specific surface area that means the higher energy dissipation through molecular flow at carbon black surfaces, as discussed previously in carbon black loading effect.

Mechanical properties

Mechanical properties of HNBR vulcanisates as functions of carbon black loading and specific surface area are shown in Table 4. It becomes evident that the tension values at 100 % elongation (M100) of cured HNBR increases with increasing carbon black loading and/or specific surface area. There are two main factors controlling the modulus M100, namely, the crosslink density of the rubber and the effect of filler reinforcement. According to Table 3, the degree of crosslink density apparently increases with carbon black loading, and the increased crosslink density would then yield the greater resistance to deformation via covalent bonds between rubber chains. Based on the results of the viscoelastic

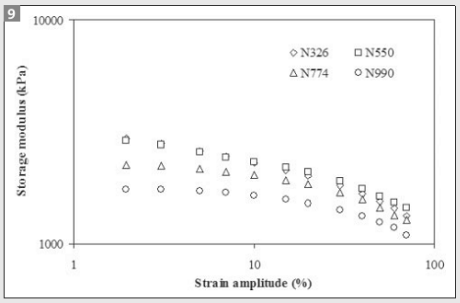

9 Storage modulus (G') as a function of strain amplitude of cured HNBR specimens (vulcanisates) with various carbon black specific surface area (measured at 1 rad/s and 60 °C)

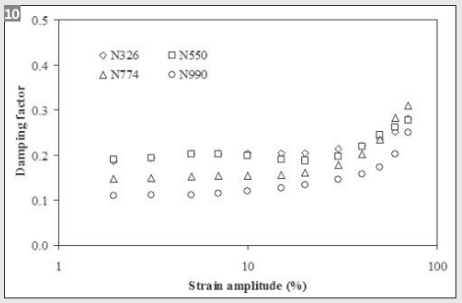

10 Damping factor (tanδ) as a function of strain amplitude of cured HNBR specimens (vulcanisates) with various carbon black specific surface area (measured at 1 rad/s and 60 °C)

behavour (Figs. 5 and 10), the increase in damping factor as a functions of both, the carbon black loading and the specific surface area is in good agreement with the increase in the M100 values of the corresponding vulcanisates. The increased carbon black loading and specific surface area mean a rise in contacting positions available for interactions between rubber molecules and the surface of carbon black. Also, the obstruction of rubber molecules by solid filler particlea or the hydrodynamic reinforcement could be another part of reason for an enhancement in the M100 values. Notably, the M100 values of vulcanisate with CB N550 appears to be close to that of CB N326 and becomes greater at high carbon black loading (60 phr) despite the relatively small specific surface area of CB N550. The results trend is similar to the one observed for G′ results discussed earlier. Thus, it is proposed that the reinforcement provided by N550 is governed by the crosslink density enhancement rather than the rubber-filler interaction.

The values obtained for tensile strength of filled HNBR vulcanisates are shown in Table 4. It is evident that strength of HNBR vulcanisates increases with increasing carbon black loading, which could be explained by filler reinforcement and/or crosslink density effects. Furthermore, it can be seen that tensile strength of HNBR filled with high specific surface area blacks is superior to the ones observed for small specific surface area blacks. Evidently, this is caused by filler reinforcement, as mentioned previously. However, an excessive crosslink density found particularly in vulcanisate with CB N550 might restrict molecular mobility, and thus a reduction in energy dissipation during being strained. This would end up with a decrease in mechanical strength [35]. One might notice that the strength of vulcanisate with CB N774 at high loading (60 phr) is highest among vulcanisates with CBN326, CB N550 and CB N990. The lowest strength found in CB N990 is not surprising as this black possesses relatively small specific surface area and low structure (low DBPA value) and thus low rubber-filler interaction. The apparently low strength observed in CB N326 at high loading is probably attributed to its relatively poor dispersion in HNBR. It is known that the capability of carbon black incorporation, distribution and dispersion is reduced with increasing specific surface area of the filler. Thus, some of undispersed CB N326 agglomerates might act as flaws in specimens leading to a reduction in tensile strength. In the case of CB N550, the excessive crosslink density might be responsible for a relatively low mechanical strength. Results of elongation at break (%EB) as illustrated in Table 4 agree well with the tensile strength result. From these results it holds: the greater the reinforcement, the lower the %EB. High extent of crosslink density and rubber-filler interaction would restrict molecular deformation and thus leading to a decrease in %EB.

In the case of carbon black loading and specific surface area effects on hardness of HNBR vulcanisates, it is apparent that the hardness increases with increasing carbon black loading. It is acknowledged that the relative deformation taking place in hardness test is relatively small. Consequently, the transient filler network in highly filled vulcanisates (i.e., HNBR vulcanisates with 60 phr N326 carbon black) might still influence the modulus at low strain (or hardness), and its effect is comparable to the crosslink density effect found in vulcanisates with CB N550.

The abrasion resistance of HNBR vulcanisates filled with various carbon black loadings is expressed as abrasion volume loss. It appears from Table 4 that, at a given specific surface area of carbon black, abrasion resistance is not significantly affected by carbon black loading. By contrast, at high carbon black loadings of 40 and 60 phr, both vulcanisates with N326 and N990 carbon black exhibit relatively low abrasion resistance. This phenomenon is probably due to poor filler dispersion at high loading of CB N326 having large specific surface area, and due to low magnitude of rubber-filler interaction of CB N990 possessing relatively low structure and specific surface area.

Conclusions

HNBR compounds and vulcanisates with various carbon black loadings and specific surface areas (or particle size) were prepared, and their cure, viscoelastic and mechanical properties were measured. Results obtained exhibit a significant dependence of cure behaviour (i.e., scorch time, optimum cure time and crosslink density) on carbon black loading and specific surface area. This dependence is explained in terms of thermal history, surface chemistry and thermal conductivity as a function of carbon black loading and specific surface area. Storage modulus and damping factor significantly increase with increasing carbon black specific surface area and loading of the blacks. The combined effect of hydrodynamic effect, filler transient network, molecular slippage at carbon black interfaces and crosslink density are proposed to be responsible for the viscoelastic properties. Mechanical properties are found to be governed by such combined effect associated probably with incomplete carbon black dispersion at high loading of carbon black (particularly in the case of relatively large specific surface area of carbon black, i.e., CB N326. The overall results imply a close correlation of viscoelastic and mechanical properties via energy dissipation process caused by molecular slippage at carbon black surfaces.

Acknowledgement

The authors thank The Royal Golden Jubilee Ph.D. Program, the Thailand Research Fund (IUG5080004) and Thai Industrial Rollers Co., Ltd. for their financial support of this research.

The authors

Ms. P. Wongwitthayakool is a Ph.D. research student in the Department of Chemistry, Faculty of Science, Mahidol University. Dr. P. Saeoui is a researcher at the National Metal and Materials Technology Center. Dr. C. Sirisinha is a lecturer in the Department of Chemistry, Faculty of Science, Mahidol University, and researcher based in the Research and Development Centre for Thai Rubber Industry at Mahidol University.

References

[1] K. C. Baranwal and H. L. Stephens, "Basic Elastomer Technology", The Rubber Division American Chemical Society, Akron (2001).
[2] J. S. Dick, "Rubber Technology: Compounding and Testing for Performance", Hanser, Munich (2001).
[3] C. R. G. Furtado, J. L. Leblanc and R. C. R. Nunes, Eur. Polym. J. **35** (1999) 1319.
[4] F. Yatsuyanagi, N. Suziki, M. Ito and H. Kaidou, Polymer **42** (2001) 9523.
[5] J. Sosnowski and W. A. Zmuda, Elastomery **11** (2007) 26.
[6] A. A. Wazzan, Intern. Polym. Mater. **54** (2005) 783.
[7] H. Tan and A. I. Isayev, J. Appl. Polym. Sci. **109** (2008) 767.
[8] B. T. Poh, H. Ismail and K. S. Tan, Polym. Test. **21** (2002) 801.
[9] S. Manroshan and A. Baharin, J. Appl. Polym. Sci. **96** (2005) 1550.
[10] P. Sae-oui, C. Sirisinha, T. Wantana and K. Hatthapanit, J. Appl. Polym. Sci. **104** (2007) 3478.
[11] J. Ansu, K. Philip and A. A. Santhosh, Int. J. P. Mater. **56** (2007) 593.
[12] P. Antony, S. K. De and M. van Duin, Rubber Chem. Technol. **74** (2001) 376.
[13] D. Achten and C. Wrana, Kautsch. Gummi Kunstst. **58** (2005) 298.
[14] D. Xu, J. Karger-Kocsis and A. K. Schlarb, eXPRESS Polym. Lett. **3** (2009) 126.

APPENDIX G
PUBLICATION
PREDICTION OF HEAT BUILD-UP BEHAVIOUR UNDER HIGH LOAD BY USE OF CONVENTIONAL VISCOELASTIC RESULTS IN CARBON BLACK FILLED HYDROGENATED NITRILE RUBBER

Prediction of heat build-up behaviour under high load by use of conventional viscoelastic results in carbon black filled hydrogenated nitrile rubber

P. Wongwitthayakool[1], P. Saeoui[2] and C. Sirisinha*[1,3]

Viscoelastic and heat build-up (HBU) properties of hydrogenated acrylonitrile butadiene rubber filled with various loadings and characteristics of carbon black were determined using RPA2000 and Gabometer 4000 flexometer equipped with high load cell respectively. A correlation of the viscoelastic results measured routinely with the HBU results is drawn. Reinforcement mechanism is proposed as an interplay of hydrodynamic effect, filler transient network, molecular slippage and cross-link density. In addition, the HBU significantly increases with increasing carbon black loading and/or surface area, which is probably the result of hysteretic process. As a prediction of HBU under high load, the loss modulus is superior to the damping factor.

Keywords: Reinforcement, Viscoelastic properties, Carbon black, Heat build-up, Hydrogenated nitrile rubber

Introduction

Hydrogenated acrylonitrile butadiene rubber (HNBR) is a high performance rubber specifically used in applications where high resistances to hydrocarbon oil and thermal aging are required. Consequently, HNBR is widely adopted in automotive, industrial and assorted, performance demanding applications. Despites its high mechanical properties, further reinforcement with the uses of reinforcing fillers is still of interest in order to gain HNBR vulcanisates having excellent mechanical properties and in conjunction with reduced production cost in some circumstances.

Carbon black (CB) is the most popular filler used in rubber industries as reinforcing filler. Particle size, structure, surface chemistry and loading of CB are known to be important factors affecting the properties of CB filled rubber products. Carbon black characteristics (i.e. specific surface area and structure) have been reported to significantly influence the reinforcement magnitude, which could be determined from the viscoelastic properties, as expressed in terms of storage modulus G', loss modulus G'' and damping factor tan δ. Numerous works[1–5] reveal that CB surface areas and loadings play strong roles in the viscoelastic behaviour of filled rubber.

Basically, the reinforcement mechanism of CB filled rubber is believed to be caused by hydrodynamic effect and CB–CB together with rubber–CB interactions.[6] Although the presence of rubber–CB interaction leads to a high extent of reinforcement, such interaction gives rise to the high magnitude of heat build-up (HBU) found in rubber products. This is because of the fact that the rubber–CB interaction is dominated by the physical over chemical interactions,[7] allowing molecular flow at rubber/CB interfaces and thus greater energy dissipation via hysteretic process.[8]

In CB filled rubber such as natural rubber, the HBU increases with increasing hysteresis loss, implying a correlation of HBU with the viscoelastic behaviour to some extent.[9] Consequently, the present study aims to investigate the interconnection between HBU and the viscoelastic properties of HNBR filled with CBs having different surface areas and structures. Generally, HBU measurement is carried out using a conventional Goodrich flexometer under low static stress (0·99 MPa), which is not suitable for such high modulus rubber vulcanisates as industrial roll products. The stress controlled flexometer provided with high load force, i.e. the Gabometer 4000 in this case, was therefore used. To measure the viscoelastic properties of HNBR vulcanisates as routine tests, a rubber process analyser (RPA2000) was utillised. The prediction of HBU by the routine measurement of viscoelastic properties was conducted and discussed.

Experimental

Materials

Raw HNBR (Therban VP KA 8837) having acrylonitrile and unsaturation contents of 34 and 18% respectively was purchased from Lanxess Co., Ltd (Bangkok,

[1]Department of Chemistry, Faculty of Science, Mahidol University, Rama 6 Rd., Bangkok 10400, Thailand
[2]National Metal and Materials Technology Center, 114 Thailand Science Park, Paholyothin Rd., Klong 1, Klong Luang, Pathumthani 12120, Thailand
[3]Research and Development Centre for Thai Rubber Industry (RDCTRI), Faculty of Science, Mahidol University, Salaya Campus, Phutthamonthon 4 Rd., Salaya, Nakhon Pathom 73170, Thailand

*Corresponding author, email sccsr@mahidol.ac.th

Published by Maney on behalf of the Institute
Received 7 July 2010; accepted 9 November 2010
DOI 10.1179/174328981OY.0000000028

Thailand). Four grades of CBs (N326, N550, N774 and N990) with different characteristics (i.e. surface area and structure) supplied by Loxley Public Co., Ltd (Bangkok, Thailand) and Siam Luck Trading Co., Ltd (Bangkok, Thailand) were used as reinforcing filler. Referred to ASTM D1765-00,[10] the specific surface area as specified by iodine adsorption value and the degree of structure as determined by dibutylphthalate absorption test are shown in Table 1. The specific surface areas of CBs used in this work are in the following order: N326> N550>N774>N990, while the degree of structure is in the following order: N550>N326 ~ N774>N990. The tri-2-ethylhexyl trimellitate as plasticiser was purchased from Behn Meyer Chemical (Thailand) Co., Ltd (Bangkok, Thailand). Dicumyl peroxide (98% active) as a curing gent was supplied by Petchthai Chemical Co., Ltd (Bangkok, Thailand).

Samples preparation

The formulation of HNBR compounds prepared is listed in Table 2. The mixing process was commenced on a laboratory scale open mill (LabTech Co., Ltd, Bangkok, Thailand) at a set temperature of 40°C. Then, the masticated HNBR was compounded with prepared CB and chemicals, as illustrated in Table 2, on the mill for 20 min. To be cylindrical in shape, having diameters of $17{\cdot}8 \pm 0{\cdot}1$ mm and heights of $25 \pm 0{\cdot}15$ mm, in accordance with ASTM D623-93 for the HBU measurement,[10] the compounds prepared were compression moulded at 145°C under moulding pressure of 150 kg cm^{-2} for 120 min.

Characterisations

Viscoelastic properties

The viscoelastic behaviours of HNBR vulcanisates were measured using a rubber process analyser (RPA2000, Alpha Technologies, Akron, OH, USA). The ~5 g of rubber compound was placed in the test cavity clamped by pseumatic pressure. The strain sweep test was then conducted under a test angular frequency of 1 rad s^{-1}. The test temperature was kept constant at 60°C according to the actual service temperature of this rubber roll application. The resultant storage modulus or elastic modulus G', loss modulus or viscous modulus G'' and damping factor or loss factor tan δ were recorded. It must be noted that the time sweep test was initially performed to monitor the thermal stability of the test specimens, so that it could be ensured that any change in results of the strain sweep tests is not caused mainly by thermal degradation.

Heat build-up behaviour

Gabometer 4000 was utillised to determine the magnitude of HBU in HNBR vulcanisates under high static stress of 1·97 MPa under frequency and dynamic displacement of 15 Hz and 2·2 mm respectively, for 25 min. The test temperature of 100°C was selected because of two main reasons: this temperature is the widely used test temperature for HBU measurement in both tyre and rubber roll industries, and this temperature could facilitate the deformation of test specimens with high hardness of vulcanisates, compared with the test temperature of 60°C used in the RPA2000 experiment.

Table 1 Carbon black properties

Properties	N326	N550	N774	N990
Iodine adsorption no. D 1510/g kg^{-1}	82	43	29	…
Dibutylphthalate no. D 2414/10^{-5} m^3 kg^{-1}	72	121	72	43

Results and discussion

To investigate the viscoelastic properties of HNBR vulcanisates filled with different types and loadings of CB, the RPA2000 as the oscillatory rheometer specially designed for the elastomer was used. RPA2000 has gained interest from rubber technologists due to its ease of operation and precise data measured. In general, the time, strain and frequency sweep tests are usually performed, giving valuable data correlating to the rubber processing aspect. In view of the dynamic mechanical properties of vulcanisates, particularly the HBU behaviour, the conventional Goodrich flexometer is usually utilised. However, in some industrial roll products in which high stress is applied to the rolls, the high modulus of the rubber vulcanisates covering the metal cores is required in order to prevent excessive deformation. This means that the high modulus of roll products is needed. The precise prediction of HBU behaviour of this high modulus rubber vulcanisate is not practical with the use of conventional Goodrich flexometer under the static stress of only 0·99 MPa. Consequently, the stress controlled flexometer equipped with high load cell (up to 4000 N), namely, Gabometer 4000, was used to measure the HBU of rubber vulcanisates in the present work. It is of interest to establish a correlation between the HBU under high applied stress and the viscoelastic results measured from RPA2000. It must be noted that the test temperature of 60°C was used in the RPA2000 experiment, which is analogous to the actual service temperature of this rubber roll product, while that of 100°C was utilised for the HBU test because of the fact that this temperature is a widely used test temperature in tyre and rubber roll industries. By this means, if such a correlation is significant, then it is possible to extend the usefulness of RPA2000 routine test results via the prediction of HBU behaviours.

Viscoelastic properties

Effect of CB loading

The dynamic mechanical properties of cured HNBR with various CB loadings, as determined from RPA2000, are shown in Figs. 1–3. It is evident from Fig. 1 that an unfilled compound possesses the lowest G' and the broadest plateau of linear viscoelastic region of up to 20% strain. A further increase in strain leads to the drop in G' due to the molecular flow of the uncured portion existing in the HNBR vulcanisates. In addition,

Table 2 Compounding ingredients used in present study

Chemical name	Function	Amount/phr
HNBR	Rubber matrix	100
CB	Reinforcing filler	Varied: 0–60
TMQ*	Antioxidant	1
Zinc oxide (ZnO)	Cure activator/filler	5
Stearic acid	Cure activator/softener	1
TOTM†	Plasticiser	5
Dicumyl peroxide (DCP)	Curing agent	2

*2,2,4-trimethyl-1,2-dihydroquinoline.
†Tri-2-ethylhexyl trimellitate.

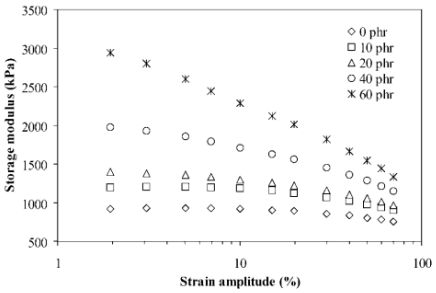

1 Storage modulus as function of strain amplitude of cured HNBR specimens (vulcanisates) with various N326 loadings (measured at 1 rad s^{-1} and 60°C)

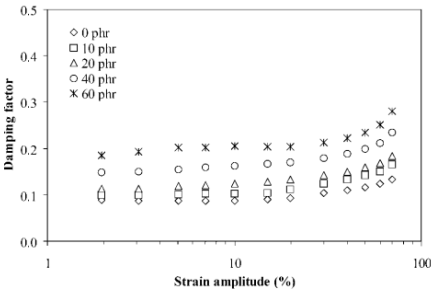

3 Damping factor as function of strain amplitude of cured HNBR specimens (vulcanisates) with various N326 loadings (measured at 1 rad s^{-1} and 60°C)

G' increases with increasing CB loading, which is due mainly to three main reasons, as follows:

(i) flow field obstruction of rubber molecules by undeformable CB aggregates usually known as a hydrodynamic effect
(ii) flow restriction caused by a strong filler–rubber interaction at the surfaces of the CB aggregates
(iii) molecular flow reduction by the formation of transient network of CB (or the so called percolated CB network).[4,8]

However, such a transient network could be disrupted by high deformation, yielding a strain softening phenomenon at high strain or the so called Payne effect.[8] The magnitude of the Payne effect appears to increase with increasing CB loading, which is in line with previous work.[4,11]

Figure 2 reveals the results of loss modulus G'', in which G'' of all compounds increases with increasing CB loading. This is because of the hydrodynamic effect, the filler–rubber interaction as well as filler–filler interaction, as discussed in G' results. It is reported that G'' is dependent on rates of transient network breakdown and reformation under dynamic strain. The processes of filler network breakdown and reformation cause additional energy dissipation.[8] In HNBR vulcanisates filled CB loading up to 20 phr, where the magnitude of the percolated CB network is relatively small (*see* Fig. 1), G'' appears to be independent of strain up to 20% and then slightly increases with increasing shear strain, which could be caused by the viscous dissipation via molecular flow. By contrast, with further CB loading, the HNBR vulcanisates initially reveal the reduction in G'' with strain amplitude followed by the somewhat rise in G'' at high strain. The reduction in G'' is in good accordance with the fact that the percolated CB network is destroyed and could not be reconstructed. At high strain of deformation, where the filler transient network is already disrupted, the viscous dissipation via molecular flow at CB surfaces is believed to be responsible for the slight increase in G''.

Figure 3 demonstrates the change in damping factor or tan δ, which is the ratio of loss to storage moduli as a function of deformation strain. In general, the damping factor could be used to imply the magnitude of the viscous response per unit of elastic response. It is evident that the damping factor of all vulcanisates increases with increasing strain amplitude, indicating the rise in magnitude of the viscous contribution dominating over the elastic one. The increase in damping factor is reported to be the result of energy dissipation through a molecular slippage associated with the breakdown of percolated CB network. This phenomenon is sometimes known as a hysteretic process.[4]

Effect of CB specific surface area (particle size)

In this section, the influence of CB surface area (or particle size) on the viscoelastic properties of HNBR

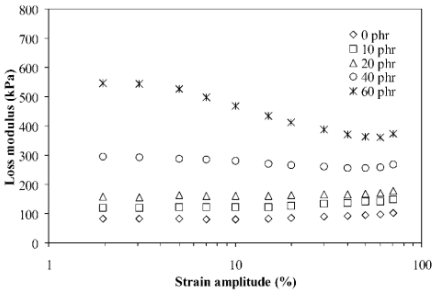

2 Loss modulus as function of strain amplitude of cured HNBR specimens (vulcanisates) with various N326 loadings (measured at 1 rad s^{-1} and 60°C)

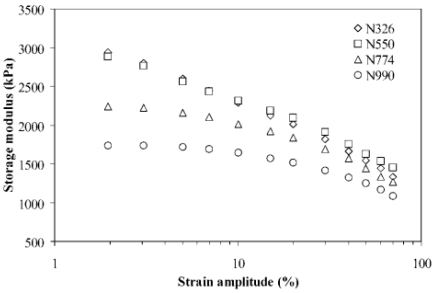

4 Storage modulus as function of strain amplitude of cured HNBR specimens (vulcanisates) with various CB surface areas (measured at 1 rad s^{-1} and 60°C)

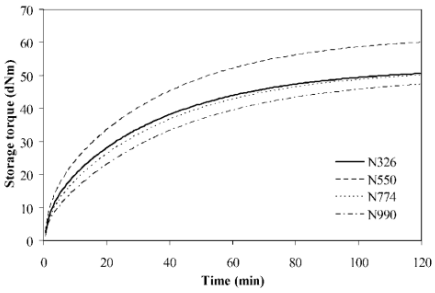

5 Cure curves of HNBR vulcanisates filled with various types of CB

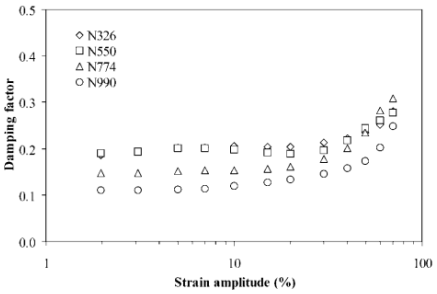

7 Damping factor as function of strain amplitude of cured HNBR specimens (vulcanisates) with various CB surface areas (measured at 1 rad s^{-1} and 60°C)

vulcanisates at a given black loading of 60 phr is focused. Figure 4 exhibits G' rise with increasing CB surface area, which could be explained by the greater contacting area available for interaction between rubber and CB as well as between filler particles (i.e. the percolated CB network). It is noticeable that, although N550 CB possesses a lower specific surface area than N326 CB, the vulcanisate with N550 shows comparable G' with that with N326. This phenomenon could be explained by two main reasons: the high structure of N550 yields a large amount of occluded rubber, providing the effective reinforcement effect, and the relatively high cross-link density in the vulcanisates with N550 CB as evidenced by the high value of torque difference (i.e. the discrepancy in torques between maximum and minimum torque determined from cure curves),[12] as shown in Fig. 5. Such high cross-link density found in the vulcanisates with N550 is believed to cause a large amount of tightly bound rubber, which has been reported to obstruct the curative absorption on filler surfaces. This means that a migration of free curatives to the free rubber matrix is promoted, leading to the increased cross-link density.[13] It is also obvious that G' of the vulcanisate with N550 shows less strain dependence than that with N326, supporting the effect of the cross-link density. The results of G'' as a function of strain amplitude are presented in Fig. 6. It is evident that the strain dependent G'' is clearly observed in all cured compounds, with the greater magnitude found in compounds filled with CB having higher surface area. At a deformation strain smaller than 30%, except for N990 thermal black having a small surface area, G'' appears to decrease with strain due to the disruption of the transient filler network. Specimens with high surface CB demonstrate high G'' due to the high magnitude of the filler network, as discussed previously in Fig. 2. The somewhat increase in G'' at high strain is attributed to the viscous dissipation via molecular flow after the filler network is broken up.

Figure 7 reveals the tan δ results of HNBR vulcanisates in a way that tan δ increases as the specific surface area of CB increases. As mentioned in the CB loading effect, the increase in contacting area (by increasing surface area in this case) available for the physical interaction between rubber and CB would lead to the rise in energy dissipation via molecular flow at the CB interfaces. Again, the increment in tan δ as a function of strain is due to the disruption of filler transient network facilitating the molecular mobility of HNBR molecules. The strain onset for the rise in tan δ is smaller in specimens with lower surface areas.

Heat build-up behaviour

As mentioned earlier, the high applied stress is required to measure the HBU behaviour of HNBR vulcanisates having high modulus designed for the roll covering applications to be used in steel and paper mills. A specially designed flexometer capable of offering high load applied

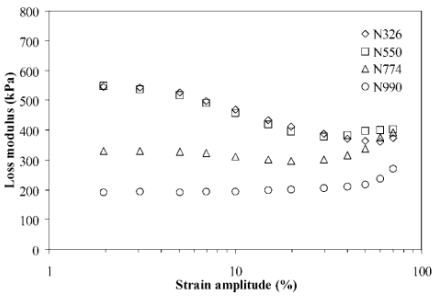

6 Loss modulus as function of strain amplitude of cured HNBR specimens (vulcanisates) with various CB surface areas (measured at 1 rad s^{-1} and 60°C)

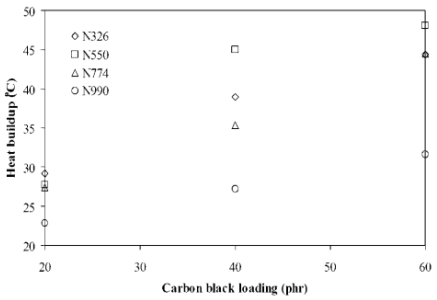

8 Relationship among HBU, CB loading and surface area of HNBR vulcanisates

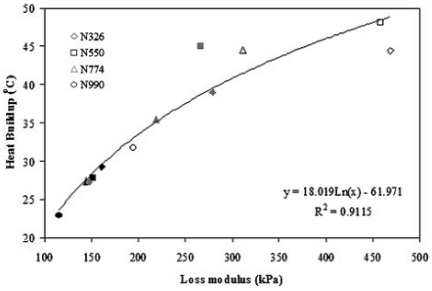

9 Relationship between HBU and loss modulus measured at 10% strain and 60°C of cured HNBR (vulcanisates) with various CB surface areas and loadings: 20 phr (black solid symbol); 40 phr (gray solid symbol); 60 phr (unfilled symbol)

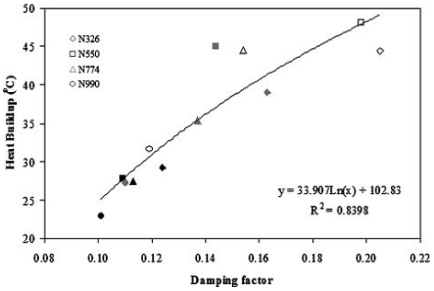

10 Relationship between HBU and damping factor measured at 10% strain and 60°C of cured HNBR (vulcanisates) with various CB surface areas and loadings: 20 phr (black solid symbol); 40 phr (gray solid symbol); 60 phr (unfilled symbol)

to the test specimens is required. In this work, Gabometer 4000 was utilised at the test temperature of 100°C. Figure 8 reveals the HBU behaviour of black filled HNBR vulcanisates. By increasing the CB loading, HBU significantly increases, and the magnitude of HBU rise is more pronounced in specimens with high surface area and/or structure of CB. Such an increase in HBU is anticipated to be the results of hysteretic process via the disruption of transient filler network and molecular flow at the CB interfaces.[8,9] Exceptionally, the HBU is found to be the highest in HNBR filled with N550, which is due probably to its relatively high extent of developed structure. At a given CB loading, the increases in surface area and structure of CB would increase the filler transient network. Under deformation, these transient networks are disrupted, leading to the increase in hysteresis loss and thus higher HBU in rubber vulcanisates.

From Fig. 8, it is clear that the HBU behaviour depends significantly on the CB characteristics and is needed to be measured for ensuring the acceptable performance of the rubber product. However, the HBU measurement using the flexometer equipped with high load cell and powerful shaker is rather costly. Thus, one of the objectives of the present work is to draw the correlation between viscoelastic results measured from oscillatory RPA2000 as a routine test and the HBU monitored from the specially designed flexometer. By this means, it is possible to estimate the HBU from the RPA2000 results. Figure 9 illustrates the relationship between loss modulus G'' as a hysteresis loss and HBU behaviour of cured HNBR (vulcanisates) filled with various CB surface areas. Evidently, regardless of the CB characteristics, the HBU increases with increasing hysteresis loss and their correlation to logarithmically agree well with the expression, as shown in equation (1) with R^2=0·9115. In other words, hysteresis loss plays a strong role in the HBU of HNBR vulcanisates studied. Apart from G'', one might consider the loss factor tan δ as an indication of HBU at a given G' (or stiffness). Figure 10 reveals the change in HBU as a function of tan δ in a similar trend to that of HBU against G'', as illustrated in equation (2), but with the lower R^2 of 0·8398. The results imply clearly that, as an indication of HBU under high load applied, G'' is superior to tan δ. Table 3 demonstrates that changing the chosen conditions (amplitude and frequency) does not influence the conclusion about the ranking of the R^2 factors

$$\mathrm{HBU} = 18{\cdot}019 \ln(G'') - 61{\cdot}971 \quad (1)$$

$$\mathrm{HBU} = 33{\cdot}907 \ln(\tan\delta) + 102{\cdot}83 \quad (2)$$

where HBU is determined from the Gabometer 4000, while G'' and tan δ are loss modulus and loss factor respectively, as measured routinely from RPA2000.

Table 3 Comparison of R^2 values as determined from regression of G'' versus HBU and tan δ versus HBU plots at various test frequencies and strains

Conditions used		R^2 values	
Angular frequency/rad s^{-1}	Strain/%	G'' versus HBU	tan δ versus HBU
1	2	0·8881	0·8023
1	10	0·9115	0·8398
1	70	0·8635	0·7117
10	10	0·9143	0·8491
50	10	0·9108	0·8325
100	10	0·9106	0·8280

Conclusions

Hydrogenated acrylonitrile butadiene rubber vulcanisates with various CB loadings and characteristics (i.e. specific surface area and structure) were prepared. Viscoelastic properties as determined from oscillatory rheometer (RPA2000) were discussed. The HBU behaviour was monitored using a stress controlled flexometer equipped with high load cell (up to 4000 N), namely, Gabometer 4000. Attempts to establish a relationship among filler characteristics, magnitude of reinforcement and viscoelastic as well as HBU behaviours were made.

The results of viscoelastic behaviour demonstrate that, by increasing CB loading and surface area, the elastic modulus G' associated with the damping factor tan δ increases significantly. Mechanisms of CB reinforcement in HNBR are proposed as combined effects of hydrodynamic effect, filler transient network, molecular slippage at CB interfaces and cross-link density. In addition, the HBU significantly increases with increasing

CB loading and/or surface area, and the magnitude of HBU rise is more pronounced in specimens with high surface area and/or structure. Last, it is possible to estimate the HBU generally measured from the high load flexometer from the RPA2000 results as a routine test; G'' is a more effective indication of HBU than tan δ.

Acknowledgements

The authors would like to thank The Royal Golden Jubilee PhD Program, The Thailand Research Fund (grant no. IUG5080004) and Thai Industrial Rollers Co., Ltd, for the financial support on this research.

References

1. A. I. Medalia: *Rubber Chem. Technol.*, 1973, **46**, 877.
2. N. K. Dutta, D. Khastgir and D.K.Tripathy: *J. Mater. Sci.*, 1991, **26**, 177.
3. P. Thavamani and A. K. Bhowmick: *J. Mater. Sci.*, 1992, **27**, 3243.
4. T. Sajjayanukul, P. Saeoui and C. Sirisinha: *J. Appl. Polym. Sci.*, 2005, **97**, 2197.
5. E. Demirhan, F. Kandemirli and M. Kandemirli: *Mater. Des.*, 2007, **28**, 1326.
6. G. Kohls and G. Beaucage: *Curr. Opin. Solid State Mater. Sci.*, 2002, **6**, 183.
7. S. K. De and J. R. White: 'Rubber technologist's handbook'; 2001, Shropshire, Rapra Technology.
8. M. J. Wang: *Rubber Chem. Technol.*, 1998, **71**, 520.
9. D. M. Park, W. H.Hong, S. G. Kim and H. J. Kim: *Eur. Polym. J.*, 2000, **36**, 2429.
10. 'Annual book of ASTM standards: rubber, natural and synthetic – general test methods', ASTM, West Conshohocken, PA, USA, 2003.
11. J. Fröhlich, W. Niedermeier and H. D. Luginsland: *Composites A*, 2005, **36A**, 449.
12. P. Phewphong, P. Saeoui and C. Sirisinha: *Polym. Test.*, 2008, **27**, 873.
13. S. S. Choi, K. J. Hwang and B. T. Kim: *J. Appl. Polym. Sci.*, 2005, **98**, 2282.

BIOGRAPHY

NAME Miss Panjaporn Wongwitthayakool

DATE OF BIRTH September 16, 1980

PLACE OF BIRTH Bangkok, Thailand

INSTITUTIONS ATTENDED Silpakorn University, 1998-2002
Bachelor of Science (Chemistry)
Mahidol University, 2003-2007
Master of Science
(Polymer Science)
Mahidol University, 2007-2009
Doctor of Philosophy
(Polymer Science and Technology)

RESEARCH GRANTS The Royal Golden Jubilee PhD program

HOME ADDRESS 40/94, Phetkasem Road, Nongkangplu, Nongkhaem, Bangkok, Thailand 10160
Tel. +66 81 932 1501, +66 2 420 1586
E-mail: panjap_w@hotmail.com, marnmok@hotmail.com

PUBLICATION / PRESENTATION

1. P. Wongwitthayakool, P. Saeoui, C. Sirisinha, "Correlation of Phase Morphology and Rheological Properties in CPE Blended with a Low-cost Grade of NR", Proceeding of the 1st World Rubber Summit at Impact Convention Center, Pathumthani, Thailand, 2006.
2. P. Wongwitthayakool, P. Saeoui, C. Sirisinha, "Correlation of Phase Morphology and Rheological Properties in CPE Blended NR", Proceeding of the 1st Polymer Graduate Conference of Thailand at Mahidol University, Salaya, Nakhonpathom, Thailand, 2007.

3. P. Wongwitthayakool, P. Saeoui, C. Sirisinha, “Viscoelastic Behaviour of Carbon Black-Filled Hydrogenated Acrylonitrile Butadiene Rubber”, Proceeding of The Fifth Thailand Materials Science and Technology Conference (MSAT-5) at Miracle Grand Hotel, Bangkok, Thailand, 2008.
4. P. Wongwitthayakool, P. Saeoui, C. Sirisinha, “Rheological Properties of Chlorinated Polyethylene Blended with Low-cost Grade Natural Rubber”, International Polymer Processing, 24 (1), pp. 9-15, 2009.
5. P. Wongwitthayakool, P. Saeoui, C. Sirisinha, “Effect of Carbon Black Hybrid System on Cure Behaviour and Dynamic Mechanical Properties of Hydrogenated Acrylonitrile Butadiene Rubber”, Proceeding of Asian Conference on Thermal Analysis and Applications (ASTA 2009) at Pullman King Power Hotel, Bangkok, Thailand, 2009.
6. P. Wongwitthayakool, P. Saeoui, C. Sirisinha, “Cure and Viscoelastic Properties of HNBR”, KGK Kautschuk Gummi Kunststoffe, 63 (11), pp. 506-512, 2010.
7. P. Wongwitthayakool, P. Saeoui, C. Sirisinha, “Prediction of Heat Build-up Behaviour under High Load by Use of Conventional Viscoelastic Results in Carbon Black Filled Hydrogenated Nitrile Rubber”, Plastics, Rubber and Composites, 40 (5), pp. 234-239, 2011.
8. P. Wongwitthayakool, J.L. Leblanc, P. Saeoui, C. Sirisinha, “Non-linear Viscoelastic Characterization of Carbon Black Hybrid System Filled Hydrogenated Acrylonitrile Butadiene Rubber through Large Amplitude Harmonic Experiment”, Proceeding of RGJ – PH.D. Congress XII at Jomtien Plam Beach Resort, Pattaya, Chonburi, Thailand, 2011.
9. P. Wongwitthayakool, J.L. Leblanc, C. Sirisinha, “A Study of Heat Build-up Behavior of Carbon Black Filled HNBR Compounds using Closed Cavity Torsional Rheometers”, Proceeding of The 12th Pacific Polymer Conference (PPC12) The 12th Pacific Polymer Conference (PPC12) at Jeju Shilla Hotel, Jeju Island, Korea, 2011.